



(51) International Patent Classification:

A61K 31/40 (2006.01) A61K 31/4035 (2006.01)
A61K 31/4015 (2006.01)

(21) International Application Number:

PCT/US2018/025507

(22) International Filing Date:

30 March 2018 (30.03.2018)

(25) Filing Language:

English

(26) Publication Language:

English

(30) Priority Data:

62/480,407 01 April 2017 (01.04.2017) US
62/519,784 14 June 2017 (14.06.2017) US
62/567,153 02 October 2017 (02.10.2017) US
62/573,117 16 October 2017 (16.10.2017) US
62/588,025 17 November 2017 (17.11.2017) US
62/595,327 06 December 2017 (06.12.2017) US
62/630,158 13 February 2018 (13.02.2018) US

02139 (US). DANA-FARBER CANCER INSTITUTE, INC. [US/US]; 450 Brookline Avenue, Boston, MA 02215 (US).

(72) Inventors; and

(71) Applicants: REGEV, Aviv [US/US]; c/o 415 Main Street, Cambridge, MA 02142 (US). ROZENBLATT-ROSEN, Orit [US/US]; c/o 415 Main Street, Cambridge, MA 02142 (US). JERBY, Livnat [US/US]; c/o 450 Brookline Avenue, Boston, MA 02215 (US).

(72) Inventors: IZAR, Benjamin; c/o 450 Brookline Avenue, Boston, MA 02215 (US). ROTEM, Asaf; c/o 450 Brookline Avenue, Boston, MA 02215 (US).

(74) Agent: SCHER, Michael, B.; Johnson, Marcou & Isaacs, LLC, P.O. Box 691, Hoschton, GA 30548 (US).

(81) Designated States (unless otherwise indicated, for every kind of national protection available): AE, AG, AL, AM, AO, AT, AU, AZ, BA, BB, BG, BH, BN, BR, BW, BY, BZ, CA, CH, CL, CN, CO, CR, CU, CZ, DE, DJ, DK, DM, DO, DZ, EC, EE, EG, ES, FI, GB, GD, GE, GH, GM, GT, HN, HR, HU, ID, IL, IN, IR, IS, JO, JP, KE, KG, KH, KN, KP, KR, KW, KZ, LA, LC, LK, LR, LS, LU, LY, MA, MD, ME, MG, MK, MN, MW, MX, MY, MZ, NA, NG, NI, NO, NZ,

(71) Applicants: THE BROAD INSTITUTE, INC. [US/US]; 450 Main Street, Cambridge, MA 02142 (US). MASSACHUSETTS INSTITUTE OF TECHNOLOGY [US/US]; 77 Massachusetts Avenue, Cambridge, MA

(54) Title: METHODS AND COMPOSITIONS FOR DETECTING AND MODULATING AN IMMUNOTHERAPY RESISTANCE GENE SIGNATURE IN CANCER

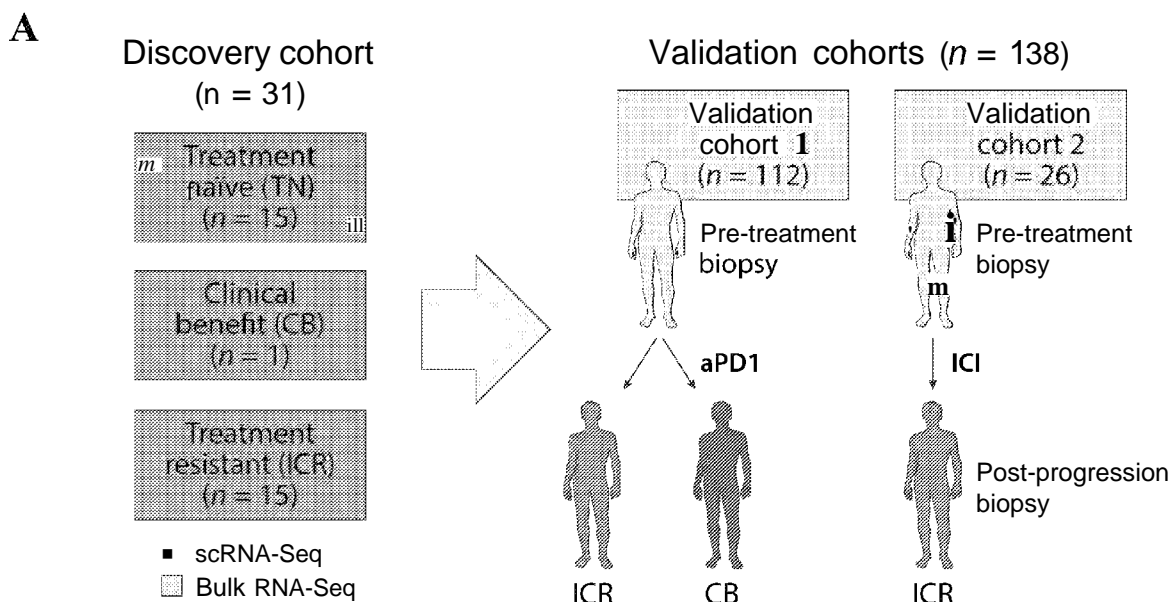


FIG. 1A

(57) Abstract: The subject matter disclosed herein is generally directed to detecting and modulating novel gene signatures for the treatment and prognosis of cancer. The novel gene signatures predict overall survival in cancer and can be targeted therapeutically.

WO 2018/183921 A1

OM, PA, PE, PG, PH, PL, PT, QA, RO, RS, RU, RW, SA, SC, SD, SE, SG, SK, SL, SM, ST, SV, SY, TH, TJ, TM, TN, TR, TT, TZ, UA, UG, US, UZ, VC, VN, ZA, ZM, ZW.

- (84) Designated States** (*unless otherwise indicated, for every kind of regional protection available*): ARIPO (BW, GH, GM, KE, LR, LS, MW, MZ, NA, RW, SD, SL, ST, SZ, TZ, UG, ZM, ZW), Eurasian (AM, AZ, BY, KG, KZ, RU, TJ, TM), European (AL, AT, BE, BG, CH, CY, CZ, DE, DK, EE, ES, FI, FR, GB, GR, HR, HU, IE, IS, IT, LT, LU, LV, MC, MK, MT, NL, NO, PL, PT, RO, RS, SE, SI, SK, SM, TR), OAPI (BF, BJ, CF, CG, CI, CM, GA, GN, GQ, GW, KM, ML, MR, NE, SN, TD, TG).

Published:

- *with international search report (Art. 21(3))*
- *before the expiration of the time limit for amending the claims and to be republished in the event of receipt of amendments (Rule 48.2(h))*
- *with sequence listing part of description (Rule 5.2(a))*

METHODS AND COMPOSITIONS FOR DETECTING AND MODULATING AN IMMUNOTHERAPY RESISTANCE GENE SIGNATURE IN CANCER

CROSS-REFERENCE TO RELATED APPLICATIONS

[0001] This application claims the benefit of U.S. Provisional Application Nos. 62/480,407, filed April 1, 2017, 62/519,784, filed June 14, 2017, 62/567,153, filed October 2, 2017, 62/573,117, filed October 16, 2017, 62/588,025, filed November 17, 2017, 62/595,327, filed December 6, 2017 and 62/630,158, filed February 13, 2018. The entire contents of the above-identified applications are hereby fully incorporated herein by reference.

STATEMENT REGARDING FEDERALLY SPONSORED RESEARCH

[0002] This invention was made with government support under grant Nos. CA222663, CA180922, CA202820 and CA14051 awarded by the National Institutes of Health. The government has certain rights in the invention.

TECHNICAL FIELD

[0003] The subject matter disclosed herein is generally directed to detecting and modulating novel gene signatures for the treatment and prognosis of cancer.

BACKGROUND

[0004] One reason that cancer cells thrive is because they are able to hide from the immune system. Certain cancer cells avoid the immune system better than others and could be a factor in determining survival. Immunotherapies have been developed to enhance immune responses against cancer and lead to prolonged survival. Immunotherapies have transformed the therapeutic landscape of several cancer types. In particular, immune checkpoint inhibitors (ICI) lead to durable responses in ~35% of patients with metastatic melanoma by unleashing T cells from oncogenic suppression (1, 2). Nonetheless, the tumors of most melanoma patients manifest either intrinsic or acquired ICI resistance (ICR). ICR is often unpredictable and poorly understood (3), hampering appropriate selection of patients for therapies, rational enrollment to clinical trials and the development of new therapeutic strategies that could overcome ICR (1).

[0005] Recent clinical studies attempted to characterize and predict ICR based on analyses of Whole Exome Sequencing (WES) and transcriptional profiles of tumors at the bulk level (4, 5). These studies demonstrated that tumors with a high mutational load (4) or

high immune cell infiltration (6, 7) are more likely to respond, and linked ICR in patients to functional immune evasion phenotypes, including defects in the JAK/STAT pathway (8) and interferon gamma (IFN- γ) response (8, 9), impaired antigen presentation (5, 8), PTEN loss (10), and increased WNT-B-catenin signaling (77). However, thus far, the predictive power of these and other (72) approaches has been limited, either because they report on only some facets of the causes of resistance (WES) and/or because they are highly confounded by tumor composition (RNA and copy-number variations). Indeed, because ICI targets the interactions between different cells in the tumor, its impact depends on multicellular circuits of malignant and non-malignant cells (73), which are challenging to study in bulk tumor specimens. Single-cell genomics, especially single cell RNA-Seq (scRNA-Seq), provides a unique tool to comprehensively map the tumor ecosystem (73-77), but has thus far not been used to study ICR. Thus, there is a need to better understand tumor immunity and resistance to immunotherapy.

[0006] Citation or identification of any document in this application is not an admission that such document is available as prior art to the present invention.

SUMMARY

[0007] Immune checkpoint inhibitors (*ICI*) produce durable responses in some patients with melanoma. Yet most patients derive no clinical benefit, and molecular underpinnings of ICI resistance (ICR) are elusive.

[0008] It is an objective of the present invention to identify molecular signatures for diagnosis, prognosis and treatment of subjects suffering from cancer. It is a further objective to understand tumor immunity and to leverage this knowledge for treating subjects suffering from cancer. It is another objective for identifying gene signatures for predicting response to checkpoint blockade therapy. It is another objective, for modulating the molecular signatures in order to increase efficacy of immunotherapy (e.g., checkpoint blockade therapy).

[0009] Here, Applicants leveraged single-cell RNA-seq (scRNA-seq) from 31 melanoma tumors and novel computational methods to systematically interrogate malignant cell states that promote immune evasion. Applicants identified a resistance program expressed by malignant cells that is strongly associated with T cell exclusion and direct evasion from immunity. The program is present prior to immunotherapy, is apparent *in situ*, and predicts clinical responses to anti-PD-1 therapy in an independent cohort of 112 melanoma patients.

CDK4/6-inhibition represses this program in individual malignant cells and induces a Senescence Associated Secretory Phenotype (SASP). This study provides a high-resolution landscape of ICI resistant cell states, identifies clinically predictive signatures, and forms a basis to develop novel therapeutic strategies that could overcome immunotherapy resistance. Applicants additionally applied single-nuclei RNA-seq (sNuc-seq) to characterize thousands of cells from estrogen-receptor-positive metastatic breast cancer (MBC). ER+ MBC is currently treated with CDK4/6-inhibitors (see, e.g., Vasan et al., State-of-the-Art Update: CDK4/6 Inhibitors in ER+ Metastatic Breast Cancer, *AJHO*. 2017;13(4):16-22). Finally, Applicants applied single-cell RNA-seq (scRNA-seq) to characterize thousands of cells from colon cancer.

[0010] In one aspect, the present invention provides for a method of detecting an immune checkpoint inhibitor resistance (ICR) gene signature in a tumor comprising, detecting in tumor cells obtained from a subject in need thereof the expression or activity of a malignant cell gene signature comprising: one or more genes or polypeptides selected from the group consisting of C1QBP, CCT2, CCT6A, DCAF13, EIF4A1, ILF2, MAGEA4, NONO, PA2G4, PGAM1, PPA1, PPIA, RPL18A, RPL26, RPL31, RPS1 1, RPS15, RPS21, RPS5, RUVBL2, SAE1, SNRPE, UBA52, UQCRH, VDAC2, AEBP1, AHNAK, APOC2, APOD, APOE, B2M, C10orf54, CD63, CTSD, EEA1, EMP1, FBX032, FYB, GATSL3, HCP5, HLA-A, HLA-B, HLA-C, HLA-E, HLA-F, HLA-H, ITGA3, LAMP2, LYRM9, MFGE8, MIA, NPC2, NSG1, PROS1, RDH5, SERPINA1, TAPBP, TIMP2, TNFSF4 and TRIML2 (refined uICR, see table S6); or one or more genes or polypeptides selected from the group consisting of ACAT1, ACP5, ACTB, ACTG1, ADSL, AEN, AK2, ANP32E, APP, ASAP1, ATP5A1, ATP5D, ATP5G2, BANC1, BCAN, BZW2, C17orf76-AS1, C1QBP, C20orf12, C6orf48, CA14, CBX5, CCT2, CCT3, CCT6A, CDK4, CEP170, CFL1, CHP1, CNRIP1, CRABP2, CS, CTPS1, CYC1, DAP3, DCAF13, DCT, DDX21, DDX39B, DLL3, EDNRB, EEF1D, EEF1G, EEF2, EIF1AX, EIF2S3, EIF3E, EIF3K, EIF3L, EIF4A1, EIF4EBP2, ESRP1, FAM174B, FAM178B, FAM92A1, FBL, FBLN1, FOXRED2, FTL, FUS, GABARAP, GAS5, GNB2L1, GPATCH4, GPI, GRWD1, GSTO1, H3F3A, H3F3AP4, HMGA1, HNRNPA1, HNRNPAIPIO, HNRNPC, HSPA8, IDH2, IFI16, ILF2, IMPDH2, ISYNA1, ITM2C, KIAA0101, LHFPL3-AS1, LOC100190986, LYPLA1, MAGEA4, MARCKS, MDH2, METAP2, MIDI, MIR4461, MLLT1 1, MPZL1, MRPL37, MRPS12, MRPS21, MYC, NACA, NCL, NDUFS2, NF2, NIDI, NOLC1, NONO, NPML, NUCKS1, OAT, PA2G4, PABPC1, PAFAH1B3, PAICS, PFDN2, PFN1, PGAM1, PIH1D1, PLTP, PPA1,

PPIA, PPP2R1A, PSAT1, PSMD4, PTMA, PYCARD, RAN, RASA3, RBM34, RNF2, RPAIN, RPL10, RPL10A, RPL11, RPL12, RPL13, RPL13A, RPL13AP5, RPL14, RPL17, RPL18, RPL18A, RPL21, RPL26, RPL28, RPL29, RPL3, RPL30, RPL31, RPL35, RPL36A, RPL37, RPL37A, RPL39, RPL4, RPL41, RPL5, RPL6, RPL7, RPL7A, RPL8, RPLPO, RPLP1, RPSIO, RPS11, RPS12, RPS15, RPS15A, RPS16, RPS17, RPS17L, RPS18, RPS19, RPS2, RPS21, RPS23, RPS24, RPS26, RPS27, RPS27A, RPS3, RPS3A, RPS4X, RPS5, RPS6, RPS7, RPS8, RPS9, RPSA, RSL1D1, RUVBL2, SAE1, SCD, SCNM1, SERBP1, SERPINF1, SET, SF3B4, SHMT2, SKP2, SLC19A1, SLC25A3, SLC25A5, SLC25A6, SMS, SNAI2, SNHG16, SNHG6, SNRPE, SORD, SOX4, SRP14, SSR2, TIMM13, TIMM50, TMC6, TOP1MT, TP53, TRAP1, TRPM1, TSR1, TUBA1B, TUBB, TUBB4A, TULP4, TXLNA, TYRP1, UBA52, UCK2, UQCRFS1, UQCRH, USP22, VCY1B, VDAC2, VPS72, YWHAE, ZFAS1, ZNF286A, A2M, ACSL3, ACSL4, ADM, AEBP1, AGA, AHNAK, ANGPTL4, ANXA1, ANXA2, APLP2, APOC2, APOD, APOE, ARF5, ARL6IP5, ATF3, ATP1A1, ATP1B1, ATP1B3, ATRAID, B2M, BACE2, BBX, BCL6, C10orf54, C4A, CALU, CASP1, CAST, CAV1, CBLB, CCND3, CD151, CD44, CD47, CD58, CD59, CD63, CD9, CDH19, CHI3L1, CHN1, CLIC4, CLU, CPVL, CRELD1, CRYAB, CSGALNACT1, CSPG4, CST3, CTSA, CTSB, CTSD, CTSL1, DAG1, DCBLD2, DDR1, DDX5, DPYSL2, DSCR8, DUSP4, DUSP6, DYNLRB1, ECM1, EEA1, EGR1, EMP1, EPHX2, ERBB3, EVA1A, EZH1, EZR, FAM3C, FBX032, FCGR2C, FCRLA, FGFR1, FLJ43663, FOS, FYB, GAA, GADD45B, GATSL3, GEM, GOLGB1, GPNMB, GRN, GSN, HCP5, HLA-A, HLA-B, HLA-C, HLA-E, HLA-F, HLA-H, HPCAL1, HSPA1A, HSPA1B, HTATIP2, ID2, IFI27L2, IFI35, IGF1R, ILIRAP, IL6ST, ISCU, ITGA3, ITGA6, ITGA7, ITGB1, ITGB3, ITM2B, JUN, KCNN4, KLF4, KLF6, KRT10, LAMP2, LEPROT, LGALS1, LGALS3, LGALS3BP, LOC100506190, LPL, LRPAP1, LTBP3, LYRM9, MAEL, MAGEC2, MAPIB, MATN2, MFGE8, MFI2, MIA, MRPS6, MT1E, MT1M, MTIX, MT2A, NDRG1, NEAT1, NFKBIA, NFKBIZ, NNMT, NPC1, NPC2, NR4A1, NSG1, OCIAD2, PAGE5, PDK4, PERP, PKM, PLP2, PRKCDBP, PRNP, PROS1, PRSS23, PSAP, PSMB9, PTRF, RDH5, RNF145, RPS4Y1, S100A13, S100A6, S100B, SAT1, SCARB2, SCCPDH, SDC3, SEL1L, SEMA3B, SERPINA1, SERPINA3, SERPINE2, SGCE, SGK1, SLC20A1, SLC26A2, SLC39A14, SLC5A3, SNX9, SOD1, SPON2, SPRY2, SQSTM1, SRPX, STOM, SYNGR2, SYPL1, TAPBP, TAPBPL, TF, TGOLN2, THBD, TIMP1, TIMP2, TIMP3, TIPARP, TM4SF1, TMBIM6, TMED10, TMED9, TMEM66, TMX4, TNC, TNFSF4, TPP1, TRIML2, TSC22D3, TSPYL2, TXNIP, TYR, UBC, UPP1,

XAGE1A, XAGE1B, XAGE1C, XAGE1D, XAGE1E, ZBTB20 and ZBTB38 (uICR, see table S6); or one or more genes or polypeptides selected from the group consisting of ANP32E, CTPS1, DDX39B, EIF4A1, ESRP1, FBL, FUS, HNRNPA1, ILF2, KIAA0101, NUCKS1, PTMA, RPL21, RUVBL2, SET, SLC25A5, TP53, TUBA1B, UCK2, YWHAE, APLP2, ARL6IP5, CD63, CLU, CRELD1, CTSD, CTSL1, FOS, GAA, GRN, HLA-F, ITM2B, LAMP2, MAPIB, NPC2, PSAP, SCARB2, SDC3, SEL1L, TMEDIO and TSC22D3 (uICR, see Fig. 3C); or one or more genes or polypeptides selected from the group consisting of MTIE, MTIM, MTIX and MT2A.

[0011] In certain embodiments, the ICR signature may comprise a ICR-down signature, said signature comprising one or more genes selected from the group consisting of: AEBP1, AHNAK, APOC2, APOD, APOE, B2M, C10orf54, CD63, CTSD, EEAI, EMP1, FBX032, FYB, GATSL3, HCP5, HLA-A, HLA-B, HLA-C, HLA-E, HLA-F, HLA-H, ITGA3, LAMP2, LYRM9, MFGE8, MIA, NPC2, NSG1, PROS1, RDH5, SERPINA1, TAPBP, TIMP2, TNFSF4 and TRIML2 (refined uICR-down, see table S6); or A2M, ACSL3, ACSL4, ADM, AEBP1, AGA, AHNAK, ANGPTL4, ANXA1, ANXA2, APLP2, APOC2, APOD, APOE, ARF5, ARL6IP5, ATF3, ATP1A1, ATP1B1, ATP1B3, ATRAID, B2M, BACE2, BBX, BCL6, C10orf54, C4A, CALU, CASP1, CAST, CAV1, CBLB, CCND3, CD151, CD44, CD47, CD58, CD59, CD63, CD9, CDH19, CHI3L1, CHN1, CLIC4, CLU, CPVL, CRELD1, CRYAB, CSGALNACT1, CSPG4, CST3, CTSA, CTSB, CTSD, CTSL1, DAG1, DCBLD2, DDRI, DDX5, DPYSL2, DSCR8, DUSP4, DUSP6, DYNLRB1, ECMI, EEAI, EGR1, EMP1, EPHX2, ERBB3, EVA1A, EZH1, EZR, FAM3C, FBX032, FCGR2C, FCRLA, FGFR1, FLJ43663, FOS, FYB, GAA, GADD45B, GATSL3, GEM, GOLGB1, GPNMB, GRN, GSN, HCP5, HLA-A, HLA-B, HLA-C, HLA-E, HLA-F, HLA-H, HPCAL1, HSPA1A, HSPA1B, HTATIP2, ID2, IFI27L2, IFI35, IGF1R, ILIRAP, IL6ST, ISCU, ITGA3, ITGA6, ITGA7, ITGB1, ITGB3, ITM2B, JUN, KCNN4, KLF4, KLF6, KRT10, LAMP2, LEPROT, LGALS1, LGALS3, LGALS3BP, LOC100506190, LPL, LRPAP1, LTBP3, LYRM9, MAEL, MAGEC2, MAPIB, MATN2, MFGE8, MFI2, MIA, MRPS6, MTIE, MTIM, MTIX, MT2A, NDRG1, NEAT1, NFKBIA, NFKBIZ, NNMT, NPC1, NPC2, NR4A1, NSG1, OCIAD2, PAGE5, PDK4, PERP, PKM, PLP2, PRKCDBP, PRNP, PROS1, PRSS23, PSAP, PSMB9, PTRF, RDH5, RNF145, RPS4Y1, S100A13, S100A6, S100B, SAT1, SCARB2, SCCPDH, SDC3, SEL1L, SEMA3B, SERPINA1, SERPINA3, SERPINE2, SGCE, SGK1, SLC20A1, SLC26A2, SLC39A14, SLC5A3, SNX9, SOD1, SPON2, SPRY2, SQSTM1, SRPX, STOM, SYNGR2, SYPL1, TAPBP, TAPBPL, TF,

TGOLN2, THBD, TIMP1, TIMP2, TIMP3, TIPARP, TM4SF1, TMBIM6, TMED10, TMED9, TMEM66, TMX4, TNC, TNFSF4, TPP1, TRIML2, TSC22D3, TSPYL2, TXNIP, TYR, UBC, UPP1, XAGE1A, XAGE1B, XAGE1C, XAGE ID, XAGEIE, ZBTB20 and ZBTB38 (uICR-down, see table S6); or APLP2, ARL6IP5, CD63, CLU, CRELD1, CTSD, CTSL1, FOS, GAA, GRN, HLA-F, ITM2B, LAMP2, MAP1B, NPC2, PSAP, SCARB2, SDC3, SEL1L, TMED10 and TSC22D3 (uICR-down, see Fig. 3C), wherein said ICR-down signature is downregulated in a tumor with a high ICR score and upregulated in a tumor with a low ICR score.

[0012] In certain embodiments, the ICR signature comprises a ICR-up signature, said signature comprising one or more genes selected from the group consisting of: C1QBP, CCT2, CCT6A, DCAF13, EIF4A1, ILF2, MAGEA4, NONO, PA2G4, PGAM1, PPA1, PPIA, RPL18A, RPL26, RPL31, RPS11, RPS15, RPS21, RPS5, RUVBL2, SAE1, SNRPE, UBA52, UQCRH and VDAC2 (refined uICR-up, see table S6); or ACAT1, ACP5, ACTB, ACTG1, ADSL, AEN, AK2, ANP32E, APP, ASAP1, ATP5A1, ATP5D, ATP5G2, BANC1, BCAN, BZW2, C17orf76-AS1, C1QBP, C20orf12, C6orf48, CA14, CBX5, CCT2, CCT3, CCT6A, CDK4, CEP170, CFL1, CHP1, CNRIP1, CRABP2, CS, CTPS1, CYC1, DAP3, DCAF13, DCT, DDX21, DDX39B, DLL3, EDNRB, EEF1D, EEF1G, EEF2, EIF1AX, EIF2S3, EIF3E, EIF3K, EIF3L, EIF4A1, EIF4EBP2, ESRP1, FAM174B, FAM178B, FAM92A1, FBL, FBLN1, FOXRED2, FTL, FUS, GABARAP, GAS5, GNB2L1, GPATCH4, GPI, GRWD1, GSTO1, H3F3A, H3F3AP4, HMGA1, HNRNPAL, HNRNPAPIO, HNRNPC, HSPA8, IDH2, IFI16, ILF2, IMPDH2, ISYNA1, ITM2C, KIAA0101, LHFPL3-AS1, LOC100190986, LYPLA1, MAGEA4, MARCKS, MDH2, METAP2, MIDI, MIR4461, MLLT11, MPZL1, MRPL37, MRPS12, MRPS21, MYC, NACA, NCL, NDUFS2, NF2, NID1, NOLCI, NONO, NPML, NUCKS1, OAT, PA2G4, PABPC1, PAFAH1B3, PAICS, PFDN2, PFNI, PGAM1, PIH1D1, PLTP, PPA1, PPIA, PPP2R1A, PSAT1, PSMD4, PTMA, PYCARD, RAN, RASA3, RBM34, RNF2, RPAIN, RPL10, RPL10A, RPL11, RPL12, RPL13, RPL13A, RPL13AP5, RPL14, RPL17, RPL18, RPL18A, RPL21, RPL26, RPL28, RPL29, RPL3, RPL30, RPL31, RPL35, RPL36A, RPL37, RPL37A, RPL39, RPL4, RPL41, RPL5, RPL6, RPL7, RPL7A, RPL8, RPLPO, RPLP1, RPS10, RPS11, RPS12, RPS15, RPS15A, RPS16, RPS17, RPS17L, RPS18, RPS19, RPS2, RPS21, RPS23, RPS24, RPS26, RPS27, RPS27A, RPS3, RPS3A, RPS4X, RPS5, RPS6, RPS7, RPS8, RPS9, RPSA, RSL1D1, RUVBL2, SAE1, SCD, SCNM1, SERBP1, SERPIN1, SET, SF3B4, SHMT2, SKP2, SLC19A1, SLC25A3, SLC25A5, SLC25A6,

SMS, SNAI2, SNHG16, SNHG6, SNRPE, SORD, SOX4, SRP14, SSR2, TIMM13, TIMM50, TMC6, TOP1MT, TP53, TRAP1, TRPM1, TSR1, TUBAIB, TUBB, TUBB4A, TULP4, TXLNA, TYRP1, UBA52, UCK2, UQCRFS1, UQCRH, USP22, VCY1B, VDAC2, VPS72, YWHAE, ZFAS1 and ZNF286A (uICR-up, see table S6); or ANP32E, CTPS1, DDX39B, EIF4A1, ESRP1, FBL, FUS, HNRNPA1, ILF2, KIAA0101, NUCKS1, PTMA, RPL21, RUVBL2, SET, SLC25A5, TP53, TUBAIB, UCK2 and YWHAE (uICR-up, see Fig. 3C), wherein said ICR-up signature is upregulated in a tumor with a high ICR score and downregulated in a tumor with a low ICR score.

[0013] In another aspect, the present invention provides for a method of detecting an immune checkpoint inhibitor resistance (ICR) gene signature in a tumor comprising, detecting in tumor cells obtained from a subject in need thereof the expression or activity of a malignant cell gene signature comprising: one or more genes or polypeptides selected from the group consisting of ACTB, AEN, ANP32E, ATP5A1, ATP5G2, BZW2, C17orf76-AS1, C1QBP, C20orf12, CA14, CBX5, CCT2, CCT3, CDK4, CFL1, CNRIP1, CRABP2, CS, CTPS1, DCAF13, DCT, DDX39B, DLL3, EEF1G, EIF2S3, EIF3K, EIF4A1, EIF4EBP2, FAM174B, FBL, FBLN1, FOXRED2, FTL, FUS, GABARAP, GAS5, GNB2L1, GPATCH4, GPI, GRWD1, H3F3A, H3F3AP4, HMGA1, HNRNPA1, HNRNPA1P10, HNRNPC, HSPA8, IDH2, ILF2, ISYNA1, ITM2C, KIAA0101, MAGEA4, MDH2, METAP2, MIDI, MIR4461, MLLT1 1, MPZL1, MRPS21, NACA, NCL, NDUFS2, NOLC1, NONO, PA2G4, PABPC1, PAFAH1B3, PFDN2, PFN1, PGAM1, PIH1D1, PPA1, PPIA, PPP2R1A, PSMD4, PTMA, RAN, RBM34, RNF2, RPAIN, RPL10A, RPL1 1, RPL12, RPL13, RPL13A, RPL13AP5, RPL17, RPL18, RPL18A, RPL21, RPL26, RPL28, RPL29, RPL3, RPL31, RPL36A, RPL37, RPL37A, RPL39, RPL4, RPL41, RPL5, RPL6, RPL8, RPLPO, RPLP1, RPS10, RPS1 1, RPS12, RPS15A, RPS16, RPS17, RPS17L, RPS18, RPS19, RPS21, RPS23, RPS24, RPS26, RPS27, RPS27A, RPS3, RPS4X, RPS5, RPS6, RPS7, RPS8, RPS9, RPSA, RUVBL2, SAE1, SCD, SCNMI, SERPINF1, SET, SF3B4, SHMT2, SKP2, SLC25A3, SMS, SNAI2, SNHG6, SNRPE, SOX4, SRP14, SSR2, TIMM50, TMC6, TP53, TRPM1, TSR1, TUBAIB, TUBB, TULP4, UBA52, UQCRFS1, UQCRH, USP22, VCY1B, VDAC2, VPS72, YWHAE, ZNF286A, A2M, ACSL3, ACSL4, ADM, AEBP1, AGA, AHNAK, ANGPTL4, ANXA1, ANXA2, APLP2, APOD, APOE, ARL6IP5, ATF3, ATP1A1, ATP1B1, ATP1B3, B2M, BACE2, BBX, BCL6, CALU, CASP1, CAST, CAV1, CCND3, CD151, CD44, CD47, CD58, CD59, CD63, CD9, CDH19, CHI3L1, CLIC4, CRELD1, CRYAB, CSGALNACT1, CSPG4, CST3, CTSA, CTSB, CTSD, CTS1, DAG1,

DCBLD2, DDR1, DDX5, DPYSL2, DUSP4, DUSP6, ECM1, EEA1, EGR1, EMP1, EPHX2, ERBB3, EVA1A, EZH1, FAM3C, FBX032, FCGR2C, FCRLA, FGFR1, FLJ43663, FOS, GAA, GADD45B, GEM, GOLGB1, GPNMB, GRN, GSN, HLA-A, HLA-B, HLA-C, HLA-E, HLA-F, HLA-H, HPCAL1, HSPA1A, HTATIP2, IFI35, IGF1R, ILIRAP, IL6ST, ITGA3, ITGA6, ITGB1, ITGB3, ITM2B, JUN, KCNN4, KLF4, KLF6, LAMP2, LEPROT, LGALS1, LGALS3, LGALS3BP, LPL, LRPAP1, MAGEC2, MFGE8, MFI2, MIA, MTIE, MTIM, MTIX, MT2A, NEAT1, NFKBIA, NFKBIZ, NNMT, NPC1, NPC2, NR4A1, NSG1, PDK4, PLP2, PRKCDBP, PRNP, PROS1, PRSS23, PSAP, PSMB9, PTRF, RNF145, RPS4Y1, S100A6, S100B, SAT1, SCARB2, SCCPDH, SDC3, SEL1L, SEMA3B, SERPINA3, SERPINE2, SGCE, SGK1, SLC20A1, SLC26A2, SLC39A14, SLC5A3, SOD1, SPRY2, SQSTM1, SRPX, STOM, SYNGR2, SYPL1, TAPBP, TAPBPL, TF, TGOLN2, TIMP1, TIMP2, TIMP3, TIPARP, TM4SF1, TMED10, TMED9, TMEM66, TMX4, TNC, TPP1, TSC22D3, TYR, UBC, UPP1, ZBTB20 and ZBTB38 (oncogenic ICR, see table S6); or one or more genes or polypeptides selected from the group consisting of AEN, ATP5A1, C20orf12, CCT2, DCAF13, DDX39B, ISYNA1, NDUFS2, NOLC1, PA2G4, PPP2R1A, RBM34, RNF2, RPL6, RPL21, SERPINF1, SF3B4, SMS, TMC6, VPS72, ANXA1, ATF3, BCL6, CD58, CD9, CTSB, DCBLD2, EMP1, HLA-F, HTATIP2, ILIRAP, ITGA6, KCNN4, KLF4, MTIE, MTIM, MTIX, MT2A, NNMT, PRKCDBP, S100A6 and TSC22D3 (oncogenic ICR, see Fig. 2B); or one or more genes or polypeptides selected from the group consisting of ACTB, ANP32E, CBX5, FUS, HNRNP1A1, IDH2, KIAA0101, NCL, PFN1, PPIA, PTMA, RAN, RPLPO, TUBA1B, TUBB, VCY1B, A2M, APOD, BCL6, CD44, CD59, CD63, CDH19, CHI3L1, CTSA, CTSB, CTSD, FOS, GPNMB, GRN, HLA-A, HLA-B, HLA-H, ITM2B, LGALS3BP, NEAT1, PDK4, PSAP, SCARB2, SERPINA3, SLC26A2, TAPBPL, TMEM66 and TYR (oncogenic ICR, see Fig. 10B); or one or more genes or polypeptides selected from the group consisting of MTIE, MTIM, MTIX and MT2A.

[0014] In certain embodiments, the ICR signature comprises an ICR-down signature, said signature comprising one or more genes selected from the group consisting of: A2M, ACSL3, ACSL4, ADM, AEBP1, AGA, AHNAK, ANGPTL4, ANXA1, ANXA2, APLP2, APOD, APOE, ARL6IP5, ATF3, ATP1A1, ATP1B1, ATP1B3, B2M, BACE2, BBX, BCL6, CALU, CASP1, CAST, CAV1, CCND3, CD151, CD44, CD47, CD58, CD59, CD63, CD9, CDH19, CHI3L1, CLIC4, CRELD1, CRYAB, CSGALNACT1, CSPG4, CST3, CTSA, CTSB, CTSD, CTSL1, DAG1, DCBLD2, DDR1, DDX5, DPYSL2, DUSP4, DUSP6, ECM1, EEA1, EGR1, EMP1, EPHX2, ERBB3, EVA1A, EZH1, FAM3C, FBX032, FCGR2C,

FCRLA, FGFR1, FLJ43663, FOS, GAA, GADD45B, GEM, GOLGB1, GPNMB, GRN, GSN, HLA-A, HLA-B, HLA-C, HLA-E, HLA-F, HLA-H, HPCAL1, HSPA1A, HTATIP2, IFI35, IGF1R, ILIRAP, IL6ST, ITGA3, ITGA6, ITGB1, ITGB3, ITM2B, JUN, KCNN4, KLF4, KLF6, LAMP2, LEPROT, LGALS1, LGALS3, LGALS3BP, LPL, LRPAP1, MAGEC2, MFGE8, MFI2, MIA, MT1E, MTIM, MTIX, MT2A, NEAT1, NFKBIA, NFKBIZ, NNMT, NPC1, NPC2, NR4A1, NSG1, PDK4, PLP2, PRKCDBP, PRNP, PROS1, PRSS23, PSAP, PSMB9, PTRF, RNF145, RPS4Y1, S100A6, S100B, SAT1, SCARB2, SCCPDH, SDC3, SEL1L, SEMA3B, SERPINA3, SERPINE2, SGCE, SGK1, SLC20A1, SLC26A2, SLC39A14, SLC5A3, SOD1, SPRY2, SQSTM1, SRPX, STOM, SYNGR2, SYPL1, TAPBP, TAPBPL, TF, TGOLN2, TIMP1, TIMP2, TIMP3, TIPARP, TM4SF1, TMED10, TMED9, TMEM66, TMX4, TNC, TPP1, TSC22D3, TYR, UBC, UPP1, ZBTB20 and ZBTB38 (oncogenic ICR down, see table S6); or ANXA1, ATF3, BCL6, CD58, CD9, CTSB, DCBLD2, EMP1, HLA-F, HTATIP2, ILIRAP, ITGA6, KCNN4, KLF4, MT1E, MTIM, MTIX, MT2A, NNMT, PRKCDBP, S100A6 and TSC22D3 (oncogenic ICR down, see Fig. 2B); or A2M, APOD, BCL6, CD44, CD59, CD63, CDH19, CHI3L1, CTSA, CTSB, CTSD, FOS, GPNMB, GRN, HLA-A, HLA-B, HLA-H, ITM2B, LGALS3BP, NEAT1, PDK4, PSAP, SCARB2, SERPINA3, SLC26A2, TAPBPL, TMEM66 and TYR (oncogenic ICR down, see Fig. 10B), wherein said ICR-down signature is downregulated in a tumor with a high ICR score and upregulated in a tumor with a low ICR score.

[0015] In certain embodiments, the ICR signature comprises an ICR-up signature, said signature comprising one or more genes selected from the group consisting of: ACTB, AEN, ANP32E, ATP5A1, ATP5G2, BZW2, C17orf76-AS1, C1QBP, C20orf12, CA14, CBX5, CCT2, CCT3, CDK4, CFL1, CNRIP1, CRABP2, CS, CTPS1, DCAF13, DCT, DDX39B, DLL3, EEF1G, EIF2S3, EIF3K, EIF4A1, EIF4EBP2, FAM174B, FBL, FBLN1, FOXRED2, FTL, FUS, GABARAP, GAS5, GNB2L1, GPATCH4, GPI, GRWD1, H3F3A, H3F3AP4, HMGA1, HNRNPA1, HNRNPA1P1, HNRNPC, HSPA8, IDH2, ILF2, ISYNA1, ITM2C, KIAA0101, MAGEA4, MDH2, METAP2, MIDI, MIR4461, MLLT1, MPZL1, MRPS21, NACA, NCL, NDUFS2, NOLC1, NONO, PA2G4, PABPC1, PAFAH1B3, PFDN2, PFN1, PGAM1, PIH1D1, PPA1, PPIA, PPP2R1A, PSMD4, PTMA, RAN, RBM34, RNF2, RPAIN, RPL10A, RPL1, RPL12, RPL13, RPL13A, RPL13AP5, RPL17, RPL18, RPL18A, RPL21, RPL26, RPL28, RPL29, RPL3, RPL31, RPL36A, RPL37, RPL37A, RPL39, RPL4, RPL41, RPL5, RPL6, RPL8, RPLPO, RPLP1, RPS10, RPS1, RPS12, RPS15A, RPS16, RPS17, RPS17L, RPS18, RPS19, RPS21, RPS23, RPS24, RPS26, RPS27, RPS27A, RPS3, RPS4X,

RPS5, RPS6, RPS7, RPS8, RPS9, RPSA, RUVBL2, SAE1, SCD, SCNM 1, SERPINFI, SET, SF3B4, SHMT2, SKP2, SLC25A3, SMS, SNAI2, SNHG6, SNRPE, SOX4, SRP14, SSR2, TIMM50, TMC6, TP53, TRPM1, TSR1, TUBA1B, TUBB, TULP4, UBA52, UQCRFS1, UQCRH, USP22, VCY1B, VDAC2, VPS72, YWHAE and ZNF286A (oncogenic ICR up, see table S6); or AEN, ATP5A1, C20orf12, CCT2, DCAF13, DDX39B, ISYNA1, NDUFS2, NOLCI, PA2G4, PPP2R1A, RBM34, RNF2, RPL6, RPL21, SERPINFI, SF3B4, SMS, TMC6, VPS72 (oncogenic ICR up, see Fig. 2B); or ACTB, ANP32E, CBX5, FUS, HNRNP1A1, IDH2, KIAA0101, NCL, PFN1, PPIA, PTMA, RAN, RPLPO, TUBA1B, TUBB and VCY1B (oncogenic ICR up, see Fig. 10B), wherein said ICR-up signature is upregulated in a tumor with a high ICR score and downregulated in a tumor with a low ICR score. In certain embodiments, the ICR signature is detected in cycling cells.

[0016] In another aspect, the present invention provides for a method of detecting an immune cell exclusion gene signature in a tumor comprising, detecting in tumor cells obtained from a subject in need thereof the expression or activity of a malignant cell gene signature comprising: one or more genes or polypeptides selected from the group consisting of ACAT1, ACP5, ACTG1, ADSL, AK2, APP, ASAP1, ATP5D, BANC1, BCAN, BZW2, C17orf76-AS1, C1QBP, C6orf48, CA14, CCT3, CCT6A, CEP170, CHP1, CTPS1, CYC1, DAP3, DCT, DDX21, EDNRB, EEF1D, EEF1G, EEF2, EIF1AX, EIF2S3, EIF3E, EIF3K, EIF3L, EIF4A1, ESRP1, FAM178B, FAM92A1, FTL, GAS5, GNB2L1, GPI, GSTO1, IFI16, ILF2, IMPDH2, LHFPL3-AS1, LOC100190986, LYPLA1, MARCKS, MDH2, MRPL37, MRPS12, MYC, NCL, NF2, NIDI, NOLCI, NPM1, NUCKS1, OAT, PABPC1, PAICS, PLTP, PSAT1, PYCARD, RASA3, RPL10, RPL10A, RPL11, RPL12, RPL13, RPL13A, RPL13AP5, RPL14, RPL17, RPL18, RPL18A, RPL28, RPL29, RPL3, RPL30, RPL35, RPL37A, RPL39, RPL4, RPL5, RPL6, RPL7, RPL7A, RPL8, RPLPO, RPLP1, RPS10, RPS11, RPS15, RPS15A, RPS16, RPS17, RPS17L, RPS18, RPS19, RPS2, RPS24, RPS27, RPS3, RPS3A, RPS4X, RPS5, RPS7, RPS8, RPS9, RPSA, RSL1D1, SCD, SERBP1, SERPINFI, SLC19A1, SLC25A5, SLC25A6, SNAI2, SNHG16, SNHG6, SORD, SOX4, TIMM13, TIMM50, TOP1MT, TRAP1, TUBB4A, TXLNA, TYRP1, UCK2, UQCRFS1, ZFAS1, A2M, AGA, AHNAK, ANXA1, APLP2, APOC2, ARF5, ATP1A1, ATP1B1, ATRAID, B2M, C10orf54, C4A, CBLB, CCND3, CD151, CD47, CD58, CD59, CDH19, CHN1, CLU, CPVL, CST3, CTSB, CTSD, CTSL1, DDR1, DPYSL2, DSCR8, DUSP6, DYNLRB1, EMP1, EZR, FAM3C, FGFR1, FYB, GAA, GATSL3, GRN, GSN, HCP5, HLA-B, HLA-C, HLA-F, HLA-H, HSPA1A, HSPA1B, ID2, IFI27L2, ISCU, ITGA3,

ITGA7, ITGB3, KCNN4, KRT10, LOC100506190, LTBP3, LYRM9, MAEL, MAPIB, MATN2, MFGE8, MFI2, MIA, MRPS6, MT2A, NDRG1, NFKBIA, NPC1, OCIAD2, PAGE5, PERP, PKM, RDH5, S100A13, S100A6, SERPINA1, SERPINA3, SERPINE2, SGCE, SLC26A2, SLC5A3, SNX9, SPON2, THBD, TIMP1, TM4SF1, TMBIM6, TNFSF4, TPP1, TRIML2, TSC22D3, TSPYL2, TXNIP, UBC, XAGEIA, XAGEIB, XAGEIC, XAGEID and XAGEIE (exclusion, see table S6); or one or more genes or polypeptides selected from the group consisting of ACTG1, ADSL, C17orf76-AS1, C1QBP, CTPS1, EIF2S3, EIF3E, ILF2, NCL, NF2, NOLCI, PABPCI, PAICS, RPLIOA, RPL18, RPL6, RPS24, RSL1D1, SERPINF1, SOX4, AHNAK, ANXA1, CCND3, CD151, CD47, CD58, CST3, CTSB, CTSD, EMP1, FGFR1, HLA-C, HLA-F, ITGB3, KCNN4, MIA, MT2A, S100A6, SLC5A3, TIMP1 and TSC22D3 (exclusion, see fig. 2H); or one or more genes or polypeptides selected from the group consisting of C17orf76-AS1, C1QBP, CTPS1, EIF2S3, ILF2, NCL, NOLCI, PABPCI, RPLIOA, RPL18, RPL6, RPS24, SERPINF1, SOX4, AHNAK, ANXA1, CCND3, CD151, CD47, CD58, CST3, CTSB, CTSD, EMP1, FGFR1, HLA-C, HLA-F, ITGB3, KCNN4, MIA, MT2A, S100A6, SLC5A3, TIMP1 and TSC22D3 (exclusion, see fig. 2H).

[0017] In certain embodiments, the exclusion signature comprises an exclusion-down signature, said signature comprising one or more genes selected from the group consisting of: A2M, AGA, AHNAK, ANXA1, APLP2, APOC2, ARF5, ATP1A1, ATP1B1, ATRAID, B2M, C10orf54, C4A, CBLB, CCND3, CD151, CD47, CD58, CD59, CDH19, CHN1, CLU, CPVL, CST3, CTSB, CTSD, CTSL1, DDR1, DPYSL2, DSCR8, DUSP6, DYNLRB1, EMP1, EZR, FAM3C, FGFR1, FYB, GAA, GATSL3, GRN, GSN, HCP5, HLA-B, HLA-C, HLA-F, HLA-H, HSPA1A, HSPA1B, ID2, IFI27L2, ISCU, ITGA3, ITGA7, ITGB3, KCNN4, KRT10, LOC100506190, LTBP3, LYRM9, MAEL, MAPIB, MATN2, MFGE8, MFI2, MIA, MRPS6, MT2A, NDRG1, NFKBIA, NPC1, OCIAD2, PAGE5, PERP, PKM, RDH5, S100A13, S100A6, SERPINA1, SERPINA3, SERPINE2, SGCE, SLC26A2, SLC5A3, SNX9, SPON2, THBD, TIMP1, TM4SF1, TMBIM6, TNFSF4, TPP1, TRIML2, TSC22D3, TSPYL2, TXNIP, UBC, XAGEIA, XAGEIB, XAGEIC, XAGEID and XAGEIE (exclusion-down, see table S6); or AHNAK, ANXA1, CCND3, CD151, CD47, CD58, CST3, CTSB, CTSD, EMP1, FGFR1, HLA-C, HLA-F, ITGB3, KCNN4, MIA, MT2A, S100A6, SLC5A3, TIMP1 and TSC22D3 (exclusion-down, see fig. 2H), wherein said exclusion-down signature is downregulated in a tumor with T cell exclusion and is upregulated in a tumor with T cell infiltration.

[0018] In certain embodiments, the exclusion signature comprises an exclusion-up signature, said signature comprising one or more genes selected from the group consisting of: ACAT1, ACP5, ACTG1, ADSL, AK2, APP, ASAP1, ATP5D, BANC1, BCAN, BZW2, C17orf76-AS1, C1QBP, C6orf48, CA14, CCT3, CCT6A, CEP170, CHP1, CTPS1, CYC1, DAP3, DCT, DDX21, EDNRB, EEF1D, EEF1G, EEF2, EIF1AX, EIF2S3, EIF3E, EIF3K, EIF3L, EIF4A1, ESRP1, FAM178B, FAM92A1, FTL, GAS5, GNB2L1, GPI, GSTO1, IFI16, ILF2, IMPDH2, LHFPL3-AS1, LOC100190986, LYPLA1, MARCKS, MDH2, MRPL37, MRPS12, MYC, NCL, NF2, NIDI, NOLC1, NPM1, NUCKS1, OAT, PABPC1, PAICS, PLTP, PSAT1, PYCARD, RASA3, RPL10, RPL10A, RPL11, RPL12, RPL13, RPL13A, RPL13AP5, RPL14, RPL17, RPL18, RPL18A, RPL28, RPL29, RPL3, RPL30, RPL35, RPL37A, RPL39, RPL4, RPL5, RPL6, RPL7, RPL7A, RPL8, RPLPO, RPLP1, RPS10, RPS11, RPS15, RPS15A, RPS16, RPS17, RPS17L, RPS18, RPS19, RPS2, RPS24, RPS27, RPS3, RPS3A, RPS4X, RPS5, RPS7, RPS8, RPS9, RPSA, RSL1D1, SCD, SERBP1, SERPINF1, SLC19A1, SLC25A5, SLC25A6, SNAI2, SNHG16, SNHG6, SORD, SOX4, TIMM13, TIMM50, TOPIMT, TRAP1, TUBB4A, TXLNA, TYRPI, UCK2, UQCRCF1 and ZFAS1 (exclusion-up, see table S6); or ACTG1, ADSL, C17orf76-AS1, C1QBP, CTPS1, EIF2S3, EIF3E, ILF2, NCL, NF2, NOLC1, PABPC1, PAICS, RPL10A, RPL18, RPL6, RPS24, RSL1D1, SERPINF1 and SOX4 (exclusion-up, see fig. 2H); or C17orf76-AS1, C1QBP, CTPS1, EIF2S3, ILF2, NCL, NOLC1, PABPC1, RPL10A, RPL18, RPL6, RPS24, SERPINF1 and SOX4 (exclusion-up, see fig. 2H), wherein said exclusion-up signature is upregulated in a tumor with T cell exclusion and is downregulated in a tumor with T cell infiltration.

[0019] In certain embodiments, the method according to any embodiment herein further comprises detecting tumor infiltrating lymphocytes (TIL). Not being bound by a theory, detecting tumor infiltration of immune cells is an independent indicator of immunotherapy resistance and progression free survival and combining detection of TILs with any of the above signatures may increase the prognostic value.

[0020] In certain embodiments, the gene signature according to any embodiment herein is detected in a bulk tumor sample, whereby the gene signature is detected by deconvolution of bulk expression data such that gene expression is assigned to malignant cells and non-malignant cells in said tumor sample.

[0021] In certain embodiments, detecting the gene signature comprises detecting downregulation of the down signature and/or upregulation of the up signature. In certain

embodiments, not detecting the gene signature comprises detecting upregulation of the down signature and/or downregulation of the up signature. In certain embodiments, detecting the signature and/or TILs indicates lower progression free survival and/or resistance to checkpoint blockade therapy. In certain embodiments, not detecting the signature and/or TILs indicates higher progression free survival and/or sensitivity to checkpoint blockade therapy. In certain embodiments, detecting the gene signature indicates a 10-year survival rate less than 40% and wherein not detecting the signature indicates a 10-year survival rate greater than 60%.

[0022] In certain embodiments, detecting an ICR signature in a tumor further comprises detecting in tumor infiltrating lymphocytes (TIL) obtained from the subject in need thereof the expression or activity of a CD8 T cell gene signature, said signature comprising one or more genes or polypeptides selected from the group consisting of CEP19, EX05, FAM153C, FCRL6, GBP2, GBP5, HSPA1B, IER2, IRF1, KLRK1, LDHA, LOC100506083, MBOAT1, SEMA4D, SIRT3, SPDYE2, SPDYE2L, STAT1, STOM, UBE2Q2P3, ACP5, AKNA, BTN3A2, CCDC141, CD27, CDC42SE1, DDIT4, FAU, FKBP5, GPR56, HAVCR2, HLA-B, HLA-C, HLA-F, IL6ST, ITGA4, KIAA1551, KLF12, MIR155HG, MTA2, MTRNR2L1, MTRNR2L3, PIK3IP1, RPL26, RPL27, RPL27A, RPL35A, RPS1 1, RPS16, RPS20, RPS26, SPOCK2, SYTL3, TOB1, TPT1, TTN, TXNIP, WNK1 and ZFP36L2. In certain embodiments, detecting an ICR signature in a tumor further comprises detecting in macrophages obtained from the subject in need thereof the expression or activity of a macrophage gene signature, said signature comprising one or more genes or polypeptides selected from the group consisting of APOL1, CD274, CSTB, DCN, HLA-DPB2, HLA-DQA1, HLA-G, HSPA8, HSPB1, IL18BP, TMEM176A, UBD, A2M, ADAP2, ADORA3, ARL4C, ASPH, BCAT1, C11orf1, C3, C3AR1, C6orf62, CAPN2, CD200R1, CD28, CD9, CD99, COMT, CREM, CRTAP, CYFIP1, DDOST, DHRS3, EGFL7, EIF1AY, ETS2, FCGR2A, FOLR2, GATM, GBP3, GNG2, GSTT1, GYPC, HIST1H1E, HPGDS, IFI44L, IGFBP4, ITGA4, KCTD12, LGMN, LOC441081, LTC4S, LYVE1, MERTK, METTL7B, MS4A4A, MS4A7, MTSS1, NLRP3, OLFML3, PLA2G15, PLXDC2, PMP22, POR, PRDX2, PTGS1, RNASE1, ROCK1, RPS4Y1, S100A9, SCAMP2, SEPP1, SESN1, SLC18B1, SLC39A1, SLC40A1, SLC7A8, SORL1, SPP1, STAB1, TMEM106C, TMEM86A, TMEM9, TNFRSF1B, TNFRSF21, TPD52L2, ULK3 and ZFP36L2.

[0023] In another aspect, the present invention provides for a method of stratifying cancer patients into a high survival group and a low survival group comprising detecting the

expression or activity of an ICR and/or exclusion signature in a tumor according to any embodiment herein, wherein if the signature is detected the patient is in the low survival group and if the signature is not detected the patient is in the high survival group. The patients in the high survival group may be immunotherapy responders and patients in the low survival group may be immunotherapy non-responders.

[0024] In another aspect, the present invention provides for a method of treating a cancer in a subject in need thereof comprising detecting the expression or activity of an ICR and/or exclusion signature according to any embodiment herein in a tumor obtained from the subject and administering a treatment, wherein if an ICR and/or exclusion signature is detected the treatment comprises administering an agent capable of reducing expression or activity of said signature, and wherein if an ICR and/or exclusion signature is not detected the treatment comprises administering an immunotherapy. The agent capable of reducing expression or activity of said signature may comprise a CDK4/6 inhibitor, a drug selected from Table 3, a cell cycle inhibitor, a PKC activator, an inhibitor of the NF κ B pathway, an IGF1R inhibitor, or Reserpine. The agent capable of reducing expression or activity of said signature may comprise an agent capable of modulating expression or activity of a gene selected from the group consisting of MAZ, NFKBIZ, MYC, ANXA1, SOX4, MT2A, PTP4A3, CD59, DLL3, SERPINE2, SERPINF1, PERP, EGR1, SERPINA3, SEMA3B, SMARCA4, IFNGR2, B2M, and PDL1. The agent capable of reducing expression or activity of said signature may comprise an agent capable of targeting or binding to one or more up-regulated secreted or cell surface exposed ICR and/or exclusion signature genes or polypeptides. The method may further comprise detecting the expression or activity of an ICR and/or exclusion signature according to any embodiment herein in a tumor obtained from the subject after the treatment and administering an immunotherapy if said signature is reduced or below a reference level. The agent capable of reducing expression or activity of said signature may be a CDK4/6 inhibitor. The method may further comprise detecting the expression or activity of an ICR and/or exclusion signature according to any embodiment herein in a tumor obtained from the subject before the treatment and administering an immunotherapy if said signature is not detected or below a reference level.

[0025] In certain embodiments, the method further comprises administering an immunotherapy to the subject administered an agent capable of reducing the expression or activity of said signature. The immunotherapy may comprise a check point inhibitor or adoptive cell transfer (ACT). The adoptive cell transfer may comprise a CAR T cell or

activated autologous T cells. The checkpoint inhibitor may comprise anti-CTLA4, anti-PD-L1 and/or anti-PD1 therapy.

[0026] In another aspect, the present invention provides for a method of treating a cancer in a subject in need thereof comprising detecting the expression or activity of an ICR and/or exclusion signature according to any embodiment herein in a tumor obtained from the subject, wherein if an ICR and/or exclusion signature is detected the treatment comprises administering an agent capable of modulating expression or activity of one or more genes or polypeptides in a network of genes disrupted by perturbation of a gene selected from the group consisting of MAZ, NFKBIZ, MYC, ANXA1, SOX4, MT2A, PTP4A3, CD59, DLL3, SERPINE2, SERPINF1, PERP, EGRI, SERPINA3, SEMA3B, SMARCA4, IFNGR2, B2M, and PDL1.

[0027] In another aspect, the present invention provides for a method of treating a cancer in a subject in need thereof comprising administering to the subject a therapeutically effective amount of an agent: capable of modulating the expression or activity of one or more ICR and/or exclusion signature genes or polypeptides according to any embodiment herein; or capable of targeting or binding to one or more cell surface exposed ICR and/or exclusion signature genes or polypeptides, wherein the gene or polypeptide is up-regulated in the ICR and/or exclusion signature; or capable of targeting or binding to one or more receptors or ligands specific for a cell surface exposed ICR and/or exclusion signature gene or polypeptide, wherein the gene or polypeptide is up-regulated in the ICR and/or exclusion signature; or comprising a secreted ICR and/or exclusion signature gene or polypeptide, wherein the gene or polypeptide is down-regulated in the ICR and/or exclusion signature; or capable of targeting or binding to one or more secreted ICR and/or exclusion signature genes or polypeptides, wherein the genes or polypeptides are up-regulated in the ICR and/or exclusion signature; or capable of targeting or binding to one or more receptors specific for a secreted ICR and/or exclusion signature gene or polypeptide, wherein the secreted gene or polypeptide is up-regulated in the ICR and/or exclusion signature; or comprising a CDK4/6 inhibitor, a drug selected from Table 3, a cell cycle inhibitor, a PKC activator, an inhibitor of the **NFKB** pathway, an IGF1R inhibitor, or Reserpine.

[0028] In certain embodiments, the agent comprises a therapeutic antibody, antibody fragment, antibody-like protein scaffold, aptamer, protein, CRISPR system or small molecule.

[0029] In certain embodiments, the agent capable of targeting or binding to one or more

cell surface exposed ICR and/or exclusion signature polypeptides or one or more receptors specific for a secreted ICR and/or exclusion signature gene or polypeptide comprises a CAR T cell capable of targeting or binding to one or more cell surface exposed ICR and/or exclusion signature genes or polypeptides or one or more receptors specific for a secreted ICR and/or exclusion signature gene or polypeptide.

[0030] In certain embodiments, the agent capable of modulating the expression or activity of one or more ICR and/or exclusion signature genes or polypeptides comprises a CDK4/6 inhibitor. The CDK4/6 inhibitor may comprise Abemaciclib.

[0031] In certain embodiments, the method further comprises administering an immunotherapy to the subject. The immunotherapy may comprise a check point inhibitor. The checkpoint inhibitor may comprise anti-CTLA4, anti-PD-L1 and/or anti-PD1 therapy.

[0032] In another aspect, the present invention provides for a method of monitoring a cancer in a subject in need thereof comprising detecting the expression or activity of an ICR and/or exclusion gene signature according to any embodiment herein in tumor samples obtained from the subject for at least two time points. The at least one sample may be obtained before treatment. The at least one sample may be obtained after treatment.

[0033] In certain embodiments, the cancer according to any embodiment herein is melanoma.

[0034] In certain embodiments, the ICR and/or exclusion signature is expressed in response to administration of an immunotherapy.

[0035] In another aspect, the present invention provides for a method of detecting an ICR signature in a tumor comprising, detecting in tumor cells obtained from a subject in need thereof who has been treated with an immunotherapy the expression or activity of a malignant cell gene signature comprising: a) one or more down regulated genes selected from the group consisting of genes associated with coagulation, apoptosis, TNF- α signaling via NF κ b, Antigen processing and presentation, metallothionein and IFNGR2; and/or b) one or more up regulated genes selected from the group consisting of genes associated with negative regulation of angiogenesis and MYC targets.

[0036] In another aspect, the present invention provides for a kit comprising reagents to detect at least one ICR and/or exclusion signature gene or polypeptide according to any embodiment herein. The kit may comprise at least one antibody, antibody fragment, or aptamer. The kit may comprise primers and/or probes for quantitative RT-PCR or fluorescently bar-coded oligonucleotide probes for hybridization to RNA.

[0037] In another aspect, the present invention provides for a CD8 T cell specific cycling signature (see Table S8). In certain embodiments, modulating target genes in this signature can allow boosting T cell proliferation without activating tumor growth. Not being bound by a theory proliferating CD8 T cells express features that are not present in proliferating malignant cells. In certain embodiments, induction of oxidative phosphorylation and/or repression of hematopoietic lineage genes (e.g., CD37, IL11RA, and IL7R) may increase CD8 T cell proliferation without affecting tumor proliferation.

[0038] In another aspect, the present invention provides for a method of detecting an immunotherapy resistance (ITR) gene signature in a tumor comprising, detecting in tumor cells obtained from a subject in need thereof the expression or activity of a malignant cell gene signature comprising:

a) one or more genes or polypeptides selected from the group consisting of ACOT7, ACSL3, ACTN1, ADAM15, ADI1, AEBP1, AGPAT1, AGRN, AHCY, AIF1L, AKAP12, AKT3, ANXA5, APOAIBP, APOD, APOE, ARL2, ARNT2, ARPC1A, ASPH, ATP1A1, ATP1B1, ATP6V0A1, B3GNT1, BACE2, BAIAP2, BCAN, BIRC7, BTBD3, C11orf24, C17orf89, Clorf198, Clorf21, Clorf85, CALD1, CALU, CAPN3, CAV1, CBR1, CCND1, CCT3, CD151, CD276, CD59, CD63, CD9, CDC42BPA, CDC42EP4, CDH19, CDK2, CDK2AP1, CECR7, CELSR2, CERCAM, CERS2, CHCHD6, CHL1, CHPF, CLDN12, CLIC4, CNIH4, CNN3, CNP, CNPY2, COA3, COL16A1, COMT, CRIP2, CRNDE, CRTAP, CRYAB, CSAG1, CSAG3, CSPG4, CSRP1, CTDSPL, CTHRC1, CTNNAL1, CTNNB1, CTSF, CTSK, CTTN, CYB5R1, CYP27A1, CYSTM1, CYTH3, DAAM2, DCBLD2, DCT, DDR1, DDR2, DIP2C, DLC1, DNAH14, DOCK7, DST, DSTN, DUSP6, ECMI, EDNRB, EFNA5, EIF4EBP1, EMP1, ENTPD6, EPS8, ERBB3, ETV4, ETV5, EVA1A, EXOSC4, FAM127A, FAM127B, FAM167B, FARP1, FARP2, FASN, FKBPIO, FKBP4, FKBP9, FNI, FNBPIL, FRMD6, FSTL1, FXYD3, G6PC3, GALE, GCSH, GDF15, GJB1, GLI3, GNG12, GOLM1, GPM6B, GPR143, GPRC5B, GSTA4, GSTP1, GULP1, GYG2, H1FO, HIBADH, HMCN1, HMG20B, HOXB7, HOXC10, HSBP1, HSP90AB1, HSPB1, HSPD1, HSPG2, IFI27, IGF1R, IGFBP7, IGSF1, IGSF3, IGSF8, IMPDH2, ISYNA1, ITFG3, ITGA3, ITGB3, KIRREL, LAMB1, LAMB2, LAMC1, LAPTM4A, LAPTM4B, LDLRAD3, LGALS1, LGALS3BP, LINC00473, LINC00673, LMNA, LOC100126784, LOC100130370, LOC645166, LOXL4, LRP6, MAGEA12, MAGEA2B, MAGEA3, MAGEA6, MAGED1, MAGED2, MAPIB, MARCKSL1, MDK, MFAP2, MFGE8, MFI2, MGST3, MIA, MIF, MITF, MLANA, MLPH, MMP14,

MORF4L2, MORN2, MPZL1, MRPL24, MT2A, MTUS1, MXI1, MYH10, MYO10, MYO1D, NAV2, NCKAP1, NDST1, NENF, NES, NGFRAP1, NGRN, NHSL1, NIDI, NME1, NME2, NME4, NRP2, NRSN2, NSG1, OSBPLIA, P4HA2, PACSIN2, PAX3, PCDHGC3, PEG10, PFDN2, PFKM, PFN2, PGRMC1, PHB, PHLDB1, PIR, PKNOX2, PLEKHB1, PLK2, PLOD1, PLOD3, PLP1, PLS3, PLXNA1, PLXNB3, PMEL, PMP22, POLR2F, POLR2L, PON2, PPT2, PRAME, PRDX4, PRDX6, PRKCDBP, PROS1, PRSS23, PSMB5, PTGFRN, PTGR1, PTK2, PTPLAD1, PTPRM, PTPRS, PTRH2, PTTG1IP, PYCR1, PYGB, PYGL, QDPR, QPCT, RAB13, RAB17, RAB34, RAB38, RAI14, RBFOX2, RCAN1, RCN1, RCN2, RDX, RGS20, RND3, ROBO1, ROPN1, ROPN1B, RTKN, S100A1, S100A13, S100A16, S100B, SCARB1, SCCPDH, SCD, SDC3, SDC4, SDCBP, SELENBP1, SEMA3B, SEMA3C, SEMA6A, SEPT10, SERPINA3, SERPINE2, SERPINH1, SGCD, SGCE, SHC1, SHC4, SLC19A2, SLC24A5, SLC25A13, SLC25A4, SLC35B2, SLC39A1, SLC39A6, SLC45A2, SLC6A15, SLC7A8, SMARCA1, SNAI2, SNCA, SNHG16, SNRPE, SORT1, SOX10, SOX13, SOX4, SPARC, SPR, SPRY4, SPTBN1, SRPX, SSFA2, ST3GAL4, ST5, ST6GALNAC2, STK32A, STMN1, STXBP1, SYNGR1, TANC1, TBC1D16, TBC1D7, TCEAL4, TEAD1, TENC1, TEX2, TFAP2A, TIMP2, TIMP3, TJP1, TMEM147, TMEM14C, TMEM9, TMEM98, TNFRSF19, TOM1L1, TRIM2, TRIM63, TSC22D1, TSPAN3, TSPAN4, TSPAN6, TLL4, TUBB2A, TUBB2B, TUBB3, TYR, UBL3, VAT1, VIM, VKORC1, WASL, WBP5, WIPI1, WLS, XAGE1A, XAGE1B, XAGE1C, XAGE1D, XAGE1E, XYLB, YWHAE and ZNF462; or

b) one or more genes or polypeptides selected from Figure 3C; or

c) one or more genes or polypeptides selected from the group consisting of ABHD2, ACSL4, AHNAK, AHR, AIM2, ANGPTL4, ANXA1, ANXA2, APOD, ATF3, ATP1A1, ATP1B3, BBX, BCL6, BIRC3, BSG, C16orf45, C8orf40, CALU, CARD16, CAV1, CBF3, CCDC109B, CCND3, CD151, CD200, CD44, CD46, CD47, CD58, CD59, CD9, CD97, CDH19, CERS5, CFB, CHI3L2, CLEC2B, CLIC4, COL16A1, COL5A2, CREG1, CRELD1, CRYAB, CSPG4, CST3, CTNNA1, CTSA, CTSB, CTSD, DCBLD2, DCTN6, EGRI, EMPI, EPDR1, FAM114A1, FAM46A, FCRLA, FNI, FNDC3B, FXYD3, G6PD, GAA, GADD45B, GALNS, GBP2, GEM, GRAMD3, GSTM2, HLA-A, HLA-C, HLA-E, HLA-F, HPCAL1, HSP90B1, HTATIP2, IFI27L2, IFI44, IFI6, IFITM3, IGFIR, IGFBP3, IGFBP7, ILIRAP, ITGA6, ITGB3, ITM2B, JUNB, KCNN4, KIAA1551, KLF4, KLF6, LAMB1, LAMP2, LGALS1, LGALS3BP, LINC00116, LOC100127888, LOXL2, LOXL3, LPL, LXN, MAGEC2, MFI2, MIA, MT1E, MT1F, MT1G, MT1M, MT1X, MT2A,

NFE2L1, NFKBIZ, NNMT, NOTCH2, NR4A1, OS9, P4HA2, PDE4B, PELI1, PIGT, PMAIP1, PNPLA8, PPAPDCIB, PRKCDBP, PRNP, PROS1, PRSS23, PSMB9, PSME1, PTPMT1, PTRF, RAMP1, RND3, RNH1, RPN2, S100A10, S100A6, SCCPDH, SERINC1, SERPINA3, SERPINE1, SERPINE2, SLC20A1, SLC35A5, SLC39A14, SLC5A3, SMIM3, SPARC, SPRY2, SQRDL, STAT1, SUMF1, TAPI, TAPBP, TEK4P2, TF, TFAP2C, TMEM43, TMX4, TNC, TNFRSF10B, TNFRSF12A, TSC22D3, TSPAN31, UBA7, UBC, UBE2L6, XP07, ZBTB20, ZDHHC5, ZMYM6NB, ACAA2, ADSL, AEN, AHCY, ALDHIB1, ARHGEF1, ARPC5, ATXN10, ATXN2L, B4GALT3, BCCIP, BGN, C10orf32, C16orf88, C17orf76-AS1, C20orf12, CDCA7, CECR5, CPSF1, CS, CTCFL, CTPS1, DLL3, DTD2, ECHDC1, ECHS1, EIF4A1, EIF4EBP2, EIF6, EML4, ENY2, ESRG, FAM174B, FAM213A, FBL, FBLN1, FDXR, FOXRED2, FXN, GALT, GEMIN8, GLOD4, GPATCH4, HDAC2, HMG3, HSD17B14, IDH2, ILF2, ISYNA1, KIAA0020, KLHDC8B, LMCD1, LOC100505876, LYPLA1, LZTS2, MAZ, METAP2, MIDI, MIR4461, MPDUI, MPZL1, MRPS16, MSTO1, MTG1, MYADM, MYBBPIA, MYL6B, NARS2, NCBP1, NDUFAF6, NDUFS2, NF2, NHEJ1, NME6, NNT, NOLC1, NTHL1, OAZ2, OXAIL, PABPC1, PAICS, PAK1IP1, PFN1, POLR2A, PPA1, PRAME, PRDX3, PSTPIP2, PTGDS, PTP4A3, RBM34, RBM4, RPL10A, RPL17, RPP30, RPS3, RPS7, RPSA, RUVBL2, SAMM50, SBNO1, SERPINF1, SKP2, SLC45A2, SMC3, SMG7, SMS, SNAI2, SORD, SOX4, SRCAP, SRSF7, STARD10, TBXA2R, THOC5, TIMM22, TIMM23, TMC6, TOMM22, TPM1, TSNAX, TSR1, TSTA3, TULP4, UBAP2L, UCHL5, UROS, VPS72, WDR6, XPNPEP1, XRCC5, YDJC, ZFP36L1, and ZNF286A; or

d) one or more genes or polypeptides selected from the group consisting of AHNK, AHR, ANXA1, ATP1B3, BBX, BCL6, BIN3, C16orf45, CARD16, CAST, CAV1, CAV2, CD59, CD9, CDH19, CLEC2B, CRYAB, CYSTM1, FAM114A1, FAM46A, FCRLA, FXD3, G6PD, GBP2, HLA-A, HLA-E, HLA-F, IGF1R, ILIRAP, IL6ST, ITGB1, ITM2B, KCNN4, KLF4, KLF6, LAMP2, LEPROT, LGALS1, LOC100127888, MT1X, MT2A, MVP, NFAT5, NFE2L1, NFKBIZ, PLP2, PROS1, PRSS23, RNF145, S100A10, SEL1L, SERINC1, SERPINA3, SERPINE2, SPRY2, SQRDL, SQSTM1, TAPBP, TF, TM6IM1, TNFRSF10B, TNFRSF12A, UBE2B, and ZBTB20; or

e) one or more genes or polypeptides selected from the group consisting of TM4SF1, ANXA1, MT2A, SERPINA3, EMP1, MIA, ITGA3, CDH19, CTSB, SERPINE2, MFI2, APOC2, ITGB8, S100A6, NNMT, SLC5A3, SEMA3B, TSC22D3, ITGB3, MATN2, CRYAB, PERP, CSPG4, SGCE, CD9, A2M, FGFR1, CST3, DDR1, CD59, DPYSL2,

KCNN4, SLC26A2, CD151, SLC39A14, AHNAK, ATP1A1, PROS1, TIMP1, TRIML2, EGR1, TNC, DCBLD2, DUSP4, DUSP6, CD58, FAM3C, ATP1B1, MT1E, TNFRSF12A, FXYD3, SCCPDH, GAA, TIMP3, LEF1-AS1, CAV1, MFGE8, NR4A1, LGALS3, CCND3, CALU, RDH5, APOD, LINC00116, ILIRAP, SERPINA1, NFKBIZ, HSPA1A, PRSS23, MAP1B, ITGA7, PLP2, IGFBP7, GSN, LOXL3, PTRF, LGALS1, IGF1R, SERPINE1, MTIX, ATP1B3, SDC3, ZBTB38, NSG1, FCGR2A, KLF4, EGR3, DAG1, CTSD, CPVL, EEAI, SLC20A1, CLU, GBP2, SPON2, TNFSF4, NPC1, PRKCDBP, HTATIP2, C16orf45, SERPINF1, DCT, SNAI2, PTP4A3, RPS19, BCAN, FOXRED2, FAM174B, TRPM1, ESRP1, PABPC1, CA14, TMC6, C17orf76-AS1, RPL13AP5, TP53, BANCR, RPL28, IDH2, LOC100133445, TYRP1, DLL3, LHFPL3-AS1, SCIN, EIF4EBP2, TIMM50, CD68, GPI, MIR4461, RPS27, C1QBP, EGFL8, RPL21, FAM178B, RPS24, SAE1, KLHDC8B, KCNAB2, RPLPO, SCD, TULP4, IL6R, LINC00439, TSTD1, NF2, TUBB4A, SOX4, RPS3, NAPRT1, RPS6, LIMD2, CDKN2A, PTGDS, ISYNA1, ARHGDIB, CNRIP1, H3F3A, TBXA2R, PSTPIP2, SERPINB9, TMEM204, SORD, RPS5, CDH3, RPL18A, RPL8, VPS53, RBM34, FES, ESRG, RPS7, HSD17B14, TTC39A, FBLN1, SLC45A2, AEN, ACP5, BCL11A, CHP1, XIST, MAZ, FAM92A1, CTPS1, ASAP1, RPL6, MARCKS, MAGEA4, NPL, RPS16, NENF, SLC19A1, FTL, RNF2, MYBBP1A, PPAP2C, GRWD1, SKP2, WDR81, DCUN1D2, LAMP2 and MPZL1; or

f) one or more genes or polypeptides selected from the group consisting of TM4SF1, MT2A, SERPINA3, CDH19, SERPINE2, CRYAB, SGCE, A2M, DDR1, CD59, DPYSL2, DUSP6, MFGE8, NFKBIZ, and PRSS23; or

g) one or more genes or polypeptides selected from the group consisting of SERPINA3, MT2A, SERPINF1, SERPINE2, SOX4, DDR1, CD59, DUSP6, PERP, SEMA3B, PTP4A3, BANCR, DLL3, and LAMP2; or

h) one or more genes or polypeptides selected from the group consisting of MT2A, MT1E, MTIX, MT1M, MT1F, MT1G, MTX1 and MTG1.

[0039] In one embodiment, the ITR signature further comprises one or more genes or polypeptides selected from the group consisting of IFNGR2, B2M, and PDL1.

[0040] In one embodiment, said ITR signature comprises a post-immunotherapy signature-down (PIT-down) module, said module comprising one or more genes selected from the group consisting of: ABHD2, ACSL4, AHNAK, AHR, AIM2, ANGPTL4, ANXA1, ANXA2, APOD, ATF3, ATP1A1, ATP1B3, BBX, BCL6, BIRC3, BSG, C16orf45, C8orf40, CALU, CARD16, CAV1, CBF3, CCDC109B, CCND3, CD151, CD200, CD44, CD46,

CD47, CD58, CD59, CD9, CD97, CDH19, CERS5, CFB, CHI3L2, CLEC2B, CLIC4, COL16A1, COL5A2, CREG1, CRELD1, CRYAB, CSPG4, CST3, CTNNAL1, CTSA, CTSB, CTSD, DCBLD2, DCTN6, EGR1, EMP1, EPDR1, FAM114A1, FAM46A, FCRLA, FN1, FNDC3B, FXYD3, G6PD, GAA, GADD45B, GALNS, GBP2, GEM, GRAMD3, GSTM2, HLA-A, HLA-C, HLA-E, HLA-F, HPCAL1, HSP90B1, HTATIP2, IFI27L2, IFI44, IFI6, IFITM3, IGFIR, IGFBP3, IGFBP7, ILIRAP, ITGA6, ITGB3, ITM2B, JUNB, KCNN4, KIAA1551, KLF4, KLF6, LAMB1, LAMP2, LGALS1, LGALS3BP, LINC00116, LOC100127888, LOXL2, LOXL3, LPL, LXN, MAGEC2, MFI2, MIA, MT1E, MT1F, MTIG, MTIM, MTIX, MT2A, NFE2L1, NFKBIZ, NNMT, NOTCH2, NR4A1, OS9, P4HA2, PDE4B, PELI1, PIGT, PMAIP1, PNPLA8, PPAPDCIB, PRKCDBP, PRNP, PROS1, PRSS23, PSMB9, PSME1, PTPMT1, PTRF, RAMP1, RND3, RNH1, RPN2, S100A10, S100A6, SCCPDH, SERINC1, SERPINA3, SERPINE1, SERPINE2, SLC20A1, SLC35A5, SLC39A14, SLC5A3, SMIM3, SPARC, SPRY2, SQRDL, STAT1, SUMF1, TAPI, TAPBP, TEKT4P2, TF, TFAP2C, TMEM43, TMX4, TNC, TNFRSF10B, TNFRSF12A, TSC22D3, TSPAN31, UBA7, UBC, UBE2L6, XP07, ZBTB20, ZDHHC5 and ZMYM6NB; or TM4SF1, ANXA1, MT2A, SERPINA3, EMP1, MIA, ITGA3, CDH19, CTSB, SERPINE2, MFI2, APOC2, ITGB8, S100A6, NNMT, SLC5A3, SEMA3B, TSC22D3, ITGB3, MATN2, CRYAB, PERP, CSPG4, SGCE, CD9, A2M, FGFR1, CST3, DDR1, CD59, DPYSL2, KCNN4, SLC26A2, CD151, SLC39A14, AHNAK, ATP1A1, PROS1, TIMP1, TRIML2, EGR1, TNC, DCBLD2, DUSP4, DUSP6, CD58, FAM3C, ATP1B1, MT1E, TNFRSF12A, FXYD3, SCCPDH, GAA, TIMP3, LEF1-AS1, CAV1, MFGE8, NR4A1, LGALS3, CCND3, CALU, RDH5, APOD, LINC00116, ILIRAP, SERPINA1, NFKBIZ, HSPA1A, PRSS23, MAPIB, ITGA7, PLP2, IGFBP7, GSN, LOXL3, PTRF, LGALS1, IGFIR, SERPINE1, MTIX, ATP1B3, SDC3, ZBTB38, NSG1, FCGR2A, KLF4, EGR3, DAG1, CTSD, CPVL, EEA1, SLC20A1, CLU, GBP2, SPON2, TNFSF4, NPC1, PRKCDBP, HTATIP2, and C16orf45; or an miCR down gene in Figure 3C, wherein said PIT-down module is downregulated in a tumor resistant to immunotherapy and upregulated in a tumor sensitive to immunotherapy as compared to a reference level.

[0041] In one embodiment, said ITR signature comprises a post-immunotherapy signature-up (PIT-up) module, said module comprising one or more genes selected from the group consisting of: ACAA2, ADSL, AEN, AHCY, ALDH1B1, ARHGEF1, ARPC5, ATXN10, ATXN2L, B4GALT3, BCCIP, BGN, C10orf32, C16orf88, C17orf76-AS1, C20orf112, CDCA7, CECR5, CPSF1, CS, CTCFL, CTPS1, DLL3, DTD2, ECHDC1,

ECHS1, EIF4A1, EIF4EBP2, EIF6, EML4, ENY2, ESRG, FAM174B, FAM213A, FBL, FBLN1, FDXR, FOXRED2, FXN, GALT, GEMIN8, GLOD4, GPATCH4, HDAC2, HMGN3, HSD17B14, IDH2, ILF2, ISYNA1, KIAA0020, KLHDC8B, LMCD1, LOC100505876, LYPLA1, LZTS2, MAZ, METAP2, MIDI, MIR4461, MPDUI, MPZLI, MRPS16, MSTO1, MTG1, MYADM, MYBBPIA, MYL6B, NARS2, NCBPI, NDUFAF6, NDUFS2, NF2, NHEJ1, NME6, NNT, NOLCI, NTHL1, OAZ2, OXAIL, PABPC1, PAICS, PAK1IP1, PFN1, POLR2A, PPA1, PRAME, PRDX3, PSTPIP2, PTGDS, PTP4A3, RBM34, RBM4, RPL10A, RPL17, RPP30, RPS3, RPS7, RPSA, RUVBL2, SAMM50, SBNO1, SERPINF1, SKP2, SLC45A2, SMC3, SMG7, SMS, SNAI2, SORD, SOX4, SRCAP, SRSF7, STARD10, TBXA2R, THOC5, TIMM22, TIMM23, TMC6, TOMM22, TPM1, TSNAX, TSR1, TSTA3, TULP4, UBAP2L, UCHL5, UROS, VPS72, WDR6, XPNPEPI, XRCC5, YDJC, ZFP36L1 and ZNF286A; or SERPINF1, DCT, SNAI2, PTP4A3, RPS19, BCAN, FOXRED2, FAM174B, TRPM1, ESRP1, PABPC1, CA14, TMC6, C17orf76-AS1, RPL13AP5, TP53, BANC1, RPL28, IDH2, LOC100133445, TYRP1, DLL3, LHFPL3-AS1, SCIN, EIF4EBP2, TIMM50, CD68, GPI, MIR4461, RPS27, C1QBP, EGFL8, RPL21, FAM178B, RPS24, SAE1, KLHDC8B, KCNAB2, RPLPO, SCD, TULP4, IL6R, LINC00439, TSTD1, NF2, TUBB4A, SOX4, RPS3, NAPRT1, RPS6, LIMD2, CDKN2A, PTGDS, ISYNA1, ARHGDIB, CNRIP1, H3F3A, TBXA2R, PSTPIP2, SERPINB9, TMEM204, SORD, RPS5, CDH3, RPL18A, RPL8, VPS53, RBM34, FES, ESRG, RPS7, HSD17B14, TTC39A, FBLN1, SLC45A2, AEN, ACP5, BCL11A, CHP1, XIST, MAZ, FAM92A1, CTPS1, ASAP1, RPL6, MARCKS, MAGEA4, NPL, RPS16, NENF, SLC19A1, FTL, RNF2, MYBBPIA, PPAP2C, GRWD1, SKP2, WDR81, DCUN1D2, and MPZLI; or an miCR up gene in Figure 3C, wherein said PIT-up module is upregulated in a tumor resistant to immunotherapy and downregulated in a tumor sensitive to immunotherapy as compared to a reference level.

[0042] Detecting an immunotherapy resistance gene signature in a tumor may further comprise detecting in tumor infiltrating lymphocytes (TIL) obtained from the subject in need thereof the expression or activity of a CD8 T cell gene signature, said signature comprising one or more genes or polypeptides selected from the group consisting of APOBEC3G, CBLB, CCL4, CCL4L1, CCL4L2, CCL5, CD27, CD8A, CD8B, CST7, CTSW, CXCL13, CXCR6, DTHD1, DUSP2, EOMES, FASLG, FCRL3, GBP5, GZMA, GZMB, GZMH, GZMK, HCST, HLA-A, HLA-B, HLA-H, ID2, IFNG, IL2RB, KLRC3, KLRC4, KLRC4-

KLRK1, KLRD1, KLRK1, LAG3, LSP1, LYST, NKG7, PDCD1, PRF1, PSTPIP1, PYHIN1, RARRES3, SH2D1A, SH2D2A, TARP, TIGIT, TNFRSF9 and TOX.

[0043] Detecting an immunotherapy resistance gene signature in a tumor may further comprise detecting in tumor infiltrating lymphocytes (TIL) obtained from the subject in need thereof the expression or activity of a CD4 T cell gene signature, said signature comprising one or more genes or polypeptides selected from the group consisting of AIM1, ANK3, AQP3, CAMK4, CCR4, CCR8, CD28, CD40LG, DGKA, EML4, FAAH2, FBLN7, FKBP5, FLT3LG, FOXP3, FXYD5, IL6R, IL7R, ITGB2-AS1, JUNB, KLRB1, LEPROTL1, LOC100128420, MAL, OXNAD1, PBXIP1, PIK3IP1, PIM2, PRKCQ-AS1, RORA, RPL35A, RPL4, RPL6, RPS15A, RPS27, RPS28, 6-Sep, SLAMF1, SORL1, SPOCK2, SUSP3, TCF7, TMEM66, TNFRSF18, TNFRSF25, TNFRSF4, TNFSF8, TRABD2A, TSC22D3 and TXK.

[0044] Detecting an immunotherapy resistance gene signature in a tumor may further comprise detecting in macrophages obtained from the subject in need thereof the expression or activity of a macrophage gene signature, said signature comprising one or more genes or polypeptides selected from the group consisting of AIF1, ALDH2, ANPEP, C15orf48, Clorf162, C1QA, C1QB, C1QC, C3AR1, CCR1, CD14, CD163, CD300A, CD300C, CD300LF, CD33, CD86, CFP, CLEC10A, CLEC12A, CLEC4A, CLEC5A, CMKLR1, CSF1R, CSF2RB, CSF3R, CSTA, CXCL9, CXCR2P1, DSC2, FAM26F, FBP1, FCER1G, FCGRIA, FCGRIB, FCGRIC, FCGR3A, FCGR3B, FCN1, FOLR2, FPRI, FPR2, FPR3, GGTA1P, GNA15, GPR84, HCK, HK3, IGSF6, IL1B, IL1RN, IL4I1, ITGAM, KYNU, LGALS2, LILRA1, LILRA2, LILRA3, LILRA4, LILRB2, LILRB4, LILRB5, LST1, MAFB, MARCO, MNDA, MRC1, MS4A4A, MS4A6A, MSR1, NCF2, OLR1, P2RY13, PILRA, PLAU, PLBD1, PLXDC2, PRAM1, RAB20, RAB31, RASSF4, RBM47, RGS18, S100A8, S100A9, SECTM1, SIGLEC1, SIGLEC7, SIGLEC9, SLAMF8, SLC31A2, SLC43A2, SLC7A7, SLC8A1, SLC02B1, SPI1, STAB1, TBXAS1, TFEC, TGFBI, TLR2, TLR4, TLR8, TMEM176A, TMEM176B, TNFSF13, TNFSF13B, TREM2, TYROBP, VSIG4 and ZNF385A.

[0045] Detecting an immunotherapy resistance gene signature in a tumor may further comprise detecting in B cells obtained from the subject in need thereof the expression or activity of a B cell gene signature, said signature comprising one or more genes or polypeptides selected from the group consisting of ADAM19, AKAP2, BACH2, BANK1, BCL11A, BLK, CD19, CD1C, CD22, CD79A, CD79B, CLEC17A, CNR2, COL19A1,

COL4A3, CPNE5, CR2, CXCR5, EBF1, ELK2AP, FAM129C, FAM177B, FCER2, FCRL1, FCRL2, FCRL5, FCRLA, HLA-DOB, IGJ, IGLL1, IGLL3P, IGLL5, KIAA0125, KIAA0226L, LOC283663, MS4A1, P2RX5, PAX5, PNOC, POU2AF1, POU2F2, RASGRP3, SEL1L3, SNX29P1, ST6GAL1, STAPI, SWAP70, TCLIA, TMEM154 and VPREB3.

[0046] The gene signature may be detected in a bulk tumor sample, whereby the gene signature is detected by deconvolution of bulk expression data such that gene expression is assigned to malignant cells and non-malignant cells in said tumor sample.

[0047] Detecting the ITR gene signature may comprise detecting downregulation of the PIT-down module and/or upregulation of the PIT-up module. Not detecting the ITR gene signature may comprise detecting upregulation of the PIT-down module and/or downregulation of the PIT-up module. The detecting an ITR gene signature may indicate a 10-year survival rate less than 40% and wherein not detecting said signature may indicate a 10-year survival rate greater than 60%. The detecting an ITR gene signature may indicate exclusion of T cells from a tumor and wherein not detecting said signature may indicate infiltration of T cells in a tumor.

[0048] In another aspect, the present invention provides for a method of stratifying cancer patients into a high survival group and a low survival group comprising detecting the expression or activity of an immunotherapy resistance gene signature in a tumor, wherein if an immunotherapy resistance gene signature is detected the patient is in the low survival group and if an immunotherapy resistance gene signature is not detected the patient is in the high survival group. The patients in the high survival group may be immunotherapy responders and patients in the low survival group may be immunotherapy non-responders.

[0049] In another aspect, the present invention provides for a method of treating a cancer in a subject in need thereof comprising detecting the expression or activity of an immunotherapy resistance gene signature according to any of claims 1 to 10 in a tumor obtained from the subject and administering a treatment, wherein if an immunotherapy resistance signature is detected the treatment comprises administering an agent capable of reducing expression or activity of said signature, and wherein if an immunotherapy resistance signature is not detected the treatment comprises administering an immunotherapy. The agent capable of reducing expression or activity of said signature may comprise a drug selected from Table 3, a PKC activator, an inhibitor of the **NFKB** pathway, an IGFIR inhibitor, or Reserpine. The agent capable of reducing expression or activity of said signature may

comprise an agent capable of modulating expression or activity of a gene selected from the group consisting of MAZ, NFKBIZ, MYC, ANXA1, SOX4, MT2A, PTP4A3, CD59, DLL3, SERPINE2, SERPINF1, PERP, EGR1, SERPINA3, SEMA3B, SMARCA4, IFNGR2, B2M, and PDL1. The agent capable of reducing expression or activity of said signature may comprise an agent capable of targeting or binding to one or more up-regulated secreted or cell surface exposed immunotherapy resistance signature genes or polypeptides. The method may further comprise detecting the expression or activity of an immunotherapy resistance gene signature in a tumor obtained from the subject after the treatment and administering an immunotherapy if said signature is not detected. The method may further comprise administering an immunotherapy to the subject administered an agent capable of reducing the expression or activity of said signature. The immunotherapy may comprise a check point inhibitor or adoptive cell transfer (ACT). The adoptive cell transfer may comprise a CAR T cell or activated autologous T cells. The checkpoint inhibitor may comprise anti-CTLA4, anti-PD-L1 and/or anti-PD1 therapy.

[0050] In another aspect, the present invention provides for a method of treating a cancer in a subject in need thereof comprising detecting the expression or activity of an immunotherapy resistance gene signature according to any embodiment herein in a tumor obtained from the subject, wherein if an immunotherapy resistance signature is detected the treatment comprises administering an agent capable of modulating expression or activity of one or more genes or polypeptides in a network of genes disrupted by perturbation of a gene selected from the group consisting of MAZ, NFKBIZ, MYC, ANXA1, SOX4, MT2A, PTP4A3, CD59, DLL3, SERPINE2, SERPINF1, PERP, EGR1, SERPINA3, SEMA3B, SMARCA4, IFNGR2, B2M, and PDL1.

[0051] In another aspect, the present invention provides for a method of treating a cancer in a subject in need thereof comprising administering to the subject a therapeutically effective amount of an agent: capable of modulating the expression or activity of one or more immunotherapy resistance signature genes or polypeptides; or capable of targeting or binding to one or more cell surface exposed immunotherapy resistance signature genes or polypeptides, wherein the gene or polypeptide is up-regulated in the ITR signature; or capable of targeting or binding to one or more receptors or ligands specific for a cell surface exposed immunotherapy resistance signature gene or polypeptide, wherein the gene or polypeptide is up-regulated in the ITR signature; or comprising a secreted immunotherapy resistance signature gene or polypeptide, wherein the gene or polypeptide is down-regulated

in the ITR signature; or capable of targeting or binding to one or more secreted immunotherapy resistance signature genes or polypeptides, wherein the genes or polypeptides are up-regulated in the ITR signature; or capable of targeting or binding to one or more receptors specific for a secreted immunotherapy resistance signature gene or polypeptide, wherein the secreted gene or polypeptide is up-regulated in the ITR signature; or comprising a drug selected from Table 3, a PKC activator, an inhibitor of the NF κ B pathway, an IGF1R inhibitor, or Reserpine. The agent capable of modulating the expression or activity of one or more immunotherapy resistance signature genes or polypeptides may comprise a CDK4/6 inhibitor. The CDK4/6 inhibitor may comprise Abemaciclib. The method may further comprise administering an immunotherapy to the subject. The immunotherapy may comprise a check point inhibitor. The checkpoint inhibitor may comprise anti-CTLA4, anti-PD-L1 and/or anti-PD1 therapy. Not being bound by a theory, the CDK4/6 inhibitor may sensitize a subject to checkpoint blockade therapy. The agent may comprise a therapeutic antibody, antibody fragment, antibody-like protein scaffold, aptamer, protein, CRISPR system or small molecule. The agent capable of targeting or binding to one or more cell surface exposed immunotherapy resistance signature polypeptides or one or more receptors specific for a secreted immunotherapy resistance signature gene or polypeptide may comprise a CAR T cell capable of targeting or binding to one or more cell surface exposed immunotherapy resistance signature genes or polypeptides or one or more receptors specific for a secreted immunotherapy resistance signature gene or polypeptide.

[0052] In another aspect, the present invention provides for a method of monitoring a cancer in a subject in need thereof comprising detecting the expression or activity of an immunotherapy resistance gene signature according to any embodiment herein in tumor samples obtained from the subject for at least two time points. The at least one sample may be obtained before treatment. The at least one sample may be obtained after treatment.

[0053] The cancer according to any embodiment may be melanoma. The ITR gene signature may be expressed in response to administration of an immunotherapy.

[0054] In another aspect, the present invention provides for a method of detecting T cell infiltration of a tumor comprising detection in malignant cells expression or activity of one or more genes selected from the group consisting of: HLA-C, FGFR1, ITGB3, CD47, AHNAK, CTSD, TIMP1, SLC5A3, CST3, CD151, CCND3, MIA, CD58, CTSB, S100A6, EMP1, HLA-F, TSC22D3, ANXA1, KCNN4 and MT2A; or A2M, AEBP1, AHNAK, ANXA1, APOC2, APOD, APOE, ATP1A1, ATP1B1, C4A, CAPN3, CAV1, CD151, CD59, CD63,

CDH19, **CRYAB**, **CSPG4**, CSRP1, **CST3**, CTSB, CTSD, **DAG1**, DDR1, DUSP6, ETV5, **EVA1A**, FBX032, FCGR2A, FGFRI, GAA, GATSL3, GJBI, GRN, GSN, HLA-B, HLA-C, HLA-F, **HLA-H**, **IFI35**, IGFBP7, IGSF8, ITGA3, ITGA7, **ITGB3**, LAMP2, **LGALS3**, LOXL4, LRPAP1, LY6E, **LYRM9**, **MATN2**, MFGE8, MIA, MPZ, MT2A, **MTRNR2L3**, MTRNR2L6, NPC1, NPC2, NSG1, PERP, PKM, PLEKHB1, PROS1, PRSS23, PYGB, **RDH5**, ROPN1, SIOOAI, S100A13, S100A6, S100B, SCARB2, SCCPDH, **SDC3**, SEMA3B, SERPINA1, SERPINA3, SERPINE2, SGCE, SGK1, SLC26A2, SLC5A3, SPON2, SPPI, **TIMP1**, TIMP2, TIMP3, **TM4SF1**, TMEM255A, TMX4, TNFSF4, TPPI, TRIML2, TSC22D3, **TXNIP**, TYR, UBC and WBP2; or HLA-A, HLA-B, HLA-C, B2M, TAPBP, **IFI27**, **IFI35**, IRF4, IRF9 and STAT2; or B2M, CTSB, CTSL1, HLA-B/C/F, HSPA1A, HSPA1B, NFKBIA and CD58, wherein detection indicates sensitivity to immunotherapy.

[0055] In another aspect, the present invention provides for a method of detecting T cell exclusion of a tumor comprising detection in malignant cells expression or activity of one or more genes selected from the group consisting of: **SERPINF1**, RPL6, NOLC1, RSL1D1, ILF2, SOX4, ACTG1, C17orf76-AS1, PABPC1, RPS24, ADSL, C1QBP, PAICS, CTPS1, NF2, EIF2S3, RPL18 and RPL10A; or **AHCY**, BZW2, CCNBIPI, CCT6A, EEF2, EIF3B, GGCT, ILF3, IMPDH2, MDH2, MYBBPIA, NT5DC2, PAICS, PFKM, POLD2, PTK7, **SLC19A1**, SMARCA4, STRAP, TIMM13, TOPIMT, TRAP1 and **USP22**; or MYC, STRAP and SMARCA4; or MYC, **SNA12** and SOX4, wherein detection indicates resistance to immunotherapy.

[0056] In another aspect, the present invention provides for a method of detecting an immunotherapy resistance gene signature in a tumor comprising, detecting in tumor cells obtained from a subject in need thereof who has been treated with an immunotherapy the expression or activity of a malignant cell gene signature comprising: one or more down regulated genes selected from the group consisting of genes associated with coagulation, apoptosis, TNF- α signaling via NF κ b, Antigen processing and presentation, metallothionein and IFNGR2; and/or one or more up regulated genes selected from the group consisting of genes associated with negative regulation of angiogenesis and MYC targets.

[0057] In another aspect, the present invention provides for a kit comprising reagents to detect at least one immunotherapy resistance signature gene or polypeptide according to the present invention. The kit may comprise at least one antibody, antibody fragment, or

aptamer. The kit may comprise primers and/or probes for quantitative RT-PCR or fluorescently bar-coded oligonucleotide probes for hybridization to RNA.

[0058] It is noted that in this disclosure and particularly in the claims and/or paragraphs, terms such as "comprises", "comprised", "comprising" and the like can have the meaning attributed to it in U.S. Patent law; e.g., they can mean "includes", "included", "including", and the like; and that terms such as "consisting essentially of" and "consists essentially of" have the meaning ascribed to them in U.S. Patent law, e.g., they allow for elements not explicitly recited, but exclude elements that are found in the prior art or that affect a basic or novel characteristic of the invention.

[0059] These and other aspects, objects, features, and advantages of the example embodiments will become apparent to those having ordinary skill in the art upon consideration of the following detailed description of illustrated example embodiments.

BRIEF DESCRIPTION OF THE DRAWINGS

[0060] The following detailed description, given by way of example, but not intended to limit the invention solely to the specific embodiments described, may best be understood in conjunction with the accompanying drawings.

[0061] **Figure 1** illustrates the study design and T cell analysis of ICR. **(A)** Overview. 31 samples from patients with metastatic melanoma (discovery cohort) were profiled by scRNA-sequencing (left), of which 15 were TN, 15 had ICI resistance (ICR) and one had clinical benefit (CB). Signatures were tested in two validation cohorts collected independently (right), with bulk RNA-seq of melanoma tumors from 112 patients who underwent biopsies prior to receiving pembrolizumab (anti-PD-1; cohort 1) and from 26 patients, 12 with matched pre-treatment and post-progression (ICR) biopsies (cohort 2). **(B-C)** Distinct profiles of malignant and non-malignant cells. Shown are tSNE plots of single cell profiles (dots) from malignant **(B)** or non-malignant **(C)** cells, shaded by *post-hoc* annotation (**materials and methods**) or by patient. **(D)** Variation in T cells ICR. Shown is a tSNE plot of CD8 T cells that Applicants generated based on the genes of the tICR signatures, with cells shaded by treatment category (right), overall expression (OE) of the tICR signature (middle), and clonality (right). Larger dots: cells from large (> 20 cells) clones. **(E)** Similar relationship between exhaustion and cytotoxicity signatures in TN and ICR CD8 T cells. For each cell (dot), the exhaustion (y axis) and cytotoxicity (x axis) scores are shown (**materials and methods**): TN; ICR; CB. Cells from the CB patient have lower than expected

exhaustion scores. **(F)** CD8 T cell clones. Shown is the distribution of clone sizes. Tumors with large (>20 cells) clones are marked. **(G)** Expanded clones have higher tICR expression. Box plots show the distribution of tICR OE scores (y axis) in CD8 T-cells from patients stratified by clinical context and by overall clonality level. Left: only CD8 T-cells with reconstructed TCRs are shown; Right: only CD8 T-cells that were not from the three ICR patients with major clonal expansion are shown (right). Box-plots: the middle line represents the median; box edges are the 25th and 75th percentiles, and whiskers represent the most extreme points that do not exceed $\pm IQR * 1.5$; points beyond the distance are plotted as single points. **(H)** CD8 T cell specific cell-cycle program. Shown are the distribution of OE scores for the CD8 specific cell cycle program in malignant cells (left) and CD8 T cells (right). The p-values were computed by comparing the cycling and non-cycling cells in each cell type with a one-sided t-test.

[0062] **Figure 2** illustrates the Malignant cell ICR programs. **(A)** Robust classification by the oncogenic-ICR signature. Left: Box-plot shows the distribution of OE scores for the oncogenic-ICR signature in malignant cells from ICR (blue) and TN (grey) patients, when obtained in a cross-validation (CV) procedure and tested on withheld data. Middle line: median; box edges: 25th and 75th percentiles, whiskers: most extreme points that do not exceed $\pm IQR * 1.5$; further outliers are marked individually. Right: Receiver Operating Characteristic (ROC) curve of the performances of different signatures in classifying cells as ICR or TN; the CV oncogenic-ICR signature was obtained by leave-one (patient) out CV; the first and second Area under the curve (AUC) values are for classification of cells and samples, respectively. **(B)** Genes in the oncogenic-ICR program. Heatmap shows the (centered and scaled) expression of the top 40 oncogenic-ICR-up and oncogenic-ICR-down genes (columns) across the malignant cells (rows), sorted by TN or ICR tumors (shaded bar, left) and clustered within each class. Leftmost bar: cycling and non-cycling cells within each group. Right: The OE of the oncogenic-ICR signature for each cell. **(C)** Differentially expressed gene sets in ICR vs. TN malignant cells. Box-plots (formatted as in (A)) show the distribution of OE scores for each signature in malignant cells from ICR vs. TN tumors. **(D-E)** Inverse relationship of the oncogenic-ICR-down and -up programs. Shown are the OE scores of the oncogenic-ICR-down (y-axis) and oncogenic-ICR-up (x-axis) programs in (D) the single cell profiles from TN (grey) and ICR (blue) tumors, and in (E) lesions of cutaneous (grey) and uveal melanoma. The Pearson correlation coefficient (r) and p-value are marked.

(F) Workflow for identification of the exclusion signatures. (G-H) Congruence between the oncogenic-ICR and exclusion programs. (G) Violin plots of the distribution of OE scores of exclusion signatures across malignant cells from ICR (blue) and TN (grey) patients. (H) Left: Heat map of the (centered and scaled) expression of the 40 most differentially expressed exclusion-up and exclusion-down (black) genes (columns) in the malignant cells (rows), sorted by ICR and TN tumors (left shaded bar) and clustered within class. Leftmost shaded bar labels cycling and non-cycling (black) cells within each group. Gene names in the oncogenic-ICR-up or oncogenic-ICR-down signatures (**table S6**) are marked by shading, respectively. Right: OE scores of the exclusion signature in each cell.

[0063] **Figure 3** illustrates that the uICR program has immune evasion properties, and can be reversed by CDK4/6 inhibition. (A-C) Reversal of resistance programs by a CDK4/6 inhibitor, abemaciclib. (A) Significance (y axis, $-\log_{10}(\text{p-value})$, Wilcoxon rank sum test) of induction (dark green) or repression (light green) of each signatures in tumors from abemaciclib treated mice compared to vehicle (37). (B) Distribution of uICR OE scores in breast cancer cell lines (M361, MCF and M453) treated with abemaciclib ("abe") or with DMSO vehicle ("con"). Box-plots: the middle line represents the median; box edges are the 25th and 75th percentiles, and whiskers represent the most extreme points that do not exceed $\pm\text{IQR} \times 1.5$; points beyond the distance are plotted as single points. (C) The relative expression of the 40 most differentially expressed uICR genes (rows) in abemaciclib-treated (green) and control (purple) breast cancer cells lines (columns). Expression values are normalized according to the cell-line specific expression in the control state or denote over- or under-expression, respectively. Bottom: OE scores of the uICR signature for each cell line. (D) Higher uICR scores in uveal melanoma. Shown are the distributions of OE scores of the uICR program in cutaneous (black) vs. uveal melanoma tumors from TCGA, scored after filtering TME contributions (**materials and methods**). P-value: t-test. (E) Suppression of cell-cell interactions in ICR. Bar plots show for each malignant signature (x-axis) the number of genes (y-axis, top) in the signature that can engage in a physical interaction with other cell types and the corresponding statistical enrichment (y-axis, $-\log_{10}(\text{P-value})$, hypergeometric test, bottom). Values above the dashed line are statistically significant.

[0064] **Figure 4** illustrates that the resistance signatures in malignant cells are prognostic and predictive in validation cohorts. (A) Resistance signatures predict melanoma patient survival based in bulk RNA-seq from TCGA (37). Kaplan-Meier (KM) plots are stratified by

high (top 25%), low (bottom 25%), or intermediate (neither high nor low) expression of the respective signature. *P* *c* p-values test if the signature further enhances the predictive power of models with T-cell infiltration levels as a covariate. See **fig. 11** for additional signatures. **(B, C)** Resistance signatures distinguish clinical benefit (CB) and non-CB in mouse models and melanoma patients. Box plots show the distribution of the OE score of the uICR in bulk RNA-Seq from a lung cancer mouse model treated with anti-CTLA-4 therapy (35) **(B)** or from biopsies of melanoma patients prior to treatment with pembrolizumab (5). Middle line: median; box edges: 25th and 75th percentiles, whiskers: most extreme points that do not exceed $\pm IQR * 1.5$; further outliers are marked individually. P-value: one-sided t-test. **(D-F)** Resistance signatures predict melanoma patient outcomes following pembrolizumab treatment from pre-treatment RNA-Seq in an independent cohort of 112 patients. **(D)** KM plots of progression-free survival (PFS) for the 104 patients in the cohort with available PFS data, when the patients are stratified by high (top 25%), low (bottom 25%), or intermediate (neither high nor low) expression of the respective signature. Prediction is enhanced when controlling for cell cycle as a confounder (two right plots, **materials and methods**). See **figs. 12 to 13**. **(E)** Bar plot shows predictive value for PFS for the 104 patients as in **(D)** with a COX regression model that accounts for inferred T-cell infiltration levels ($-\log_{10}(p\text{-value})$, x axis). Light blue bars: enhances PFS; grey bars: reduces PFS. Bars with black border denote the new signatures identified in this study for malignant resistance. Dashed line: $p < 0.05$. Resistance signatures are significantly more predictive compared to others ($P = 3.37 * 10^{-6}$, Wilcoxon-ranksum test). **(F)** Distribution of OE scores (y axis) of each signature in the pre-treatment bulk RNA-Seq profiles, showing patients with either intrinsic resistance (Non-CB, n=49) or with clinical benefit (CB, n=39), with the latter also further stratified based on duration of response (CB < 6mo, n=5; 6mo < CB < 1 year, n=9; CB > 1 year, n=25). Twenty-four patients with unknown response or stable disease are not shown here (see **fig. 14**). Distinctions are enhanced when accounting for inferred T-cell infiltration levels (right). *P1* and *P2* are the one-sided t-test p-value obtained when comparing the non-CB patients to the CB or CB > 1yr patients, respectively. The AUC at the top was obtained when predicting long-term CB (CB > 1yr) in all patients with a recorder response (n =101). Box plots formatted as in **(B)**. **(G)** Box-plots show the distribution of OE scores (y axis) of each signature in the pre-treatment bulk RNA-Seq profiles, for patients with complete response (CR, n=14), partial response (PR, n=25), or progressive disease (PD, n=49). *P* is the one-sided t-test p-value obtained when comparing the CR patients to the PR and PD patients. The

AUC at the top was obtained when predicting CR in all patients with a recorder response (n =101). (H) Bar plot shows predictive value for predicting complete response with the different signatures (4ogio(t-test p-value), x-axis) in 101 patients with a recorded response. Light blue bars: positive impact; grey bars: negative impact. Bars with black border denote the new signatures identified in this study for malignant resistance. Dashed line: $p = 0.05$. Resistance signatures are significantly more predictive compared to other signatures ($P = 1.64 \times 10^{-8}$, Wilcoxon ranksum test). AUC values are marked next to the bar for each significant association. (I) Model for ICR based on this study.

[0065] **Figure 5** illustrates the classification of malignant and non-malignant cells. (A) Inferred large-scale CNVs distinguish malignant (right) from nonmalignant (left) cells. Shown are the inferred CNVs (amplification, blue, deletion) along the chromosomes (x axis) for cells (y axis) in two representative tumors. (B-E) Congruence between different assignment methods. (B) Each plot shows the relation between two different scorings, by showing for CD45⁻ cells the distribution of scores (y axis) by one scheme, stratified to two categories by another scheme. CNV: inference of malignant and non-malignant CD45⁻ cells as in (A, **materials and methods**); signature based: assignment of CD45⁻ cells as malignant or stroma by scoring the corresponding expression signatures (**materials and methods**); differential similarity to melanoma: assignment of CD45⁻ cells as malignant or non-malignant by similarity to bulk melanoma tumors compared to normal tissue. Middle line: median; box edges: 25th and 75th percentiles; whiskers: most extreme points that do not exceed $\pm IQR \times 1.5$; points beyond the distance: single points. (C) Distribution of CNV-R-score for cells identified as malignant and non-malignant. The CNV-R-score of a cell is defined as the Spearman correlation coefficient (r) between the cell's CNV profile and its tumor's inferred CNV profile (**materials and methods**). (D) The distribution of CNV-R-scores across each identified cell type. (E) The CNV-R-score (y axis) at each overall CNV signal (**materials and methods**) for malignant and non-malignant cells; Non-malignant cells with values that exceed the dashed lines were considered unresolved and were omitted from further analyses.

[0066] **Figure 6** illustrates non-malignant cells. Shown are tSNE plots of all non-malignant cells (dots), shaded by (A) OE scores (bar) of well-established cell type markers (**table S3**), or (B) detection of *CD4* or *CD8* (*CD8A* or *CD8B*).

[0067] **Figure 7** illustrates cell type specific ICR signatures. Left panels: Box-plots show the distribution of OE scores for the ICR signature in each cell type in ICR (blue) and TN (grey) patients. Middle line: median; box edges: 25th and 75th percentiles; whiskers: most

extreme points that do not exceed $\pm IQR * 1.5$; points beyond the distance: single points. Middle and right panels: Receiver Operating Characteristic (ROC) curves of the performances of different signatures in classifying cells (middle) or samples (left) as ICR or TN. (A) Malignant cells, (B) CD4 T cells, (C) CD8 T cells, (D) B cells, (E) macrophages.

[0068] **Figure 8** illustrates the shift in the balance of cytotoxicity and exhaustion states in CD8 T-cells in the patient with CB. (A) The distribution of expression levels of each of five key checkpoint genes in CD8 T cells from ICR, TN, and CB tumors. (B) Distinct relationship between exhaustion and cytotoxicity signatures in CD8 T cells from a CB patient. For each cell (dot) shown are the cytotoxicity (x-axis) and exhaustion (y-axis) scores (**materials and methods**), using different exhaustion signatures from (7) and (77). TN; ICR; CB. Cells from the CB patient have lower than expected exhaustion scores (p-values, hypergeometric test **materials and methods**).

[0069] **Figure 9** illustrates clonal expansion of CD8 T cells. (A) TCR reconstruction. Shown is the fraction (y-axis) of T-cells with one (α or β), both or no TCR chain reconstructed at full length (**materials and methods**). (B) Variation in CD8 T cell expansion across tumors. Violin plots show the distribution of estimated proportions of CD8 T cell clones in each tumor. Tumors are shaded by treatment group. The tumors of ICR patients have higher T-cell clonal expansion ($P = 3.2 * 10^{-2}$, one-sided Wilcoxon ranksum test). (C,D) Persistence of clones over time in one patient (Mel75). Shown are the number (C) and relative proportions (D) of cells in each clone for two post-ICI lesions collected, a year apart, from patient Mel75.

[0070] **Figure 10** illustrates the relationship between the malignant ICR program and cell cycle. (A, B) Higher ICR in cycling cells. (A) Box plots of the distribution of OE scores of the oncogenic-ICR signatures (y-axis) in cycling and non-cycling cells from ICR and TN tumors (x-axis). The middle line represents the median; box edges are the 25th and 75th percentiles, and whiskers represent the most extreme points that do not exceed $\pm IQR * 1.5$; points beyond the distance are plotted as single points. (B) Heatmap of the expression of ICR-up (bar) and down (black bar) genes (rows) that are also induced (repressed) in cycling vs. non-cycling malignant cells. Cells (columns) are sorted by TN and ICR tumors and clustered within each set (bar on top); the cells' cycling status in each category is marked by the bar on top. Bottom: Oncogenic ICR signature score (y axis) in each cell (x axis). (C) Abemaciclib represses the uICR program in breast cancer

cell lines. Heatmap of the relative expression of all the uICR genes (rows) in Abemaciclib-treated and control breast cancer cells lines (columns), based on the data in (24). Gene expression is relative to the basal expression level in each cell line. Bottom: OE scores (y axis) of the uICR signature for each cell line (x axis).

[0071] **Figure 11** illustrates that the resistance signatures score in TCGA tumors predict survival of melanoma patients. Kaplan-Meier (KM) plots stratified by high, intermediate or low OE of the respective signature in bulk RNA-Seq of TCGA tumors. *P_c* p-values test if the signature further enhances the predictive power of models with inferred T-cell infiltration levels as a covariate.

[0072] **Figure 12** illustrates that the resistance signature scores in pre-treatment biopsies predict response to anti-PD-1 therapy in an independent cohort. KM plots of progression-free survival (PFS) for the 104 of 112 patients in validation cohort 1 with PFS data, with patients stratified by high, intermediate and low OE score of the respective signature. *P_c* p-values test if the signature further enhances the predictive power of models with inferred T cell infiltration levels as a covariate.

[0073] **Figure 13** illustrates that the predictive performance of resistance signatures is enhanced when controlling for the cell cycle. KM plots of progression-free survival (PFS) for the 104 of 112 patients in validation cohort 1 with PFS data, with patients stratified by high, intermediate and low OE score of the respective, after controlling for cell cycle as a confounding factor (**materials and methods**).

[0074] **Figure 14** illustrates the expression of the resistance signatures in 101 melanoma patients, stratified according to their clinical response to pembrolizumab. Distribution of OE scores (y axis) of each signature in the pre-treatment bulk RNA-Seq profiles, showing overall 101 patients with complete response (CR, n = 14), partial response or stable disease (PR/SD, n = 38), or progressive disease (PD, n = 49). *P* is the one-sided t-test p-value obtained when comparing the CR patients to the PR, SD and PD patients. AUC is also marked on top. Middle line: median; box edges: 25th and 75th percentiles; whiskers: most extreme points that do not exceed $\pm IQR * 1.5$.

[0075] **Figure 15** illustrates pan-cancer analysis of the resistance signatures. Box-plots of the distribution of OE scores (x-axis) of the uICR signature in bulk RNA-seq profiles of 9,559 tumors across 33 cancer types (y-axis) from TCGA either scored (A) "as-is" or (B) with a regression-based process to control for TME-related signals (**materials and methods**). Middle line: median; box edges: 25th and 75th percentiles;

whiskers: most extreme points that do not exceed $\pm IQR * 1.5$; points beyond the distance: single points.

[0076] **Figure 16** illustrates that an unbiased analysis reveals a malignant cell state linked to ICR.

[0077] **Figure 17** illustrates an overview of the patients analyzed.

[0078] **Figure 18** illustrates the separation of immunotherapy treated and untreated tumors by Principle Component (PC) analysis.

[0079] **Figure 19** illustrates the correlation between the resistance signature and patients that are naive or resistant to immunotherapy.

[0080] **Figure 20** illustrates a leave-one-out cross validation analysis.

[0081] **Figure 21** illustrates mutual exclusive expression of the ITR up and down genes across malignant cells, and their anti-correlation in TCGA.

[0082] **Figure 22** illustrates the correlation between the resistance signature and MHC-I expression.

[0083] **Figure 23** illustrates the association of metallothionein expression and treated and untreated subjects.

[0084] **Figure 24** illustrates the association of the resistance signature with prognosis.

[0085] **Figure 25** illustrates the resistance signature compared to other single-cell based signatures.

[0086] **Figure 26** illustrates that the ITR signature is predictive of eventual outcome in both mouse and human data.

[0087] **Figure 27** illustrates the association of complete responders and non-complete responders to genes up-regulated post-treatment with immunotherapy.

[0088] **Figure 28** illustrates the association of complete responders and non-complete responders to genes down-regulated post-treatment with immunotherapy.

[0089] **Figure 29** illustrates that malignant cells ITR signatures have higher exclusion signatures and treatment naive malignant cells have higher infiltration signatures.

[0090] **Figure 30** illustrates analysis of CD8 T cells.

[0091] **Figure 31** illustrates analysis of CD8 T cells.

[0092] **Figure 32** illustrates analysis of CD8 T cells.

[0093] **Figure 33** illustrates that the CD8 ITR signature is strongly associated with clonal expansion.

[0094] **Figure 34** illustrates an interaction map of genes in the ITR signature and immune and stromal genes.

[0095] **Figure 35** illustrates the number of interactions between differentially expressed malignant genes and immune and stromal genes.

[0096] **Figure 36** illustrates ITR versus T cell scores in different cancers.

[0097] **Figure 37** illustrates ITR scores in two melanomas.

[0098] **Figure 38** illustrates tSNE analysis of ER+ metastatic breast cancer using single nuclei RNA-seq (snRNA-seq) on fresh and frozen tissue samples.

[0099] **Figure 39** illustrates tSNE analysis of 22 colon cancer samples using scRNA-seq.

[0100] **Figure 40** illustrates that the expanded T cell state is highly correlated with the overall T cell infiltration level of tumors in an independent lung cancer cohort (**Table SII**).

[0101] **Figure 41** illustrates that CDK4/6 inhibitors sensitize melanoma cells.

[0102] **Figure 42** illustrates that CDK4/6 inhibitors induce markers of differentiation, senescence and immunogenicity in melanoma.

[0103] **Figure 43** illustrates that CDK4/6 inhibitors eliminate a resistant subpopulation of melanoma cells.

[0104] **Figure 44. Identification of a T cell exclusion program in malignant cells.** (A) Study overview. 31 tumors from melanoma patients (discovery cohort) were profiled by scRNA-seq (left, tan) and integrated analytically with bulk RNA-Seq data from TCGA (473 melanoma tumors). The discovered program was tested in two validation cohorts of bulk RNA-Seq collected independently (right). (B) Analysis approach to discover malignant cell programs associated with immune cell infiltration or exclusion. (C-D) Distinct profiles of malignant and nonmalignant cells. tSNE plots of single cell profiles (dots) from malignant (C) or nonmalignant (D) cells, shaded by *post-hoc* annotation (**Methods**, D left) or by tumor (C, D right). (E) Exclusion program. Expression (centered and scaled; bar) of the top genes (columns) in the exclusion program across the malignant cells (rows), sorted by untreated or post-treatment tumors (blue/grey bar, left) and clustered within each class. Leftmost bar: cycling and non-cycling cells within each group. Right: The overall expression (**Methods**) of the exclusion program in each cell. See also **Figure 51** and **Tables S1-S3**.

[0105] **Figure 45. Exclusion and resistance programs characterizing individual malignant cells from patients who failed immunotherapy.** (A) Post-treatment program in malignant cells. Left: The Overall expression (**Methods**) of the post-treatment program in malignant cells from post-treatment (blue) and untreated (grey) patients, when obtained in a

cross-validation (CV) procedure and tested on withheld data. Middle line: median; box edges: 25th and 75th percentiles, whiskers: most extreme points that do not exceed $\pm IQR * 1.5$; further outliers are marked individually. Right: Receiver Operating Characteristic (ROC) curve of the performances of different programs in classifying cells as post-treatment or untreated; the CV post-treatment signature was obtained by leave-one (patient) out CV; the first and second Area Under the Curve (AUC) values are for classification of cells and samples, respectively. (B) Significant overlap between the exclusion and post-treatment programs. Venn diagram of the number of genes in each program and in their overlap. P-value: hypergeometric test. (C) Program genes. Expression (centered and scaled, bar) of the top genes (columns) in the post-treatment program across the malignant cells (rows), sorted by untreated or post-treatment tumors (bar, left) and clustered within each class. Leftmost bar: cycling and non-cycling cells within each group. Right: overall expression of the post-treatment program in each cell. (D) Repressed and induced processes. The distribution of overall expression scores of differentially expressed gene sets in malignant cells from post-treatment (blue) and untreated (gray) tumors (formatted as in (A)). (E) The exclusion program is higher in post-treatment malignant cells. The distribution of overall expression scores of the exclusion program in malignant cells from post-treatment (blue) and untreated (gray) tumors. See also **Tables S6 and S9**.

[0106] Figure 46. The resistance program is a coherently regulated module that represses cell-cell interactions. (A) The immune resistance program is higher in uveal vs. cutaneous melanoma. The distribution of overall expression scores of the immune resistance program in cutaneous vs. uveal melanoma tumors from TCGA, scored after filtering tumor microenvironment contributions (**Methods**). (B) Cell-cell interaction genes are repressed in the immune resistance program. The number of genes (y axis, top) in each part of the program encoding proteins that engage in a physical interaction with other cell types and the significance of the corresponding enrichment (y axis, $-\log_{10}(P\text{-value})$, hypergeometric test, bottom). Values above the dashed line are statistically significant. (C-D) Co-regulation of the immune resistance program. (C) The overall expression of the induced (x axis) and repressed (y axis) parts of the immune resistance programs in each malignant cell (top, scRNA-seq data) and in cutaneous melanoma tumors (bottom, TCGA RNA-Seq data, after filtering tumor microenvironment signals). The Pearson correlation coefficient (r) and p-value are marked. (D) Gene-gene Pearson correlation coefficients (bar) between the genes in the

resistance program, across individual malignant cells from the same tumor (top, average coefficient) or across cutaneous melanoma tumors from TCGA skin (bottom, after filtering tumor microenvironment effects). See also **Figure 52**.

[0107] **Figure 47. The resistance program is associated with the cold niche *in situ*.** (A-B) Multiplex imaging relates resistance program genes to hot or cold niches. Malignant cells expressing high or low/moderate protein levels of HLA-A (A) and c-Jun (B) and their proximity to CD3⁺ T cells (blue) or CD3⁺CD8⁺ T cells (cyan) in three representative tumors. (C) Congruence of multiplex protein and scRNA-seq profiles. Left and middle: tSNE plots of co-embedding of cells from the scRNA-seq data and the images of a specific tumor (Mel 112; others shown in **Figure 53**), with cells shaded by clusters (top left), data source (bottom left), and source and cell type (right). Right: Log-odds ratio (bar, **Methods**) assessing for each pair of cell types (rows, columns) if they are assigned to the same cluster significantly more (>0) or less (<0) than expected by chance. See also **Figure 53**.

[0108] **Figure 48. The resistance program is prognostic and predictive in validation cohorts.** (A) The program predicts melanoma patient survival based on bulk RNA-Seq from TCGA (Akbari et al., 2015). Kaplan-Meier (KM) plots stratified by high (top 25%), low (bottom 25%), or intermediate (remainder) expression of the respective program subset. *P*: COX regression p-value; *Pc*: COX regression p-value that tests if the program further enhances the predictive power of a model with inferred T cell infiltration levels as a covariate. (B, C) Resistance signatures distinguish responders and non-responders in mouse models and melanoma patients. The distribution of overall expression of the resistance program in bulk RNA-Seq from (B) a lung cancer mouse model treated with anti-CTLA-4 therapy (Lesterhuis et al., 2015) or (C) biopsies of melanoma patients collected prior to treatment with pembrolizumab (Hugo et al., 2016). Middle line: median; box edges: 25th and 75th percentiles, whiskers: most extreme points that do not exceed $\pm IQR \cdot 1.5$; further outliers are marked individually. (D-F) The program predicts melanoma patient outcomes following pembrolizumab treatment from pre-treatment RNA-Seq in an independent cohort of 112 patients. (D) KM plots of progression-free survival (PFS) for the 104 patients in the cohort with available PFS data, stratified by high (top 25%), low (bottom 25%), or intermediate (remainder) expression of the respective program subset. (E) Predictive value for PFS (-log₁₀(p-value), x axis, COX regression model that accounts for inferred T cell infiltration levels) for the 104 patients in (D). Blue/grey bars: positive/negative correlation between

expression and PFS. Black border: subsets of the resistance program. Dashed line: $p = 0.05$. **(F)** Overall expression of the resistance program (y axis) in the pre-treatment bulk RNA-Seq profiles of patients with intrinsic resistance (Non-CB, $n=49$) or clinical benefit (CB, $n=39$), latter further stratified by response duration (CB < 6mo, $n=5$; 6mo < CB < 1 year, $n=9$; CB > 1 year, $n=25$). Twenty four patients with unknown response or stable disease are not shown here. *PI* and *P2*: one-tailed t-test p-value when comparing the non-CB patients to the CB or to CB > 1yr patients, respectively. AUC for predicting CB > 1yr in all patients with a recorded response ($n = 101$) is denoted. Box plots formatted as in (B). **(G)** Overall expression values of the resistance program (y axis) in the pre-treatment bulk RNA-Seq profiles of patients with complete response (CR, $n = 14$), partial response (PR, $n = 25$), or progressive disease (PD, $n = 49$). *P*: one-tailed t-test p-value comparing CR patients to PR and PD patients. AUC for predicting CR in all patients with a recorded response ($n = 101$). **(H)** Predictive value of different signatures for complete response ($4\log_{10}(\text{t-test p-value})$, x axis) in 101 patients with a recorded response. Blue/grey bars: expression associated with CR/non-CR, respectively. Black border: subsets of the resistance program. Dashed line: $p = 0.05$. AUC values are marked next to the bar for each significant association. See also **Figures 54, 55, 57** and **Table S10**.

[0109] Figure 49. The resistance program can be reversed by CDK4/6 inhibition. (A-C) Impact on breast cancer tumors and cell lines. **(A)** Significance (y axis, $-\log_{10}(\text{p-value})$, Wilcoxon rank sum test) of induction (dark green) or repression (light green) of the program subsets in breast cancer tumors from abemaciclib treated mice compared to vehicle (Goel et al., 2017). **(B)** Overall expression of the program in breast cancer cell lines (M361, MCF and M453) treated with abemaciclib ("abe") or with DMSO vehicle ("con"). Middle line: median; box edges: 25th and 75th percentiles, whiskers: most extreme points that do not exceed $\pm\text{IQR} \times 1.5$; further outliers are marked individually. P-value: paired t-test. **(C)** Expression of 40 program genes (columns; shaded bar) that were most differentially expressed in abemaciclib-treated vs. control breast cancer cells lines (rows). Expression is normalized to each cell line's control. Right: overall expression values of the program for each cell line. **(D-G)** CDK4/6 inhibition reverses the program in melanoma cell lines and induces the SASP. **(D,E)** tSNE plots of 4,024 IGR137 **(D)** and 7,340 UACC257 **(E)** melanoma cells, shaded by (left to right): treatment, clusters, or the expression of a cell cycle signature, resistance program, MITF signature, SASP signature and *DNMT1*. **(F)** Concentration (pg/ml, y axis) of

secreted chemokines in the supernatant of melanoma cells treated for 7 days with abemaciclib (500 nM) or with DMSO control. ** $P < 0.01$, *** $P < 0.001$ *t*-test. **(G)** Senescence associated alpha-galactosidase activity (green) and morphological alterations in melanoma cells treated for 10 days with abemaciclib (500 nM, right) vs. DMSO control (left). See also **Figure 56** and **Table S12**.

[0110] Figure 50. Immune resistance model. Malignant cells that evade the immune system have a unique transcriptional state, which distinguishes between responders and non-responders to immunotherapy. This state is tightly linked to the exclusion of T cells from the tumor, the repression of SASP and cell-cell communication routes, and the inhibition of cytokine secretion. CDK4/6 inhibition can reverse this state in malignant cells.

[0111] Figure 51. Assignment of cells into cell types by scRNA-seq; related to Figure 44. **(A)** Inferred large-scale CNVs distinguish malignant from nonmalignant cells. Shown are the inferred CNVs (amplification, deletion) along the chromosomes (x axis) for cells (y axis) in two representative tumors partitioned as malignant (left) or nonmalignant (right) by CD45 sorting and transcriptional features. **(B-E)** Congruence between different assignment methods. **(B)** Each plot shows the relation between two different scorings, by showing for CD45⁻ cells the distribution of scores (y axis) by one scheme, stratified to two categories by another scheme. CNV: inference of malignant and nonmalignant CD45⁻ cells (as in A, **Methods**); signature based: assignment of CD45⁻ cells as malignant or stroma by scoring the corresponding expression signatures (**Methods**); differential similarity to melanoma: assignment of CD45⁻ cells as malignant or nonmalignant by similarity to bulk melanoma tumors compared to normal tissue. Middle line: median; box edges: 25th and 75th percentiles, whiskers: most extreme points that do not exceed $\pm IQR * 1.5$; further outliers are marked individually. **(C)** Distribution of CNV-R-scores for cells called as malignant or nonmalignant. The CNV-R-score of a cell is the Spearman correlation coefficient (*r*) between the cell's CNV profile and its tumor's inferred CNV profile (**Methods**). **(D)** The distribution of CNV-R-scores across each identified cell subset. Box plots as in (B). **(E)** The CNV-R-score (y axis) vs. the overall CNV signal (x axis, **Methods**) for malignant and nonmalignant cells; Nonmalignant cells with values that exceed the dashed lines were considered unresolved and were omitted from further analyses. **(F-G)** tSNE plots of all nonmalignant cells (dots), shaded by **(F)** overall expression (bar) of well-established cell type markers (**Table S3**), or **(G)** detection of *CD4* or *CD8* (*CD8A* or *CD8B*).

[0112] **Figure 52. Co-variation of the resistance signature genes across single cells within each tumor; related to Figure 46.** Gene-gene Pearson correlation coefficients (bar) between the genes in the resistance program, across individual malignant cells from each specific tumor (as labeled). Genes are sorted in the same order in all heatmaps (and in Figure 46D). The consistent intra-tumor correlation suggests shared regulation.

[0113] **Figure 53. Integrative analysis of scRNA-seq and spatial multiplex protein IHC data; related to Figure 47.** (A-D) Integrative analysis of scRNA-seq and CyCIF multiplex protein data from each of four tumors: (A) Mel79, (B) Mel80, (C) Mel74, and (D) Mel89. Left: tSNE plots of co-embedding of cells from scRNA-seq and images of each tumors, with cells shaded by (from left): clusters, data source, or source and cell type. Right: Log-odds ratio (bar, **Methods**) assessing for each pair of cell types (rows, columns) if they are assigned to the same cluster significantly more (>0) or less (<0) than expected by chance.

[0114] **Figure 54. The immune resistance program predicts survival of TCGA melanoma patients; related to Figure 48.** Kaplan-Meier (KM) plots stratified by high, intermediate or low Over expression of the respective signature in bulk RNA-Seq of TCGA tumors. *P*: COX regression p-value; *P_c*: COX regression p-value that tests if the program further enhances the predictive power of a model with inferred T cell infiltration levels as a covariate.

[0115] **Figure 55. The immune resistance program predicts response to anti-PD-1 therapy in an independent cohort; related to Figure 48.** (A-E) KM plots of progression-free survival (PFS) for the 104 of 112 patients in validation cohort 2 with PFS data, with patients stratified by high, intermediate and low over expression values of the respective signature, after controlling for cell cycle as a confounding factor (**Methods**). *P_c* p-values test if the signature further enhances the predictive power of models with inferred T cell infiltration levels as a covariate. (F) Distribution of overall expression values (y axis) of each signature in the pre-treatment bulk RNA-Seq profiles, showing overall 101 patients with either complete response (CR, *n* = 14), partial response/stable disease (PR/SD, *n* = 38), or progressive disease (PD, *n* = 49). *P* is the one-sided t-test p-value obtained when comparing CR patients vs. PR, SD and PD patients. AUC is also marked on top. Middle line: median; box edges: 25th and 75th percentiles, whiskers: most extreme points that do not exceed $\pm IQR * 1.5$; further outliers are marked individually.

[0116] **Figure 56. Relationship between the resistance program and cell cycle; related to Figure 49.** (A, B) Higher expression of the resistance program in cycling cells. (A) Distribution of overall expression values of the resistance program (y axis) in cycling (grey) and non-cycling (blue) cells from either post-treatment or untreated tumors (x axis). Solid line: mean of the respective distribution; dashed line: mean across *all* malignant cells. (B) Expression of genes from the resistance program (rows) that are also differentially expressed in cycling vs. non-cycling malignant cells. Cells (columns) are sorted by untreated and post-treatment tumors and clustered within each set (bar on top); the cells' cycling status in each category is marked by the bar on top. (C) Abemaciclib represses the resistance program in breast cancer cell lines. The relative expression of all genes in the resistance program (rows) in abemaciclib-treated and control breast cancer cells lines (columns), based on the data in (Goel et al., 2017). Expression levels are relative to the basal expression level in each cell line. Bottom: overall expression (y axis) of the resistance program in each cell line (x axis).

[0117] **Figure 57. Pan-cancer analysis of the resistance program; related to Figure 48.** (A-B) Overall expression of the resistance program (x axis) in 9,559 tumors from 33 cancer types (y axis) from TCGA. In (B) a regression-based approach controls for tumor microenvironment-related signals (**Methods**). Middle line: median; box edges: 25th and 75th percentiles, whiskers: most extreme points that do not exceed $\pm IQR * 1.5$; further outliers are marked individually.

DETAILED DESCRIPTION OF THE EXAMPLE EMBODIMENTS

General Definitions

[0118] Unless defined otherwise, technical and scientific terms used herein have the same meaning as commonly understood by one of ordinary skill in the art to which this disclosure pertains. Definitions of common terms and techniques in molecular biology may be found in *Molecular Cloning: A Laboratory Manual*, 2nd edition (1989) (Sambrook, Fritsch, and Maniatis); *Molecular Cloning: A Laboratory Manual*, 4th edition (2012) (Green and Sambrook); *Current Protocols in Molecular Biology* (1987) (F.M. Ausubel et al. eds.); the series *Methods in Enzymology* (Academic Press, Inc.); *PCR 2: A Practical Approach* (1995) (M.J. MacPherson, B.D. Hames, and G.R. Taylor eds.); *Antibodies, A Laboratory Manual* (1988) (Harlow and Lane, eds.); *Antibodies A Laboratory Manual*, 2nd edition 2013 (E.A.

Greenfield ed.); Animal Cell Culture (1987) (R.I. Freshney, ed.); Benjamin Lewin, Genes IX, published by Jones and Bartlet, 2008 (ISBN 0763752223); Kendrew *et al.* (eds.), The Encyclopedia of Molecular Biology, published by Blackwell Science Ltd., 1994 (ISBN 0632021829); Robert A. Meyers (ed.), Molecular Biology and Biotechnology: a Comprehensive Desk Reference, published by VCH Publishers, Inc., 1995 (ISBN 9780471 185710); Singleton *et al.*, Dictionary of Microbiology and Molecular Biology 2nd ed., J. Wiley & Sons (New York, N.Y. 1994), March, Advanced Organic Chemistry Reactions, Mechanisms and Structure 4th ed., John Wiley & Sons (New York, N.Y. 1992); and Marten H. Hofker and Jan van Deursen, Transgenic Mouse Methods and Protocols, 2nd edition (2011) .

[0119] As used herein, the singular forms "a", "an", and "the" include both singular and plural referents unless the context clearly dictates otherwise.

[0120] The term "optional" or "optionally" means that the subsequent described event, circumstance or substituent may or may not occur, and that the description includes instances where the event or circumstance occurs and instances where it does not.

[0121] The recitation of numerical ranges by endpoints includes all numbers and fractions subsumed within the respective ranges, as well as the recited endpoints.

[0122] The terms "about" or "approximately" as used herein when referring to a measurable value such as a parameter, an amount, a temporal duration, and the like, are meant to encompass variations of and from the specified value, such as variations of +/-10% or less, +/-5% or less, +/-1% or less, and +/-0.1% or less of and from the specified value, insofar such variations are appropriate to perform in the disclosed invention. It is to be understood that the value to which the modifier "about" or "approximately" refers is itself also specifically, and preferably, disclosed.

[0123] Reference throughout this specification to "one embodiment", "an embodiment," "an example embodiment," means that a particular feature, structure or characteristic described in connection with the embodiment is included in at least one embodiment of the present invention. Thus, appearances of the phrases "in one embodiment," "in an embodiment," or "an example embodiment" in various places throughout this specification are not necessarily all referring to the same embodiment, but may. Furthermore, the particular features, structures or characteristics may be combined in any suitable manner, as would be apparent to a person skilled in the art from this disclosure, in one or more embodiments. Furthermore, while some embodiments described herein include some but not other features

included in other embodiments, combinations of features of different embodiments are meant to be within the scope of the invention. For example, in the appended claims, any of the claimed embodiments can be used in any combination.

[0124] All publications, published patent documents, and patent applications cited in this application are indicative of the level of skill in the art(s) to which the application pertains. All publications, published patent documents, and patent applications cited herein are hereby incorporated by reference to the same extent as though each individual publication, published patent document, or patent application was specifically and individually indicated as being incorporated by reference.

Overview

[0125] Embodiments disclosed herein provide methods and compositions for detecting and modulating an immunotherapy resistance gene signature in cancer. Embodiments disclosed herein also provide for diagnosing, prognosing, monitoring and treating tumors based on detection of an immunotherapy resistance gene signature.

[0126] As used herein, the immunotherapy resistance signature is referred to as "ITR", "immunotherapy resistance signature", "ICR", "immune checkpoint inhibitor resistance", "mICR", "malignant immune checkpoint inhibitor resistance", "PIT", "post-immunotherapy", "oncogenic-ICR", "unified-ICR", "uICR", "uICR-up", "uICR-down", "refined uICR", "immune resistant", "refined immune resistant", "post treatment", "exclusion-up", or "exclusion-down". All of these terms may be used in reference to a gene signature in malignant cells from a subject that is resistant to immune checkpoint inhibitors (ICI). In regards to the exclusion signatures, these signatures refer to signatures in malignant cells that correlate to immune cell exclusion. In other words, exclusion-up refers to genes that are upregulated in malignant cells and that are correlated with exclusion, while exclusion-down refer to genes downregulated in malignant cells that are correlated with exclusion. In certain embodiments, exclusion-down refers to genes upregulated when there is immune cell infiltration and thus can be referred to as the infiltration signature. In regards to "oncogenic ICR", "mICR", "malignant immune checkpoint inhibitor resistance", "Post-treatment", "PIT", or "post-immunotherapy", these terms all refer to genes differentially expressed in malignant cells after immunotherapy. "Immune resistance", "unified-ICR" or "uICR" refers to all genes in the exclusion signature and post treatment signature. The "refined uICR" and "refined immune resistant" are shortened lists from the immune resistance signature that include the best performing genes from the exclusion and post treatment signatures for

predicting immunotherapy sensitivity. In regards to CD8 T cells "tICR" refers to T cell immune checkpoint inhibitor resistance signature.

[0127] As used herein the term "cancer-specific survival" refers to the percentage of patients with a specific type and stage of cancer who have not died from their cancer during a certain period of time after diagnosis. The period of time may be 1 year, 2 years, 5 years, etc., with 5 years being the time period most often used. Cancer-specific survival is also called disease-specific survival. In most cases, cancer-specific survival is based on causes of death listed in medical records.

[0128] As used herein the term "relative survival" refers to a method used to estimate cancer-specific survival that does not use information about the cause of death. It is the percentage of cancer patients who have survived for a certain period of time after diagnosis compared to people who do not have cancer.

[0129] As used herein the term "overall survival" refers to the percentage of people with a specific type and stage of cancer who have not died from any cause during a certain period of time after diagnosis.

[0130] As used herein the term "disease-free survival" refers to the percentage of patients who have no signs of cancer during a certain period of time after treatment. Other names for this statistic are recurrence-free or progression-free survival.

[0131] As used herein a "signature" may encompass any gene or genes, protein or proteins, or epigenetic element(s) whose expression profile or whose occurrence is associated with a specific cell type, subtype, or cell state of a specific cell type or subtype within a population of cells (e.g., immune evading tumor cells, immunotherapy resistant tumor cells, tumor infiltrating lymphocytes, macrophages). In certain embodiments, the expression of the immunotherapy resistant, T cell signature and/or macrophage signature is dependent on epigenetic modification of the genes or regulatory elements associated with the genes. Thus, in certain embodiments, use of signature genes includes epigenetic modifications that may be detected or modulated. For ease of discussion, when discussing gene expression, any of gene or genes, protein or proteins, or epigenetic element(s) may be substituted. As used herein, the terms "signature", "expression profile", or "expression program" may be used interchangeably. It is to be understood that also when referring to proteins (e.g. differentially expressed proteins), such may fall within the definition of "gene" signature. Levels of expression or activity may be compared between different cells in order to characterize or identify for instance signatures specific for cell (sub)populations. Increased or decreased

expression or activity or prevalence of signature genes may be compared between different cells in order to characterize or identify for instance specific cell (sub)populations. The detection of a signature in single cells may be used to identify and quantitate for instance specific cell (sub)populations. A signature may include a gene or genes, protein or proteins, or epigenetic element(s) whose expression or occurrence is specific to a cell (sub)population, such that expression or occurrence is exclusive to the cell (sub)population. A gene signature as used herein, may thus refer to any set of up- and/or down-regulated genes that are representative of a cell type or subtype. A gene signature as used herein, may also refer to any set of up- and/or down-regulated genes between different cells or cell (sub)populations derived from a gene-expression profile. For example, a gene signature may comprise a list of genes differentially expressed in a distinction of interest.

[0132] The signature as defined herein (being it a gene signature, protein signature or other genetic or epigenetic signature) can be used to indicate the presence of a cell type, a subtype of the cell type, the state of the microenvironment of a population of cells, a particular cell type population or subpopulation, and/or the overall status of the entire cell (sub)population. Furthermore, the signature may be indicative of cells within a population of cells *in vivo*. The signature may also be used to suggest for instance particular therapies, or to follow up treatment, or to suggest ways to modulate immune systems. The signatures of the present invention may be discovered by analysis of expression profiles of single-cells within a population of cells from isolated samples (e.g. tumor samples), thus allowing the discovery of novel cell subtypes or cell states that were previously invisible or unrecognized. The presence of subtypes or cell states may be determined by subtype specific or cell state specific signatures. The presence of these specific cell (sub)types or cell states may be determined by applying the signature genes to bulk sequencing data in a sample. Not being bound by a theory the signatures of the present invention may be microenvironment specific, such as their expression in a particular spatio-temporal context. Not being bound by a theory, signatures as discussed herein are specific to a particular pathological context. Not being bound by a theory, a combination of cell subtypes having a particular signature may indicate an outcome. Not being bound by a theory, the signatures can be used to deconvolute the network of cells present in a particular pathological condition. Not being bound by a theory the presence of specific cells and cell subtypes are indicative of a particular response to treatment, such as including increased or decreased susceptibility to treatment. The signature may indicate the presence of one particular cell type. In one embodiment, the novel

signatures are used to detect multiple cell states or hierarchies that occur in subpopulations of cells that are linked to particular pathological condition, or linked to a particular outcome or progression of the disease, or linked to a particular response to treatment of the disease (e.g. resistance to immunotherapy).

[0133] The signature according to certain embodiments of the present invention may comprise or consist of one or more genes, proteins and/or epigenetic elements, such as for instance 1, 2, 3, 4, 5, 6, 7, 8, 9, 10 or more. In certain embodiments, the signature may comprise or consist of two or more genes, proteins and/or epigenetic elements, such as for instance 2, 3, 4, 5, 6, 7, 8, 9, 10 or more. In certain embodiments, the signature may comprise or consist of three or more genes, proteins and/or epigenetic elements, such as for instance 3, 4, 5, 6, 7, 8, 9, 10 or more. In certain embodiments, the signature may comprise or consist of four or more genes, proteins and/or epigenetic elements, such as for instance 4, 5, 6, 7, 8, 9, 10 or more. In certain embodiments, the signature may comprise or consist of five or more genes, proteins and/or epigenetic elements, such as for instance 5, 6, 7, 8, 9, 10 or more. In certain embodiments, the signature may comprise or consist of six or more genes, proteins and/or epigenetic elements, such as for instance 6, 7, 8, 9, 10 or more. In certain embodiments, the signature may comprise or consist of seven or more genes, proteins and/or epigenetic elements, such as for instance 7, 8, 9, 10 or more. In certain embodiments, the signature may comprise or consist of eight or more genes, proteins and/or epigenetic elements, such as for instance 8, 9, 10 or more. In certain embodiments, the signature may comprise or consist of nine or more genes, proteins and/or epigenetic elements, such as for instance 9, 10 or more. In certain embodiments, the signature may comprise or consist of ten or more genes, proteins and/or epigenetic elements, such as for instance 10, 11, 12, 13, 14, 15, or more. It is to be understood that a signature according to the invention may for instance also include genes or proteins as well as epigenetic elements combined.

[0134] In certain embodiments, a signature is characterized as being specific for a particular cell or cell (sub)population if it is upregulated or only present, detected or detectable in that particular cell or cell (sub)population, or alternatively is downregulated or only absent, or undetectable in that particular cell or cell (sub)population. In this context, a signature consists of one or more differentially expressed genes/proteins or differential epigenetic elements when comparing different cells or cell (sub)populations, including comparing different immune cells or immune cell (sub)populations (e.g., T cells), as well as comparing immune cells or immune cell (sub)populations with other immune cells or

immune cell (sub)populations. It is to be understood that "differentially expressed" genes/proteins include genes/proteins which are up- or down-regulated as well as genes/proteins which are turned on or off. When referring to up- or down-regulation, in certain embodiments, such up- or down-regulation is preferably at least two-fold, such as two-fold, three-fold, four-fold, five-fold, or more, such as for instance at least ten-fold, at least 20-fold, at least 30-fold, at least 40-fold, at least 50-fold, or more. Alternatively, or in addition, differential expression may be determined based on common statistical tests, as is known in the art.

[0135] As discussed herein, differentially expressed genes/proteins, or differential epigenetic elements may be differentially expressed on a single cell level, or may be differentially expressed on a cell population level. Preferably, the differentially expressed genes/ proteins or epigenetic elements as discussed herein, such as constituting the gene signatures as discussed herein, when as to the cell population level, refer to genes that are differentially expressed in all or substantially all cells of the population (such as at least 80%, preferably at least 90%, such as at least 95% of the individual cells). This allows one to define a particular subpopulation of cells. As referred to herein, a "subpopulation" of cells preferably refers to a particular subset of cells of a particular cell type (e.g., resistant) which can be distinguished or are uniquely identifiable and set apart from other cells of this cell type. The cell subpopulation may be phenotypically characterized, and is preferably characterized by the signature as discussed herein. A cell (sub)population as referred to herein may constitute of a (sub)population of cells of a particular cell type characterized by a specific cell state.

[0136] When referring to induction, or alternatively reducing or suppression of a particular signature, preferable is meant induction or alternatively reduction or suppression (or upregulation or downregulation) of at least one gene/protein and/or epigenetic element of the signature, such as for instance at least two, at least three, at least four, at least five, at least six, or all genes/proteins and/or epigenetic elements of the signature.

[0137] Various aspects and embodiments of the invention may involve analyzing gene signatures, protein signature, and/or other genetic or epigenetic signature based on single cell analyses (e.g. single cell RNA sequencing) or alternatively based on cell population analyses, as is defined herein elsewhere.

[0138] The invention further relates to various uses of the gene signatures, protein signature, and/or other genetic or epigenetic signature as defined herein, as well as various

uses of the immune cells or immune cell (sub)populations as defined herein. Particular advantageous uses include methods for identifying agents capable of inducing or suppressing particular immune cell (sub)populations based on the gene signatures, protein signature, and/or other genetic or epigenetic signature as defined herein. The invention further relates to agents capable of inducing or suppressing particular immune cell (sub)populations based on the gene signatures, protein signature, and/or other genetic or epigenetic signature as defined herein, as well as their use for modulating, such as inducing or repressing, a particular gene signature, protein signature, and/or other genetic or epigenetic signature. In one embodiment, genes in one population of cells may be activated or suppressed in order to affect the cells of another population. In related aspects, modulating, such as inducing or repressing, a particular gene signature, protein signature, and/or other genetic or epigenetic signature may modify overall immune composition, such as immune cell composition, such as immune cell subpopulation composition or distribution, or functionality.

[0139] The signature genes of the present invention were discovered by analysis of expression profiles of single-cells within a population of tumor cells, thus allowing the discovery of novel cell subtypes that were previously invisible in a population of cells within a tumor. The presence of subtypes may be determined by subtype specific signature genes. The presence of these specific cell types may be determined by applying the signature genes to bulk sequencing data in a patient. Not being bound by a theory, many cells that make up a microenvironment, whereby the cells communicate and affect each other in specific ways. As such, specific cell types within this microenvironment may express signature genes specific for this microenvironment. Not being bound by a theory the signature genes of the present invention may be microenvironment specific, such as their expression in a tumor. The signature genes may indicate the presence of one particular cell type. In one embodiment, the expression may indicate the presence of immunotherapy resistant cell types. Not being bound by a theory, a combination of cell subtypes in a subject may indicate an outcome (e.g., resistant cells, cytotoxic T cells, Tregs).

[0140] In certain embodiments, the present invention provides for gene signature screening. The concept of signature screening was introduced by Stegmaier et al. (Gene expression-based high-throughput screening (GE-HTS) and application to leukemia differentiation. *Nature Genet.* 36, 257-263 (2004)), who realized that if a gene-expression signature was the proxy for a phenotype of interest, it could be used to find small molecules that effect that phenotype without knowledge of a validated drug target. The signature of the

present may be used to screen for drugs that reduce the signature in cancer cells or cell lines having a resistant signature as described herein. The signature may be used for GE-HTS. In certain embodiments, pharmacological screens may be used to identify drugs that are selectively toxic to cancer cells having an immunotherapy resistant signature. In certain embodiments, drugs selectively toxic to cancer cells having an immunotherapy resistant signature are used for treatment of a cancer patient. In certain embodiments, cells having an immunotherapy resistant signature as described herein are treated with a plurality of drug candidates not toxic to non-tumor cells and toxicity is assayed.

[0141] The Connectivity Map (cmap) is a collection of genome-wide transcriptional expression data from cultured human cells treated with bioactive small molecules and simple pattern-matching algorithms that together enable the discovery of functional connections between drugs, genes and diseases through the transitory feature of common gene-expression changes (see, Lamb et al., *The Connectivity Map: Using Gene-Expression Signatures to Connect Small Molecules, Genes, and Disease*. *Science* 29 Sep 2006: Vol. 313, Issue 5795, pp. 1929-1935, DOI: 10.1126/science.1132939; and Lamb, J., *The Connectivity Map: a new tool for biomedical research*. *Nature Reviews Cancer* January 2007: Vol. 7, pp. 54-60). Cmap can be used to screen for a signature in silico.

[0142] In one embodiment, the signature genes may be detected by immunofluorescence, immunohistochemistry, fluorescence activated cell sorting (FACS), mass cytometry (CyTOF), Drop-seq, RNA-seq, scRNA-seq, InDrop, single cell qPCR, MERFISH (multiplex (in situ) RNA FISH) and/or by in situ hybridization. Other methods including absorbance assays and colorimetric assays are known in the art and may be used herein.

[0143] All gene name symbols refer to the gene as commonly known in the art. The examples described herein refer to the human gene names and it is to be understood that the present invention also encompasses genes from other organisms (e.g., mouse genes). Gene symbols may be those referred to by the HUGO Gene Nomenclature Committee (HGNC) or National Center for Biotechnology Information (NCBI). Any reference to the gene symbol is a reference made to the entire gene or variants of the gene. The signature as described herein may encompass any of the genes described herein. In certain embodiments, the gene signature includes surface expressed and secreted proteins. Not being bound by a theory, surface proteins may be targeted for detection and isolation of cell types, or may be targeted therapeutically to modulate an immune response.

[0144] As used herein, "modulating" or "to modulate" generally means either reducing or inhibiting the expression or activity of, or alternatively increasing the expression or activity of a target gene. In particular, "modulating" or "to modulate" can mean either reducing or inhibiting the activity of, or alternatively increasing a (relevant or intended) biological activity of, a target or antigen as measured using a suitable *in vitro*, cellular or *in vivo* assay (which will usually depend on the target involved), by at least 5%, at least 10%, at least 25%, at least 50%, at least 60%, at least 70%, at least 80%, at least 90%, or more, compared to activity of the target in the same assay under the same conditions but without the presence of an agent. An "increase" or "decrease" refers to a statistically significant increase or decrease respectively. For the avoidance of doubt, an increase or decrease will be at least 10% relative to a reference, such as at least 10%, at least 20%, at least 30%, at least 40%, at least 50%, at least 60%, at least 70%, at least 80%, at least 90%, at least 95%, at least 97%, at least 98%, or more, up to and including at least 100% or more, in the case of an increase, for example, at least 2-fold, at least 3-fold, at least 4-fold, at least 5-fold, at least 6-fold, at least 7-fold, at least 8-fold, at least 9-fold, at least 10-fold, at least 50-fold, at least 100-fold, or more. "Modulating" can also involve effecting a change (which can either be an increase or a decrease) in affinity, avidity, specificity and/or selectivity of a target or antigen, such as a receptor and ligand. "Modulating" can also mean effecting a change with respect to one or more biological or physiological mechanisms, effects, responses, functions, pathways or activities in which the target or antigen (or in which its substrate(s), ligand(s) or pathway(s) are involved, such as its signaling pathway or metabolic pathway and their associated biological or physiological effects) is involved. Again, as will be clear to the skilled person, such an action as an agonist or an antagonist can be determined in any suitable manner and/or using any suitable assay known or described herein (e.g., *in vitro* or cellular assay), depending on the target or antigen involved.

[0145] Modulating can, for example, also involve allosteric modulation of the target and/or reducing or inhibiting the binding of the target to one of its substrates or ligands and/or competing with a natural ligand, substrate for binding to the target. Modulating can also involve activating the target or the mechanism or pathway in which it is involved. Modulating can for example also involve effecting a change in respect of the folding or conformation of the target, or in respect of the ability of the target to fold, to change its conformation (for example, upon binding of a ligand), to associate with other (sub)units, or to

disassociate. Modulating can for example also involve effecting a change in the ability of the target to signal, phosphorylate, dephosphorylate, and the like.

Modulating Agents

[0146] As used herein, an "agent" can refer to a protein-binding agent that permits modulation of activity of proteins or disrupts interactions of proteins and other biomolecules, such as but not limited to disrupting protein-protein interaction, ligand-receptor interaction, or protein-nucleic acid interaction. Agents can also refer to DNA targeting or RNA targeting agents. Agents may include a fragment, derivative and analog of an active agent. The terms "fragment," "derivative" and "analog" when referring to polypeptides as used herein refers to polypeptides which either retain substantially the same biological function or activity as such polypeptides. An analog includes a proprotein which can be activated by cleavage of the proprotein portion to produce an active mature polypeptide. Such agents include, but are not limited to, antibodies ("antibodies" includes antigen-binding portions of antibodies such as epitope- or antigen-binding peptides, paratopes, functional CDRs; recombinant antibodies; chimeric antibodies; humanized antibodies; nanobodies; tribodies; midibodies; or antigen-binding derivatives, analogs, variants, portions, or fragments thereof), protein-binding agents, nucleic acid molecules, small molecules, recombinant protein, peptides, aptamers, avimers and protein-binding derivatives, portions or fragments thereof. An "agent" as used herein, may also refer to an agent that inhibits expression of a gene, such as but not limited to a DNA targeting agent (e.g., CRISPR system, TALE, Zinc finger protein) or RNA targeting agent (e.g., inhibitory nucleic acid molecules such as RNAi, miRNA, ribozyme).

[0147] The agents of the present invention may be modified, such that they acquire advantageous properties for therapeutic use (e.g., stability and specificity), but maintain their biological activity.

[0148] It is well known that the properties of certain proteins can be modulated by attachment of polyethylene glycol (PEG) polymers, which increases the hydrodynamic volume of the protein and thereby slows its clearance by kidney filtration. (See, e.g., Clark et al., J. Biol. Chem. 271: 21969-21977 (1996)). Therefore, it is envisioned that certain agents can be PEGylated (e.g., on peptide residues) to provide enhanced therapeutic benefits such as, for example, increased efficacy by extending half-life *in vivo*. In certain embodiments, PEGylation of the agents may be used to extend the serum half-life of the agents and allow for particular agents to be capable of crossing the blood-brain barrier.

[0149] In regards to peptide PEGylation methods, reference is made to Lu et al., *Int. J. Pept. Protein Res.* 43: 127-38 (1994); Lu et al., *Pept. Res.* 6: 140-6 (1993); Felix et al., *Int. J. Pept. Protein Res.* 46: 253-64 (1995); Gaertner et al., *Bioconjug. Chem.* 7: 38-44 (1996); Tsutsumi et al., *Thromb. Haemost.* 77: 168-73 (1997); Francis et al., *Int. J. Hematol.* 68: 1-18 (1998); Roberts et al., *J. Pharm. Sci.* 87: 1440-45 (1998); and Tan et al., *Protein Expr. Purif.* 12: 45-52 (1998). Polyethylene glycol or PEG is meant to encompass any of the forms of PEG that have been used to derivatize other proteins, including, but not limited to, mono-(Cl-10) alkoxy or aryloxy-polyethylene glycol. Suitable PEG moieties include, for example, 40 kDa methoxy poly(ethylene glycol) propionaldehyde (Dow, Midland, Mich.); 60 kDa methoxy poly(ethylene glycol) propionaldehyde (Dow, Midland, Mich.); 40 kDa methoxy poly(ethylene glycol) maleimido-propionamide (Dow, Midland, Mich.); 31 kDa alpha-methyl-w-(3-oxopropoxy), polyoxyethylene (NOF Corporation, Tokyo); mPEG2-NHS-40k (Nektar); mPEG2-MAL-40k (Nektar), SUNBRIGHT GL2-400MA ((PEG)240kDa) (NOF Corporation, Tokyo), SUNBRIGHT ME-200MA (PEG20kDa) (NOF Corporation, Tokyo). The PEG groups are generally attached to the peptide (e.g., neuromedin U receptor agonists or antagonists) via acylation or alkylation through a reactive group on the PEG moiety (for example, a maleimide, an aldehyde, amino, thiol, or ester group) to a reactive group on the peptide (for example, an aldehyde, amino, thiol, a maleimide, or ester group).

[0150] The PEG molecule(s) may be covalently attached to any Lys, Cys, or K(CO(CH₂)₂SH) residues at any position in a peptide. In certain embodiments, the neuromedin U receptor agonists described herein can be PEGylated directly to any amino acid at the N-terminus by way of the N-terminal amino group. A "linker arm" may be added to a peptide to facilitate PEGylation. PEGylation at the thiol side-chain of cysteine has been widely reported (see, e.g., Caliceti & Veronese, *Adv. Drug Deliv. Rev.* 55: 1261-77 (2003)). If there is no cysteine residue in the peptide, a cysteine residue can be introduced through substitution or by adding a cysteine to the N-terminal amino acid.

[0151] Substitutions of amino acids may be used to modify an agent of the present invention. The phrase "substitution of amino acids" as used herein encompasses substitution of amino acids that are the result of both conservative and non-conservative substitutions. Conservative substitutions are the replacement of an amino acid residue by another similar residue in a polypeptide. Typical but not limiting conservative substitutions are the replacements, for one another, among the aliphatic amino acids Ala, Val, Leu and Ile; interchange of Ser and Thr containing hydroxy residues, interchange of the acidic residues

Asp and Glu, interchange between the amide-containing residues Asn and Gin, interchange of the basic residues Lys and Arg, interchange of the aromatic residues Phe and Tyr, and interchange of the small-sized amino acids Ala, Ser, Thr, Met, and Gly. Non-conservative substitutions are the replacement, in a polypeptide, of an amino acid residue by another residue which is not biologically similar. For example, the replacement of an amino acid residue with another residue that has a substantially different charge, a substantially different hydrophobicity, or a substantially different spatial configuration.

[0152] The term "antibody" is used interchangeably with the term "immunoglobulin" herein, and includes intact antibodies, fragments of antibodies, e.g., Fab, F(ab')₂ fragments, and intact antibodies and fragments that have been mutated either in their constant and/or variable region (e.g., mutations to produce chimeric, partially humanized, or fully humanized antibodies, as well as to produce antibodies with a desired trait, e.g., enhanced binding and/or reduced FcR binding). The term "fragment" refers to a part or portion of an antibody or antibody chain comprising fewer amino acid residues than an intact or complete antibody or antibody chain. Fragments can be obtained via chemical or enzymatic treatment of an intact or complete antibody or antibody chain. Fragments can also be obtained by recombinant means. Exemplary fragments include Fab, Fab', F(ab')₂, Fabc, Fd, dAb, VHH and scFv and/or Fv fragments.

[0153] As used herein, a preparation of antibody protein having less than about 50% of non-antibody protein (also referred to herein as a "contaminating protein"), or of chemical precursors, is considered to be "substantially free." 40%, 30%, 20%, 10% and more preferably 5% (by dry weight), of non-antibody protein, or of chemical precursors is considered to be substantially free. When the antibody protein or biologically active portion thereof is recombinantly produced, it is also preferably substantially free of culture medium, i.e., culture medium represents less than about 30%, preferably less than about 20%, more preferably less than about 10%, and most preferably less than about 5% of the volume or mass of the protein preparation.

[0154] The term "antigen-binding fragment" refers to a polypeptide fragment of an immunoglobulin or antibody that binds antigen or competes with intact antibody (i.e., with the intact antibody from which they were derived) for antigen binding (i.e., specific binding). As such these antibodies or fragments thereof are included in the scope of the invention, provided that the antibody or fragment binds specifically to a target molecule.

[0155] It is intended that the term "antibody" encompass any Ig class or any Ig subclass (e.g. the IgG1, IgG2, IgG3, and IgG4 subclasses of IgG) obtained from any source (e.g., humans and non-human primates, and in rodents, lagomorphs, caprines, bovines, equines, ovines, etc.).

[0156] The term "Ig class" or "immunoglobulin class", as used herein, refers to the five classes of immunoglobulin that have been identified in humans and higher mammals, IgG, IgM, IgA, IgD, and IgE. The term "Ig subclass" refers to the two subclasses of IgM (H and L), three subclasses of IgA (IgA1, IgA2, and secretory IgA), and four subclasses of IgG (IgG1, IgG2, IgG3, and IgG4) that have been identified in humans and higher mammals. The antibodies can exist in monomeric or polymeric form; for example, IgM antibodies exist in pentameric form, and IgA antibodies exist in monomeric, dimeric or multimeric form.

[0157] The term "IgG subclass" refers to the four subclasses of immunoglobulin class IgG - IgG1, IgG2, IgG3, and IgG4 that have been identified in humans and higher mammals by the heavy chains of the immunoglobulins, $\text{VI} - \gamma_4$, respectively. The term "single-chain immunoglobulin" or "single-chain antibody" (used interchangeably herein) refers to a protein having a two-polypeptide chain structure consisting of a heavy and a light chain, said chains being stabilized, for example, by interchain peptide linkers, which has the ability to specifically bind antigen. The term "domain" refers to a globular region of a heavy or light chain polypeptide comprising peptide loops (e.g., comprising 3 to 4 peptide loops) stabilized, for example, by β pleated sheet and/or intrachain disulfide bond. Domains are further referred to herein as "constant" or "variable", based on the relative lack of sequence variation within the domains of various class members in the case of a "constant" domain, or the significant variation within the domains of various class members in the case of a "variable" domain. Antibody or polypeptide "domains" are often referred to interchangeably in the art as antibody or polypeptide "regions". The "constant" domains of an antibody light chain are referred to interchangeably as "light chain constant regions", "light chain constant domains", "CL" regions or "CL" domains. The "constant" domains of an antibody heavy chain are referred to interchangeably as "heavy chain constant regions", "heavy chain constant domains", "CH" regions or "CH" domains). The "variable" domains of an antibody light chain are referred to interchangeably as "light chain variable regions", "light chain variable domains", "VL" regions or "VL" domains). The "variable" domains of an antibody heavy chain are referred to interchangeably as "heavy chain constant regions", "heavy chain constant domains", "VH" regions or "VH" domains).

[0158] The term "region" can also refer to a part or portion of an antibody chain or antibody chain domain (e.g., a part or portion of a heavy or light chain or a part or portion of a constant or variable domain, as defined herein), as well as more discrete parts or portions of said chains or domains. For example, light and heavy chains or light and heavy chain variable domains include "complementarity determining regions" or "CDRs" interspersed among "framework regions" or "FRs", as defined herein.

[0159] The term "conformation" refers to the tertiary structure of a protein or polypeptide (e.g., an antibody, antibody chain, domain or region thereof). For example, the phrase "light (or heavy) chain conformation" refers to the tertiary structure of a light (or heavy) chain variable region, and the phrase "antibody conformation" or "antibody fragment conformation" refers to the tertiary structure of an antibody or fragment thereof.

[0160] The term "antibody-like protein scaffolds" or "engineered protein scaffolds" broadly encompasses proteinaceous non-immunoglobulin specific-binding agents, typically obtained by combinatorial engineering (such as site-directed random mutagenesis in combination with phage display or other molecular selection techniques). Usually, such scaffolds are derived from robust and small soluble monomeric proteins (such as Kunitz inhibitors or lipocalins) or from a stably folded extra-membrane domain of a cell surface receptor (such as protein A, fibronectin or the ankyrin repeat).

[0161] Such scaffolds have been extensively reviewed in Binz et al. (Engineering novel binding proteins from nonimmunoglobulin domains. *Nat Biotechnol* 2005, 23:1257-1268), Gebauer and Skerra (Engineered protein scaffolds as next-generation antibody therapeutics. *Curr Opin Chem Biol.* 2009, 13:245-55), Gill and Damle (Biopharmaceutical drug discovery using novel protein scaffolds. *Curr Opin Biotechnol* 2006, 17:653-658), Skerra (Engineered protein scaffolds for molecular recognition. *J Mol Recognit* 2000, 13:167-187), and Skerra (Alternative non-antibody scaffolds for molecular recognition. *Curr Opin Biotechnol* 2007, 18:295-304), and include without limitation affibodies, based on the Z-domain of staphylococcal protein A, a three-helix bundle of 58 residues providing an interface on two of its alpha-helices (Nygren, Alternative binding proteins: Affibody binding proteins developed from a small three-helix bundle scaffold. *FEBS J* 2008, 275:2668-2676); engineered Kunitz domains based on a small (ca. 58 residues) and robust, disulphide-crosslinked serine protease inhibitor, typically of human origin (e.g. LACI-D1), which can be engineered for different protease specificities (Nixon and Wood, Engineered protein inhibitors of proteases. *Curr Opin Drug Discov Dev* 2006, 9:261-268); monobodies or adnectins based on the 10th

extracellular domain of human fibronectin III (10Fn3), which adopts an Ig-like beta-sandwich fold (94 residues) with 2-3 exposed loops, but lacks the central disulphide bridge (Koide and Koide, *Monobodies: antibody mimics based on the scaffold of the fibronectin type III domain. Methods Mol Biol* 2007, 352:95-109); anticalins derived from the lipocalins, a diverse family of eight-stranded beta-barrel proteins (ca. 180 residues) that naturally form binding sites for small ligands by means of four structurally variable loops at the open end, which are abundant in humans, insects, and many other organisms (Skerra, *Alternative binding proteins: Anticalins—harnessing the structural plasticity of the lipocalin ligand pocket to engineer novel binding activities. FEBS J* 2008, 275:2677-2683); DARPins, designed ankyrin repeat domains (166 residues), which provide a rigid interface arising from typically three repeated beta-turns (Stumpp et al., *DARPins: a new generation of protein therapeutics. Drug Discov Today* 2008, 13:695-701); avimers (multimerized LDLR-A module) (Silverman et al., *Multivalent avimer proteins evolved by exon shuffling of a family of human receptor domains. Nat Biotechnol* 2005, 23:1556-1561); and cysteine-rich knottin peptides (Kolmar, *Alternative binding proteins: biological activity and therapeutic potential of cysteine-knot miniproteins. FEBS J* 2008, 275:2684-2690).

[0162] "Specific binding" of an antibody means that the antibody exhibits appreciable affinity for a particular antigen or epitope and, generally, does not exhibit significant cross reactivity. "Appreciable" binding includes binding with an affinity of at least 25 μM . Antibodies with affinities greater than $1 \times 10^7 \text{ M}^{-1}$ (or a dissociation coefficient of $1 \mu\text{M}$ or less or a dissociation coefficient of 1 nM or less) typically bind with correspondingly greater specificity. Values intermediate of those set forth herein are also intended to be within the scope of the present invention and antibodies of the invention bind with a range of affinities, for example, 100 nM or less, 75 nM or less, 50 nM or less, 25 nM or less, for example 10 nM or less, 5 nM or less, 1 nM or less, or in embodiments 500 pM or less, 100 pM or less, 50 pM or less or 25 pM or less. An antibody that "does not exhibit significant crossreactivity" is one that will not appreciably bind to an entity other than its target (e.g., a different epitope or a different molecule). For example, an antibody that specifically binds to a target molecule will appreciably bind the target molecule but will not significantly react with non-target molecules or peptides. An antibody specific for a particular epitope will, for example, not significantly crossreact with remote epitopes on the same protein or peptide. Specific binding can be determined according to any art-recognized means for determining such binding.

Preferably, specific binding is determined according to Scatchard analysis and/or competitive binding assays.

[0163] As used herein, the term "affinity" refers to the strength of the binding of a single antigen-combining site with an antigenic determinant. Affinity depends on the closeness of stereochemical fit between antibody combining sites and antigen determinants, on the size of the area of contact between them, on the distribution of charged and hydrophobic groups, etc. Antibody affinity can be measured by equilibrium dialysis or by the kinetic BIACORE™ method. The dissociation constant, K_d , and the association constant, K_a , are quantitative measures of affinity.

[0164] As used herein, the term "monoclonal antibody" refers to an antibody derived from a clonal population of antibody-producing cells (e.g., B lymphocytes or B cells) which is homogeneous in structure and antigen specificity. The term "polyclonal antibody" refers to a plurality of antibodies originating from different clonal populations of antibody-producing cells which are heterogeneous in their structure and epitope specificity but which recognize a common antigen. Monoclonal and polyclonal antibodies may exist within bodily fluids, as crude preparations, or may be purified, as described herein.

[0165] The term "binding portion" of an antibody (or "antibody portion") includes one or more complete domains, e.g., a pair of complete domains, as well as fragments of an antibody that retain the ability to specifically bind to a target molecule. It has been shown that the binding function of an antibody can be performed by fragments of a full-length antibody. Binding fragments are produced by recombinant DNA techniques, or by enzymatic or chemical cleavage of intact immunoglobulins. Binding fragments include Fab, Fab', F(ab')₂, Fabc, Fd, dAb, Fv, single chains, single-chain antibodies, e.g., scFv, and single domain antibodies.

[0166] "Humanized" forms of non-human (e.g., murine) antibodies are chimeric antibodies that contain minimal sequence derived from non-human immunoglobulin. For the most part, humanized antibodies are human immunoglobulins (recipient antibody) in which residues from a hypervariable region of the recipient are replaced by residues from a hypervariable region of a non-human species (donor antibody) such as mouse, rat, rabbit or nonhuman primate having the desired specificity, affinity, and capacity. In some instances, FR residues of the human immunoglobulin are replaced by corresponding non-human residues. Furthermore, humanized antibodies may comprise residues that are not found in the recipient antibody or in the donor antibody. These modifications are made to further refine

antibody performance. In general, the humanized antibody will comprise substantially all of at least one, and typically two, variable domains, in which all or substantially all of the hypervariable regions correspond to those of a non-human immunoglobulin and all or substantially all of the FR regions are those of a human immunoglobulin sequence. The humanized antibody optionally also will comprise at least a portion of an immunoglobulin constant region (Fc), typically that of a human immunoglobulin.

[0167] Examples of portions of antibodies or epitope-binding proteins encompassed by the present definition include: (i) the Fab fragment, having **VL**, **CL**, **VH** and **CHI** domains; (ii) the Fab' fragment, which is a Fab fragment having one or more cysteine residues at the C-terminus of the **CHI** domain; (iii) the Fd fragment having **VH** and **CHI** domains; (iv) the Fd' fragment having **VH** and **CHI** domains and one or more cysteine residues at the C-terminus of the **CHI** domain; (v) the Fv fragment having the **VL** and **VH** domains of a single arm of an antibody; (vi) the dAb fragment (Ward et al., 341 Nature 544 (1989)) which consists of a **VH** domain or a **VL** domain that binds antigen; (vii) isolated CDR regions or isolated CDR regions presented in a functional framework; (viii) F(ab')₂ fragments which are bivalent fragments including two Fab' fragments linked by a disulphide bridge at the hinge region; (ix) single chain antibody molecules (e.g., single chain Fv; scFv) (Bird et al., 242 Science 423 (1988); and Huston et al., 85 PNAS 5879 (1988)); (x) "diabodies" with two antigen binding sites, comprising a heavy chain variable domain (**VH**) connected to a light chain variable domain (**VL**) in the same polypeptide chain (see, e.g., EP 404,097; WO 93/1 1161; Hollinger et al., 90 PNAS 6444 (1993)); (xi) "linear antibodies" comprising a pair of tandem Fd segments (**VH-Chl-VH-Chl**) which, together with complementary light chain polypeptides, form a pair of antigen binding regions (Zapata et al., Protein Eng. 8(10): 1057-62 (1995); and U.S. Patent No. 5,641,870).

[0168] As used herein, a "blocking" antibody or an antibody "antagonist" is one which inhibits or reduces biological activity of the antigen(s) it binds. In certain embodiments, the blocking antibodies or antagonist antibodies or portions thereof described herein completely inhibit the biological activity of the antigen(s).

[0169] Antibodies may act as agonists or antagonists of the recognized polypeptides. For example, the present invention includes antibodies which disrupt receptor/ligand interactions either partially or fully. The invention features both receptor-specific antibodies and ligand-specific antibodies. The invention also features receptor-specific antibodies which do not prevent ligand binding but prevent receptor activation. Receptor activation (i.e., signaling)

may be determined by techniques described herein or otherwise known in the art. For example, receptor activation can be determined by detecting the phosphorylation (e.g., tyrosine or serine/threonine) of the receptor or of one of its down-stream substrates by immunoprecipitation followed by western blot analysis. In specific embodiments, antibodies are provided that inhibit ligand activity or receptor activity by at least 95%, at least 90%, at least 85%, at least 80%, at least 75%, at least 70%, at least 60%, or at least 50% of the activity in absence of the antibody.

[0170] The invention also features receptor-specific antibodies which both prevent ligand binding and receptor activation as well as antibodies that recognize the receptor-ligand complex. Likewise, encompassed by the invention are neutralizing antibodies which bind the ligand and prevent binding of the ligand to the receptor, as well as antibodies which bind the ligand, thereby preventing receptor activation, but do not prevent the ligand from binding the receptor. Further included in the invention are antibodies which activate the receptor. These antibodies may act as receptor agonists, i.e., potentiate or activate either all or a subset of the biological activities of the ligand-mediated receptor activation, for example, by inducing dimerization of the receptor. The antibodies may be specified as agonists, antagonists or inverse agonists for biological activities comprising the specific biological activities of the peptides disclosed herein. The antibody agonists and antagonists can be made using methods known in the art. See, e.g., PCT publication WO 96/40281; U.S. Pat. No. 5,811,097; Deng et al., *Blood* 92(6):1981-1988 (1998); Chen et al., *Cancer Res.* 58(16):3668-3678 (1998); Harrop et al., *J. Immunol.* 161(4):1786-1794 (1998); Zhu et al., *Cancer Res.* 58(15):3209-3214 (1998); Yoon et al., *J. Immunol.* 160(7):3170-3179 (1998); Prat et al., *J. Cell. Sci.* 111(Pt2):237-247 (1998); Pitard et al., *J. Immunol. Methods* 205(2):177-190 (1997); Liautard et al., *Cytokine* 9(4):233-241 (1997); Carlson et al., *J. Biol. Chem.* 272(17):11295-11301 (1997); Taryman et al., *Neuron* 14(4):755-762 (1995); Muller et al., *Structure* 6(9):1153-1167 (1998); Bartunek et al., *Cytokine* 8(1):14-20 (1996).

[0171] The antibodies as defined for the present invention include derivatives that are modified, i.e., by the covalent attachment of any type of molecule to the antibody such that covalent attachment does not prevent the antibody from generating an anti-idiotypic response. For example, but not by way of limitation, the antibody derivatives include antibodies that have been modified, e.g., by glycosylation, acetylation, pegylation, phosphorylation, amidation, derivatization by known protecting/blocking groups, proteolytic cleavage, linkage to a cellular ligand or other protein, etc. Any of numerous chemical

modifications may be carried out by known techniques, including, but not limited to specific chemical cleavage, acetylation, formylation, metabolic synthesis of tunicamycin, etc. Additionally, the derivative may contain one or more non-classical amino acids.

[0172] Simple binding assays can be used to screen for or detect agents that bind to a target protein, or disrupt the interaction between proteins (e.g., a receptor and a ligand). Because certain targets of the present invention are transmembrane proteins, assays that use the soluble forms of these proteins rather than full-length protein can be used, in some embodiments. Soluble forms include, for example, those lacking the transmembrane domain and/or those comprising the IgV domain or fragments thereof which retain their ability to bind their cognate binding partners. Further, agents that inhibit or enhance protein interactions for use in the compositions and methods described herein, can include recombinant peptido-mimetics.

[0173] Detection methods useful in screening assays include antibody-based methods, detection of a reporter moiety, detection of cytokines as described herein, and detection of a gene signature as described herein.

[0174] Another variation of assays to determine binding of a receptor protein to a ligand protein is through the use of affinity biosensor methods. Such methods may be based on the piezoelectric effect, electrochemistry, or optical methods, such as ellipsometry, optical wave guidance, and surface plasmon resonance (SPR).

[0175] The disclosure also encompasses nucleic acid molecules, in particular those that inhibit a signature gene. Exemplary nucleic acid molecules include aptamers, siRNA, artificial microRNA, interfering RNA or RNAi, dsRNA, ribozymes, antisense oligonucleotides, and DNA expression cassettes encoding said nucleic acid molecules. Preferably, the nucleic acid molecule is an antisense oligonucleotide. Antisense oligonucleotides (ASO) generally inhibit their target by binding target mRNA and sterically blocking expression by obstructing the ribosome. ASOs can also inhibit their target by binding target mRNA thus forming a DNA-RNA hybrid that can be a substrate for RNase H. Preferred ASOs include Locked Nucleic Acid (LNA), Peptide Nucleic Acid (PNA), and morpholinos. Preferably, the nucleic acid molecule is an RNAi molecule, i.e., RNA interference molecule. Preferred RNAi molecules include siRNA, shRNA, and artificial miRNA. The design and production of siRNA molecules is well known to one of skill in the art (e.g., Hajeri PB, Singh SK. *Drug Discov Today*. 2009 14(17-18):851-8). The nucleic acid molecule inhibitors may be chemically synthesized and provided directly to cells of interest.

The nucleic acid compound may be provided to a cell as part of a gene delivery vehicle. Such a vehicle is preferably a liposome or a viral gene delivery vehicle.

Adoptive Cell Therapy

[0176] In certain embodiments, tumor cells are targeted by using Adoptive cell therapy. As used herein, "ACT", "adoptive cell therapy" and "adoptive cell transfer" may be used interchangeably. Adoptive cell therapy (ACT) can refer to the transfer of cells, most commonly immune-derived cells, back into the same patient or into a new recipient host with the goal of transferring the immunologic functionality and characteristics into the new host. If possible, use of autologous cells helps the recipient by minimizing GVHD issues. The adoptive transfer of autologous tumor infiltrating lymphocytes (TIL) (Besser et al., (2010) Clin. Cancer Res 16 (9) 2646-55; Dudley et al., (2002) Science 298 (5594): 850-4; and Dudley et al., (2005) Journal of Clinical Oncology 23 (10): 2346-57.) or genetically re-directed peripheral blood mononuclear cells (Johnson et al., (2009) Blood 114 (3): 535-46; and Morgan et al., (2006) Science 314(5796) 126-9) has been used to successfully treat patients with advanced solid tumors, including melanoma and colorectal carcinoma, as well as patients with CD19-expressing hematologic malignancies (Kalos et al., (2011) Science Translational Medicine 3 (95): 95ra73).

[0177] Aspects of the invention involve the adoptive transfer of immune system cells, such as T cells, specific for selected antigens, such as tumor associated antigens or tumor specific neoantigens (see Maus et al., 2014, Adoptive Immunotherapy for Cancer or Viruses, Annual Review of Immunology, Vol. 32: 189-225; Rosenberg and Restifo, 2015, Adoptive cell transfer as personalized immunotherapy for human cancer, Science Vol. 348 no. 6230 pp. 62-68; Restifo et al., 2015, Adoptive immunotherapy for cancer: harnessing the T cell response. Nat. Rev. Immunol. 12(4): 269-281; and Jenson and Riddell, 2014, Design and implementation of adoptive therapy with chimeric antigen receptor-modified T cells. Immunol Rev. 257(1): 127-144; and Rajasagi et al., 2014, Systematic identification of personal tumor-specific neoantigens in chronic lymphocytic leukemia. Blood. 2014 Jul 17;124(3):453-62).

[0178] In certain embodiments, an antigen (such as a tumor antigen) to be targeted in adoptive cell therapy (such as particularly CAR or TCR T-cell therapy) of a disease (such as particularly of tumor or cancer) may be selected from a group consisting of: B cell maturation antigen (BCMA); PSA (prostate-specific antigen); prostate-specific membrane antigen (PSMA); PSCA (Prostate stem cell antigen); Tyrosine-protein kinase transmembrane

receptor ROR1; fibroblast activation protein (FAP); Tumor-associated glycoprotein 72 (TAG72); Carcinoembryonic antigen (CEA); Epithelial cell adhesion molecule (EPCAM); Mesothelin; Human Epidermal growth factor Receptor 2 (ERBB2 (Her2/neu)); Prostase; Prostatic acid phosphatase (PAP); elongation factor 2 mutant (ELF2M); Insulin-like growth factor 1 receptor (IGF-1R); gp100; BCR-ABL (breakpoint cluster region-Abelson); tyrosinase; New York esophageal squamous cell carcinoma 1 (NY-ESO-1); κ -light chain, LAGE (L antigen); MAGE (melanoma antigen); Melanoma-associated antigen 1 (MAGE-A1); MAGE A3; MAGE A6; legumain; Human papillomavirus (HPV) E6; HPV E7; prostein; survivin; PCTA1 (Galectin 8); Melan-A/MART-1; Ras mutant; TRP-1 (tyrosinase related protein 1, or gp75); Tyrosinase-related Protein 2 (TRP2); TRP-2/INT2 (TRP-2/intron 2); RAGE (renal antigen); receptor for advanced glycation end products 1 (RAGE1); Renal ubiquitous 1, 2 (RU1, RU2); intestinal carboxyl esterase (iCE); Heat shock protein 70-2 (HSP70-2) mutant; thyroid stimulating hormone receptor (TSHR); CD123; CD171; CD19; CD20; CD22; CD26; CD30; CD33; CD44v7/8 (cluster of differentiation 44, exons 7/8); CD53; CD92; CD100; CD148; CD150; CD200; CD261; CD262; CD362; CS-1 (CD2 subset 1, CRACC, SLAMF7, CD319, and 19A24); C-type lectin-like molecule-1 (CLL-1); ganglioside GD3 (aNeu5Ac(2-8)aNeu5Ac(2-3)bDGalp(1-4)bDGlc(1-1)Cer); Tn antigen (Tn Ag); Fms-Like Tyrosine Kinase 3 (FLT3); CD38; CD138; CD44v6; B7H3 (CD276); KIT (CD117); Interleukin-13 receptor subunit alpha-2 (IL-13Ra2); Interleukin 11 receptor alpha (IL-1 IRa); prostate stem cell antigen (PSCA); Protease Serine 21 (PRSS21); vascular endothelial growth factor receptor 2 (VEGFR2); Lewis(Y) antigen; CD24; Platelet-derived growth factor receptor beta (PDGFR-beta); stage-specific embryonic antigen-4 (SSEA-4); Mucin 1, cell surface associated (MUC1); mucin 16 (MUC16); epidermal growth factor receptor (EGFR); epidermal growth factor receptor variant III (EGFRvIII); neural cell adhesion molecule (NCAM); carbonic anhydrase IX (CAIX); Proteasome (Prosome, Macropain) Subunit, Beta Type, 9 (LMP2); ephrin type-A receptor 2 (EphA2); Ephrin B2; Fucosyl GM1; sialyl Lewis adhesion molecule (sLe); ganglioside GM3 (aNeu5Ac(2-3)bDGalp(1-4)bDGlc(1-1)Cer); TGS5; high molecular weight-melanoma-associated antigen (HMWMAA); o-acetyl-GD2 ganglioside (OAcGD2); Folate receptor alpha; Folate receptor beta; tumor endothelial marker 1 (TEM1/CD248); tumor endothelial marker 7-related (TEM7R); claudin 6 (CLDN6); G protein-coupled receptor class C group 5, member D (GPCR5D); chromosome X open reading frame 61 (CXORF61); CD97; CD179a; anaplastic lymphoma kinase (ALK); Polysialic acid; placenta-specific 1 (PLAC1); hexasaccharide

portion of globoH glycosphingolipid (GloboH); mammary gland differentiation antigen (NY-BR-1); uroplakin 2 (UPK2); Hepatitis A virus cellular receptor 1 (HAVCR1); adrenoceptor beta 3 (ADRB3); pannexin 3 (PANX3); G protein-coupled receptor 20 (GPR20); lymphocyte antigen 6 complex, locus K 9 (LY6K); Olfactory receptor 51E2 (OR51E2); TCR Gamma Alternate Reading Frame Protein (TARP); Wilms tumor protein (WT1); ETS translocation-variant gene 6, located on chromosome 12p (ETV6-AML); sperm protein 17 (SPA17); X Antigen Family, Member 1A (XAGE1); angiopoietin-binding cell surface receptor 2 (Tie 2); CT (cancer/testis (antigen)); melanoma cancer testis antigen-1 (MAD-CT-1); melanoma cancer testis antigen-2 (MAD-CT-2); Fos-related antigen 1; p53; p53 mutant; human Telomerase reverse transcriptase (hTERT); sarcoma translocation breakpoints; melanoma inhibitor of apoptosis (ML-IAP); ERG (transmembrane protease, serine 2 (TMPRSS2) ETS fusion gene); N-Acetyl glucosaminyl-transferase V (NA17); paired box protein Pax-3 (PAX3); Androgen receptor; Cyclin B1; Cyclin D1; v-myc avian myelocytomatosis viral oncogene neuroblastoma derived homolog (MYCN); Ras Homolog Family Member C (RhoC); Cytochrome P450 1B1 (CYP1B1); CCCTC-Binding Factor (Zinc Finger Protein-Like (BORIS); Squamous Cell Carcinoma Antigen Recognized By T Cells-1 or 3 (SART1, SART3); Paired box protein Pax-5 (PAX5); proacrosin binding protein sp32 (OY-TES1); lymphocyte-specific protein tyrosine kinase (LCK); A kinase anchor protein 4 (AKAP-4); synovial sarcoma, X breakpoint- 1, -2, -3 or -4 (SSX1, SSX2, SSX3, SSX4); CD79a; CD79b; CD72; Leukocyte-associated immunoglobulin-like receptor 1 (LAIR1); Fc fragment of IgA receptor (FCAR); Leukocyte immunoglobulin-like receptor subfamily A member 2 (LILRA2); CD300 molecule-like family member f (CD300LF); C-type lectin domain family 12 member A (CLEC12A); bone marrow stromal cell antigen 2 (BST2); EGF-like module-containing mucin-like hormone receptor-like 2 (EMR2); lymphocyte antigen 75 (LY75); Glypican-3 (GPC3); Fc receptor-like 5 (FCRL5); mouse double minute 2 homolog (MDM2); livin; alphafetoprotein (AFP); transmembrane activator and CAML Interactor (TACI); B-cell activating factor receptor (BAFF-R); V-Ki-ras2 Kirsten rat sarcoma viral oncogene homolog (KRAS); immunoglobulin lambda-like polypeptide 1 (IGLL1); 707-AP (707 alanine proline); ART-4 (adenocarcinoma antigen recognized by T4 cells); BAGE (B antigen; b-catenin/m, b-catenin/mutated); CAMEL (CTL-recognized antigen on melanoma); CAPI (carcinoembryonic antigen peptide 1); CASP-8 (caspase-8); CDC27m (cell-division cycle 27 mutated); CDK4/m (cyclin-dependent kinase 4 mutated); Cyp-B (cyclophilin B); DAM (differentiation antigen melanoma); EGP-2 (epithelial glycoprotein 2); EGP-40 (epithelial

glycoprotein 40); Erbb2, 3, 4 (erythroblastic leukemia viral oncogene homolog-2, -3, 4); FBP (folate binding protein); fAChR (Fetal acetylcholine receptor); G250 (glycoprotein 250); GAGE (G antigen); GnT-V (N-acetylglucosaminyltransferase V); HAGE (helicose antigen); ULA-A (human leukocyte antigen-A); HST2 (human signet ring tumor 2); KIAA0205; KDR (kinase insert domain receptor); LDLR/FUT (low density lipid receptor/GDP L-fucose: b-D-galactosidase 2-a-L fucosyltransferase); LICAM (LI cell adhesion molecule); MC1R (melanocortin 1 receptor); Myosin/m (myosin mutated); MUM-1, -2, -3 (melanoma ubiquitous mutated 1, 2, 3); NA88-A (NA cDNA clone of patient M88); KG2D (Natural killer group 2, member D) ligands; oncofetal antigen (h5T4); pi90 minor bcr-abl (protein of 190KD bcr-abl); Pml/RARa (promyelocytic leukaemia/retinoic acid receptor a); PRAME (preferentially expressed antigen of melanoma); SAGE (sarcoma antigen); TEL/AML1 (translocation Ets-family leukemia/acute myeloid leukemia 1); TPI/m (triosephosphate isomerase mutated); and any combination thereof.

[0179] In certain embodiments, an antigen to be targeted in adoptive cell therapy (such as particularly CAR or TCR T-cell therapy) of a disease (such as particularly of tumor or cancer) is a tumor-specific antigen (TSA).

[0180] In certain embodiments, an antigen to be targeted in adoptive cell therapy (such as particularly CAR or TCR T-cell therapy) of a disease (such as particularly of tumor or cancer) is a neoantigen.

[0181] In certain embodiments, an antigen to be targeted in adoptive cell therapy (such as particularly CAR or TCR T-cell therapy) of a disease (such as particularly of tumor or cancer) is a tumor-associated antigen (TAA).

[0182] In certain embodiments, an antigen to be targeted in adoptive cell therapy (such as particularly CAR or TCR T-cell therapy) of a disease (such as particularly of tumor or cancer) is a universal tumor antigen. In certain preferred embodiments, the universal tumor antigen is selected from the group consisting of: a human telomerase reverse transcriptase (hTERT), survivin, mouse double minute 2 homolog (MDM2), cytochrome P450 IB 1 (CYP1B), HER2/neu, Wilms' tumor gene 1 (WT1), livin, alphafetoprotein (AFP), carcinoembryonic antigen (CEA), mucin 16 (MUC16), MUC1, prostate-specific membrane antigen (PSMA), p53, cyclin (D1), and any combinations thereof.

[0183] In certain embodiments, an antigen (such as a tumor antigen) to be targeted in adoptive cell therapy (such as particularly CAR or TCR T-cell therapy) of a disease (such as particularly of tumor or cancer) may be selected from a group consisting of: CD19, BCMA,

CLL-1, MAGE A3, MAGE A6, HPV E6, HPV E7, WT1, CD22, CD171, ROR1, MUC16, and SSX2. In certain preferred embodiments, the antigen may be CD19. For example, CD19 may be targeted in hematologic malignancies, such as in lymphomas, more particularly in B-cell lymphomas, such as without limitation in diffuse large B-cell lymphoma, primary mediastinal b-cell lymphoma, transformed follicular lymphoma, marginal zone lymphoma, mantle cell lymphoma, acute lymphoblastic leukemia including adult and pediatric ALL, non-Hodgkin lymphoma, indolent non-Hodgkin lymphoma, or chronic lymphocytic leukemia. For example, BCMA may be targeted in multiple myeloma or plasma cell leukemia. For example, CLL1 may be targeted in acute myeloid leukemia. For example, MAGE A3, MAGE A6, SSX2, and/or KRAS may be targeted in solid tumors. For example, HPV E6 and/or HPV E7 may be targeted in cervical cancer or head and neck cancer. For example, WT1 may be targeted in acute myeloid leukemia (AML), myelodysplastic syndromes (MDS), chronic myeloid leukemia (CML), non-small cell lung cancer, breast, pancreatic, ovarian or colorectal cancers, or mesothelioma. For example, CD22 may be targeted in B cell malignancies, including non-Hodgkin lymphoma, diffuse large B-cell lymphoma, or acute lymphoblastic leukemia. For example, CD171 may be targeted in neuroblastoma, glioblastoma, or lung, pancreatic, or ovarian cancers. For example, ROR1 may be targeted in ROR1+ malignancies, including non-small cell lung cancer, triple negative breast cancer, pancreatic cancer, prostate cancer, ALL, chronic lymphocytic leukemia, or mantle cell lymphoma. For example, MUC16 may be targeted in MUC16ecto+ epithelial ovarian, fallopian tube or primary peritoneal cancer.

[0184] Various strategies may for example be employed to genetically modify T cells by altering the specificity of the T cell receptor (TCR) for example by introducing new TCR α and β chains with selected peptide specificity (see U.S. Patent No. 8,697,854; PCT Patent Publications: WO2003020763, WO2004033685, WO2004044004, WO2005114215, WO2006000830, WO2008038002, WO2008039818, WO2004074322, WO2005113595, WO2006125962, WO2013166321, WO2013039889, WO2014018863, WO2014083173; U.S. Patent No. 8,088,379).

[0185] As an alternative to, or addition to, TCR modifications, chimeric antigen receptors (CARs) may be used in order to generate immunoresponsive cells, such as T cells, specific for selected targets, such as malignant cells, with a wide variety of receptor chimera constructs having been described (see U.S. Patent Nos. 5,843,728; 5,851,828; 5,912,170;

6,004,811; 6,284,240; 6,392,013; 6,410,014; 6,753,162; 8,211,422; and, PCT Publication W09215322).

[0186] In general, CARs are comprised of an extracellular domain, a transmembrane domain, and an intracellular domain, wherein the extracellular domain comprises an antigen-binding domain that is specific for a predetermined target. While the antigen-binding domain of a CAR is often an antibody or antibody fragment (e.g., a single chain variable fragment, scFv), the binding domain is not particularly limited so long as it results in specific recognition of a target. For example, in some embodiments, the antigen-binding domain may comprise a receptor, such that the CAR is capable of binding to the ligand of the receptor. Alternatively, the antigen-binding domain may comprise a ligand, such that the CAR is capable of binding the endogenous receptor of that ligand.

[0187] The antigen-binding domain of a CAR is generally separated from the transmembrane domain by a hinge or spacer. The spacer is also not particularly limited, and it is designed to provide the CAR with flexibility. For example, a spacer domain may comprise a portion of a human Fc domain, including a portion of the CH3 domain, or the hinge region of any immunoglobulin, such as IgA, IgD, IgE, IgG, or IgM, or variants thereof. Furthermore, the hinge region may be modified so as to prevent off-target binding by FcRs or other potential interfering objects. For example, the hinge may comprise an IgG4 Fc domain with or without a S228P, L235E, and/or N297Q mutation (according to Kabat numbering) in order to decrease binding to FcRs. Additional spacers/hinges include, but are not limited to, CD4, CD8, and CD28 hinge regions.

[0188] The transmembrane domain of a CAR may be derived either from a natural or from a synthetic source. Where the source is natural, the domain may be derived from any membrane bound or transmembrane protein. Transmembrane regions of particular use in this disclosure may be derived from CD8, CD28, CD3, CD45, CD4, CD5, CD8, CD9, CD16, CD22, CD33, CD37, CD64, CD80, CD86, CD134, CD137, CD154, TCR. Alternatively, the transmembrane domain may be synthetic, in which case it will comprise predominantly hydrophobic residues such as leucine and valine. Preferably a triplet of phenylalanine, tryptophan and valine will be found at each end of a synthetic transmembrane domain. Optionally, a short oligo- or polypeptide linker, preferably between 2 and 10 amino acids in length may form the linkage between the transmembrane domain and the cytoplasmic signaling domain of the CAR. A glycine-serine doublet provides a particularly suitable linker.

[0189] Alternative CAR constructs may be characterized as belonging to successive generations. First-generation CARs typically consist of a single-chain variable fragment of an antibody specific for an antigen, for example comprising a VL linked to a VH of a specific antibody, linked by a flexible linker, for example by a CD8a hinge domain and a CD8a transmembrane domain, to the transmembrane and intracellular signaling domains of either CD3C or FcR γ (scFv-CD3C or scFv-FcR γ ; see U.S. Patent No. 7,741,465; U.S. Patent No. 5,912,172; U.S. Patent No. 5,906,936). Second-generation CARs incorporate the intracellular domains of one or more costimulatory molecules, such as CD28, OX40 (CD134), or 4-1BB (CD137) within the endodomain (for example scFv-CD28/OX40/4-1BB-CD3Q see U.S. Patent Nos. 8,911,993; 8,916,381; 8,975,071; 9,101,584; 9,102,760; 9,102,761). Third-generation CARs include a combination of costimulatory endodomains, such as CD3 ζ -chain, CD97, GDI la-CD18, CD2, ICOS, CD27, CD154, CDS, OX40, 4-1BB, CD2, CD7, LIGHT, LFA-1, NKG2C, B7-H3, CD30, CD40, PD-1, or CD28 signaling domains (for example scFv-CD28-4-1BB-CD3C or scFv-CD28-OX40-CD3Q see U.S. Patent No. 8,906,682; U.S. Patent No. 8,399,645; U.S. Pat. No. 5,686,281; PCT Publication No. WO2014134165; PCT Publication No. WO2012079000). In certain embodiments, the primary signaling domain comprises a functional signaling domain of a protein selected from the group consisting of CD3 zeta, CD3 gamma, CD3 delta, CD3 epsilon, common FcR gamma (FCERIG), FcR beta (Fc Epsilon Rib), CD79a, CD79b, Fc gamma RIIa, DAPIO, and DAP12. In certain preferred embodiments, the primary signaling domain comprises a functional signaling domain of CD3 ζ or FcR γ . In certain embodiments, the one or more costimulatory signaling domains comprise a functional signaling domain of a protein selected, each independently, from the group consisting of: CD27, CD28, 4-1BB (CD137), OX40, CD30, CD40, PD-1, ICOS, lymphocyte function-associated antigen-1 (LFA-1), CD2, CD7, LIGHT, NKG2C, B7-H3, a ligand that specifically binds with CD83, CDS, ICAM-1, GITR, BAFFR, HVEM (LIGHTR), SLAMF7, NKp80 (KLRF1), CD160, CD19, CD4, CD8 alpha, CD8 beta, IL2R beta, IL2R gamma, IL7R alpha, ITGA4, VLA1, CD49a, ITGA4, IA4, CD49D, ITGA6, VLA-6, CD49f, ITGAD, CD11d, ITGAE, CD103, ITGAL, CD11a, LFA-1, ITGAM, CD11b, ITGAX, CD11c, ITGB1, CD29, ITGB2, CD18, ITGB7, TNFR2, TRANCE/RANKL, DNAM1 (CD226), SLAMF4 (CD244, 2B4), CD84, CD96 (Tactile), CEACAM1, CRTAM, Ly9 (CD229), CD160 (BY55), PSGL1, CD100 (SEMA4D), CD69, SLAMF6 (NTB-A, Lyl08), SLAM (SLAMF1, CD150, IPO-3), BLAME (SLAMF8), SELPLG (CD162), LTBR, LAT, GADS, SLP-76, PAG/Cbp, NKp44, NKp30, NKp46, and NKG2D. In certain embodiments,

the one or more costimulatory signaling domains comprise a functional signaling domain of a protein selected, each independently, from the group consisting of: 4-1BB, CD27, and CD28. In certain embodiments, a chimeric antigen receptor may have the design as described in U.S. Patent No. 7,446,190, comprising an intracellular domain of CD3 ζ chain (such as amino acid residues 52-163 of the human CD3 zeta chain, as shown in SEQ ID NO: 14 of US 7,446,190), a signaling region from CD28 and an antigen-binding element (or portion or domain; such as scFv). The CD28 portion, when between the zeta chain portion and the antigen-binding element, may suitably include the transmembrane and signaling domains of CD28 (such as amino acid residues 114-220 of SEQ ID NO: 10, full sequence shown in SEQ ID NO: 6 of US 7,446,190; these can include the following portion of CD28 as set forth in Genbank identifier NM_006139 (sequence version 1, 2 or 3):
 IEVMYPPPYLDNEKSNGTIIHVKGKHLCPSPLEPGPSKPFWVLVVV
 GGVLACYLLVTVAFIIFWVRSKRSLHSDYMNMTPRRPGPTRKHYQPYAPPRDFA
 AYRS) SEQ ID No: 1). Alternatively, when the zeta sequence lies between the CD28 sequence and the antigen-binding element, intracellular domain of CD28 can be used alone (such as amino sequence set forth in SEQ ID NO: 9 of US 7,446,190). Hence, certain embodiments employ a CAR comprising (a) a zeta chain portion comprising the intracellular domain of human CD3 ζ chain, (b) a costimulatory signaling region, and (c) an antigen-binding element (or portion or domain), wherein the costimulatory signaling region comprises the amino acid sequence encoded by SEQ ID NO: 6 of US 7,446,190.

[0190] Alternatively, costimulation may be orchestrated by expressing CARs in antigen-specific T cells, chosen so as to be activated and expanded following engagement of their native aPTCR, for example by antigen on professional antigen-presenting cells, with attendant costimulation. In addition, additional engineered receptors may be provided on the immunoresponsive cells, for example to improve targeting of a T-cell attack and/or minimize side effects

[0191] By means of an example and without limitation, Kochenderfer et al., (2009) *J Immunother.* 32 (7): 689-702 described anti-CD19 chimeric antigen receptors (CAR). FMC63-28Z CAR contained a single chain variable region moiety (scFv) recognizing CD19 derived from the FMC63 mouse hybridoma (described in Nicholson et al., (1997) *Molecular Immunology* 34: 1157-1165), a portion of the human CD28 molecule, and the intracellular component of the human TCR- ζ molecule. FMC63-CD828BBZ CAR contained the FMC63 scFv, the hinge and transmembrane regions of the CD8 molecule, the cytoplasmic portions of

CD28 and 4-1BB, and the cytoplasmic component of the TCR- ζ molecule. The exact sequence of the CD28 molecule included in the FMC63-28Z CAR corresponded to Genbank identifier NM_006139; the sequence included all amino acids starting with the amino acid sequence IEVMYPPPY and continuing all the way to the carboxy-terminus of the protein. To encode the anti-CD 19 scFv component of the vector, the authors designed a DNA sequence which was based on a portion of a previously published CAR (Cooper et al., (2003) Blood 101: 1637-1644). This sequence encoded the following components in frame from the 5' end to the 3' end: an XhoI site, the human granulocyte-macrophage colony-stimulating factor (GM-CSF) receptor α -chain signal sequence, the FMC63 light chain variable region (as in Nicholson et al., *supra*), a linker peptide (as in Cooper et al., *supra*), the FMC63 heavy chain variable region (as in Nicholson et al., *supra*), and a NotI site. A plasmid encoding this sequence was digested with XhoI and NotI. To form the MSGV-FMC63-28Z retroviral vector, the XhoI and NotI-digested fragment encoding the FMC63 scFv was ligated into a second XhoI and NotI-digested fragment that encoded the MSGV retroviral backbone (as in Hughes et al., (2005) Human Gene Therapy 16: 457-472) as well as part of the extracellular portion of human CD28, the entire transmembrane and cytoplasmic portion of human CD28, and the cytoplasmic portion of the human TCR- ζ molecule (as in Maher et al., 2002) Nature Biotechnology 20: 70-75). The FMC63-28Z CAR is included in the KTE-C19 (axicabtagene ciloleucel) anti-CD 19 CAR-T therapy product in development by Kite Pharma, Inc. for the treatment of *inter alia* patients with relapsed/refractory aggressive B-cell non-Hodgkin lymphoma (NHL). Accordingly, in certain embodiments, cells intended for adoptive cell therapies, more particularly immunoresponsive cells such as T cells, may express the FMC63-28Z CAR as described by Kochenderfer et al. (*supra*). Hence, in certain embodiments, cells intended for adoptive cell therapies, more particularly immunoresponsive cells such as T cells, may comprise a CAR comprising an extracellular antigen-binding element (or portion or domain; such as scFv) that specifically binds to an antigen, an intracellular signaling domain comprising an intracellular domain of a CD3 ζ chain, and a costimulatory signaling region comprising a signaling domain of CD28. Preferably, the CD28 amino acid sequence is as set forth in Genbank identifier NM_006139 (sequence version 1, 2 or 3) starting with the amino acid sequence IEVMYPPPY (SEQ ID No: 2) and continuing all the way to the carboxy-terminus of the protein. The sequence is reproduced herein:

IEVMYPPPYLDNEKSNGTIIHVKGKHLCPSPFPGPSKPFWVLVVVGGVLACYSLLVT

VAFIIFWVRSKRSRLHSDYMNMTPRRPGPTRKHYPYAPPRDFAAYRS (SEQ. ID. No: 3). Preferably, the antigen is CD 19, more preferably the antigen-binding element is an anti-CD 19 scFv, even more preferably the anti-CD 19 scFv as described by Kochenderfer et al. *(supra)*.

[0192] Additional anti-CD19 CARs are further described in WO2015187528. More particularly Example 1 and Table 1 of WO2015187528, incorporated by reference herein, demonstrate the generation of anti-CD 19 CARs based on a fully human anti-CD 19 monoclonal antibody (47G4, as described in US20100104509) and murine anti-CD 19 monoclonal antibody (as described in Nicholson et al. and explained above). Various combinations of a signal sequence (human CD8-alpha or GM-CSF receptor), extracellular and transmembrane regions (human CD8-alpha) and intracellular T-cell signalling domains (CD28-CD3Q 4-1BB-CD3Q CD27-CD3Q CD28-CD27-CD3C, 4-1BB-CD27-CD3Q CD27-4-1BB-CD3 ζ ; CD28-CD27-FcsRI gamma chain; or CD28-FcsRI gamma chain) were disclosed. Hence, in certain embodiments, cells intended for adoptive cell therapies, more particularly immunoresponsive cells such as T cells, may comprise a CAR comprising an extracellular antigen-binding element that specifically binds to an antigen, an extracellular and transmembrane region as set forth in Table 1 of WO2015187528 and an intracellular T-cell signalling domain as set forth in Table 1 of WO2015187528. Preferably, the antigen is CD 19, more preferably the antigen-binding element is an anti-CD 19 scFv, even more preferably the mouse or human anti-CD 19 scFv as described in Example 1 of WO2015187528. In certain embodiments, the CAR comprises, consists essentially of or consists of an amino acid sequence of SEQ ID NO: 1, SEQ ID NO: 2, SEQ ID NO: 3, SEQ ID NO: 4, SEQ ID NO: 5, SEQ ID NO: 6, SEQ ID NO: 7, SEQ ID NO: 8, SEQ ID NO: 9, SEQ ID NO: 10, SEQ ID NO: 11, SEQ ID NO: 12, or SEQ ID NO: 13 as set forth in Table 1 of WO2015187528.

[0193] In certain embodiments, the immune cell may, in addition to a CAR or exogenous TCR as described herein, further comprise a chimeric inhibitory receptor (inhibitory CAR) that specifically binds to a second target antigen and is capable of inducing an inhibitory or immunosuppressive or repressive signal to the cell upon recognition of the second target antigen. In certain embodiments, the chimeric inhibitory receptor comprises an extracellular antigen-binding element (or portion or domain) configured to specifically bind to a target antigen, a transmembrane domain, and an intracellular immunosuppressive or repressive

signaling domain. In certain embodiments, the second target antigen is an antigen that is not expressed on the surface of a cancer cell or infected cell or the expression of which is downregulated on a cancer cell or an infected cell. In certain embodiments, the second target antigen is an MHC-class I molecule. In certain embodiments, the intracellular signaling domain comprises a functional signaling portion of an immune checkpoint molecule, such as for example PD-1 or CTLA4. Advantageously, the inclusion of such inhibitory CAR reduces the chance of the engineered immune cells attacking non-target (e.g., non-cancer) tissues.

[0194] Alternatively, T-cells expressing CARs may be further modified to reduce or eliminate expression of endogenous TCRs in order to reduce off-target effects. Reduction or elimination of endogenous TCRs can reduce off-target effects and increase the effectiveness of the T cells (U.S. 9,181,527). T cells stably lacking expression of a functional TCR may be produced using a variety of approaches. T cells internalize, sort, and degrade the entire T cell receptor as a complex, with a half-life of about 10 hours in resting T cells and 3 hours in stimulated T cells (von Essen, M. et al. 2004. *J. Immunol.* 173:384-393). Proper functioning of the TCR complex requires the proper stoichiometric ratio of the proteins that compose the TCR complex. TCR function also requires two functioning TCR zeta proteins with ITAM motifs. The activation of the TCR upon engagement of its MHC-peptide ligand requires the engagement of several TCRs on the same T cell, which all must signal properly. Thus, if a TCR complex is destabilized with proteins that do not associate properly or cannot signal optimally, the T cell will not become activated sufficiently to begin a cellular response.

[0195] Accordingly, in some embodiments, TCR expression may be eliminated using RNA interference (e.g., shRNA, siRNA, miRNA, etc.), CRISPR, or other methods that target the nucleic acids encoding specific TCRs (e.g., TCR- α and TCR- β) and/or CD3 chains in primary T cells. By blocking expression of one or more of these proteins, the T cell will no longer produce one or more of the key components of the TCR complex, thereby destabilizing the TCR complex and preventing cell surface expression of a functional TCR.

[0196] In some instances, CAR may also comprise a switch mechanism for controlling expression and/or activation of the CAR. For example, a CAR may comprise an extracellular, transmembrane, and intracellular domain, in which the extracellular domain comprises a target-specific binding element that comprises a label, binding domain, or tag that is specific for a molecule other than the target antigen that is expressed on or by a target cell. In such embodiments, the specificity of the CAR is provided by a second construct that comprises a target antigen binding domain (e.g., an scFv or a bispecific antibody that is specific for both

the target antigen and the label or tag on the CAR) and a domain that is recognized by or binds to the label, binding domain, or tag on the CAR. See, e.g., WO 2013/044225, WO 2016/000304, WO 2015/057834, WO 2015/057852, WO 2016/070061, US 9,233,125, US 2016/0129109. In this way, a T-cell that expresses the CAR can be administered to a subject, but the CAR cannot bind its target antigen until the second composition comprising an antigen-specific binding domain is administered.

[0197] Alternative switch mechanisms include CARs that require multimerization in order to activate their signaling function (see, e.g., US 2015/0368342, US 2016/0175359, US 2015/0368360) and/or an exogenous signal, such as a small molecule drug (US 2016/0166613, Yung et al., *Science*, 2015), in order to elicit a T-cell response. Some CARs may also comprise a "suicide switch" to induce cell death of the CAR T-cells following treatment (Buddee et al., *PLoS One*, 2013) or to downregulate expression of the CAR following binding to the target antigen (WO 2016/01 1210).

[0198] Alternative techniques may be used to transform target immunoresponsive cells, such as protoplast fusion, lipofection, transfection or electroporation. A wide variety of vectors may be used, such as retroviral vectors, lentiviral vectors, adenoviral vectors, adeno-associated viral vectors, plasmids or transposons, such as a Sleeping Beauty transposon (see U.S. Patent Nos. 6,489,458; 7,148,203; 7,160,682; 7,985,739; 8,227,432), may be used to introduce CARs, for example using 2nd generation antigen-specific CARs signaling through CD3 ζ and either CD28 or CD137. Viral vectors may for example include vectors based on HIV, SV40, EBV, HSV or BPV.

[0199] Cells that are targeted for transformation may for example include T cells, Natural Killer (NK) cells, cytotoxic T lymphocytes (CTL), regulatory T cells, human embryonic stem cells, tumor-infiltrating lymphocytes (TIL) or a pluripotent stem cell from which lymphoid cells may be differentiated. T cells expressing a desired CAR may for example be selected through co-culture with γ -irradiated activating and propagating cells (AaPC), which co-express the cancer antigen and co-stimulatory molecules. The engineered CAR T-cells may be expanded, for example by co-culture on AaPC in presence of soluble factors, such as IL-2 and IL-21. This expansion may for example be carried out so as to provide memory CAR⁺ T cells (which may for example be assayed by non-enzymatic digital array and/or multi-panel flow cytometry). In this way, CAR T cells may be provided that have specific cytotoxic activity against antigen-bearing tumors (optionally in conjunction with production of desired

chemokines such as interferon- γ). CAR T cells of this kind may for example be used in animal models, for example to treat tumor xenografts.

[0200] In certain embodiments, ACT includes co-transferring CD4⁺ Th1 cells and CD8⁺ CTLs to induce a synergistic antitumour response (see, e.g., Li et al., Adoptive cell therapy with CD4⁺ T helper 1 cells and CD8⁺ cytotoxic T cells enhances complete rejection of an established tumour, leading to generation of endogenous memory responses to non-targeted tumour epitopes. *Clin Transl Immunology*. 2017 Oct; 6(10): e160).

[0201] In certain embodiments, Th17 cells are transferred to a subject in need thereof. Th17 cells have been reported to directly eradicate melanoma tumors in mice to a greater extent than Th1 cells (Muranski P, et al., Tumor-specific Th17-polarized cells eradicate large established melanoma. *Blood*. 2008 Jul 15; 112(2):362-73; and Martin-Orozco N, et al., T helper 17 cells promote cytotoxic T cell activation in tumor immunity. *Immunity*. 2009 Nov 20; 31(5):787-98). Those studies involved an adoptive T cell transfer (ACT) therapy approach, which takes advantage of CD4⁺ T cells that express a TCR recognizing tyrosinase tumor antigen. Exploitation of the TCR leads to rapid expansion of Th17 populations to large numbers *ex vivo* for reinfusion into the autologous tumor-bearing hosts.

[0202] In certain embodiments, ACT may include autologous iPSC-based vaccines, such as irradiated iPSCs in autologous anti-tumor vaccines (see e.g., Kooreman, Nigel G. et al., Autologous iPSC-Based Vaccines Elicit Anti-tumor Responses In Vivo, *Cell Stem Cell* 22, 1-13, 2018, doi.org/10.1016/j.stem.2018.01.016).

[0203] Unlike T-cell receptors (TCRs) that are MHC restricted, CARs can potentially bind any cell surface-expressed antigen and can thus be more universally used to treat patients (see Irving et al., Engineering Chimeric Antigen Receptor T-Cells for Racing in Solid Tumors: Don't Forget the Fuel, *Front. Immunol.*, 03 April 2017, doi.org/10.3389/fimmu.2017.00267). In certain embodiments, in the absence of endogenous T-cell infiltrate (e.g., due to aberrant antigen processing and presentation), which precludes the use of TIL therapy and immune checkpoint blockade, the transfer of CAR T-cells may be used to treat patients (see, e.g., Hinrichs CS, Rosenberg SA. Exploiting the curative potential of adoptive T-cell therapy for cancer. *Immunol Rev* (2014) 257(1):56-71. doi:10.1111/imr.12132).

[0204] Approaches such as the foregoing may be adapted to provide methods of treating and/or increasing survival of a subject having a disease, such as a neoplasia, for example by administering an effective amount of an immunoresponsive cell comprising an antigen

recognizing receptor that binds a selected antigen, wherein the binding activates the immunoresponsive cell, thereby treating or preventing the disease (such as a neoplasia, a pathogen infection, an autoimmune disorder, or an allogeneic transplant reaction).

[0205] In certain embodiments, the treatment can be administered after lymphodepleting pretreatment in the form of chemotherapy (typically a combination of cyclophosphamide and fludarabine) or radiation therapy. Initial studies in ACT had short lived responses and the transferred cells did not persist in vivo for very long (Houot et al., T-cell-based immunotherapy: adoptive cell transfer and checkpoint inhibition. *Cancer Immunol Res* (2015) 3(10): 1115-22; and Kamta et al., Advancing Cancer Therapy with Present and Emerging Immuno-Oncology Approaches. *Front. Oncol.* (2017) 7:64). Immune suppressor cells like Tregs and MDSCs may attenuate the activity of transferred cells by outcompeting them for the necessary cytokines. Not being bound by a theory lymphodepleting pretreatment may eliminate the suppressor cells allowing the TILs to persist.

[0206] In one embodiment, the treatment can be administered into patients undergoing an immunosuppressive treatment. The cells or population of cells, may be made resistant to at least one immunosuppressive agent due to the inactivation of a gene encoding a receptor for such immunosuppressive agent. Not being bound by a theory, the immunosuppressive treatment should help the selection and expansion of the immunoresponsive or T cells according to the invention within the patient.

[0207] In certain embodiments, the treatment can be administered before primary treatment (e.g., surgery or radiation therapy) to shrink a tumor before the primary treatment. In another embodiment, the treatment can be administered after primary treatment to remove any remaining cancer cells.

[0208] In certain embodiments, immunometabolic barriers can be targeted therapeutically prior to and/or during ACT to enhance responses to ACT or CAR T-cell therapy and to support endogenous immunity (see, e.g., Irving et al., Engineering Chimeric Antigen Receptor T-Cells for Racing in Solid Tumors: Don't Forget the Fuel, *Front. Immunol.*, 03 April 2017, doi.org/10.3389/fimmu.2017.00267).

[0209] The administration of cells or population of cells, such as immune system cells or cell populations, such as more particularly immunoresponsive cells or cell populations, as disclosed herein may be carried out in any convenient manner, including by aerosol inhalation, injection, ingestion, transfusion, implantation or transplantation. The cells or population of cells may be administered to a patient subcutaneously, intradermally,

intratumorally, intranodally, intramedullary, intramuscularly, intrathecally, by intravenous or intralymphatic injection, or intraperitoneally. In some embodiments, the disclosed CARs may be delivered or administered into a cavity formed by the resection of tumor tissue (i.e. intracavity delivery) or directly into a tumor prior to resection (i.e. intratumoral delivery). In one embodiment, the cell compositions of the present invention are preferably administered by intravenous injection.

[0210] The administration of the cells or population of cells can consist of the administration of 10^4 - 10^9 cells per kg body weight, preferably 10^5 to 10^6 cells/kg body weight including all integer values of cell numbers within those ranges. Dosing in CAR T cell therapies may for example involve administration of from 10^6 to 10^9 cells/kg, with or without a course of lymphodepletion, for example with cyclophosphamide. The cells or population of cells can be administered in one or more doses. In another embodiment, the effective amount of cells are administered as a single dose. In another embodiment, the effective amount of cells are administered as more than one dose over a period time. Timing of administration is within the judgment of managing physician and depends on the clinical condition of the patient. The cells or population of cells may be obtained from any source, such as a blood bank or a donor. While individual needs vary, determination of optimal ranges of effective amounts of a given cell type for a particular disease or conditions are within the skill of one in the art. An effective amount means an amount which provides a therapeutic or prophylactic benefit. The dosage administered will be dependent upon the age, health and weight of the recipient, kind of concurrent treatment, if any, frequency of treatment and the nature of the effect desired.

[0211] In another embodiment, the effective amount of cells or composition comprising those cells are administered parenterally. The administration can be an intravenous administration. The administration can be directly done by injection within a tumor.

[0212] To guard against possible adverse reactions, engineered immunoresponsive cells may be equipped with a transgenic safety switch, in the form of a transgene that renders the cells vulnerable to exposure to a specific signal. For example, the herpes simplex viral thymidine kinase (TK) gene may be used in this way, for example by introduction into allogeneic T lymphocytes used as donor lymphocyte infusions following stem cell transplantation (Greco, et al., Improving the safety of cell therapy with the TK-suicide gene. *Front. Pharmacol.* 2015; 6: 95). In such cells, administration of a nucleoside prodrug such as ganciclovir or acyclovir causes cell death. Alternative safety switch constructs include

inducible caspase 9, for example triggered by administration of a small-molecule dimerizer that brings together two nonfunctional icasp9 molecules to form the active enzyme. A wide variety of alternative approaches to implementing cellular proliferation controls have been described (see U.S. Patent Publication No. 20130071414; PCT Patent Publication WO2011146862; PCT Patent Publication WO2014011987; PCT Patent Publication WO2013040371; Zhou et al. BLOOD, 2014, 123/25:3895 - 3905; Di Stasi et al., The New England Journal of Medicine 2011; 365:1673-1683; Sadelain M, The New England Journal of Medicine 2011; 365:1735-173; Ramos et al., Stem Cells 28(6): 1107-15 (2010)).

[0213] In a further refinement of adoptive therapies, genome editing may be used to tailor immunoresponsive cells to alternative implementations, for example providing edited CAR T cells (see Poirot et al., 2015, Multiplex genome edited T-cell manufacturing platform for "off-the-shelf" adoptive T-cell immunotherapies, Cancer Res 75 (18): 3853; Ren et al., 2016, Multiplex genome editing to generate universal CAR T cells resistant to PD1 inhibition, Clin Cancer Res. 2016 Nov 4; and Qasim et al., 2017, Molecular remission of infant B-ALL after infusion of universal TALEN gene-edited CAR T cells, Sci Transl Med. 2017 Jan 25;9(374)). Cells may be edited using any CRISPR system and method of use thereof as described herein. CRISPR systems may be delivered to an immune cell by any method described herein. In preferred embodiments, cells are edited ex vivo and transferred to a subject in need thereof. Immunoresponsive cells, CAR T cells or any cells used for adoptive cell transfer may be edited. Editing may be performed for example to insert or knock-in an exogenous gene, such as an exogenous gene encoding a CAR or a TCR, at a preselected locus in a cell; to eliminate potential alloreactive T-cell receptors (TCR) or to prevent inappropriate pairing between endogenous and exogenous TCR chains, such as to knock-out or knock-down expression of an endogenous TCR in a cell; to disrupt the target of a chemotherapeutic agent in a cell; to block an immune checkpoint, such as to knock-out or knock-down expression of an immune checkpoint protein or receptor in a cell; to knock-out or knock-down expression of other gene or genes in a cell, the reduced expression or lack of expression of which can enhance the efficacy of adoptive therapies using the cell; to knock-out or knock-down expression of an endogenous gene in a cell, said endogenous gene encoding an antigen targeted by an exogenous CAR or TCR; to knock-out or knock-down expression of one or more MHC constituent proteins in a cell; to activate a T cell; to modulate cells such that the cells are resistant to exhaustion or dysfunction; and/or increase the differentiation and/or proliferation of functionally exhausted or dysfunctional CD8+ T-cells (see PCT Patent

Publications: WO2013 176915, WO2014059173, WO2014172606, WO2014184744, and WO2014191 128). Editing may result in inactivation of a gene.

[0214] By inactivating a gene it is intended that the gene of interest is not expressed in a functional protein form. In a particular embodiment, the CRISPR system specifically catalyzes cleavage in one targeted gene thereby inactivating said targeted gene. The nucleic acid strand breaks caused are commonly repaired through the distinct mechanisms of homologous recombination or non-homologous end joining (NHEJ). However, NHEJ is an imperfect repair process that often results in changes to the DNA sequence at the site of the cleavage. Repair via non-homologous end joining (NHEJ) often results in small insertions or deletions (Indel) and can be used for the creation of specific gene knockouts. Cells in which a cleavage induced mutagenesis event has occurred can be identified and/or selected by well-known methods in the art.

[0215] Hence, in certain embodiments, editing of cells (such as by CRISPR/Cas), particularly cells intended for adoptive cell therapies, more particularly immunoresponsive cells such as T cells, may be performed to insert or knock-in an exogenous gene, such as an exogenous gene encoding a CAR or a TCR, at a preselected locus in a cell. Conventionally, nucleic acid molecules encoding CARs or TCRs are transfected or transduced to cells using randomly integrating vectors, which, depending on the site of integration, may lead to clonal expansion, oncogenic transformation, variegated transgene expression and/or transcriptional silencing of the transgene. Directing of transgene(s) to a specific locus in a cell can minimize or avoid such risks and advantageously provide for uniform expression of the transgene(s) by the cells. Without limitation, suitable 'safe harbor' loci for directed transgene integration include CCR5 or AAVS1. Homology-directed repair (HDR) strategies are known and described elsewhere in this specification allowing to insert transgenes into desired loci.

[0216] Further suitable loci for insertion of transgenes, in particular CAR or exogenous TCR transgenes, include without limitation loci comprising genes coding for constituents of endogenous T-cell receptor, such as T-cell receptor alpha locus (TRA) or T-cell receptor beta locus (TRB), for example T-cell receptor alpha constant (TRAC) locus, T-cell receptor beta constant 1 (TRBC1) locus or T-cell receptor beta constant 2 (TRBC2) locus. Advantageously, insertion of a transgene into such locus can simultaneously achieve expression of the transgene, potentially controlled by the endogenous promoter, and knock-out expression of the endogenous TCR. This approach has been exemplified in Eyquem et al., (2017) Nature 543: 113-117, wherein the authors used CRISPR/Cas9 gene editing to

knock-in a DNA molecule encoding a CD19-specific CAR into the TRAC locus downstream of the endogenous promoter; the CAR-T cells obtained by CRISPR were significantly superior in terms of reduced tonic CAR signaling and exhaustion.

[0217] T cell receptors (TCR) are cell surface receptors that participate in the activation of T cells in response to the presentation of antigen. The TCR is generally made from two chains, α and β , which assemble to form a heterodimer and associates with the CD3-transducing subunits to form the T cell receptor complex present on the cell surface. Each α and β chain of the TCR consists of an immunoglobulin-like N-terminal variable (V) and constant (C) region, a hydrophobic transmembrane domain, and a short cytoplasmic region. As for immunoglobulin molecules, the variable region of the α and β chains are generated by V(D)J recombination, creating a large diversity of antigen specificities within the population of T cells. However, in contrast to immunoglobulins that recognize intact antigen, T cells are activated by processed peptide fragments in association with an MHC molecule, introducing an extra dimension to antigen recognition by T cells, known as MHC restriction. Recognition of MHC disparities between the donor and recipient through the T cell receptor leads to T cell proliferation and the potential development of graft versus host disease (GVHD). The inactivation of TCRA or TCRP can result in the elimination of the TCR from the surface of T cells preventing recognition of alloantigen and thus GVHD. However, TCR disruption generally results in the elimination of the CD3 signaling component and alters the means of further T cell expansion.

[0218] Hence, in certain embodiments, editing of cells (such as by CRISPR/Cas), particularly cells intended for adoptive cell therapies, more particularly immunoresponsive cells such as T cells, may be performed to knock-out or knock-down expression of an endogenous TCR in a cell. For example, NHEJ-based or HDR-based gene editing approaches can be employed to disrupt the endogenous TCR alpha and/or beta chain genes. For example, gene editing system or systems, such as CRISPR/Cas system or systems, can be designed to target a sequence found within the TCR beta chain conserved between the beta 1 and beta 2 constant region genes (TRBC1 and TRBC2) and/or to target the constant region of the TCR alpha chain (TRAC) gene.

[0219] Allogeneic cells are rapidly rejected by the host immune system. It has been demonstrated that, allogeneic leukocytes present in non-irradiated blood products will persist for no more than 5 to 6 days (Boni, Muranski et al. 2008 Blood 1;1 12(12):4746-54). Thus, to prevent rejection of allogeneic cells, the host's immune system usually has to be suppressed

to some extent. However, in the case of adoptive cell transfer the use of immunosuppressive drugs also have a detrimental effect on the introduced therapeutic T cells. Therefore, to effectively use an adoptive immunotherapy approach in these conditions, the introduced cells would need to be resistant to the immunosuppressive treatment. Thus, in a particular embodiment, the present invention further comprises a step of modifying T cells to make them resistant to an immunosuppressive agent, preferably by inactivating at least one gene encoding a target for an immunosuppressive agent. An immunosuppressive agent is an agent that suppresses immune function by one of several mechanisms of action. An immunosuppressive agent can be, but is not limited to a calcineurin inhibitor, a target of rapamycin, an interleukin-2 receptor α -chain blocker, an inhibitor of inosine monophosphate dehydrogenase, an inhibitor of dihydrofolic acid reductase, a corticosteroid or an immunosuppressive antimetabolite. The present invention allows conferring immunosuppressive resistance to T cells for immunotherapy by inactivating the target of the immunosuppressive agent in T cells. As non-limiting examples, targets for an immunosuppressive agent can be a receptor for an immunosuppressive agent such as: CD52, glucocorticoid receptor (GR), a FKBP family gene member and a cyclophilin family gene member.

[0220] In certain embodiments, editing of cells (such as by CRISPR/Cas), particularly cells intended for adoptive cell therapies, more particularly immunoresponsive cells such as T cells, may be performed to block an immune checkpoint, such as to knock-out or knock-down expression of an immune checkpoint protein or receptor in a cell. Immune checkpoints are inhibitory pathways that slow down or stop immune reactions and prevent excessive tissue damage from uncontrolled activity of immune cells. In certain embodiments, the immune checkpoint targeted is the programmed death-1 (PD-1 or CD279) gene (PDCD1). In other embodiments, the immune checkpoint targeted is cytotoxic T-lymphocyte-associated antigen (CTLA-4). In additional embodiments, the immune checkpoint targeted is another member of the CD28 and CTLA4 Ig superfamily such as BTLA, LAG3, ICOS, PDL1 or KIR. In further additional embodiments, the immune checkpoint targeted is a member of the TNFR superfamily such as CD40, OX40, CD137, GITR, CD27 or TIM-3.

[0221] Additional immune checkpoints include Src homology 2 domain-containing protein tyrosine phosphatase 1 (SHP-1) (Watson HA, et al., SHP-1: the next checkpoint target for cancer immunotherapy? *Biochem Soc Trans.* 2016 Apr 15;44(2):356-62). SHP-1 is a widely expressed inhibitory protein tyrosine phosphatase (PTP). In T-cells, it is a negative

regulator of antigen-dependent activation and proliferation. It is a cytosolic protein, and therefore not amenable to antibody-mediated therapies, but its role in activation and proliferation makes it an attractive target for genetic manipulation in adoptive transfer strategies, such as chimeric antigen receptor (CAR) T cells. Immune checkpoints may also include T cell immunoreceptor with Ig and ITIM domains (TIGIT/Vstm3/WUCAM/VSIG9) and VISTA (Le Mercier I, et al., (2015) Beyond CTLA-4 and PD-1, the generation Z of negative checkpoint regulators. *Front. Immunol.* 6:418).

[0222] WO20 14 172606 relates to the use of MT1 and/or MT2 inhibitors to increase proliferation and/or activity of exhausted CD8+ T-cells and to decrease CD8+ T-cell exhaustion (e.g., decrease functionally exhausted or unresponsive CD8+ immune cells). In certain embodiments, metallothioneins are targeted by gene editing in adoptively transferred T cells.

[0223] In certain embodiments, targets of gene editing may be at least one targeted locus involved in the expression of an immune checkpoint protein. Such targets may include, but are not limited to CTLA4, PPP2CA, PPP2CB, PTPN6, PTPN22, PDCD1, ICOS (CD278), PDL1, KIR, LAG3, HAVCR2, BTLA, CD160, TIGIT, CD96, CRTAM, LAIR1, SIGLEC7, SIGLEC9, CD244 (2B4), TNFRSF10B, TNFRSF10A, CASP8, CASP10, CASP3, CASP6, CASP7, FADD, FAS, TGFBR2, TGFBR1, SMAD2, SMAD3, SMAD4, SMAD1, SKI, SKIL, TGIF1, IL10RA, IL10RB, HMOX2, IL6R, IL6ST, EIF2AK4, CSK, PAG1, SIT1, FOXP3, PRDM1, BATF, VISTA, GUCY1A2, GUCY1A3, GUCY1B2, GUCY1B3, MT1, MT2, CD40, OX40, CD137, GITR, CD27, SHP-1, TIM-3, CEACAM-1, CEACAM-3, or CEACAM-5. In preferred embodiments, the gene locus involved in the expression of PD-1 or CTLA-4 genes is targeted. In other preferred embodiments, combinations of genes are targeted, such as but not limited to PD-1 and TIGIT.

[0224] By means of an example and without limitation, WO2016196388 concerns an engineered T cell comprising (a) a genetically engineered antigen receptor that specifically binds to an antigen, which receptor may be a CAR; and (b) a disrupted gene encoding a PD-L1, an agent for disruption of a gene encoding a PD-L1, and/or disruption of a gene encoding PD-L1, wherein the disruption of the gene may be mediated by a gene editing nuclease, a zinc finger nuclease (ZFN), CRISPR/Cas9 and/or TALEN. WO20 15 142675 relates to immune effector cells comprising a CAR in combination with an agent (such as CRISPR, TALEN or ZFN) that increases the efficacy of the immune effector cells in the treatment of cancer, wherein the agent may inhibit an immune inhibitory molecule, such as

PDI, PD-L1, CTLA-4, TIM-3, LAG-3, VISTA, BTLA, TIGIT, LAIR1, CD 160, 2B4, TGF β , CEACAM-1, CEACAM-3, or CEACAM-5. Ren et al., (2017) Clin Cancer Res 23 (9) 2255-2266 performed lentiviral delivery of CAR and electro-transfer of Cas9 mRNA and gRNAs targeting endogenous TCR, β -2 microglobulin (B2M) and PDI simultaneously, to generate gene-disrupted allogeneic CAR T cells deficient of TCR, HLA class I molecule and PDI.

[0225] In certain embodiments, cells may be engineered to express a CAR, wherein expression and/or function of methylcytosine dioxygenase genes (TET1, TET2 and/or TET3) in the cells has been reduced or eliminated, such as by CRISPR, ZNF or TALEN (for example, as described in WO20 17049 16).

[0226] In certain embodiments, editing of cells (such as by CRISPR/Cas), particularly cells intended for adoptive cell therapies, more particularly immunoresponsive cells such as T cells, may be performed to knock-out or knock-down expression of an endogenous gene in a cell, said endogenous gene encoding an antigen targeted by an exogenous CAR or TCR, thereby reducing the likelihood of targeting of the engineered cells. In certain embodiments, the targeted antigen may be one or more antigen selected from the group consisting of CD38, CD138, CS-1, CD33, CD26, CD30, CD53, CD92, CD100, CD148, CD150, CD200, CD261, CD262, CD362, human telomerase reverse transcriptase (hTERT), survivin, mouse double minute 2 homolog (MDM2), cytochrome P450 1B1 (CYP1B), HER2/neu, Wilms' tumor gene 1 (WT1), livin, alphafetoprotein (AFP), carcinoembryonic antigen (CEA), mucin 16 (MUC16), MUC1, prostate-specific membrane antigen (PSMA), p53, cyclin (D1), B cell maturation antigen (BCMA), transmembrane activator and CAML Interactor (TACI), and B-cell activating factor receptor (BAFF-R) (for example, as described in WO201601 1210 and WO20 170 11804).

[0227] In certain embodiments, editing of cells (such as by CRISPR/Cas), particularly cells intended for adoptive cell therapies, more particularly immunoresponsive cells such as T cells, may be performed to knock-out or knock-down expression of one or more MHC constituent proteins, such as one or more HLA proteins and/or beta-2 microglobulin (B2M), in a cell, whereby rejection of non-autologous (e.g., allogeneic) cells by the recipient's immune system can be reduced or avoided. In preferred embodiments, one or more HLA class I proteins, such as HLA-A, B and/or C, and/or B2M may be knocked-out or knocked-down. Preferably, B2M may be knocked-out or knocked-down. By means of an example, Ren et al., (2017) Clin Cancer Res 23 (9) 2255-2266 performed lentiviral delivery of CAR

and electro-transfer of Cas9 mRNA and gRNAs targeting endogenous TCR, β -2 microglobulin (B2M) and PDI simultaneously, to generate gene-disrupted allogeneic CAR T cells deficient of TCR, HLA class I molecule and PDI.

[0228] In other embodiments, at least two genes are edited. Pairs of genes may include, but are not limited to PDI and TCRA, PDI and TCRp, CTLA-4 and TCRA, CTLA-4 and TCRp, LAG3 and TCRA, LAG3 and TCRp, Tim3 and TCRA, Tim3 and TCRp, BTLA and TCRA, BTLA and TCRp, BY55 and TCRA, BY55 and TCRp, TIGIT and TCRA, TIGIT and TCRp, B7H5 and TCRA, B7H5 and TCRp, LAIR1 and TCRA, LAIR1 and TCRp, SIGLEC10 and TCRA, SIGLEC10 and TCRp, 2B4 and TCRA, 2B4 and TCRp.

[0229] In certain embodiments, a cell may be multiply edited (multiplex genome editing) as taught herein to (1) knock-out or knock-down expression of an endogenous TCR (for example, TRBC1, TRBC2 and/or TRAC), (2) knock-out or knock-down expression of an immune checkpoint protein or receptor (for example PDI, PD-L1 and/or CTLA4); and (3) knock-out or knock-down expression of one or more MHC constituent proteins (for example, HLA-A, B and/or C, and/or B2M, preferably B2M).

[0230] Whether prior to or after genetic modification of the T cells, the T cells can be activated and expanded generally using methods as described, for example, in U.S. Patents 6,352,694; 6,534,055; 6,905,680; 5,858,358; 6,887,466; 6,905,681; 7,144,575; 7,232,566; 7,175,843; 5,883,223; 6,905,874; 6,797,514; 6,867,041; and 7,572,631. T cells can be expanded in vitro or in vivo.

[0231] Immune cells may be obtained using any method known in the art. In one embodiment T cells that have infiltrated a tumor are isolated. T cells may be removed during surgery. T cells may be isolated after removal of tumor tissue by biopsy. T cells may be isolated by any means known in the art. In one embodiment, the method may comprise obtaining a bulk population of T cells from a tumor sample by any suitable method known in the art. For example, a bulk population of T cells can be obtained from a tumor sample by dissociating the tumor sample into a cell suspension from which specific cell populations can be selected. Suitable methods of obtaining a bulk population of T cells may include, but are not limited to, any one or more of mechanically dissociating (e.g., mincing) the tumor, enzymatically dissociating (e.g., digesting) the tumor, and aspiration (e.g., as with a needle).

[0232] The bulk population of T cells obtained from a tumor sample may comprise any suitable type of T cell. Preferably, the bulk population of T cells obtained from a tumor sample comprises tumor infiltrating lymphocytes (TILs).

[0233] The tumor sample may be obtained from any mammal. Unless stated otherwise, as used herein, the term "mammal" refers to any mammal including, but not limited to, mammals of the order Logomorpha, such as rabbits; the order Carnivora, including Felines (cats) and Canines (dogs); the order Artiodactyla, including Bovines (cows) and Swines (pigs); or of the order Perssodactyla, including Equines (horses). The mammals may be non-human primates, e.g., of the order Primates, Ceboids, or Simoids (monkeys) or of the order Anthropoids (humans and apes). In some embodiments, the mammal may be a mammal of the order Rodentia, such as mice and hamsters. Preferably, the mammal is a non-human primate or a human. An especially preferred mammal is the human.

[0234] T cells can be obtained from a number of sources, including peripheral blood mononuclear cells, bone marrow, lymph node tissue, spleen tissue, and tumors. In certain embodiments of the present invention, T cells can be obtained from a unit of blood collected from a subject using any number of techniques known to the skilled artisan, such as Ficoll separation. In one preferred embodiment, cells from the circulating blood of an individual are obtained by apheresis or leukapheresis. The apheresis product typically contains lymphocytes, including T cells, monocytes, granulocytes, B cells, other nucleated white blood cells, red blood cells, and platelets. In one embodiment, the cells collected by apheresis may be washed to remove the plasma fraction and to place the cells in an appropriate buffer or media for subsequent processing steps. In one embodiment of the invention, the cells are washed with phosphate buffered saline (PBS). In an alternative embodiment, the wash solution lacks calcium and may lack magnesium or may lack many if not all divalent cations. Initial activation steps in the absence of calcium lead to magnified activation. As those of ordinary skill in the art would readily appreciate a washing step may be accomplished by methods known to those in the art, such as by using a semi-automated "flow-through" centrifuge (for example, the Cobe 2991 cell processor) according to the manufacturer's instructions. After washing, the cells may be resuspended in a variety of biocompatible buffers, such as, for example, Ca-free, Mg-free PBS. Alternatively, the undesirable components of the apheresis sample may be removed and the cells directly resuspended in culture media.

[0235] In another embodiment, T cells are isolated from peripheral blood lymphocytes by lysing the red blood cells and depleting the monocytes, for example, by centrifugation through a PERCOLL™ gradient. A specific subpopulation of T cells, such as CD28+, CD4+, CDC, CD45RA+, and CD45RO+ T cells, can be further isolated by positive or negative

selection techniques. For example, in one preferred embodiment, T cells are isolated by incubation with anti-CD3/anti-CD28 (i.e., 3x28)-conjugated beads, such as DYNABEADS® M-450 CD3/CD28 T, or XCYTE DYNABEADS™ for a time period sufficient for positive selection of the desired T cells. In one embodiment, the time period is about 30 minutes. In a further embodiment, the time period ranges from 30 minutes to 36 hours or longer and all integer values there between. In a further embodiment, the time period is at least 1, 2, 3, 4, 5, or 6 hours. In yet another preferred embodiment, the time period is 10 to 24 hours. In one preferred embodiment, the incubation time period is 24 hours. For isolation of T cells from patients with leukemia, use of longer incubation times, such as 24 hours, can increase cell yield. Longer incubation times may be used to isolate T cells in any situation where there are few T cells as compared to other cell types, such in isolating tumor infiltrating lymphocytes (TIL) from tumor tissue or from immunocompromised individuals. Further, use of longer incubation times can increase the efficiency of capture of CD8+ T cells.

[0236] Enrichment of a T cell population by negative selection can be accomplished with a combination of antibodies directed to surface markers unique to the negatively selected cells. A preferred method is cell sorting and/or selection via negative magnetic immunoadherence or flow cytometry that uses a cocktail of monoclonal antibodies directed to cell surface markers present on the cells negatively selected. For example, to enrich for CD4+ cells by negative selection, a monoclonal antibody cocktail typically includes antibodies to CD14, CD20, CD11b, CD16, HLA-DR, and CD8.

[0237] Further, monocyte populations (i.e., CD14+ cells) may be depleted from blood preparations by a variety of methodologies, including anti-CD 14 coated beads or columns, or utilization of the phagocytotic activity of these cells to facilitate removal. Accordingly, in one embodiment, the invention uses paramagnetic particles of a size sufficient to be engulfed by phagocytotic monocytes. In certain embodiments, the paramagnetic particles are commercially available beads, for example, those produced by Life Technologies under the trade name Dynabeads™. In one embodiment, other non-specific cells are removed by coating the paramagnetic particles with "irrelevant" proteins (e.g., serum proteins or antibodies). Irrelevant proteins and antibodies include those proteins and antibodies or fragments thereof that do not specifically target the T cells to be isolated. In certain embodiments the irrelevant beads include beads coated with sheep anti-mouse antibodies, goat anti-mouse antibodies, and human serum albumin.

[0238] In brief, such depletion of monocytes is performed by preincubating T cells isolated from whole blood, apheresed peripheral blood, or tumors with one or more varieties of irrelevant or non-antibody coupled paramagnetic particles at any amount that allows for removal of monocytes (approximately a 20:1 bead:cell ratio) for about 30 minutes to 2 hours at 22 to 37 degrees C, followed by magnetic removal of cells which have attached to or engulfed the paramagnetic particles. Such separation can be performed using standard methods available in the art. For example, any magnetic separation methodology may be used including a variety of which are commercially available, (e.g., DYNAL® Magnetic Particle Concentrator (DYNAL MPC®)). Assurance of requisite depletion can be monitored by a variety of methodologies known to those of ordinary skill in the art, including flow cytometric analysis of CD14 positive cells, before and after depletion.

[0239] For isolation of a desired population of cells by positive or negative selection, the concentration of cells and surface (e.g., particles such as beads) can be varied. In certain embodiments, it may be desirable to significantly decrease the volume in which beads and cells are mixed together (i.e., increase the concentration of cells), to ensure maximum contact of cells and beads. For example, in one embodiment, a concentration of 2 billion cells/ml is used. In one embodiment, a concentration of 1 billion cells/ml is used. In a further embodiment, greater than 100 million cells/ml is used. In a further embodiment, a concentration of cells of 10, 15, 20, 25, 30, 35, 40, 45, or 50 million cells/ml is used. In yet another embodiment, a concentration of cells from 75, 80, 85, 90, 95, or 100 million cells/ml is used. In further embodiments, concentrations of 125 or 150 million cells/ml can be used. Using high concentrations can result in increased cell yield, cell activation, and cell expansion. Further, use of high cell concentrations allows more efficient capture of cells that may weakly express target antigens of interest, such as CD28-negative T cells, or from samples where there are many tumor cells present (i.e., leukemic blood, tumor tissue, etc). Such populations of cells may have therapeutic value and would be desirable to obtain. For example, using high concentration of cells allows more efficient selection of CD8+ T cells that normally have weaker CD28 expression.

[0240] In a related embodiment, it may be desirable to use lower concentrations of cells. By significantly diluting the mixture of T cells and surface (e.g., particles such as beads), interactions between the particles and cells is minimized. This selects for cells that express high amounts of desired antigens to be bound to the particles. For example, CD4+ T cells express higher levels of CD28 and are more efficiently captured than CD8+ T cells in dilute

concentrations. In one embodiment, the concentration of cells used is 5×10^6 /ml. In other embodiments, the concentration used can be from about 1×10^5 /ml to 1×10^6 /ml, and any integer value in between.

[0241] T cells can also be frozen. Wishing not to be bound by theory, the freeze and subsequent thaw step provides a more uniform product by removing granulocytes and to some extent monocytes in the cell population. After a washing step to remove plasma and platelets, the cells may be suspended in a freezing solution. While many freezing solutions and parameters are known in the art and will be useful in this context, one method involves using PBS containing 20% DMSO and 8% human serum albumin, or other suitable cell freezing media, the cells then are frozen to -80°C at a rate of 1° per minute and stored in the vapor phase of a liquid nitrogen storage tank. Other methods of controlled freezing may be used as well as uncontrolled freezing immediately at -20°C . or in liquid nitrogen.

[0242] T cells for use in the present invention may also be antigen-specific T cells. For example, tumor-specific T cells can be used. In certain embodiments, antigen-specific T cells can be isolated from a patient of interest, such as a patient afflicted with a cancer or an infectious disease. In one embodiment neopeptides are determined for a subject and T cells specific to these antigens are isolated. Antigen-specific cells for use in expansion may also be generated in vitro using any number of methods known in the art, for example, as described in U.S. Patent Publication No. US 20040224402 entitled, Generation and Isolation of Antigen-Specific T Cells, or in U.S. Pat. Nos. 6,040,177. Antigen-specific cells for use in the present invention may also be generated using any number of methods known in the art, for example, as described in Current Protocols in Immunology, or Current Protocols in Cell Biology, both published by John Wiley & Sons, Inc., Boston, Mass.

[0243] In a related embodiment, it may be desirable to sort or otherwise positively select (e.g. via magnetic selection) the antigen specific cells prior to or following one or two rounds of expansion. Sorting or positively selecting antigen-specific cells can be carried out using peptide-MHC tetramers (Altman, et al., Science. 1996 Oct. 4; 274(5284):94-6). In another embodiment the adaptable tetramer technology approach is used (Andersen et al., 2012 Nat Protoc. 7:891-902). Tetramers are limited by the need to utilize predicted binding peptides based on prior hypotheses, and the restriction to specific HLAs. Peptide-MHC tetramers can be generated using techniques known in the art and can be made with any MHC molecule of interest and any antigen of interest as described herein. Specific epitopes to be used in this context can be identified using numerous assays known in the art. For example, the ability of

a polypeptide to bind to MHC class I may be evaluated indirectly by monitoring the ability to promote incorporation of 125I labeled P2-microglobulin (β_2m) into MHC class I/p2m/peptide heterotrimeric complexes (see Parker et al., J. Immunol. 152:163, 1994).

[0244] In one embodiment cells are directly labeled with an epitope-specific reagent for isolation by flow cytometry followed by characterization of phenotype and TCRs. In one T cells are isolated by contacting the T cell specific antibodies. Sorting of antigen-specific T cells, or generally any cells of the present invention, can be carried out using any of a variety of commercially available cell sorters, including, but not limited to, MoFlo sorter (DakoCytomation, Fort Collins, Colo.), FACSAria™, FACSArray™, FACSVantage™, BD™ LSR II, and FACSCalibur™ (BD Biosciences, San Jose, Calif).

[0245] In a preferred embodiment, the method comprises selecting cells that also express CD3. The method may comprise specifically selecting the cells in any suitable manner. Preferably, the selecting is carried out using flow cytometry. The flow cytometry may be carried out using any suitable method known in the art. The flow cytometry may employ any suitable antibodies and stains. Preferably, the antibody is chosen such that it specifically recognizes and binds to the particular biomarker being selected. For example, the specific selection of CD3, CD8, TIM-3, LAG-3, 4-1BB, or PD-1 may be carried out using anti-CD3, anti-CD8, anti-TIM-3, anti-LAG-3, anti-4-1BB, or anti-PD-1 antibodies, respectively. The antibody or antibodies may be conjugated to a bead (e.g., a magnetic bead) or to a fluorochrome. Preferably, the flow cytometry is fluorescence-activated cell sorting (FACS). TCRs expressed on T cells can be selected based on reactivity to autologous tumors. Additionally, T cells that are reactive to tumors can be selected for based on markers using the methods described in patent publication Nos. WO2014133567 and WO2014133568, herein incorporated by reference in their entirety. Additionally, activated T cells can be selected for based on surface expression of CD 107a.

[0246] In one embodiment of the invention, the method further comprises expanding the numbers of T cells in the enriched cell population. Such methods are described in U.S. Patent No. 8,637,307 and is herein incorporated by reference in its entirety. The numbers of T cells may be increased at least about 3-fold (or 4-, 5-, 6-, 7-, 8-, or 9-fold), more preferably at least about 10-fold (or 20-, 30-, 40-, 50-, 60-, 70-, 80-, or 90-fold), more preferably at least about 100-fold, more preferably at least about 1,000 fold, or most preferably at least about 100,000-fold. The numbers of T cells may be expanded using any suitable method known in the art. Exemplary methods of expanding the numbers of cells are described in patent publication

No. WO 2003057171, U.S. Patent No. 8,034,334, and U.S. Patent Application Publication No. 2012/0244133, each of which is incorporated herein by reference.

[0247] In one embodiment, ex vivo T cell expansion can be performed by isolation of T cells and subsequent stimulation or activation followed by further expansion. In one embodiment of the invention, the T cells may be stimulated or activated by a single agent. In another embodiment, T cells are stimulated or activated with two agents, one that induces a primary signal and a second that is a co-stimulatory signal. Ligands useful for stimulating a single signal or stimulating a primary signal and an accessory molecule that stimulates a second signal may be used in soluble form. Ligands may be attached to the surface of a cell, to an Engineered Multivalent Signaling Platform (EMSP), or immobilized on a surface. In a preferred embodiment both primary and secondary agents are co-immobilized on a surface, for example a bead or a cell. In one embodiment, the molecule providing the primary activation signal may be a CD3 ligand, and the co-stimulatory molecule may be a CD28 ligand or 4-1BB ligand.

[0248] In certain embodiments, T cells comprising a CAR or an exogenous TCR, may be manufactured as described in WO2015120096, by a method comprising: enriching a population of lymphocytes obtained from a donor subject; stimulating the population of lymphocytes with one or more T-cell stimulating agents to produce a population of activated T cells, wherein the stimulation is performed in a closed system using serum-free culture medium; transducing the population of activated T cells with a viral vector comprising a nucleic acid molecule which encodes the CAR or TCR, using a single cycle transduction to produce a population of transduced T cells, wherein the transduction is performed in a closed system using serum-free culture medium; and expanding the population of transduced T cells for a predetermined time to produce a population of engineered T cells, wherein the expansion is performed in a closed system using serum-free culture medium. In certain embodiments, T cells comprising a CAR or an exogenous TCR, may be manufactured as described in WO2015120096, by a method comprising: obtaining a population of lymphocytes; stimulating the population of lymphocytes with one or more stimulating agents to produce a population of activated T cells, wherein the stimulation is performed in a closed system using serum-free culture medium; transducing the population of activated T cells with a viral vector comprising a nucleic acid molecule which encodes the CAR or TCR, using at least one cycle transduction to produce a population of transduced T cells, wherein the transduction is performed in a closed system using serum-free culture medium; and

expanding the population of transduced T cells to produce a population of engineered T cells, wherein the expansion is performed in a closed system using serum-free culture medium. The predetermined time for expanding the population of transduced T cells may be 3 days. The time from enriching the population of lymphocytes to producing the engineered T cells may be 6 days. The closed system may be a closed bag system. Further provided is population of T cells comprising a CAR or an exogenous TCR obtainable or obtained by said method, and a pharmaceutical composition comprising such cells.

[0249] In certain embodiments, T cell maturation or differentiation in vitro may be delayed or inhibited by the method as described in WO2017070395, comprising contacting one or more T cells from a subject in need of a T cell therapy with an AKT inhibitor (such as, e.g., one or a combination of two or more AKT inhibitors disclosed in claim 8 of WO2017070395) and at least one of exogenous Interleukin-7 (IL-7) and exogenous Interleukin-15 (IL-15), wherein the resulting T cells exhibit delayed maturation or differentiation, and/or wherein the resulting T cells exhibit improved T cell function (such as, e.g., increased T cell proliferation; increased cytokine production; and/or increased cytolytic activity) relative to a T cell function of a T cell cultured in the absence of an AKT inhibitor.

[0250] In certain embodiments, a patient in need of a T cell therapy may be conditioned by a method as described in WO2016191756 comprising administering to the patient a dose of cyclophosphamide between 200 mg/m²/day and 2000 mg/m²/day and a dose of fludarabine between 20 mg/m²/day and 900 mg/m²/day.

Diseases

[0251] It will be understood by the skilled person that treating as referred to herein encompasses enhancing treatment, or improving treatment efficacy. Treatment may include inhibition of tumor regression as well as inhibition of tumor growth, metastasis or tumor cell proliferation, or inhibition or reduction of otherwise deleterious effects associated with the tumor.

[0252] Efficaciousness of treatment is determined in association with any known method for diagnosing or treating the particular disease. The invention comprehends a treatment method comprising any one of the methods or uses herein discussed.

[0253] The phrase "therapeutically effective amount" as used herein refers to a sufficient amount of a drug, agent, or compound to provide a desired therapeutic effect.

[0254] As used herein "patient" refers to any human being receiving or who may receive medical treatment and is used interchangeably herein with the term "subject".

[0255] Therapy or treatment according to the invention may be performed alone or in conjunction with another therapy, and may be provided at home, the doctor's office, a clinic, a hospital's outpatient department, or a hospital. Treatment generally begins at a hospital so that the doctor can observe the therapy's effects closely and make any adjustments that are needed. The duration of the therapy depends on the age and condition of the patient, the stage of the cancer, and how the patient responds to the treatment.

[0256] The disclosure also provides methods for reducing resistance to immunotherapy and treating disease. Not being bound by a theory, cancer cells have many strategies of avoiding the immune system and by reducing the signature of the present invention cancer cells may be unmasked to the immune system. Not being bound by a theory, reducing a gene signature of the present invention may be used to treat a subject who has not been administered an immunotherapy, such that the subject's tumor becomes unmasked to their natural or unamplified immune system. In other embodiments, the cancer is resistant to therapies targeting the adaptive immune system (see e.g., Rooney et al., Molecular and genetic properties of tumors associated with local immune cytolytic activity, Cell. 2015 January 15; 160(1-2): 48-61). In one embodiment, modulation of one or more of the signature genes are used for reducing an immunotherapy resistant signature for the treatment of a subpopulation of tumor cells that are linked to resistance to targeted therapies and progressive tumor growth.

[0257] In general, the immune system is involved with controlling all cancers and the present application is applicable to treatment of all cancers. Not being bound by a theory, the signature of the present invention is applicable to all cancers and may be used for treatment, as well as for determining a prognosis and stratifying patients. The cancer may include, without limitation, liquid tumors such as leukemia (e.g., acute leukemia, acute lymphocytic leukemia, acute myelocytic leukemia, acute myeloblastic leukemia, acute promyelocytic leukemia, acute myelomonocytic leukemia, acute monocytic leukemia, acute erythroleukemia, chronic leukemia, chronic myelocytic leukemia, chronic lymphocytic leukemia), polycythemia vera, lymphoma (e.g., Hodgkin's disease, non-Hodgkin's disease), Waldenstrom's macroglobulinemia, heavy chain disease, or multiple myeloma.

[0258] The cancer may include, without limitation, solid tumors such as sarcomas and carcinomas. Examples of solid tumors include, but are not limited to fibrosarcoma, myxosarcoma, liposarcoma, chondrosarcoma, osteogenic sarcoma, chordoma, angiosarcoma, endotheliosarcoma, lymphangiosarcoma, lymphangioendotheliosarcoma, synovioma,

mesothelioma, Ewing's tumor, leiomyosarcoma, rhabdomyosarcoma, squamous cell carcinoma, basal cell carcinoma, adenocarcinoma, sweat gland carcinoma, sebaceous gland carcinoma, papillary carcinoma, papillary adenocarcinomas, cystadenocarcinoma, medullary carcinoma, epithelial carcinoma, bronchogenic carcinoma, hepatoma, colorectal cancer (e.g., colon cancer, rectal cancer), anal cancer, pancreatic cancer (e.g., pancreatic adenocarcinoma, islet cell carcinoma, neuroendocrine tumors), breast cancer (e.g., ductal carcinoma, lobular carcinoma, inflammatory breast cancer, clear cell carcinoma, mucinous carcinoma), ovarian carcinoma (e.g., ovarian epithelial carcinoma or surface epithelial-stromal tumour including serous tumour, endometrioid tumor and mucinous cystadenocarcinoma, sex-cord-stromal tumor), prostate cancer, liver and bile duct carcinoma (e.g., hepatocellular carcinoma, cholangiocarcinoma, hemangioma), choriocarcinoma, seminoma, embryonal carcinoma, kidney cancer (e.g., renal cell carcinoma, clear cell carcinoma, Wilm's tumor, nephroblastoma), cervical cancer, uterine cancer (e.g., endometrial adenocarcinoma, uterine papillary serous carcinoma, uterine clear-cell carcinoma, uterine sarcomas and leiomyosarcomas, mixed mullerian tumors), testicular cancer, germ cell tumor, lung cancer (e.g., lung adenocarcinoma, squamous cell carcinoma, large cell carcinoma, bronchioloalveolar carcinoma, non-small-cell carcinoma, small cell carcinoma, mesothelioma), bladder carcinoma, signet ring cell carcinoma, cancer of the head and neck (e.g., squamous cell carcinomas), esophageal carcinoma (e.g., esophageal adenocarcinoma), tumors of the brain (e.g., glioma, glioblastoma, medullablastoma, astrocytoma, medulloblastoma, craniopharyngioma, ependymoma, pinealoma, hemangioblastoma, acoustic neuroma, oligodendroglioma, schwannoma, meningioma), neuroblastoma, retinoblastoma, neuroendocrine tumor, melanoma, cancer of the stomach (e.g., stomach adenocarcinoma, gastrointestinal stromal tumor), or carcinoids. Lymphoproliferative disorders are also considered to be proliferative diseases.

Administration it will be appreciated that administration of therapeutic entities in accordance with the invention will be administered with suitable carriers, excipients, and other agents that are incorporated into formulations to provide improved transfer, delivery, tolerance, and the like. A multitude of appropriate formulations can be found in the formulary known to all pharmaceutical chemists: Remington's Pharmaceutical Sciences (15th ed, Mack Publishing Company, Easton, PA (1975)), particularly Chapter 87 by Blaug, Seymour, therein. These formulations include, for example, powders, pastes, ointments, jellies, waxes, oils, lipids, lipid (cationic or anionic) containing vesicles (such as Lipofectin™), DNA conjugates, anhydrous

absorption pastes, oil-in-water and water-in-oil emulsions, emulsions carbowax (polyethylene glycols of various molecular weights), semi-solid gels, and semi-solid mixtures containing carbowax. Any of the foregoing mixtures may be appropriate in treatments and therapies in accordance with the present invention, provided that the active ingredient in the formulation is not inactivated by the formulation and the formulation is physiologically compatible and tolerable with the route of administration. *See also* Baldrick P. "Pharmaceutical excipient development: the need for preclinical guidance." *Regul. Toxicol Pharmacol.* 32(2):210-8 (2000), Wang W. "Lyophilization and development of solid protein pharmaceuticals." *Int. J. Pharm.* 203(1-2): 1-60 (2000), Charman WN "Lipids, lipophilic drugs, and oral drug delivery—some emerging concepts." *J Pharm Sci.* 89(8):967-78 (2000), Powell *et al.* "Compendium of excipients for parenteral formulations" *PDA J Pharm Sci Technol.* 52:238-311 (1998) and the citations therein for additional information related to formulations, excipients and carriers well known to pharmaceutical chemists.

[0260] The medicaments of the invention are prepared in a manner known to those skilled in the art, for example, by means of conventional dissolving, lyophilizing, mixing, granulating or confectioning processes. Methods well known in the art for making formulations are found, for example, in *Remington: The Science and Practice of Pharmacy*, 20th ed., ed. A. R. Gennaro, 2000, Lippincott Williams & Wilkins, Philadelphia, and *Encyclopedia of Pharmaceutical Technology*, eds. J. Swarbrick and J. C. Boylan, 1988-1999, Marcel Dekker, New York.

[0261] Administration of medicaments of the invention may be by any suitable means that results in a compound concentration that is effective for treating or inhibiting (e.g., by delaying) the development of a disease. The compound is admixed with a suitable carrier substance, e.g., a pharmaceutically acceptable excipient that preserves the therapeutic properties of the compound with which it is administered. One exemplary pharmaceutically acceptable excipient is physiological saline. The suitable carrier substance is generally present in an amount of 1-95% by weight of the total weight of the medicament. The medicament may be provided in a dosage form that is suitable for administration. Thus, the medicament may be in form of, e.g., tablets, capsules, pills, powders, granulates, suspensions, emulsions, solutions, gels including hydrogels, pastes, ointments, creams, plasters, drenches, delivery devices, injectables, implants, sprays, or aerosols.

[0262] The agents disclosed herein (e.g., antibodies) may be used in a pharmaceutical composition when combined with a pharmaceutically acceptable carrier. Such compositions

comprise a therapeutically-effective amount of the agent and a pharmaceutically acceptable carrier. Such a composition may also further comprise (in addition to an agent and a carrier) diluents, fillers, salts, buffers, stabilizers, solubilizers, and other materials well known in the art. Compositions comprising the agent can be administered in the form of salts provided the salts are pharmaceutically acceptable. Salts may be prepared using standard procedures known to those skilled in the art of synthetic organic chemistry.

[0263] The term "pharmaceutically acceptable salts" refers to salts prepared from pharmaceutically acceptable non-toxic bases or acids including inorganic or organic bases and inorganic or organic acids. Salts derived from inorganic bases include aluminum, ammonium, calcium, copper, ferric, ferrous, lithium, magnesium, manganic salts, manganous, potassium, sodium, zinc, and the like. Particularly preferred are the ammonium, calcium, magnesium, potassium, and sodium salts. Salts derived from pharmaceutically acceptable organic non-toxic bases include salts of primary, secondary, and tertiary amines, substituted amines including naturally occurring substituted amines, cyclic amines, and basic ion exchange resins, such as arginine, betaine, caffeine, choline, N,N'-dibenzylethylenediamine, diethylamine, 2-diethylaminoethanol, 2-dimethylaminoethanol, ethanolamine, ethylenediamine, N-ethyl-morpholine, N-ethylpiperidine, glucamine, glucosamine, histidine, hydrabamine, isopropylamine, lysine, methylglucamine, morpholine, piperazine, piperidine, polyamine resins, procaine, purines, theobromine, triethylamine, trimethylamine, tripropylamine, tromethamine, and the like. The term "pharmaceutically acceptable salt" further includes all acceptable salts such as acetate, lactobionate, benzenesulfonate, laurate, benzoate, malate, bicarbonate, maleate, bisulfate, mandelate, bitartrate, mesylate, borate, methylbromide, bromide, methylnitrate, calcium edetate, methyl sulfate, camsylate, mucate, carbonate, napsylate, chloride, nitrate, clavulanate, N-methylglucamine, citrate, ammonium salt, dihydrochloride, oleate, edetate, oxalate, edisylate, pamoate (embonate), estolate, palmitate, esylate, pantothenate, fumarate, phosphate/diphosphate, gluceptate, polygalacturonate, gluconate, salicylate, glutamate, stearate, glycollylarsanilate, sulfate, hexylresorcinate, subacetate, hydrabamine, succinate, hydrobromide, tannate, hydrochloride, tartrate, hydroxynaphthoate, teoate, iodide, tosylate, isothionate, triethiodide, lactate, pantoate, valerate, and the like which can be used as a dosage form for modifying the solubility or hydrolysis characteristics or can be used in sustained release or pro-drug formulations. It will be understood that, as used herein, references to

specific agents (e.g., neuromedin U receptor agonists or antagonists), also include the pharmaceutically acceptable salts thereof.

[0264] Methods of administering the pharmacological compositions, including agonists, antagonists, antibodies or fragments thereof, to an individual include, but are not limited to, intradermal, intrathecal, intramuscular, intraperitoneal, intravenous, subcutaneous, intranasal, epidural, by inhalation, and oral routes. The compositions can be administered by any convenient route, for example by infusion or bolus injection, by absorption through epithelial or mucocutaneous linings (for example, oral mucosa, rectal and intestinal mucosa, and the like), ocular, and the like and can be administered together with other biologically-active agents. Administration can be systemic or local. In addition, it may be advantageous to administer the composition into the central nervous system by any suitable route, including intraventricular and intrathecal injection. Pulmonary administration may also be employed by use of an inhaler or nebulizer, and formulation with an aerosolizing agent. It may also be desirable to administer the agent locally to the area in need of treatment; this may be achieved by, for example, and not by way of limitation, local infusion during surgery, topical application, by injection, by means of a catheter, by means of a suppository, or by means of an implant.

[0265] Various delivery systems are known and can be used to administer the pharmacological compositions including, but not limited to, encapsulation in liposomes, microparticles, microcapsules; minicells; polymers; capsules; tablets; and the like. In one embodiment, the agent may be delivered in a vesicle, in particular a liposome. In a liposome, the agent is combined, in addition to other pharmaceutically acceptable carriers, with amphipathic agents such as lipids which exist in aggregated form as micelles, insoluble monolayers, liquid crystals, or lamellar layers in aqueous solution. Suitable lipids for liposomal formulation include, without limitation, monoglycerides, diglycerides, sulfatides, lysolecithin, phospholipids, saponin, bile acids, and the like. Preparation of such liposomal formulations is within the level of skill in the art, as disclosed, for example, in U.S. Pat. No. 4,837,028 and U.S. Pat. No. 4,737,323. In yet another embodiment, the pharmacological compositions can be delivered in a controlled release system including, but not limited to: a delivery pump (See, for example, Saudek, et al., *New Engl. J. Med.* 321: 574 (1989) and a semi-permeable polymeric material (See, for example, Howard, et al., *J. Neurosurg.* 71: 105 (1989)). Additionally, the controlled release system can be placed in proximity of the therapeutic target (e.g., a tumor), thus requiring only a fraction of the systemic dose. See, for

example, Goodson, In: Medical Applications of Controlled Release, 1984. (CRC Press, Boca Raton, Fla.).

[0266] The amount of the agents which will be effective in the treatment of a particular disorder or condition will depend on the nature of the disorder or condition, and may be determined by standard clinical techniques by those of skill within the art. In addition, *in vitro* assays may optionally be employed to help identify optimal dosage ranges. The precise dose to be employed in the formulation will also depend on the route of administration, and the overall seriousness of the disease or disorder, and should be decided according to the judgment of the practitioner and each patient's circumstances. Ultimately, the attending physician will decide the amount of the agent with which to treat each individual patient. In certain embodiments, the attending physician will administer low doses of the agent and observe the patient's response. Larger doses of the agent may be administered until the optimal therapeutic effect is obtained for the patient, and at that point the dosage is not increased further. In general, the daily dose range of a drug lie within the range known in the art for a particular drug or biologic. Effective doses may be extrapolated from dose-response curves derived from *in vitro* or animal model test systems. Ultimately the attending physician will decide on the appropriate duration of therapy using compositions of the present invention. Dosage will also vary according to the age, weight and response of the individual patient.

[0267] Methods for administering antibodies for therapeutic use is well known to one skilled in the art. In certain embodiments, small particle aerosols of antibodies or fragments thereof may be administered (see e.g., Piazza et al., J. Infect. Dis., Vol. 166, pp. 1422-1424, 1992; and Brown, Aerosol Science and Technology, Vol. 24, pp. 45-56, 1996). In certain embodiments, antibodies are administered in metered-dose propellant driven aerosols. In certain embodiments, antibodies may be administered in liposomes, i.e., immunoliposomes (see, e.g., Maruyama et al., Biochim. Biophys. Acta, Vol. 1234, pp. 74-80, 1995). In certain embodiments, immunoconjugates, immunoliposomes or immunospheres containing an agent of the present invention is administered by inhalation.

[0268] In certain embodiments, antibodies may be topically administered to mucosa, such as the oropharynx, nasal cavity, respiratory tract, gastrointestinal tract, eye such as the conjunctival mucosa, vagina, urogenital mucosa, or for dermal application. In certain embodiments, antibodies are administered to the nasal, bronchial or pulmonary mucosa. In order to obtain optimal delivery of the antibodies to the pulmonary cavity in particular, it may

be advantageous to add a surfactant such as a phosphoglyceride, e.g. phosphatidylcholine, and/or a hydrophilic or hydrophobic complex of a positively or negatively charged excipient and a charged antibody of the opposite charge.

[0269] Other excipients suitable for pharmaceutical compositions intended for delivery of antibodies to the respiratory tract mucosa may be a) carbohydrates, e.g., monosaccharides such as fructose, galactose, glucose, D-mannose, sorbitol, and the like; disaccharides, such as lactose, trehalose, cellobiose, and the like; cyclodextrins, such as 2-hydroxypropyl- β -cyclodextrin; and polysaccharides, such as raffinose, maltodextrins, dextrans, and the like; b) amino acids, such as glycine, arginine, aspartic acid, glutamic acid, cysteine, lysine and the like; c) organic salts prepared from organic acids and bases, such as sodium citrate, sodium ascorbate, magnesium gluconate, sodium gluconate, tromethamine hydrochloride, and the like; d) peptides and proteins, such as aspartame, human serum albumin, gelatin, and the like; e) alditols, such as mannitol, xylitol, and the like, and f) polycationic polymers, such as chitosan or a chitosan salt or derivative.

[0270] For dermal application, the antibodies of the present invention may suitably be formulated with one or more of the following excipients: solvents, buffering agents, preservatives, humectants, chelating agents, antioxidants, stabilizers, emulsifying agents, suspending agents, gel-forming agents, ointment bases, penetration enhancers, and skin protective agents.

[0271] Examples of solvents are e.g. water, alcohols, vegetable or marine oils (e.g. edible oils like almond oil, castor oil, cacao butter, coconut oil, corn oil, cottonseed oil, linseed oil, olive oil, palm oil, peanut oil, poppy seed oil, rapeseed oil, sesame oil, soybean oil, sunflower oil, and tea seed oil), mineral oils, fatty oils, liquid paraffin, polyethylene glycols, propylene glycols, glycerol, liquid polyalkylsiloxanes, and mixtures thereof.

[0272] Examples of buffering agents are e.g. citric acid, acetic acid, tartaric acid, lactic acid, hydrogenphosphoric acid, diethyl amine etc. Suitable examples of preservatives for use in compositions are parabens, such as methyl, ethyl, propyl p-hydroxybenzoate, butylparaben, isobutylparaben, isopropylparaben, potassium sorbate, sorbic acid, benzoic acid, methyl benzoate, phenoxyethanol, bronopol, bronidox, MDM hydantoin, iodopropynyl butylcarbamate, EDTA, benzalconium chloride, and benzylalcohol, or mixtures of preservatives.

[0273] Examples of humectants are glycerin, propylene glycol, sorbitol, lactic acid, urea, and mixtures thereof.

[0274] Examples of antioxidants are butylated hydroxy anisole (BHA), ascorbic acid and derivatives thereof, tocopherol and derivatives thereof, cysteine, and mixtures thereof.

[0275] Examples of emulsifying agents are naturally occurring gums, e.g. gum acacia or gum tragacanth; naturally occurring phosphatides, e.g. soybean lecithin, sorbitan monooleate derivatives: wool fats; wool alcohols; sorbitan esters; monoglycerides; fatty alcohols; fatty acid esters (e.g. triglycerides of fatty acids); and mixtures thereof.

[0276] Examples of suspending agents are e.g. celluloses and cellulose derivatives such as, e.g., carboxymethyl cellulose, hydroxyethylcellulose, hydroxypropylcellulose, hydroxypropylmethylcellulose, carraghenan, acacia gum, arabic gum, tragacanth, and mixtures thereof.

[0277] Examples of gel bases, viscosity-increasing agents or components which are able to take up exudate from a wound are: liquid paraffin, polyethylene, fatty oils, colloidal silica or aluminum, zinc soaps, glycerol, propylene glycol, tragacanth, carboxyvinyl polymers, magnesium-aluminum silicates, Carbopol®, hydrophilic polymers such as, e.g. starch or cellulose derivatives such as, e.g., carboxymethylcellulose, hydroxyethylcellulose and other cellulose derivatives, water-swallowable hydrocolloids, carragenans, hyaluronates (e.g. hyaluronate gel optionally containing sodium chloride), and alginates including propylene glycol alginate.

[0278] Examples of ointment bases are e.g. beeswax, paraffin, cetanol, cetyl palmitate, vegetable oils, sorbitan esters of fatty acids (Span), polyethylene glycols, and condensation products between sorbitan esters of fatty acids and ethylene oxide, e.g. polyoxyethylene sorbitan monooleate (Tween).

[0279] Examples of hydrophobic or water-emulsifying ointment bases are paraffins, vegetable oils, animal fats, synthetic glycerides, waxes, lanolin, and liquid polyalkylsiloxanes. Examples of hydrophilic ointment bases are solid macrogols (polyethylene glycols). Other examples of ointment bases are triethanolamine soaps, sulphated fatty alcohol and polysorbates.

[0280] Examples of other excipients are polymers such as carmelose, sodium carmelose, hydroxypropylmethylcellulose, hydroxyethylcellulose, hydroxypropylcellulose, pectin, xanthan gum, locust bean gum, acacia gum, gelatin, carbomer, emulsifiers like vitamin E, glyceryl stearates, cetanyl glucoside, collagen, carrageenan, hyaluronates and alginates and chitosans.

[0281] The dose of antibody required in humans to be effective in the treatment cancer differs with the type and severity of the cancer to be treated, the age and condition of the patient, etc. Typical doses of antibody to be administered are in the range of 1 μg to 1 g, preferably 1-1000 μg , more preferably 2-500, even more preferably 5-50, most preferably 10-20 μg per unit dosage form. In certain embodiments, infusion of antibodies of the present invention may range from 10-500 mg/m^2 .

[0282] There are a variety of techniques available for introducing nucleic acids into viable cells. The techniques vary depending upon whether the nucleic acid is transferred into cultured cells *in vitro*, or *in vivo* in the cells of the intended host. Techniques suitable for the transfer of nucleic acid into mammalian cells *in vitro* include the use of liposomes, electroporation, microinjection, cell fusion, DEAE-dextran, the calcium phosphate precipitation method, etc. The currently preferred *in vivo* gene transfer techniques include transduction with viral (typically lentivirus, adeno associated virus (AAV) and adenovirus) vectors.

[0283] In certain embodiments, an agent that reduces a gene signature as described herein is used to treat a subject in need thereof having a cancer.

[0284] In one embodiment, the agent is a protein kinase C (PKC) activator. By "protein kinase C activator" is meant any compound that increases the catalytic activity of any protein kinase C (PKC) isoform (see, e.g., WO1998017299A1). The preferred catalytic activity that is enhanced is the kinase activity. Protein kinase C ("PKC") is a key enzyme in signal transduction involved in a variety of cellular functions, including cell growth, regulation of gene expression, and ion channel activity. The PKC family of isozymes includes at least 11 different protein kinases that can be divided into at least three subfamilies based on their homology and sensitivity to activators. Each isozyme includes a number of homologous ("conserved" or "C") domains interspersed with isozyme-unique ("variable" or "V") domains. Members of the "classical" or "cPKC" subfamily, α , β_1 , β_2 and γ PKC, contain four homologous domains (C1, C2, C3 and C4) and require calcium, phosphatidylserine, and diacylglycerol or phorbol esters for activation. In members of the "novel" or "nPKC" subfamily, δ , ϵ , η and θ PKC, a C2-like domain precedes the C1 domain. However, that C2 domain does not bind calcium and therefore the nPKC subfamily does not require calcium for activation. Finally, members of the "atypical" or "aPKC" subfamily, ζ and λ PKC, lack both the C2 and one-half of the C1 homologous domains and are insensitive to diacylglycerol, phorbol esters and calcium. Studies on the subcellular distribution of PKC isozymes

demonstrate that activation of PKC results in its redistribution in the cells (also termed trans location), such that activated PKC isozymes associate with the plasma membrane, cytoskeletal elements, nuclei, and other subcellular compartments (Saito, N. et al, Proc. Natl. Acad. Sci. USA 86:3409-3413 (1989); Papadopoulos, V. and Hall, P.F. J. Cell Biol. 108:553-567 (1989); Mochly-Rosen, D., et al., Molec. Biol. Cell (formerly Cell Reg.) 1 :693-706, (1990)).

[0285] Mochly-Rosen, D., et al. discusses activation of PKC (Nat Rev Drug Discov. 2012 Dec; 11(12): 937-957). PKC isozymes are activated by a variety of hormones, such as adrenalin and angiotensin, by growth factors, including epidermal growth factor and insulin, and by neurotransmitters such as dopamine and endorphin; these stimulators, when bound to their respective receptors, activate members of the phospholipase C family, which generates diacylglycerol, a lipid-derived second messenger. The novel isozymes (PKC δ , ϵ , θ and η) are activated by diacylglycerol alone, whereas the four conventional PKC isozymes (PKC α , β I, β II and γ) also require calcium for their activation. Cellular calcium levels are elevated along with diacylglycerol, because the latter is often co-produced with inositol trisphosphate (IP3), which triggers calcium release into the cytosol from internal stores. Activation of PKC can also occur in the absence of the above second messengers. High levels of cytosolic calcium can directly activate phospholipase C, thus leading to PKC activation in the absence of receptor activation. A number of post-translational modifications of PKC were also found to lead to activation of select PKC isozymes both in normal and disease states. These include activation by proteolysis between the regulatory and the catalytic domain that was noted to occur for PKC5, for example. Phosphorylation of a number of sites may be required for maturation of the newly synthesized enzyme, but also for activation of mature isozymes, e.g. H2O2-induced tyrosine phosphorylation of PKC5. Other modifications including oxidation, acetylation and nitration have also been found to activate PKC.

[0286] In one embodiment, the agent is an inhibitor of the **NFKB** pathway. Inhibitors of the **NFKB** pathway have been described (see, e.g., Gilmore and Herscovitch, Inhibitors of **NF-kappaB** signaling: 785 and counting. Oncogene (2006) 25, 6887-6899). These compounds include chemicals, metals, metabolites, synthetic compounds, antioxidants, peptides, small RNA/DNA, microbial and viral proteins, small molecules, and engineered dominant-negative or constitutively active polypeptides.

[0287] In one embodiment, the agent is an IGF1R inhibitor. IGF1R inhibitors are well known in the art (see, e.g., King et al., Can we unlock the potential of IGF-1R inhibition in

cancer therapy? Cancer Treat Rev. 2014 Oct; 40(9): 1096-1105). IGF1R inhibitors may include, but are not limited to monoclonal anti-IGF1R antibodies, small molecule tyrosine kinase inhibitors (TKIs), and IGF ligand antibodies.

[0288] In one embodiment, the agent is Reserpine (methyl 18P-hydroxy-1,17 a-dimethoxy-3p, 20a-yohimban-16P-carboxylate 3,4,5-trimethoxybenzoate) or derivative thereof. Reserpine is an alkaloid first isolated from *Rauwolfia serpentina*. Reserpine (also known by trade names Raudixin, Serpalan, Serpasil) is an indole alkaloid, antipsychotic, and antihypertensive drug that has been used for the control of high blood pressure and for the relief of psychotic symptoms, although because of the development of better drugs for these purposes and because of its numerous side-effects, it is rarely used today. The antihypertensive actions of reserpine are a result of its ability to deplete catecholamines (among other monoamine neurotransmitters) from peripheral sympathetic nerve endings. These substances are normally involved in controlling heart rate, force of cardiac contraction and peripheral vascular resistance. The daily dose of reserpine in antihypertensive treatment is as low as 0.1 to 0.25 mg. In certain embodiments, the dose is significantly higher for the treatment of cancer. A skilled practitioner would know to adjust the dose based on response to the drug. For example, reduction of an immunotherapy resistance signature or decrease in tumor size and/or proliferation. In certain embodiments, Reserpine is administered directly to a tumor. In certain embodiments, reserpine is administered over the course of a single day or week or month.

[0289] Typical of the known rauwolfia alkaloids are deserpidine, alperaxylon, reserpine, and rauwolfia serpentina. Oral dosage of the rauwolfia alkaloid should be carefully adjusted according to individual tolerance and response, using the lowest possible effective dosage. Typically, the amount of rauwolfia alkaloid administered daily is from about 0.001 to about 0.01 mg per kg of body weight.

[0290] In certain embodiments, the agent capable of modulating a signature as described herein is a cell cycle inhibitor (see e.g., Dickson and Schwartz, Development of cell-cycle inhibitors for cancer therapy, Curr Oncol. 2009 Mar; 16(2): 36-43). In one embodiment, the agent capable of modulating a signature as described herein is a CDK4/6 inhibitor, such as LEE011, palbociclib (PD-0332991), and Abemaciclib (LY2835219) (see, e.g., US9259399B2; WO2016025650A1; US Patent Publication No. 20140031325; US Patent Publication No. 20140080838; US Patent Publication No. 20130303543; US Patent Publication No. 2007/0027147; US Patent Publication No. 2003/0229026; US Patent

Publication No 2004/0048915; US Patent Publication No. 2004/0006074; US Patent Publication No. 2007/01791 18; each of which is incorporated by reference herein in its entirety). Currently there are three CDK4/6 inhibitors that are either approved or in late-stage development: palbociclib (PD-0332991; Pfizer), ribociclib (LEE011; Novartis), and abemaciclib (LY2835219; Lilly) (see e.g., Hamilton and Infante, Targeting CDK4/6 in patients with cancer, Cancer Treatment Reviews, Volume 45, April 2016, Pages 129-138).

[0291] In certain embodiments, an agent that reduces an immunotherapy resistance signature is co-administered with an immunotherapy or is administered before administration of an immunotherapy. The immunotherapy may be adoptive cell transfer therapy, as described herein or may be an inhibitor of any check point protein described herein. Specific check point inhibitors include, but are not limited to anti-CTLA4 antibodies (e.g., Ipilimumab), anti-PD-1 antibodies (e.g., Nivolumab, Pembrolizumab), and anti-PD-L1 antibodies (e.g., Atezolizumab).

[0292] In another aspect, provided is a pharmaceutical pack or kit, comprising one or more containers filled with one or more of the ingredients of the pharmaceutical compositions.

[0293] In another aspect, provided is a kit for detecting the gene signature as described herein.

[0294] With respect to general information on CRISPR-Cas Systems, components thereof, and delivery of such components, including methods, materials, delivery vehicles, vectors, particles, AAV, and making and using thereof, including as to amounts and formulations, all useful in the practice of the instant invention, reference is made to: US Patents Nos. 8,999,641, 8,993,233, 8,945,839, 8,932,814, 8,906,616, 8,895,308, 8,889,418, 8,889,356, 8,871,445, 8,865,406, 8,795,965, 8,771,945 and 8,697,359; US Patent Publications US 2014-0310830 (US APP. Ser. No. 14/105,031), US 2014-0287938 A1 (U.S. App. Ser. No. 14/213,991), US 2014-0273234 A1 (U.S. App. Ser. No. 14/293,674), US2014-0273232 A1 (U.S. App. Ser. No. 14/290,575), US 2014-0273231 (U.S. App. Ser. No. 14/259,420), US 2014-0256046 A1 (U.S. App. Ser. No. 14/226,274), US 2014-0248702 A1 (U.S. App. Ser. No. 14/258,458), US 2014-0242700 A1 (U.S. App. Ser. No. 14/222,930), US 2014-0242699 A1 (U.S. App. Ser. No. 14/183,512), US 2014-0242664 A1 (U.S. App. Ser. No. 14/104,990), US 2014-0234972 A1 (U.S. App. Ser. No. 14/183,471), US 2014-0227787 A1 (U.S. App. Ser. No. 14/256,912), US 2014-0189896 A1 (U.S. App. Ser. No. 14/105,035), US 2014-0186958 (U.S. App. Ser. No. 14/105,017), US 2014-0186919 A1 (U.S. App. Ser.

No. 14/104,977), US 2014-0186843 A1 (U.S. App. Ser. No. 14/104,900), US 2014-0179770 A1 (U.S. App. Ser. No. 14/104,837) and US 2014-0179006 A1 (U.S. App. Ser. No. 14/183,486), US 2014-0170753 (US App Ser No 14/183,429); European Patents EP 2 784 162 B1 and EP 2 771 468 B1; European Patent Applications EP 2 771 468 (EP13818570.7), EP 2 764 103 (EP13824232.6), and EP 2 784 162 (EP 14 1703 83.5); and PCT Patent Publications PCT Patent Publications WO 2014/093661 (PCT/US20 13/074743), WO 2014/093694 (PCT/US20 13/074790), WO 2014/093595 (PCT/US20 13/0746 11), WO 2014/093718 (PCT/US20 13/074825), WO 2014/093709 (PCT/US20 13/0748 12), WO 2014/093622 (PCT/US20 13/074667), WO 2014/093635 (PCT/US20 13/074691), WO 2014/093655 (PCT/US20 13/07473 6), WO 2014/093712 (PCT/US20 13/0748 19), WO20 14/093 701 (PCT/US20 13/074800), WO20 14/0 18423 (PCT/US2013/051418), WO 2014/204723 (PCT/US20 14/04 1790), WO 2014/204724 (PCT/US20 14/04 1800), WO 2014/204725 (PCT/US20 14/04 1803), WO 2014/204726 (PCT/US20 14/04 1804), WO 2014/204727 (PCT/US20 14/04 1806), WO 2014/204728 (PCT/US20 14/04 1808), WO 2014/204729 (PCT/US2014/041809). Reference is also made to US provisional patent applications 61/758,468; 61/802,174; 61/806,375; 61/814,263; 61/819,803 and 61/828,130, filed on January 30, 2013; March 15, 2013; March 28, 2013; April 20, 2013; May 6, 2013 and May 28, 2013 respectively. Reference is also made to US provisional patent application 61/836,123, filed on June 17, 2013. Reference is additionally made to US provisional patent applications 61/835,931, 61/835,936, 61/836,127, 61/836, 101, 61/836,080 and 61/835,973, each filed June 17, 2013. Further reference is made to US provisional patent applications 61/862,468 and 61/862,355 filed on August 5, 2013; 61/871,301 filed on August 28, 2013; 61/960,777 filed on September 25, 2013 and 61/961,980 filed on October 28, 2013. Reference is yet further made to: PCT Patent applications Nos: PCT/US2014/041803, PCT/US20 14/04 1800, PCT/US20 14/04 1809, PCT/US20 14/04 1804 and PCT/US20 14/04 1806, each filed June 10, 2014 6/10/14; PCT/US20 14/04 1808 filed June 11, 2014; and PCT/US2014/62558 filed October 28, 2014, and US Provisional Patent Applications Serial Nos.: 61/915,150, 61/915,301, 61/915,267 and 61/915,260, each filed December 12, 2013; 61/757,972 and 61/768,959, filed on January 29, 2013 and February 25, 2013; 61/835,936, 61/836,127, 61/836,101, 61/836,080, 61/835,973, and 61/835,931, filed June 17, 2013; 62/010,888 and 62/010,879, both filed June 11, 2014; 62/010,329 and 62/010,441, each filed June 10, 2014; 61/939,228 and 61/939,242, each filed February 12, 2014; 61/980,012, filed April 15,2014; 62/038,358, filed August 17, 2014; 62/054,490,

62/055,484, 62/055,460 and 62/055,487, each filed September 25, 2014; and 62/069,243, filed October 27, 2014. Reference is also made to US provisional patent applications Nos. 62/055,484, 62/055,460, and 62/055,487, filed September 25, 2014; US provisional patent application 61/980,012, filed April 15, 2014; and US provisional patent application 61/939,242 filed February 12, 2014. Reference is made to PCT application designating, inter alia, the United States, application No. PCT/US14/41806, filed June 10, 2014. Reference is made to US provisional patent application 61/930,214 filed on January 22, 2014. Reference is made to US provisional patent applications 61/915,251; 61/915,260 and 61/915,267, each filed on December 12, 2013. Reference is made to US provisional patent application USSN 61/980,012 filed April 15, 2014. Reference is made to PCT application designating, inter alia, the United States, application No. PCT/US 14/4 1806, filed June 10, 2014. Reference is made to US provisional patent application 61/930,214 filed on January 22, 2014. Reference is made to US provisional patent applications 61/915,251; 61/915,260 and 61/915,267, each filed on December 12, 2013.

[0295] Mention is also made of US application 62/091,455, filed, 12-Dec-14, PROTECTED GUIDE RNAS (PGRNAS); US application 62/096,708, 24-Dec-14, PROTECTED GUIDE RNAS (PGRNAS); US application 62/091,462, 12-Dec-14, DEAD GUIDES FOR CRISPR TRANSCRIPTION FACTORS; US application 62/096,324, 23-Dec-14, DEAD GUIDES FOR CRISPR TRANSCRIPTION FACTORS; US application 62/091,456, 12-Dec-14, ESCORTED AND FUNCTIONALIZED GUIDES FOR CRISPR-CAS SYSTEMS; US application 62/091,461, 12-Dec-14, DELIVERY, USE AND THERAPEUTIC APPLICATIONS OF THE CRISPR-CAS SYSTEMS AND COMPOSITIONS FOR GENOME EDITING AS TO HEMATOPOETIC STEM CELLS (HSCs); US application 62/094,903, 19-Dec-14, UNBIASED IDENTIFICATION OF DOUBLE-STRAND BREAKS AND GENOMIC REARRANGEMENT BY GENOME-WISE INSERT CAPTURE SEQUENCING; US application 62/096,761, 24-Dec-14, ENGINEERING OF SYSTEMS, METHODS AND OPTIMIZED ENZYME AND GUIDE SCAFFOLDS FOR SEQUENCE MANIPULATION; US application 62/098,059, 30-Dec-14, RNA-TARGETING SYSTEM; US application 62/096,656, 24-Dec-14, CRISPR HAVING OR ASSOCIATED WITH DESTABILIZATION DOMAINS; US application 62/096,697, 24-Dec-14, CRISPR HAVING OR ASSOCIATED WITH AAV; US application 62/098,158, 30-Dec-14, ENGINEERED CRISPR COMPLEX INSERTIONAL TARGETING SYSTEMS; US application 62/151,052, 22-Apr-15, CELLULAR TARGETING FOR

EXTRACELLULAR EXOSOMAL REPORTING; US application 62/054,490, 24-Sep-14, DELIVERY, USE AND THERAPEUTIC APPLICATIONS OF THE CRISPR-CAS SYSTEMS AND COMPOSITIONS FOR TARGETING DISORDERS AND DISEASES USING PARTICLE DELIVERY COMPONENTS; US application 62/055,484, 25-Sep-14, SYSTEMS, METHODS AND COMPOSITIONS FOR SEQUENCE MANIPULATION WITH OPTIMIZED FUNCTIONAL CRISPR-CAS SYSTEMS; US application 62/087,537, 4-Dec-14, SYSTEMS, METHODS AND COMPOSITIONS FOR SEQUENCE MANIPULATION WITH OPTIMIZED FUNCTIONAL CRISPR-CAS SYSTEMS; US application 62/054,651, 24-Sep-14, DELIVERY, USE AND THERAPEUTIC APPLICATIONS OF THE CRISPR-CAS SYSTEMS AND COMPOSITIONS FOR MODELING COMPETITION OF MULTIPLE CANCER MUTATIONS *IN VIVO*; US application 62/067,886, 23-Oct-14, DELIVERY, USE AND THERAPEUTIC APPLICATIONS OF THE CRISPR-CAS SYSTEMS AND COMPOSITIONS FOR MODELING COMPETITION OF MULTIPLE CANCER MUTATIONS *IN VIVO*; US application 62/054,675, 24-Sep-14, DELIVERY, USE AND THERAPEUTIC APPLICATIONS OF THE CRISPR-CAS SYSTEMS AND COMPOSITIONS IN NEURONAL CELLS/TISSUES; US application 62/054,528, 24-Sep-14, DELIVERY, USE AND THERAPEUTIC APPLICATIONS OF THE CRISPR-CAS SYSTEMS AND COMPOSITIONS IN IMMUNE DISEASES OR DISORDERS; US application 62/055,454, 25-Sep-14, DELIVERY, USE AND THERAPEUTIC APPLICATIONS OF THE CRISPR-CAS SYSTEMS AND COMPOSITIONS FOR TARGETING DISORDERS AND DISEASES USING CELL PENETRATION PEPTIDES (CPP); US application 62/055,460, 25-Sep-14, MULTIFUNCTIONAL-CRISPR COMPLEXES AND/OR OPTIMIZED ENZYME LINKED FUNCTIONAL-CRISPR COMPLEXES; US application 62/087,475, 4-Dec-14, FUNCTIONAL SCREENING WITH OPTIMIZED FUNCTIONAL CRISPR-CAS SYSTEMS; US application 62/055,487, 25-Sep-14, FUNCTIONAL SCREENING WITH OPTIMIZED FUNCTIONAL CRISPR-CAS SYSTEMS; US application 62/087,546, 4-Dec-14, MULTIFUNCTIONAL CRISPR COMPLEXES AND/OR OPTIMIZED ENZYME LINKED FUNCTIONAL-CRISPR COMPLEXES; and US application 62/098,285, 30-Dec-14, CRISPR MEDIATED *IN VIVO* MODELING AND GENETIC SCREENING OF TUMOR GROWTH AND METASTASIS.

[0296] Each of these patents, patent publications, and applications, and all documents cited therein or during their prosecution ("appln cited documents") and all documents cited or

referenced in the appln cited documents, together with any instructions, descriptions, product specifications, and product sheets for any products mentioned therein or in any document therein and incorporated by reference herein, are hereby incorporated herein by reference, and may be employed in the practice of the invention. All documents (e.g., these patents, patent publications and applications and the appln cited documents) are incorporated herein by reference to the same extent as if each individual document was specifically and individually indicated to be incorporated by reference.

[0297] Also with respect to general information on CRISPR-Cas Systems, mention is made of the following (also hereby incorporated herein by reference):

- Multiplex genome engineering using CRISPR/Cas systems. Cong, L., Ran, F.A., Cox, D., Lin, S., Barretto, R., Habib, N., Hsu, P.D., Wu, X., Jiang, W., Marraffini, L.A., & Zhang, F. *Science* Feb 15;339(6121):819-23 (2013);
- > RNA-guided editing of bacterial genomes using CRISPR-Cas systems. Jiang W., Bikard D., Cox D., Zhang F, Marraffini LA. *Nat Biotechnol* Mar;31(3):233-9 (2013);
- One-Step Generation of Mice Carrying Mutations in Multiple Genes by CRISPR/Cas-Mediated Genome Engineering. Wang H., Yang H., Shivalila CS., Dawlaty MM., Cheng AW., Zhang F., Jaenisch R. *Cell* May 9;153(4):910-8 (2013);
- Optical control of mammalian endogenous transcription and epigenetic states. Konermann S, Brigham MD, Trevino AE, Hsu PD, Heidenreich M, Cong L, Piatt RJ, Scott DA, Church GM, Zhang F. *Nature*. Aug 22;500(7463):472-6. doi: 10.1038/Nature12466. Epub 2013 Aug 23 (2013);
- > Double Nicking by RNA-Guided CRISPR Cas9 for Enhanced Genome Editing Specificity. Ran, FA., Hsu, PD., Lin, CY., Gootenberg, JS., Konermann, S., Trevino, AE., Scott, DA., Inoue, A., Matoba, S., Zhang, Y., & Zhang, F. *Cell* Aug 28. pii: S0092-8674(13)01015-5 (2013-A);
- > DNA targeting specificity of RNA-guided Cas9 nucleases. Hsu, P., Scott, D., Weinstein, J., Ran, FA., Konermann, S., Agarwala, V., Li, Y., Fine, E., Wu, X., Shalem, O., Cradick, TJ., Marraffini, LA., Bao, G., & Zhang, F. *Nat Biotechnol* doi:10.1038/nbt.2647 (2013);

- Genome engineering using the CRISPR-Cas9 system. Ran, FA., Hsu, PD., Wright, J., Agarwala, V., Scott, DA., Zhang, F. *Nature Protocols* Nov;8(11):2281-308 (2013-B);
- Genome-Scale CRISPR-Cas9 Knockout Screening in Human Cells. Shalem, O., Sanjana, NE., Hartenian, E., Shi, X., Scott, DA., Mikkelsen, T., Heckl, D., Ebert, BL., Root, DE., Doench, JG., Zhang, F. *Science* Dec 12. (2013). [Epub ahead of print];
- Crystal structure of cas9 in complex with guide RNA and target DNA. Nishimasu, H., Ran, FA., Hsu, PD., Konermann, S., Shehata, SI., Dohmae, N., Ishitani, R., Zhang, F., Nureki, O. *Cell* Feb 27, 156(5):935-49 (2014);
- Genome-wide binding of the CRISPR endonuclease Cas9 in mammalian cells. Wu X., Scott DA., Kriz AJ., Chiu AC, Hsu PD., Dadon DB., Cheng AW., Trevino AE., Konermann S., Chen S., Jaenisch R., Zhang F., Sharp PA. *Nat Biotechnol.* Apr 20. doi: 10.1038/nbt.2889 (2014);
- CRISPR-Cas9 Knockin Mice for Genome Editing and Cancer Modeling. Piatt RJ, Chen S, Zhou Y, Yim MJ, Swiech L, Kempton HR, Dahlman JE, Parnas O, Eisenhaure TM, Jovanovic M, Graham DB, Jhunjhunwala S, Heidenreich M, Xavier RJ, Langer R, Anderson DG, Hacohen N, Regev A, Feng G, Sharp PA, Zhang F. *Cell* 159(2): 440-455 DOI: 10.1016/j.cell.2014.09.014(2014);
- Development and Applications of CRISPR-Cas9 for Genome Engineering, Hsu PD, Lander ES, Zhang F., *Cell.* Jun 5;157(6): 1262-78 (2014).
- Genetic screens in human cells using the CRISPR/Cas9 system, Wang T, Wei JJ, Sabatini DM, Lander ES., *Science.* January 3; 343(6166): 80-84. doi: 10.1126/science.1246981 (2014);
- Rational design of highly active sgRNAs for CRISPR-Cas9-mediated gene inactivation, Doench JG, Hartenian E, Graham DB, Tothova Z, Hegde M, Smith I, Sullender M, Ebert BL, Xavier RJ, Root DE., (published online 3 September 2014) *Nat Biotechnol.* Dec;32(12): 1262-7 (2014);
- *In vivo* interrogation of gene function in the mammalian brain using CRISPR-Cas9, Swiech L, Heidenreich M, Banerjee A, Habib N, Li Y, Trombetta J, Sur M, Zhang F., (published online 19 October 2014) *Nat Biotechnol.* Jan;33(1): 102-6 (2015);

- Genome-scale transcriptional activation by an engineered CRISPR-Cas9 complex, Konermann S, Brigham MD, Trevino AE, Joung J, Abudayyeh O, Barcena C, Hsu PD, Habib N, Gootenberg JS, Nishimasu H, Nureki O, Zhang F., Nature. Jan 29;517(7536):583-8 (2015).
- A split-Cas9 architecture for inducible genome editing and transcription modulation, Zetsche B, Volz SE, Zhang F., (published online 02 February 2015) Nat Biotechnol. Feb;33(2): 139-42 (2015);
- Genome-wide CRISPR Screen in a Mouse Model of Tumor Growth and Metastasis, Chen S, Sanjana NE, Zheng K, Shalem O, Lee K, Shi X, Scott DA, Song J, Pan JQ, Weissleder R, Lee H, Zhang F, Sharp PA. Cell 160, 1246-1260, March 12, 2015 (multiplex screen in mouse), and
- > *In vivo* genome editing using Staphylococcus aureus Cas9, Ran FA, Cong L, Yan WX, Scott DA, Gootenberg JS, Kriz AJ, Zetsche B, Shalem O, Wu X, Makarova KS, Koonin EV, Sharp PA, Zhang F., (published online 01 April 2015), Nature. Apr 9;520(7546): 186-91 (2015).
- Shalem et al., "High-throughput functional genomics using CRISPR-Cas9," Nature Reviews Genetics 16, 299-311 (May 2015).
- Xu et al., "Sequence determinants of improved CRISPR sgRNA design," Genome Research 25, 1147-1157 (August 2015).
- Parnas et al., "A Genome-wide CRISPR Screen in Primary Immune Cells to Dissect Regulatory Networks," Cell 162, 675-686 (July 30, 2015).
- Ramanan et al., "CRISPR/Cas9 cleavage of viral DNA efficiently suppresses hepatitis B virus," Scientific Reports 5:10833. doi: 10.1038/srep10833 (June 2, 2015)
- > Nishimasu et al., "Crystal Structure of Staphylococcus aureus Cas9," Cell 162, 1113-1126 (Aug. 27, 2015)
- > BCL11A enhancer dissection by Cas9-mediated in situ saturating mutagenesis, Canver et al., Nature 527(7577): 192-7 (Nov. 12, 2015) doi: 10.1038/nature15521. Epub 2015 Sep 16.
- *Cpf1 Is a Single RNA-Guided Endonuclease of a Class 2 CRISPR-Cas System*, Zetsche et al., Cell 163, 759-771 (Sep 25, 2015).

- *Discovery and Functional Characterization of Diverse Class 2 CRISPR-Cas Systems*, Shmakov et al., *Molecular Cell*, 60(3), 385-397 doi: 10.1016/j.molcel.2015.10.008 Epub October 22, 2015.
- *Rationally engineered Cas9 nucleases with improved specificity*, Slaymaker et al., *Science* 2016 Jan 1 351(6268): 84-88 doi: 10.1126/science.125227. Epub 2015 Dec 1.
- Gao *et al.*, "Engineered Cpf1 Enzymes with Altered PAM Specificities," bioRxiv 091611; doi: <http://dx.doi.org/10.1101/091611> (Dec. 4, 2016).

each of which is incorporated herein by reference, may be considered in the practice of the instant invention, and discussed briefly below:

- Cong et al. engineered type II CRISPR-Cas systems for use in eukaryotic cells based on both *Streptococcus thermophilus* Cas9 and also *Streptococcus pyogenes* Cas9 and demonstrated that Cas9 nucleases can be directed by short RNAs to induce precise cleavage of DNA in human and mouse cells. Their study further showed that Cas9 as converted into a nicking enzyme can be used to facilitate homology-directed repair in eukaryotic cells with minimal mutagenic activity. Additionally, their study demonstrated that multiple guide sequences can be encoded into a single CRISPR array to enable simultaneous editing of several at endogenous genomic loci sites within the mammalian genome, demonstrating easy programmability and wide applicability of the RNA-guided nuclease technology. This ability to use RNA to program sequence specific DNA cleavage in cells defined a new class of genome engineering tools. These studies further showed that other CRISPR loci are likely to be transplantable into mammalian cells and can also mediate mammalian genome cleavage. Importantly, it can be envisaged that several aspects of the CRISPR-Cas system can be further improved to increase its efficiency and versatility.
- Jiang et al. used the clustered, regularly interspaced, short palindromic repeats (CRISPR)-associated Cas9 endonuclease complexed with dual-RNAs to introduce precise mutations in the genomes of *Streptococcus pneumoniae* and *Escherichia coli*. The approach relied on dual-RNA:Cas9-directed cleavage at the targeted genomic site to kill unmutated cells and circumvents the need for selectable markers or counter-selection systems. The study reported reprogramming dual-RNA:Cas9 specificity by changing the sequence of short CRISPR RNA (crRNA)

to make single- and multinucleotide changes carried on editing templates. The study showed that simultaneous use of two crRNAs enabled multiplex mutagenesis. Furthermore, when the approach was used in combination with recombineering, in *S. pneumoniae*, nearly 100% of cells that were recovered using the described approach contained the desired mutation, and in *E. coli*, 65% that were recovered contained the mutation.

- Wang et al. (2013) used the CRISPR/Cas system for the one-step generation of mice carrying mutations in multiple genes which were traditionally generated in multiple steps by sequential recombination in embryonic stem cells and/or time-consuming intercrossing of mice with a single mutation. The CRISPR/Cas system will greatly accelerate the *in vivo* study of functionally redundant genes and of epistatic gene interactions.
- Konermann et al. (2013) addressed the need in the art for versatile and robust technologies that enable optical and chemical modulation of DNA-binding domains based CRISPR Cas9 enzyme and also Transcriptional Activator Like Effectors
- Ran et al. (2013-A) described an approach that combined a Cas9 nickase mutant with paired guide RNAs to introduce targeted double-strand breaks. This addresses the issue of the Cas9 nuclease from the microbial CRISPR-Cas system being targeted to specific genomic loci by a guide sequence, which can tolerate certain mismatches to the DNA target and thereby promote undesired off-target mutagenesis. Because individual nicks in the genome are repaired with high fidelity, simultaneous nicking via appropriately offset guide RNAs is required for double-stranded breaks and extends the number of specifically recognized bases for target cleavage. The authors demonstrated that using paired nicking can reduce off-target activity by 50- to 1,500-fold in cell lines and to facilitate gene knockout in mouse zygotes without sacrificing on-target cleavage efficiency. This versatile strategy enables a wide variety of genome editing applications that require high specificity.
- Hsu et al. (2013) characterized SpCas9 targeting specificity in human cells to inform the selection of target sites and avoid off-target effects. The study evaluated >700 guide RNA variants and SpCas9-induced indel mutation levels at >100 predicted genomic off-target loci in 293T and 293FT cells. The authors that

SpCas9 tolerates mismatches between guide RNA and target DNA at different positions in a sequence-dependent manner, sensitive to the number, position and distribution of mismatches. The authors further showed that SpCas9-mediated cleavage is unaffected by DNA methylation and that the dosage of SpCas9 and sgRNA can be titrated to minimize off-target modification. Additionally, to facilitate mammalian genome engineering applications, the authors reported providing a web-based software tool to guide the selection and validation of target sequences as well as off-target analyses.

- Ran et al. (2013-B) described a set of tools for Cas9-mediated genome editing via non-homologous end joining (NHEJ) or homology-directed repair (HDR) in mammalian cells, as well as generation of modified cell lines for downstream functional studies. To minimize off-target cleavage, the authors further described a double-nicking strategy using the Cas9 nickase mutant with paired guide RNAs. The protocol provided by the authors experimentally derived guidelines for the selection of target sites, evaluation of cleavage efficiency and analysis of off-target activity. The studies showed that beginning with target design, gene modifications can be achieved within as little as 1-2 weeks, and modified clonal cell lines can be derived within 2-3 weeks.
- Shalem et al. described a new way to interrogate gene function on a genome-wide scale. Their studies showed that delivery of a genome-scale CRISPR-Cas9 knockout (GeCKO) library targeted 18,080 genes with 64,751 unique guide sequences enabled both negative and positive selection screening in human cells. First, the authors showed use of the GeCKO library to identify genes essential for cell viability in cancer and pluripotent stem cells. Next, in a melanoma model, the authors screened for genes whose loss is involved in resistance to vemurafenib, a therapeutic that inhibits mutant protein kinase BRAF. Their studies showed that the highest-ranking candidates included previously validated genes NF1 and MED12 as well as novel hits NF2, CUL3, TADA2B, and TADA1. The authors observed a high level of consistency between independent guide RNAs targeting the same gene and a high rate of hit confirmation, and thus demonstrated the promise of genome-scale screening with Cas9.
- Nishimasu et al. reported the crystal structure of *Streptococcus pyogenes* Cas9 in complex with sgRNA and its target DNA at 2.5 Å resolution. The structure

revealed a bilobed architecture composed of target recognition and nuclease lobes, accommodating the sgRNA:DNA heteroduplex in a positively charged groove at their interface. Whereas the recognition lobe is essential for binding sgRNA and DNA, the nuclease lobe contains the HNH and RuvC nuclease domains, which are properly positioned for cleavage of the complementary and non-complementary strands of the target DNA, respectively. The nuclease lobe also contains a carboxyl-terminal domain responsible for the interaction with the protospacer adjacent motif (PAM). This high-resolution structure and accompanying functional analyses have revealed the molecular mechanism of RNA-guided DNA targeting by Cas9, thus paving the way for the rational design of new, versatile genome-editing technologies.

- Wu et al. mapped genome-wide binding sites of a catalytically inactive Cas9 (dCas9) from *Streptococcus pyogenes* loaded with single guide RNAs (sgRNAs) in mouse embryonic stem cells (mESCs). The authors showed that each of the four sgRNAs tested targeted dCas9 to between tens and thousands of genomic sites, frequently characterized by a 5-nucleotide seed region in the sgRNA and an NGG protospacer adjacent motif (PAM). Chromatin inaccessibility decreases dCas9 binding to other sites with matching seed sequences; thus 70% of off-target sites are associated with genes. The authors showed that targeted sequencing of 295 dCas9 binding sites in mESCs transfected with catalytically active Cas9 identified only one site mutated above background levels. The authors proposed a two-state model for Cas9 binding and cleavage, in which a seed match triggers binding but extensive pairing with target DNA is required for cleavage.
- Piatt et al. established a Cre-dependent Cas9 knockin mouse. The authors demonstrated *in vivo* as well as *ex vivo* genome editing using adeno-associated virus (AAV)-, lentivirus-, or particle-mediated delivery of guide RNA in neurons, immune cells, and endothelial cells.
- Hsu et al. (2014) is a review article that discusses generally CRISPR-Cas9 history from yogurt to genome editing, including genetic screening of cells.
- Wang et al. (2014) relates to a pooled, loss-of-function genetic screening approach suitable for both positive and negative selection that uses a genome-scale lentiviral single guide RNA (sgRNA) library.

- > Doench et al. created a pool of sgRNAs, tiling across all possible target sites of a panel of six endogenous mouse and three endogenous human genes and quantitatively assessed their ability to produce null alleles of their target gene by antibody staining and flow cytometry. The authors showed that optimization of the PAM improved activity and also provided an on-line tool for designing sgRNAs.
- Swiech et al. demonstrate that AAV-mediated SpCas9 genome editing can enable reverse genetic studies of gene function in the brain.
- > Konermann et al. (2015) discusses the ability to attach multiple effector domains, e.g., transcriptional activator, functional and epigenomic regulators at appropriate positions on the guide such as stem or tetraloop with and without linkers.
- Zetsche et al. demonstrates that the Cas9 enzyme can be split into two and hence the assembly of Cas9 for activation can be controlled.
- > Chen et al. relates to multiplex screening by demonstrating that a genome-wide *in vivo* CRISPR-Cas9 screen in mice reveals genes regulating lung metastasis.
- Ran et al. (2015) relates to SaCas9 and its ability to edit genomes and demonstrates that one cannot extrapolate from biochemical assays.
- Shalem et al. (2015) described ways in which catalytically inactive Cas9 (dCas9) fusions are used to synthetically repress (CRISPRi) or activate (CRISPRa) expression, showing advances using Cas9 for genome-scale screens, including arrayed and pooled screens, knockout approaches that inactivate genomic loci and strategies that modulate transcriptional activity.
- Xu et al. (2015) assessed the DNA sequence features that contribute to single guide RNA (sgRNA) efficiency in CRISPR-based screens. The authors explored efficiency of CRISPR/Cas9 knockout and nucleotide preference at the cleavage site. The authors also found that the sequence preference for CRISPRi/a is substantially different from that for CRISPR/Cas9 knockout.
- Parnas et al. (2015) introduced genome-wide pooled CRISPR-Cas9 libraries into dendritic cells (DCs) to identify genes that control the induction of tumor necrosis factor (Tnf) by bacterial lipopolysaccharide (LPS). Known regulators of Tlr4 signaling and previously unknown candidates were identified and classified into three functional modules with distinct effects on the canonical responses to LPS.

- Ramanan et al (2015) demonstrated cleavage of viral episomal DNA (cccDNA) in infected cells. The HBV genome exists in the nuclei of infected hepatocytes as a 3.2kb double-stranded episomal DNA species called covalently closed circular DNA (cccDNA), which is a key component in the HBV life cycle whose replication is not inhibited by current therapies. The authors showed that sgRNAs specifically targeting highly conserved regions of HBV robustly suppresses viral replication and depleted cccDNA.
- > Nishimasu et al. (2015) reported the crystal structures of SaCas9 in complex with a single guide RNA (sgRNA) and its double-stranded DNA targets, containing the 5'-TTGAAT-3' PAM and the 5'-TTGGGT-3' PAM. A structural comparison of SaCas9 with SpCas9 highlighted both structural conservation and divergence, explaining their distinct PAM specificities and orthologous sgRNA recognition.
- Canver *et al.* (2015) demonstrated a CRISPR-Cas9-based functional investigation of non-coding genomic elements. The authors developed pooled CRISPR-Cas9 guide RNA libraries to perform *in situ* saturating mutagenesis of the human and mouse BCL1 1A enhancers which revealed critical features of the enhancers.
- Zetsche et al. (2015) reported characterization of Cpf1, a class 2 CRISPR nuclease from *Francisella novicida* U 112 having features distinct from Cas9. Cpf1 is a single RNA-guided endonuclease lacking tracrRNA, utilizes a T-rich protospacer-adjacent motif, and cleaves DNA via a staggered DNA double-stranded break.
- Shmakov et al. (2015) reported three distinct Class 2 CRISPR-Cas systems. Two system CRISPR enzymes (C2c1 and C2c3) contain RuvC-like endonuclease domains distantly related to Cpf1. Unlike Cpf1, C2c1 depends on both crRNA and tracrRNA for DNA cleavage. The third enzyme (C2c2) contains two predicted HEPN RNase domains and is tracrRNA independent.
- Slaymaker et al (2016) reported the use of structure-guided protein engineering to improve the specificity of *Streptococcus pyogenes* Cas9 (SpCas9). The authors developed "enhanced specificity" SpCas9 (eSpCas9) variants which maintained robust on-target cleavage with reduced off-target effects.

[0298] Also, "Dimeric CRISPR RNA-guided FokI nucleases for highly specific genome editing", Shengdar Q. Tsai, Nicolas Wyvekens, Cyd Khayter, Jennifer A. Foden, Vishal Thapar, Deepak Reyon, Mathew J. Goodwin, Martin J. Aryee, J. Keith Joung *Nature Biotechnology* 32(6): 569-77 (2014), relates to dimeric RNA-guided FokI Nucleases that

recognize extended sequences and can edit endogenous genes with high efficiencies in human cells.

[0299] The methods and tools provided herein are may be designed for use with or Cas13, a type II nuclease that does not make use of tracrRNA. Orthologs of Cas13 have been identified in different bacterial species as described herein. Further type II nucleases with similar properties can be identified using methods described in the art (Shmakov et al. 2015, 60:385-397; Abudayeh et al. 2016, Science, 5;353(6299)). In particular embodiments, such methods for identifying novel CRISPR effector proteins may comprise the steps of selecting sequences from the database encoding a seed which identifies the presence of a CRISPR Cas locus, identifying loci located within 10 kb of the seed comprising Open Reading Frames (ORFs) in the selected sequences, selecting therefrom loci comprising ORFs of which only a single ORF encodes a novel CRISPR effector having greater than 700 amino acids and no more than 90% homology to a known CRISPR effector. In particular embodiments, the seed is a protein that is common to the CRISPR-Cas system, such as Cas1. In further embodiments, the CRISPR array is used as a seed to identify new effector proteins.

[0300] One type of programmable DNA-binding domain is provided by artificial zinc-finger (ZF) technology, which involves arrays of ZF modules to target new DNA-binding sites in the genome. Each finger module in a ZF array targets three DNA bases. A customized array of individual zinc finger domains is assembled into a ZF protein (ZFP).

[0301] ZFPs can comprise a functional domain. The first synthetic zinc finger nucleases (ZFNs) were developed by fusing a ZF protein to the catalytic domain of the Type IIS restriction enzyme FokI. (Kim, Y. G. et al., 1994, Chimeric restriction endonuclease, Proc. Natl. Acad. Sci. U.S.A. 91, 883-887; Kim, Y. G. et al., 1996, Hybrid restriction enzymes: zinc finger fusions to Fok I cleavage domain. Proc. Natl. Acad. Sci. U.S.A. 93, 1156-1160). Increased cleavage specificity can be attained with decreased off target activity by use of paired ZFN heterodimers, each targeting different nucleotide sequences separated by a short spacer. (Doyon, Y. et al., 2011, Enhancing zinc-finger-nuclease activity with improved obligate heterodimeric architectures. Nat. Methods 8, 74-79). ZFPs can also be designed as transcription activators and repressors and have been used to target many genes in a wide variety of organisms.

[0302] In advantageous embodiments of the invention, the methods provided herein use isolated, non-naturally occurring, recombinant or engineered DNA binding proteins that comprise TALE monomers or TALE monomers or half monomers as a part of their

organizational structure that enable the targeting of nucleic acid sequences with improved efficiency and expanded specificity.

[0303] Naturally occurring TALEs or "wild type TALEs" are nucleic acid binding proteins secreted by numerous species of proteobacteria. TALE polypeptides contain a nucleic acid binding domain composed of tandem repeats of highly conserved monomer polypeptides that are predominantly 33, 34 or 35 amino acids in length and that differ from each other mainly in amino acid positions 12 and 13. In advantageous embodiments the nucleic acid is DNA. As used herein, the term "polypeptide monomers", "TALE monomers" or "monomers" will be used to refer to the highly conserved repetitive polypeptide sequences within the TALE nucleic acid binding domain and the term "repeat variable di-residues" or "RVD" will be used to refer to the highly variable amino acids at positions 12 and 13 of the polypeptide monomers. As provided throughout the disclosure, the amino acid residues of the RVD are depicted using the IUPAC single letter code for amino acids. A general representation of a TALE monomer which is comprised within the DNA binding domain is $X1-1-(X12X13)-X14-33$ or 34 or 35, where the subscript indicates the amino acid position and X represents any amino acid. X12X13 indicate the RVDs. In some polypeptide monomers, the variable amino acid at position 13 is missing or absent and in such monomers, the RVD consists of a single amino acid. In such cases the RVD may be alternatively represented as X^* , where X represents X12 and (*) indicates that X13 is absent. The DNA binding domain comprises several repeats of TALE monomers and this may be represented as $(X1-1-(X12X13)-X14-33$ or 34 or 35) $_z$, where in an advantageous embodiment, z is at least 5 to 40. In a further advantageous embodiment, z is at least 10 to 26.

[0304] The TALE monomers have a nucleotide binding affinity that is determined by the identity of the amino acids in its RVD. For example, polypeptide monomers with an RVD of NI preferentially bind to adenine (A), monomers with an RVD of NG preferentially bind to thymine (T), monomers with an RVD of HD preferentially bind to cytosine (C) and monomers with an RVD of NN preferentially bind to both adenine (A) and guanine (G). In yet another embodiment of the invention, monomers with an RVD of IG preferentially bind to T. Thus, the number and order of the polypeptide monomer repeats in the nucleic acid binding domain of a TALE determines its nucleic acid target specificity. In still further embodiments of the invention, monomers with an RVD of NS recognize all four base pairs and may bind to A, T, G or C. The structure and function of TALEs is further described in, for example, Moscou et al., Science 326:1501 (2009); Boch et al., Science 326:1509-1512

(2009); and Zhang et al., Nature Biotechnology 29:149-153 (2011), each of which is incorporated by reference in its entirety.

[0305] The polypeptides used in methods of the invention are isolated, non-naturally occurring, recombinant or engineered nucleic acid-binding proteins that have nucleic acid or DNA binding regions containing polypeptide monomer repeats that are designed to target specific nucleic acid sequences.

[0306] As described herein, polypeptide monomers having an RVD of HN or NH preferentially bind to guanine and thereby allow the generation of TALE polypeptides with high binding specificity for guanine containing target nucleic acid sequences. In a preferred embodiment of the invention, polypeptide monomers having RVDs RN, NN, NK, SN, NH, KN, HN, NQ, HH, RG, KH, RH and SS preferentially bind to guanine. In a much more advantageous embodiment of the invention, polypeptide monomers having RVDs RN, NK, NQ, HH, KH, RH, SS and SN preferentially bind to guanine and thereby allow the generation of TALE polypeptides with high binding specificity for guanine containing target nucleic acid sequences. In an even more advantageous embodiment of the invention, polypeptide monomers having RVDs HH, KH, NH, NK, NQ, RH, RN and SS preferentially bind to guanine and thereby allow the generation of TALE polypeptides with high binding specificity for guanine containing target nucleic acid sequences. In a further advantageous embodiment, the RVDs that have high binding specificity for guanine are RN, NH, RH and KH. Furthermore, polypeptide monomers having an RVD of NV preferentially bind to adenine and guanine. In more preferred embodiments of the invention, monomers having RVDs of H*, HA, KA, N*, NA, NC, NS, RA, and S* bind to adenine, guanine, cytosine and thymine with comparable affinity.

[0307] The predetermined N-terminal to C-terminal order of the one or more polypeptide monomers of the nucleic acid or DNA binding domain determines the corresponding predetermined target nucleic acid sequence to which the polypeptides of the invention will bind. As used herein the monomers and at least one or more half monomers are "specifically ordered to target" the genomic locus or gene of interest. In plant genomes, the natural TALE-binding sites always begin with a thymine (T), which may be specified by a cryptic signal within the non-repetitive N-terminus of the TALE polypeptide; in some cases, this region may be referred to as repeat 0. In animal genomes, TALE binding sites do not necessarily have to begin with a thymine (T) and polypeptides of the invention may target DNA sequences that begin with T, A, G or C. The tandem repeat of TALE monomers always ends

with a half-length repeat or a stretch of sequence that may share identity with only the first 20 amino acids of a repetitive full length TALE monomer and this half repeat may be referred to as a half-monomer. Therefore, it follows that the length of the nucleic acid or DNA being targeted is equal to the number of full monomers plus two.

[0308] As described in Zhang et al., *Nature Biotechnology* 29:149-153 (2011), TALE polypeptide binding efficiency may be increased by including amino acid sequences from the "capping regions" that are directly N-terminal or C-terminal of the DNA binding region of naturally occurring TALEs into the engineered TALEs at positions N-terminal or C-terminal of the engineered TALE DNA binding region. Thus, in certain embodiments, the TALE polypeptides described herein further comprise an N-terminal capping region and/or a C-terminal capping region.

[0309] As used herein the predetermined "N-terminus" to "C terminus" orientation of the N-terminal capping region, the DNA binding domain comprising the repeat TALE monomers and the C-terminal capping region provide structural basis for the organization of different domains in the d-TALEs or polypeptides of the invention.

[0310] The entire N-terminal and/or C-terminal capping regions are not necessary to enhance the binding activity of the DNA binding region. Therefore, in certain embodiments, fragments of the N-terminal and/or C-terminal capping regions are included in the TALE polypeptides described herein.

[0311] In certain embodiments, the TALE polypeptides described herein contain a N-terminal capping region fragment that included at least 10, 20, 30, 40, 50, 54, 60, 70, 80, 87, 90, 94, 100, 102, 110, 117, 120, 130, 140, 147, 150, 160, 170, 180, 190, 200, 210, 220, 230, 240, 250, 260 or 270 amino acids of an N-terminal capping region. In certain embodiments, the N-terminal capping region fragment amino acids are of the C-terminus (the DNA-binding region proximal end) of an N-terminal capping region. As described in Zhang et al., *Nature Biotechnology* 29:149-153 (2011), N-terminal capping region fragments that include the C-terminal 240 amino acids enhance binding activity equal to the full length capping region, while fragments that include the C-terminal 147 amino acids retain greater than 80% of the efficacy of the full length capping region, and fragments that include the C-terminal 117 amino acids retain greater than 50% of the activity of the full-length capping region.

[0312] In some embodiments, the TALE polypeptides described herein contain a C-terminal capping region fragment that included at least 6, 10, 20, 30, 37, 40, 50, 60, 68, 70, 80, 90, 100, 110, 120, 127, 130, 140, 150, 155, 160, 170, 180 amino acids of a C-terminal

capping region. In certain embodiments, the C-terminal capping region fragment amino acids are of the N-terminus (the DNA-binding region proximal end) of a C-terminal capping region. As described in Zhang et al., Nature Biotechnology 29:149-153 (2011), C-terminal capping region fragments that include the C-terminal 68 amino acids enhance binding activity equal to the full length capping region, while fragments that include the C-terminal 20 amino acids retain greater than 50% of the efficacy of the full length capping region.

[0313] In certain embodiments, the capping regions of the TALE polypeptides described herein do not need to have identical sequences to the capping region sequences provided herein. Thus, in some embodiments, the capping region of the TALE polypeptides described herein have sequences that are at least 50%, 60%, 70%, 80%, 85%, 90%, 91%, 92%, 93%, 94%, 95%, 96%, 97%, 98% or 99% identical or share identity to the capping region amino acid sequences provided herein. Sequence identity is related to sequence homology. Homology comparisons may be conducted by eye, or more usually, with the aid of readily available sequence comparison programs. These commercially available computer programs may calculate percent (%) homology between two or more sequences and may also calculate the sequence identity shared by two or more amino acid or nucleic acid sequences. In some preferred embodiments, the capping region of the TALE polypeptides described herein have sequences that are at least 95% identical or share identity to the capping region amino acid sequences provided herein.

[0314] Sequence homologies may be generated by any of a number of computer programs known in the art, which include but are not limited to BLAST or FASTA. Suitable computer program for carrying out alignments like the GCG Wisconsin Bestfit package may also be used. Once the software has produced an optimal alignment, it is possible to calculate % homology, preferably % sequence identity. The software typically does this as part of the sequence comparison and generates a numerical result.

[0315] In advantageous embodiments described herein, the TALE polypeptides of the invention include a nucleic acid binding domain linked to the one or more effector domains. The terms "effector domain" or "regulatory and functional domain" refer to a polypeptide sequence that has an activity other than binding to the nucleic acid sequence recognized by the nucleic acid binding domain. By combining a nucleic acid binding domain with one or more effector domains, the polypeptides of the invention may be used to target the one or more functions or activities mediated by the effector domain to a particular target DNA sequence to which the nucleic acid binding domain specifically binds.

[0316] In some embodiments of the TALE polypeptides described herein, the activity mediated by the effector domain is a biological activity. For example, in some embodiments the effector domain is a transcriptional inhibitor (i.e., a repressor domain), such as an mSin interaction domain (SID). SID4X domain or a Kriippel-associated box (KRAB) or fragments of the KRAB domain. In some embodiments, the effector domain is an enhancer of transcription (i.e. an activation domain), such as the VP 16, VP64 or p65 activation domain. In some embodiments, the nucleic acid binding is linked, for example, with an effector domain that includes but is not limited to a transposase, integrase, recombinase, resolvase, invertase, protease, DNA methyltransferase, DNA demethylase, histone acetylase, histone deacetylase, nuclease, transcriptional repressor, transcriptional activator, transcription factor recruiting, protein nuclear-localization signal or cellular uptake signal.

[0317] In some embodiments, the effector domain is a protein domain which exhibits activities which include but are not limited to transposase activity, integrase activity, recombinase activity, resolvase activity, invertase activity, protease activity, DNA methyltransferase activity, DNA demethylase activity, histone acetylase activity, histone deacetylase activity, nuclease activity, nuclear-localization signaling activity, transcriptional repressor activity, transcriptional activator activity, transcription factor recruiting activity, or cellular uptake signaling activity. Other preferred embodiments of the invention may include any combination the activities described herein.

[0318] In certain embodiments, the invention involves targeted nucleic acid profiling (e.g., sequencing, quantitative reverse transcription polymerase chain reaction, and the like) (see e.g., Geiss GK, et al., Direct multiplexed measurement of gene expression with color-coded probe pairs. *Nat Biotechnol.* 2008 Mar;26(3):3 17-25). In certain embodiments, a target nucleic acid molecule (e.g., RNA molecule), may be sequenced by any method known in the art, for example, methods of high-throughput sequencing, also known as next generation sequencing or deep sequencing. A nucleic acid target molecule labeled with a barcode (for example, an origin-specific barcode) can be sequenced with the barcode to produce a single read and/or contig containing the sequence, or portions thereof, of both the target molecule and the barcode. Exemplary next generation sequencing technologies include, for example, Illumina sequencing, Ion Torrent sequencing, 454 sequencing, SOLiD sequencing, and nanopore sequencing amongst others. Methods for constructing sequencing libraries are known in the art (see, e.g., Head et al., Library construction for next-generation sequencing: Overviews and challenges. *Biotechniques.* 2014; 56(2): 61-77).

[0319] In certain embodiments, the invention involves plate based single cell RNA sequencing (see, e.g., Picelli, S. et al., 2014, "Full-length RNA-seq from single cells using Smart-seq2" *Nature protocols* 9, 171-181, doi:10.1038/nprot.2014.006).

[0320] In certain embodiments, the invention involves high-throughput single-cell RNA-seq and/or targeted nucleic acid profiling where the RNAs from different cells are tagged individually, allowing a single library to be created while retaining the cell identity of each read. In this regard reference is made to Macosko et al., 2015, "Highly Parallel Genome-wide Expression Profiling of Individual Cells Using Nanoliter Droplets" *Cell* 161, 1202-1214; International patent application number PCT/US20 15/049 178, published as WO2016/040476 on March 17, 2016; Klein et al., 2015, "Droplet Barcoding for Single-Cell Transcriptomics Applied to Embryonic Stem Cells" *Cell* 161, 1187-1201; International patent application number PCT/US20 16/027734, published as WO2016168584A1 on October 20, 2016; Zheng, et al., 2016, "Haplotyping germline and cancer genomes with high-throughput linked-read sequencing" *Nature Biotechnology* 34, 303-311; Zheng, et al., 2017, "Massively parallel digital transcriptional profiling of single cells" *Nat. Commun.* 8, 14049 doi: 10.1038/ncomms14049; International patent publication number WO 2014210353 A2; Zilionis, et al., 2017, "Single-cell barcoding and sequencing using droplet microfluidics" *Nat Protoc.* Jan;12(1):44-73; Cao et al., 2017, "Comprehensive single cell transcriptional profiling of a multicellular organism by combinatorial indexing" *bioRxiv* preprint first posted online Feb. 2, 2017, doi: dx.doi.org/10.1101/104844; Rosenberg et al., 2017, "Scaling single cell transcriptomics through split pool barcoding" *bioRxiv* preprint first posted online Feb. 2, 2017, doi: dx.doi.org/10.1101/105163; Vitak, et al., "Sequencing thousands of single-cell genomes with combinatorial indexing" *Nature Methods*, 14(3):302-308, 2017; Cao, et al., Comprehensive single-cell transcriptional profiling of a multicellular organism. *Science*, 357(6352):661-667, 2017; and Gierahn et al., "Seq-Well: portable, low-cost RNA sequencing of single cells at high throughput" *Nature Methods* 14, 395-398 (2017), all the contents and disclosure of each of which are herein incorporated by reference in their entirety.

[0321] In certain embodiments, the invention involves single nucleus RNA sequencing (sn-RNA-seq). In this regard reference is made to Swiech et al., 2014, "In vivo interrogation of gene function in the mammalian brain using CRISPR-Cas9" *Nature Biotechnology* Vol. 33, pp. 102-106; Habib et al., 2016, "Div-Seq: Single-nucleus RNA-Seq reveals dynamics of rare adult newborn neurons" *Science*, Vol. 353, Issue 6302, pp. 925-928; and Habib et al.,

2017, "Massively parallel single-nucleus RNA-seq with DroNc-seq" Nat Methods. 2017 Oct;14(10):955-958, which are herein incorporated by reference in their entirety.

[0322] In certain embodiments, the immunotherapy resistance signature comprises EGRI and/or MAZ. In other embodiments, EGRI and/or MAZ are targeted for therapeutic intervention. In one embodiment, EGRI and/or MAZ are targeted to reduce a resistance signature. EGRI and MAZ are zinc finger transcription factors (TF). EGRI is down regulated in malignant cells of the post-treatment tumors, and MAZ (Myc-associated *zinc* finger protein) is up-regulated. These TFs may be connected to the decrease in metallothioneins post-treatment and availability to metal ions. Applicants saw an enrichment in EGRI targets in the genes which are down-regulated post-treatment. Applicants also saw an overlap with a signature identified in synovial sarcoma. In synovial sarcoma EGRI is repressed. Mutations in the BAF complex are strongly associated with the response to immunotherapy/resistance to T-cells, and is related to the present invention.

[0323] In certain embodiments, the gene signatures described herein are screened by perturbation of target genes within said signatures. In certain embodiments, perturbation of any signature gene or gene described herein may reduce or induce the immunotherapy resistance signature. In preferred embodiments, the perturbed genes include MAZ, NFKBIZ, MYC, ANXA1, SOX4, MT2A, PTP4A3, CD59, DLL3, SERPINE2, SERPINF1, PERP, EGRI, SERPINA3, IFNGR2, B2M, and PDL1. In certain embodiments, after perturbation, gene expression may be evaluated to determine whether the gene signature is reduced.

[0324] Methods and tools for genome-scale screening of perturbations in single cells using CRISPR-Cas9 have been described, herein referred to as perturb-seq (see e.g., Dixit et al., "Perturb-Seq: Dissecting Molecular Circuits with Scalable Single-Cell RNA Profiling of Pooled Genetic Screens" 2016, Cell 167, 1853-1866; Adamson et al., "A Multiplexed Single-Cell CRISPR Screening Platform Enables Systematic Dissection of the Unfolded Protein Response" 2016, Cell 167, 1867-1882; and International publication serial number WO/2017/075294). The present invention is compatible with perturb-seq, such that signature genes may be perturbed and the perturbation may be identified and assigned to the proteomic and gene expression readouts of single cells. In certain embodiments, signature genes may be perturbed in single cells and gene expression analyzed. Not being bound by a theory, networks of genes that are disrupted due to perturbation of a signature gene may be determined. Understanding the network of genes effected by a perturbation may allow for a gene to be linked to a specific pathway that may be targeted to modulate the signature and

treat a cancer. Thus, in certain embodiments, perturb-seq is used to discover novel drug targets to allow treatment of specific cancer patients having the gene signature of the present invention.

[0325] The perturbation methods and tools allow reconstructing of a cellular network or circuit. In one embodiment, the method comprises (1) introducing single-order or combinatorial perturbations to a population of cells, (2) measuring genomic, genetic, proteomic, epigenetic and/or phenotypic differences in single cells and (3) assigning a perturbation(s) to the single cells. Not being bound by a theory, a perturbation may be linked to a phenotypic change, preferably changes in gene or protein expression. In preferred embodiments, measured differences that are relevant to the perturbations are determined by applying a model accounting for co-variates to the measured differences. The model may include the capture rate of measured signals, whether the perturbation actually perturbed the cell (phenotypic impact), the presence of subpopulations of either different cells or cell states, and/or analysis of matched cells without any perturbation. In certain embodiments, the measuring of phenotypic differences and assigning a perturbation to a single cell is determined by performing single cell RNA sequencing (RNA-seq). In preferred embodiments, the single cell RNA-seq is performed by any method as described herein (e.g., Drop-seq, InDrop, 10X genomics). In certain embodiments, unique barcodes are used to perform Perturb-seq. In certain embodiments, a guide RNA is detected by RNA-seq using a transcript expressed from a vector encoding the guide RNA. The transcript may include a unique barcode specific to the guide RNA. Not being bound by a theory, a guide RNA and guide RNA barcode is expressed from the same vector and the barcode may be detected by RNA-seq. Not being bound by a theory, detection of a guide RNA barcode is more reliable than detecting a guide RNA sequence, reduces the chance of false guide RNA assignment and reduces the sequencing cost associated with executing these screens. Thus, a perturbation may be assigned to a single cell by detection of a guide RNA barcode in the cell. In certain embodiments, a cell barcode is added to the RNA in single cells, such that the RNA may be assigned to a single cell. Generating cell barcodes is described herein for single cell sequencing methods. In certain embodiments, a Unique Molecular Identifier (UMI) is added to each individual transcript and protein capture oligonucleotide. Not being bound by a theory, the UMI allows for determining the capture rate of measured signals, or preferably the binding events or the number of transcripts captured. Not being bound by a theory, the data is more significant if the signal observed is derived from more than one protein binding

event or transcript. In preferred embodiments, Perturb-seq is performed using a guide RNA barcode expressed as a polyadenylated transcript, a cell barcode, and a UMI.

[0326] Perturb-seq combines emerging technologies in the field of genome engineering, single-cell analysis and immunology, in particular the CRISPR-Cas9 system and droplet single-cell sequencing analysis. In certain embodiments, a CRISPR system is used to create an INDEL at a target gene. In other embodiments, epigenetic screening is performed by applying CRISPRa/i/x technology (see, e.g., Konermann et al. "Genome-scale transcriptional activation by an engineered CRISPR-Cas9 complex" *Nature*. 2014 Dec 10. doi: 10.1038/nature14136; Qi, L. S., et al. (2013). "Repurposing CRISPR as an RNA-guided platform for sequence-specific control of gene expression". *Cell*. 152 (5): 1173-83; Gilbert, L. A., et al., (2013). "CRISPR-mediated modular RNA-guided regulation of transcription in eukaryotes". *Cell*. 154 (2): 442-51; Konior et al., 2016, Programmable editing of a target base in genomic DNA without double-stranded DNA cleavage, *Nature* 533, 420-424; Nishida et al., 2016, Targeted nucleotide editing using hybrid prokaryotic and vertebrate adaptive immune systems, *Science* 353(6305); Yang et al., 2016, Engineering and optimising deaminase fusions for genome editing, *Nat Commun.* 7:13330; Hess et al., 2016, Directed evolution using dCas9-targeted somatic hypermutation in mammalian cells, *Nature Methods* 13, 1036-1042; and Ma et al., 2016, Targeted AID-mediated mutagenesis (TAM) enables efficient genomic diversification in mammalian cells. *Nature Methods* 13, 1029-1035). Numerous genetic variants associated with disease phenotypes are found to be in non-coding region of the genome, and frequently coincide with transcription factor (TF) binding sites and non-coding RNA genes. Not being bound by a theory, CRISPRa/i/x approaches may be used to achieve a more thorough and precise understanding of the implication of epigenetic regulation. In one embodiment, a CRISPR system may be used to activate gene transcription. A nuclease-dead RNA-guided DNA binding domain, dCas9, tethered to transcriptional repressor domains that promote epigenetic silencing (e.g., KRAB) may be used for "CRISPRi" that represses transcription. To use dCas9 as an activator (CRISPRa), a guide RNA is engineered to carry RNA binding motifs (e.g., MS2) that recruit effector domains fused to RNA-motif binding proteins, increasing transcription. A key dendritic cell molecule, p65, may be used as a signal amplifier, but is not required.

[0327] In certain embodiments, other CRISPR-based perturbations are readily compatible with Perturb-seq, including alternative editors such as CRISPR/Cpf1. In certain embodiments, Perturb-seq uses Cpf1 as the CRISPR enzyme for introducing perturbations.

Not being bound by a theory, Cpf1 does not require Tracr RNA and is a smaller enzyme, thus allowing higher combinatorial perturbations to be tested.

[0328] The cell(s) may comprise a cell in a model non-human organism, a model non-human mammal that expresses a Cas protein, a mouse that expresses a Cas protein, a mouse that expresses Cpf1, a cell in vivo or a cell ex vivo or a cell in vitro (see e.g., WO 2014/093622 (PCT/US 13/074667); US Patent Publication Nos. 20120017290 and 20110265198 assigned to Sangamo Biosciences, Inc.; US Patent Publication No. 20130236946 assigned to Collectis; Piatt et al., "CRISPR-Cas9 Knockin Mice for Genome Editing and Cancer Modeling" *Cell* (2014), 159(2): 440-455; "Oncogenic models based on delivery and use of the CRISPR-Cas systems, vectors and compositions" WO2014204723A1 "Delivery and use of the CRISPR-Cas systems, vectors and compositions for hepatic targeting and therapy" WO2014204726A1; "Delivery, use and therapeutic applications of the CRISPR-Cas systems and compositions for modeling mutations in leukocytes" WO2016049251; and Chen et al., "Genome-wide CRISPR Screen in a Mouse Model of Tumor Growth and Metastasis" 2015, *Cell* 160, 1246-1260). The cell(s) may also comprise a human cell. Mouse cell lines may include, but are not limited to neuro-2a cells and EL4 cell lines (ATCC TIB-39). Primary mouse T cells may be isolated from C57/BL6 mice. Primary mouse T cells may be isolated from Cas9-expressing mice.

[0329] In one embodiment, CRISPR/Cas9 may be used to perturb protein-coding genes or non-protein-coding DNA. CRISPR/Cas9 may be used to knockout protein-coding genes by frameshifts, point mutations, inserts, or deletions. An extensive toolbox may be used for efficient and specific CRISPR/Cas9 mediated knockout as described herein, including a double-nicking CRISPR to efficiently modify both alleles of a target gene or multiple target loci and a smaller Cas9 protein for delivery on smaller vectors (Ran, F.A., et al., In vivo genome editing using *Staphylococcus aureus* Cas9. *Nature*. 520, 186-191 (2015)). A genome-wide sgRNA mouse library (-10 sgRNAs/gene) may also be used in a mouse that expresses a Cas9 protein (see, e.g., WO2014204727A1).

[0330] In one embodiment, perturbation is by deletion of regulatory elements. Non-coding elements may be targeted by using pairs of guide RNAs to delete regions of a defined size, and by tiling deletions covering sets of regions in pools.

[0331] In one embodiment, perturbation of genes is by RNAi. The RNAi may be shRNA's targeting genes. The shRNA's may be delivered by any methods known in the art.

In one embodiment, the shRNA's may be delivered by a viral vector. The viral vector may be a lentivirus, adenovirus, or adeno associated virus (AAV).

[0332] A CRISPR system may be delivered to primary mouse T-cells. Over 80% transduction efficiency may be achieved with Lenti-CRISPR constructs in CD4 and CD8 T-cells. Despite success with lentiviral delivery, recent work by Hendel et al, (Nature Biotechnology 33, 985-989 (2015) doi:10.1038/nbt.3290) showed the efficiency of editing human T-cells with chemically modified RNA, and direct RNA delivery to T-cells via electroporation. In certain embodiments, perturbation in mouse primary T-cells may use these methods.

[0333] In certain embodiments, whole genome screens can be used for understanding the phenotypic readout of perturbing potential target genes. In preferred embodiments, perturbations target expressed genes as defined by a gene signature using a focused sgRNA library. Libraries may be focused on expressed genes in specific networks or pathways. In other preferred embodiments, regulatory drivers are perturbed. In certain embodiments, Applicants perform systematic perturbation of key genes that regulate T-cell function in a high-throughput fashion. In certain embodiments, Applicants perform systematic perturbation of key genes that regulate cancer cell function in a high-throughput fashion (e.g., immune resistance or immunotherapy resistance). Applicants can use gene expression profiling data to define the target of interest and perform follow-up single-cell and population RNA-seq analysis. Not being bound by a theory, this approach will accelerate the development of therapeutics for human disorders, in particular cancer. Not being bound by a theory, this approach will enhance the understanding of the biology of T-cells and tumor immunity, and accelerate the development of therapeutics for human disorders, in particular cancer, as described herein.

[0334] Not being bound by a theory, perturbation studies targeting the genes and gene signatures described herein could (1) generate new insights regarding regulation and interaction of molecules within the system that contribute to suppression of an immune response, such as in the case within the tumor microenvironment, and (2) establish potential therapeutic targets or pathways that could be translated into clinical application.

[0335] In certain embodiments, after determining Perturb-seq effects in cancer cells and/or primary T-cells, the cells are infused back to the tumor xenograft models (melanoma, such as B16F10 and colon cancer, such as CT26) to observe the phenotypic effects of genome editing. Not being bound by a theory, detailed characterization can be performed

based on (1) the phenotypes related to tumor progression, tumor growth, immune response, etc. (2) the TILs that have been genetically perturbed by CRISPR-Cas9 can be isolated from tumor samples, subject to cytokine profiling, qPCR/RNA-seq, and single-cell analysis to understand the biological effects of perturbing the key driver genes within the tumor-immune cell contexts. Not being bound by a theory, this will lead to validation of TILs biology as well as lead to therapeutic targets.

[0336] The invention is further described in the following examples, which do not limit the scope of the invention described in the claims.

EXAMPLES

Example 1 - Identifying Signatures of Resistance

[0337] Applicants leveraged single-cell RNA-sequencing (scRNA-Seq) of thousands of cells from melanoma tumors and a novel data-driven method to systematically map cancer programs that promote ICR and T cell exclusion. Applicants collected 10,123 scRNA-seq profiles from the tumors of 31 patients, consisting of 15 treatment naive (TN) patients, and 16 post-ICI tumors. Of these 16 post-ICI specimens, 15 had clinical resistance and were therefore termed ICI-resistant (ICR), and one had a partial response (PR) according to the RECIST criteria (18) (Fig. 1A, table SI), and was termed as having clinical benefit (CB). Applicants filtered lower-quality cells to retain 7,186 high-quality transcriptomes, including 4,199 cells from 16 patients that Applicants previously reported (13), and 2,987 cells from 16 newly collected patient tumors (table SI).

[0338] Applicants first aimed to determine the effects ICI has on different cell types in the tumor at the time of post-ICI progression, by comparing between the ICR and TN tumors. Although the specimens in the different treatment groups were not from the same patients, Applicants reasoned that the high resolution and large number of cells profiled will provide sufficient power to detect some of these effects.

[0339] It revealed that, despite the lack of clinical response, CD8 T-cells in the ICR tumors manifested heterogeneous phenotypes of T-cell activation. Conversely, the malignant cells of ICR tumors had a distinct transcriptional state that was substantially less frequent in the TN tumors.

[0340] Next, for any such transcriptional program that may reflect ICI effects, Applicants examined its potential causal connection to immune evasion or resistance. Applicants acknowledged the possibility that malignant cells derived from TN tumors could contain both

treatment-sensitive and intrinsically resistant cells. Thus, Applicants tested the malignant signatures in two independent validation cohorts (**Fig. 1A**), where pre-ICI patient biopsies were profiled with bulk RNA-Seq, and the response to ICI therapy was monitored. Applicants demonstrated that this oncogenic state is tightly linked to immune evasion and exclusion, and that it can be used to predict ICR based on the bulk RNA-seq of the pre-ICI biopsy.

[0341] Applicants collected scRNA-Seq of dissociated individual cells from fresh tumor resections, sorted into immune and non-immune cells based on the CD45 expression, and profiled them with a modified full-length SMART-Seq2 protocol (**materials and methods, table S2**). Applicants distinguished different cell subsets and clones both by their expression profiles and by their inferred genetic features. In the non-immune compartment (**Fig. 1B**), Applicants distinguished malignant from non-malignant cells (**materials and methods**) according to (1) their inferred CNV profiles (13) (**fig. 5**); (2) under-expression of different non-malignant cell-type signatures (**fig. 5B**); and (3) high similarity to bulk RNA-Seq profiles of melanoma tumors compared to adjacent normal tissue. The cell assignments by the different criteria were highly consistent (hypergeometric p -value $< 10^{-17}$, **fig. 5, materials and methods**). Within non-malignant cells, Applicants used unsupervised clustering to identify (**materials and methods**) CD8 and CD4 T cells, B cells, NK cells, macrophages, Cancer Associated Fibroblasts (CAFs) and endothelial cells (**Fig. 1C, fig. 6, table S4**). Overall, malignant cells clustered first by their tumor of origin (**Fig. 1B**), while the non-malignant cells clustered primarily by their cell type, and only then by their tumor of origin (**Fig. 1C**).

[0342] Applicants identified transcriptional features that distinguish between the cells of TN and ICR tumors, analyzing separately each cell type with a sufficient number (>100) of cells: malignant cells, macrophages, B cells, CD8 T cells, and CD4 T cells. Applicants applied a subsampling procedure to prevent tumors with a particularly large number of cells of a given type from dominating the results and to mitigate the effects of outliers. For each cell type Applicants defined an ICR-up and ICR-down signature, consisting of genes that were significantly up or down regulated in the cells from the ICR tumors, respectively (19). Applicants used a mixed-effect model to test the ability of a given gene signature to distinguish between cells from ICR and TN tumors, while accounting for potential confounders, including other clinical characteristics and cell quality (**materials and methods**).

[0343] The CD8 T cells and malignant cells subset derived from ICR patients were markedly different from their TN counterparts (**fig. 7, tables S5 and S6**), and are the focus of this analysis. Macrophages also showed ICR associated expression programs (**table S5**), but due to their relatively small number in the dataset, Applicants did not pursue them further. Conversely, very few genes were differentially expressed between the ICR vs. TN groups when analyzing B cells or CD4 T cells (**table S5**). Deeper sampling of these and other cell types might identify significant distinctions.

[0344] The CD8 T-cell-ICR signatures (**Fig. ID**) revealed the induction of cytotoxicity genes and the repression of some exhaustion features. Compared to TN CD8 T cells, ICR CD8 T cells up regulated the T cell activation markers STAT1, GBP2, GBP5 and IRF1, and down regulated WNK1. Inhibition of WNK1 has been shown to increase T cell infiltration and accumulation in tumors in an in vivo shRNA screen (20). Lactate dehydrogenase A (LDHA) was also up regulated in the ICR CD8 T cells, suggesting that the cells may have infiltrated the hypoxic tumor microenvironment. Among the immune checkpoints, HAVCR2 (TIM3) and CD27 are significantly, though modestly, down-regulated. Although the inhibitory checkpoints CTLA-4, TIGIT, LAG-3, PD-1, and TIM3 co-vary across cells (along with the transcription factor PRDM1), as Applicants previously reported (13, 21), Applicants did not detect a significant difference in their expression between TN and ICR cells (**fig. 8A**). Rather, CD8 T cells from both TN and ICR tumor specimens spanned a spectrum of states in the exhaustion-cytotoxicity space, even within the CD8 T cells of the same tumor (13), with a strong association between dysfunction ("exhaustion") and cytotoxicity scores at the single cell level (**Fig. IE, fig. 8B**), as Applicants previously reported (13). Notably, the CD8 T cells of the one ICI responder patient are both highly cytotoxic and significantly less dysfunctional than cells of other patients (**Fig. IE**, $P = 1.31 \times 10^{-6}$, hypergeometric test). However, since a similar trend was observed in one of the ICR patients (Mell26, $P = 4.08 \times 10^{-13}$, hypergeometric test), such an enhanced cytotoxic state may not necessarily mark clinical response. These findings were robust when using different T cell dysfunction signatures (**materials and methods**), including single-cell signatures that were recently identified in T cells from hepatocellular carcinoma tumors (22) (**fig. 8B**, $P < 2.46 \times 10^{-4}$, hypergeometric test). A list of differentially expressed genes obtained when comparing the CD8 T cells of the CB patients to those from the ICR patients is provided in **table S7**.

[0345] To examine the association between CD8 T cell profiles and clonal expansion Applicants reconstructed full-length T cell receptors (TCR) and identified 137 CD8 T cell

clones of varying sizes (23) (**Fig. 1F, fig. 9**). Three patients, all of them ICR, had exceptionally large clonal expansions, with 39-51% of the CD8 T cells in these tumors as members of large (>20 cells) clonotypes (Fig. 1F). These three ICR patients had extremely expanded CD8 T cells, even after controlling for the number of CD8 T cells profiled and the success rate of TCR reconstruction (**materials and methods**, $P = 4.54 * 10^{-3}$, one-sided Wilcoxon ranksum, **fig. 9B**). For one ICR patient with extreme clonal expansions, Applicants obtained two lesions a year apart: 15 of the 28 clones identified in these specimens included cells from both lesions, such that 71% and 52% of the CD8 T cells in the early and late samples, respectively, were in the shared clones, demonstrating their stability and persistence (**fig. 9C,D**). T cell clonality pre-treatment has previously been identified as a potential predictive marker of response to anti-PD-1 therapy (6); the results herein suggest that the extent of clonal expansion post ICI may not be coupled to clinical response.

[0346] The expression of the ICR signature is higher in expanded CD8 T cells within each subset of patients, with the clonally expanded ICR CD8 T cells scoring highest (**Fig. 1D,G**, left, $P = 3.23 * 10^{-5}$, mixed-effects test). Nonetheless, even when completely removing the T cells of the three ICR patients with the large T cell clonal expansion, the T-cell-ICR signature still significantly distinguished between the TN and ICR CD8 T cells (**Fig. 1G**, right, $P = 5.56 * 10^{-53}$ and $7.41 * 10^{-3}$, t-test and mixed effects test, respectively). The expanded T cells had a gene signature that included significant down-regulation of KLRG1 (**table SII**).

[0347] According to the expression of cell cycle signatures in each cell (**materials and methods**), five patients had a significantly larger fraction of cycling CD8 T cells (hypergeometric p-value <0.01), four of them were ICR patients. Proliferating CD8 T cells expressed some unique genes compared to proliferating malignant cells (**Fig. 1H, table S8**), including induction of oxidative phosphorylation ($P = 7.89 * 10^{-6}$, hypergeometric test) and repression of the hematopoietic lineage genes CD37, IL11RA, and IL7R ($P = 1.28 * 10^{-4}$, hypergeometric test). Thus, it may be possible to perturb T cell proliferation specifically, without affecting tumor cells (i.e. tumor growth).

[0348] Taken together, these findings demonstrate that even in ICR patients CD8 T cells following ICI can show some indicators of enhanced functionality, such as expansion and transcriptional changes. In other words, these findings demonstrate that ICI can promote the expansion and functionality of the CD8 T cells without leading to a clinical response. Additional data from ICI responders is needed to examine if insufficient T cell functionality nonetheless limited the clinical response in such ICR patients. Nevertheless, Applicants

hypothesized that the malignant cell compartment may contribute to ICR in these patients, at least in part.

[0349] Applicants thus turned to examine the effect of ICI on the malignant cell profiles, and identified signatures that distinguish malignant cells from ICR vs. TN tumors: oncogenic-ICR-up and oncogenic-ICR-down (**Fig. 2A,B, table S6**). The signatures were robust and generalizable in cross-validation (withholding data from each patient in turn and classifying the withheld test set; **materials and methods, Fig. 2A**, AUC=0.86). The variation in the expression of the oncogenic-ICR signatures in either this data or across TCGA melanoma bulk tumors was not significantly associated with potential confounders (**materials and methods**, mixed-effect model and ANOVA, respectively). Finally, a proportion of malignant cells in TN tumors manifested the oncogenic-ICR state (**Fig. 2B, right**), suggesting that it may precede ICI at least in some patients. This is discussed further below.

[0350] The oncogenic-ICR-down signature genes were enriched both in pathways that reflect established mechanisms of resistance, including downregulation of IFN- signaling and MHC class I presentation (8), and in additional processes, not previously implicated in ICR (**Fig. 2B, tables S6 and S9, materials and methods**). These include suppression of other innate immune responses, such as TNF-mediated NF B signaling, apoptosis, response to the complement system, IL2/STAT5 signaling, and the reduced expression of metallothioneins. NFkB pathway activation can induce expression of cytokines with either negative or positive immune-modulatory effects (24, 25). Our results suggest that under-expression of TNF-mediated NFkB signaling genes may be detrimental for response. The oncogenic-ICR-up genes include several transcriptional and chromatin regulators (e.g., SNAI2, HMGA1), and are enriched for Myc and CDK7/8 targets ($P < 10^{-11}$, hypergeometric p-value). Myc-activation has been previously linked to increased expression of immunosuppressive signals, including the upregulation of PD-L1 and β -catenin, which in turn inhibits dendritic cell recruitment to the tumor microenvironment via CCL4 (11). Similar results were obtained when comparing pre-defined gene modules directly between malignant cells of ICR and TN patients (**Fig. 2C, materials and methods**), including repression of the IL6/JAK/STAT3 pathway; mutations in this pathway were recently reported as an escape mechanism to anti-PD-1 therapy (8).

[0351] Gene modules are more robust to noise and provide more coherent signals than the expression of single genes. Applicants thus applied the mixed-effect models to test which

biological pathways are differentially expressed between the two groups. The analysis revealed similar pathways to those outlined above, as well as the repression of the JAK/STAT pathway. Mutations in this pathway were previously reported as an escape mechanism to anti-PD-1 therapy.

[0352] Several lines of evidence suggest that the oncogenic-ICR-up and oncogenic-ICR-down signatures are under shared control by one or few master regulators with opposing effects on these two programs. First, the expression of the oncogenic-ICR-up and oncogenic-ICR-down signatures is anti-correlated within the malignant cells of the same tumor and across hundreds of (TCGA) melanoma tumors (**Fig. 2D,E**). Second, in the Connectivity Map (26), there is a significant overlap between the genetic perturbations that induce the oncogenic-ICR-down signature and those that repress the oncogenic-ICR-up signature (hypergeometric p -value = 1.9×10^{-6}), including overexpression of IFN- γ and IFN- β and the knockdown of MYC. Indeed, MYC knockdown is the top perturbation to repress oncogenic-ICR-up, which is enriched for Myc targets. Moreover, there are 1,583 protein-protein interactions within and between the genes in the two oncogenic-ICR signatures ($P < 10^{-3}$, empirical test), consistent with participation in convergent biological processes. Applicants therefore defined the oncogenic-ICR state as a concurrent induction of the oncogenic-ICR-up signature and repression of the oncogenic-ICR-down signature, which Applicants quantify by the overall expression (**materials and methods**) of the oncogenic-ICR-up signature minus the overall expression of the oncogenic-ICR-down signature.

[0353] Next, Applicants hypothesized that the oncogenic-ICR signatures reflect an active resistance program, rather than only a post-ICI malignant cell state. This would be consistent with the presence of cells expressing the program in TN patients. In particular, to resist ICI, malignant cells may not only evade the immune cells (e.g., through the repression of MHC I and IFN- γ in oncogenic-ICR-down) but may also actively exclude the immune cells. The latter will impact the extent of CD8 T cell infiltration, which is a known pre-treatment predictor of ICI response (6, 27). To explore this possibility, Applicants developed a data-driven approach that characterizes malignant cells in non-infiltrated niches or tumors (**Fig. 2F**). In this approach, Applicants combined single cell profiles (irrespective of treatment status) with 473 melanoma bulk expression profiles from TCGA. First, Applicants used the single-cell profiles to define a T cell specific signature of 143 genes, and a signature of 332 genes that were primarily expressed by malignant cells (**table S4**). Then Applicants estimated the T cell infiltration level of the TCGA tumors based on their expression of the T cell

signature (**materials and methods**), and identified malignant genes whose expression was correlated to the estimated T cell infiltration levels. Six and 20 of the 332 malignant cell genes were significantly correlated or anti-correlated to the T cell infiltration level, respectively, which Applicants termed the seed T cell exclusion (Exclusion)-down and -up modules, respectively. However, the seed modules would neglect genes that are expressed also by other, non-malignant cells in the tumor (as MHC I, IFN- γ). To recover these, Applicants correlated the expression of each gene to the expression of the seed Exclusion modules across the entire malignant single-cell profiles. This yielded the final Exclusion-up and down modules, with 101 and 134 genes, respectively (**table S6**).

[0354] The Exclusion-down module was enriched for antigen processing and presentation genes (B2M, CTSB, CTSL1, HLA-B/C/F, HSPA1A, HSPA1B, $P = 4.19 \times 10^{-7}$, hypergeometric test), immune modulation genes ($P = 3.84 \times 10^{-9}$, as CD58 and the NFKB inhibitor, NFKBIA), and genes involved in the response to the Complement system ($P = 2.26 \times 10^{-7}$, e.g., CD59 and C4A). CD58 KO in malignant cells was recently shown to enhance the survival of melanoma cells in a genome-scale CRISPR screen of melanoma/T cell co-cultures (28), and its genetic loss or epigenetic inactivation are frequent immune evasion drivers in diffuse large B cell lymphoma (29). The Exclusion-up module included MYC itself and Myc targets ($P = 6.8 \times 10^{-12}$), as well as the transcription factors SNAI2 and SOX4.

[0355] Even though the Exclusion modules were identified without considering the treatment status of the tumors (TN or ICR), they significantly overlapped the corresponding oncogenic-ICR signatures (64 and 52 overlapping genes in oncogenic-ICR-up and -down, respectively, $P < 10^{-16}$, hypergeometric test, **Fig. 2G,H**). Both oncogenic-ICR (AUC = 0.83, in cross-validation) and the Exclusion signatures (AUC = 0.86) robustly classified individual cells as TN or ICR (**Fig. 2A,G**). In light of this congruence, Applicants defined a unified resistance program (uICR-up and uICRdown) as the union of the corresponding oncogenic-ICR and Exclusion signatures.

[0356] Importantly, there was no significant difference between the fraction of cycling cells in ICR vs. TN tumors ($P = 0.696$, t-test), and the oncogenic-ICR signatures were identical when identified only based on non-cycling cells. Interestingly however, the oncogenic-ICR state was more pronounced in cycling cells, both within the same patient group and among cells of the same tumor (**Fig. 2B,H, fig- 10A,B**, $P < 10^{-16}$, mixed effects model). Thus, cycling malignant cells may have induced stronger immune evasion capacities compared to their non-cycling counterparts. Moreover, CDK4 was a member of the of the

induced resistance program (uICRup). Applicants thus hypothesized that its targeted inhibition could shift the malignant cells to a less resistant state.

[0357] Unlike other biomarkers, such as PDL1 expression, mutational load, or T cell infiltration levels, the immune resistance signature could potentially provide a basis to develop novel treatment strategies. Next, Applicants explored therapeutic strategies to overcome resistance by reversing the uICR cell state in cancer cells. As CDK4 and multiple CDK target were members of the of the induced resistance program (uICR-up) and as the ICR state was more pronounced in cycling cells, Applicants hypothesized that cell cycle arrest through CDK4/6 inhibition could shift the malignant cells to a less resistant state. Additionally, CDK4/6 inhibitors could potentially increase tumor cell immunogenicity by inducing SASP, which was significantly repressed in the cancer cells from the ICR tumors compared to those from the untreated ones.

[0358] To test this assumption, Applicants first analyzed a recently published data set (30) in breast cancer cell lines and *in vivo* models and showed that CDK4/6 inhibition through abemaciclib treatment represses the ICR state defined by our signatures (**Fig. 3A-B, fig. IOC**). Applicants found that the CDK4/6 inhibitor abemaciclib strongly repressed uICR-up (which includes CDK4) and induced uICR-down (which includes the D-cyclin, CCND3). Indeed, abemaciclib, approved for the treatment of *i3RC4*-mutated breast cancer, was recently shown to trigger anti-tumor activity by inducing type III interferon production and suppressing T regulatory cells (30). Furthermore it was shown to sensitize solid tumors to anti-PDL1 in mouse models (30) in an RB-dependent manner.

[0359] To determine this effect in melanoma, Applicants identified melanoma cell lines in the Cancer Cell Line Encyclopedia (CCLE) with the strongest expression of the uICR signature, including IGR37, UACC257 (both RB-sufficient) and A2058 (RB-deficient). Applicants performed scRNA-seq on these cell lines before and after treatment with abemaciclib for 1 week (**Fig. 41**). In both IGR37 and UACC257, Applicants saw a decrease in the expression of the uICR state ($P < 3.59 \times 10^{-34}$, one-sided t-test). The single-cell resolution of the data revealed that in IGR37 there was a subpopulation of cells with an exceptionally strong expression of the uICR signature prior to the treatment with abemaciclib (**Fig. 43**). This population decreased from 10% before treatment (2,454 cells) to 2% in the post-treatment condition (1,570 cells). In contrast, the RB-deficient cell line A2058 did not show changes in the uICR expression, consistent with the hypothesis that this effect depends on RB-sufficiency.

[0360] Interestingly, Applicants found that DNMT1 is repressed while ERV-3 is induced in IGR37 and UACC257 cells post-treatment. These findings support previous observations that CDK4/6 inhibition leads to DNMT1 repression, allowing the methylation of endogenous retroviral genes (ERVs). The induction of ERVs triggers 'viral mimicry' and a double-stranded RNA (dsRNA) response, which stimulates type III IFN production to activate IFN-stimulated genes. Interestingly, Applicants also find that abemaciclib induces the expression of an MITF signature (Tirosh I, et al., Science. 2016 Apr 8;352(6282): 189-96) and of the SASP module (**Fig. 42**). The resistant cells, which are eradicated or altered by abemaciclib, had the lowest expression of the MITF and SASP signatures. While this pattern is decoupled from the expression of the MITF gene itself, it nonetheless indicates that, unlike the mechanism described in breast cancer cells (30), abemaciclib might trigger SASP and cell differentiation in melanoma cells.

[0361] To explore the potential of abemaciclib to induce T cell mediated toxicity to tumor cells, Applicants leveraged a patient-derived co-culture model of melanoma cells and ex-vivo expanded tumor infiltrating lymphocytes (TILs) from a metastatic melanoma lesion. Following one week of treatment of tumor cells with abemaciclib, cells were treated with their autologous TILs vs. control, and surviving tumor cells were submitted to scRNA-seq. The exposure to TILs reduced the expression of the uICR signature, both in the control and abemaciclib-treated cells ($P < 4.91 * 10^{-13}$). The treatment with abemaciclib further intensifies these effects, such that in the abemaciclib-treated cells there was an increase in a sensitive (ICR-low) subpopulation of cells post-TILs (**Fig. 42**). These sensitive cells are also characterized by a low expression of DNMT1, overexpression of ERV-3, and higher expression of the MITF and SASP modules. Furthermore, Applicants measured 40 human cytokines/chemokines in the conditioned media of abemaciclib treated cancer cells (before co-culture) and found the induction of several secreted factors (**Fig. 42**): macrophage inhibition factor (MIF), CX3CL1 a chemokine that induces migration and adhesion of T and NK cells and is linked to clinical outcomes in immunotherapy treatment (38, 39), and CCL20, an important factor for T cell differentiation that may enhance immunity in melanoma (40).

[0362] The relevance of the uICR as a resistance program is further supported by several lines of evidence. First, the induced uICR is overexpressed in uveal melanoma, which resides in an immune-privileged environment and has very low response rates to immunotherapy (31, 32), compared to cutaneous melanoma (**Fig. 3D**). Second, perturbations of genes from

the repressed resistance program (uICR-down) in malignant melanoma cells conferred resistance to cytotoxic CD8 T cells in a genome-wide CRISPR KO screen ($P = 6.37 \times 10^{-3}$, hypergeometric test). Third, malignant cells in the resistant state substantially repress interaction routes with other cell types in the tumor (**Fig. 3E**), as defined by cognate pairs of interacting surface molecules (**materials and methods**), including MHC I:TCR (T cells), CD58:CD2 (T cells), and ILIRAPTLIB (macrophages).

[0363] These results support a model, in which malignant cells from ICR tumors either had active resistance programs prior to treatment or induced the resistance program upon ICI exposure. Because some of the malignant cells from the TN patients expressed the resistance programs (**Fig. 2B,H**) Applicants next tested their prognostic value in independent datasets and cohorts. To this end, Applicants used both the full uICR and further filtered/refined uICR signatures. The refined signatures include only uICR genes that were also co-regulated with genes whose inhibition enhanced melanoma cell resistance to T cell mediated killing in functional screens (28) (**table S6, materials and methods**); the oncogenic-ICR and Exclusion signatures show the same behavior (**Fig 4E-H, figs. 11-13**).

[0364] The uICR programs are prognostic and predictive for response in external data sets. First, the signatures strongly associated with survival in 431 TCGA melanoma patients (who did not receive ICI, **Fig. 4A, fig. 11**), even after controlling for tumor purity and T cell infiltration, a known prognostic marker in melanoma (33, 34). Furthermore, combining resistance signatures and T cell infiltration levels yielded a significantly stronger association of patient survival than either alone (COX p-value = 1.4×10^{-8} , **Fig. 4A, right**). Other proposed mechanisms, such as dedifferentiation of melanoma cells (35), as reflected by an MITF-low signature, and other malignant signatures from the single cell profiles (e.g., cell cycle and the AXL program) (13), did not show an association to patient survival, indicating that mere variation across malignant cells is insufficient as a prognostic signature. Second, the signatures were associated with benefit of ICI in published pre-treatment and early on-treatment bulk expression profiles. In a lung cancer mouse model, which was mostly free of confounding genetic variability, the uICR clearly separated anti-CTLA-4 responders from non-responders based on early on-treatment profiles ($P = 3.6 \times 10^{-7}$, one-sided t-test, **Fig. 4B**) (36). In bulk pre-treatment RNA-Seq data from 27 melanoma patients that were subsequently treated with Pembrolizumab (5), the uICR program was lower in the five complete responders, though just above statistical significance ($P=6.3 \times 10^{-2}$, **Fig. 4C**). In bulk pre-treatment RNA-Seq data from 42 melanoma patients that were subsequently treated with the

CTLA-4 inhibitor ipilimumab (4), the uICR program was significantly lower in the two complete responders ($P = 5.2 * 10^{-3}$).

[0365] To test the predictive value of the resistance program in a larger independent setting, Applicants assembled a validation cohort of 112 patients with metastatic melanoma who underwent pretreatment biopsy and bulk RNA-Seq followed by Pembrolizumab (anti-PD-1) therapy (**Fig. 1A, table SI**). The cohort was collected in a different hospital and country (Germany), and samples were processed and sequenced on the same platform at the Broad Institute (**materials and methods**). Applicants evaluated the performances of the malignant resistance modules in predicting anti-PD-1 responses, with respect to three parameters (**materials and methods**): (1) progression-free survival (PFS, recorded for 104 of the 112 patients), (2) clinical benefit (CB, defined as either partial or complete response by RECIST criteria), and (3) complete response (CR). To compare the performance of the predictors to prior knowledge and clinically used markers, Applicants assembled a set of 32 other transcriptional signatures, including the top hits of two ICR functional CRISPR screens (28, 37) (**table S10**).

[0366] Our malignant cell resistance signatures were predictive of PFS in the validation cohort (**Fig. 4D,E, figs. 12 and 13**). Their predictive value was significant even when accounting for other known predictors of ICI response, including inferred T cell infiltration levels and PD-L1 expression (**figs. 12E and 13E**). Although cell cycle alone is not associated with CB (COX $P > 0.25$), filtering the cell-cycle component from the uICR overexpression score (**materials and methods**) further improved the PFS predictions (**Fig. 4D, right**), suggesting that a tumor ICR level should be evaluated conditioning on its proliferation level. The additional predictive value of the malignant resistance signatures beyond T cell infiltration was significantly higher than that of other signatures ($P = 3.37 * 10^{-6}$, Wilcoxon-ranksum test), and they were the only ones negatively associated with PFS. Other alternative predictors were either not predictive or highly associated with T cell infiltration levels, such that they did not provide an additive predictive value once accounting for T cell infiltration levels (**Fig. 4E**).

[0367] The uICR state was overexpressed in patients with CB vs. no-CB (**Fig. 4F**). Applicants noted however that some CB patients had high pre-treatment uICR expression and hypothesized that these patients, while experiencing an initial CB, might cease to respond quickly. Indeed, when stratifying patients with CB based on the duration of their response (>12 months, <12 months but >6 months, and <6 months), Applicants found that patients

with an initial CB but high uICR score pretreatment were significantly more likely to experience subsequent progressive disease (**Fig. 4F**). Indeed, patients with rapid progression, that is CB<6 months had the highest uICR score, even compared to those with no-CB. Consistently, the resistance signatures were most accurate in predicting patients with complete responses ($P < 6.3 \times 10^{-3}$, one-sided t-test, **Fig. 4G, fig. 14**). In this task, they were superior to all the other alternative predictors ($P = 1.64 \times 10^{-8}$, Wilcoxon ranksum test), all of which, including the clinically used markers, failed to predict complete response (**Fig. 4H**).

[0368] Finally, Applicants explored intrinsic vs. acquired uICR programs in an additional independent cohort, collected in yet another hospital (**materials and methods**), consisting of 90 samples from 26 patients with metastatic melanoma who underwent both pre-treatment and post-progression biopsies with bulk RNA-Seq, including 17 patients with on-treatment biopsy (**Fig. 1A**). The ICR state was induced following ICI compared to pre-ICI lesions from the same patient ($P = 1.26 \times 10^{-4}$ and 0.01, for the refined uICR and uICR-up, respectively; mixed-effect test, **materials and methods**). However, inter-patient variation in uICR expression was significantly higher than intra-patient changes ($P < 10^{-8}$, ANOVA). This suggests that one pre-treatment sample per patient may suffice to evaluate ICR for many patients, and that intrinsic resistance may be more prevalent than acquired resistance, consistent with clinical observations (3). Notably, Applicants did not observe an induction in uICR expression following RAF/MEK-inhibition (**materials and methods**), indicating that the ICR state is specific to ICI therapy and not merely a marker of a generally drug resistant tumor ecosystem.

Discussion

[0369] Applicants discovered new features linked to response and resistance to immunotherapy in metastatic melanoma with a strong prognostic and predictive value in independent patient cohorts. T cell profiles from ICR patients reflect variability in T cell responses, which are often decoupled from the clinical response. In some ICR patients, T cells manifest substantial clonal expansions, in others higher frequency of T cell proliferation, or a shift in the cytotoxicity/exhaustion balance. While more data is needed to distinguish between proper and insufficient T cell response to ICI, the results suggest that malignant cell-autonomous programs may be another key contributor to ICR, even in the presence of properly activated T cells (**Fig. 4I**).

[0370] Malignant cell programs that suppress interactions with the tumor microenvironment, modulate key inflammatory pathways and activate mechanisms of T cell

exclusion were distinguishing features of ICR tumors. These may be jointly controlled as a single coherent resistance program to confer ICR, through master regulators like Myc and CDK4/6. While these programs were initially identified in post-progression samples using scRNA-Seq, Applicants validated their predictive value in a pre-ICI cohort and explored their expression in matched pre/post specimens of ICI-treated patients. The ICR signatures Applicants identified were superior to a comprehensive and diverse set of alternative predictors in several ways, especially in predicting complete responders and patients that responded for more than 6 months. Unlike other predictors, the ICR signatures have a significant additional predictive value beyond pre-treatment T cell infiltration levels, indicating that they highlight new and yet unappreciated aspects of ICR. In light of these results, the signatures may help stratify patients for ICI beyond currently used biomarkers.

[0371] The pathways represented in the resistance program also highlight potential mechanistic causes of ICR that could be reversed by combining ICI with other drugs. Combination of ICI with CDK4/6 inhibitors (such as abemaciclib) may be particularly attractive in light of the findings that abemaciclib reverses the resistant oncogenic state and that there are distinctions between the cell cycle programs of malignant cells and T cells.

[0372] The malignant resistance programs may be relevant in other subtypes of melanoma and even in other lineage-independent cancer types. Among different types of melanoma, uveal melanoma has more active resistance programs compared to cutaneous melanoma (**Fig. 3D**); across cancers, the resistance program is higher in some cancer types that are less responsive to immunotherapy and/or arise from immune-privileged tissues (eye, testis) and lower in some of the more responsive tissues (head and neck, kidney, skin, lung) (**fig. 15**). This distinction, however, is imperfect, and additional, tumor-specific resistance programs may be discovered by similar strategies. Our study uncovers an improved, potentially clinically applicable biomarker for patient selection, provides a rationale to examine novel mechanisms of ICR, and reveals guiding principles to further dissect and repress mechanistic underpinnings that mediate ICI resistance.

[0373] Applicants demonstrated that cancer cell-autonomous ICR programs identified by scRNA-Seq predict clinical response (per RECIST criteria) and progression-free survival in two independent cohorts: one of patients who underwent RNA-seq of matched pre-treatment and progression (ICR) specimens; and another of 112 melanoma patients with pre-treatment RNA-seq who receive anti-PD-1 monotherapy. Applicants also validated the prognostic value of these cell programs in TCGA. Lastly, Applicants demonstrated that pharmacological

reversal of these oncogenic cell states can be achieved by CDK4/6-inhibition, and explored the impact of this treatment in melanoma at the single cell level. To determine the role of T cell exclusion from the TME as a potential mechanism of ICR, Applicants performed spatially resolved 30-plex single-cell protein analysis of matching FFPE specimens from 16 of the patients who also underwent scRNA-seq. Thus, the presented analytical platforms provide a promising approach to understanding drug resistance within preserved tumor ecosystems.

[0374] In conclusion, this study provides a high-resolution landscape of oncogenic ICR states, identifies clinically predictive signatures, and forms a basis to develop novel therapeutic strategies that could overcome immunotherapy resistance in melanoma.

Table SI. Clinical characteristics of the patients and samples in the scRNA-Seq cohort, and in the two validation cohorts.

scRNA-Seq cohort

Sample	Cohort	Age	Sex	Treatment	Treatment group	Lesion type	Site
Mel53	Tirosh et al. 2016	77	F	None	TN	metastasis	Subcutaneous back lesion
Mel58	Tirosh et al. 2016	83	M	Ipilimumab	ICR	metastasis	Subcutaneous leg lesion
Mel60	Tirosh et al. 2016	60	M	Trametinib, ipilimumab	ICR	metastasis	Spleen
Mel71	Tirosh et al. 2016	79	M	None	TN	metastasis	Transverse colon
Mel72	Tirosh et al. 2016	57	F	IL-2, nivolumab, ipilimumab + anti-KIR-Ab	ICR	metastasis	External iliac lymph node
Mel74	Tirosh et al. 2016	63	M	Nivolumab	ICR	metastasis	Terminal ileum
Mel75	Tirosh et al. 2016	80	M	Ipilimumab + nivolumab, WDVAX	ICR	metastasis	Subcutaneous leg lesion
Mel78	Tirosh et al. 2016	73	M	WDVAX, ipilimumab + nivolumab	ICR	metastasis	Small bowel
Mel79	Tirosh et al. 2016	74	M	None	TN	metastasis	Axillary lymph node
Mel80	Tirosh et al. 2016	86	F	None	TN	metastasis	Axillary lymph node
Mel81	Tirosh et al. 2016	43	F	None	TN	metastasis	Axillary lymph node
Mel82	Tirosh et al. 2016	73	F	None	TN	metastasis	Axillary lymph node
Mel84	Tirosh et al. 2016	67	M	None	TN	primary tumor	Acral primary
Mel88	Tirosh et al. 2016	54	F	Tremelimumab + MEDI3617	ICR	metastasis	Cutanous met
Mel89	Tirosh et al. 2016	67	M	None	TN	metastasis	Axillary lymph node
Mel94	Tirosh et al. 2016	54	F	IFN, ipilimumab + nivolumab	ICR	metastasis	Iliac lymph node
Mel126	Additional	63	M	Ipilimumab, nivolumab	ICR	metastasis	Soft tissue

Sample	Cohort	Age	Sex	Treatment	Treatment group	Lesion type	Site
Mel04.3	Additional	81	M	Ipilimumab	CB	metastasis	Skin
Mel110	Additional	74	M	ipilimumab + angiopoietin 2 inhibitor, Temezlolamide, Pembrolizumab	ICR	metastasis	R adrenal metastasis
Mel121.1	Additional	74	M	S/p Pembrolizumab	ICR	metastasis	Skin
Mel106	Additional	67	M	Prior treatment: nivolumab + ipilimumab	ICR	metastasis	Necrotic L axillary lymph nodes
Mel75.1	Additional	81	M	Ipilimumab + nivolumab, WDVAX, Pembrolizumab	ICR	metastasis	Soft tissue
Mel98	Additional	47	F	S/p IFN, s/p ipilimumab+GMCSF	ICR	metastasis	L thigh soft tissue metastasis
Mel102	Additional	72	F	S/p nivolumab + ipilimumab	ICR	metastasis	Fragmented pieces of (R) adrenal gland metastasis
Mel129PA	Additional	63	M	None	TN	primary tumor	Skin
Mel129PB	Additional	63	M	None	TN	primary tumor	Skin
Mel116	Additional	85	M	None	TN	metastasis	Lymph node
Mel103	Additional	58	M	None	TN	metastasis	Lymph node
Mel105	Additional	77	M	None	TN	primary tumor	Skin
Mel112	Additional	76	M	None	TN	metastasis	Bulky (L) axillary metastasis
Mel194	Additional	68	M	Nivolumab + lirilumab (anti-kit), Nivolumab, Ipilimumab, Pan-RAF-inhibitor, Pembrolizumab	ICR	metastasis	L anterior shoulder subcutaneous
Mel478	Additional	54	F	None	TN	metastasis	Transanal rectal mass
Mel128	Additional	37	M	None	TN	metastasis	Lymph node

Cohort 1	Sex, n	Number of therapies prior to anti-PD-1 therapy, n	RECIST category
Patients 1-112	Female, 49	No prior treatment, 49	PD, 49
	Male, 56	1, 34	SD, 13
	n/a, 7	2, 14	PR, 25
		3, 6	CR, 14
		7, 2	n/a, 11
		n/a, 7	

Cohort 2	Number of samples per patient, n
Patients 1-26	2, 10
90 samples	3, 8
	4, 3
	6, 2
	7, 2
	8, 1

Table S2

Table S2. Quality measures of scRNA-Seq experiment					
Cell type	Median no. of detected genes	Median no. of aligned reads	No. of TN cells	No. of ICR cells	Total no. of cells
B.cell	3774	164400	463	355	818
CAF	5518	357423	61	45	106
Endothelial cell	5057	304326	87	17	104
Macrophage	5670	654482	161	259	420
Mai	5482	335563	1193	825	2018
NK	3909	147376	44	48	92
CD4 T cell	4036	220614	420	436	856
CD8 T cell	4064	264494	720	1039	1759
T cell (unresolved)	3827	234410	298	408	706
Low quality cell	732	24991	1386	1551	2937
?	3433	221421	183	124	307
All cells	3559	377141	5016	5107	10123

Table S4

Table S4. Cell type signatures that were derived from the analysis of the scRNA-seq data (see section Data-driven signatures of specific cell types).												
B cell	CAF	Endothelial cell	Macrophage	Malignant cell	NK cell	T cell	CD4 T cell	CD8 T cell	Immune cell		Lymphocyte	Stroma cell
ADAM19	ABI3BP	A2M	ACP5	AATF	CCL4	AAK1	AQP3	AKAP5	AAK1	HLA-DRB6	AAK1	A2M
ADAM28	ACTA2	ADAM15	ACSL1	ACN9	CD244	ACAP1	CCR4	APOBEC3C	ACAP1	HMHA1	ACAP1	ABI3BP
AFF3	ADAM12	ADAMTS9	ADAMDEC1	ACSL3	CST7	AKNA	CD28	APOBEC3G	ACP5	HMOX1	ADAM19	ACTA2
BANK1	ADAMTS2	ADCY4	ADAP2	AHCY	CTSW	APOBEC3G	CD4	ARHGA P9	ACSL1	HNRNP A1P10	ADAM28	ADAM12
BCL11A	ANTXR1	AFAP1L1	ADORA3	AIF1L	GNLY	ARAP2	CD40LG	ATP8A1	ADAM19	HOPX	AFF3	ADAM15
BIRC3	ASPN	APLNR	ADPGK	AK2	GZMA	ARHGEF1	CD5	BTN3A1	ADAM28	HSH2D	AKAP5	ADAMTS2
BLK	CIS	AQP1	AIF1	ALX1	GZMB	ASB2	DGKA	CBLB	ADAMDEC1	HSPA6	AKNA	ADAMTS9
BLNK	CALD1	ARHGEF15	AKR1A1	AMD1	HOPX	ATHL1	F5	CCL4	ADAP2	HSPA7	ANKRD44	ADCY4
BTLA	CCDC80	CALCRL	ALDH2	ANKRD20A12P	ID2	BCL11B	FAAH2	CCL4L1	ADORA3	HVCN1	APOBEC3C	AFAP1L1
CCR6	CD248	CCL14	ALDH3B1	ANKRD54	IL2RB	BTN3A2	FOX P3	CCL4L2	ADPGK	ICOS	APOBEC3D	ANTXR1
CCR7	CDH11	CD200	AMICA1	AP1S2	KLRB1	CBLB	ICOS	CCL5	AFF3	ID2	APOBEC3G	APLNR
CD19	CERCAM	CD34	ANKRD22	AP0A1BP	KLRCI	CCL4	IL6R	CD27	AIF1	IFI30	AQP3	APP
CD1C	COL12A1	CD93	AP1B1	AP0C2	KLRD1	CCL5	IL7R	CD7	AKAP5	IFNG	ARAP2	AQP1
CD22	COL14A1	CDH5	AQP9	APOD	KLRF1	CD2	PASK	CD8A	AKNA	IFNGR1	ARHGA P15	ARHGEF15
CD24	COL1A1	CFI	ATF5	APOE	KLRK1	CD247	PBXIP1	CD8B	AKR1A1	IFNGR2	ARHGA P9	ASPN
CD37	COL1A2	CLDN5	ATG3	ATP1A1	NCAM1	CD27	SLAMF1	CD96	ALDH2	IGFLR1	ARHGEF1	BGN
CD52	COL3A1	CLEC14A	ATG7	ATP1B1	NKG7	CD28	SPOCK2	CLEC2D	ALDH3B1	IGLL1	ASB2	C1R
CD79A	COL5A1	COL15A1	ATP6V0B	ATP5C1	PRF1	CD3D	TCF7	CRTAM	ALOX5	IGLL3P	ATHL1	CIS

Table S4. Cell type signatures that we derived from the analysis of the scRNA-seq data (see section Data-driven signatures of specific cell-types)

B cell	CAF	Endothelial cell	Macrophage	Malignant cell	NK cell	T cell	CD4 T cell	CD8 T cell	Immune cell		Lymphocyte	Stroma cell
CD79B	COL5A2	COL4A1	ATP6V0D1	ATP5G1	PTGDR	CD3E	TNFSF8	CST7	ALOX5AP	IIGL5	ATP2A3	CALCRL
CD82	COL6A1	COL4A2	ATP6V1B2	ATP5G2	SH2DIB	CD3G		CTSW	AMIC A1	IGSF6	ATP8A1	CALD1
CHMP7	COL6A2	CRIP2	BCL2A1	ATP6V0E2	XCL1	CD5		CXCL13	ANKRD22	IKZF1	BANK1	CCDC80
CIITA	COL6A3	CXorf36	BID	ATP6V1CI		CD6		CXCR6	ANKRD44	IKZF3	BCL11A	CCL14
CLEC17A	COL8A1	CYYR1	BLVRA	ATP6V1E1		CD7		DTHD1	AOAH	IL1ORA	BCL11B	CD200
CNR2	CREB3L1	DARC	BLVRB	ATP6V1GI		CD8A		DUSP2	AP1B1	IL12RB1	BIRC3	CD248
COL19A1	CXCL14	DCHS1	C1orf75	AZGP1		CD8B		EOMES	APOBEC3C	IL16	BLK	CD34
COL4A3	CYBRD1	DOCK6	C15orf48	BAIAP2		CD96		FASLG	APOBEC3D	IL18	BLNK	CD93
CR2	DCN	DOCK9	C19orf38	BANCR		CDC42SE2		FYN	APOBEC3G	IL1B	BTLA	CDH11
CXCR5	DPT	DYSF	C1orf62	BCAN		CELF2		GPR171	AQP3	IL1RN	BTN3A1	CDH5
ELK2AP	EFEMP2	ECE1	C1QA	BCAS3		CLEC2D		GZMA	AQP9	IL2RB	BTN3A2	CERCAM
FAIM3	FBLN1	ECSCR	C1QB	BCHE		CNOT6L		GZMB	ARAP2	IL2RG	C16orf54	CFI
FAM129C	FBLN5	EGFL7	C1QC	BIRC7		CST7		GZMH	ARHGAP15	IL32	CBLB	CLDN5
FCER2	FGF7	ELK3	C2	BZW2		CTLA4		GZMK	ARHGAP30	IL4I1	CCL4	CLEC14A
FCRL1	GPR176	ELTD1	C3AR1	C10orf90		CTSW		ID2	ARHGAP4	IL6R	CCL4L1	COL12A1
FCRL2	HSPB6	EMCN	C5AR1	C1orf11		CXCL13		IFNG	ARHGAP9	IL7R	CCL4L2	COL14A1
FCRL5	INHBA	ENG	C9orf72	C12orf76		CXCR3		IKZF3	ARHGDI B	IL8	CCL5	COL15A1
FCRLA	ISLR	EPAS1	CAPG	C17orf89		CXCR6		IL2RB	ARHGEF1	INPP4B	CCR4	COL1A1
HLA-DOB	ITGA11	EPHB4	CARD9	C1orf43		DEF6		ITGA4	ARPC3	INPP5D	CCR6	COL1A2
HLA-DQA2	LOX	ERG	CASP1	C1orf85		DENND2D		ITGB7	ARRB2	IPCEF1	CCR7	COL3A1
HVCN1	LPAR1	ESAM	CCR1	C4orf48		DGKA		JAKMIP1	ASB2	IRF5	CD19	COL4A1
IIGL1	LTBP2	FGD5	CCR2	CA14		DTHD1		KIR2DL4	ATF5	IRF8	CD1C	COL4A2
IIGL3P	LUM	FKBP1A	CD14	CA8		DUSP2		KLRC1	ATG3	ISG20	CD2	COL5A1
IIGL5	MAP1A	FLT4	CD163	CACYBP		EMB		KLRC2	ATG7	ITGA4	CD22	COL5A2
IRF8	MEG3	GALNT18	CD274	CAPN3		EVL		KLRC3	ATHL1	ITGAL	CD24	COL6A1
KBTBD8	MIR100HG	GPR116	CD300C	CBX3		FASLG		KLRC4	ATP2A3	ITGAM	CD244	COL6A2
KIAA0125	MRC2	HERC2P2	CD300E	CCDC47		FYN		KLRC4-KLRK1	ATP6VOB	ITGAX	CD247	COL6A3
KIAA0226L	MXRA8	HSPG2	CD300LB	CCND1		GATA3		KLRD1	ATP6V0D1	ITGB2	CD27	COL8A1
LOC283663	MYL9	HYAL2	CD300LF	CCT2		GPR171		KLRK1	ATP6V1B2	ITGB7	CD28	CREB3L1
LRMP	NID2	ICA1	CD302	CCT3		GPR174		LAG3	ATP8A1	ITK	CD37	CRIP2
LTB	OLFML3	ID1	CD33	CCT6A		GPRIN3		LOC100506776	BANK1	JAK3	CD3D	CXCL14
MS4A1	PALLD	IL3RA	CD4	CCT8		GRAP2		LYST	BCL11A	JAKMIP1	CD3E	CXorf36

Table S4. Cell type signatures that we derived from the analysis of the scRNA-seq data (see section Data-driven signatures of specific cell types).

B cell	CAF	Endothelial cell	Macrophage	Malignant cell	NK cell	T cell	CD4 T cell	CD8 T cell	Immune cell		Lymphocyte	Stroma cell
NAPS B	PCDH18	ITGB4	CD68	CDH19		GZMA		MIR155HG	BCL11B	KBTBD8	CD3G	CYBRD1
NCOA3	PCOLCE	KDR	CD80	CDH3		GZMB		NELL2	BCL2A1	KCNMA1	CD4	CYYR1
P2RX5	PDGFRA	LAMA5	CD86	CDK2		GZMH		NGK7	BID	KIAA0125	CD40LG	DARC
PAX5	PDGFRB	LDB2	CECR1	CHCHD6		GZMK		OASL	BIN2	KIAA0226L	CD5	DCHS1
PLEKHF2	PDGFRL	LOC100505495	CFP	CITED1		GZMM		PARP8	BIRC3	KIR2DL4	CD52	DCN
PNOC	PLAC9	MALL	CLEC10A	CLCN7		HNRNP A1P10		PDCD1	BLK	KLRB1	CD6	DOCK6
POLD4	PDN	MMRN1	CLEC12A	CLNS1A		ICOS		PIP4K2A	BLNK	KLRC1	CD69	DOCK9
POU2AF1	PRRX1	MMRN2	CLEC4A	CMC2		IFNG		PRF1	BLVRA	KLRC2	CD7	DPT
POU2F2	RARRS2	MYCT1	CLEC4E	COA6		IKZF1		PRKCH	BLVRB	KLRC3	CD79A	DYSF
QRSL1	RCN3	NOS3	CLEC5A	COX5B		IKZF3		PSTPIP1	BTK	KLRC4	CD79B	ECE1
RALGPS2	SDC2	NOTCH4	CLEC7A	COX7A2		IL12RB1		PTPN22	BTLA	KLRC4-KLKR1	CD82	ECSCR
RPL13	SFRP2	NPDC1	CMKLR1	COX7C		IL2RB		PVRIG	BTN3A1	KLRD1	CD8A	EFEMP2
RPS20	SLIT3	PALMD	CNPY3	CRYL1		IL2RG		PYHIN1	BTN3A2	KLRF1	CD8B	EGFL7
RPS23	SMOC2	PCDH17	COTL1	CSAG1		IL32		RAB27A	Clorf75	KLKR1	CD96	EHD2
SEL1L3	SPOCK1	PDE2A	CPVL	CSAG2		IL7R		RARRS3	C15orf48	KYNU	CDC42SE2	ELK3
SELL	SULF1	PDLIM1	CREG1	CSAG3		INPP4B		RUNX3	C16orf54	LAG3	CELF2	ELTD1
SMIM14	SVEP1	PECAM1	CSF1R	CSPG4		IPCEF1		SAMD3	C19orf38	LAIR1	CHMP7	EMCN
SNX29	TAGLN	PLVAP	CSF2RA	CTNNA1		ITGAL		SH2D1A	Clorf162	LAPTM5	CIITA	ENG
SNX29P1	THBS2	PLXND1	CSF3R	CYC1		ITK		SLA2	C1QA	LAT	CLEC17A	EPAS1
SPIB	THY1	PODXL	CSTA	CYP27A1		JAK3		SLAMF6	C1QB	LAT2	CLEC2D	EPHB4
ST6GAL1	TMEM119	PRCP	CTSB	DAAM2		JAKMIP1		SYTL3	C1QC	LBH	CNOT6L	ERG
STAG3	TPM1	PREX2	CTSC	DANCR		KLRC4		TARP	C2	LCK	CNR2	ESAM
STAP1	TPM2	PTPRB	CTSD	DAP3		KLRD1		THEMIS	C3AR1	LCP1	COL19A1	FBLN1
TCL1A		PVRL2	CTSH	DCT		KLRK1		TIGIT	C5AR1	LCP2	COL4A3	FBLN5
TLR10		RAMP2	CTSS	DCXR		LAG3		TNFRSF9	C9orf72	LEPROTLI	CORO1A	FBN1
TMEM154		RAMP3	CXCL10	DDIT3		LAT		TNIP3	CAPG	LGALS2	CR2	FGD5
TNFRSF13B		RHOJ	CXCL16	DDT		LCK		TOX	CARD9	LGMN	CRTAM	FGF7
VPREB3		ROB4	CXCL9	DFNB31		LEPROTLI		TTC24	CASP1	LILRA1	CST7	FKBP1A
WDFY4		S1PR1	CXCR2PI	DLL3		LIME1		WIPF1	CBLB	LILRA2	CTLA4	FLT4
ZCCHC7		SDPR	CYBB	DNAH14		LOC100130231		XCL1	CCL3	LILRA3	CTSW	FSTL1
		SELP	CYP2S1	DNAJA4		MAP4K1		XCL2	CCL4	LILRA5	CXCL13	GALNT18
		SHROOM4	DAPK1	DSCR8		MIAT			CCL4LI	LILRA6	CXCR3	GNG11

Table S4. Cell type signatures that we've derived from the analysis of the scRNA-seq data (see section Data-driven signatures of specific cell types).

B cell	CAF	Endothelial cell	Macrophage	Malignant cell	NK cell	T cell	CD4 T cell	CD8 T cell	Immune cell	Lymphocyte	Stroma cell	
		SLC02A1	DHRS9	DUSP4		NELL2			CCL4L2	LILRB1	CXCR4	GPR116
		SMAD1	DMXL2	EDNRB		NKG7			CCL5	LILRB2	CXCR5	GPR176
		STOM	DNAJC5B	EIF3C		NLRC3			CCR1	LILRB3	CXCR6	HERC2P2
		SYNPO	EBI3	EIF3D		NLRC5			CCR2	LILRB4	CYFIP2	HSPB6
		TAOK2	EMR2	EIF3E		OXNAD1			CCR4	LILRB5	CYTIP	HSPG2
		TEK	EPSTI1	EIF3H		PAG1			CCR6	LIMD2	DEF6	HYAL2
		TENC1	F13A1	EIF3L		PARP8			CCR7	LIME1	DENND2D	ICA1
		TGFBR2	FAM157B	ENO1		PCED1B			CD14	LIPA	DGKA	ID1
		TGM2	FAM26F	ENO2		PCED1B-AS1			CD163	LITAF	DTHD1	ID3
		THBD	FBP1	ENTHD1		PDCD1			CD19	LOC100130231	DUSP2	IFITM3
		TIE1	FCER1G	ENTPD6		PIK3IP1			CD1C	LOC100506776	ELK2AP	IGFBP4
		TM4SF1	FCGR1A	ERBB3		PIM2			CD2	LOC283663	EMB	IGFBP7
		TM4SF18	FCGR1B	ESRP1		PIP4K2A			CD22	LOC729737	EOMES	IL3RA
		TMEM255B	FCGR1C	ETV4		PPP2R5C			CD24	LPXN	EVL	INHBA
		TSPAN18	FCGR2A	ETV5		PRDM1			CD244	LRMP	EZR	ISLR
		TSPAN7	FCGR2C	EXOSC4		PRF1			CD247	LRRC25	F5	ITGA11
		VWF	FCN1	EXTL1		PRKCQ			CD27	LSP1	FAAH2	ITGA5
		ZNF385D	FGL2	FAHD2B		PSTPIP1			CD274	LST1	FAIM3	ITGB4
			FOLR2	FAM103A1		PTPN22			CD28	LTA4H	FAM129C	KDR
			FPR1	FAM178B		PTPN7			CD30QA	LTB	FAM65B	LAMA5
			FPR2	FANCL		PVRIG			CD30OC	LY86	FASLG	LAMB1
			FPR3	FARP2		PYHIN1			CD30OE	LY9	FCER2	LDB2
			FTH1	FASN		RAB27A			CD30OLB	LYN	FCRL1	LOC100505495
			FTL	FBX032		RAPGEF6			CD30OLF	LYST	FCRL2	LOX
			FUCA1	FBX07		RARRES3			CD302	LYZ	FCRL3	LPAR1
			FUOM	FDFT1		RASAL3			CD33	M6PR	FCRL5	LTBP2
			GABARAP	FKBP4		RASGRP1			CD37	MAFB	FCRLA	LUM
			GATM	FMN1		RGS1			CD38	MAN2B1	FOXP3	MALL
			GBP1	FXYD3		RHOF			CD3D	MAP4K1	FYB	MAP1A
			GCA	GALE		RNF213			CD3E	1-Mar	FYN	MEG3
			GK	GAPDH		RUNX3			CD3G	MARCO	GATA3	MIR100HG
			GLA	GAPDHS		SCML4			CD4	MFSD1	GNLY	MMP2

Table S4. Cell type signatures that we've derived from the analysis of the srRNA-seq data (see section Data-driven signatures of specific cell types)												
B cell	CAF	Endothelial cell	Macrophage	Malignant cell	NK cell	T cell	CD4 T cell	CD8 T cell	Immune cell		Lymphocyte	Stroma cell
			GLRX	GAS2L3		SEMA4D			CD40LG	MIAT	GPR171	MMRN1
			GLUL	GAS5		1-Sep			CD48	MILR1	GPR174	MMRN2
			GM2A	GAS7		SH2D1A			CD5	MIR155HG	GPRIN3	MRC2
			GNA15	GDF15		SH2D2A			CD52	MNDA	GRAP2	MXRA8
			GPBAR1	GJB1		SIRPG			CD53	MOB1A	GZMA	MYCT1
			GPR34	GPATC H4		SIT1			CD6	MPEG1	GZMB	MYL9
			GPR84	GPM6B		SKAP1			CD68	MPP1	GZMH	NFIB
			GPX1	GPNMB		SLA2			CD69	MS4A1	GZMK	NID2
			CRN	GPR137B		SPATA13			CD7	MS4A4A	GZMM	NNMT
			HCAR2	GPR143		SPN			CD72	MS4A6A	HLA-DOB	NOS3
			HCAR3	GPS1		SPOCK2			CD74	MS4A7	HLA-DQA2	NOTCH4
			HCK	GSTP1		STAT4			CD79A	MSR1	HMHA1	NPDC1
			HK2	GYG2		SYTL3			CD79B	MTMR14	HNRNP A1P10	OLFML3
			HK3	H2AFZ		TARP			CD80	MYD88	HOPX	PALLD
			HLA-DMA	HAX1		TBC1D10C			CD82	MYOIF	HSH2D	PALMD
			HLA-DMB	HIST1H2BD		TC2N			CD83	NAAA	HVCN1	PCDH17
			HLA-DPA1	HIST3H2A		TESPA1			CD84	NADK	ICOS	PCDH18
			HLA-DPB1	HMG20B		THEMIS			CD86	NAGA	ID2	PCOLCE
			HLA-DPB2	HMGA1		TIGIT			CD8A	NAGK	IFNG	PDE2A
			HLA-DRA	HPGD		TNFAIP3			CD8B	NAIP	IIGLL1	PDGFR A
			HLA-DRB1	HPS4		TNFRSF9			CD96	NAPSB	IIGLL3P	PDGFR B
			HLA-DRB5	HPS5		TOX			CD97	NCAM1	IIGLL5	PDGFRL
			HLA-DRB6	HSP90A A1		TRAF1			CDC42SE2	NCF1	IKZF1	PDLIM1
			HMOX1	HSP90A B1		TRATI			CECR1	NCF1B	IKZF3	PECAM1
			HSPA6	HSPA9		TTC39C			CELF2	NCF1C	IL12RB1	PLAC9
			HSPA7	HSPD1		UBASH3A			CFP	NCF2	IL16	PLVAP
			IFI30	HSPE1		WIPF1			CHMP7	NCF4	IL2RB	PLXND1
			IFNGR1	IGSF11		ZAP70			CIITA	NCKAP1L	IL2RG	PODN
			IFNGR2	IGSF3		ZC3HAV1			CLEC10A	NCOA3	IL32	PODXL
			IGFLR1	IGSF8					CLEC12A	NCOA4	IL6R	PPIC
			IGSF6	INPP5F					CLEC17A	NELL2	IL7R	PRCP
			IL18	IRF4					CLEC2D	NFAM1	INPP4B	PREX2

Table S4. Cell type signatures that were derived from the analysis of the scRNA-seq data (see section Data-driven signatures of specific cell-types).												
B cell	CAF	Endothelial cell	Macrophage	Malignant cell	NK cell	T cell	CD4 T cell	CD8 T cell	Immune cell		Lymphocyte	Stroma cell
			IL1B	ISYNA1					CLEC4A	NINJ1	IPCEF1	PRRX1
			IL1RN	KCNJ13					CLEC4E	NKG7	IRF8	PTPRB
			IL4I1	LAGE3					CLEC5A	NLRC3	ISG20	PTRF
			IL8	LDHB					CLEC7A	NLRC4	ITGA4	PVRL2
			IRF5	LDLRA D3					CMKLR1	NLRC5	ITGAL	PXDN
			KCNMA1	LEF1-AS1					CNOT6L	NLRP3	ITGB7	RAMP2
			KYNU	LHFPL3-AS1					CNPY3	NMI	ITK	RAMP3
			LAIR1	LINC00473					CNR2	NPC2	JAK3	RARRES2
			LGALS2	LINC00518					COL19A1	NPL	JAKMIP1	RCN3
			LGMN	LINC00673					COL4A3	OAS1	KBTBD8	RHOJ
			LILRA1	LOC100126784					CORO1A	OASL	KIAA0125	ROBO4
			LILRA2	LOC100127888					COTL1	OAZ1	KIAA0226L	S1PR1
			LILRA3	LOC100130370					CPVL	OLR1	KIR2DL4	SDC2
			LILRA5	LOC100133445					CR2	OSCAR	KLRB1	SDPR
			LILRA6	LOC100505865					CREG1	OXNAD1	KLRC1	SELP
			LILRB1	LOC146481					CRTAM	P2RX5	KLRC2	SFRP2
			LILRB2	LOC340357					CSF1R	P2RY12	KLRC3	SHROOM4
			LILRB3	LONP2					CSF2RA	P2RY13	KLRC4	SLCO2A1
			LILRB4	LOXL4					CSF3R	PAG1	KLRC4-KLRK1	SLIT3
			LILRB5	LZTS1					CST7	PAK1	KLRD1	SMAD1
			LIPA	MAGEA1					CSTA	PARP15	KLRF1	SMOC2
			LOC729737	MAGEA12					CTLA4	PARP8	KLRK1	SPARC
			LRRC25	MAGEA2					CTSB	PARVG	LAG3	SPARCL1
			LST1	MAGEA2B					CTSC	PASK	LAT	SPOCK1
			LTA4H	MAGEA3					CTSD	PAX5	LBH	STOM
			LYZ	MAGEA4					CTSH	PBXIP1	LCK	SULF1
			MAFB	MAGEA6					CTSS	PCED1B	LEPROTL1	SVEP1
			MAN2B1	MAGEC1					CTSW	PCED1B-AS1	LIMD2	SYNPO
			MARCO	MDH1					CXCL10	PCK2	LIME1	TAGLN
			MFSD1	MDH2					CXCL13	PDCD1	LOC100130231	TAOK2
			MILR1	MFI2					CXCL16	PIK3AP1	LOC100506776	TEK
			MNDA	MFSD12					CXCL9	PIK3IP1	LOC283663	TENC1

Table S4. Cell type signatures that we've derived from the analysis of the scRNA-seq data (see section Data-driven signatures of specific cell types)

B cell	CAF	Endothelial cell	Macrophage	Malignant cell	NK cell	T cell	CD4 T cell	CD8 T cell	Immune cell	Lymphocyte	Stroma cell	
			MOB1A	MIA					CXCR2P1	PIK3R5	LRMP	TGFBR2
			MPEG1	MIF					CXCR3	PILRA	LTB	TGM2
			MPP1	MITF					CXCR4	PIM2	LY9	THBD
			MS4A4A	MLANA					CXCR5	PION	LYST	THBS2
			MS4A6A	MLPH					CXCR6	PIP4K2A	MAP4K1	THY1
			MS4A7	MOK					CYBA	PLA2G7	MIAT	TIE1
			MSR1	MRPS21					CYBB	PLAC8	MIR155HG	TM4SF1
			MTMR14	MRPS25					CYFIP2	PLAUR	MS4A1	TM4SF18
			MYD88	MRPS26					CYP2SI	PLBD1	NAPSB	TMEM119
			NAAA	MRPS6					CYTH4	PLCB2	NCAM1	TMEM255B
			NADK	MSI2					CYTIP	PLEK	NCOA3	TPM1
			NAGA	MXI1					DAPK1	PLEKH A2	NELL2	TPM2
			NAGK	MYO10					DAPP1	PLEKHF2	NKG7	TSPAN18
			NAIP	NAV2					DEF6	PLEKH01	NLRC3	TSPAN7
			NCF2	NDUFA4					DENN D2D	PLIN2	NLRC5	VWF
			NCF4	NDUFB9					DGKA	PNOC	OASL	ZNF385D
			NCOA4	NDUFS2					DHRS9	POLD4	OXNAD1	
			NFAM1	NEDD4L					DMXL2	POU2AF1	P2RX5	
			NINJ1	NELFCD					DNAJ C5B	POU2F2	PAG1	
			NLRC4	NHP2					DOCK2	PPM1K	PARP15	
			NLRP3	NME1					DOCK8	PPP2R5C	PARP8	
			NMI	NOP58					DOK2	PPT1	PASK	
			NPC2	NPM1					DOK3	PRAMI	PAX5	
			NPL	NSG1					DTHD1	PRDM1	PBXIP1	
			OAS1	NT5C3					DUSP2	PRF1	PCED1B	
			OAZ1	NT5DC3					EBI3	PRKCB	PCED1B-AS1	
			OLR1	OSTM1					ELK2AP	PRKCD	PDCD1	
			OSCAR	PACSIN2					EMB	PRKCH	PIK3IP1	
			P2RY12	PAGE5					EMR2	PRKCQ	PIM2	
			P2RY13	PAICS					EOMES	PSAP	PIP4K2A	
			PAK1	PAX3					EPSTI1	PSMB10	PLAC8	
			PCK2	PEBP1					EVI2A	PSTPIP1	PLEKH A2	

Table S4. Cell type signatures that were derived from the analysis of the scRNA-seq data (see section Data-driven signatures of specific cell-types).

B cell	CAF	Endothelial cell	Macrophage	Malignant cell	NK cell	T cell	CD4 T cell	CD8 T cell	Immune cell		Lymphocyte	Stroma cell
			PILRA	PEG10					EVI2B	PTAFR	PLEKHF2	
			PLA2G7	PFDN2					EVL	PTGDR	PNOC	
			PLAUR	PHB					EZR	PTK2B	POLD4	
			PLBD1	PHLDA1					F13A1	PTPN22	POU2AF1	
			PLEKH01	PIGY					F5	PTPN6	POU2F2	
			PLIN2	PIR					FAAH2	PTPN7	PPM1K	
			PPT1	PLEKH B1					FAIM3	PTPRC	PPP2R5C	
			PRAM1	PLP1					FAM105A	PTPRCA P	PRDM1	
			PRKCD	PMEL					FAM129C	PVRIG	PRF1	
			PSAP	POLR2F					FAM157B	PYCARD	PRKCH	
			PTAFR	PPIL1					FAM26F	PYHIN1	PRKCQ	
			PYCARD	PRAME					FAM49B	QRSL1	PSTPIP1	
			RAB20	PSMB4					FAM65B	RAB20	PTGDR	
			RASSF4	PSMD4					FASLG	RAB27A	PTPN22	
			RBM47	PUF60					FBP1	RAC2	PTPN7	
			RELT	PYGB					FCER1G	RALGPS2	PTPRC	
			RGS10	PYURF					FCER2	RAPGEF6	PTPRCA P	
			RGS18	QDPR					FCGR1A	RARRES3	PVRIG	
			RGS19	RAB17					FCGR1B	RASAL3	PYHIN1	
			RGS2	RAB38					FCGR1C	RASGRP1	QRSL1	
			RHBD F2	RAN					FCGR2A	RASSF4	RAB27A	
			RILPL2	RAP1GA P					FCGR2C	RASSF5	RAC2	
			RIPK2	RGS20					FCGR3A	RBM47	RALGPS2	
			RNASE6	ROPN1					FCGR3B	RCSD1	RAPGEF6	
			RNASE T2	ROPN1 B					FCN1	RELT	RARRES3	
			RNF13	RPL38					FCRL1	RGS1	RASAL3	
			RNF130	RPS6KA5					FCRL2	RGS10	RASGRP1	
			RNF144B	RSL1D1					FCRL3	RGS18	RGS1	
			RTN1	RTKN					FCRL5	RGS19	RHOF	
			S100A8	S100A1					FCRLA	RGS2	RHOH	
			S100A9	S100B					FERM T3	RHBDF2	RNF213	
			SAMHD1	SCD					FGD2	RHOF	RPL13	

Table S4. Cell type signatures that were derived from the analysis of the scRNA-seq data (see section Data-driven signatures of specific cell-types).

B cell	CAF	Endothelial cell	Macrophage	Malignant cell	NK cell	T cell	CD4 T cell	CD8 T cell	Immune cell		Lymphocyte	Stroma cell
			SAT1	SDC3					FGD3	RHOG	RPS20	
			SDS	SEC11C					FGL2	RHOH	RPS23	
			SECTM1	SEMA3B					FGR	RILPL2	RUNX3	
			SEMA4A	SERPINA3					FOLR2	RIPK2	SAMD3	
			SERPINA1	SERPINE2					FOXP3	RNASE6	SCML4	
			SIGLEC1	SGCD					FPR1	RNASET2	SEL1L3	
			SIGLEC5	SGK1					FPR2	RNF13	SELL	
			SIGLEC9	SHC4					FPR3	RNF130	SEMA4D	
			SIRPB1	SLC19A2					FTH1	RNF144B	1-Sep	
			SIRPB2	SLC24A5					FTL	RNF213	SH2D1A	
			SLAMF8	SLC25A13					FUCA1	RPL13	SH2D1B	
			SLC11A1	SLC25A4					FUOM	RPS20	SH2D2A	
			SLC15A3	SLC26A2					FYB	RPS23	SIRPG	
			SLC1A3	SLC3A2					FYN	RPS6KA1	SIT1	
			SLC29A3	SLC45A2					GABARAP	RTN1	SKAP1	
			SLC31A2	SLC5A3					GATA3	RUNX3	SLA2	
			SLC7A7	SLC6A15					GATM	S100A8	SLAMF1	
			SLCO2B1	SLC7A5					GBP1	S100A9	SLAMF6	
			SMPDL3A	SNCA					GBP5	SAMD3	SMIM14	
			SNX10	SNHG16					GCA	SAMHD1	SNX29	
			SOD2	SNHG6					GK	SAMSN1	SNX29P1	
			SPI1	SNRPC					GLA	SASH3	SP140	
			SPINT2	SNRPD1					GLRX	SAT1	SPATA13	
			STAT1	SNRPE					GLUL	SCIMP	SPIB	
			STX11	SOD1					GM2A	SCML4	SPN	
			TBXAS1	SORD					GNA15	SDS	SPOCK2	
			TGFBI	SORT1					GPLY	SECTM1	ST6GAL1	
			THEMS2	SOX10					GPBAR1	SEL1L3	STAG3	
			TIFAB	SPCS1					GPR171	SELL	STAP1	
			TLR1	SPRY4					GPR174	SELPLG	STAT4	
			TLR2	ST13					GPR183	SEMA4A	STK17B	
			TLR5	ST3GAL4					GPR34	SEMA4D	STK4	

Table S4. Cell type signatures that were derived from the analysis of the scRNA-seq data (see section Data-driven signatures of specific cell-types).

B cell	CAF	Endothelial cell	Macrophage	Malignant cell	NK cell	T cell	CD4 T cell	CD8 T cell	Immune cell		Lymphocyte	Stroma cell
			TLR8	ST3GAL6					GPR84	1-Sep	SYTL3	
			TMEM106A	ST3GAL6-AS1					GPRI N3	SERPIN A1	TARP	
			TMEM176A	ST6GAL NAC2					GPSM3	SH2D1A	TBC1D10C	
			TMEM176B	STIP1					GPX1	SH2D1B	TC2N	
			TMEM37	STK32A					GRAP2	SH2D2A	TCF7	
			TNFAIP2	STMN1					GRB2	SIGLEC1	TCL1A	
			TNFAIP8L2	STX7					GRN	SIGLEC14	TESPA1	
			TNFSF13	STXBP1					GZMA	SIGLEC5	THEMIS	
			TNFSF13B	SYNGR1					GZMB	SIGLEC7	TIGIT	
			TPP1	TBC1D7					GZMH	SIGLEC9	TLR10	
			TREM1	TBCA					GZMK	SIRPB1	TMC8	
			TREM2	TEX2					GZMM	SIRPB2	TMEM154	
			TWF2	TFAP2A					HAVCR2	SIRPG	TNFAIP3	
			TYMP	TFAP2C					HCAR2	SIT1	TNFRSF13B	
			TYROBP	TMEM147					HCAR3	SKAP1	TNFRSF9	
			UBE2D1	TMEM14B					HCK	SLA	TNFSF8	
			VAMP8	TMEM177					HCLS1	SLA2	TNIP3	
			VMO1	TMEM251					HCST	SLAMF1	TOX	
			VSIG4	TMX4					HK2	SLAMF6	TRAF1	
			ZNF385A	TNFRSF21					HK3	SLAMF7	TRAF3IP3	
				TOM1L1					HLA-DMA	SLAMF8	TRAT1	
				TOMM20					HLA-DMB	SLC11A1	TSC22D3	
				TOMM22					HLA-DOB	SLC15A3	TTC24	
				TOMM6					HLA-DPA1	SLC1A3	TTC39C	
				TOMM7					HLA-DPB1	SLC29A3	UBASH3A	
				TOP1MT					HLA-DPB2	SLC31A2	VPREB3	
				TRIB2					HLA-DQA1	SLC7A7	WDFY4	
				TRIM2					HLA-DQA2	SLCO2B1	WIPF1	
				TRIM63					HLA-DQB1	SMAP2	XCL1	
				TRIML2					HLA-DQB2	SMIM14	XCL2	
				TRMT112					HLA-DRA	SMPDL3A	ZAP70	
				TSNAX					HLA-DRB1	SNX10	ZC3HAV1	

Table S4. Cell type signatures that we've derived from the analysis of the scRNA-seq data (see section Data-driven signatures of specific cell types).												
B cell	CAF	Endothelial cell	Macrophage	Malignant cell	NK cell	T cell	CD4 T cell	CD8 T cell	Immune cell		Lymphocyte	Stroma cell
				TTL4					HLA-DRB5	SNX20	ZCCHC7	
				TTYH2					SNX29	TMEM176A		
				TUBB2B					SNX29P1	TMEM176B		
				TUBB4A						TMEM37		
				TYR					SP140	TNFAIP2		
				TYRP1					SPATA13	TNFAIP3		
				UBL3					SPI1	TNFAIP8		
				UQCRH					SPIB	TNFAIP8L2		
				UTP18					SPINT2	TNFRSF13B		
				VAT1					SPN	TNFRSF9		
				VDAC1					SPOCK2	TNFSF13		
				VPS72					SRGN	TNFSF13B		
				WBSCR22					ST6GAL1	TNFSF8		
				XAGE1A					STAG3	TNIP3		
				XAGE1B					STAP1	TOX		
				XAGE1C					STAT1	TPP1		
				XAGE1D					STAT4	TRAF1		
				XAGE1E					STK17B	TRAF3IP3		
				XRCC6					STK4	TRAT1		
				XYLB					STX11	TREM1		
				ZCCHC17					STXB2	TREM2		
				ZFAS1					SYK	TSC22D3		
				ZFP106					SYTL3	TTC24		
				ZNF280B					TAGAP	TTC39C		
				ZNF330					TARP	TWF2		
				ZNF692					TBC1D10C	TYMP		
									TBXAS1	TYROBP		
									TC2N	UBASH3A		
									TCF7	UBE2D1		
									TCL1A	UCP2		
									TESPA1	VAMP8		
									TGFBI	VAV1		

Table S4. Cell type signatures that were derived from the analysis of the scRNA-seq data (see section Data-driven signatures of specific cell types).

B cell	CAF	Endothelial cell	Macrophage	Malignant cell	NK cell	T cell	CD4 T cell	CD8 T cell	Immune cell	Lymphocyte	Stroma cell
									THEMIS	VMO1	
									THEMIS2	VPREB3	
									TIFAB	VSIG4	
									TIGIT	WDFY4	
									TLR1	WIPF1	
									TLR10	XCL1	
									TLR2	XCL2	
									TLR5	ZAP70	
									TLR8	ZC3HAV1	
									TMC8	ZCCHC7	
									TME M106A	ZNF385A	
									TME M154		

Table S5

Table S5. The CRISPRi silencing of L100 different immune cell types: B-cells, macrophages, CD4+ and CD8+ T cells.

CD8-T-cell-up	CD8-T-cell-down	macrophage-up	macrophage-down	B-cell-up	B-cell-down	CD4-T-cell-up	CD4-T-cell-down
CEP19	ACP5	APOL1	A2M	C6orf62	MTRNR2L1	PRDM1	CHI3L2
EX05	AKNA	CD274	ADAP2	CDC42	MTRNR2L10		RPL13A
FAM153C	BTN3A2	CSTB	ADORA3	CNN2	MTRNR2L3		
FCRL6	CCDC141	DCN	ARL4C	FOXP1	MTRNR2L4		
GBP2	CD27	HLA-DPB2	ASPH	FYB	RGS2		
GBP5	CDC42SE1	HLA-DQA1	BCAT1	GRB2			
HSPA1B	DDIT4	HLA-G	C11orf1				
IER2	FAU	HSPA8	C3				
IRF1	FKBP5	HSPB1	C3AR1				
KLRK1	GPR56	IL18BP	C6orf62				
LDHA	HAVCR2	TMEM176A	CAPN2				
LOC100506083	HLA-B	UBD	CD200R1				
MBOAT1	HLA-C		CD28				
SEMA4D	HLA-F		CD9				
SIRT3	IL6ST		CD99				
SPDYE2	ITGA4		COMT				
SPDYE2L	KIAA1551		CREM				
STAT1	KLF12		CRTAP				
STOM	MIR155HG		CYFIP1				
UBE2Q2P3	MTA2		DDOST				
	MTRNR2L1		DHRS3				
	MTRNR2L3		EGFL7				
	PIK3IP1		EIF1AY				
	RPL26		ETS2				
	RPL27		FCGR2A				
	RPL27A		FOLR2				

	RPL35A		GATM				
	RPS11		GBP3				
	RPS16		GNB2				
	RPS20		GSTT1				
	RPS26		GYPC				
	SPOCK2		HIST1H1E				
	SYTL3		HPGDS				
	TOB1		IFI44L				
	TPT1		IGFBP4				
	TTN		ITGA4				
	TXNIP		KCTD12				
	WNK1		LGMN				
	ZFP36L2		LOC441081				
			LTC4S				
			LYVE1				
			MERTK				
			METTL7B				
			MS4A4A				
			MS4A7				
			MTSS1				
			NLRP3				
			OLFML3				
			PLA2G15				
			PLXDC2				
			PMP22				
			POR				
			PRDX2				
			PTGS1				
			RNASE1				
			ROCK1				
			RPS4Y1				
			S100A9				
			SCAMP2				
			SEPP1				
			SESN1				
			SLC18B1				
			SLC39A1				
			SLC40A1				
			SLC7A8				
			SORL1				
			SPP1				
			STAB1				
			TMEM106C				
			TMEM86A				
			TMEM9				
			TNFRSF1B				
			TNFRSF21				
			TPD52L2				
			ULK3				
			ZFP36L2				

Table S6

Table S6. The oncogenic resistance signatures: oncogenic-ICR, exclusion, uICR, and the refined uICR							
Genes up-regulated in ICR malignant cells (1 denotes the gene is included in the signature, and 0 otherwise)				Genes down-regulated in ICR malignant cells (1 denotes the gene is included in the signature, and 0 otherwise)			
uICR-up genes (immune resistance)	oncogenic-ICR-up (post treatment)	Exclusion-on-up	uICR-up (refined)	uICR-down genes	oncogenic-ICR-down	Exclusion-down	uICR-down (refined)
ACAT1	0	1	0	A2M	1	1	0
ACP5	0	1	0	ACSL3	1	0	0
ACTB	1	0	0	ACSL4	1	0	0
ACTG1	0	1	0	ADM	1	0	0
ADSL	0	1	0	AEBP1	1	0	1
AEN	1	0	0	AGA	1	1	0
AK2	0	1	0	AHNAK	1	1	1

Table S6. The oncogenic resistance signatures: oncogenic-ICR, exclusion, uICR, and the refined uICR.

Genes up-regulated in ICR malignant cells (1 denotes the gene is included in the signature, and 0 otherwise)				Genes down-regulated in ICR malignant cells (1 denotes the gene is included in the signature, and 0 otherwise)			
uICR-up genes (immune resistance)	oncogenic-ICR-up (post treatment)	Exclusion-up	uICR-up (refined)	uICR-down genes	oncogenic-ICR-down	Exclusion-down	uICR-down (refined)
ANP32E	1	0	0	ANGPTL4	1	0	0
APP	0	1	0	ANXA1	1	1	0
ASAP1	0	1	0	ANXA2	1	0	0
ATP5A1	1	0	0	APLP2	1	1	0
ATP5D	0	1	0	APOC2	0	1	1
ATP5G2	1	0	0	APOD	1	0	1
BANCR	0	1	0	APOE	1	0	1
BCAN	0	1	0	ARF5	0	1	0
BZW2	1	1	0	ARL6IP5	1	0	0
C17orf76-AS1	1	1	0	ATF3	1	0	0
C1QBP	1	1	1	ATP1A1	1	1	0
C20orf112	1	0	0	ATP1B1	1	1	0
C6orf48	0	1	0	ATP1B3	1	0	0
CA14	1	1	0	ATRAID	0	1	0
CBX5	1	0	0	B2M	1	1	1
CCT2	1	0	1	BACE2	1	0	0
CCT3	1	1	0	BBX	1	0	0
CCT6A	0	1	1	BCL6	1	0	0
CDK4	1	0	0	C10orf54	0	1	1
CEP170	0	1	0	C4A	0	1	0
CFL1	1	0	0	CALU	1	0	0
CHP1	0	1	0	CASP1	1	0	0
CNRIP1	1	0	0	CAST	1	0	0
CRABP2	1	0	0	CAV1	1	0	0
CS	1	0	0	CBLB	0	1	0
CTPS1	1	1	0	CCND3	1	1	0
CYC1	0	1	0	CD151	1	1	0
DAP3	0	1	0	CD44	1	0	0
DCAF13	1	0	1	CD47	1	1	0
DCT	1	1	0	CD58	1	1	0
DDX21	0	1	0	CD59	1	1	0
DDX39B	1	0	0	CD63	1	0	1
DLL3	1	0	0	CD9	1	0	0
EDNRB	0	1	0	CDH19	1	1	0
EEF1D	0	1	0	CHI3L1	1	0	0
EEF1G	1	1	0	CHN1	0	1	0
EEF2	0	1	0	CLIC4	1	0	0
EIF1AX	0	1	0	CLU	0	1	0
EIF2S3	1	1	0	CPVL	0	1	0
EIF3E	0	1	0	CRELD1	1	0	0
EIF3K	1	1	0	CRYAB	1	0	0
EIF3L	0	1	0	CSGALNACT1	1	0	0
EIF4A1	1	1	1	CSPG4	1	0	0
EIF4EBP2	1	0	0	CST3	1	1	0
ESRP1	0	1	0	CTSA	1	0	0
FAM174B	1	0	0	CTSB	1	1	0
FAM178B	0	1	0	CTSD	1	1	1
FAM92A1	0	1	0	CTSL1	1	1	0
FBL	1	0	0	DAG1	1	0	0
FBLN1	1	0	0	DCBLD2	1	0	0
FOXRED2	1	0	0	DDR1	1	1	0
FTL	1	1	0	DDX5	1	0	0
FUS	1	0	0	DPYSL2	1	1	0
GABARAP	1	0	0	DSCR8	0	1	0
GAS5	1	1	0	DUSP4	1	0	0
GNB2L1	1	1	0	DUSP6	1	1	0
GPATCH4	1	0	0	DYNLRB1	0	1	0
GPI	1	1	0	ECM1	1	0	0
GRWD1	1	0	0	EEA1	1	0	1
GSTO1	0	1	0	EGR1	1	0	0

Table S6. The oncogenic resistance signatures: oncogenic-ICR, exclusion, uICR, and the refined uICR.							
Genes up-regulated in ICR malignant cells (1 denotes the gene is included in the signature, and 0 otherwise)				Genes down-regulated in ICR malignant cells (1 denotes the gene is included in the signature, and 0 otherwise)			
uICR-up genes (immune resistance)	oncogenic-ICR-up (post treatment)	Exclusion-up	uICR-up (refined)	uICR-down genes	oncogenic-ICR-down	Exclusion-down	uICR-down (refined)
H3F3A	1	0	0	EMP1	1	1	1
H3F3AP4	1	0	0	EPHX2	1	0	0
HMG1A1	1	0	0	ERBB3	1	0	0
HNRNPA1	1	0	0	EVA1A	1	0	0
HNRNPA1P10	1	0	0	EZH1	1	0	0
HNRNPC	1	0	0	EZR	0	1	0
HSPA8	1	0	0	FAM3C	1	1	0
IDH2	1	0	0	FBXO32	1	0	1
IFI16	0	1	0	FCGR2C	1	0	0
ILF2	1	1	1	FCRLA	1	0	0
IMPDH2	0	1	0	FGFR1	1	1	0
ISYNA1	1	0	0	FLJ43663	1	0	0
ITM2C	1	0	0	FOS	1	0	0
KIAA0101	1	0	0	FYB	0	1	1
LHFPL3-AS1	0	1	0	GAA	1	1	0
LOC100190986	0	1	0	GADD45B	1	0	0
LYPLA1	0	1	0	GATSL3	0	1	1
MAGEA4	1	0	1	GEM	1	0	0
MARCKS	0	1	0	GOLGB1	1	0	0
MDH2	1	1	0	GPNUMB	1	0	0
METAP2	1	0	0	GRN	1	1	0
MID1	1	0	0	GSN	1	1	0
MIR4461	1	0	0	HCP5	0	1	1
MLLT11	1	0	0	HLA-A	1	0	1
MPZL1	1	0	0	HLA-B	1	1	1
MRPL37	0	1	0	HLA-C	1	1	1
MRPS12	0	1	0	HLA-E	1	0	1
MRPS21	1	0	0	HLA-F	1	1	1
MYC	0	1	0	HLA-H	1	1	1
NACA	1	0	0	HPCAL1	1	0	0
NCL	1	1	0	HSPA1A	1	1	0
NDUFS2	1	0	0	HSPA1B	0	1	0
NF2	0	1	0	HTATIP2	1	0	0
NID1	0	1	0	ID2	0	1	0
NOLC1	1	1	0	IFI27L2	0	1	0
NONO	1	0	1	IFI35	1	0	0
NPM1	0	1	0	IGF1R	1	0	0
NUCKS1	0	1	0	IL1RAP	1	0	0
OAT	0	1	0	IL6ST	1	0	0
PA2G4	1	0	1	ISCU	0	1	0
PABPC1	1	1	0	ITGA3	1	1	1
PAFAH1B3	1	0	0	ITGA6	1	0	0
PAICS	0	1	0	ITGA7	0	1	0
PFDN2	1	0	0	ITGB1	1	0	0
PFN1	1	0	0	ITGB3	1	1	0
PGAM1	1	0	1	ITM2B	1	0	0
PIH1D1	1	0	0	JUN	1	0	0
PLTP	0	1	0	KCNN4	1	1	0
PPA1	1	0	1	KLF4	1	0	0
PPIA	1	0	1	KLF6	1	0	0
PPP2R1A	1	0	0	KRT10	0	1	0
PSAT1	0	1	0	LAMP2	1	0	1
PSMD4	1	0	0	LEPROT	1	0	0
PTMA	1	0	0	LGALS1	1	0	0
PYCARD	0	1	0	LGALS3	1	0	0
RAN	1	0	0	LGALS3BP	1	0	0
RASA3	0	1	0	LOC100506190	0	1	0
RBM34	1	0	0	LPL	1	0	0

Table S6. The non-immune resistance signatures: oncogenic-ICR, exclusion, uICR, and the refined uICR.							
Genes up-regulated in ICR malignant cells (1 denotes the gene is included in the signature, and 0 otherwise)				Genes down-regulated in ICR malignant cells (1 denotes the gene is included in the signature, and 0 otherwise)			
uICR-up genes (immune resistance)	oncogenic-ICR-up (post treatment)	Exclusion-up	uICR-up (refined)	uICR-down genes	oncogenic-ICR-down	Exclusion-down	uICR-down (refined)
RNF2	1	0	0	LRPAP1	1	0	0
RPAIN	1	0	0	LTBP3	0	1	0
RPL10	0	1	0	LYRM9	0	1	1
RPL10A	1	1	0	MAEL	0	1	0
RPL11	1	1	0	MAGEC2	1	0	0
RPL12	1	1	0	MAP1B	0	1	0
RPL13	1	1	0	MATN2	0	1	0
RPL13A	1	1	0	MFGE8	1	1	1
RPL13AP5	1	1	0	MF12	1	1	0
RPL14	0	1	0	MIA	1	1	1
RPL17	1	1	0	MRPS6	0	1	0
RPL18	1	1	0	MT1E	1	0	0
RPL18A	1	1	1	MT1M	1	0	0
RPL21	1	0	0	MT1X	1	0	0
RPL26	1	0	1	MT2A	1	1	0
RPL28	1	1	0	NDRG1	0	1	0
RPL29	1	1	0	NEAT1	1	0	0
RPL3	1	1	0	NFKBIA	1	1	0
RPL30	0	1	0	NFKBIZ	1	0	0
RPL31	1	0	1	NNMT	1	0	0
RPL35	0	1	0	NPC1	1	1	0
RPL36A	1	0	0	NPC2	1	0	1
RPL37	1	0	0	NR4A1	1	0	0
RPL37A	1	1	0	NSG1	1	0	1
RPL39	1	1	0	OCIAD2	0	1	0
RPL4	1	1	0	PAGE5	0	1	0
RPL41	1	0	0	PDK4	1	0	0
RPL5	1	1	0	PERP	0	1	0
RPL6	1	1	0	PKM	0	1	0
RPL7	0	1	0	PLP2	1	0	0
RPL7A	0	1	0	PRKCDBP	1	0	0
RPL8	1	1	0	PRNP	1	0	0
RPLPO	1	1	0	PROS1	1	0	1
RPLP1	1	1	0	PRSS23	1	0	0
RPS10	1	1	0	PSAP	1	0	0
RPS11	1	1	1	PSMB9	1	0	0
RPS12	1	0	0	PTRF	1	0	0
RPS15	0	1	1	RDH5	0	1	1
RPS15A	1	1	0	RNF145	1	0	0
RPS16	1	1	0	RPS4Y1	1	0	0
RPS17	1	1	0	S100A13	0	1	0
RPS17L	1	1	0	S100A6	1	1	0
RPS18	1	1	0	S100B	1	0	0
RPS19	1	1	0	SAT1	1	0	0
RPS2	0	1	0	SCARB2	1	0	0
RPS21	1	0	1	SCCPDH	1	0	0
RPS23	1	0	0	SDC3	1	0	0
RPS24	1	1	0	SEL1L	1	0	0
RPS26	1	0	0	SEMA3B	1	0	0
RPS27	1	1	0	SERPINA1	0	1	1
RPS27A	1	0	0	SERPINA3	1	1	0
RPS3	1	1	0	SERPINE2	1	1	0
RPS3A	0	1	0	SGCE	1	1	0
RPS4X	1	1	0	SGK1	1	0	0
RPS5	1	1	1	SLC20A1	1	0	0
RPS6	1	0	0	SLC26A2	1	1	0
RPS7	1	1	0	SLC39A1	1	0	0

Table S6. The non-co-inhibitory signaling: oncogenic-K.R, exclusion, uICR, and the refined uICR.							
Genes up-regulated in ICR malignant cells (1 denotes the gene is included in the signature, and 0 otherwise)				Genes down-regulated in ICR malignant cells (1 denotes the gene is included in the signature, and 0 otherwise)			
uICR-up genes (immune resistance)	oncogenic-ICR-up (post treatment)	Exclusion-on-up	uICR-up (refined)	uICR-down genes	oncogenic-ICR-down	Exclusion-down	uICR-down (refined)
				4			
RPS8	1	1	0	SLC5A3	1	1	0
RPS9	1	1	0	SNX9	0	1	0
RPSA	1	1	0	SOD1	1	0	0
RSL1D1	0	1	0	SPON2	0	1	0
RUVBL2	1	0	1	SPRY2	1	0	0
SAE1	1	0	1	SQSTM1	1	0	0
SCD	1	1	0	SRPX	1	0	0
SCNM1	1	0	0	STOM	1	0	0
SERBP1	0	1	0	SYNGR2	1	0	0
SERPINF1	1	1	0	SYPL1	1	0	0
SET	1	0	0	TAPBP	1	0	1
SF3B4	1	0	0	TAPBPL	1	0	0
SHMT2	1	0	0	TF	1	0	0
SKP2	1	0	0	TGOLN2	1	0	0
SLC19A1	0	1	0	THBD	0	1	0
SLC25A3	1	0	0	TIMP1	1	1	0
SLC25A5	0	1	0	TIMP2	1	0	1
SLC25A6	0	1	0	TIMP3	1	0	0
SMS	1	0	0	TIPARP	1	0	0
SNAI2	1	1	0	TM4SF1	1	1	0
SNHG16	0	1	0	TMBIM6	0	1	0
SNHG6	1	1	0	TMED10	1	0	0
SNRPE	1	0	1	TMED9	1	0	0
SORD	0	1	0	TMEM66	1	0	0
SOX4	1	1	0	TMX4	1	0	0
SRP14	1	0	0	TNC	1	0	0
SSR2	1	0	0	TNFSF4	0	1	1
TIMM13	0	1	0	TPP1	1	1	0
TIMM50	1	1	0	TRIML2	0	1	1
TMC6	1	0	0	TSC22D3	1	1	0
TOP1MT	0	1	0	TSPYL2	0	1	0
TP53	1	0	0	TXNIP	0	1	0
TRAP1	0	1	0	TYR	1	0	0
TRPM1	1	0	0	UBC	1	1	0
TSR1	1	0	0	UPP1	1	0	0
TUBA1B	1	0	0	XAGE1A	0	1	0
TUBB	1	0	0	XAGE1B	0	1	0
TUBB4A	0	1	0	XAGE1C	0	1	0
TULP4	1	0	0	XAGE1D	0	1	0
TXLNA	0	1	0	XAGE1E	0	1	0
TYRP1	0	1	0	ZBTB20	1	0	0
UBA52	1	0	1	ZBTB38	1	0	0
UCK2	0	1	0				
UQCERS1	1	1	0				
UQCRH	1	0	1				
USP22	1	0	0				
VCY1B	1	0	0				
VDAC2	1	0	1				
VPS72	1	0	0				
YWHAE	1	0	0				
ZFAS1	0	1	0				
ZNF286A	1	0	0				

Table S7. Genes differentially expressed in CD8 T cells of the CB patient compared to those of the ICR patients.

Up-regulated in CB vs. ICR	Down-regulated in CB vs. ICR
ALOX5AP	AKIRIN2
C1D	APIP
C3orf14	ARL5A
CCL5	ASF1B
CCR2	ATP6V0C
CD52	ATP9B
CDC26	BRAT1
CIDECP	BRD7
CISH	C17orf89
C0X5B	C1GALT1C1
CRIP1	C4orf48
CTSW	CALR
CXCR6	CCDC137
DDX3Y	CDC73
EDF1	CDCA7
EIF1AY	CDK1
FAM127B	CENPM
FASLG	CEP78
FAU	CHMP6
FCGR3A	CITED2
FTL	CUNT1
GZMA	CMTM7
GZMB	COTL1
GZMH	CRIP1
HCG26	CSNK1G3
HCST	CYB5R4
HLA-A	DCPS
HLA-C	DNAJB14
HLA-DQA2	DND1
HLA-H	DPH3
HSPA1B	EFR3A
ID2	EMC2
KDM5D	EML3
LAIR2	FAM160B1
MIR4461	FAM168B
MTRNR2L1	FAM46C
MTRNR2L10	FAM53C
MTRNR2L6	FAM69A
NACA	FARSB
NCF4	FBX022
NDUFA13	FEM1A
NDUFS5	FTSJD1
NDUFV2	GATAD2A
RBPJ	GET4
RNASEK	GGA3
RPL10	GLTSCR2
RPL11	GNL3
RPL12	GOLT1B
RPL13	GPR137B
RPL13AP5	GTDC1
RPL15	HIST1H1E
RPL17	HMGA1
RPL18	HMHA1
RPL18A	HSF1
RPL19	IARS2
RPL21	IL6ST
RPL23	JUNB

Up-regulated in CB vs. ICR	Down-regulated in CB vs. ICR
RPL23A	KATNA1
RPL24	KIAA1429
RPL26	LATS1
RPL29	LOC100294145
RPL30	LRIG2
RPL32	MAN2A1
RPL35	MAP3K2
RPL35A	MB21D1
RPL36	MCM2
RPL36AL	MCM4
RPL37A	MED23
RPL4	MGEA5
RPL41	MPLKIP
RPL6	MRPS33
RPL7	MZT1
RPL7A	NAGK
RPL9	NEK1
RPLP1	NOA1
RPLP2	NPC2
RPS10	NUDT1
RPS11	NUP107
RPS12	OSGEP
RPS13	PARP10
RPS14	PEU1
RPS15	PGS1
RPS15A	PITHD1
RPS16	PLEKHF2
RPS18	POLR3E
RPS19	PPIF
RPS20	PPP1R21
RPS24	PRKAB1
RPS25	PSMD2
RPS27	PTGDR
RPS27A	PYG02
RPS3	RAB11B
RPS3A	RABEP1
RPS4X	RALB
RPS4Y1	REC8
RPS5	REEP4
RPS6	RNF216P1
RPS8	RNF219
SAMD3	RPIA
SELM	RPS6KA5
SH3BGRL3	RPSAP58
SYMPK	SFSWAP
TMSB10	SGSM2
TMSB4X	SLC1A5
TNFSF4	SLC25A26
TPT1	SLC33A1
TXLNG2P	SLC39A3
	SLC7A5
	SMC1A
	SMC4
	SNX4
	SPPL2A
	STAT1
	STX17

Up-regulated in CB vs. ICR	Down-regulated in CB vs. ICR
	SYPL1
	TAF1B
	TAF6
	TCERG1
	TCF7
	TEKT4P2
	TERF2IP
	TIMM44
	TMEM161B
	TMEM170A
	TMEM189
	TMEM69
	TMX4
	TNIP1
	TNPOI
	TOP2A
	TPX2
	TRIS2
	TSC22D1
	TUBGCP3
	TYMS
	UBA5
	UBE2J1
	UBE2Q2
	UBE2T
	USP38
	UVRAG
	WDR18
	ZBED6
	ZBTB20
	ZFYVE28
	ZNF259
	ZNF511

Table S8

Table S8. Cell-cycle signatures specific to CD8 T cells.	
Up-regulated in cycling CD8 T cells	Down-regulated in cycling CD8 T cells
ACTG1	AOAH
ANXA5	ATHL1
ARHGD1B	C11orf21
ARL6IP1	CCL3L1
ARPC2	CD37
ATP5L	CISH
CD74	CX3CR1
CNTRL	DENND2D
CORO1A	GNPDA1
COTL1	GZMM
COX6A1	IL11RA
COX6C	IL7R
COX8A	KLRB1
DDOST	LDLRAP1
GALM	LINC00612
GMFG	LY9
GNG5	NR4A3

HLA-DRA	PDGFD
HP1BP3	PLCB2
LCP1	PTGDR
LRRFIP1	RAB37
MPC2	RPS27
MT2A	S0RL1
NDUFA4	TRIM22
NDUFC2	TRMU
NUP50	TTN
PCBP1	UPRT
PKM	ZNF121
P0LR2A	
PSMB2	
SNX1	
SRRM1	
TMA7	
VIM	
YWHAE	
YWHAQ	

Table S9. The topmost differentially expressed gene sets in the malignant cells from ICR vs. TN tumors

Gene set	t-test p-value (-log10(p)), positive = higher in ICR, negative = lower in ICR		N = No. of genes in the gene set	N _{ICR} = No. of used genes	N/N _{ICR}
	t-test p-value	mixed effects p-value			
GO_RESPONSE_TO_ENDOPLASMIC_RETICULUM_STRESS	-36.49	-4.05	233	147	0.63
GO_CELLULAR_COPPER_ION_HOMEOSTASIS	-44.3	-4.04	13	9	0.69
GO_CELLULAR_RESPONSE_TO_ZINC_ION	-215.84	-4	16	7	0.44
ENDOPLASMIC_RETICULUM_MEMBRANE	-42.56	-3.93	85	55	0.65
GO_REGULATION_OF_ENDOTHELIAL_CELL_APOPTOTIC_PROCESS	-52.39	-3.79	42	14	0.33
METALLOTHIONEINS	-208.11	-3.72	13	6	0.46
GO_INTRAMOLECULAR_OXIDOREDUCTASE_ACTIVITY_TRANSPOSING_S_S_BONDS	-40.53	-3.64	22	14	0.64
NUCLEAR_ENVELOPE_ENDOPLASMIC_RETICULUM_NETWORK	-38.41	-3.59	94	62	0.66
GO_CELLULAR_RESPONSE_TO_VITAMIN_D	-78.74	-3.56	14	4	0.29
KEGG_SNARE_INTERACTIONS_IN_VESICULAR_TRANSPORT	-17.6	-3.43	38	23	0.61
ENDOPLASMIC_RETICULUM_PART	-44.43	-3.43	97	65	0.67
GO_COPPER_ION_HOMEOSTASIS	-38.11	-3.38	16	12	0.75
KEGG_ECM_RECEPTOR_INTERACTION	-163.89	-3.35	84	35	0.42
GO_ENDOPLASMIC_RETICULUM_GOLGI_INTERMEDIATE_COMPARTMENT	-40.27	-3.3	105	64	0.61
GO_BLOOD_VESSEL_MORPHOGENESIS	-153.28	-3.3	364	117	0.32
GO_PLATELET_DERIVED_GROWTH_FACTOR_RECEPTOR_BINDING	-62.32	-3.24	15	5	0.33
GO_ANGIOGENESIS	-148.37	-3.23	293	102	0.35
GO_RESPONSE_TO_ZINC_ION	-76.24	-3.22	55	21	0.38
PID_INTEGRIN_CS_PATHWAY	-172.58	-3.19	26	9	0.35
GOLGI_MEMBRANE	-53.05	-3.13	45	26	0.58
GO_TRANSITION_METAL_ION_TRANSMEMBRANE_TRANSPORTER_ACTIVITY	-61.25	-3.12	39	19	0.49
POSITIVE_REGULATION_OF_CELL_PROLIFERATION	-31.46	-3.11	149	48	0.32
GO_MUSCLE_CELL_MIGRATION	-164.41	-3.11	18	10	0.56
NUCLEAR_ORPHAN_RECEPTOR	-83.44	-3.09	3	2	0.67
GO_POSITIVE_REGULATION_OF_EXTRINSIC_APOPTOTIC_SIGNALING_PATHWAY	-75.37	-3.08	17	11	0.65

Gene set	t-test p-value (-log10(p)), positive = higher in ICR, negative = lower in ICR)		N = No. of genes in the gene set	N/qc = No. of used genes	N/N.qc
	t-test p-value	mixed effects p-value			
ATHWAY_VIA_DEATH_DOMAIN_RECEPTORS					
GO_PHOSPHOTRANSFERASE_ACTIVITY_FOR_OTHER_SUBSTITUTED_PHOSPHATE_GROUPS	-32.33	-3.07	19	11	0.58
ST_INTERLEUKIN_13_PATHWAY	-2.38	-3.03	7	2	0.29
WOUND_HEALING	-148	-3.02	54	13	0.24
C/EBP	-38.85	-3	10	3	0.3
GO_INSULIN_LIKE_GROWTH_FACTOR_BINDING	-62.71	-2.98	25	11	0.44
MUSCLE_DEVELOPMENT	-122.53	-2.98	93	29	0.31
GO_PLATELET_ALPHA_GRANULE_MEMBRANE	-104.99	-2.96	13	7	0.54
GO_MANNOSIDASE_ACTIVITY	-28.46	-2.95	15	5	0.33
GO_POSITIVE_REGULATION_OF_ADHERENS_JUNCTION_ORGANIZATION	-61.36	-2.95	21	9	0.43
GO_NEGATIVE_REGULATION_OF_EPITHELIAL_CELL_APOPTOTIC_PROCESSES	-70.48	-2.95	35	8	0.23
ENDOPLASMIC_RETICULUM	-50.01	-2.94	294	180	0.61
CELL_FATE_COMMITMENT	-72.59	-2.94	13	3	0.23
GO_ENDOPLASMIC_RETICULUM_GOLGI_INTERMEDIATE_COMPARTMENT_MEMBRANE	-65.43	-2.93	63	38	0.6
GO_NEGATIVE_REGULATION_OF_INTERLEUKIN_8_PRODUCTION	-126.57	-2.93	15	5	0.33
PID_TNF_PATHWAY	-73	-2.92	46	22	0.48
GO_RECEPTOR_REGULATOR_ACTIVITY	-92.97	-2.92	45	10	0.22
GO_EXTRACELLULAR_STRUCTURE_ORGANIZATION	-107.25	-2.92	304	111	0.37
ER_GOLGI_INTERMEDIATE_COMPARTMENT	-12.41	-2.91	24	20	0.83
GO_RESPONSE_TO_CADMIUM_ION	-124.5	-2.9	40	25	0.62
GO_HEPARAN_SULFATE_PROTEOGLYCAN_BIOSYNTHETIC_PROCESS	-31.95	-2.89	23	8	0.35
GO_AXON_REGENERATION	-144.4	-2.88	24	9	0.38
ENDOMEMBRANE_SYSTEM	-21.95	-2.87	220	137	0.62
HALLMARK_IL6_JAK_STAT3_SIGNALING	-170.22	-2.87	87	40	0.46
GO_HEPARAN_SULFATE_PROTEOGLYCAN_METABOLIC_PROCESS	-30.74	-2.86	28	8	0.29
GO_POSITIVE_REGULATION_OF_CELL_JUNCTION_ASSEMBLY	-88.33	-2.85	24	11	0.46
GO_VASCULATURE_DEVELOPMENT	-143.79	-2.84	469	153	0.33
CELLULAR_CATION_HOMEOSTASIS	-96.84	-2.83	106	32	0.3
GO_CELL_SUBSTRATE_JUNCTION_ASSEMBLY	-79.64	-2.82	41	19	0.46
PID_FRA_PATHWAY	-55.92	-2.81	37	17	0.46
GO_REGULATION_OF_ADHERENS_JUNCTION_ORGANIZATION	-63.38	-2.81	50	22	0.44
GO_CELL_ADHESION_MEDIATED_BY_INTEGRIN	-81.75	-2.81	12	8	0.67
GO_SARCOLEMMMA	-216.58	-2.81	125	37	0.3
GO_NEGATIVE_REGULATION_OF_ENDOTHELIAL_CELL_APOPTOTIC_PROCESSES	-38.24	-2.8	27	7	0.26
GO_CORECEPTOR_ACTIVITY	-68.21	-2.79	38	11	0.29
GO_REGULATION_OF_INTERLEUKIN_8_BIOSYNTHETIC_PROCESS	-12.85	-2.78	12	3	0.25
REACTOME_EXTRINSIC_PATHWAY_FOR_APOPTOSIS	-55.38	-2.78	13	8	0.62
HALLMARK_HYPOXIA	-112.24	-2.78	200	116	0.58
GO_ER_NUCLEUS_SIGNALING_PATHWAY	-28.31	-2.75	34	25	0.74
HOMOPHILIC_CELL_ADHESION	-55	-2.74	16	4	0.25
GO_SNAP_RECEPTOR_ACTIVITY	-20.16	-2.73	38	22	0.58
HALLMARK_EPITHELIAL_MESENCHYMAL_TRANSITION	-128.55	-2.73	200	110	0.55
GO_CELLULAR_RESPONSE_TO_CADMIUM_ION	-155.05	-2.73	15	9	0.6
GO_BASAL_LAMINA	-27.9	-2.72	21	6	0.29
CELL_CELL_ADHESION	-40.27	-2.72	86	19	0.22
POSITIVE_REGULATION_OF_MULTICELLULAR_ORGANISMAL_PROCESS	-45.51	-2.71	66	18	0.27
FIBROBLAST	-73.88	-2.71	6	3	0.5
GO_ATPASE_COMPLEX	-80.46	-2.7	24	7	0.29
GO_INTRINSIC_COMPONENT_OF_EXTERNAL_SIDE_OF_PLASMA_MEMBRANE	-68.1	-2.69	27	7	0.26
PID_INTEGRIN3_PATHWAY	-78.14	-2.68	43	22	0.51
CATION_HOMEOSTASIS	-93.05	-2.68	109	32	0.29
GO_CELL_SUBSTRATE_ADHESION	-162.02	-2.68	164	58	0.35
GO_INTRINSIC_APOPTOTIC_SIGNALING_PATHWAY_IN_RESPONSE_TO_ENDOPLASMIC_RETICULUM_STRESS	-37.62	-2.67	32	18	0.56
GO_POSITIVE_REGULATION_OF_CELL_MATRIX_ADHESION	-57.1	-2.66	40	15	0.38

Gene set	t-test p-value (-log10(p)), positive = higher in ICR, negative = lower in ICR)		N = No. of genes in the gene set	N,qc = No. of used genes	N/N,qc
	t-test p-value	mixed effects p-value			
GO_NEGATIVE_REGULATION_OF_GLYCOPROTEIN_METABOLIC_PROCESSES	-60.19	-2.66	15	10	0.67
GO_NEGATIVE_REGULATION_OF_TYPE_2_IMMUNE_RESPONSE	-162.47	-2.66	11	4	0.36
REACTOME_ACTIVATION_OF_CHAPERONES_BY_ATF6_ALPHA	-22.85	-2.64	13	8	0.62
GO_NEGATIVE_REGULATION_OF_DNA_RECOMBINATION	-13.63	-2.63	16	8	0.5
GO_CELLULAR_RESPONSE_TO_TOPOLOGICALLY_INCORRECT_PROTEIN	-22.73	-2.63	122	81	0.66
GO_CELLULAR_RESPONSE_TO_CALCIUM_ION	-69.45	-2.63	49	18	0.37
GO_SECRETORY_GRANULE_MEMBRANE	-133.42	-2.63	78	28	0.36
GOLGI_VESICLE_TRANSPORT	-13.68	-2.62	48	37	0.77
REACTOME_DIABETES_PATHWAYS	-20.26	-2.62	133	80	0.6
GO_NEGATIVE_REGULATION_OF_GLYCOPROTEIN_BIOSYNTHETIC_PROCESS	-23.98	-2.61	12	9	0.75
CAHOY_ASTROGLIAL	-197.11	-2.61	100	37	0.37
GO_HEMIDESMOSOME_ASSEMBLY	-95.2	-2.6	12	5	0.42
GO_FIBRINOLYSIS	-98.47	-2.6	21	6	0.29
GO_PROTEIN_COMPLEX_INVOLVED_IN_CELL_ADHESION	-171.74	-2.6	30	10	0.33
ST_IL_13_PATHWAY	-1.56	-2.59	7	2	0.29
POSITIVE_REGULATION_OF_PROTEIN_MODIFICATION_PROCESS	-37.38	-2.58	29	9	0.31
HALLMARK_UV_RESPONSE_UP	-67.14	-2.57	158	93	0.59
CELL_MIGRATION	-87.02	-2.57	96	34	0.35
ATPASE_ACTIVITY_COUPLED_TO_TRANSMEMBRANE_MOVEMENT_OF_IONS_PHOSPHORYLATIVE_MECHANISM	-130.2	-2.57	20	5	0.25
GO_INTEGRIN_BINDING	-94.95	-2.56	105	48	0.46
HALLMARK_TNFA_SIGNALING_VIA_NFKB	-154.11	-2.56	200	108	0.54
GO_PLATELET_ALPHA_GRANULE	-164.05	-2.56	75	35	0.47
PID_INTEGRIN1_PATHWAY	-89.65	-2.55	66	34	0.52
GO_CATION_TRANSPORTING_ATPASE_COMPLEX	-119.68	-2.55	16	4	0.25
PROTEIN_AMINO_ACID_LIPIDATION	-35.59	-2.54	24	19	0.79
GO_NEGATIVE_REGULATION_OF_LIPID_STORAGE	-92.01	-2.54	17	6	0.35
GO_BASEMENT_MEMBRANE_ORGANIZATION	-26.24	-2.53	11	7	0.64
POSITIVE_REGULATION_OF_CYTOKINE_PRODUCTION	-41.65	-2.53	15	5	0.33
BIOCARTA_SODD_PATHWAY	-37.42	-2.52	10	8	0.8
GO_PERK_MEDIATED_UNFOLDED_PROTEIN_RESPONSE	-39.21	-2.52	12	10	0.83
PHOSPHOLIPID_METABOLIC_PROCESS	-44.83	-2.52	74	42	0.57
Targets of NFAT_Q6	-53.2	-2.52	246	80	0.33
BIOCARTA_STRESS_PATHWAY	-71.76	-2.52	25	10	0.4
CYTOPLASM_ORGANIZATION_AND_BIOGENESIS	-67.96	-2.51	15	7	0.47
Targets of FREAC3_01	-23.28	-2.5	251	65	0.26
GO_COLLAGEN_BINDING	-84.49	-2.5	65	27	0.42
PID_INTEGRIN4_PATHWAY	-35.75	-2.49	11	4	0.36
CELL_SURFACE	-42.55	-2.49	79	27	0.34
GO_PHOSPHATE_TRANSMEMBRANE_TRANSPORTER_ACTIVITY	-14.32	-2.48	30	16	0.53
NAIVE_VS_ACTIVATED_CD8_TCELL_DN	-38.5	-2.48	200	81	0.4
MEMBRANE_LIPID_BIOSYNTHETIC_PROCESS	-20.36	-2.47	49	29	0.59
GO_GLYCEROPHOSPHOLIPID_CATABOLIC_PROCESS	-27.95	-2.47	13	7	0.54
GO_INTERSTITIAL_MATRIX	-81.96	-2.47	14	3	0.21
GO_REGULATION_OF_EXTRINSIC_APOPTOTIC_SIGNALING_PATHWAY_VIA_DEATH_DOMAIN_RECEPTORS	-103.8	-2.47	55	32	0.58
INORGANIC_ANION_TRANSPORT	-151.85	-2.47	18	4	0.22
REACTOME_CLASS_B_2_SECRETIN_FAMILY_RECEPTORS	-62.64	-2.46	88	19	0.22
GO_DECIDUALIZATION	-99.39	-2.46	21	7	0.33
GO_MULTI_MULTICELLULAR_ORGANISM_PROCESS	-129.03	-2.46	213	62	0.29
NABA_BASEMENT_MEMBRANES	-19.18	-2.45	40	12	0.3
GO_PROTEINACEOUS_EXTRACELLULAR_MATRIX	-60.88	-2.45	356	86	0.24
GO_EXTRACELLULAR_MATRIX	-121.18	-2.45	426	116	0.27
GO_INTEGRIN_MEDIATED_SIGNALING_PATHWAY	-129.11	-2.45	82	36	0.44
SECRETION	-34.16	-2.44	178	68	0.38
GO_CARBOHYDRATE_DERIVATIVE_CATABOLIC_PROCESS	-62.72	-2.44	174	76	0.44
HALLMARK_APOPTOSIS	-184.35	-2.44	161	111	0.69
LIPOPROTEIN_METABOLIC_PROCESS	-34.84	-2.43	33	21	0.64

Gene set	t-test p-value (-log10(p)), positive = higher in ICR, negative = lower in ICR)		N = No. of genes in the gene set	N/qc = No. of used genes	N/N.qc
	t-test p-value	mixed effects p-value			
LIPOPROTEIN_BIOSYNTHETIC_PROCESS	-36.48	-2.43	26	19	0.73
GO_BASEMENT_MEMBRANE	-54.56	-2.43	93	32	0.34
REACTOME_UNFOLDED_PROTEIN_RESPONSE	-13.89	-2.42	80	58	0.72
GO_LIPOPROTEIN_BIOSYNTHETIC_PROCESS	-63.03	-2.42	85	40	0.47
GO_HYDROLASE_ACTIVITY_ACTING_ON_GLYCOSYL_BONDS	-65.4	-2.42	122	44	0.36
GO_REGULATION_OF_VIRAL_ENTRY_INTO_HOST_CELL	-72.07	-2.42	28	12	0.43
BIOCARTA_IL1R_PATHWAY	-72.17	-2.41	33	12	0.36
HALLMARK_IL2_STAT5_SIGNALING	-199.12	-2.41	200	91	0.46
GO_NEGATIVE_REGULATION_OF_SMALL_GTPASE_MEDIATED_SIGNAL_TRANSDUCTION	-72.25	-2.4	40	14	0.35
GO_GROWTH_FACTOR_BINDING	-107.54	-2.39	123	46	0.37
GO_METALLOENDOPEPTIDASE_INHIBITOR_ACTIVITY	-118.81	-2.39	14	5	0.36
TTAYRTAA_Targets of E4BP4_01	-133.15	-2.39	265	74	0.28
GO_REGULATION_OF_T_HELPER_2_CELL_DIFFERENTIATION	-200.19	-2.39	11	3	0.27
CELL_ACTIVATION	-24.51	-2.38	77	17	0.22
GO_EXTRACELLULAR_MATRIX_COMPONENT	-46.21	-2.38	125	47	0.38
GO_RESPONSE_TO_AXON_INJURY	-138.03	-2.38	48	19	0.4
GO_FORMATION_OF_PRIMARY_GERM_LAYER	-93.37	-2.37	110	33	0.3
HYDROLASE_ACTIVITY_ACTING_ON_ACID_ANHYDRIDESCATALYZING_TRANSMEMBRANE_MOVEMENT_OF_SUBSTANCES	-126.69	-2.37	39	14	0.36
GO_CELLULAR_RESPONSE_TO_PROSTAGLANDIN_STIMULUS	-41.78	-2.36	24	10	0.42
GO_NEGATIVE_REGULATION_OF_MULTICELLULAR_ORGANISMAL_METABOLIC_PROCESS	-55.1	-2.36	12	6	0.5
GO_NEGATIVE_REGULATION_OF_GROWTH	-96.42	-2.36	236	85	0.36
GO_REGULATION_OF_ERK1_AND_ERK2_CASCADE	-121.13	-2.36	238	74	0.31
GO_CELL_MATRIX_ADHESION	-156.53	-2.36	119	42	0.35
PID_P38_MKK3_6PATHWAY	-11.76	-2.35	26	9	0.35
GO_ACROSOMAL_MEMBRANE	-98.54	-2.35	22	8	0.36
BLOOD_COAGULATION	-133.89	-2.35	43	12	0.28
GO_REGULATION_OF_INTERLEUKIN_2_PRODUCTION	-134.5	-2.35	48	19	0.4
GO_JRE1_MEDIATED_UNFOLDED_PROTEIN_RESPONSE	-17.39	-2.34	56	44	0.79
GO_PROTEIN_HETEROOLIGOMERIZATION	-31.48	-2.34	113	44	0.39
GO_NEGATIVE_REGULATION_OF_SODIUM_ION_TRANSPORT	-110.08	-2.34	11	4	0.36
MEMBRANE_FUSION	-27.59	-2.33	28	15	0.54
KEGG_GLYCOSPHINGOLIPID_BIOSYNTHESIS_GANGLIO_SERIES	-46.27	-2.33	15	6	0.4
GO_REGULATION_OF_CELL_SUBSTRATE_ADHESION	-62.07	-2.33	173	67	0.39
GO_REGULATION_OF_PROTEIN_GLYCOSYLATION	-18.5	-2.32	14	5	0.36
GO_PLASMA_MEMBRANE_FUSION	-40.77	-2.32	26	8	0.31
GO_COMPACT_MYELIN	-55.03	-2.31	15	8	0.53
Targets of CDPCR1_01	-74.82	-2.31	130	33	0.25
AMINO_ACID_DERIVATIVE_BIOSYNTHETIC_PROCESS	-10.41	-2.3	10	4	0.4
KEGG_GLYCOSAMINOGLYCAN_BIOSYNTHESIS_CHONDROITIN_SULFATE	-61.3	-2.3	22	6	0.27
GO_REGULATION_OF_CELL_MATRIX_ADHESION	-63.63	-2.3	90	34	0.38
GO_ANTIMICROBIAL_HUMORAL_RESPONSE	-81.25	-2.3	52	14	0.27
GO_NEGATIVE_REGULATION_OF_PROTEIN_KINASE_B_SIGNALING	-47.66	-2.29	36	16	0.44
GO_RESPONSE_TO_OXYGEN_LEVELS	-69.16	-2.29	311	127	0.41
GO_RESPONSE_TO_TRANSITION_METAL_NANOPARTICLE	-89.78	-2.29	148	63	0.43
GO_FIBRONECTIN_BINDING	-106.39	-2.29	28	16	0.57
GO_POSITIVE_REGULATION_OF_INTERLEUKIN_2_PRODUCTION	-147.35	-2.29	31	12	0.39
GO_ENDOPLASMIC_RETICULUM_LUMEN	-32.2	-2.28	201	84	0.42
GO_POSITIVE_REGULATION_OF_EXTRINSIC_APOPTOTIC_SIGNALING_PATHWAY	-52.86	-2.28	53	35	0.66
GO_CELLULAR_RESPONSE_TO_OXYGEN_LEVELS	-58.67	-2.28	143	55	0.38
REACTOME_INTEGRIN_CELL_SURFACE_INTERACTIONS	-89.69	-2.28	79	37	0.47
EXTRACELLULAR_REGION_PART	-125.68	-2.28	338	88	0.26
GO_SECRETORY_GRANULE_LUMEN	-157.29	-2.28	85	31	0.36
GO_SNARE_COMPLEX	-17.36	-2.27	53	28	0.53
KEGG_GLYCOSAMINOGLYCAN_DEGRADATION	-47	-2.27	21	9	0.43
ATPASE_ACTIVITY_COUPLED_TO_TRANSMEMBRANE_MOVEMENT_OF_IONS	-133.35	-2.27	24	9	0.38
GO_NEGATIVE_REGULATION_OF_COAGULATION	-196.17	-2.27	48	13	0.27

Gene set	t-test p-value (-log10(p)), positive = higher in ICR, negative = lower in ICR)		N = No. of genes in the gene set	N/gc = No. of used genes	N/N/gc
	t-test p-value	mixed effects p-value			
REACTOME_TRANSPORT_OF_VITAMINS_NUCLEOSIDES_AND_RELATED_MOLECULES	-10.14	-2.26	31	9	0.29
GO_IRON_ION_BINDING	-18.16	-2.26	163	42	0.26
GO_ACETYLGUCOSAMINYLTRANSFERASE_ACTIVITY	-38.97	-2.26	49	19	0.39
GO_POSITIVE_REGULATION_OF_RECEPTOR_MEDIATED_ENDOCYTOSIS	-75.46	-2.26	47	13	0.28
HALLMARK_UV_RESPONSE_DN	-95.37	-2.26	144	64	0.44
GO_CELL_ADHESION_MOLECULE_BINDING	-113.26	-2.26	186	74	0.4
REACTOME_CELL_SURFACE_INTERACTIONS_AT_THE_VASCULAR_WALL	-148.37	-2.26	91	38	0.42
GO_UBIQUITIN_UBIQUITIN_LIGASE_ACTIVITY	-10.5	-2.25	13	7	0.54
GO_N_GLYCAN_PROCESSING	-37.67	-2.25	20	5	0.25
GO_BRANCH_ELONGATION_OF_AN_EPITHELIUM	-38.53	-2.25	17	4	0.24
REACTOME_TRANSPORT_OF_GLUCOSE_AND_OTHER_SUGARS_BILE_SALTS_AND_ORGANIC_ACIDS_METAL_IONS_AND_AMINE_COMPOUNDS	-70.87	-2.25	89	18	0.2
GO_BASAL_PLASMA_MEMBRANE	-102.25	-2.25	33	9	0.27
GO_PLATELET_DEGRANULATION	-156.77	-2.25	107	51	0.48
PDZ_DOMAIN_BINDING	-29.47	-2.24	14	4	0.29
BIOCARTA_GATA3_PATHWAY	-52.32	-2.24	16	4	0.25
GO_NEGATIVE_REGULATION_OF_CELL_SUBSTRATE_ADHESION	-81.77	-2.24	53	25	0.47
AMINE_BIOSYNTHETIC_PROCESS	-12.25	-2.23	15	7	0.47
GO_REGULATION_OF_RECEPTOR_ACTIVITY	-13.59	-2.23	117	30	0.26
GO_PYRIMIDINE_NUCLEOSIDE_CATABOLIC_PROCESS	-79.61	-2.23	21	8	0.38
GO_CIRCULATORY_SYSTEM_DEVELOPMENT	-132.21	-2.23	788	233	0.3
GO_MATURE_B_CELL_DIFFERENTIATION	-21.54	-2.22	17	7	0.41
GO_OLIGOSACCHARIDE_CATABOLIC_PROCESS	-24.14	-2.22	12	7	0.58
GO_RESPONSE_TO_PROSTAGLANDIN	-38.47	-2.22	34	11	0.32
GO_OXIDOREDUCTASE_ACTIVITY_ACTING_ON_THE_CH_NH2_GROUP_OF_DONORS_OXYGEN_AS_ACCEPTOR	-60.87	-2.22	15	5	0.33
ST_TUMOR_NECROSIS_FACTOR_PATHWAY	-96.67	-2.22	29	17	0.59
GO_REGULATION_OF_INTERLEUKIN_8_SECRETION	-101.51	-2.22	19	8	0.42
GO_REGULATION_OF_MEMBRANE_PROTEIN_ECTODOMAIN_PROTEOLYSIS	-157.88	-2.22	21	9	0.43
ER_TO_GOLGI_VESICLE_MEDIATED_TRANSPORT	-4.83	-2.21	18	15	0.83
PID_TCR_JNK_PATHWAY	-26.53	-2.21	14	6	0.43
REACTOME_IL1_SIGNALING	-34.94	-2.21	39	16	0.41
GO_POSITIVE_REGULATION_OF_IMMUNOGLOBULIN_SECRETION	-97.18	-2.21	11	4	0.36
PID_API1_PATHWAY	-129.76	-2.2	70	31	0.44
Targets of LMO2COM_01	-20.1	-2.19	264	72	0.27
GO_RESPONSE_TO_STARVATION	-41.8	-2.19	154	70	0.45
GO_MEMBRANE_RAFT_ORGANIZATION	-114.17	-2.19	17	12	0.71
COAGULATION	-131.28	-2.19	44	12	0.27
GO_SULFATE_TRANSPORT	-73.24	-2.18	14	3	0.21
Targets of STAT5A_02	-73.82	-2.18	141	42	0.3
GO_SECRETORY_GRANULE	-145.5	-2.18	352	114	0.32
GO_REGULATION_OF_COAGULATION	-149.09	-2.18	88	26	0.3
GO_CELL_SURFACE	-169.9	-2.18	757	217	0.29
GO_NUCLEOTIDE_TRANSMEMBRANE_TRANSPORT	-6.85	-2.17	12	7	0.58
PROTEIN_TRANSPORTER_ACTIVITY	-7.67	-2.17	14	7	0.5
ENDOPLASMIC_RETICULUM_LUMEN	-16.08	-2.17	14	12	0.86
GO_REGULATION_OF_PEPTIDYL_SERINE_PHOSPHORYLATION	-34.4	-2.17	118	37	0.31
LIPID_RAFT	-83.19	-2.17	29	16	0.55
GO_CELLULAR_RESPONSE_TO_EXTERNAL_STIMULUS	-74.77	-2.16	264	114	0.43
GO_REGULATION_OF_EXTRINSIC_APOPTOTIC_SIGNALING_PATHWAY	-97.55	-2.16	153	77	0.5
GO_RESPONSE_TO_DRUG	-144.63	-2.16	431	159	0.37
GO_REGULATION_OF_EXTRACELLULAR_MATRIX_DISASSEMBLY	-147.71	-2.16	14	4	0.29
REACTOME_ACTIVATION_OF_CHAPERONE_GENES_BY_XBP1S	-15.37	-2.15	46	35	0.76
GO_DENDRITE_MORPHOGENESIS	-17.1	-2.15	42	12	0.29
GO_MATURE_B_CELL_DIFFERENTIATION_INVOLVED_IN_IMMUNE_RESPONSE	-27.87	-2.15	13	6	0.46
GO_CELLULAR_RESPONSE_TO_MECHANICAL_STIMULUS	-133.12	-2.15	80	32	0.4
GO_HETEROTYPIC_CELL_CELL_ADHESION	-138.66	-2.15	27	9	0.33
BIOCARTA_LYM_PATHWAY	-58.96	-2.14	11	7	0.64

Gene set	t-test p-value (-log10(p)), positive = higher in ICR, negative = lower in ICR)		N = No. of genes in the gene set	N/qc = No. of used genes	N/N.qc
	t-test p-value	mixed effects p-value			
HINATA_NFKB_MATRIX	-78.15	-2.14	10	7	0.7
GO_NEGATIVE_REGULATION_OF_RHO_PROTEIN_SIGNAL_TRANSDUCTION	-83.78	-2.14	14	8	0.57
GO_TELOMERE_LOCALIZATION	-8.52	-2.13	11	4	0.36
INTRINSIC_TO_ENDOPLASMIC_RETICULUM_MEMBRANE	-11.39	-2.13	24	14	0.58
CELLULAR_HOMEOSTASIS	-61.96	-2.13	147	45	0.31
GO_CELL_MIGRATION_INVOLVED_IN_SPROUTING_ANGIOGENESIS	-87.08	-2.13	15	4	0.27
GO_GASTRULATION	-36.59	-2.12	155	46	0.3
PID_IL1_PATHWAY	-68.25	-2.12	34	15	0.44
GO_ENDOPEPTIDASE_ACTIVITY	-81.63	-2.12	448	135	0.3
INTEGRAL_TO_ENDOPLASMIC_RETICULUM_MEMBRANE	-9.58	-2.11	24	14	0.58
REACTOME_ACTIVATION_OF_CHAPERONE_GENES_BY_ATF6_ALPHA	-16.39	-2.11	11	7	0.64
GO_ZINC_II_ION_TRANSPORT	-38.12	-2.11	26	13	0.5
RYAAAKNNNNNTTGW_UNKNOWN	-51.33	-2.11	84	22	0.26
GGARNTKYCCA_UNKNOWN	-56.64	-2.11	78	24	0.31
GO_MEMBRANE_HYPERPOLARIZATION	-86.71	-2.11	11	3	0.27
PID_INTEGRIN_A9B1_PATHWAY	-88.11	-2.11	25	11	0.44
GO_MEMBRANE_ASSEMBLY	-113.44	-2.11	25	10	0.4
GO_ALCOHOL_TRANSMEMBRANE_TRANSPORTER_ACTIVITY	-135.7	-2.11	24	5	0.21
LEUKOCYTE_ACTIVATION	-21.62	-2.1	69	16	0.23
GO_POSITIVE_REGULATION_OF_PEPTIDYL_SERINE_PHOSPHORYLATION	-60.49	-2.1	88	29	0.33
GO_OXALATE_TRANSPORT	-81.43	-2.09	12	3	0.25
GO_MEMBRANE_BIOGENESIS	-92.93	-2.09	30	12	0.4
GO_SECRETORY_VESICLE	-133.02	-2.09	461	143	0.31
REACTOME_EXTRACELLULAR_MATRIX_ORGANIZATION	-29.23	-2.08	87	25	0.29
Targets of ATargets of 01	-45.86	-2.08	259	109	0.42
ATPASE_ACTIVITY_COUPLED_TO_MOVEMENT_OF_SUBSTANCES	-130.08	-2.08	40	14	0.35
GO_ENDOPLASMIC_RETICULUM_CHAPERONE_COMPLEX	-3.32	-2.07	11	8	0.73
GO_CIS_GOLGI_NETWORK	-25.98	-2.07	40	23	0.57
GO_RESPONSE_TO_OXIDATIVE_STRESS	-58.41	-2.07	352	165	0.47
Targets of FOXD3_01	-77.69	-2.07	199	45	0.23
HYDROLASE_ACTIVITY_HYDROLYZING_O_GLYCOSYL_COMPOUNDS	-37.78	-2.06	37	13	0.35
Targets of CEBP_Q2_01	-52.02	-2.06	267	76	0.28
GO_REGULATION_OF_CELL_JUNCTION_ASSEMBLY	-53.46	-2.06	68	27	0.4
GO_PEPTIDASE_ACTIVITY	-53.89	-2.06	663	202	0.3
GO_REGULATION_OF_EPITHELIAL_CELL_APOPTOTIC_PROCESS	-88.51	-2.06	59	20	0.34
ACTIVE_TRANSMEMBRANE_TRANSPORTER_ACTIVITY	-98.29	-2.06	122	31	0.25
GO_REGULATION_OF_PEPTIDASE_ACTIVITY	-127.28	-2.06	392	176	0.45
GO_RESPONSE_TO_FOOD	-15.02	-2.05	19	5	0.26
GO_PROTEIN_DEGLYCOSYLATION	-21.99	-2.05	21	13	0.62
GO_AMINOGLYCAN_CATABOLIC_PROCESS	-66.41	-2.05	68	27	0.4
INTEGRAL_TO_ORGANELLE_MEMBRANE	-12.43	-2.04	50	27	0.54
LYMPHOCYTE_ACTIVATION	-16.18	-2.04	61	15	0.25
BIOCARTA_VITCB_PATHWAY	-23.55	-2.04	11	6	0.55
NEGATIVE_REGULATION_OF_SECRETION	-25.56	-2.04	13	5	0.38
MEMBRANE_LIPID_METABOLIC_PROCESS	-61.37	-2.04	101	55	0.54
GO_CELL_CELL_CONTACT_ZONE	-91.65	-2.04	64	21	0.33
KEGG_COMPLEMENT_AND_COAGULATION_CASCADES	-112.22	-2.04	69	28	0.41
GO_NEGATIVE_REGULATION_OF_WOUND_HEALING	-182.92	-2.04	58	13	0.22
NUCLEOTIDE_KINASE_ACTIVITY	-0.4	-2.03	13	5	0.38
GO_ENDODERM_FORMATION	-52.71	-2.03	50	20	0.4
GO_GLYCOLIPID_BIOSYNTHETIC_PROCESS	-58.12	-2.03	62	33	0.53
M1_MACROPHAGES	-77.24	-2.03	54	25	0.46
RESPONSE_TO_WOUNDING	-137.23	-2.03	190	58	0.31
GO_REGULATION_OF_ASTROCYTE_DIFFERENTIATION	-149.91	-2.03	27	7	0.26
GO_HOST	-4.29	-2.02	12	8	0.67
GO_REGULATION_OF_CHOLESTEROL_HOMEOSTASIS	-29.21	-2.02	11	4	0.36
GO_REGULATION_OF_SODIUM_ION_TRANSMEMBRANE_TRANSPORT	-67.2	-2.02	48	14	0.29
TIL_HCC_C9_CD4_GZMK	-75.21	-2.02	10	5	0.5
SUGAR_BINDING	-98.2	-2.02	34	7	0.21

Gene set	t-test p-value (-log10(p)), positive = higher in ICR, negative = lower in ICR)		N = No. of genes in the gene set	N/gc = No. of used genes	N/N/gc
	t-test p-value	mixed effects p-value			
GO_APICAL_PLASMA_MEMBRANE	-139.37	-2.02	292	74	0.25
GO_REGULATION_OF_SODIUM_ION_TRANSPORT	-143	-2.02	77	22	0.29
GO_UDP_GLYCOSYLTRANSFERASE_ACTIVITY	-33.38	-2.01	139	38	0.27
GO_OXIDOREDUCTASE_ACTIVITY_ACTING_ON_THE_CH_NH2_GROUP_OF_DONORS	-37.81	-2.01	19	6	0.32
GO_ENDODERM_DEVELOPMENT	-49.7	-2.01	71	21	0.3
GO_CARBOHYDRATE_BINDING	-65.62	-2.01	277	72	0.26
Targets of OCT1_Q5_01	-69.32	-2.01	273	64	0.23
GO_MATERNAL_PROCESS_INVOLVED_IN_FEMALE_PREGNANCY	-72.71	-2.01	60	21	0.35
GO_SODIUM_POTASSIUM_EXCHANGING_ATPASE_COMPLEX	-141.23	-2.01	11	3	0.27
HALLMARK_COAGULATION	-166.89	-2.01	138	64	0.46
SULFURIC_ESTER_HYDROLASE_ACTIVITY	-49.62	-2	16	4	0.25
GO_RESPONSE_TO_UV	39.84	2	126	60	0.48
FATTY_ACID_OXIDATION	17.45	2	18	12	0.67
GO_PROTEIN_SUMOYLATION	74.55	2.01	115	68	0.59
GO_POSITIVE_REGULATION_OF_DNA_REPAIR	59.89	2.01	38	17	0.45
GO_CHROMOSOMAL_REGION	54.33	2.01	330	159	0.48
GO_NEGATIVE_REGULATION_OF_DEFENSE_RESPONSE_TO_VIRUS	42.57	2.01	18	8	0.44
KEGG_LIMONENE_AND_PINENE_DEGRADATION	40.9	2.01	10	7	0.7
NUCLEAR_HORMONE_RECEPTOR_BINDING	39.05	2.01	28	15	0.54
CELLULAR_PROTEIN_COMPLEX_DISASSEMBLY	35.57	2.01	13	7	0.54
BIOCARTA_VEGF_PATHWAY	21.87	2.01	29	15	0.52
GO_FILAMENTOUS_ACTIN	8.26	2.01	20	6	0.3
GO_DNA_METHYLATION_OR_DEMETHYLATION	2.5	2.01	59	22	0.37
GO_REGULATION_OF_TELOMERASE_ACTIVITY	68.25	2.02	43	17	0.4
GO_HORMONE_RECEPTOR_BINDING	23.76	2.02	168	73	0.43
GO_REGULATION_OF_MITOCHONDRIAL_OUTER_MEMBRANE_PERMEABILIZATION_INVOLVED_IN_APOPTOTIC_SIGNALING_PATHWAY	17.67	2.02	43	23	0.53
GO_DNA_HELICASE_COMPLEX	50.82	2.03	14	9	0.64
GO_VIRAL_GENOME_REPLICATION	28.4	2.03	21	13	0.62
GO_REGULATION_OF_SPINDLE_ASSEMBLY	8.3	2.03	15	11	0.73
TAAYNRNNTCC_UNKNOWN	3.81	2.03	172	44	0.26
GO_REGULATION_OF_TELOMERE_MAINTENANCE_VIA_TELOMERE_LENGTHENING	108.58	2.04	50	26	0.52
BIOCARTA_EIF2_PATHWAY	19.87	2.04	11	7	0.64
GO_REGULATION_OF_CHROMATIN_SILENCING	70.9	2.05	21	9	0.43
GO_MICROTUBULE	70.74	2.05	405	173	0.43
GO_POSITIVE_REGULATION_OF_PROTEIN_LOCALIZATION_TO_NUCLEUS	60.95	2.05	129	53	0.41
GO_NEGATIVE_REGULATION_OF_TELOMERE_MAINTENANCE_VIA_TELOMERE_LENGTHENING	59.17	2.05	17	12	0.71
Targets of E2F_Q6_01	44.57	2.05	240	111	0.46
PROTEIN_COMPLEX_DISASSEMBLY	32.97	2.05	14	7	0.5
GO_PEROXISOME_PROLIFERATOR_ACTIVATED_RECEPTOR_BINDING	23	2.05	15	4	0.27
GO_FEMALE_MEIOTIC_DIVISION	19.4	2.05	26	10	0.38
GO_POSITIVE_REGULATION_OF_MRNA_PROCESSING	7.84	2.05	32	20	0.62
GO_MICROTUBULE_CYTOSKELETON_ORGANIZATION	7.79	2.05	348	134	0.39
Targets of AP4_Q6_01	21.61	2.06	255	71	0.28
REACTOME_TRANSPORT_OF_MATURE_MRNA_DERIVED_FROM_AN_INTRONLESS_TRANSCRIPT	36.77	2.07	33	26	0.79
AUXILIARY_TRANSPORT_PROTEIN_ACTIVITY	9.03	2.07	26	6	0.23
GO_POSITIVE_REGULATION_OF_TELOMERE_MAINTENANCE_VIA_TELOMERE_LENGTHENING	96.96	2.08	33	14	0.42
GO_NEGATIVE_REGULATION_OF_CHROMOSOME_ORGANIZATION	77.33	2.08	96	49	0.51
RNA_DEPENDENT_ATPASE_ACTIVITY	48.48	2.08	18	14	0.78
GO_MIRNA_BINDING	31.2	2.08	16	5	0.31
GO_G1_DNA_DAMAGE_CHECKPOINT	31.15	2.08	73	44	0.6
GO_TELOMERE_ORGANIZATION	47.03	2.09	104	49	0.47
DNA_INTEGRITY_CHECKPOINT	25.86	2.09	24	11	0.46
GO_CYTOPLASMIC_MICROTUBULE	33.85	2.1	57	27	0.47
GO_UBIQUITIN_LIKE_PROTEIN_LIGASE_BINDING	27.06	2.1	264	154	0.58

Gene set	t-test p-value (-log10(p)), positive = higher in ICR, negative = lower in ICR)		N = No. of genes in the gene set	N/qc = No. of used genes	N/N.qc
	t-test p-value	mixed effects p-value			
GO_POSITIVE_REGULATION_OF_ERYTHROCYTE_DIFFERENTIATION	12.02	2.1	23	7	0.3
GO_REGULATION_OF_HISTONE_H3_K9_ACETYLATION	27.95	2.11	14	4	0.29
GO_DNA_BINDING_BENDING	19.1	2.11	20	6	0.3
GO_MACROPHAGE_ACTIVATION_INVOLVED_IN_IMMUNE_RESPONSE	10.16	2.11	11	3	0.27
NEGATIVE_REGULATION_OF_IMMUNE_SYSTEM_PROCESS	8.83	2.11	14	3	0.21
GO_DNA_INTEGRITY_CHECKPOINT	37.37	2.12	146	72	0.49
GO_REGULATION_OF_SPINDLE_ORGANIZATION	15.42	2.12	20	14	0.7
GO_CHROMATIN_BINDING	78.09	2.13	435	148	0.34
GO_VIRAL_LATENCY	68.81	2.13	11	9	0.82
DNA_HELICASE_ACTIVITY	52.6	2.13	25	15	0.6
GO_NUCLEAR_CHROMOSOME_TELOMERIC_REGION	62.34	2.14	132	66	0.5
GO_POSITIVE_REGULATION_OF_GLUCOSE_IMPORT_IN_RESPONSE_TO_INSULIN_STIMULUS	13.76	2.14	12	4	0.33
GO_CELL_CELL_RECOGNITION	92.12	2.15	60	13	0.22
GO_RIBONUCLEOPROTEIN_GRANULE	90.49	2.15	148	87	0.59
CONTRACTILE_FIBER_PART	82.69	2.15	23	8	0.35
GO_MITOTIC_NUCLEAR_DIVISION	44.49	2.15	361	187	0.52
GO_CELL_CYCLE_PHASE_TRANSITION	35.91	2.16	255	127	0.5
Targets of OCT1_O2	29.34	2.16	214	50	0.23
GO_BINDING_OF_SPERM_TO_ZONA_PELLUCIDA	99.01	2.17	33	9	0.27
GO_POSITIVE_REGULATION_OF_DNA_BIOSYNTHETIC_PROCESS	81.19	2.17	59	23	0.39
TRANSLATION_FACTOR_ACTIVITY_NUCLEIC_ACID_BINDING	69.02	2.17	39	29	0.74
REACTOME_CELL_DEATH_SIGNALLING_VIA_NRAGE_NRIF_AND_NADE	32.08	2.17	60	22	0.37
GO_EMBRYONIC_HEMOPOIESIS	17.18	2.17	20	6	0.3
GO_POSITIVE_REGULATION_OF_TELOMERE_MAINTENANCE	98.25	2.18	47	24	0.51
GO_ADENYL_NUCLEOTIDE_BINDING	83.66	2.19	1514	548	0.36
GO_DAMAGED_DNA_BINDING	66.18	2.19	63	38	0.6
GO_SPINDLE_POLE	31.43	2.19	126	54	0.43
GO_CENTROSOME_CYCLE	7.5	2.19	45	18	0.4
CONTRACTILE_FIBER	88.84	2.2	25	8	0.32
AEROBIC_RESPIRATION	53.17	2.2	15	13	0.87
RESPONSE_TO_RADIATION	39	2.2	60	16	0.27
PID_IL3_PATHWAY	9.65	2.2	27	10	0.37
GO_TRANSCRIPTION_EXPORT_COMPLEX	52.59	2.21	13	12	0.92
GO_POSITIVE_REGULATION_OF_DNA_TEMPLATED_TRANSCRIPTION_ELONGATION	47.81	2.21	23	16	0.7
PID_INSULIN_GLUCOSE_PATHWAY	18.14	2.22	26	11	0.42
GO_POSITIVE_REGULATION_OF_MRNA_METABOLIC_PROCESS	17.19	2.22	45	27	0.6
ZF-MIZ	11.83	2.22	7	4	0.57
GO_MRNA_3_UTR_BINDING	52.16	2.23	48	26	0.54
REACTOME_PURINE_METABOLISM	48.02	2.23	33	22	0.67
DNA_REPLICATION_INITIATION	9.15	2.23	16	7	0.44
GO_REGULATION_OF_CHROMATIN_ORGANIZATION	70.88	2.24	152	61	0.4
GO_NEGATIVE_REGULATION_OF_GENE_SILENCING	42.63	2.24	19	5	0.26
BIOCARTA_G1_PATHWAY	41.82	2.24	28	10	0.36
GO_CELL_CYCLE_CHECKPOINT	54.94	2.25	194	93	0.48
GO_PROTEIN_N_TERMINUS_BINDING	25.88	2.25	103	64	0.62
GO_ENDODEOXYRIBONUCLEASE_ACTIVITY	48.57	2.26	51	21	0.41
GO ASPARTATE METABOLIC PROCESS	31.42	2.26	11	5	0.45
GO_POSITIVE_REGULATION_OF_CELLULAR_RESPONSE_TO_INSULIN_STIMULUS	16.99	2.26	23	6	0.26
GO_RESPONSE_TO_ACIDIC_PH	16.79	2.26	21	5	0.24
GO_ENDOLYSOSOME_MEMBRANE	16.29	2.27	11	5	0.45
GO_MYOFILAMENT	82.74	2.28	24	6	0.25
GO_REGULATION_OF_SIGNAL_TRANSDUCTION_BY_P53_CLASS_MEDIA TOR	53.98	2.28	162	73	0.45
MACROMOLECULAR_COMPLEX_DISASSEMBLY	38.21	2.28	15	8	0.53
PID_P73PATHWAY	17.96	2.28	79	41	0.52
GO_RIBONUCLEOTIDE_BINDING	81.21	2.29	1860	694	0.37
GO_REGULATION_OF_PROTEIN_ACETYLATION	48.57	2.29	64	27	0.42

Gene set	t-test p-value (-log10(p)), positive = higher in ICR, negative = lower in ICR)		N = No. of genes in the gene set	N/qc = No. of used genes	N/N.qc
	t-test p-value	mixed effects p-value			
GO_NEGATIVE_REGULATION_OF_CELL_CYCLE_PROCESS	44.5	2.29	214	104	0.49
GO_MEIOTIC_CELL_CYCLE	22.02	2.3	186	58	0.31
GO_ALDEHYDE_CATABOLIC_PROCESS	17.84	2.3	13	9	0.69
M_PHASE_OF_MITOTIC_CELL_CYCLE	46.52	2.31	85	47	0.55
PID_CMYB_PATHWAY	41.73	2.31	84	36	0.43
REACTOME_DOUBLE_STRAND_BREAK_REPAIR	40.26	2.31	24	9	0.38
REGULATION_OF_MITOSIS	40.4	2.32	41	20	0.49
GO_CELL_CYCLE_G2_M_PHASE_TRANSITION	28.36	2.32	138	77	0.56
TCCCRNRTGC_UNKNOWN	23.51	2.32	213	111	0.52
GO_NUCLEAR_CHROMOSOME	70.81	2.33	523	222	0.42
GO_CHROMATIN_DNA_BINDING	69.13	2.33	80	35	0.44
Targets of COUP_DR1_Q6	66.25	2.33	247	94	0.38
ATP_DEPENDENT_DNA_HELICASE_ACTIVITY	62.62	2.33	11	8	0.73
GO_MITOTIC_DNA_INTEGRITY_CHECKPOINT	39.42	2.33	100	56	0.56
GO_PROTEIN_C_TERMINUS_BINDING	25.24	2.33	186	81	0.44
GO_P53_BINDING	85.62	2.34	67	23	0.34
M_PHASE	45.04	2.35	114	55	0.48
GO_CORONARY_VASCULATURE_DEVELOPMENT	30.33	2.35	37	9	0.24
GO_NEGATIVE_REGULATION_OF_DNA_DEPENDENT_DNA_REPLICATION	9.47	2.35	16	5	0.31
Targets of E2F1_Q4_01	60.41	2.36	228	90	0.39
MICROTUBULE_CYTOSKELETON_ORGANIZATION_AND_BIOGENESIS	50.93	2.36	35	18	0.51
GO_NEGATIVE_REGULATION_OF_VIRAL_RELEASE_FROM_HOST_CELL	21.79	2.37	16	9	0.56
REACTOME_APOPTOSIS_INDUCED_DNA_FRAGMENTATION	13.69	2.37	13	8	0.62
GO_CHROMOSOME	75.27	2.38	880	390	0.44
DNA_DEPENDENT_ATPASE_ACTIVITY	64.91	2.38	22	13	0.59
GO_NUCLEOSOMAL_DNA_BINDING	79.26	2.39	30	22	0.73
GO_DNA_DOUBLE_STRAND_BREAK_PROCESSING	21.71	2.39	20	9	0.45
GO_MICROTUBULE_ORGANIZING_CENTER_ORGANIZATION	15.43	2.39	84	40	0.48
Targets of E2F_Q4_01	69.24	2.4	237	100	0.42
GO_ORGANELLE_ASSEMBLY	55.85	2.4	495	214	0.43
GO_REGULATION_OF_PROTEIN_INSERTION_INTO_MITOCHONDRIAL_MEMBRANE_INVOLVED_IN_APOPTOTIC_SIGNALING_PATHWAY	13.8	2.4	29	15	0.52
PID_PI3KCI_AKT_PATHWAY	5.36	2.41	35	16	0.46
REACTOME_DESTABILIZATION_OF_MRNA_BY_BRF1	57.41	2.42	17	13	0.76
GO_POSITIVE_REGULATION_OF_CHROMATIN_MODIFICATION	52.36	2.42	85	35	0.41
HISTONE_METHYLTRANSFERASE_ACTIVITY	26.67	2.42	11	4	0.36
REACTOME_PLATELET_SENSITIZATION_BY_LDL	22.83	2.42	16	6	0.38
PROTEIN_AMINO_ACID_ADP_RIBOSYLATION	20.94	2.42	10	3	0.3
PROTEIN_PHOSPHATASE_TYPE_2A_REGULATOR_ACTIVITY	37.57	2.43	14	7	0.5
CONDENSED_CHROMOSOME	47.3	2.44	34	16	0.47
GTRYCATRR_UNKNOWN	16.7	2.44	172	45	0.26
MITOCHONDRIAL_TRANSPORT	44.92	2.45	21	19	0.9
REACTOME_INTEGRATION_OF_PROVIRUS	80.22	2.46	16	6	0.38
GO_POSITIVE_REGULATION_OF_MRNA_SPLICING_VIA_SPLICEOSOME	46.81	2.46	14	6	0.43
GO_NEGATIVE_REGULATION_OF_MITOTIC_CELL_CYCLE	36.32	2.46	199	100	0.5
ST_FAS_SIGNALING_PATHWAY	29.53	2.46	65	31	0.48
GO_POSITIVE_REGULATION_OF_DNA_REPLICATION	68.55	2.47	86	31	0.36
GO_NEGATIVE_REGULATION_OF_DNA_REPLICATION	64.35	2.47	55	25	0.45
RRCCGTTA_UNKNOWN	36.84	2.47	87	52	0.6
GO_CHROMATIN	66.61	2.48	441	168	0.38
GO_RESPONSE_TO_FUNGICIDE	17.51	2.48	11	4	0.36
GO_GLOBAL_GENOME_NUCLEOTIDE_EXCISION_REPAIR	16.24	2.49	32	25	0.78
GO_DNA_CATABOLIC_PROCESS	16.38	2.5	27	13	0.48
GO_ATP_DEPENDENT_DNA_HELICASE_ACTIVITY	54.77	2.51	34	19	0.56
MRNA_BINDING	90.95	2.52	23	17	0.74
PID_AURORA_B_PATHWAY	31.45	2.52	39	19	0.49
CELL_CYCLE_PHASE	53	2.53	170	78	0.46
GO_AU_RICH_ELEMENT_BINDING	29.36	2.54	23	12	0.52
GO_REGULATION_OF_MICROTUBULE_POLYMERIZATION_OR_DEPOLY	19.11	2.54	178	88	0.49

Gene set	t-test p-value (-log10(p)), positive = higher in CR, negative = lower in CR)		N = No. of genes in the gene set	N/gc = No. of used genes	N/N/gc
	t-test p-value	mixed effects p-value			
MERIZATION					
GO_SUMO_BINDING	13.84	2.54	14	5	0.36
Targets of CEBPGAMMA_Q6	46.47	2.55	257	78	0.3
HMG	13.08	2.55	51	17	0.33
GO_REGULATION_OF_PROTEIN_PHOSPHATASE_TYPE_2A_ACTIVITY	33.51	2.57	24	11	0.46
KEGG_BETA_ALANINE_METABOLISM	64.25	2.58	22	11	0.5
GO_RNA_POLYMERASE_II_DISTAL_ENHANCER_SEQUENCE_SPECIFIC_DNA_BINDING	55.57	2.59	65	28	0.43
GO_PEPTIDYL_AMINO_ACID_MODIFICATION	43.76	2.59	841	340	0.4
GO_NEGATIVE_REGULATION_OF_TELOMERASE_ACTIVITY	29.05	2.59	15	7	0.47
Targets of AP2REP_01	27.21	2.61	178	57	0.32
GO_MITOTIC_SPINDLE_ORGANIZATION	21.78	2.61	69	32	0.46
KEGG_GLYOXYLATE_AND_DICARBOXYLATE_METABOLISM	60.42	2.62	16	10	0.62
GO_MITOTIC_CELL_CYCLE_CHECKPOINT	53.4	2.62	139	75	0.54
GO_REGULATION_OF_CELL_CYCLE_ARREST	50.41	2.62	108	52	0.48
GO_REGULATION_OF_DNA_TEMPLATED_TRANSCRIPTION_ELONGATION	46.41	2.62	44	25	0.57
GO_RESPONSE_TO_AMMONIUM_ION	32.19	2.62	51	11	0.22
GO_REGULATION_OF_THYMOCYTE_APOPTOTIC_PROCESS	49.18	2.63	12	4	0.33
GO_POSITIVE_REGULATION_OF_MITOCHONDRIAL_OUTER_MEMBRANE_PERMEABILIZATION_INVOLVED_IN_APOPTOTIC_SIGNALING_PATHWAY	19.54	2.63	36	19	0.53
GO_NEGATIVE_REGULATION_OF_TELOMERE_MAINTENANCE	62.11	2.64	26	17	0.65
GO_CHROMOSOME_TELOMERIC_REGION	64.33	2.65	162	79	0.49
GO_REGULATION_OF_GENE_SILENCING	48.57	2.65	52	16	0.31
PID_ATM_PATHWAY	33.28	2.66	34	12	0.35
REACTOME_E2F_ENABLED_INHIBITION_OF_PRE_REPLICATION_COMPLEX_FORMATION	17.78	2.66	10	6	0.6
GO_REGULATION_OF_EXECUTION_PHASE_OF_APOPTOSIS	88.61	2.67	24	11	0.46
MICROTUBULE	51.63	2.67	32	22	0.69
BIOCARTA_ATRBRCA_PATHWAY	37.5	2.67	21	8	0.38
GO_NEGATIVE_REGULATION_OF_RESPONSE_TO_BIOTIC_STIMULUS	20.91	2.68	30	14	0.47
GO_POSITIVE_REGULATION_OF_PROTEIN_IMPORT_INTO_NUCLEUS_TRANSLOCATION	7.78	2.69	13	5	0.38
GO_NEGATIVE_REGULATION_OF_EPITHELIAL_CELL_MIGRATION	6.17	2.7	53	21	0.4
Targets of E2F1_Q6_01	71.47	2.71	238	98	0.41
GO_ORGANIC_ACID_BINDING	25.77	2.71	209	68	0.33
GO_AMINO_ACID_BINDING	78.19	2.73	108	36	0.33
MITOTIC_SPINDLE_ORGANIZATION_AND_BIOGENESIS	41.3	2.73	10	5	0.5
CHROMOSOME PERICENTRIC_REGION	29.45	2.74	31	14	0.45
GO_REGULATION_OF_DNA_REPLICATION	86.77	2.75	161	66	0.41
YAATNRNNNNYNATT_UNKNOWN	70.49	2.75	104	27	0.26
GO_LYMPHOID_PROGENITOR_CELL_DIFFERENTIATION	77.56	2.78	11	3	0.27
Targets of E2F_Q3_01	60.66	2.79	235	89	0.38
PID_P38_MK2_PATHWAY	31.15	2.82	21	12	0.57
REACTOME_RECRUITMENT_OF_NUMA_TO_MITOTIC_CENTROSOMES	26.59	2.82	10	7	0.7
DNA_RECOMBINATION	70.64	2.85	47	18	0.38
GO_GLYOXYLATE_METABOLIC_PROCESS	55.35	2.86	28	14	0.5
MITOTIC_CELL_CYCLE_CHECKPOINT	22.04	2.86	21	10	0.48
Targets of EFC_Q6	17.64	2.86	268	84	0.31
Targets of E2F_Q3	45.09	2.87	227	91	0.4
REACTOME_E2F_MEDIATED_REGULATION_OF_DNA_REPLICATION	40.93	2.87	35	13	0.37
Targets of ER_Q6_02	15.46	2.87	252	79	0.31
GO_POSITIVE_REGULATION_OF_PROTEIN_ACETYLATION	43.79	2.88	36	12	0.33
CELL_CYCLE_PROCESS	52.7	2.89	193	87	0.45
Targets of E2F1_Q6	63.66	2.9	232	101	0.44
GO_MODULATION_BY_SYMBIONT_OF_HOST_CELLULAR_PROCESS	8.45	2.92	28	11	0.39
REACTOME_EARLY_PHASE_OF_HIV_LIFE_CYCLE	76.06	2.94	21	10	0.48
SPINDLE_POLE	22.59	2.94	18	9	0.5
GO_POSITIVE_REGULATION_OF_PROTEIN_EXPORT_FROM_NUCLEUS	44.14	2.95	19	7	0.37
GO_GTPASE_ACTIVATING_PROTEIN_BINDING	21.58	2.95	14	7	0.5

Gene set	t-test p-value (-log10(p)), positive = higher in ICR, negative = lower in ICR)		N = No. of genes in the gene set	N/qc = No. of used genes	N/N/qc
	t-test p-value	mixed effects p-value			
TRANSCRIPTION_ELONGATION_REGULATOR_ACTIVITY	23.11	2.99	12	7	0.58
GO_POSITIVE_REGULATION_OF_DNA_METABOLIC_PROCESS	102.41	3.01	185	76	0.41
KEGG_BUTANOATE_METABOLISM	29.15	3.01	34	17	0.5
GO_NUCLEAR_CHROMATIN	52.27	3.03	291	111	0.38
GO_REGULATION_OF_MICROTUBULE_BASED_PROCESS	24.01	3.04	243	106	0.44
GO_FOLIC_ACID_BINDING	53.44	3.06	14	3	0.21
Targets of E2F1DP1RB_01	65.74	3.1	231	96	0.42
Targets of E2F4DP1_01	60.9	3.1	239	100	0.42
BIOCARTA_RB_PATHWAY	33.67	3.1	13	7	0.54
GO_POSITIVE_REGULATION_OF_PROTEIN_IMPORT	26.61	3.11	104	35	0.34
SGCGSSAAA_Targets of E2F1DP2_01	57.9	3.12	168	77	0.46
SPINDLE_ORGANIZATION_AND_BIOGENESIS	51.5	3.13	11	6	0.55
Targets of E2F1DP1_01	71.16	3.17	235	97	0.41
GO_POSITIVE_REGULATION_OF_NUCLEOCYTOPLASMIC_TRANSPORT	29.3	3.19	121	40	0.33
REACTOME_TGF_BETA_RECEPTOR_SIGNALING_IN_EMT_EPITHELIAL_T_O_MESENCHYMAL_TRANSITION	66.6	3.2	16	6	0.38
BIOCARTA_TEL_PATHWAY	35.54	3.21	18	10	0.56
Targets of E2F1DP2_01	71.9	3.22	235	97	0.41
DNA_DAMAGE_RESPONSESIGNAL_TRANSDUCTION	42.9	3.24	35	13	0.37
Targets of E2F_02	70.15	3.28	235	98	0.42
BIOCARTA_CHREBP2_PATHWAY	19.81	3.28	42	17	0.4
PID_BARD1_PATHWAY	56.99	3.32	29	15	0.52
GO_NEGATIVE_REGULATION_OF_ORGANELLE_ORGANIZATION	54.33	3.34	387	184	0.48
REACTOME_MITOTIC_G2_G2_M_PHASES	45.21	3.36	81	47	0.58
Targets of E2F4DP2_01	72.15	3.4	235	97	0.41
DNA_DAMAGE_RESPONSESIGNAL_TRANSDUCTION_BY_P53_CLASS_ME DIATOR	39.26	3.44	13	7	0.54
REACTOME_TGF_BETA_RECEPTOR_SIGNALING_ACTIVATES_SMADS	40.84	3.46	26	12	0.46
Targets of E2F1_Q3	79.97	3.47	244	97	0.4
NEGATIVE_REGULATION_OF_ANGIOGENESIS	107.96	3.51	13	3	0.23
Targets of CMYB_01	41.11	3.52	249	106	0.43
GO_RNA_CAP_BINDING_COMPLEX	25.05	3.54	14	6	0.43
PROTEIN_N_TERMINUS_BINDING	65.41	3.56	38	22	0.58
GO_PONUCLEUS	49.72	3.57	15	9	0.6
PID_DNA_PK_PATHWAY	69.37	3.63	16	9	0.56
GO_RESPONSE_TO_COBALT_ION	77.24	3.64	13	7	0.54
GGAMTNNNNNTCCY_UNKNOWN	108.65	3.67	117	41	0.35
Targets of SMAD3_Q6	25.73	3.74	239	56	0.23
Targets of E2F_Q4	70.57	3.77	234	99	0.42
REACTOME_LOSS_OF_NLP_FROM_MITOTIC_CENTROSOMES	64.59	3.84	59	34	0.58
REACTOME_RECRUITMENT_OF_MITOTIC_CENTROSOME_PROTEINS_A ND_COMPLEXES	67.72	3.9	66	39	0.59
Targets of E2F_Q6	72.88	3.99	232	97	0.42
Targets of MYC_MAX_B (Myc and MAX targets)	138.78	4.02	268	108	0.4
GO_NEGATIVE_REGULATION_OF_ENDOTHELIAL_CELL_MIGRATION	13.25	4.42	39	16	0.41
GO_RESPONSE_TO_ARSENIC_CONTAINING_SUBSTANCE	68.55	4.46	29	18	0.62
GO_REGULATION_OF_CIRCADIAN_RHYTHM	93.03	5.08	103	29	0.28
GO_ENDODEOXYRIBONUCLEASE_ACTIVITY_PRODUCING_5_PHOSPHO MONOESTERS	26.73	5.36	12	4	0.33

Table S10. Signatures that were used as alternative ICR predictors.

Description	
Signature name	Reference
AXL (Tirosh)	Tirosh et al Science 2016
Melanoma cell cycle (Tirosh)	Tirosh et al Science 2016
G1 S (Tirosh)	Tirosh et al Science 2016
G2 M (Tirosh)	Tirosh et al Science 2016

Melanoma cells (Tirosh)	Tirosh et al Science 2016
MITF (Tirosh)	Tirosh et al Science 2016
TME B cell	Tumor microenvironment (TME): Current study
TME CAF	TME: Current study
TME Endo	TME: Current study
TME Mai	TME: Current study
TME NK	TME: Current study
TME Neutrophil	TME: Current study
TME T cells	TME: Current study
TME T CD4	TME: Current study
TME T CD8	TME: Current study
TME Macrophage	TME: Current study
TME immune cells	TME: Current study
TME lymphocytes	TME: Current study
TME meylold	TME: Current study
TME stroma	TME: Current study
Fluidgm Panel A	www.fluidigm.com/applications/advanta-immuno-oncology-gene-expression-assay
Fluidgm Panel B	www.fluidigm.com/applications/advanta-immuno-oncology-gene-expression-assay
in-vivo screen GVAXPDI vs TCRaKO depleted	Manguso et al. Cell 2017
in-vivo screen GVAX vs TCRaKO depleted	Manguso et al. Cell 2017
in-vivo screen TCRaKO vs in-vitro depleted	Manguso et al. Cell 2017
in-vivo screen GVAXPDI vs TCRaKO enriched	Manguso et al. Cell 2017
in-vivo screen GVAX vs TCRaKO enriched	Manguso et al. Cell 2017
in-vivo screen TCRaKO vs in-vitro enriched	Manguso et al. Cell 2017
co-culture screen top 10 hits	Patel et al. Nature 2017
co-culture screen top 50 hits	Patel et al. Nature 2017
Ayers IFNg sig	Ayers et al. JCI 2017
Ayers immune sig	Ayers et al. JCI 2017

TME B cell	TME CAF	TME Endo	TME Mai	TME NK	TME T cells	TME T CD4	TME T CD8	TME Macrophage	TME immune	TME lymphocytes	TME meylold	TME stroma
ADAM19	ABI3BP	A2M	ABTB2	CCL4	CXCL13	AQP3	APOBEC3C	ACP5	ACAP1	ADAM28	ADAP2	ABI3BP
ADAM28	ACTA2	ADAM15	ACN9	CD244	CST7	CCR4	APOBEC3G	ACRBP	ADAM28	APOBEC3G	AIF1	ACTA2
AFF3	ADAM12	ADCY4	ACSL3	CST7	RARRES3	CCR8	CBLB	ADAMDEC1	ADAP2	BANK1	AMICA1	ADAM12
BANK1	ADAMTS2	AFAP1L1	AHCY	CTSW	KLRK4	CD28	CCL4	ADAP2	AFF3	BCL11A	BCL2A1	ADCY4
BCL11A	ANTXR1	AQP1	AIF1L	GNLY	EMB	CD4	CCL4L1	ADORA3	AIF1	BCL11B	C1orf162	AFAP1L1
BIRC3	ASPN	ARHGF15	AK2	GZMA	TESPA1	CD40LG	CCL4L2	ALDH2	AKNA	BIRC3	C1QA	APP
BLK	AXL	CALCRL	ALX1	GZMB	LAT	CD5	CCL5	ANKRD22	ALOX5	BLK	C1QB	AQP1
BLNK	BGN	CCL14	ANKRD54	HOPX	CD28	DGKA	CD8A	C1QA	ALOX5AP	BLNK	C1QC	ARHGAP29
BTLA	C1R	CD200	AP1S2	ID2	IL2RG	FAAH2	CD8B	C1QB	AMICA1	CBLB	C3AR1	BGN
CCR6	C1S	CD34	APOA1BP	IL2RB	DUSP2	FOXP3	CRTAM	C1QC	ANKRD44	CCL4	C5AR1	C1R
CCR7	C3	CD93	APOC2	KLRB1	PAG1	ICOS	CST7	C1orf162	AOAH	CCL4L1	CASP1	C1S
CD19	CALD1	CDH5	APOD	KLRK1	TRAT1	IL7R	CTSW	C3AR1	APOBEC3G	CCL4L2	CCR1	CALCRL
CD1C	CCDC80	CFI	APOE	KLRD1	PPP2R5C	LOC100128420	CXCL13	CAPG	ARHGAP15	CCL5	CD14	CALD1
CD22	CD248	CLDN5	ATP1A1	KLRF1	SKAP1	MAL	DTHD1	CARD9	ARHGAP30	CD19	CD163	CCDC80
CD24	CDH11	CLEC14A	ATP1B1	KLRK1	CD96	PASK	DUSP2	CASP1	ARHGAP9	CD2	CD33	CD200
CD37	CERCAM	COL4A2	ATP5C1	NKG7	GPRIN3	PBXIP1	EOMES	CCR2	ARHGAP9	CD22	CD4	CD248
CD79A	CKAP4	CRIP2	ATP5G1	PRF1	CDC42SE2	SLAMF1	FCRL6	CD163	ARRB2	CD247	CD68	CD34
CD79B	COL12A1	CXorf36	ATP5G2	PTGDR	GRAP2	SPOCK2	GZMA	CD300C	B2M	CD27	CD86	CDH11
CHMP7	COL14A1	CYYR1	ATP6V0E2	SH2D1B	GZMM		GZMB	CD33	BANK1	CD28	CECR1	CDH5
CHTA	COL1A1	DARC	ATP6V1C1		RGS1		GZMH	CD4	BCL11A	CD37	CLEC4A	CFH

TME B cell	TME CAF	TME Endo	TME Mal	TME NK	TME T cells	TME T CD4	TME T CD8	TME Macrophage	TME immune	TME lymphocytes	TME myeloid	TME stroma
CLEC17A	COL1A2	DOCK6	ATP6V1E1		SLA2		GZMK	CD68	BCL11B	CD3D	CLEC7A	CFI
CNR2	COL3A1	DOCK9	ATP6V1G1		LOC100130231		ID2	CD86	BCL2A1	CD3E	CPVL	CLDN5
COL19A1	COL5A1	ECE1	AZGP1		PDCD1		IFNG	CEBPA	BIN2	CD3G	CSF1R	CLEC14A
CR2	COL5A2	ECSCR	BAIAP2		ICOS		IKZF3	CECR1	BIRC3	CD5	CSF2RA	COL12A1
CXCR5	COL6A1	EGFL7	BANCR		EVL		ITGAE	CLEC10A	BLK	CD52	CSF3R	COL14A1
ELK2AP	COL6A2	ELK3	BCAN		TC2N		JAKMIP1	CLEC5A	BLNK	CD6	CSTA	COL15A1
FAIM3	COL6A3	ELTD1	BCAS3		LAG3		KLRC4	CMKLR1	BTK	CD7	CTSB	COL1A1
FAM129C	COL8A1	EMCN	BCHE		CBLB		KLRC4-KLRK1	CPVL	C16orf54	CD79A	CTSS	COL1A2
FCER2	CREB3L1	ENG	BIRC7		LCK		KLRD1	CSF1R	C1orf162	CD79B	CXCL16	COL3A1
FCRL1	CTSK	EPHB4	BZW2		TTC39C		KLRK1	CTSB	C1QA	CD8A	CYBB	COL4A1
FCRL2	CXCL12	ERG	C10orf90		NLR5		MIR155HG	CTSC	C1QB	CD8B	EPST11	COL4A2
FCRL5	CXCL14	ESAM	C11orf31		CD5		NKG7	CTSH	C1QC	CD96	FAM26F	COL5A1
FCRLA	CYBRD1	FGD5	C17orf89		ASB2		PRF1	CXCL10	C3AR1	CLEC2D	FBP1	COL5A2
HLA-DOB	CYP1B1	FLT4	C1orf43		PTPN22		RAB27A	CXCL9	C5AR1	CST7	FCGR1A	COL6A1
HLA-DQA2	DLCK1	GALNT18	C1orf85		RAPGEF6		RUNX3	CXCR2P1	CASP1	CTSW	FCGR1B	COL6A2
HVCN1	DCN	GNG11	C4orf48		TNFRSF9		TARP	CYBB	CBLB	CXCR5	FCGR2A	COL6A3
IGLL1	DPT	GPR116	CA14		SH2D2A		TNFRSF9	CYP2S1	CCL3	DENND2D	FCGR2C	CRIP2
IGLL3P	ECM2	GPR146	CA8		GPR174		TOX	DMXL2	CCL4	DGKA	FCGR3B	CTGF
IGLL5	EFEMP2	HSPG2	CACYBP		ITK			DNAJC5B	CCL4L1	DUSP2	FCN1	CXCL12
IRF8	FAM114A1	HYAL2	CAPN3		PCED1B			EBI3	CCL4L2	EEF1A1	FGL2	CXorf36
KIAA0125	FAT1	ICA1	CBX3		CD247			EPST11	CCL5	EZR	FPR1	CYBRD1
KIAA0226L	FBLN1	ID1	CCDC47		DGKA			F13A1	CCR1	FAIM3	FPR2	CYR61
LOC283663	FBLN2	IL3RA	CCT2		AAK1			FAM26F	CCR6	FAM129C	FPR3	DCHS1
LTB	FBLN5	ITGB4	CCT3		SH2D1A			FBP1	CD14	FCER2	FTH1	DCN
MS4A1	FGF7	KDR	CCT6A		BTN3A2			FCER1G	CD163	FCRL1	FTL	DOCK6
NAPSB	FSTL1	LAMA5	CCT8		PTPN7			FCGR1A	CD19	FCRLA	GOS2	DPT
P2RX5	GPR176	LDB2	CDH19		UBASH3A			FCGR1C	CD2	FYN	GLUL	ECSCR
PAX5	GPX8	LOC100505495	CDH3		ACAP1			FOLR2	CD22	GNLY	GPX1	EFEMP1
PLEKHF2	HSPB6	MALL	CDK2		FASLG			FPR3	CD244	GZMA	HCK	EFEMP2
PNOC	IGFBP6	MMRN1	CELSR2		INPP4B			FUCA1	CD247	GZMB	HK3	EGFL7
POU2AF1	INHBA	MMRN2	CHCHD6		ARAP2			FUOM	CD27	GZMK	HLA-C	EHD2
POU2F2	ISLR	MYCT1	CITED1		CD3G			GATM	CD28	HLA-DOB	HLA-DMA	ELK3
QRSL1	ITGA11	NOS3	CLCN7		IL7R			GM2A	CD300A	HOPX	HLA-DMB	ELN
RALGPS2	ITGBL1	NOTCH4	CLNS1A		1-Sep			GNA15	CD33	HVCN1	HLA-DRB1	ELTD1
SEL1L3	LOX	NPDC1	CMC2		SCML4			GPBAR1	CD37	ID2	HLA-DRB5	EMCN
SNX29P1	LPAR1	PALMD	COA6		IKZF3			GPR34	CD38	IGLL5	IFI30	ENG
SPIB	LRP1	PCDH17	COX7A2		GATA3			GPX1	CD3D	IKZF3	IGSF6	EPAS1
ST6GAL1	LTBP2	PDE2A	CRYL1		PIM2			HLA-DMA	CD3E	IL2RB	IL1RN	EPHB4
STAG3	LUM	PECAM1	CSAG1		NKG7			HLA-DMB	CD3G	IL32	IL411	ERG
STAP1	MAP1A	PLVAP	CSAG2		KLRK1			HLA-DPB2	CD4	IL7R	IL8	ESAM
TCL1A	MEG3	PLXND1	CSAG3		SIT1			HLA-DRB1	CD48	IRF8	IRF5	FAM114A1
TLR10	MFAP4	PODXL	CSAG4		DEF6			HLA-	CD5	ITK	KYNU	FAP

TME B cell	TME CAF	TME Endo	TME Mal	TME NK	TME T cells	TME T CD4	TME T CD8	TME Macrop hage	TME immune	TME lympho cytes	TME myeloid	TME stroma
								DRB5				
VPREB 3	MFAP5	PRCP	CSPG4		GZMH			HLA-DRB6	CD52	JAK3	LAIR1	FBLN1
WDFY 4	MIRIOHG	PTPRB	CYC1		LIME1			HMOX1	CD53	KLRB1	LILRA1	FBLN2
	MMP2	PVRL2	CYP27A1		GZMA			IFI30	CD6	KLRC4	LILRA2	FBLN5
	MRC2	RAMP2	DAAM2		JAK3			IL4I1	CD68	KLRD1	LILRA3	FBN1
	MXRA5	RAMP3	DANCR		DENND2D			IRF5	CD69	KLRK1	LILRA6	FGF7
	MXRA8	RHOJ	DAP3		SEMA4D			KCNMA1	CD7	LAG3	LILRB1	FHL1
	MYL9	R0B04	DCT		SIRPG			KYNU	CD72	LAT	LILRB2	FN1
	NID2	S1PR1	DCXR		CLEC2D			LAIR1	CD74	LCK	LILRB3	FSTL1
	NUPR1	SDPR	DDT		CD8B			LGALS2	CD79A	LOC283663	LILRB4	GNG11
	OLFML2B	SELP	DLGAP1		THEM1S			LILRB1	CD79B	LTB	LRRC25	GPR116
	OLFML3	SHROOM4	DLL3		NLRC3			LILRB4	CD83	LY9	LST1	HSPG2
	PALLD	SLC02A1	DNAH14		ZAP70			LILRB5	CD86	MAP4K1	LYZ	HTRA1
	PCDH18	SMAD1	DNAJA4		IL12RB1			LIPA	CD8A	MS4A1	MAFB	HYAL2
	PCOLCE	STOM	DSCR8		CTSW			MAFB	CD8B	NAPSB	MAN2B1	ID1
	PDGFRA	TEK	DUSP4		MAP4K1			MAN2B1	CD96	NGG7	MFSD1	ID3
	PDGFRB	TGM2	EDNRB		IFNG			MARCO	CDC42SE2	PARP15	MNDA	IFITM3
	PDGFRL	THBD	EIF3C		SPOCK2			MFSD1	CECR1	PAX5	MPEG1	IGFBP4
	PLAC9	TIE1	EIF3D		DTHD1			MPEG1	CELF2	PCED1B-AS1	MPP1	IGFBP7
	PODN	TM4SF1	EIF3E		APOBEC3G			MS4A4A	CIITA	PDCD1	MS4A4A	IL33
	PRRX1	TM4SF18	EIF3H		PSTPIP1			MS4A6A	CLEC2D	PLAC8	MS4A6A	ISLR
	RARRES2	TMEM25B	EIF3L		CD2			MS4A7	CLEC4A	POU2AF1	MS4A7	KDR
	RCN3	TSPAN18	ENO1		PRF1			MSR1	CLEC7A	POU2F2	MSR1	LAMA5
	SDC1	TSPAN7	EN02		BCL11B			MTMR14	COR01A	PRDM1	MXD1	LAMB1
	SDC2	VWF	ENTHD1		PARP8			NAGA	CPVL	PRF1	NAIP	LAMC1
	SEC24D	ZNF385D	ENTPD6		CXCR3			NPC2	CSF1R	PTPN7	NCF2	LDB2
	SERPINF1		ERBB3		CELF2			OAS1	CSF2RA	PTPRCA-P	NINJ1	LHFP
	SFRP2	ESRP1			CCL5			OLR1	CSF3R	PYHIN1	NPC2	LIMA1
	SFRP4	ETV4			IL32			PLA2G7	CST7	RHOH	NPL	LIMS2
	SLIT3	ETV5			PRKCCQ			PPT1	CSTA	RNF213	PILRA	LOX
	SMOC2	EXOSC4			WIPF1			PTPRO	CTSB	RPL13	PPT1	LOXL2
	SPARC	EXTL1			GZMK			RASSF4	CTSC	RPS27	PSAP	LPAR1
	SPOCK1	FAHD2B			ATHL1			RGS10	CTSD	RPS3A	PTAFR	LTBP2
	SPON1	FAM103A1			ZC3HA-V1			RHBDF2	CTSS	RPS6	PYCARD	LUM
	SULF1	FAM178B			CD7			RNASE6	CTSW	RUNX3	RAB20	MAP1B
	SVEP1		FANCL		CD3D			RNASET2	CXCL16	1-Sep	RASSF4	MEG3
	TAGLN		FARP2		RASGRP1			RTN1	CXCR4	SH2D1A	RBM47	MFAP4
	THBS2		FASN		TBC1D10C			SDS	CXCR5	SH2D2A	RGS2	MGP
	THY1		FBX032		TRAF1			SIGLECI	CYBA	SIRPG	RNASE6	MMP2
	TMEM119		FBX07		ARHGEF1			SLAMF8	CYBB	SIT1	RNF130	MXRA8
	TPM1		FDFT1		TARP			SLC15A3	CYFIP2	SKAP1	RNF144B	MYCT1
	TPM2		FKBP4		SPATA13			SLC6A12	CYTH4	SP140	S100A8	MYL9
	VCAN		FMN1		PCED1B-AS1			SLC7A7	CYTIP	SPOCK2	S100A9	NFIB
			FOXO3		RUNX3			SLC02B1	DENND2D	STAP1	SAT1	NID2
			FXYD3		CD6			SPINT2	DGKA	STAT4	SERPINA1	NNMT
			GAPDH		CD8A			TFEC	DOCK2	TARP	SIGLECI	NPDC1
			GAPDHS		NELL2			TIFAB	DOCK8	TIGIT	SIGLEC9	OLFML3
			GAS2L3		TNFAIP3			TNFSF13	DOK2	TMC8	SIRPB1	PALLD
			GAS5		IPCEF1			TPP1	DOK3	TOX	SLAMF8	PCOLCE

TME B cell	TME CAF	TME Endo	TME Mal	TME NK	TME T cells	TME T CD4	TME T CD8	TME Macrophage	TME immune	TME lymphocytes	TME myeloid	TME stroma
			GAS7		CXCR6			TREM2	DUSP2	VPREB3	SLC7A7	PDGFR A
			GDF15		ITGAL			TYMP	EEF1A1	ZAP70	SLCO2B 1	PDGFR B
			GJB1		RHOF			VAMP8	EPST11		SPI1	PDLIM1
			GPATCH4		STAT4			VSIG4	EVI2A		SPINT2	PLAC9
			GPM6B		PVRIG			ZNF385 A	EVI2B		TBXAS1	PLVAP
			GPNCB		TIGIT				EZR		TFEC	PLXND 1
			GPR137B		CD27				FAIM3		THEMIS 2	PODN
			GPR143		ZNF83 1				FAM129C		TLR2	PODXL
			GSTP1		RNF21 3				FAM26F		TNFRSF 10C	PPAP2 A
			GYG2		SYTL3				FAM49B		TNFSF1 3	PPIC
			H2AFZ		CNOT6 L				FAM65B		TPP1	PRCP
			HIST1H2 BD		SPN				FBP1		TREM1	PRRX1
			HIST3H2 A		GPR17 1				FCER1G		VSIG4	PRSS23
			HMG20B		AKNA				FCER2		ZNF385 A	PTPRB
			HMGA1		FYN				FCGR1A			PTRF
			HPGD		RASAL 3				FCGR1B			PXDN
			HPS4		CCL4				FCGR2A			RAMP2
			HPS5		TOX				FCGR2C			RAMP3
			HSP90AA 1		PRDM1				FCGR3A			RARRE S2
			HSP90AB 1		PIP4K2 A				FCGR3B			RCN3
			HSPA9		CTLA4				FCN1			RHOJ
			HSPD1		GZMB				FCRL1			ROBO4
			HSPE1		HNRNP A1P10				FCRLA			S100A1 6
			IGSF11		CD3E				FERMT3			S1PR1
			IGSF3		IKZF1				FGD2			SELM
			IGSF8		JAKMIP 1				FGD3			SERPIN H1
			INPP5F		PYHIN 1				FGL2			SLCO2A 1
			ISYNA1		MIAT				FGR			SMAD1
			KCNJ13		LEPRO TL1				FPR1			SPARC
			LAGE3		OXNAD 1				FPR2			SPARCL 1
			LDHB		RAB27 A				FPR3			SULF1
			LDLRAD3		IL2RB				FTH1			SYNPO
			LEF1-AS1		KLRD1				FTL			TAGLN
			LHFPL3-AS1		PIK3IP 1				FYB			TEK
			LINC004 73						FYN			TFPI
			LINC005 18						G0S2			TGFB1 1
			LINC006 73						GBP5			THBS1
			LOC1001 26784						GLUL			THBS2
			LOC1001 27888						GNA15			THY1
			LOC1001 30370						GNLY			TIE1
			LOC1001 33445						GPR183			TM4SF 1
			LOC1005 05865						GPSM3			TMEM2 04
			LOC1464 81						GPX1			TMEM2 55B
			LOC3403 57						GRB2			TNS1
			LONP2						GZMA			TPM1
			LOXL4						GZMB			TPM2
			LZTS1						GZMK			VCL
			MAGEA1						HAVCR2			VWF
			MAGEA1 2						HCK			

TME B cell	TME CAF	TME Endo	TME Mal	TME NK	TME T cells	TME T CD4	TME T CD8	TME Macrop hage	TME immune	TME lympho cytes	TME meyltoid	TME stroma
			MAGEA2						HCLS1			
			MAGEA2 B						HCST			
			MAGEA3						HK3			
			MAGEA4						HLA-B			
			MAGEA6						HLA-C			
			MAGEC1						HLA-DMA			
			MDH1						HLA-DMB			
			MF12						HLA-DOB			
			MFSD12						HLA-DPA1			
			MIA						HLA-DPB1			
			MIF						HLA-DPB2			
			MITF						HLA-DQA1			
			MLANA						HLA-DQA2			
			MLPH						HLA-DQB1			
			MOK						HLA-DQB2			
			MRPS21						HLA-DRA			
			MRPS25						HLA-DRB1			
			MRPS26						HLA-DRB5			
			MRPS6						HLA-G			
			MSI2						HMHA1			
			MXI1						HOPX			
			MYO10						HVCN1			
			NAV2						ID2			
			NDUFA4						IFI30			
			NDUFB9						IGFLR1			
			NEDD4L						IGLL5			
			NELFCD						IGSF6			
			NHP2						IKZF1			
			NME1						IKZF3			
			NOP58						IL10RA			
			NPM1						IL16			
			NSG1						IL1RN			
			NT5DC3						IL2RB			
			OSTM1						IL2RG			
			PACSN2						IL32			
			PAGE5						IL41			
			PAICS						IL7R			
			PAX3						IL8			
			PEG10						INPP5D			
			PFDN2						IRF5			
			PHB						IRF8			
			PHLDA1						ITGAL			
			PIGY						ITGAM			
			PIR						ITGAX			
			PKNOX2						ITGB2			
			PLEKHB1						ITK			
			PLP1						JAK3			
			PLXNB3						KLRB1			
			PMEL						KLRC4			
			POLR2F						KLRD1			
			PPIL1						KLRK1			
			PPM1H						KYNU			
			PRAME						LAG3			
			PSMB4						LAIR1			
			PUF60						LAPTM5			
			PYGB						LAT			
			PYURF						LAT2			
			QDPR						LCK			
			RAB17						LCP1			
			RAB38						LCP2			
			RAP1GAP						LILRA1			
			RGS20						LILRA2			
			RNF43						LILRA3			
			ROPN1						LILRA6			
			ROPN1B						LILRB1			
			RPL38						LILRB2			
			RSL1D1						LILRB3			
			RTKN						LILRB4			
			S100A1						LIMD2			
			S100B						LITAF			
			SCD						LOC283663			
			SDC3						LRRC25			
			SEC11C						LSP1			
			SEMA3B						LST1			
			SERPINA 3						LTB			
			SERPINE 2						LY86			
			SGCD						LY9			

TME B cell	TME CAF	TME Endo	TME Mal	TME NK	TME T cells	TME T CD4	TME T CD8	TME Macrop hage	TME immune	TME lympho cytes	TME meylold	TME stroma
			SGK1						LYN			
			SH3D21						LYST			
			SHC4						LYZ			
			SLC19A2						M6PR			
			SLC24A5						MAFB			
			SLC25A1 3						MAN2B1			
			SLC25A4						MAP4K1			
			SLC26A2						1-Mar			
			SLC3A2						MFSD1			
			SLC45A2						MNDA			
			SLC5A3						MPEG1			
			SLC6A15						MPP1			
			SLC6A8						MS4A1			
			SLC7A5						MS4A4A			
			SNCA						MS4A6A			
			SNHG16						MS4A7			
			SNHG6						MSR1			
			SNRPC						MXD1			
			SNRPD1						MYO1F			
			SNRPE						NAIP			
			SOD1						NAPSB			
			SORD						NCF1			
			SORT1						NCF1B			
			SOX10						NCF1C			
			SOX6						NCF2			
			SPCS1						NCF4			
			SPRY4						NCKAP1L			
			ST13						NINJ1			
			ST3GAL4						NKG7			
			ST3GAL6						NPC2			
			ST3GAL6 -AS1						NPL			
			ST6GALN AC2						PAG1			
			STIP1						PARP15			
			STK32A						PARVG			
			STMN1						PAX5			
			STX7						PCED1B- AS1			
			STXBP1						PDCD1			
			SYNGR1						PIK3AP1			
			TBC1D7						PIK3R5			
			TBCA						PILRA			
			TEX2						PIM2			
			TFAP2A						PION			
			TFAP2C						PLAC8			
			TMEM14 7						PLCB2			
			TMEM14 B						PLEK			
			TMEM17 7						PLEKHA2			
			TMEM25 1						POU2AF1			
			TMX4						POU2F2			
			TNFRSF2 1						PPT1			
			TOM1L1						PRDM1			
			TOMM20						PRF1			
			TOMM22						PSAP			
			TOMM6						PSMB10			
			TOMM7						PSTPIP1			
			TOP1MT						PTAFR			
			TRIB2						PTK2B			
			TRIM2						PTPN6			
			TRIM63						PTPN7			
			TRIM9						PTPRC			
			TRIML2						PTPRCAP			
			TRMT11 2						PYCARD			
			TSPAN10						PYHIN1			
			TTL4						RAB20			
			TTYH2						RAC2			
			TUBB2B						RASSF4			
			TUBB4A						RBM47			
			TYR						RGS1			
			TYRP1						RGS19			
			UBL3						RGS2			
			UQCRH						RHOF			

TME B cell	TME CAF	TME Endo	TME Mal	TME NK	TME T cells	TME T CD4	TME T CD8	TME Macrophage	TME immune	TME lymphocytes	TME myeloid	TME stroma
			UTP18						RHOG			
			VAT1						RHOH			
			VDAC1						RNASE6			
			VPS72						RNASET2			
			WBSR22						RNF130			
			XAGE1A						RNF144B			
			XAGE1B						RNF213			
			XAGE1C						RPL13			
			XAGE1D						RPS27			
			XAGE1E						RPS3A			
			XYLB						RPS6			
			ZCCHC17						RPS6KA1			
			ZFP106						RUNX3			
			ZNF280B						S100A8			
			ZNF330						S100A9			
									SAMHD1			
									SAMSN1			
									SASH3			
									SAT1			
									SCIMP			
									SELL			
									SELP1G			
									1-Sep			
									SERPINA1			
									SH2D1A			
									SH2D2A			
									SIGLEC1			
									SIGLEC14			
									SIGLEC7			
									SIGLEC9			
									SIRPB1			
									SIRPG			
									SIT1			
									SKAP1			
									SLA			
									SLAMF6			
									SLAMF7			
									SLAMF8			
									SLC7A7			
									SLCO2B1			
									SNX10			
									SP140			
									SPI1			
									SPINT2			
									SPN			
									SPOCK2			
									SRGN			
									STAP1			
									STAT4			
									STK17B			
									STXBP2			
									SYK			
									TAGAP			
									TARP			
									TBC1D10C			
									TBXAS1			
									TFEC			
									THEMIS2			
									TIGIT			
									TLR1			
									TLR2			
									TMC8			
									TNFRSF10C			
									TNFRSF9			
									TNFSF13			
									TOX			
									TPP1			
									TRAF3IP3			
									TREM1			
									TYROBP			
									UCP2			
									VAMP8			
									VAV1			
									VNN2			
									VPREB3			
									VSIG4			
									WIPF1			
									ZAP70			
									ZNF385A			

Table SII. Signatures of Expanded T cells

Up/down regulated in expanded T cells compared to non-expanded T cells.					
up (expanded)	down (expanded)	up (all)		down (all)	
ABCD2	ALOX5AP	ABCD2	NABI	AAK1	MCM5
ADAM28	ANXA1	ADAM28	NCALD	AHNAK	MRPS24
AIM2	ARL4C	AIM2	NEK7	ALOX5AP	MRPS34
AKAP5	C12orf75	AKAP5	NFAT5	ANAPC15	MUTYH
APIAR	CAMK4	AKAP8L	NMB	ANXA1	MXD4
ARID5A	CD200R1	ANAPC4	NOD2	AP5S1	MYH9
ARNT	CD44	APIAR	NOTCH1	APOBEC3G	NDUFB9
ATHL1	CD5	AQR	NSUN2	ARL4C	NEDD8
ATP2C1	COX7A2	ARID5A	OPA1	ASF1B	NFKBIZ
BCOR	DBF4	ARNT	ORMDL3	ATG16L2	NR4A3
CADM1	EMP3	ATHL1	OSBPL3	AURKA	NUP37
CCL3L3	FAM46C	ATM	PAPOLA	BOLA3	PCK2
DGKD	FOSB	ATP2C1	PARP11	BUB1	PCNA
DTHD1	GZMH	ATXN7L1	PCED1B	C12orf75	PDCD5
ETV1	HMGA1	BCOR	PCM1	C3orf38	PDE4B
G3BP1	KIAA0101	C17orf59	PDE7B	CAMK4	PFDN2
HSPA1B	KLRG1	C18orf25	PDGFD	CARD16	PHLDA1
ID3	LIME1	CADM1	PDXDC2P	CCR5	POLR2K
ITM2A	LMNB1	CAV1	PIK3AP1	CCR7	PRDX3
KCNK5	MAB21L3	CCL3L3	PIKFYVE	CD200R1	PRPF4
KLRC2	NR4A3	CD200	PJA2	CD44	PRR5L
KLRC3	PCK2	CDC73	PRKCH	CD5	PXN
KLRC4	PCNA	CEP85L	PROSER1	CD97	RDH11
KLRK1	PDCD5	DDX3Y	PSTPIP1	CKS1B	REXO2
LOC220729	PDE4B	DDX6	PTPN6	COX7A2	RNASEH2C
LONP2	PFDN2	DGKD	PYHIN1	DBF4	RNASEK
LRBA	RDH11	DGKH	RALGDS	DNAJC9	RPUSD3
LYST	S100A10	DNAJA2	RCBTB2	DTYMK	RTCA
NABI	S100A4	DTHD1	RGS2	ECE1	S100A10
NMB	SAMD3	ELF1	RGS4	ECHS1	S100A4
PAPOLA	SPOCK2	ELMO1	RHOB	ELL	S100A6
PDE7B	TKT	ETNK1	RIN3	EMP3	S1PR1
PIK3AP1	TNF	ETV1	RNF19A	F2R	SAMD3
PRKCH	TOB1	FAIM3	RWDD2B	FAM46C	SELL
PROSER1	TOMM7	FBXW11	S100PBP	FAM50B	SLIRP
PTPN6	TUBA1C	FCRL3	SATB1	FOSB	SPOCK2
PYHIN1	UGDH-AS1	FOXL2	SDAD1	FOXP1	STX16
RGS2		G3BP1	SEC24C	GMCL1	TANK
RGS4		GALT	SERINC3	GNPTAB	TKT
S100PBP		GFOD1	SFI1	GPR183	TMEM173
SH2D1B		GNG4	SH2D1B	GTF3C6	TNF
SNAP47		HIF1A	SKIV2L	GYPC	TNFAIP3
SPDYE8P		HIST1H2BG	SLC30A7	GZMA	TNFSF4
SPRY2		HIST2H2BE	SLC7A5P1	GZMH	TOB1
SYVN1		HSPA1B	SLFN11	HAUS4	TOMM5
TACO1		HSPB1	SNAP47	HMGA1	TOMM7
THADA		ID3	SOD1	HMOX2	TPT1
TP53INP1		IL6ST	SPATA13	INSIG1	TUBA1B
TSC22D1		INPP5B	SPDYE8P	ITM2C	TUBA1C
UBA7		INPP5F	SPRY2	KIAA0101	TUBB4B
ZMYM2		IRF8	STT3B	KLF6	TXN
		ITM2A	SYVN1	KLRB1	UBE2Q2P3
		KCNK5	TACO1	KLRG1	UCHL3
		KDM4C	TBC1D23	LEF1	UGDH-AS1
		KLRC2	TBC1D4	LIME1	UQCRB

up/down regulated in expanded T cells		compared to turn-expanded T cells.			
up (expanded)	down (expanded)	up (all)	down (all)	down (fall)	up (fall)
		KLRC3	THADA	LMNB1	VIM
		KLRC4	TNFRSF9	LTB	WBP11
		KLRD1	TNIP1	LY6E	ZNF683
		KLRK1	TP53INP1	MAB21L3	
		LOC100190986	TRAF5		
		LOC220729	TSC22D1		
		LOC374443	TTI2		
		LONP2	TTY15		
		LRBA	TXNDC11		
		LRRC8D	UBA7		
		LSM14A	VMA21		
		LY9	VPRBP		
		LYST	WWC3		
		MBP	ZBED5		
		MED13	ZMYM2		
		MGA	ZMYM5		
		MGEA5	ZNF384		
		MS4A1	ZNF468		
		MST4	ZNF83		
		NAA16			

Example 2 - Immunotherapy Resistance Signature from 26 Melanoma Tumors

[0375] Applicants performed single-cell RNA-seq on 26 melanoma tumors (12 treatment naive, 14 post immunotherapy) (Figure 17). Applicants discovered that immunotherapy leads to profound transcriptional alterations in both the malignant and immune cells. Applicants also discovered that these transcriptional programs are associated the response to immunotherapy by analyzing prior data sets (Hugo et al. Cell. 2016 Mar 24;165(1):35-44. doi: 10.1016/j.cell.2016.02.065; and Riaz et al. Nature Genetics 48, 1327-1329 (2016) doi:10.1038/ng.3677). Applicants also discovered that these transcriptional programs are associated Intra-tumor: heterogeneity, location, and antigen presentation. Applicants explored and characterized the effect immunotherapies have on different cell types within the tumor (i.e., Malignant cells, CD8/CD4 T-cells, B cells and Macrophages). The data includes twenty six samples (14 post immunotherapy, 8 anti-CTLA4 & anti-PD-1, 2 anti-PDI(Nivolumab), 4 anti-CTLA4 (Ipilimumab), and 12 treatment naive (Figure 17).

[0376] Applicants performed principal component analysis on the expression data. The second Principle Component (PC) separates between immunotherapy resistant and untreated tumors (Figure 18). Applicants discovered that treatment is the main source of variation in malignant cells between tumors, reflected by the difference in the score of malignant cells from treatment naive and resistant tumors on the second principle component.

[0377] Applicants analyzed the transcriptome of the malignant cells to identify cell states that are associated with immunotherapy. To this end, Applicants identified differentially

expressed genes and derived two post-immunotherapy (PIT) modules, consisting of genes that are up (PIT-up) or down (PIT-down) regulated in PIT malignant cells compared to the untreated ones. In comparison to the treatment naive tumors, all the PIT tumors overexpress the PIT-up module and underexpress the PIT-down module, such that there is a spectrum of expression levels also within each patient group and within the malignant cell population of a single tumor (**Figure 19**). The genes within each module are co-expressed, while the two modules are anti-correlated with each other, not only across tumors but also within the malignant cell population of a single tumor. Additionally, the two modules have heavy and opposite weights in the first principle components of the malignant single-cell expression profiles, indicating that immunotherapy is one of the main sources of inter-tumor heterogeneity in the data.

[0378] Applicants applied down sampling and cross-validation to confirm that the PIT modules are robust and generalizable (**Figure 20**). More specifically, Applicants repeatedly identified the signatures without accounting for the data of one of the tumors, and showed that the modules were similar to those derived with the full dataset. Furthermore, the modules that were derived based on a *training* data could still correctly classify the *test* tumor as either PIT or treatment naive. The signature is very robust. If Applicants leave out all the malignant cells from a given tumor, recalculate it and then assign the cells, Applicants make only one "error" when guessing if the tumor is treatment naive or ITR. This one tumor has a particularly high T cell infiltration. These results testify that, while more data and samples will enable us to refine these modules, the resulting modules are not likely to change substantially. The signature is also supported by the mutual exclusive expression of the up and down genes across malignant cells, and their anti-correlation in TCGA (**Figure 21**).

[0379] Gene set enrichment analysis of the PIT programs highlights well-established immune-evasion mechanisms as the down-regulation of MHC class I antigen presentation machinery and interferon gamma signaling in PIT cells (**Table 1**). Cells with less MHC-I expression are more resistant to immunotherapy (**Figure 22**). Additionally, it has been recently shown that melanoma tumors that are resistant to ipilimumab therapy contain genomic defects in IFN-gamma pathway genes, and that the knockdown of IFNGR1 promotes tumor growth and reduces mouse survival in response to anti-CTLA-4 therapy. The PIT-down program is also enriched with genes involved in coagulation, IL2-STAT5 signaling, TNFa signaling via NFkB, hypoxia, and apoptosis. The PIT-up program is tightly linked to MYC. It is enriched with MYC targets and according to the connectivity map data

(c-map) - MYC knockout alone is able to repress the expression of the entire PIT-up signature. Supporting these findings, it has been shown that MYC modulates immune regulatory molecules, such that its inactivation in mouse tumors enhances the antitumor immune response. Interestingly, Applicants find that metallothioneins (MTs) are overrepresented in the PIT-down program, and show that their expression alone separates between the PIT and untreated samples (**Figure 23**). MTs are a family of metal-binding proteins that function as immune modulators and zinc regulators. The secretion of MTs to the extracellular matrix can suppress T-cells and promote T-cell chemotaxis. Interestingly, it has been recently shown that MT2A is a key regulator of CD8 T-cells, such that its inhibition promotes T-cell functionality in the immunosuppressive tumor microenvironment (Singer et al. Cell. 2016 Sep 8;166(6): 1500-1511). The underexpression of MTs in the malignant cells of post-immunotherapy tumors could potentially be linked to the role of MT2A in T-cells and to the abundance of zinc in the tumor microenvironment.

Table 1. Functional classification of PIT module genes.

Pathway	Genes
MHC class I antigen presentation machinery	<i>CTSB, HLA-A, HLA-C, HLA-E, HLA-F, PSME1, TAP1, TAPBP</i>
Coagulation	<i>ANXA1, CD9, CFB, CTSB, FN1, ITGB3, LAMP2, PROS1, PRSS23, SERPINE1, SPARC, TF</i>
TNF α signaling via NF κ B	<i>ATF3, BCL6, BIRC3, CD44, EGR1, GADD45B, GEM, JUNB, KLF4, KLF6, NR4A1, PDE4B, SERPINE1, TAP1, TNC</i>
IL2/STAT5 signaling	<i>AHNAK, AHR, CCND3, CD44, EMP1, GADD45B, IFITM3, IGF1R, ITGA6, KLF6, NFKBIZ, PRNP, RNH1</i>
Metallothioneins	<i>MT1E, MT1F, MT1G, MT1M, MT1X, MT2A</i>
MYC targets	<i>EIF4A1, FBL, HDAC2, ILF2, NCBP1, NOLC1, PABPC1, PRDX3, RPS3, RUVBL2, SRSF7</i>

[0380] Applicants identified an immunotherapy resistance signature by identifying genes that were up and down regulated in immunotherapy treated subjects as compared to untreated subjects (**Table 2, 3**). The signature was compared to clinical data of subjects that were complete responders to immunotherapy, partial responders and non-responders. The data was also compared to subjects with high survival and low survival.

Table 2. Analysis of all gene expression data and clinical data

	clinic.R.in ore	clinic.R. less	sc.All	sc.Old	sc.New	sc.Bul k	sc.Q.gene	tcga.Increased. risk	tcga.Increased.risk .beyond.T.cells
ANXA1	7.58E-02	8.19E-01	202.40	-2.44	-200.00	-3.02	FALSE	-2.64	-1.37
EMP1	4.92E-01	8.96E-02	189.84	-20.93	-75.82	-2.58	FALSE	0.69	0.60
TSC22D3	4.26E-01	4.63E-01	175.14	-13.19	-82.60	-2.43	FALSE	-1.52	-0.32
MT2A	4.06E-02	7.81E-01	174.76	-18.16	-67.52	-4.41	FALSE	-2.83	-1.80
CTSB	4.03E-01	5.87E-01	165.96	-25.70	-112.90	-2.50	FALSE	-0.44	0.56
TM4SF1	1.76E-01	7.74E-01	164.10	5.621836 397	165.507 1875	-1.14	FALSE	0.45	0.32
CDH19	4.35E-02	4.15E-01	155.59	-3.79	-42.42	-1.53	FALSE	-2.24	-1.86
MIA	3.62E-01	4.96E-01	152.98	-4.22	-60.91	-1.53	FALSE	-1.60	-0.91
SERPINE2	2.27E-02	1.70E-01	151.17	-31.78	-46.03	-1.68	FALSE	-3.66	-3.12
SERPINA3	1.43E-01	4.64E-01	148.25	13.63	-229.59	-1.37	FALSE	-2.64	-2.04
S100A6	2.91E-01	2.01E-01	128.57	-12.30	-49.34	-2.42	FALSE	-0.40	-0.47
ITGA3	3.35E-02	9.20E-01	123.57	1.882158 19	83.8067 0184	-0.97	FALSE	-0.51	-0.49
SLC5A3	4.64E-01	4.71E-01	119.83	1.06	-96.80	-1.71	FALSE	-6.19	-4.10
A2M	3.01E-02	4.38E-01	118.06	15.73720 409	30.2916 1959	-1.07	FALSE	-2.81	-1.47
MF12	3.67E-01	4.22E-01	117.29	-3.06	-44.01	-1.41	FALSE	0.46	0.38
CSPG4	7.50E-01	2.24E-01	112.90	-5.56	-30.13	-1.87	FALSE	-1.60	-1.41
AHNAK	5.70E-02	7.09E-01	112.83	-12.69	-13.16	-2.03	FALSE	-0.45	-0.38
APOC2	6.76E-01	1.57E-01	111.01	4.108007 818	92.3401 2794	-0.52	FALSE	-0.55	0.51
ITGB3	1.66E-01	3.79E-01	110.25	0.79	-109.99	-1.75	FALSE	-2.25	-1.42
NNMT	4.47E-01	6.63E-01	110.12	-1.62	-122.65	-2.51	FALSE	-2.28	-0.87
ATP1A1	2.34E-01	4.92E-01	107.58	-19.25	-26.63	-1.40	FALSE	0.52	0.30
SEMA3B	8.03E-02	9.69E-01	106.75	2.022007 432	74.1899 8319	-1.06	FALSE	-1.65	-1.08
CD59	3.34E-02	7.57E-01	101.92	-16.59	-40.13	-1.86	FALSE	-1.71	-0.90
PERP	1.03E-01	9.58E-01	-99.65	2.618926 27	123.085 1115	-1.13	FALSE	0.78	-0.77
EGR1	1.98E-01	8.54E-01	-96.70	-1.43	-25.74	-1.30	FALSE	-0.80	0.30
LGALS3	2.66E-01	6.41E-01	-96.06	57.79606 403	1.17499 1366	-1.19	FALSE	-0.42	-0.50
SLC26A2	1.86E-01	2.65E-01	-95.69	0.615403 346	34.7461 3485	-0.92	FALSE	-3.62	-2.73
CRYAB	2.26E-02	5.72E-01	-94.74	0.85	-139.66	-1.89	FALSE	-0.84	-0.63
HLA-F	4.70E-02	9.62E-01	-94.42	-12.84	-23.07	-1.82	FALSE	-4.49	-1.03
MT1E	1.78E-01	5.89E-01	-92.61	-14.66	-27.25	-3.00	FALSE	-1.20	-1.19
KCNN4	1.88E-01	7.63E-01	-92.09	-1.36	-108.90	-2.56	FALSE	-4.61	-2.92
CST3	1.87E-01	6.36E-01	-90.32	-3.11	-43.51	-2.19	FALSE	-1.31	0.32

	clinic.R.in ore	clinic.R. less	sc.All	sc.Old	sc.New	sc.Bul k	sc.Q.gene	tcga.Increased. risk	tcga.Increased.risk .beyond.T.cells
CD9	6.23E-01	4.58E-01	-89.32	-9.57	-19.34	-2.77	FALSE	0.35	-0.79
TNC	3.59E-01	6.45E-01	-87.60	-6.21	-88.45	-1.78	FALSE	-2.72	-1.10
SGCE	2.19E-02	3.21E-01	-87.28	0.302176 627	62.8095 8661	-1.02	FALSE	-3.12	-1.69
NFKBIZ	2.32E-02	9.71E-01	-86.67	-4.35	-30.64	-2.89	FALSE	-2.40	-1.85
PROS1	2.16E-02	4.37E-01	-86.35	-0.52	-28.78	-1.72	FALSE	-0.40	-0.71
CAV1	6.55E-02	3.13E-01	-85.42	-24.08	-6.13	-1.34	FALSE	-1.43	-0.72
MFGE8	2.64E-01	3.77E-01	-84.81	12.26983 949	19.3346 1436	-1.07	FALSE	-1.84	-1.29
IGFBP7	7.97E-01	9.60E-02	-83.96	-22.46	-27.89	-1.37	FALSE	-0.37	0.88
SLC39A14	1.73E-01	8.74E-01	-83.65	0.52	-37.30	-1.97	FALSE	-0.52	-0.67
CD151	2.53E-01	3.98E-01	-83.63	-2.11	-33.44	-1.90	FALSE	-0.56	-0.63
SCCPDH	5.51E-01	3.85E-01	-83.37	-3.18	-20.08	-1.68	FALSE	-1.26	-1.07
MATN2	6.66E-01	2.81E-01	-82.90	0.523529 704	70.3656 0095	-1.17	FALSE	-0.34	0.68
DUSP4	2.30E-01	3.73E-01	-82.27	6.193791 11	19.3740 1872	-1.18	FALSE	0.58	0.60
APOD	3.39E-01	5.42E-01	-81.89	-9.70	-15.76	-1.58	FALSE	-1.62	-1.49
GAA	1.72E-01	6.87E-01	-81.55	-2.56	-27.32	-1.50	FALSE	-1.23	-0.56
CD58	1.48E-01	5.02E-01	-81.12	-1.03	-40.89	-2.52	FALSE	-2.40	-3.24
HLA-E	5.00E-02	9.47E-01	-79.92	-25.19	-23.50	-1.86	FALSE	-3.54	0.48
TIMP3	4.17E-01	8.28E-02	-79.58	6.278620 205	2.72829 0317	-1.11	FALSE	-1.13	-1.19
NR4A1	1.22E-01	6.52E-01	-79.47	-14.82	-8.42	-1.37	FALSE	0.32	-0.51
FXYD3	2.31E-02	8.64E-01	-78.83	-3.88	-17.90	-1.81	FALSE	-0.47	-0.96
TAPBP	9.56E-02	9.33E-01	-78.23	-9.90	-25.67	-1.40	FALSE	-3.06	0.45
CTSD	2.10E-01	4.50E-01	-76.29	-35.68	-12.15	-1.73	FALSE	0.51	1.21
NSG1	2.25E-01	5.26E-02	-75.54	6.885019 5	45.2569 0934	-0.59	FALSE	NA	NA
DCBLD2	1.51E-01	3.97E-01	-75.17	-2.70	-30.36	-2.50	FALSE	-0.93	-1.69
GBP2	3.33E-02	4.65E-01	-74.58	-6.60	-112.34	-3.42	FALSE	-9.49	-2.53
FAM3C	2.17E-02	3.24E-01	-73.79	1.099557 442	34.2099 212	-0.80	FALSE	-4.22	-2.95
CALU	7.70E-01	2.45E-01	-73.21	-2.96	-22.58	-1.44	FALSE	0.34	-0.56
DDR1	1.30E-02	9.47E-01	-72.94	1.320302 264	41.9364 9931	-0.93	FALSE	-0.66	-1.98
TIMP1	2.44E-01	1.95E-01	-72.66	0.832732 502	44.3146 5375	-1.27	FALSE	-2.53	-0.80
LRPAP1	3.26E-01	5.82E-01	-72.03	8.741825 947	33.2840 9269	-1.12	FALSE	0.55	0.62
CD44	1.20E-01	7.83E-01	-71.20	-42.03	-7.56	-1.31	FALSE	-1.20	-0.70

	clinic.R.in ore	clinic.R. less	sc.All	sc.Old	sc.New	sc.Bul k	sc.Q.gene	tcga.Increased. risk	tcga.Increased.risk .beyond.T.cells
GSN	1.83E-01	9.76E-02	-71.17	7.066367 901	8.37910 9684	-1.25	FALSE	-0.48	-0.40
PTRF	1.20E-01	1.26E-01	-70.87	-11.99	-21.89	-2.19	FALSE	-0.81	-0.88
CAPG	3.42E-01	4.17E-01	-70.60	17.12110 776	3.79280 4113	-1.21	FALSE	-0.42	0.69
CD47	1.14E-01	8.55E-01	-68.77	-5.84	-21.44	-2.75	FALSE	-5.65	-3.19
CCND3	1.48E-01	7.90E-01	-68.60	-0.85	-62.30	-2.43	FALSE	-0.65	0.43
HLA-C	1.63E-01	4.28E-01	-68.47	-22.92	-13.18	-1.33	FALSE	-4.97	-1.10
CARD16	3.15E-02	9.14E-01	-68.09	-1.20	-51.51	-1.48	FALSE	-0.65	0.50
DUSP6	3.52E-01	3.46E-01	-67.35	1.443530 586	32.1707 1544	-0.53	FALSE	-4.33	-2.45
IL1RAP	6.76E-03	4.53E-01	-66.82	-2.25	-24.21	-3.64	FALSE	-1.77	-1.51
FGFR1	7.25E-02	1.31E-01	-66.47	9.950506 533	57.9295 1091	-1.14	FALSE	-0.49	-0.62
TRIML2	8.90E-01	1.20E-01	-66.24	21.84557 542	68.4092 2705	-0.49	FALSE	-1.47	-1.52
ZBTB38	7.00E-01	3.77E-01	-65.84	-6.25	-8.44	-1.64	FALSE	-3.18	-3.11
PRSS23	6.42E-01	8.53E-02	-63.62	-0.34	-35.59	-1.53	FALSE	-0.54	0.37
S100B	4.64E-01	6.74E-01	-63.21	18.39689 161	0.98953 4032	-1.08	FALSE	-1.72	-0.73
PLP2	1.29E-02	7.48E-01	-63.01	-3.16	-7.46	-1.46	FALSE	0.34	-0.80
LAMP2	2.64E-01	6.13E-01	-62.96	-5.73	-13.68	-1.48	FALSE	-1.19	-1.06
FCGR2A	8.31E-04	8.38E-01	-62.40	0.623470 411	28.6430 2633	-0.93	FALSE	-6.97	-2.82
LGALS1	7.24E-02	1.72E-01	-61.40	-12.41	-1.43	-1.38	FALSE	0.77	1.02
NPC1	9.96E-02	4.70E-01	-60.93	2.330822 107	12.2470 8172	-0.83	FALSE	0.37	-0.31
UBC	6.96E-01	4.80E-01	-60.76	-6.83	-41.63	-1.69	FALSE	-1.71	-0.61
TNFRSF12 A	8.03E-02	7.99E-01	-60.31	1.73	-37.68	-1.53	FALSE	-0.63	-0.66
SPON2	1.56E-01	2.67E-01	-59.94	0.444813 435	54.2854 9635	-0.87	FALSE	-0.62	0.47
EEA1	4.38E-01	4.73E-01	-59.50	0.680184 335	13.2340 1918	-1.02	FALSE	-1.33	-2.70
CD63	7.00E-01	2.67E-01	-59.49	14.73233 445	14.2926 3209	-1.30	FALSE	1.10	0.65
SGK1	4.34E-01	3.83E-01	-59.42	2.775881 65	13.5729 112	-0.52	FALSE	0.63	0.68
HPCAL1	1.03E-01	6.53E-02	-59.22	-8.70	-10.48	-1.83	FALSE	-0.69	-0.91
HLA-B	5.22E-02	8.84E-01	-58.69	16.77311 58	7.71200 708	-1.18	FALSE	-5.85	-0.79
SERPINA1	5.48E-01	4.51E-01	-58.50	4.670124 42	61.1315 4453	-0.74	FALSE	-2.78	0.47
JUN	3.03E-01	7.09E-01	-58.42	1.182777 495	17.4316 4065	-1.18	FALSE	-0.89	0.32

	clinic.R.in ore	clinic.R. less	sc.All	sc.Old	sc.New	sc.Bul k	sc.Q.gene	tcga.Increased. risk	tcga.Increased.risk .beyond.T.cells
HLA-A	4.98E-02	9.30E-01	-58.18	-26.50	-18.12	-1.46	FALSE	-2.09	-0.34
RAMP1	5.43E-01	2.02E-01	-58.03	-11.93	-63.50	-1.60	FALSE	0.45	0.53
TPP1	7.54E-02	8.18E-01	-57.91	18.16810 565	4.42680 0522	-1.02	FALSE	-0.70	-0.41
FYB	1.49E-01	7.19E-01	-57.13	2.867192 419	45.7344 5912	-0.52	FALSE	-4.33	-0.75
RDH5	1.02E-01	8.47E-01	-56.99	1.683618 144	39.4842 3368	-0.59	FALSE	-3.18	-2.30
SDC3	1.84E-01	4.92E-01	-56.80	2.227320 442	7.93031 9849	-0.90	FALSE	-1.46	-0.67
PRKCDBP	2.03E-01	3.35E-01	-56.58	-3.45	-25.88	-2.48	FALSE	-0.69	-0.46
CSGALNAC T1	3.14E-01	1.30E-01	-56.46	1.005860 494	21.1023 4746	-1.19	FALSE	-5.34	-3.85
HLA-H	2.38E-01	7.55E-01	-56.36	26.85223 45	2.69165 9575	-0.99	FALSE	-2.77	-0.44
CLEC2B	9.68E-04	1.64E-01	-55.69	-3.93	-40.47	-1.87	FALSE	-8.63	-4.19
ATP1B1	4.75E-01	9.93E-02	-55.53	3.790248 535	73.6652 0645	-0.74	FALSE	-3.09	-1.56
DAG1	2.86E-01	6.40E-01	-55.41	-3.15	-5.62	-1.66	FALSE	-0.71	-0.52
NFKBIA	5.25E-03	5.77E-01	-55.35	7.315272 323	17.0587 2829	-1.05	FALSE	-4.18	-0.54
SRPX	3.36E-01	2.51E-01	-55.12	-7.37	-3.79	-2.09	FALSE	-0.80	-1.57
CASP1	6.92E-02	8.19E-01	-55.00	1.031280 571	66.1978 381	-0.96	FALSE	-1.32	0.38
DPYSL2	1.23E-02	7.32E-01	-54.92	1.056511 462	99.2291 6498	-1.14	FALSE	-0.77	0.34
S100A1	1.82E-01	1.09E-01	-54.68	14.25397 572	14.4242 0921	-0.63	FALSE	-0.61	-0.78
FLJ43663	Inf	Inf	-54.67	6.490292 736	10.5791 0257	-1.20	FALSE	-4.45	-4.16
UPP1	1.21E-01	7.67E-01	-54.34	7.451372 117	2.52827 6372	-1.13	FALSE	1.67	1.17
APOE	3.46E-01	1.80E-01	-54.04	4.357609 216	10.0650 0479	0.32	FALSE	0.31	1.11
LPL	1.87E-01	1.61E-01	-54.00	-6.59	-51.84	-2.19	FALSE	-0.45	-0.45
KLF4	3.63E-02	9.02E-01	-53.99	-0.31	-23.01	-2.34	FALSE	-0.55	-0.36
SLC20A1	3.66E-01	3.38E-01	-53.68	0.47	-18.37	-2.06	FALSE	-2.41	-1.61
LGALS3BP	1.92E-01	8.74E-01	-53.62	-12.98	-5.64	-1.68	FALSE	-0.61	0.43
LINC00116	4.39E-01	1.53E-01	-53.33	0.38	-29.09	-1.90	FALSE	NA	NA
RPS4Y1	8.64E-02	9.11E-01	-53.11	64.09755 214	3.82061 851	-0.66	FALSE	1.34	1.23
SQRDL	9.82E-02	8.26E-01	-52.38	-5.25	-38.28	-3.08	FALSE	-3.94	-1.26
ITM2B	2.72E-02	7.97E-01	-52.21	-10.23	-13.51	-1.63	FALSE	-5.41	-2.59
TMX4	4.28E-01	2.58E-01	-52.20	-1.16	-13.17	-1.39	FALSE	-2.83	-1.33

	clinic.R.in ore	clinic.R. less	sc.All	sc.Old	sc.New	sc.Bul k	sc.Q.gene	tcga.Increased. risk	tcga.Increased.risk .beyond.T.cells
IL6ST	1.01E-02	3.26E-01	-52.05	-2.89	-6.37	-1.61	FALSE	-1.92	-0.83
BIRC3	1.72E-01	7.32E-01	-51.42	-7.23	-41.19	-4.32	FALSE	-7.28	-2.50
ANXA2	4.45E-01	5.66E-01	-51.27	-12.18	-8.25	-2.15	FALSE	0.78	0.68
ZBTB20	2.19E-01	7.01E-01	-51.13	-1.09	-25.68	-1.43	FALSE	-0.42	0.31
GRN	9.79E-02	5.69E-01	-51.04	3.334799 04	10.5850 0961	-0.92	FALSE	0.51	0.95
SERPINE1	2.26E-01	8.94E-02	-50.78	0.45	-45.37	-2.08	FALSE	-1.78	-0.47
MT1X	9.41E-02	7.92E-01	-50.16	-2.90	-20.02	-1.51	FALSE	-1.45	-2.13
FCGR2C	6.04E-04	3.75E-01	-50.04	6.560207 399	28.2343 2948	-0.90	FALSE	-5.71	-2.00
ACSL3	4.57E-01	3.37E-01	-49.94	3.939970 091	4.77535 2737	-0.49	FALSE	-0.93	-1.32
IFI27	2.77E-01	4.25E-01	-49.91	24.12491 388	7.19393 3103	-1.12	FALSE	-3.69	-1.74
AEBP1	7.23E-03	7.36E-01	-49.86	0.652064 041	9.79151 9511	-1.24	FALSE	-0.31	0.33
TIPARP	6.67E-02	5.81E-01	-49.73	1.699010 303	20.1284 8456	-1.30	FALSE	-2.25	-1.20
VAMP8	7.89E-02	4.82E-01	-49.73	5.340727 074	25.9515 3555	-0.78	FALSE	-0.77	1.19
DST	3.55E-01	6.19E-01	-48.89	-2.44	-3.35	-1.59	FALSE	0.47	0.55
IFI35	1.88E-01	7.91E-01	-48.67	-7.02	-6.98	-2.31	FALSE	-3.05	-1.00
ITGB1	3.60E-01	2.39E-01	-48.52	-3.58	-9.62	-2.66	FALSE	-1.85	-1.87
BCL6	8.45E-02	8.06E-01	-48.50	-4.89	-22.66	-3.13	FALSE	-4.25	-1.89
ERBB3	1.90E-01	6.37E-01	-48.36	9.731344 26	0.43907 8261	-0.73	FALSE	0.53	0.33
ZMYM6NB	6.10E-01	1.14E-01	-47.89	-1.77	-21.83	-1.45	FALSE	NA	NA
CLIC4	1.22E-01	3.15E-01	-47.81	-1.16	-17.42	-1.41	FALSE	-4.55	-3.87
FOS	4.13E-01	6.43E-01	-47.57	6.386092 681	1.04213 9346	-0.73	FALSE	-0.87	-0.36
IGF1R	3.62E-01	4.41E-01	-47.19	-1.54	-23.75	-1.37	FALSE	-0.36	-0.58
PLEKHB1	2.57E-02	3.38E-01	-46.81	6.095867 912	42.4320 8655	-0.54	FALSE	-1.60	-1.68
GOLGB1	5.56E-01	4.63E-01	-46.38	4.661054 566	8.36828 4482	-1.24	FALSE	-2.84	-2.24
PSAP	1.12E-01	7.72E-01	-45.94	17.73630 528	0.39637 2679	-1.07	FALSE	-0.67	0.69
RNF145	4.06E-02	6.25E-01	-45.93	-4.00	-9.25	-2.29	FALSE	-2.59	-1.12
CTSL1	5.49E-01	2.91E-01	-45.88	13.12164 871	18.6571 7439	-0.84	FALSE	0.67	0.86
SYNGR2	2.82E-03	7.59E-01	-45.78	5.091681 04	10.4819 0321	-0.94	FALSE	-1.25	0.81
HTATIP2	8.60E-01	1.13E-01	-45.69	-2.00	-19.85	-2.43	FALSE	-1.31	-1.68

	clinic.R.in ore	clinic.R. less	sc.All	sc.Old	sc.New	sc.Bul k	sc.Q.gene	tcga.Increased. risk	tcga.Increased.risk .beyond.T.cells
KLF6	2.33E-02	6.52E-01	-45.62	-18.85	1.21	-1.57	FALSE	-0.45	-0.44
LOC54147 1	Inf	Inf	-45.38	2.644136 674	11.1496 4202	-1.23	FALSE	1.16	1.08
SAT1	2.24E-01	3.62E-01	-44.81	30.71664 031	1.26808 839	-0.55	FALSE	-0.81	0.50
FBX032	1.79E-01	2.88E-01	-44.73	0.322762 583	6.16164 8524	-0.32	FALSE	0.70	0.40
S100A10	5.31E-03	6.74E-01	-44.66	-22.95	0.42	-2.01	FALSE	0.38	0.48
ATF3	4.52E-01	3.92E-01	-44.63	1.63	-38.08	-2.50	FALSE	-1.55	0.34
SCARB2	8.77E-02	6.12E-01	-44.43	2.576905 156	2.01525 226	-1.16	FALSE	-1.06	-0.77
GPNUMB	1.82E-01	7.59E-01	-44.30	27.37333 779	0.67286 7612	-0.74	FALSE	0.44	0.73
FCRLA	7.03E-03	9.79E-01	-44.01	-10.35	-13.12	-1.87	FALSE	-0.40	0.40
CLU	6.77E-01	4.88E-01	-43.85	2.663183 144	40.0619 6504	-0.63	FALSE	-1.13	0.40
ADM	6.89E-01	6.95E-02	-43.84	4.543551 718	28.9692 9856	-0.76	FALSE	0.30	0.30
TF	5.05E-01	4.79E-01	-43.65	-8.72	-51.07	-1.33	FALSE	-1.03	-0.56
CAST	2.14E-02	8.85E-01	-43.40	-2.23	-9.80	-1.38	FALSE	-1.51	-1.09
C10orf54	2.37E-01	5.08E-01	-43.23	1.005464 269	47.2918 2888	-1.01	FALSE	-3.61	0.82
ITGA6	4.78E-01	4.15E-01	-43.18	-3.18	-12.52	-2.60	FALSE	-3.43	-1.94
PSMB9	1.02E-01	7.61E-01	-43.08	-9.75	-11.68	-1.87	FALSE	-6.40	-1.66
BACE2	3.23E-01	6.02E-01	-43.02	1.544458 411	3.81810 5651	-0.83	FALSE	2.35	1.69
GADD45B	4.04E-01	1.97E-01	-42.59	-1.28	-35.87	-1.53	FALSE	-1.56	0.60
IFI27L2	4.94E-01	1.42E-01	-42.51	-11.43	-4.73	-1.31	FALSE	-0.54	-0.68
FADS3	3.81E-01	5.31E-01	-42.38	2.307281 418	10.4877 9629	-0.84	FALSE	-0.73	-0.64
GPR155	4.45E-01	3.44E-01	-42.36	1.727392 739	9.73076 0161	-0.67	FALSE	-2.99	-1.44
IFNGR2	2.69E-02	5.64E-01	-42.34	2.678730 729	5.82450 1595	-1.16	FALSE	-2.71	-1.79
NEAT1	1.24E-03	9.34E-01	-42.32	3.957711 442	4.81657 5504	-0.65	FALSE	-2.07	-2.38
ARL6IP5	9.95E-02	8.05E-01	-42.03	5.061500 123	6.02687 7076	-1.20	FALSE	-4.08	-2.21
GJB1	6.66E-02	6.60E-01	-42.02	3.948684 44	3.63986 5415	-0.32	FALSE	-0.31	0.38
ACSL4	6.24E-01	3.88E-01	-41.97	-1.75	-14.86	-2.59	FALSE	-6.05	-3.62
ATP1B3	2.92E-02	6.43E-01	-41.66	-2.82	-21.79	-3.00	FALSE	-0.52	-0.79
ECM1	1.35E-01	5.94E-01	-41.65	-2.62	-6.36	-1.47	FALSE	2.45	1.30
APLP2	4.94E-01	1.91E-01	-41.49	1.557538 98	32.7925	-0.99	FALSE	-1.94	-2.11

	clinic.R.in ore	clinic.R. less	sc.All	sc.Old	sc.New	sc.Bul k	sc.Q.gene	tcga.Increased. risk	tcga.Increased.risk .beyond.T.cells
					2137				
ANGPTL4	4.14E-01	2.31E-01	-41.48	-0.66	-57.88	-1.62	FALSE	-0.39	0.38
GPR56	7.32E-03	6.52E-01	-41.45	18.86181027	6.113225588	0.32	FALSE	1.27	1.10
SYPL1	2.59E-01	7.74E-01	-41.38	2.204809487	11.39626417	-1.08	FALSE	-1.57	-3.14
FNDC3B	2.11E-01	3.32E-01	-41.27	-1.78	-19.28	-1.86	FALSE	-4.21	-2.77
CYBRD1	3.43E-01	9.88E-02	-41.01	-3.84	-6.47	-1.37	FALSE	-1.60	-1.51
CTSA	1.55E-01	5.79E-01	-40.89	-3.17	-15.31	-1.86	FALSE	0.49	0.68
MCL1	4.84E-01	4.49E-01	-40.82	0.665221316	21.44924463	-1.22	FALSE	-4.37	-1.75
LEF1	1.84E-01	7.45E-01	-40.69	0.409062265	22.95759126	-0.36	FALSE	-0.88	-0.46
BBX	2.43E-01	5.39E-01	-40.61	-0.61	-21.43	-1.67	FALSE	-3.83	-2.98
FKBP5	5.46E-01	2.10E-01	-40.55	9.020160799	25.90285892	-1.24	FALSE	-1.88	-0.53
FAM114A1	7.76E-01	2.18E-01	-40.47	-3.16	-18.85	-1.90	FALSE	-0.54	-0.53
LTBP3	1.66E-01	4.22E-01	-40.27	3.20667713	16.87434626	-0.99	FALSE	-2.15	-2.16
HSPA1A	9.37E-01	1.13E-01	-40.16	9.037838299	41.23649886	-0.31	FALSE	1.23	1.55
EPHX2	1.42E-01	2.31E-01	-40.08	1.222892988	48.82245871	-1.07	FALSE	0.77	0.95
ITGA7	6.60E-01	3.30E-01	-40.03	15.86332961	39.83592494	0.37	FALSE	0.61	-0.61
AGA	2.23E-01	7.32E-01	-39.91	0.536274519	9.136581859	-0.68	FALSE	-1.38	-1.08
LYRM9	7.78E-03	8.61E-01	-39.80	1.964812062	24.63102517	-0.69	FALSE	NA	NA
CREG1	2.30E-01	6.57E-01	-39.71	-1.46	-13.57	-1.52	FALSE	-3.57	-3.22
IFI6	4.46E-01	3.38E-01	-39.64	-15.10	0.69	-1.73	FALSE	-1.61	-0.66
JUNB	3.17E-01	3.06E-01	-39.64	1.25	-18.40	-1.74	FALSE	-1.43	-0.32
SPTBN1	6.95E-03	6.68E-02	-39.48	10.19774666	1.9742265	-0.96	FALSE	0.37	-0.44
PRNP	1.27E-01	7.68E-01	-39.20	-0.86	-16.57	-1.55	FALSE	-2.85	-2.80
TNFSF4	9.86E-01	3.54E-03	-38.88	16.30016407	42.88092111	-0.42	FALSE	-3.81	-2.50
C8orf40	2.61E-01	2.10E-01	-38.60	-0.90	-18.77	-2.97	FALSE	-0.99	-1.72
SEL1L	4.31E-01	4.74E-01	-38.58	-3.90	-1.91	-1.65	FALSE	-3.19	-2.36
SNX9	8.39E-02	9.43E-01	-38.40	4.21773408	17.87314667	-0.31	FALSE	-1.99	-2.10
KRT10	7.68E-01	1.86E-01	-38.33	6.615582665	27.12457887	-1.01	FALSE	2.72	0.66
EPDR1	1.94E-01	1.86E-01	-37.93	4.58	-42.43	-1.53	FALSE	-0.35	-0.76

	clinic.R.in ore	clinic.R. less	sc.All	sc.Old	sc.New	sc.Bul k	sc.Q.gene	tcga.Increased. risk	tcga.Increased.risk .beyond.T.cells
EGR2	2.42E-01	1.28E-01	-37.72	0.332043 956	14.2700 3379	-1.16	FALSE	-2.88	-0.63
GATSL3	1.63E-01	1.34E-02	-37.61	7.800143 337	24.6397 7081	-0.35	FALSE	-0.94	-0.81
COL16A1	3.73E-01	3.56E-01	-37.54	-2.47	-38.81	-1.42	FALSE	-1.72	-0.87
CD55	5.71E-01	1.64E-01	-37.49	1.970677 68	9.60416 9548	-0.97	FALSE	-1.46	-4.40
CRELD1	5.86E-01	6.12E-01	-37.35	5.47	-34.69	-1.57	FALSE	-1.13	-0.68
SVIP	5.84E-01	1.64E-01	-37.25	0.974568 455	25.3187 1464	-0.74	FALSE	-1.56	-1.15
NFE2L1	8.30E-02	8.74E-01	-37.12	-0.70	-10.29	-1.42	FALSE	1.23	0.70
PRDX1	6.51E-01	4.55E-01	-36.94	3.087427 147	24.8219 9094	-0.54	FALSE	0.70	0.62
B2M	4.43E-02	7.71E-01	-36.89	21.10505 197	26.4177 3682	-1.10	FALSE	-7.29	-2.96
PDE4DIP	5.31E-01	5.09E-02	-36.89	0.402602 515	9.20890 7424	-0.71	FALSE	0.49	0.41
APOL1	1.22E-01	6.68E-01	-36.88	1.287252 758	17.1478 7261	-0.74	FALSE	-5.74	-1.36
CREB3L2	4.17E-01	4.63E-01	-36.84	0.358284 954	2.01839 1143	-0.49	FALSE	-0.60	-0.70
EVA1A	1.57E-01	6.76E-01	-36.71	0.761040 106	18.0715 6414	-0.66	FALSE	NA	NA
TIMP2	1.13E-01	8.26E-01	-36.71	0.626230 588	4.25199 6112	-0.64	FALSE	1.22	0.72
STAT3	1.90E-01	6.70E-01	-36.62	0.369941 565	8.52937 68	-1.07	FALSE	-3.12	-0.90
EZH1	5.10E-02	3.93E-01	-36.54	0.417829 156	9.67345 54	-1.13	FALSE	-2.33	-2.81
SPRY2	1.85E-02	2.34E-01	-36.26	-1.08	-25.28	-1.61	FALSE	-2.42	-2.39
ITGA10	6.22E-01	1.93E-01	-36.13	2.056177 09	7.09359 9209	-0.71	FALSE	-1.57	-1.75
TGOLN2	2.71E-01	6.43E-01	-35.99	-1.61	-8.04	-1.52	FALSE	-2.20	-1.14
NFAT5	3.84E-02	6.11E-01	-35.92	-0.97	-7.21	-1.45	FALSE	-2.99	-2.31
CD46	7.87E-01	3.15E-01	-35.83	-11.65	-0.60	-1.53	FALSE	-4.30	-4.97
HLA-G	1.55E-01	5.82E-01	-35.67	28.13806 449	4.32458 5401	-1.15	FALSE	-2.09	-0.41
NPC2	4.63E-01	2.90E-01	-35.66	14.30417 724	0.49509 1905	-0.40	FALSE	0.54	1.18
LOC10012 7888	6.29E-02	8.12E-01	-35.63	-11.84	-3.62	-1.37	FALSE	0.83	-0.35
LXN	1.66E-01	5.62E-01	-35.60	-4.54	-40.35	-2.72	FALSE	-0.74	-0.38
MT1M	3.49E-01	2.33E-01	-35.36	-14.10	-11.08	-3.18	FALSE	-0.69	-0.68
C16orf45	3.02E-03	6.46E-01	-35.32	-0.76	-48.53	-1.56	FALSE	-2.09	-1.93
LOXL3	8.91E-01	4.37E-02	-35.03	4.82	-40.56	-1.35	FALSE	-3.28	-1.82

	clinic.R.in ore	clinic.R. less	sc.All	sc.Old	sc.New	sc.Bul k	sc.Q.gene	tcga.Increased. risk	tcga.Increased.risk .beyond.T.cells
LINC00152	5.34E-01	3.79E-01	-34.97	-5.73	-8.24	-1.32	FALSE	NA	NA
PDK4	6.52E-01	1.85E-01	-34.90	5.780192 629	25.2760 7059	-0.98	FALSE	-0.86	-0.83
GEM	4.46E-01	1.12E-02	-34.88	1.13	-32.19	-1.60	FALSE	-1.36	-0.81
CCDC47	2.14E-01	1.23E-01	-34.85	0.460464 013	4.08009 3569	-0.82	FALSE	-0.76	-0.68
SAA1	2.70E-01	6.03E-01	-34.50	14.25803 074	33.7718 886	-1.07	FALSE	-0.63	-0.54
FAP	2.46E-01	1.13E-01	-34.42	4.359167 404	41.9045 5405	-0.39	FALSE	-0.67	-0.60
IER3	9.45E-02	7.96E-01	-34.39	1.561694 536	19.8124 9058	-1.06	FALSE	-1.68	-2.71
LEPROT	6.81E-02	4.29E-01	-34.35	-3.84	-3.79	-1.37	FALSE	-1.36	-1.01
SQSTM1	3.08E-01	5.29E-01	-34.34	-8.65	-2.82	-1.56	FALSE	-0.46	-0.44
TMEM66	1.03E-01	1.17E-01	-34.23	6.335487 056	14.2478 9241	-1.11	FALSE	-2.58	-1.09
BIN3	7.84E-02	8.47E-01	-34.16	-1.04	-4.76	-1.88	FALSE	0.32	-0.68
H2AFJ	3.84E-02	5.04E-01	-34.07	25.87241 942	16.3668 4482	-1.06	FALSE	2.18	1.36
TAPBPL	1.34E-01	7.56E-01	-33.96	0.367921 789	29.9760 1261	-1.09	FALSE	-2.88	-0.43
CHPF	6.61E-01	4.31E-01	-33.88	2.895612 909	13.0886 9319	-1.15	FALSE	0.71	-0.37
KIAA1551	3.03E-01	2.58E-01	-33.84	-2.17	-10.79	-2.28	FALSE	NA	NA
CCPG1	6.35E-01	5.74E-01	-33.73	-2.59	-3.53	-1.41	FALSE	-3.84	-3.38
CHI3L1	4.46E-01	4.28E-01	-33.64	0.396603 931	50.3233 9741	-1.07	FALSE	-3.88	-1.18
TNFRSF10 B	2.48E-01	3.26E-01	-33.55	-1.29	-19.70	-1.58	FALSE	0.41	-0.32
ENDOD1	3.12E-01	7.77E-01	-33.51	2.518536 44	1.04123 2189	-1.04	FALSE	-0.45	-1.09
CLIP1	1.44E-02	6.78E-01	-33.48	2.054976 195	6.35811 2418	-1.14	FALSE	-0.55	-0.44
TMBIM1	8.50E-02	9.38E-01	-33.46	-7.42	-1.80	-1.93	FALSE	0.33	-0.34
AHR	5.02E-02	6.01E-02	-33.45	-2.02	-16.52	-2.41	FALSE	-3.48	-1.81
TMED9	7.07E-01	4.41E-01	-33.43	3.860348 819	7.45232 1879	-0.87	FALSE	0.49	0.55
NPTN	1.61E-01	6.54E-01	-33.14	-0.52	-4.89	-1.37	FALSE	-2.34	-2.31
UBE2B	1.90E-01	3.56E-01	-33.08	-4.50	-9.49	-2.60	FALSE	-3.96	-3.73
SYNE2	8.23E-02	8.84E-01	-33.05	8.739833 095	3.94233 7418	-0.55	FALSE	-0.81	0.32
MBNL1	8.92E-02	5.79E-01	-32.82	5.434241 63	0.46937 185	-1.05	FALSE	-5.55	-2.89
FAM46A	3.69E-01	2.02E-02	-32.69	3.82	-22.62	-1.63	FALSE	-1.06	-1.10
IL12RB2	4.14E-01	3.95E-01	-32.68	16.46671	5.37628	-0.96	FALSE	-0.41	0.64

	clinic.R.in ore	clinic.R. less	sc.All	sc.Old	sc.New	sc.Bul k	sc.Q.gene	tcga.Increased. risk	tcga.Increased.risk .beyond.T.cells
				472	8421				
DDIT3	7.65E-01	3.64E-02	-32.63	1.447014 332	19.2775 0288	-1.20	FALSE	-0.70	-2.12
FOSB	1.43E-01	8.00E-01	-32.49	0.796475 507	4.31272 261	-1.06	FALSE	-1.11	0.34
CAV2	1.80E-01	2.59E-01	-32.43	-3.08	-4.61	-1.36	FALSE	-1.69	-1.13
STOM	3.22E-01	4.73E-01	-32.40	4.411700 006	0.60124 6398	-0.40	FALSE	-0.52	1.09
SERINC1	6.29E-02	4.88E-01	-32.30	-3.03	-11.26	-1.69	FALSE	-1.80	-2.10
MT1F	5.29E-01	2.87E-01	-32.19	-10.67	-7.72	-1.67	FALSE	-0.35	0.31
FZD6	4.56E-02	4.75E-01	-32.14	4.466223 946	10.6108 4389	-0.42	FALSE	-2.55	-3.38
G6PD	4.37E-02	7.80E-01	-32.10	2.04	-13.40	-1.65	FALSE	-0.35	0.40
MVP	4.11E-02	9.36E-01	-32.00	-2.51	-3.07	-1.43	FALSE	-1.53	-0.51
TMED10	3.04E-01	4.70E-01	-31.94	3.937577 051	1.49110 1847	-0.72	FALSE	-0.78	-1.04
MCOLN3	5.15E-02	7.52E-01	-31.92	1.592257 374	34.9598 1505	-1.28	FALSE	0.56	0.63
C4A	5.68E-02	7.73E-01	-31.78	5.638375 4	63.9558 7021	-0.57	FALSE	-3.86	-0.65
CHPT1	1.14E-01	7.16E-01	-31.65	-1.71	-8.66	-1.96	FALSE	-0.92	-0.97
TOB1	1.63E-01	2.88E-01	-31.63	3.499775 851	9.25731 9016	-0.60	FALSE	0.32	-0.67
ELK3	2.92E-01	4.28E-01	-31.32	0.690617 385	15.6088 5115	-0.75	FALSE	-1.57	-1.23
RND3	3.53E-01	5.03E-01	-30.88	-4.70	-15.82	-2.44	FALSE	-1.33	-1.28
PHLDA1	1.23E-01	6.12E-01	-30.88	3.554078 519	12.0807 0285	-1.05	FALSE	-0.72	-1.27
TRIB1	2.16E-01	4.24E-01	-30.87	4.102846 583	7.01253 5992	-1.14	FALSE	-1.07	-0.49
PLOD3	6.85E-01	3.92E-01	-30.70	4.529043 691	0.52129 9179	-1.19	FALSE	0.50	-0.36
DUSP1	2.31E-01	1.61E-01	-30.66	0.662164 296	14.2747 394	-0.77	FALSE	-1.45	-0.31
LAMA4	3.36E-01	1.86E-01	-30.65	1.304437 005	13.7140 9326	-0.96	FALSE	-2.08	-1.15
ALCAM	1.39E-01	5.13E-01	-30.52	0.324216 688	7.23309 32	-1.26	FALSE	-0.64	0.45
PRKAR1A	6.16E-01	5.09E-01	-30.49	2.995748 369	5.80777 074	-0.36	FALSE	-2.49	-1.59
CYSTM1	1.56E-01	6.62E-01	-30.37	-5.01	-1.52	-1.52	FALSE	NA	NA
MPZ	7.95E-01	3.44E-02	-30.22	3.827991 239	17.8589 262	-0.79	FALSE	-0.98	-0.46
REEP5	4.44E-01	2.83E-01	-30.12	-5.08	-6.71	-2.22	FALSE	-0.94	-0.57
BCAP29	6.01E-02	2.85E-01	-30.07	0.788569	8.45253	-0.66	FALSE	-3.69	-3.59

	clinic.R.in ore	clinic.R. less	sc.All	sc.Old	sc.New	sc.Bul k	sc.Q.gene	tcga.Increased. risk	tcga.Increased.risk .beyond.T.cells
				825	8217				
PLEC	3.00E-01	1.49E-01	-29.99	0.32314	11.4049 6196	-1.07	FALSE	-0.70	-0.48
CBLB	4.62E-02	6.91E-01	-29.96	1.160755 876	17.2852 1246	-0.37	FALSE	-0.90	-0.37
CHI3L2	4.24E-01	3.28E-01	-29.83	4.908298 993	29.8038 7401	-1.50	FALSE	-2.40	-0.30
GRAMD3	2.24E-02	1.27E-01	-29.69	3.175491 376	32.2482 9385	-2.48	FALSE	-1.28	-0.61
CAMP	2.58E-01	2.56E-01	-29.67	6.537864 387	32.9594 1798	-1.04	FALSE	-1.50	-0.43
CSRP1	6.53E-01	4.51E-01	-29.65	3.645548 095	4.55503 6259	-1.17	FALSE	-1.00	-1.12
ARMCX3	5.62E-01	4.06E-02	-29.33	6.284817 238	0.59187 6729	-1.90	FALSE	-0.38	-0.36
CANX	2.70E-01	5.34E-01	-29.31	1.780081 404	6.18123 2682	-0.92	FALSE	-0.75	-0.53
TXNIP	1.58E-01	8.52E-01	-29.27	0.527598 171	4.21470 4474	0.37	FALSE	-0.70	1.02
S100A16	4.52E-01	6.89E-01	-29.26	0.688460 885	13.9969 7	-0.84	FALSE	-0.44	-1.03
HEXB	3.66E-01	1.28E-01	-29.23	6.435524 884	0.37105 0963	-1.21	FALSE	-1.30	-0.79
WEE1	2.40E-02	3.83E-01	-29.22	1.837664 314	10.4577 6818	-0.94	FALSE	-2.16	-1.20
CTSO	2.03E-01	3.03E-01	-29.18	0.529135 38	10.2511 7093	-0.89	FALSE	-3.34	-0.64
PLOD2	2.29E-02	2.76E-01	-29.00	1.038914 654	11.9526 9747	-0.82	FALSE	-1.68	-0.99
DAAM2	2.86E-01	8.20E-01	-28.93	0.995149 536	16.3541 3947	-0.37	FALSE	0.33	0.31
IQGAP1	2.26E-01	8.38E-01	-28.81	5.892500 327	3.99979 6242	-1.01	FALSE	-1.12	-0.63
ATP6V1B2	3.12E-02	9.33E-01	-28.81	1.236034 151	5.74856 853	-1.57	FALSE	-0.42	-0.37
PSMB8	8.52E-02	7.24E-01	-28.67	5.117567 066	8.85451 8735	-1.76	FALSE	-4.67	-1.59
TES	1.42E-01	5.00E-01	-28.64	0.478011 716	32.2155 5921	-0.44	FALSE	-0.88	0.34
ABHD2	1.04E-01	6.28E-01	-28.54	1.251595 254	10.6189 5132	-2.78	FALSE	-1.09	-0.84
AKAP9	6.09E-01	1.96E-01	-28.52	0.359183 91	5.46143 2538	-0.42	FALSE	-2.69	-2.68
LIF	6.70E-01	3.44E-01	-28.52	3.073773 887	28.0703 9375	-1.10	FALSE	-4.32	-3.08
PLK3	1.38E-01	8.45E-01	-28.49	1.464108 474	11.4461 8117	-0.99	FALSE	-0.50	-0.36
OSBPL5	6.95E-01	3.31E-02	-28.46	2.269849	8.98048	-1.32	FALSE	-0.98	-1.54

	clinic.R.in ore	clinic.R. less	sc.All	sc.Old	sc.New	sc.Bul k	sc.Q.gene	tcga.Increased. risk	tcga.Increased.risk .beyond.T.cells
				969	9184				
ADIPOR2	1.68E-01	8.80E-01	-28.35	0.839832 233	5.70682 7917	-1.02	FALSE	1.68	0.89
S100A4	7.37E-01	6.12E-02	-28.27	3.380134 016	64.0119 9908	-1.03	FALSE	-1.02	-0.40
RTKN	6.89E-01	3.62E-01	-28.22	0.492129 374	9.89222 8036	-0.92	FALSE	0.53	-0.68
NR4A2	4.92E-02	6.31E-01	-28.21	3.780760 282	0.42338 9847	-1.30	FALSE	-2.24	-1.22
PPAPDC1B	2.33E-01	9.19E-02	-28.10	1.533802 908	10.8139 9535	-1.87	FALSE	-1.98	-1.79
MAGEC2	6.50E-01	7.68E-02	-28.07	2.107111 7	41.3470 3335	-1.46	FALSE	-1.05	-1.02
PDE4B	6.64E-01	2.67E-01	-28.03	2.364902 426	35.0094 4346	-2.37	FALSE	-3.27	-0.50
AQP3	3.72E-01	7.16E-01	-28.03	9.058871 123	22.6804 4058	-1.01	FALSE	0.58	1.50
RTP4	1.96E-02	8.07E-01	-27.94	5.675337 518	6.01970 5486	-2.01	FALSE	-2.18	-0.74
NIPAL3	7.84E-02	7.37E-01	-27.58	2.025738 972	2.55974 3987	-0.76	FALSE	-3.63	-3.63
PPP4R2	5.59E-01	3.37E-01	-27.53	2.217580 79	3.37550 1383	-0.68	FALSE	-2.28	-1.72
NDRG1	3.17E-01	1.99E-01	-27.44	2.248121 009	15.8768 9568	-0.56	FALSE	-3.88	-3.05
PFKP	3.56E-02	1.73E-01	-27.42	0.422114 565	4.66026 4324	-0.49	FALSE	1.20	0.49
CD200	2.69E-01	5.64E-01	-27.40	2.559052 299	16.8901 3676	-2.02	FALSE	-2.30	-0.77
SLC2A3	5.69E-01	3.59E-01	-27.38	1.861116 025	1.24731 2253	-0.79	FALSE	0.52	0.65
TRIM51	1.23E-02	9.86E-01	-27.38	22.00677 143	5.87640 5839	-0.74	FALSE	NA	NA
TJP1	2.45E-01	2.61E-01	-27.23	0.387152 694	29.9785 7109	-0.85	FALSE	-0.81	0.36
CPVL	6.42E-01	1.96E-01	-27.04	0.662656 107	31.8573 706	-0.59	FALSE	-1.29	-0.44
IFRD1	5.23E-02	1.74E-01	-27.01	4.489953 381	27.0724 7597	-0.51	FALSE	-1.74	-3.39
LMNA	2.61E-01	7.35E-01	-26.99	14.85556 789	5.14922 2622	-0.90	FALSE	0.57	0.39
TMEM30A	8.31E-02	1.20E-01	-26.95	1.296738 123	9.65045 9473	-0.72	FALSE	-4.05	-4.59
NAMPT	2.38E-01	8.88E-01	-26.92	0.599957 745	8.35441 204	-1.27	FALSE	-3.72	-2.18
INPP5F	1.79E-01	4.31E-01	-26.90	4.825022 902	0.53646 6924	-0.49	FALSE	-2.07	-1.43
DLGAP1- AS1	9.43E-01	5.69E-02	-26.86	0.873888	5.98305	-0.56	FALSE	NA	NA

	clinic.R.in ore	clinic.R. less	sc.All	sc.Old	sc.New	sc.Bul k	sc.Q.gene	tcga.Increased. risk	tcga.Increased.risk .beyond.T.cells
				664	5739				
ENTPD6	3.39E-01	2.81E-01	-26.81	0.918823 136	9.94480 9472	-0.69	FALSE	0.64	0.62
ANKRD36B P1	3.05E-01	8.29E-01	-26.74	0.387440 246	1.45048 7926	-1.12	FALSE	-0.84	0.33
DNASE2	3.82E-01	3.30E-01	-26.66	5.792710 27	3.08760 3241	-1.13	FALSE	-0.85	-0.45
PARP9	1.77E-02	9.10E-01	-26.62	8.593426 968	3.79735 601	-3.07	FALSE	-6.05	-2.17
ETV4	4.66E-01	4.90E-01	-26.48	2.154806 287	40.7905 761	-0.37	FALSE	-0.31	-0.77
AKR1C3	1.43E-01	4.41E-01	-26.25	4.534550 779	31.8300 8396	-1.29	FALSE	-0.42	0.41
PIGT	8.38E-01	1.37E-01	-26.24	0.796637 157	21.8279 6134	-1.98	FALSE	1.11	0.71
ANKRD28	6.58E-02	8.47E-01	-26.18	0.835178 911	1.88060 5312	-1.05	FALSE	-0.34	-0.72
TCN1	2.30E-01	3.90E-01	-25.97	13.20783 241	24.9560 4114	-0.76	FALSE	0.85	0.51
SERINC5	2.86E-01	3.40E-01	-25.90	1.367509 487	2.31045 0523	-0.56	FALSE	-0.35	0.98
SLC38A2	2.45E-01	6.32E-01	-25.84	5.887885 708	14.8517 84	-0.51	FALSE	-3.06	-2.13
SLC16A3	4.77E-01	5.69E-03	-25.80	1.860338 009	2.42580 2885	-0.48	FALSE	-0.53	0.41
ENO2	7.06E-02	3.19E-01	-25.77	5.890890 828	0.71293 2382	-0.60	FALSE	0.64	-0.60
ADAM9	2.70E-02	5.60E-01	-25.74	0.496294 512	4.87067 2147	-1.45	FALSE	-0.75	-0.46
P4HA2	2.45E-01	1.78E-01	-25.73	1.590533 138	10.6894 4038	-1.54	FALSE	0.67	0.58
TRIM47	7.98E-02	9.46E-01	-25.63	1.850462 382	9.01817 8263	-0.70	FALSE	-0.52	0.36
S100A13	1.28E-01	8.69E-01	-25.59	0.978590 241	3.66591 8361	-0.34	FALSE	0.38	-0.44
SUMF2	3.63E-01	4.64E-01	-25.55	1.576955 308	9.13583 2478	-1.47	FALSE	0.43	-0.50
LONP2	7.24E-02	6.03E-01	-25.52	1.149798 332	2.11467 6254	-0.35	FALSE	-0.92	-0.99
PJA2	1.03E-01	1.27E-02	-25.34	0.664063 647	8.49029 5655	-1.46	FALSE	-4.51	-2.82
NOTCH2	6.53E-02	9.23E-01	-25.27	1.062830 302	18.1437 5992	-1.39	FALSE	1.89	1.93
FLNA	1.85E-01	6.62E-01	-25.25	1.245245 646	6.64162 0967	-0.69	FALSE	1.17	1.24
ETV5	1.03E-01	7.28E-01	-25.16	2.425088 433	2.09504 1157	-0.33	FALSE	0.56	0.31
IRF4	1.43E-01	1.55E-01	-25.14	8.149769	1.66438	-0.51	FALSE	1.06	1.71

	clinic.R.in ore	clinic.R. less	sc.All	sc.Old	sc.New	sc.Bul k	sc.Q.gene	tcga.Increased. risk	tcga.Increased.risk .beyond.T.cells
				268	9215				
RNF213	1.31E-01	8.83E-01	-25.03	2.256625 015	0.44280 1921	-0.70	FALSE	-5.53	-0.81
ACTN1	8.63E-02	6.82E-01	-24.87	2.392087 133	0.46149 3171	-0.63	FALSE	0.67	0.34
MAP1B	1.41E-01	3.16E-01	-24.85	16.48663 287	91.9037 6064	-0.75	FALSE	-1.34	-0.72
SIL1	7.50E-01	8.78E-02	-24.81	0.575261 468	7.53966 8952	-2.88	FALSE	-0.51	0.38
PNPLA2	1.42E-02	9.22E-01	-24.79	3.113307 912	6.39481 8612	-1.78	FALSE	-1.19	-0.63
TSPYL2	6.78E-01	1.52E-01	-24.72	3.778385 825	9.37033 9528	-0.51	FALSE	-0.61	0.31
SLC44A1	1.06E-01	6.28E-01	-24.69	2.380864 194	0.34964 7359	-0.92	FALSE	-0.51	-0.39
PARP4	6.46E-02	8.01E-01	-24.68	4.159339 69	4.59780 5687	-1.69	FALSE	-2.92	-1.43
THBD	3.74E-01	3.56E-01	-24.64	14.85253 744	8.81721 5143	-0.72	FALSE	0.36	0.50
ATP6AP2	2.46E-01	2.24E-01	-24.56	2.737231 423	3.50521 377	-1.49	FALSE	-4.10	-3.54
SLCO4A1	1.17E-01	4.29E-01	-24.54	12.32577 077	2.49128 5662	-1.12	FALSE	0.53	0.32
QDPR	3.87E-01	3.01E-01	-24.46	0.848626 308	1.28147 9991	-0.58	FALSE	0.93	-0.37
ACSL1	3.34E-01	7.20E-01	-24.44	1.343355 398	2.39421 8878	-0.74	FALSE	-0.52	-0.42
PHF17	1.88E-01	3.97E-01	-24.41	2.536355 562	9.66696 095	-0.67	FALSE	-1.39	-0.76
PKM	4.16E-01	3.42E-01	-24.35	2.779782 869	25.7245 4124	0.30	FALSE	NA	NA
SUMF1	4.47E-02	9.62E-01	-24.20	0.385589 079	18.6176 8978	-1.61	FALSE	-0.41	-0.67
DIP2C	1.36E-01	5.96E-01	-24.12	0.895308 56	0.45682 9866	-0.77	FALSE	0.40	-0.78
CCDC109B	1.35E-01	5.33E-01	-24.12	5.921564 373	20.8975 8313	-2.54	FALSE	-2.60	-1.01
CLCN3	3.24E-02	6.68E-01	-24.11	1.199961 056	0.42486 9674	-1.19	FALSE	0.36	-0.49
UBE2L6	1.07E-01	9.31E-01	-24.10	32.41261 04	8.30573 1147	-1.48	FALSE	-7.72	-2.59
SNCA	5.44E-02	5.43E-01	-24.09	4.640547 132	4.11479 0574	-0.52	FALSE	1.38	0.88
PCM1	8.07E-03	3.32E-01	-24.08	0.540265 66	0.72218 8884	-0.72	FALSE	-2.49	-2.26
GPR137B	6.68E-02	6.10E-01	-24.07	11.24242 878	4.38425 8609	-0.67	FALSE	0.75	-0.31
XPO7	2.20E-01	6.54E-01	-24.04	1.128305 25	11.7746 9529	-2.28	FALSE	0.54	-0.32

	clinic.R.in ore	clinic.R. less	sc.All	sc.Old	sc.New	sc.Bul k	sc.Q.gene	tcga.Increased. risk	tcga.Increased.risk .beyond.T.cells
ACTN4	2.89E-01	6.30E-01	-23.85	1.040958 249	7.66818 6482	-1.69	FALSE	-1.41	-2.22
SERINC3	5.28E-01	6.88E-02	-23.84	0.812247 624	7.88097 1405	-1.79	FALSE	-2.22	-1.93
RCAN1	4.73E-01	4.75E-01	-23.82	7.648341 32	1.42444 6662	-1.57	FALSE	-1.78	-1.20
RHOB	1.81E-01	2.40E-01	-23.80	1.511826 677	3.89608 0823	-1.25	FALSE	1.01	0.81
GNPTG	5.17E-01	5.84E-01	-23.63	2.367199 494	5.62907 5389	-1.60	FALSE	0.40	-0.35
SHC4	8.71E-02	8.28E-01	-23.63	0.761842 584	1.21341 2465	-0.41	FALSE	-0.92	-0.56
RGS2	5.33E-01	2.47E-01	-23.60	0.640530 514	35.2694 8489	-0.86	FALSE	-1.66	-0.77
LOC72901 3	Inf	Inf	-23.34	1.347015 309	7.73923 7399	-0.38	FALSE	NA	NA
SPTAN1	2.79E-01	6.02E-01	-23.28	3.516248 421	0.93349 9052	-1.09	FALSE	1.33	1.92
ROPN1B	1.96E-01	5.51E-01	-23.25	0.392244 359	3.75722 9083	-1.17	FALSE	-0.37	0.31
CD97	5.02E-02	6.09E-01	-23.17	1.828424 99	11.2144 0814	-2.60	FALSE	-4.58	-1.91
HIST1H2B D	1.36E-01	7.30E-02	-22.98	1.015586 013	7.33602 1298	-0.59	FALSE	0.44	0.52
RNH1	3.44E-01	5.51E-01	-22.98	15.57474 178	1.48976 8126	-2.73	FALSE	-0.36	-0.33
LAMB2	1.53E-01	7.07E-01	-22.88	5.223327 364	6.00551 1857	-0.66	FALSE	1.34	1.26
CFB	2.69E-01	6.21E-01	-22.75	3.336017 193	33.8193 6425	-1.72	FALSE	-5.01	-1.30
APOC1	3.51E-01	2.53E-01	-22.72	5.248454 96	10.9311 5237	0.56	FALSE	-0.97	0.35
CTTN	2.95E-02	8.62E-01	-22.68	21.47838 673	14.3723 1691	-0.93	TRUE	1.79	1.06
SERPINI1	1.94E-01	3.95E-01	-22.64	7.367752 032	20.7152 515	-0.82	FALSE	-2.81	-2.79
AQP1	3.61E-01	1.34E-02	-22.54	3.040433 37	24.5447 6544	-1.11	FALSE	-0.63	-0.40
C9orf89	1.20E-02	3.49E-01	-22.49	0.827086 987	7.74480 6672	-2.09	FALSE	-1.25	-1.19
IGSF8	6.93E-01	1.66E-02	-22.42	3.569587 79	3.52059 0252	-0.34	FALSE	1.85	0.62
LOXL4	3.71E-01	2.10E-01	-22.33	1.334897 324	7.47665 9986	0.30	FALSE	-2.35	-1.86
PARP14	5.18E-02	9.01E-01	-22.19	8.097178 503	0.32888 6759	-1.20	FALSE	-7.56	-1.95
METTL7B	8.30E-01	3.07E-01	-22.13	5.765117 863	28.5287 5728	-0.53	FALSE	-2.27	-1.03

	clinic.R.in ore	clinic.R. less	sc.All	sc.Old	sc.New	sc.Bul k	sc.Q.gene	tcga.Increased. risk	tcga.Increased.risk beyond.T.cells
DDIT4	1.02E-01	3.25E-01	-22.11	5.255322 514	6.52630 495	-0.30	FALSE	-0.73	0.42
ATP6AP1	6.86E-01	2.45E-01	-22.08	2.478485 511	4.57401 432	-1.25	FALSE	2.24	1.59
EFCAB14	1.39E-01	7.38E-01	-22.08	3.316119 059	1.51572 9612	-0.55	FALSE	NA	NA
HIPK3	9.45E-02	3.66E-01	-22.07	2.821393 944	4.28775 0809	-2.31	FALSE	-2.16	-1.20
TRAM1	1.70E-01	3.45E-01	-22.00	1.343023 324	5.81854 9856	-0.80	FALSE	-2.96	-0.93
GNG12	1.51E-01	4.34E-01	-21.98	3.285765 565	0.61041 2559	-1.15	FALSE	-0.52	-1.19
HEXIM1	3.90E-01	6.89E-01	-21.98	0.494765 627	1.20984 7864	-0.53	FALSE	0.77	0.59
ARPC1B	4.19E-01	5.02E-01	-21.95	5.014848 929	0.37872 1015	-0.51	FALSE	-0.44	0.43
TBC1D10A	7.46E-02	1.14E-01	-21.92	0.552709 866	1.47590 4674	-0.40	FALSE	-0.67	-0.35
CELF2	1.04E-03	9.09E-01	-21.91	11.30510 408	4.39802 6966	-0.65	FALSE	0.72	1.32
AASS	2.27E-02	4.80E-01	-21.87	2.599548 19	6.59686 3423	-0.58	FALSE	-1.59	-1.62
BTG1	3.04E-02	8.04E-01	-21.84	2.240405 471	2.12511 0401	0.32	FALSE	-2.35	-2.87
ITGB5	2.13E-01	3.37E-01	-21.80	1.055482 689	7.66466 3167	-1.23	FALSE	-0.39	-0.59
LRP10	2.33E-03	9.26E-01	-21.76	2.643825 963	0.57523 7992	-0.86	FALSE	0.59	0.83
APOBEC3G	3.50E-01	1.02E-01	-21.76	1.435926 819	18.5519 6462	-1.19	FALSE	-7.99	-3.16
NBR1	1.91E-01	1.24E-01	-21.73	0.401682 359	7.03012 4647	-1.45	FALSE	-2.31	-1.99
ARHGAP18	6.67E-02	5.56E-01	-21.70	1.549818 958	6.08307 845	-0.91	FALSE	-3.47	-1.51
RHBDF1	5.39E-01	3.26E-01	-21.64	1.584125 889	5.04101 6329	-2.17	FALSE	0.56	-0.47
C2orf82	8.24E-01	1.09E-01	-21.54	3.589476 747	36.0767 4841	-0.80	FALSE	-0.76	-1.03
MRPS6	8.46E-01	6.04E-02	-21.54	3.819810 3	31.1953 7764	-0.48	FALSE	-3.76	-2.64
MFSD12	7.75E-02	7.20E-01	-21.46	10.32875 944	0.84732 4385	-0.81	FALSE	NA	NA
IL17RC	3.20E-03	9.68E-01	-21.46	0.950909 415	6.90376 5831	-1.33	FALSE	0.41	1.10
ORMDL3	2.42E-01	4.01E-01	-21.35	1.028831 949	12.1218 1027	-0.82	FALSE	-1.56	-0.43
ERAP1	8.92E-03	8.00E-01	-21.33	2.020343 036	1.07433 683	-1.32	FALSE	-4.25	-0.52

	clinic.R.in ore	clinic.R. less	sc.All	sc.Old	sc.New	sc.Bul k	sc.Q.gene	tcga.Increased. risk	tcga.Increased.risk .beyond.T.cells
DHRS3	3.85E-01	1.49E-01	-21.32	3.674737 662	36.7712 5122	-0.89	FALSE	-3.81	-1.01
SMIM3	4.40E-01	1.74E-01	-21.31	0.533091 389	27.3010 335	-1.51	FALSE	NA	NA
MTRNR2L7	9.55E-01	4.31E-01	-21.30	0.641838 996	0.83825 4683	-0.36	FALSE	NA	NA
MAN2B2	8.41E-02	6.73E-01	-21.30	3.188196 571	7.23594 0374	-2.17	FALSE	-0.67	0.35
UBA7	9.53E-03	9.62E-01	-21.16	6.237460 628	12.0651 5012	-2.74	FALSE	-7.29	-1.47
LOC10012 6784	2.74E-01	6.97E-01	-21.12	0.617459 169	1.53833 8712	-0.33	FALSE	0.91	0.40
ZMYND8	6.52E-01	4.23E-01	-21.09	8.469978 89	41.0598 472	-0.84	FALSE	-0.71	-0.77
SERPINB1	7.69E-02	7.68E-01	-21.08	7.082913 363	3.51317 6367	-1.08	FALSE	-2.14	-0.81
TUG1	7.67E-01	2.24E-01	-21.08	4.463316 224	0.48440 1657	-0.88	FALSE	-0.47	-0.64
TMEM123	4.50E-01	4.45E-01	-21.02	1.608148 266	24.2828 0986	-1.17	FALSE	-3.65	-3.37
OPTN	1.75E-02	9.00E-01	-21.01	15.25331 624	6.95785 8787	-1.28	FALSE	-1.82	-0.67
SPP1	1.58E-01	2.37E-01	-20.95	29.30414 836	15.6759 2791	-0.31	FALSE	-1.62	-0.80
VAMP5	2.01E-01	2.49E-01	-20.80	18.92620 281	2.11967 2202	-2.52	TRUE	-4.70	-0.83
PFN1P2	2.26E-01	5.20E-01	-20.78	4.251955 922	0.43571 2066	-1.31	FALSE	NA	NA
STRIP2	2.90E-01	6.75E-01	-20.69	0.450218 251	16.8353 3974	0.68	FALSE	NA	NA
TERF2IP	4.19E-01	4.95E-01	-20.68	0.523959 722	4.99899 526	-1.15	FALSE	-2.47	-2.74
CALD1	4.76E-02	4.98E-01	-20.63	0.953518 04	3.24192 5514	-0.49	FALSE	-1.72	-1.22
SDC4	1.32E-01	5.67E-02	-20.63	1.191859 966	2.50048 3993	-0.76	FALSE	-1.75	-1.20
ST3GAL6	2.60E-02	4.09E-01	-20.62	3.940416 547	1.01146 6756	-0.39	FALSE	-1.54	-1.76
GABARAPL 1	8.78E-02	5.78E-01	-20.60	0.899609 729	10.6307 2995	-1.03	FALSE	-1.21	-1.70
ATP2B4	3.11E-01	3.74E-01	-20.51	4.945501 045	0.71372 8198	-0.82	FALSE	0.42	-0.73
TYR	1.62E-01	8.43E-01	-20.44	5.806227 943	8.57382 8698	0.35	FALSE	0.95	0.74
LPXN	9.73E-02	5.50E-01	-20.32	4.724249 565	6.69091 907	-2.49	FALSE	-2.90	-0.99
NT5DC3	3.85E-01	7.50E-01	-20.30	3.824113 566	9.43965 8069	0.87	FALSE	1.45	1.08
TMEM43	2.13E-01	7.61E-01	-20.29	0.777872	10.6589	-1.87	FALSE	-0.43	-0.78

	clinic.R.in ore	clinic.R. less	sc.All	sc.Old	sc.New	sc.Bul k	sc.Q.gene	tcga.Increased. risk	tcga.Increased.risk .beyond.T.cells
				969	5763				
PPFIBP1	4.24E-01	4.93E-01	-20.24	1.128627 461	0.72107 9442	-0.79	FALSE	-1.32	-2.12
HPS5	1.63E-01	5.31E-01	-20.20	4.911611 77	0.94178 8497	-0.87	FALSE	-1.99	-1.23
ST6GALNA C2	1.94E-01	4.17E-01	-20.18	15.32664 647	2.85016 0806	-0.52	FALSE	0.64	0.45
GANAB	4.65E-01	2.60E-01	-20.18	6.760249 926	6.86200 1928	-0.43	FALSE	0.73	-0.34
UBE2Z	1.30E-01	7.08E-01	-20.12	0.635275 033	4.15713 8659	-0.93	FALSE	-0.40	0.34
BHLHE40	2.74E-01	3.89E-01	-20.08	15.75869 206	0.46098 2512	-1.07	FALSE	0.49	0.41
ICAM1	1.40E-01	1.30E-01	-20.07	5.429802 78	4.22767 8526	-0.90	FALSE	-2.94	-0.81
MT1G	2.64E-01	6.28E-01	-20.07	6.619086 183	19.4536 0494	-1.78	FALSE	-1.25	-0.92
TNFRSF1A	1.73E-01	3.01E-01	-20.05	1.213887 782	9.90138 4801	-2.19	FALSE	-0.58	-0.31
CEACAM1	8.88E-02	2.21E-01	-20.04	7.679312 791	0.61886 8776	-0.70	FALSE	0.31	-0.35
ATP6V0E2	1.88E-02	4.01E-01	-20.03	1.928199 495	14.2636 5141	-0.52	FALSE	0.57	0.41
IER2	6.61E-01	4.96E-01	-20.02	4.109943 558	25.7474 651	-0.51	FALSE	-0.30	0.35
PELI1	4.39E-01	3.28E-01	-20.00	1.189921 924	35.6465 558	-2.97	FALSE	-2.64	-1.15
GLCE	1.85E-01	3.72E-01	-19.98	1.177969 643	8.82578 3231	-0.32	FALSE	-1.80	-2.12
AFAP1L2	6.59E-01	4.14E-02	-19.97	1.073567 177	0.57027 5269	-1.36	FALSE	-2.23	-1.19
SRPR	6.59E-01	3.13E-01	-19.93	0.531970 765	4.90620 2103	-2.01	FALSE	-0.93	-1.11
PEG10	6.25E-02	5.12E-01	-19.79	9.864562 142	70.6588 3456	-0.36	FALSE	-1.59	-1.00
CCND1	2.58E-01	5.24E-01	-19.79	44.94838 696	9.14444 0051	-0.44	FALSE	0.93	0.81
PDLIM5	1.61E-01	8.65E-01	-19.73	1.229814 252	4.44144 9396	-0.81	FALSE	-1.49	-0.84
PTTG1P	4.37E-01	4.41E-01	-19.73	5.840061 211	31.8167 4616	-0.46	FALSE	1.42	0.70
PIM3	1.43E-01	4.70E-01	-19.67	2.058564 12	2.93170 429	-0.43	FALSE	-1.29	-0.88
LOXL2	1.30E-01	5.07E-02	-19.66	2.227721 553	17.7578 2926	-1.59	FALSE	0.63	0.59
CASP4	4.33E-02	5.13E-01	-19.66	1.060183 077	8.33983 3791	-2.26	FALSE	-2.39	-0.56
SLC39A6	2.57E-01	2.62E-01	-19.62	7.554501	2.80882 6234	-0.42	FALSE	1.49	0.36

	clinic.R.in ore	clinic.R. less	sc.All	sc.Old	sc.New	sc.Bul k	sc.Q.gene	tcga.Increased. risk	tcga.Increased.risk .beyond.T.cells
				206					
MICA	1.60E-02	3.12E-01	-19.54	4.830115 449	3.59963 1309	-1.12	FALSE	1.47	1.02
PTPRM	4.72E-01	5.15E-01	-19.50	0.814845 29	4.35855 1311	-0.92	FALSE	0.73	0.87
IGFBP3	7.45E-01	6.80E-03	-19.50	1.314794 414	34.0976 0334	-1.44	FALSE	-1.60	-1.31
OCIAD2	6.65E-01	2.76E-01	-19.49	1.305114 076	79.9825 0015	-0.31	FALSE	-1.69	-0.93
ASAH1	4.70E-01	3.55E-01	-19.40	8.977291 847	12.3096 9044	-0.54	FALSE	1.02	0.93
BAMBI	7.62E-02	4.89E-01	-19.40	7.127650 082	0.37112 5258	-0.66	FALSE	0.37	-0.67
CHN1	4.39E-01	1.42E-02	-19.28	4.899749 645	63.0544 6674	-1.01	FALSE	-2.08	-1.63
SORT1	2.69E-01	6.04E-01	-19.05	0.346897 384	4.21423 3311	0.30	FALSE	1.07	0.79
SPARCL1	2.75E-01	7.92E-02	-19.00	5.863651 519	7.67158 9784	-0.45	FALSE	-0.51	0.84
TYMP	5.50E-02	7.40E-01	-18.99	7.727093 689	2.34370 7718	-1.57	FALSE	-2.68	0.30
LYST	3.98E-01	5.38E-01	-18.94	2.644630 966	2.41002 413	-0.84	FALSE	-0.74	0.57
PACSIN2	1.92E-01	4.29E-01	-18.93	1.371299 596	1.41169 7598	-0.54	FALSE	-0.34	-0.40
GNS	6.32E-01	5.79E-01	-18.78	4.823051 083	3.28615 7821	-1.51	FALSE	-0.32	0.38
CSTB	1.50E-01	8.41E-02	-18.77	10.13996 322	12.4589 8834	-0.64	FALSE	3.01	2.46
PRR4	5.94E-01	3.79E-02	-18.75	2.798690 96	29.6357 1458	-1.07	FALSE	-0.94	-1.61
MFNG	4.15E-01	6.44E-01	13.74	5.389614 969	7.87782 8514	0.76	FALSE	-3.24	1.32
RNMTL1	6.42E-01	2.90E-02	13.76	5.382066 026	3.63082 7576	0.81	FALSE	1.85	0.97
6-Sep	3.42E-01	4.64E-01	13.79	4.196300 143	5.14015 6942	1.00	FALSE	-1.09	1.29
TUBGCP4	1.83E-02	8.31E-01	13.81	3.017098 753	1.78840 835	1.56	FALSE	0.56	0.31
ARHGEF1	1.00E-01	4.17E-01	13.83	0.583974 655	21.5705 2633	1.53	FALSE	-0.81	0.82
11-Sep	1.16E-01	1.74E-01	13.88	1.430393 629	24.2236 7679	0.89	FALSE	0.61	0.64
PCOLCE	2.45E-01	8.53E-02	13.90	60.72202 561	6.40674 755	1.57	TRUE	-0.54	-0.79
SURF2	3.11E-01	8.17E-03	13.90	3.289195 508	4.66096 5337	0.89	FALSE	1.86	0.96
MRPL44	1.42E-01	2.49E-01	13.90	0.452623 362	9.00164 0945	0.59	FALSE	0.66	0.47
DCAF12	2.42E-01	2.44E-01	13.91	7.312065 126	0.85145 1243	1.40	FALSE	-0.37	0.47
SAT2	5.10E-01	3.73E-01	13.92	12.75708 283	5.62835 4728	1.21	FALSE	0.47	-0.33

	clinic.R in ore	clinic. i1 less	sc. All	sc. Okl	sc. New	sc. Bil k	sc. Q geije	toga. Incr <3> risk	toga. Ii increased.risk lievond. T.cells
TSNAX	2.90E-01	5.50E-01	13.92	1.805752 837	12.1279 3854	1.33	FALSE	-1.86	-2.50
THOC3	8.77E-02	5.88E-01	13.92	4.098106 348	1.95790 0047	0.65	FALSE	1.18	0.59
PDCD5	7.35E-01	4.07E-01	13.98	6.751326 589	6.83658 6916	-0.35	FALSE	0.34	-1.77
MOCS3	3.15E-01	3.56E-02	14.00	1.434370 227	2.04395 5951	0.95	FALSE	0.34	-0.66
RBM4 B	6.30E-01	1.64E-02	14.11	6.906518 123	12.5381 1823	0.59	FALSE	0.40	0.38
MTX1	6.94E-01	2.54E-01	14.12	5.917603 68	2.66763 2146	1.24	FALSE	2.66	1.38
PRPF4	5.54E-01	1.41E-01	14.16	8.189088 103	2.04496 9562	0.86	FALSE	2.38	1.76
HNRNPD	5.99E-01	2.59E-01	14.17	4.315130 309	7.50364 1237	1.01	FALSE	-0.35	0.63
MCM4	4.36E-01	2.25E-01	14.19	1.664350 763	0.95347 9445	0.93	FALSE	1.50	1.57
AP3M1	8.55E-02	5.45E-01	14.24	0.629153 205	6.41742 361	1.11	FALSE	0.51	0.84
XIST	7.44E-01	2.49E-02	14.30	29.59293 181	7.69768 9322	0.45	FALSE	-1.93	-1.51
FAM64A	6.61E-01	8.41E-02	14.31	8.330570 062	0.35104 2029	0.83	FALSE	1.24	0.88
G3BP1	4.02E-01	3.85E-01	14.31	10.54566 035	1.94380 6272	-0.40	FALSE	-0.40	0.45
SNCG	4.74E-01	1.77E-01	14.33	18.24763 977	7.52820 7908	0.97	FALSE	0.76	2.26
PI4KB	6.25E-01	2.16E-01	14.34	0.797031 323	29.5211 7947	0.41	FALSE	4.66	3.87
DDX46	5.72E-01	7.29E-02	14.35	5.884048 05	5.55290 8424	0.75	FALSE	-0.96	-0.52
NNT	3.32E-01	5.47E-01	14.37	14.45967 163	6.90551 2186	1.70	FALSE	0.34	0.45
TIMM17A	8.05E-01	5.02E-02	14.40	4.529771 377	5.27448 5432	0.98	FALSE	0.67	-0.48
FTSJ3	7.42E-01	2.64E-02	14.41	11.30594 08	2.19752 3397	0.77	FALSE	1.50	1.16
HNRNPM	8.64E-01	8.82E-02	14.42	5.210267 361	2.73802 4614	0.91	FALSE	0.90	1.26
EXOSC6	3.95E-01	7.85E-01	14.43	0.458097 878	5.66286 2445	2.19	FALSE	1.75	0.76
IDH3B	8.23E-01	8.08E-02	14.43	3.288279 147	0.69493 1133	0.49	TRUE	2.10	1.15
NHEJ1	6.12E-02	5.57E-01	14.45	0.746766 7	10.0136 6284	2.85	FALSE	3.41	2.34
COPS5	4.72E-01	2.19E-01	14.49	13.43972 244	1.10968 4877	1.29	FALSE	-3.27	-3.87
SBN01	2.70E-01	6.76E-01	14.50	11.83280 512	0.31530 709	1.51	FALSE	-0.35	0.40
TXNDC17	8.75E-01	2.11E-01	14.51	19.93469 228	1.53723 4956	0.37	FALSE	0.51	-0.73
HMG20A	4.15E-01	2.71E-01	14.51	8.768995 629	3.13868 4411	1.23	FALSE	-0.42	-0.34
TRIB2	6.31E-01	4.40E-01	14.51	1.325156 749	36.7833 1778	1.14	FALSE	0.56	0.37
CSK	1.54E-01	1.13E-01	14.53	1.783684 971	3.90860 1844	0.83	FALSE	0.84	3.57
B4GALT3	6.85E-01	3.24E-02	14.53	2.984723 465	13.9929 3996	2.23	FALSE	0.64	0.69
AIMP2	1.98E-01	2.26E-01	14.54	9.995109 565	0.58923 4557	0.68	FALSE	3.46	1.01
SUPT5H	7.15E-01	1.21E-01	14.56	0.524094 651	17.2621 3471	0.54	FALSE	2.66	1.82
POSTN	2.42E-01	9.71E-02	14.57	25.61569 592	8.58471	0.72	FALSE	0.46	0.73

	clinical score	clinical score less	score All	score Old	score New	score RUI:111:1111	score Q gene	tcga.Increased.risk	tcga.Increased.risk.beyond.T.cells
					8074				
GTF2H2C	6.04E-01	1.69E-01	14.58	0.403995243	5.926998115	2.48	FALSE	-1.77	-1.09
GNL3	3.37E-01	4.02E-01	14.61	3.602849144	4.807218992	0.66	FALSE	-1.34	-1.91
GBAS	2.19E-01	2.58E-01	14.62	3.050038089	8.165505882	1.17	FALSE	-1.66	-2.61
MEST	4.42E-01	1.23E-01	14.64	26.73500059	1.521354639	0.45	FALSE	0.43	0.43
CDH3	6.93E-02	4.14E-02	14.67	4.060021324	27.37588719	0.38	FALSE	3.88	3.59
PLEKHJ1	5.88E-01	1.16E-01	14.68	3.793428817	7.780824818	0.33	FALSE	0.67	0.70
ECHS1	1.07E-01	2.20E-01	14.72	1.041998674	13.08042231	1.96	FALSE	2.27	1.81
SLC45A2	4.80E-01	3.24E-02	14.73	11.23157773	20.34505987	1.51	FALSE	2.62	2.58
NEUROD1	5.30E-01	1.52E-01	14.75	11.86664298	10.86699078	0.69	FALSE	-0.77	-1.69
ACTR1A	2.03E-01	2.17E-02	14.76	0.616928184	16.24202821	0.49	FALSE	3.57	3.89
CD24	2.14E-01	2.06E-01	14.78	1.079125614	1.079391239	0.79	FALSE	0.64	1.79
LOC388796	Inf	Inf	14.79	0.443428997	8.562706973	-0.46	FALSE	1.60	0.61
CDC20	5.51E-01	4.34E-02	14.80	4.913073148	0.753666063	0.63	FALSE	2.89	2.24
TPI1	4.34E-01	1.30E-01	14.82	5.327916572	0.744378475	0.77	TRUE	3.41	1.46
NOC2L	6.32E-01	2.28E-01	14.83	16.2653311	1.958200998	1.14	TRUE	1.46	0.80
CHCHD1	1.48E-01	5.42E-03	14.88	2.622835248	9.47306062	0.94	FALSE	0.45	0.40
ALDH1B1	6.57E-01	3.31E-01	14.98	0.922296057	19.44016174	2.22	FALSE	0.94	0.33
NTHL1	3.95E-01	1.32E-01	15.01	10.15717558	2.446536902	1.34	FALSE	1.35	0.87
RARRES2	2.25E-01	5.11E-01	15.05	4.873224671	0.301976127	0.91	FALSE	-1.43	-0.37
SLC25A44	2.69E-01	1.85E-01	15.12	1.806177902	12.42707653	0.82	FALSE	2.81	2.10
ECD	3.16E-02	3.29E-01	15.16	0.508216518	14.92602402	1.10	FALSE	-0.56	-0.81
ACBD6	4.72E-01	9.99E-02	15.18	4.54003142	6.492731101	0.49	FALSE	1.54	-0.33
AURKA	4.90E-01	5.48E-03	15.18	4.926437071	1.29370898	1.38	FALSE	1.99	1.32
PRMT1	5.78E-01	3.22E-01	15.18	7.87390675	2.414514677	0.56	FALSE	1.52	0.88
GNB2L1	3.13E-02	4.07E-01	15.22	0.754171752	3.35276588	0.35	TRUE	0.40	-0.33
TOMM5	2.75E-01	5.50E-02	15.24	16.83196592	1.221893499	1.00	FALSE	1.00	-0.31
SNRPF	2.17E-01	1.95E-01	15.27	15.00145479	3.094281947	0.67	FALSE	1.20	0.60
KLHL9	1.47E-01	7.18E-01	15.27	0.397375031	24.81289951	0.85	FALSE	-1.85	-1.54
RNPS1	1.42E-01	4.75E-01	15.29	2.320398903	3.782271567	1.76	FALSE	1.11	0.72
RPL36	5.72E-02	3.71E-01	15.33	2.178512724	26.41709158	-0.33	FALSE	0.50	0.33
SLC25A11	6.01E-01	2.68E-01	15.38	12.13755268	0.76179644	0.69	FALSE	1.65	1.15

	clink. R in ore	clinc R less	sc.All	sc.Oil	sc.New	sc.Bul k	sc.Q.gene	cg.Increased risk	tcga.Increased.risk .beyond.T.cells
FDPS	3.64E-01	1.03E-01	15.41	3.097761 019	7.76264 8036	0.62	FALSE	4.01	2.54
PRFSA P2	4.16E-01	1.22E-01	15.41	9.218191 038	2.29874 1055	1.45	FALSE	-0.83	-1.15
HAUS1	2.26E-01	3.37E-01	15.43	5.352399 583	1.24736 9224	0.96	FALSE	-1.42	-1.32
POLR2A	2.03E-01	8.81E-01	15.51	13.15051 816	22.8032 9056	2.32	FALSE	4.89	3.89
TDG	9.85E-01	3.25E-02	15.51	6.013013 072	1.03069 4741	1.73	FALSE	-0.62	-0.69
EGLN2	1.62E-01	2.30E-01	15.51	4.254455 956	6.34470 7044	1.09	FALSE	1.99	2.30
CDC45	5.88E-01	1.06E-01	15.53	5.285026 282	0.30704 5502	0.82	FALSE	1.49	1.03
EIF2S2	6.74E-01	1.23E-02	15.55	8.293233 204	0.58456 1792	0.79	FALSE	-1.33	-2.61
CACYBP	5.67E-01	5.28E-02	15.56	2.448860 208	6.78446 5091	1.43	FALSE	-0.90	-1.21
TOMM22	5.29E-01	3.03E-03	15.57	11.70143 787	1.10512 845	1.41	FALSE	1.63	0.57
GLUL	4.19E-01	1.68E-01	15.60	0.524584 718	13.6220 7707	0.68	FALSE	-1.32	0.33
KPNA2	2.93E-01	5.18E-03	15.60	4.991817 798	6.63982 0973	0.58	FALSE	3.86	3.97
GTF2E1	2.03E-01	5.56E-01	15.64	0.783473 28	2.04871 9802	1.04	FALSE	-1.63	-1.64
LINC00665	1.28E-01	8.43E-01	15.74	1.516171 688	5.78048 6589	1.43	FALSE	NA	NA
TARS2	4.95E-01	1.64E-01	15.74	3.244718 053	7.16795 3196	1.02	FALSE	2.01	1.13
ZSWIM7	4.97E-01	4.57E-01	15.77	5.395171 027	2.00074 9052	0.66	FALSE	-0.62	-1.46
SPDYE5	2.06E-01	4.71E-01	15.80	0.748477 234	8.22009 067	1.06	FALSE	-0.85	-0.64
LSM4	6.34E-01	1.59E-01	15.82	4.470623 28	2.25169 3195	0.39	FALSE	3.16	1.48
MYL9	4.21E-01	5.72E-02	15.88	0.696709 556	7.75093 8059	0.63	FALSE	0.83	0.90
ATP5B	4.63E-01	7.46E-02	15.89	2.737412 219	3.55705 0178	1.66	FALSE	3.60	1.19
RGS3	2.55E-01	4.95E-01	15.91	6.172391 972	3.48462 9082	-0.38	FALSE	-0.57	0.57
CHTOP	6.15E-01	8.77E-02	15.91	10.10615 811	5.69056 281	0.97	FALSE	NA	NA
SMG7	5.02E-01	6.60E-03	15.93	5.209483 431	11.9910 1659	2.02	FALSE	1.66	1.06
EIF3J	2.68E-01	1.88E-01	16.00	14.28593 134	0.67422 3072	0.92	FALSE	-2.31	-3.82
MGC2752	Inf	Inf	16.00	2.904335 761	2.48840 784	0.80	FALSE	1.05	0.69
PAM	3.98E-01	5.38E-03	16.04	0.837075 37	10.5175 5539	0.48	FALSE	-0.65	-0.55
GSTO1	6.07E-02	5.15E-01	16.05	1.337030 558	62.1927 9211	0.95	FALSE	1.72	0.92
RABEP1	8.74E-01	1.42E-01	16.06	21.29284 48	4.65628 2388	0.49	FALSE	-0.59	-0.83
KIF2C	7.82E-01	4.29E-02	16.11	6.859855 363	1.85427 0407	0.97	FALSE	2.25	1.77
CCNB2	2.81E-01	2.26E-01	16.12	3.919230 216	0.97304 1322	0.76	FALSE	1.37	0.69
NEK5	1.56E-01	8.32E-01	16.17	0.324543 846	3.95830 2922	0.56	FALSE	0.47	-0.69
PPIF	3.27E-02	9.52E-02	16.22	4.347882 752	2.12935 5273	0.32	FALSE	3.33	3.00
C17orf49	8.03E-01	3.47E-01	16.22	9.736718 533	0.87005 317	0.67	FALSE	-0.49	0.64

	clinic.R.more	clinic.R.less	sc.All	sc.Old	sc.New	sc.Bulk	sc.Q.gene	tiga.Increased.risk	tiga.Increased.risk.beyond.T.cells
EXOSC5	5.33E-01	4.78E-01	16.26	4.490272 348	1.54214 2828	0.38	FALSE	0.48	-0.45
MAP1LC3C	4.65E-01	1.06E-01	16.27	1.592062 983	3.55431 3965	1.34	FALSE	0.54	1.25
TUBB4A	9.06E-02	5.47E-01	16.29	18.47518 133	78.6913 9618	0.66	TRUE	NA	NA
EIF3G	2.66E-01	4.13E-01	16.30	0.485973 534	14.9116 7008	-0.34	FALSE	0.45	0.32
KIRREL	7.10E-01	1.91E-01	16.31	1.457831 877	23.6096 0921	1.24	FALSE	1.50	2.01
ID3	4.40E-01	4.62E-02	16.33	6.385801 262	6.66187 6303	1.01	FALSE	-0.70	0.37
CCNB1IP1	9.37E-02	6.45E-01	16.37	1.083665 256	8.08759 0455	0.98	FALSE	0.41	-0.93
IL6R	1.64E-01	1.16E-01	16.40	1.548267 241	43.8525 0904	1.24	FALSE	0.72	2.10
RPS10	1.11E-01	1.50E-01	16.42	3.683944 948	16.3033 9108	0.76	FALSE	0.71	0.42
PKN1	5.51E-01	4.88E-01	16.42	13.74625 835	3.30634 5432	0.70	FALSE	-0.75	-0.56
C10orf32	7.21E-02	4.78E-01	16.43	1.253078 131	10.4182 4098	1.99	FALSE	-1.13	-0.68
SKA1	9.28E-02	2.26E-02	16.59	0.563847 042	6.49426 39	1.74	FALSE	1.34	1.20
MRPS10	4.85E-01	8.68E-02	16.61	11.13816 237	1.78064 3088	0.73	FALSE	-0.56	-1.54
CKB	7.19E-01	2.83E-01	16.62	0.943666 82	0.67307 1985	0.87	TRUE	0.91	0.69
CDCA8	6.65E-01	4.59E-02	16.62	5.935347 842	3.40903 6488	0.85	FALSE	3.42	2.98
ATP5A1	3.11E-02	3.82E-01	16.68	4.114811 371	5.51647 72	1.16	FALSE	2.11	1.65
TTYH3	8.19E-01	6.55E-02	16.68	0.839172 467	25.9981 956	0.60	FALSE	6.36	5.75
WDR6	2.40E-01	6.41E-01	16.69	2.845445 8	11.1468 2125	2.13	FALSE	0.52	0.72
SLC5A6	6.91E-01	2.34E-01	16.79	12.87746 605	0.74779 4957	0.73	FALSE	1.64	1.27
FAM213A	2.19E-01	5.17E-02	16.83	0.649223 104	18.3827 6775	1.31	FALSE	NA	NA
SNRPA1	9.48E-01	1.16E-01	16.88	8.418866 258	1.51173 8171	1.59	FALSE	0.34	-0.32
MARCKSL1	6.64E-01	2.42E-01	16.89	11.85693 628	0.32290 1855	0.35	FALSE	0.54	1.18
DDX39A	6.91E-01	1.20E-01	16.91	0.618867 402	13.2599 3888	0.54	FALSE	NA	NA
BEX1	6.18E-01	4.03E-02	16.92	15.14930 944	3.63952 7861	0.58	FALSE	0.98	0.40
ZNF526	3.02E-01	5.04E-01	16.95	0.436912 6	4.00576 9467	1.12	FALSE	1.81	0.94
SMCR7L	2.03E-01	2.97E-01	17.02	7.881351 856	5.19450 4892	2.41	FALSE	2.29	1.25
FAM126A	5.19E-01	3.75E-02	17.08	4.352744 29	8.58497 2	0.63	FALSE	-1.33	-1.06
LSM14A	5.40E-01	3.49E-01	17.11	0.425148 121	20.8603 9965	0.55	FALSE	-1.33	-1.39
FDXR	5.12E-01	4.05E-01	17.12	1.673688 01	16.3833 1044	1.47	FALSE	2.00	1.47
SLC19A1	5.55E-01	2.28E-01	17.15	5.585866 639	14.8464 6384	0.81	FALSE	2.13	2.18
GAGE12J	1.82E-01	2.36E-01	17.16	17.96014 408	14.6809 6465	0.33	FALSE	-1.39	-2.77
OCA2	1.40E-01	2.52E-01	17.16	-	28.5171	1.11	FALSE	5.56	3.33

	clinical score	clinical score less	St. All	sc.OUL	sc.Ncv	sr.Rul k	sc.Qgetic	tcga_mmr<3s> risk	tct>a.If increased.risk bevoftil.T.cells
		02		5.354814 935	977				
RBBP4	8.19E-01	1.59E-01	17.17	7.902170 54	3.95826 2309	1.72	FALSE	-0.54	0.47
NIP7	1.48E-01	4.29E-01	17.34	7.740805 625	3.79024 9229	0.73	FALSE	0.63	-0.54
PRPF31	6.36E-01	4.74E-01	17.37	3.746194 298	5.15393 4765	0.79	FALSE	1.42	0.91
MKI67IP	4.95E-01	4.41E-01	17.46	5.342737 904	3.95036 9618	0.74	FALSE	-0.37	-1.42
TRUB2	7.07E-01	7.54E-02	17.48	4.615751 42	4.89377 5965	2.04	FALSE	2.77	1.68
METTL3	3.47E-01	4.85E-02	17.49	3.105289 5	5.77183 743	0.61	FALSE	2.17	1.65
HMGBl	3.33E-01	2.08E-01	17.50	6.146315 189	2.06010 4614	0.82	FALSE	-1.52	-1.07
RCC1	6.07E-01	2.04E-01	17.52	6.917331 724	3.98125 4561	0.87	FALSE	3.62	1.69
RPA1	3.28E-01	4.21E-01	17.53	5.961074 344	5.61797 7147	1.25	FALSE	1.36	1.23
HNRNPUL1	1.01E-01	2.70E-01	17.55	0.680339 536	16.4264 6971	0.56	FALSE	3.18	3.24
NDUFV3	4.85E-01	2.61E-01	17.56	2.992981 728	18.7577 1812	1.14	FALSE	2.18	2.14
RQCD1	7.06E-01	1.40E-01	17.57	2.435033 782	2.12079 1626	-0.41	FALSE	1.93	1.80
TCF4	3.80E-01	1.16E-01	17.62	9.236103 162	2.67978 4236	0.53	FALSE	-1.45	-0.68
C20orf27	4.98E-01	4.60E-01	17.62	7.631118 695	10.6194 9581	0.86	FALSE	3.11	2.07
CCT4	3.45E-01	9.10E-02	17.65	2.170402 339	6.39931 7541	2.01	FALSE	0.42	-0.48
VPS53	1.15E-01	3.30E-01	17.69	0.335449 031	37.0197 0924	1.02	FALSE	5.99	4.71
WDR46	2.26E-01	4.31E-01	17.76	8.702406 207	1.72587 4114	1.39	FALSE	1.37	0.53
NEFL	7.01E-01	2.22E-02	17.76	11.97364 126	5.92116 5572	0.60	FALSE	1.26	0.51
TCEA3	8.40E-01	7.29E-02	17.83	0.459042 162	4.03801 4366	1.40	FALSE	0.52	-0.40
GAGE6	1.00E+00	1.00E+00	17.86	16.08931 781	14.7586 0399	0.66	FALSE	NA	NA
GALT	1.33E-01	6.34E-01	17.87	1.976498 Oil	20.9818 5221	2.04	FALSE	-0.54	0.38
SNRNP40	8.89E-01	5.60E-02	17.90	8.554249 159	4.94873 4856	0.85	FALSE	0.87	1.24
CRK	8.58E-01	1.99E-01	17.94	3.670575 611	7.55391 113	0.91	FALSE	0.87	0.76
GNL3L	5.40E-01	2.97E-01	17.96	4.387265 453	23.9081 4734	1.25	FALSE	2.02	2.37
NUF2	7.59E-01	7.74E-02	17.97	4.131933 124	3.64760 7035	1.05	FALSE	-0.49	-0.70
SERPINB9	2.32E-01	9.95E-02	17.99	2.380561 98	2.91478 6989	1.08	FALSE	-1.77	-0.41
ZFP36L1	1.21E-01	4.84E-01	18.01	5.938605 734	19.4299 0388	1.51	FALSE	-0.55	0.31
MRPS2	3.15E-02	1.72E-01	18.02	4.542140 417	7.77927 5401	2.47	FALSE	6.06	4.32
NENF	7.99E-01	2.86E-01	18.04	6.800958 187	30.6559 8274	1.02	FALSE	1.98	0.56
DUSP12	8.17E-01	2.93E-01	18.14	3.468611 254	6.13291 7887	1.25	FALSE	-0.48	-1.03
FLJ30403	7.61E-02	8.71E-01	18.15	0.598011 003	3.40798 8308	1.44	FALSE	NA	NA
APEX1	7.41E-02	1.70E-01	18.19	5.445008 003	9.91907 6697	0.96	FALSE	-0.31	-0.60
NUP62	5.48E-01	4.64E-01	18.22	2.387450	4.82254	1.22	FALSE	1.90	3.41

	clinic.R.in ore	clinic.R. less	sc.All	sc.Old	sc.New	sc.Bul k	sc.Q.gene	tcga.Increased. risk	tcga.Increased.risk beyond.T.cells
		01		184	016				
LYPLA2	4.25E-01	4.36E-01	18.23	13.82195 911	2.61593 9526	1.18	FALSE	1.38	0.79
EEF1D	3.44E-01	6.12E-01	18.28	0.985759 893	7.45131 1433	1.02	FALSE	-0.45	1.00
ABCF1	4.22E-01	1.35E-01	18.31	7.435248 233	0.35607 0614	1.34	FALSE	3.23	2.37
SKAP2	2.81E-01	3.45E-01	18.37	0.456404 247	23.7208 6612	0.76	TRUE	-5.45	-3.16
GPS2	6.67E-01	3.04E-01	18.40	4.308701 037	7.88118 5647	0.55	FALSE	0.87	-0.37
SNRPA	2.81E-01	1.16E-01	18.50	3.411530 561	7.83545 4232	1.66	FALSE	1.41	1.64
SNRPD1	5.32E-01	2.38E-02	18.60	21.15658 975	0.55411 3785	0.82	TRUE	0.74	-0.30
NR2F6	5.66E-01	3.63E-01	18.64	8.495360 144	6.72771 0363	1.64	FALSE	3.63	2.14
IMPDH2	7.55E-02	4.30E-01	18.71	0.535373 592	30.6857 4445	1.02	FALSE	1.81	1.03
PSMC4	9.11E-01	1.04E-01	18.73	8.390998 517	3.11400 1291	0.46	FALSE	1.33	0.75
GPM6B	3.21E-01	7.52E-01	18.77	4.862310 428	33.4728 9854	0.32	FALSE	-0.57	-1.24
SNRPE	7.55E-01	3.43E-02	18.80	16.92686 645	0.33193 7635	0.74	TRUE	1.03	-0.49
ASS1	4.62E-01	1.92E-01	18.80	14.90230 724	0.46335 7928	0.85	FALSE	0.92	1.15
SF3B2	2.20E-01	6.96E-01	18.81	10.70469 624	15.0156 9271	0.94	FALSE	-0.31	-0.94
NDST1	3.03E-01	6.10E-02	18.82	7.522230 908	12.7278 3941	0.34	FALSE	2.20	2.95
RBM4	5.21E-01	4.82E-01	18.84	12.59107 638	10.0007 1396	1.52	FALSE	0.55	0.52
SERPINH1	9.28E-01	8.95E-03	18.85	37.92813 3	8.20048 5704	0.49	FALSE	0.99	0.91
RBP1	8.03E-01	2.16E-01	18.86	12.31936 246	4.52201 5287	-0.31	FALSE	0.36	-0.37
SCO1	8.30E-01	2.85E-01	18.86	12.77799 115	2.97447 8737	0.72	FALSE	0.54	-0.48
RAB20	7.25E-01	1.55E-01	18.87	0.538124 767	16.5852 5585	1.08	FALSE	-0.59	1.11
CRABP2	4.46E-01	4.25E-02	18.88	5.991748 766	0.81829 6256	0.73	FALSE	2.76	1.86
AURKB	5.17E-01	1.81E-02	18.88	9.869762 355	0.85916 5871	0.75	FALSE	2.28	1.41
DCTN5	1.03E-01	3.03E-01	18.90	3.150239 057	6.14026 7676	1.32	FALSE	1.98	1.58
POLD1	4.07E-01	2.17E-01	18.90	2.322155 697	4.86595 6872	0.55	FALSE	1.04	1.35
ENY2	6.49E-01	3.68E-01	18.91	24.95069 297	0.41050 8403	1.77	FALSE	-1.25	-1.00
QARS	4.42E-02	3.13E-01	18.96	3.706877 301	9.48829 2408	2.20	FALSE	2.33	1.73
TOP1MT	7.94E-01	1.59E-01	19.00	2.138074 483	7.06162 2399	1.01	FALSE	0.46	-0.34
MPDU1	2.78E-01	1.02E-01	19.02	12.07276 379	5.75865 2693	1.46	FALSE	2.19	2.00
SMC3	1.43E-01	2.89E-01	19.04	2.200475 748	26.6551 6067	1.37	FALSE	-1.26	-1.19
DTD2	7.61E-02	7.38E-01	19.06	0.454680 038	11.4742 5732	1.86	FALSE	NA	NA
TATDN1	1.17E-01	6.67E-01	19.10	6.785825 964	2.25200 4297	1.28	FALSE	-2.97	-3.70
UQCRC2	2.53E-02	3.72E-01	19.12	7.938348 231	5.09044 0135	0.94	FALSE	0.45	-0.44

	clinic.R.in ore	clinic.R. less	sc.All	sc.Old	sc.New	sc.Bul k	sc.Q.gene	tcga.Increased. risk	tcga.Increased.risk beyond.T.cells
RPP30	1.91E-01	2.11E-01	19.13	0.301420 634	11.7773 3863	1.87	FALSE	-0.60	-1.17
ATXN10	6.94E-01	2.97E-01	19.14	15.77144 524	13.4473 554	2.30	FALSE	0.57	-0.50
WDR81	9.64E-02	8.16E-01	19.17	1.702392 177	25.9390 4876	1.27	FALSE	2.80	2.13
PEPD	5.58E-01	2.73E-01	19.18	4.936443 511	11.4957 8245	1.14	FALSE	2.63	1.77
GAGE2B	2.57E-01	4.80E-01	19.18	17.70105 474	15.3573 6178	0.61	FALSE	-0.98	-2.19
FEN1	1.07E-01	2.62E-01	19.24	8.650445 933	5.65384 7713	0.63	FALSE	1.14	0.66
MRPS12	5.69E-01	1.66E-01	19.31	5.930175 903	5.31161 9169	1.32	FALSE	2.84	1.58
FKBP4	6.18E-01	5.52E-02	19.36	10.29840 259	1.10843 4516	1.06	FALSE	3.95	2.47
ALAS1	5.54E-01	3.19E-02	19.38	5.938125 987	9.87863 5076	1.06	FALSE	1.02	1.71
DPP9	1.83E-01	1.89E-01	19.42	0.678639 926	18.4124 4692	0.58	FALSE	2.05	1.88
ELAC2	5.97E-01	2.82E-01	19.45	12.02634 776	3.28783 9364	0.85	FALSE	3.04	1.34
RPS21	3.21E-01	5.10E-02	19.59	15.48074 181	4.43365 2949	0.81	FALSE	-0.61	-0.82
HYPK	9.14E-02	8.26E-02	19.62	15.88253 495	0.54156 1047	0.94	TRUE	NA	NA
THEM4	3.55E-01	4.66E-01	19.63	2.641838 036	14.1049 993	1.04	FALSE	0.60	-0.35
NXN	9.91E-01	1.25E-02	19.72	0.570380 212	4.96539 098	0.91	FALSE	0.84	1.70
ABR	3.48E-01	6.70E-01	19.73	1.706300 196	19.3613 9174	0.77	FALSE	2.16	1.33
DARS	3.52E-01	2.45E-01	19.76	5.495581 21	7.54473 926	1.48	FALSE	-1.49	-3.22
KCNAB2	6.30E-02	6.76E-01	19.79	3.601301 043	82.1749 82	1.14	FALSE	1.31	1.95
NUSAP1	1.31E-01	1.92E-01	19.90	4.885093 685	2.57669 1979	0.97	FALSE	0.59	0.37
STOML2	3.74E-01	6.99E-02	20.04	8.770091 625	2.09821 2208	1.02	FALSE	0.98	0.41
TOP2A	7.94E-01	4.05E-02	20.04	4.271010 52	1.77593 0792	1.05	FALSE	0.51	0.43
INTS7	8.16E-01	4.00E-02	20.23	6.644441 6	3.72007 6088	0.79	FALSE	0.71	0.87
MFAP4	2.69E-01	1.24E-01	20.27	17.64876 071	2.07063 2726	1.07	FALSE	0.53	2.01
MYADM	1.93E-01	6.15E-01	20.29	10.61246 616	11.6747 5742	1.39	FALSE	0.56	0.81
POLR3C	8.17E-01	1.79E-01	20.29	1.698797 211	13.4863 1224	1.26	FALSE	2.24	0.39
OXA1L	1.12E-02	3.08E-01	20.35	0.321055 708	42.3874 6933	2.14	FALSE	1.48	0.84
RRP15	6.36E-01	1.43E-01	20.36	4.607755 076	2.11199 0874	0.77	FALSE	-0.71	-2.44
GAS5	1.29E-01	5.14E-01	20.37	0.472735 128	48.1546 2574	0.76	FALSE	0.36	-0.61
HMGN1	6.43E-01	1.36E-01	20.39	6.749846 284	4.09002 5383	2.61	FALSE	-1.19	-0.56
BIRC5	4.62E-01	2.77E-01	20.53	3.988960 147	2.58911 6396	0.84	FALSE	2.08	1.65
NEK2	8.14E-01	3.28E-02	20.55	5.416078 429	2.17649 1052	1.71	FALSE	1.32	0.82
RRS1	8.28E-01	1.39E-01	20.58	10.21643 123	1.58067 3648	0.47	FALSE	0.67	0.47
PPP5C	4.71E-01	2.16E-	20.62	1.771526	8.36898	0.76	FALSE	1.43	0.61

	clink_Rjn ore	clinic R. less	sc.All	sc.Okl	sc.New	sc.IIil k	sc.Q.gmc	tca.Increased risk	tca.Incroiscd.ri.sk beyond.T.cells
		01		742	8743				
ARPC5	1.89E-01	8.71E-02	20.70	1.972299 705	13.3833 9241	1.47	FALSE	-3.00	-2.34
TMEM206	3.87E-01	7.69E-02	20.75	8.747393 842	9.67767 2637	2.21	FALSE	0.45	-0.31
GAGE4	9.87E-02	9.02E-01	20.76	20.72965 183	14.0070 9129	0.42	FALSE	-1.23	-2.28
EML4	9.25E-01	8.77E-02	20.79	12.05217 543	6.93482 5832	1.60	FALSE	-0.36	0.76
NT5DC2	1.03E-01	3.47E-02	20.89	8.113534 256	5.66234 2879	0.87	FALSE	4.32	1.93
GAGE12H	6.82E-01	2.28E-01	20.99	18.51606 224	13.9733 8677	0.70	FALSE	NA	NA
PA2G4	1.68E-01	1.03E-01	21.05	5.497595 07	1.67997 1385	1.66	FALSE	3.15	1.29
LOC10013 3445	5.36E-01	3.78E-01	21.09	3.452678 468	36.5509 2064	0.98	FALSE	NA	NA
RRM 2	4.18E-01	5.40E-02	21.19	3.042468 097	2.54502 9055	0.55	FALSE	0.92	0.82
GAGE2D	8.73E-03	3.59E-01	21.20	20.08829 393	14.2805 9448	0.62	FALSE	-1.16	-2.67
MRPL9	8.73E-01	4.07E-03	21.35	5.975779 42	6.14648 4827	1.12	FALSE	2.40	1.13
TMEM11	4.08E-01	1.35E-01	21.40	20.12015 326	1.01846 9789	0.89	FALSE	2.30	0.92
TPM4	2.84E-01	6.94E-02	21.55	8.611761 357	10.1410 9291	-0.31	FALSE	-0.32	-0.56
ESRG	1.86E-01	7.18E-01	21.56	0.451092 433	19.1285 2841	1.43	FALSE	NA	NA
SLC25A5	1.55E-01	6.97E-02	21.57	2.102500 624	13.0975 1618	0.79	FALSE	1.48	1.20
CYP51A1	2.25E-01	6.21E-01	21.57	1.084958 837	22.7515 9578	0.35	FALSE	0.48	-0.53
TBXA2R	7.68E-01	7.92E-02	21.58	1.441369 813	22.2980 5571	1.63	FALSE	-0.58	-0.43
LOC10012 8252	Inf	Inf	21.59	25.17189 358	14.0963 2693	0.36	FALSE	NA	NA
SKA2	8.87E-01	9.62E-02	21.67	5.316547 277	9.93793 0469	1.05	FALSE	-0.60	0.37
RUSC1	4.21E-02	3.03E-01	21.75	1.660172 441	20.8932 2619	0.95	FALSE	2.59	1.08
PSTPIP2	5.69E-01	3.55E-01	21.76	1.750472 311	11.7213 1361	1.49	FALSE	-2.63	0.44
LMCD1	1.57E-01	9.29E-01	21.91	6.221082 642	20.6117 2886	2.05	FALSE	-0.68	-0.33
TIMM23	6.53E-03	8.93E-02	21.92	5.327664 989	21.5501 0632	2.07	FALSE	NA	NA
NARS2	5.28E-01	9.12E-02	21.93	7.661886 481	16.6734 0475	1.86	FALSE	2.52	0.96
STRAP	6.79E-01	3.63E-01	21.97	4.999612 565	3.18913 343	1.85	FALSE	2.08	0.65
XRCC5	7.17E-01	2.58E-01	22.00	10.20245 23	3.78386 2242	2.03	FALSE	0.45	-0.49
EEF1G	4.35E-03	6.07E-01	22.24	3.623195 074	11.3778 5233	0.69	FALSE	0.57	0.44
FLAD1	2.73E-01	9.01E-02	22.24	9.115959 046	4.88990 0661	1.14	FALSE	5.30	3.34
PRDX3	1.28E-01	7.54E-01	22.26	1.506889 444	32.2419 1804	1.77	FALSE	-2.28	-1.43
GAGE2E	1.19E-01	2.55E-01	22.36	20.18764 216	14.8056 0626	0.69	FALSE	-1.21	-2.41

	clinic R in ore	clinic R less	sc.All	sc.Old	sc.New	sc.Bul k	sc.Q.gene	tfga.Incre! sed. risk	tfga.Increased.risk beyond T.cells
TUBGCP2	1.31E-01	5.85E-02	22.66	0.633889 067	43.1529 1198	0.99	FALSE	0.85	1.13
ORC6	7.21E-01	1.58E-01	22.71	0.700919 811	7.21907 4042	1.94	FALSE	NA	NA
GAGE12G	4.76E-01	1.69E-01	22.73	21.55374 302	14.0475 5971	0.65	FALSE	NA	NA
TSTD1	3.33E-02	9.76E-01	22.77	4.022382 197	28.1798 6342	0.77	FALSE	-1.68	-0.68
GAGE12E	8.00E-01	6.52E-01	22.80	22.08978 66	14.2987 637	0.63	FALSE	NA	NA
GAGE12C	6.13E-01	4.14E-01	22.81	22.08782 445	14.3028 4956	0.63	FALSE	NA	NA
NOP56	2.92E-01	1.32E-01	22.85	5.832178 979	12.6509 4704	0.93	FALSE	1.58	0.68
HNRNPAIP 10	4.99E-01	2.94E-01	22.87	10.61174 151	6.92785 4056	1.18	FALSE	NA	NA
H3F3AP4	3.96E-01	6.95E-01	22.91	11.05089 081	0.79095 3059	1.18	FALSE	NA	NA
ALDH18A1	3.46E-01	2.20E-02	22.94	15.61796 755	10.1284 6167	0.91	FALSE	1.76	1.87
HN1	1.94E-01	5.05E-02	23.04	12.03860 552	3.77552 5297	0.96	FALSE	1.78	1.68
CPXM1	5.09E-01	3.38E-02	23.05	34.54741 553	19.2357 018	0.59	FALSE	2.24	1.64
SEMA6A	2.72E-01	2.53E-01	23.06	2.112698 771	36.8658 6147	0.89	FALSE	5.02	3.59
PLTP	1.26E-01	1.21E-01	23.23	0.705496 057	32.7770 504	-0.35	FALSE	0.93	1.16
NA PRT1	1.05E-01	7.78E-01	23.49	2.243806 067	26.6341 8143	1.37	TRUE	0.57	0.58
CPSF1	4.77E-01	5.25E-01	23.53	4.938813 475	18.9944 5597	2.32	FALSE	0.49	1.64
BUB3	5.98E-03	2.03E-01	23.57	3.787914 349	14.6604 4954	0.94	FALSE	-0.59	-0.47
RGS16	7.20E-01	1.09E-01	23.66	24.77150 312	1.06162 3763	0.59	FALSE	-1.88	-0.96
AFMID	4.63E-01	6.89E-01	23.73	3.422504 125	5.08900 0714	1.48	FALSE	0.59	-0.43
SSR2	8.95E-01	3.81E-02	23.74	3.232954 04	13.3560 7135	0.81	FALSE	1.29	0.98
NDUFAF6	1.88E-01	3.96E-01	23.75	10.75636 07	2.52781 3066	1.97	FALSE	NA	NA
HSD17B14	6.74E-01	1.51E-01	23.76	0.434598 607	25.1751 0233	1.72	FALSE	1.16	1.55
GPC3	5.12E-01	1.16E-02	23.81	28.39313 231	5.63330 805	1.17	TRUE	1.77	1.50
PGAM1	1.41E-01	1.70E-01	23.81	1.192883 052	16.0990 166	0.93	FALSE	2.85	2.14
Cl16orf88	7.89E-01	7.76E-02	23.89	16.56262 336	4.40464 8103	2.01	FALSE	2.80	0.95
MSTO1	6.69E-01	1.41E-01	23.89	4.649573 196	15.3472 1826	2.10	FALSE	2.66	2.24
TSTA3	3.55E-01	3.22E-01	23.94	3.151005 81	16.3785 3925	2.68	FALSE	1.80	2.04
UBAP2L	1.55E-01	5.08E-01	23.97	1.815656 305	18.6483 2265	1.97	FALSE	5.67	2.94
Clorf198	9.00E-01	5.96E-04	24.06	3.577483 523	22.4333 289	0.58	FALSE	0.91	0.42
MAP1LC3A	9.31E-01	1.21E-01	24.10	3.104255 127	16.3976 6697	0.32	FALSE	-0.39	-0.34
ISG20L2	4.82E-02	7.63E-02	24.21	5.979207 631	5.76521 1543	2.61	FALSE	3.40	2.02
PHB2	2.37E-01	6.02E-01	24.23	5.049553 302	6.97004 1892	0.90	FALSE	2.24	0.97

	clinic.R.in ore	clinic.R. less	sc.All	sc.Old	sc.New	sc.Bul k	sc.Q.gene	tcga.Increased. risk	tcga.Increased.risk beyond.T.cells
SETDB1	4.06E-01	2.32E-01	24.24	7.633068 319	13.3659 3165	0.89	FALSE	2.05	1.23
MRPL15	7.82E-01	2.79E-01	24.35	14.96676 665	0.58139 0132	0.63	FALSE	0.78	0.45
MRPS16	1.40E-02	1.52E-01	24.39	2.641804 679	22.5309 111	1.30	FALSE	2.35	1.47
EIF2S3	3.38E-01	1.48E-01	24.47	1.156094 853	13.3749 7764	1.03	FALSE	-0.58	-0.91
ACAA2	4.20E-01	3.56E-01	24.48	15.52042 436	6.98892 0199	3.83	FALSE	1.04	0.47
TYRP1	2.10E-01	6.41E-01	24.53	1.989085 889	12.2744 8658	0.37	TRUE	4.01	3.07
HDAC2	6.57E-01	4.07E-02	24.61	10.46242 506	1.20833 2687	1.89	FALSE	-0.33	-0.87
PIH1D1	4.87E-01	3.31E-01	24.70	6.126480 848	5.91174 4655	0.82	FALSE	0.33	-0.49
KLHDC3	5.70E-01	5.28E-01	24.75	22.33788 991	0.66400 1516	1.15	FALSE	0.64	0.44
CBX5	3.09E-01	1.03E-01	24.89	9.713726 735	0.31012 8775	1.22	FALSE	0.56	0.91
GLOD4	4.51E-01	5.04E-01	25.00	7.219301 782	20.6899 4046	1.38	FALSE	0.87	0.44
ZNF146	8.68E-01	5.38E-02	25.03	9.080673 457	6.81987 5157	1.59	FALSE	-1.63	-1.82
NOP2	5.64E-01	7.22E-02	25.08	11.43230 613	4.15808 6545	1.14	FALSE	4.00	1.65
TTC39A	7.10E-01	2.95E-01	25.13	0.597290 641	46.8381 6572	1.24	FALSE	2.76	2.75
SRSF7	7.30E-01	9.45E-02	25.21	8.342370 883	11.0214 6198	2.23	FALSE	NA	NA
LHFPL3- AS1	1.04E-01	8.00E-01	25.24	1.251309 555	100.251 4925	1.11	FALSE	NA	NA
ARHGDI1B	6.71E-01	4.56E-01	25.26	5.905664 136	2.35219 4126	0.72	FALSE	-3.46	0.38
CYC1	5.00E-01	3.51E-01	25.32	6.635231 365	2.41938 6869	0.90	FALSE	1.34	1.07
ECH1	4.73E-01	6.23E-01	25.36	1.907500 873	11.8308 27	0.92	FALSE	0.78	0.46
DECR1	2.26E-01	3.03E-01	25.39	7.937262 507	8.72511 2226	1.50	FALSE	0.45	0.66
SET	6.42E-01	2.79E-01	25.45	4.492009 689	0.83100 7838	0.72	TRUE	0.94	1.17
MTG1	9.69E-02	1.90E-01	25.55	2.947736 591	23.2724 9486	1.53	FALSE	1.11	1.61
KIAA0020	1.64E-01	7.24E-02	25.57	9.604019 31	20.8418 105	3.17	FALSE	-0.87	-0.80
TMEM204	6.97E-01	1.75E-02	25.57	1.118931 472	23.0823 9672	1.12	FALSE	1.25	1.89
TPX2	5.81E-01	1.52E-02	25.77	6.760853 407	2.94437 134	1.10	FALSE	2.34	1.50
H19	5.96E-01	5.55E-02	25.91	23.61054 168	2.06812 358	1.12	FALSE	2.09	1.92
CCT3	7.28E-01	3.59E-02	26.21	1.163472 086	9.11957 5759	0.97	TRUE	2.53	1.55
MAZ	1.20E-01	6.09E-01	26.28	2.123839 678	31.4830 4112	1.74	FALSE	3.12	2.51
UBE2T	4.62E-01	5.78E-03	26.39	5.398937 996	6.61326 871	1.01	FALSE	1.24	0.33
FES	6.27E-01	4.01E-01	26.47	3.382276 111	18.3604 6107	0.93	FALSE	-0.51	0.43
VPS72	6.31E-01	5.39E-02	26.53	3.539245 137	18.5346 2929	2.49	FALSE	2.18	0.88
GAGE2A	8.47E-01	5.06E-01	26.66	26.34578 486	- 13.9686	0.74	FALSE	-1.31	-2.19

	clinic.R.in ore	clinic.R. less	sc.All	sc.Old	sc.New	sc.Bul k	sc.Q.gene	tcga.Increased. risk	tcga.Increased.risk beyond.T.cells
					2467				
TUFM	2.00E-01	4.80E-01	26.80	8.012399 21	6.85926 7668	1.22	FALSE	3.70	2.18
ARHGAP4	5.56E-01	4.68E-01	26.84	0.711358 224	23.0672 9832	0.64	FALSE	-2.39	0.44
CCT2	4.07E-01	1.05E-01	26.85	10.05194 913	1.60194 2797	1.94	TRUE	-0.36	-1.08
CDK1	2.44E-01	1.98E-01	26.89	8.429749 705	4.57957 5038	1.09	FALSE	0.50	0.37
TIMM22	7.29E-01	2.48E-01	27.00	11.76212 824	8.69167 1484	2.40	FALSE	2.25	1.64
UHRF1	1.91E-01	7.94E-02	27.05	11.51644 137	3.21263 6756	0.59	FALSE	1.58	1.23
PTGDS	1.81E-01	3.97E-02	27.10	1.823688 286	19.0243 1831	1.54	FALSE	-0.48	2.64
RPSA	7.46E-02	4.38E-01	27.28	0.915567 272	24.1354 4158	1.43	FALSE	0.54	0.86
RPL29	4.20E-02	3.07E-01	27.64	2.972270 992	52.8346 8434	0.64	FALSE	0.92	0.78
CECR5	6.73E-02	2.16E-01	27.64	13.82231 5	12.7346 6581	1.44	FALSE	2.59	1.35
HENMT1	7.20E-01	1.17E-01	27.70	10.62719 38	2.35501 8229	0.47	FALSE	NA	NA
SAMM50	7.10E-01	2.57E-02	27.73	5.612340 388	28.9160 6056	1.76	FALSE	3.26	1.17
PPAP2C	6.46E-01	1.02E-01	27.88	13.08854 512	13.3265 9581	0.63	FALSE	0.96	0.90
TRAF7	4.61E-02	5.61E-01	28.04	6.064625 478	9.78220 488	1.01	FALSE	2.88	2.20
NPL	5.63E-01	3.07E-01	28.07	0.304899 232	41.1394 0087	0.67	FALSE	0.45	0.83
NOSIP	7.94E-01	2.53E-01	28.19	7.332252 555	5.08641 8955	0.83	FALSE	0.65	0.73
UBE2C	4.15E-01	8.94E-03	28.23	9.149834 832	3.06241 0476	1.03	FALSE	2.08	1.46
RPL13A	1.11E-01	4.09E-01	28.31	1.051589 093	14.6293 3637	0.79	TRUE	-0.32	0.45
TUBA1B	4.48E-01	4.72E-01	28.35	7.111768 95	4.01197 9889	1.64	FALSE	2.11	2.10
MPZL1	9.84E-01	1.31E-02	28.40	2.648030 647	32.9871 6246	1.58	FALSE	1.65	0.74
LINC00439	8.10E-01	7.13E-02	28.43	11.22443 52	1.28953 0792	0.65	FALSE	NA	NA
NCBP1	5.60E-01	4.63E-01	28.57	5.488108 351	20.3950 1388	3.16	FALSE	0.36	0.42
SMIM15	5.85E-01	3.47E-01	28.60	6.239127 59	8.28036 221	0.36	FALSE	NA	NA
UQCRH	5.30E-01	2.97E-01	28.67	22.16415 41	0.33728 2219	1.11	TRUE	1.42	0.46
APP	7.36E-01	7.63E-02	28.72	9.599129 023	18.6987 9539	0.43	FALSE	0.36	0.59
ADSL	3.60E-01	4.89E-02	28.74	6.114321 09	24.6252 3135	2.18	FALSE	0.56	-0.90
UCK2	4.01E-01	2.08E-01	28.95	9.052578 861	3.56694 3066	1.07	FALSE	1.80	0.82
TP53I11	7.37E-01	2.79E-01	29.06	17.31232 856	3.33708 7794	1.14	FALSE	1.19	2.37
GPATCH4	5.94E-01	1.85E-01	29.10	12.26517 954	11.0302 3118	1.48	FALSE	0.81	-0.34
C20orf112	5.78E-01	1.41E-01	29.13	30.69758 56	2.95906 0323	3.54	FALSE	-0.60	-0.46
RPL17	4.53E-02	4.62E-01	29.30	5.134546 488	21.6912 7968	1.41	FALSE	-0.53	-0.65
BGN	4.65E-01	1.30E-01	29.51	11.64816 463	0.49018 527	1.80	FALSE	1.45	2.25
BCCIP	4.09E-01	9.82E-02	29.59	5.686214 848	17.7761 4765	1.64	FALSE	-0.86	-1.00
CALM3	6.27E-01	2.48E-01	29.70	5.470474 648	20.6990 5116	0.69	FALSE	2.37	2.29
FAM178B	7.63E-01	1.55E-	29.73	-	24.8879	0.43	FALSE	0.77	0.55

	clinic. R in ore	clinic. R less	sc.Au	sc.OKI	sc.New	sc.Hil k	sc.Q gene	tcga.Increased risk	tcga.Iincreaseil.risU lieyond.T.cells
		02		0.777212 747	1609				
PAICS	3.90E-01	5.41E- 01	29.76	3.312032 659	24.2686 9834	1.74	FALSE	1.52	0.48
TSR1	5.73E-01	1.43E- 01	29.94	11.25783 989	1.50263 5952	2.19	FALSE	0.94	0.32
DDX21	5.48E-02	4.82E- 01	29.97	3.930072 862	12.6570 417	0.62	FALSE	-0.65	-0.52
METAP2	4.28E-01	4.93E- 01	30.02	11.00208 454	8.13944 0078	1.75	FALSE	-0.92	-2.24
TPM1	1.25E-01	3.35E- 01	30.15	16.47245 443	3.78054 5609	1.38	FALSE	-0.36	0.45
CHP1	1.28E-03	7.38E- 01	30.25	0.401031 609	22.8692 9931	0.99	FALSE	NA	NA
DDX50	4.87E-02	6.45E- 01	30.29	4.624495 525	16.8467 8101	1.01	FALSE	-2.74	-2.56
RPL30	3.28E-01	5.91E- 01	30.39	14.92031 239	3.61843 6257	0.77	FALSE	-0.63	-0.43
FBLN2	3.82E-01	2.03E- 03	30.66	7.803353 827	7.69571 0285	1.55	FALSE	0.87	1.75
BANCR	1.42E-01	5.48E- 01	30.82	3.861608 173	8.40273 4173	0.46	FALSE	NA	NA
SCIN	6.93E-01	5.54E- 02	31.02	2.738650 819	81.9465 8272	1.03	FALSE	0.70	1.60
C19orf48	7.07E-01	2.88E- 01	31.11	6.190544 609	6.03867 728	1.17	FALSE	2.31	1.10
RPL5	2.21E-01	4.46E- 01	31.16	6.752007 916	6.99791 5457	1.15	FALSE	-0.84	-1.18
SCD	1.21E-01	6.04E- 01	31.17	18.67992 188	88.9847 3766	0.55	TRUE	0.71	0.59
MDH2	2.90E-01	2.00E- 01	31.18	7.906322 813	3.89530 2932	1.76	TRUE	2.21	0.97
PRAME	4.80E-01	4.11E- 01	31.19	9.259758 737	33.8924 5342	2.16	FALSE	0.32	-0.41
HNRNPA1	3.07E-01	1.30E- 01	31.31	4.371453 406	3.26997 2055	1.46	TRUE	-0.33	-0.43
SCNM1	2.19E-01	1.06E- 01	31.31	3.806661 745	7.46341 7038	1.35	TRUE	1.13	0.51
TUBB	2.22E-01	2.35E- 01	31.61	3.915227 069	4.37910 9031	1.16	TRUE	2.41	1.48
KLHDC8B	1.33E-01	4.28E- 01	31.64	2.496474 168	41.3155 0213	1.51	FALSE	2.20	2.37
ASAP1	2.03E-01	3.78E- 01	31.68	3.393690 401	25.6152 7297	1.04	FALSE	0.31	1.36
CD68	1.98E-01	3.79E- 01	31.75	1.979897 879	50.2119 6829	0.57	FALSE	-1.06	0.58
ANP32E	4.92E-01	2.24E- 01	31.96	12.31896 695	6.59729 4926	0.68	FALSE	-1.10	-0.82
ITM2C	9.63E-01	1.39E- 02	32.08	8.323594 178	9.18073 0963	0.37	FALSE	0.59	0.59
VDAC2	8.01E-02	3.76E- 01	32.24	1.012942 241	29.4639 8783	0.83	FALSE	1.61	0.74
EGFL8	4.52E-01	1.29E- 01	32.55	12.73725 487	42.5645 6272	1.01	FALSE	1.36	1.54
RPS11	1.39E-01	2.94E- 01	32.62	6.172582 657	42.7020 0252	0.39	FALSE	0.32	0.36
GRWD1	4.38E-01	5.24E- 01	32.83	10.91432 61	5.02004 0199	1.24	FALSE	5.62	3.78
Cs	1.65E-01	7.41E- 01	33.27	6.422065 041	17.1233 515	2.24	FALSE	5.08	2.61
FAM92A1	1.80E-01	1.18E- 02	33.62	23.12776 574	3.34455 4005	0.74	FALSE	-1.33	-2.16
NDUFS2	7.10E-01	9.12E- 02	34.33	3.683553 625	26.4960 6832	2.86	FALSE	1.87	0.56
PPA1	1.68E-02	7.35E- 01	34.57	4.191072 237	36.2446 0964	1.33	FALSE	-3.57	-1.51
THOC5	4.22E-01	3.11E- 01	34.76	23.72211 148	8.65559 4417	1.61	FALSE	0.56	-0.39

	clink.R_in ore	clinc.R. less	sc.All	sc.Oiq	sc.New	sc.Bul k	sc.Q.gene	Ug.Increased. risk	tcga.Increased.risk beyond .ccls
NF2	2.21E-01	4.46E-01	35.44	5.935951 855	29.6830 3947	1.87	FALSE	3.24	2.59
SMS	3.48E-01	3.36E-01	35.45	10.57117 775	7.55438 5933	3.53	FALSE	0.82	0.45
MARCKS	2.18E-01	8.98E-01	35.55	1.393466 011	26.7190 5725	0.42	TRUE	-0.60	-0.35
TRPM1	2.73E-02	4.37E-01	35.72	18.29374 495	70.9018 7013	0.92	TRUE	3.10	2.37
RPL10A	4.87E-02	3.71E-01	35.75	6.395271 832	19.8959 5719	1.43	FALSE	0.56	0.44
LYPLA1	3.39E-01	5.06E-01	36.15	10.23638 354	8.32018 4641	1.87	FALSE	-2.44	-1.87
FBL	5.03E-01	3.43E-01	36.53	4.637441 097	24.8528 6255	1.35	FALSE	2.64	1.65
ZNF286A	9.41E-01	4.19E-02	36.53	14.14241 98	2.76828 4631	1.36	FALSE	-0.47	-0.77
LIMD2	5.49E-01	1.46E-01	36.60	2.122873 767	9.29510 2203	1.17	FALSE	-0.75	2.94
TULP4	2.15E-01	8.43E-02	36.72	3.566475 392	21.1174 1429	1.35	FALSE	0.87	1.16
TIMM13	5.36E-01	2.65E-01	37.26	13.78610 742	7.02180 3959	0.77	FALSE	2.20	1.24
RPAIN	5.60E-01	1.47E-01	37.35	20.39074 062	4.48494 7614	1.21	FALSE	-0.81	-1.76
RBM34	3.24E-01	2.16E-01	37.89	2.249744 298	18.8675 2144	2.58	FALSE	-1.41	-2.72
AHCY	3.78E-01	5.00E-02	38.02	10.57704 66	15.4687 9045	2.09	FALSE	2.49	1.19
MLLT11	9.77E-01	1.52E-02	38.08	44.02874 412	1.88444 4301	0.56	TRUE	0.76	0.55
MYBBP1A	6.00E-01	2.83E-01	38.23	29.53471 619	4.32435 2219	1.57	FALSE	2.43	1.71
AEN	5.21E-02	2.42E-01	38.35	14.49457 588	12.6910 7053	2.30	FALSE	3.38	2.32
TRIM28	3.81E-01	3.31E-01	38.48	14.93519 938	7.65022 211	1.28	FALSE	2.93	2.05
NOLC1	2.47E-02	2.92E-01	38.64	8.507240 496	23.2024 8731	1.84	FALSE	3.61	2.77
SHMT2	2.12E-01	1.72E-01	38.82	7.774111 14	5.09944 1692	0.97	FALSE	2.62	1.34
TYMS	4.65E-01	1.60E-01	38.85	5.796612 685	6.72125 9278	1.64	FALSE	2.02	1.91
RPS12	3.71E-02	4.01E-01	38.95	6.384081 023	4.08278 2447	1.08	FALSE	0.45	0.39
SORD	2.73E-02	3.55E-01	38.98	9.939454 508	11.4966 5193	2.10	FALSE	3.16	1.05
RPL7	4.01E-01	3.36E-01	39.04	11.15340 377	3.78274 3401	1.06	FALSE	-0.38	0.30
ESRP1	4.44E-01	4.55E-02	39.09	10.06244 484	25.1069 7937	1.20	FALSE	2.42	1.76
BZW2	6.62E-01	1.05E-01	39.22	21.62172 441	26.9244 2566	0.92	FALSE	1.37	0.90
RPL18A	8.24E-02	3.34E-01	39.43	2.878936 474	36.6984 4039	0.51	TRUE	1.13	1.24
CA14	3.81E-02	1.81E-01	39.82	3.998230 163	67.4306 5241	0.77	FALSE	2.21	1.79
SKP2	9.82E-01	1.14E-02	39.93	21.51868 872	1.28341 7716	1.83	FALSE	1.68	1.42
DCAF13	4.60E-01	2.72E-01	40.41	24.87612 305	1.56429 7695	2.88	TRUE	-1.21	-1.72
HMGA1	6.81E-02	6.40E-01	40.42	19.74301 642	5.93647 9134	0.83	FALSE	0.84	0.52
KIAA0101	4.38E-01	5.20E-02	41.14	5.177374 736	9.34349 1776	1.31	FALSE	-0.55	-0.59
CTPS1	8.43E-01	8.35E-02	41.34	24.76379 084	7.76565 0207	1.78	FALSE	NA	NA
PPP2R1A	3.35E-01	5.52E-01	42.96	5.321317 629	16.8131 3352	1.23	FALSE	5.38	2.24

	clinic.R in ore	†lnR.R. less	sc.All	sc.Old	sc.New	sc.Bul k	sc.Q.gene	g. Increased risk	tcga.Increascd.risk beyond T.cells
FBLN1	5.09E-01	4.76E-03	43.12	7.246750 299	20.2794 9953	1.92	FALSE	1.65	2.28
RNF2	8.06E-01	2.83E-02	43.71	8.672094 386	7.73690 4785	2.07	FALSE	-0.38	-0.97
CDCA7	6.15E-01	3.99E-02	43.91	5.924051 047	11.4716 3669	1.55	FALSE	0.55	0.97
RPS6	8.53E-02	5.20E-01	43.91	1.692897 361	54.0756 381	0.83	TRUE	-1.35	-1.38
ILF2	8.63E-01	1.77E-03	45.26	6.943339 213	14.8497 2817	1.39	FALSE	1.31	0.79
RPL18	9.66E-02	2.25E-01	45.37	3.114484 434	48.2506 6529	0.95	FALSE	1.39	1.27
UQCRFS1	4.79E-01	1.04E-01	45.94	2.404437 46	31.0840 894	0.72	FALSE	3.57	1.57
RUVBL2	7.03E-01	3.34E-01	46.06	9.456736 484	13.3900 2528	1.57	FALSE	2.93	1.38
RPL26	1.01E-01	1.65E-01	46.82	16.99198 955	14.0939 6856	0.84	FALSE	-2.08	-2.60
RPS27	1.47E-02	3.83E-01	47.85	6.873462 208	48.3169 4024	0.66	FALSE	-0.90	0.30
CDKN2A	5.27E-01	6.49E-01	48.20	1.937507 613	16.9016 692	0.77	TRUE	-0.46	-0.33
MIR4461	9.23E-01	1.12E-02	48.20	5.488218 285	21.5615 8776	1.49	FALSE	NA	NA
TPM2	5.40E-01	2.36E-02	48.33	47.15134 153	0.45206 8271	0.90	TRUE	-0.30	0.49
CNRIP1	4.03E-01	5.26E-01	48.87	10.22154 305	16.2593 5254	1.06	FALSE	-0.36	-0.36
PAFAH1B3	3.38E-01	4.49E-01	49.53	9.159237 785	28.8635 675	1.14	FALSE	1.48	0.86
FAM174B	6.29E-01	2.83E-01	50.07	15.22332 615	36.2291 0751	1.63	FALSE	3.44	1.88
USP22	4.57E-01	4.65E-01	51.05	32.02385 954	8.72117 1083	1.03	FALSE	2.18	1.05
GTSF1	8.47E-01	2.11E-01	51.20	89.51451 745	29.3956 8184	1.35	TRUE	-3.43	-1.39
ISYNA1	5.19E-01	3.37E-01	51.20	8.162255 211	38.3377 3761	3.05	FALSE	1.99	1.79
DLL3	8.77E-01	6.01E-02	51.70	14.88708 119	20.3077 5936	3.27	FALSE	3.09	2.42
TMC6	3.36E-01	5.51E-02	52.13	5.290669 679	67.7112 702	2.25	FALSE	2.61	3.47
RPS18	7.25E-02	7.13E-01	52.28	27.56806 633	18.6352 6549	0.69	FALSE	0.61	0.32
NREP	6.54E-01	6.71E-03	52.32	66.79439 813	16.6762 9308	0.68	TRUE	NA	NA
RPL21	3.07E-01	2.13E-01	52.38	3.737360 847	14.0661 9494	2.11	TRUE	-1.10	-1.33
RPS3	5.62E-02	3.60E-01	52.44	10.48799 182	69.4537 1116	1.37	FALSE	0.97	0.76
RPS5	2.04E-02	3.71E-01	56.38	4.847150 55	32.7126 0656	0.81	TRUE	1.33	0.83
EIF4A1	7.28E-01	1.85E-01	56.54	12.44176 552	23.7977 7896	1.45	FALSE	1.80	0.60
GPI	1.17E-01	3.72E-01	57.12	1.130371 128	45.7648 0744	1.30	TRUE	4.46	2.91
BCAN	7.45E-01	2.02E-01	57.20	2.308514 409	72.9791 1384	0.48	FALSE	3.07	3.42
FTL	2.64E-01	3.99E-01	57.23	1.205064 194	75.2369 9673	1.17	FALSE	0.51	2.31
DCT	3.01E-01	4.11E-01	58.58	1.023830 081	123.936 0976	0.58	TRUE	1.78	2.06
RPS16	2.08E-01	4.47E-02	58.91	5.580237 253	61.9000 3741	1.24	FALSE	0.90	0.61
RPL6	1.02E-01	5.40E-01	60.07	16.14902 123	9.90401 0704	2.18	TRUE	-0.35	-0.63
IDH2	6.45E-01	1.16E-01	60.71	11.44171 851	14.0597 6702	1.57	FALSE	-0.31	1.14

	clinic. R in ore	clinic. 11 less	sc.MI	sc.Old	sc.New	sc.Bil k	sc.gene	tcgilll.reisen. risk	tcga.Incroiscd.risk be.yond.T.clls
H3F3A	3.97E-01	4.63E-01	61.79	14.22533 613	3.66789 3274	1.73	TRUE	-0.70	-0.70
EIF3K	3.13E-01	9.04E-02	61.83	8.143610 635	22.7512 6648	0.89	FALSE	2.25	1.49
SAE1	7.36E-01	1.87E-01	64.08	5.547424 178	19.2009 9815	1.27	FALSE	3.78	2.16
TIMM50	6.48E-01	9.10E-02	65.03	5.084853 086	35.2953 8079	1.29	FALSE	2.94	1.91
RPS24	8.85E-02	3.75E-01	66.05	3.716330 306	98.7798 9575	1.30	FALSE	-0.64	-0.62
RPL28	1.50E-02	4.21E-01	67.31	5.833859 88	54.9536 147	0.71	TRUE	0.99	1.01
MIDI	1.41E-01	5.75E-01	68.45	30.60224 621	19.9879 4862	1.40	FALSE	1.53	1.43
MAGEA4	6.31E-01	2.50E-01	70.13	154.8532 59	37.7726 8982	0.76	TRUE	-1.19	-1.25
SOX4	4.33E-01	3.28E-01	71.11	26.06105 51	13.4306 1044	2.03	FALSE	1.15	0.82
EIF4EBP2	4.09E-02	5.48E-01	71.92	4.991883 552	41.1208 7104	1.61	FALSE	0.57	1.03
SNAI2	3.83E-01	1.30E-01	75.43	7.149559 432	49.1718 5344	1.36	FALSE	1.35	1.14
FOXRED2	2.26E-01	4.31E-01	75.45	12.49982 549	58.2133 9609	3.02	FALSE	3.28	1.62
RPL13AP5	1.17E-01	2.58E-01	77.82	2.595272 255	72.7402 9977	0.90	TRUE	NA	NA
PABPC1	1.84E-01	6.67E-01	79.27	7.945824 677	66.8858 1105	1.76	FALSE	-0.44	0.64
RPL8	1.61E-01	5.12E-01	79.52	0.613777 713	40.1608 0849	1.75	TRUE	0.73	1.10
RPS7	1.97E-01	2.87E-01	79.88	12.55655 574	40.6271 1274	1.62	FALSE	-0.52	-0.79
CIQBP	4.72E-01	1.88E-01	84.82	24.30944 797	14.3704 7936	1.82	TRUE	1.60	0.63
TP53	5.16E-01	4.69E-01	85.56	32.44957 009	13.4499 0773	1.60	TRUE	0.40	0.47
Cl7orf76- AS1	7.92E-01	9.18E-02	87.51	6.678852 726	62.5386 0033	1.51	FALSE	NA	NA
PTP4A3	5.09E-01	1.18E-01	94.12	18.75491 086	26.9741 7247	3.61	FALSE	1.56	1.83
PFN1	3.26E-01	2.42E-01	96.68	20.38345 9	27.1648 7933	2.07	FALSE	1.34	2.82
RPLPO	5.66E-02	6.51E-01	102.20	8.883720 005	57.6445 3707	1.97	TRUE	1.37	0.73
RPS19	1.31E-01	3.50E-01	116.49	8.842607 397	97.0926 3286	1.07	TRUE	1.43	1.14
SERPINF1	1.90E-01	4.68E-01	138.29	45.36545 505	71.2467 1866	3.31	FALSE	0.79	0.87

Table 3. Down-regulated and Up-regulated genes post-immunotherapy treatment in malignant cells

Down-regulated	post-treatment	Up-regulated	post-treatment
ABHD2	ITM2B	ACAA2	PRDX3
AGSL1	JUNB	ADSL	PSTPIP2
AHNAK	KCNN4	AEN	PTGDS
AHR	KIAA151	AHCY	PTP4A3
AIM2	KLF4	ALDH1B1	RBM34
ANGPTL4	KLF6	ARHGEF1	RBM4
ANXA1	LAMB1	ARPC5	RPL10A
ANXA2	LAMP2	ATXN10	RPL17
ATOL	LGALS1	ATXN2L	RPP30
ATF3	CTSL	B4GALT3	RPS3
ATMA1	ENC0116	BCCIP	RPS7
ATP1B3	LOC10127488	BGN	RPSA

Down-regulated post-treatment		Up-regulated post-treatment	
BBX	LOXL2	C10orf32	RUVBL2
BCL6	LOXL3	C16orf88	SAMM50
BIRC3	LPL	C17orf76-AS1	SBN01
BSG	LXN	C20orf112	SERPINF1
C16orf45	MAGEC2	CDCA7	SKP2
C8orf40	MF12	CECR5	SLC45A2
CALU	MIA	CPSF1	SMC3
CARD16	MT1E	CS	SMG7
CAV1	MT1F	CTCFL	SMS
CBFB	MT1G	CTPS1	SNAI2
CCDC109B	MT1M	DLL3	SORD
CCND3	MT1X	DTD2	SOX4
CD151	MT2A	ECHDC1	SRCAP
CD200	NFE2L1	ECHS1	SRSF7
CD44	NFKBIZ	EIF4A1	STARD10
CD16	NNMT	EIF4EBP2	TBXA2R
CD47	NOTCH2	EIF6	THOC5
CD58	NR4A1	EML4	TIMM22
CD59	OS9	ENY2	TIMM23
CD9	P4HA2	ESRG	TMC6
CD97	PDI4B	FAM174B	TOMM22
CDH19	PEL1	FAM213A	TPM1
CERS5	PIGT	FBL	TSNAX
CIB	PMAIP1	FBLN1	TSR1
CHI3L2	PNPLA8	FDXR	TSTA3
CLIC2B	PPAPDC1B	FOXRED2	TULP4
CLIC4	PRKCDBP	FXN	UBAP2L
COL16A1	PRNP	GALT	UCHL5
COL5A2	PROS1	GEMIN8	UROS
CREG1	PRSS23	GLOD4	VPS72
CRELD1	PSMB9	GPATCH4	WDR6
CRYAB	PSME1	HDAC2	XPNPEP1
CSPG4	PTPMT1	HMGN3	XRCC5
CST3	PTRF	HSD17B14	YDJC
CTNNA1	RAMP1	IDH2	ZFP36L1
CTSA	RND3	ILF2	ZNF286A
CTSB	RNH1	ISYNA1	
CTSD	RPN2	KIAA0020	
DCBLD2	S100A10	KLHDC8B	
DCTN6	S100A6	LMCD1	
EGR1	SCCPDH	LOC100505876	
EMP1	SERINC1	LYPLA1	
EPDR1	SERPINA3	LZTS2	
FAM114A1	SERPINE1	MAZ	
FAM46A	SERPINE2	METAP2	
FCRLA	SLC20A1	MID1	
FN1	SLC35A5	MIR4461	
FNDC3B	SLC39A14	MPDU1	
FXYD3	SLC5A3	MPZL1	
G6PD	SMIM3	MRPS16	
GAA	SPARC	MSTO1	
GADD45B	SPRY2	MTG1	
GALNS	SQRDL	MYADM	
GBP2	STAT1	MYBBP1A	
GEM	SUMF1	MYL6B	
GRAMD3	TAP1	NARS2	
GSTM2	TAPBP	NCBP1	
HLA-A	TEKT4P2	NDUFAF6	
HLA-C	TF	NDUFS2	
HLA-E	TFAP2C	NF2	

Down-regulated post-treatment		Up-regulated post-treatment	
HLA-F	TMEM43	NHEJ1	
HPCAL1	TMX4	NME6	
HSP90B1	TNC	NNT	
HTATIP2	TNFRSF10B	NOLC1	
IFI27L2	TNFRSF12A	NTHL1	
IFI44	TSC22D3	OAZ2	
IFI6	TSPAN31	OXA1L	
IFITM3	UBA7	PABPC1	
IGF1R	UBC	PAICS	
IGFBP3	UBE2L6	PAK1IP1	
IGFBP7	XPO7	PFN1	
IL1RAP	ZBTB20	POLR2A	
ITGA6	ZDHHC5	PPA1	
ITGB3	ZMYM6NB	PRAME	

[0381] The signature was down-regulated in resistant tumors for genes associated with coagulation, apoptosis, TNF-alpha signaling via NFkB (NFKBIZ), Antigen processing and presentation (e.g., MHC-I, HSPA1A), metallothioneins (e.g., MT2A, MT1E) involved in metal storage, transport, and detoxification, and IFNGR2 (Gao et al. *Cell* 2016).

[0382] The signature was up-regulated in resistant tumors for genes associated with negative regulation of angiogenesis and MYC targets.

[0383] Serine protease inhibitors (SERPINs), which are involved in protease inhibition and control of coagulation and inflammation were differentially expressed in the signature. Prior studies relate to recurrent *SERPINB3* and *SERPINB4* mutations in patients who respond to anti-CTLA4 immunotherapy (Riaz et al. *NG* 2016). *SERPINA3*, *SERPINA1*, *SERPINE2* were down-regulated in resistant tumors. *SERPINF1*, *SERPINB9* were up-regulated in resistant tumors.

[0384] The resistance signature also strongly correlated with MHC-I expression (**Figure 22**). One of the tumors in the cohort has a wide range of MHC-I expression in the malignant cells. Applicants filtered HLA genes from the resistance signature, and scored the malignant cells. The malignant cells with the highest resistance scores in this tumor under express MHC-I.

[0385] There are 13 different metallothioneins and 6 of them are moderately/highly expressed in the melanoma malignant cells. When Applicants scored the cells according to this mini-signature separation between the treated and untreated samples was observed (**Figure 23**). Therefore, a signature only including metallothioneins may be used in the methods of the present invention.

The prognostic value of the post-immunotherapy modules

[0386] Applicants discovered that the immunotherapy resistance signature was also predictive of survival rates in tumors. The prognostic value of the signature is significant ($P = 1.6e-05$), even when accounting for T-cell infiltration scores as shown by analyzing samples in the cancer genome atlas (TCGA) (**Figure 24**). The resistance signature performs better than other single-cell based signatures in predicting high and low survival rates (**Figure 25**).

[0387] To further examine the generalizability of the PIT modules Applicants analyzed the bulk gene expression data of melanoma tumors from The Cancer Genome Atlas (TCGA). As Applicants saw at the single-cell level, Applicants find that the genes within each module are co-expressed across tumors, while the two modules are negatively correlated. Applicants postulated that higher expression of the PIT-up program and a lower expression of the PIT-down program might indicate that the tumor is more resilient against immune-mediated clearing, resulting in a more aggressive disease. To test this hypothesis, Applicants scored each tumor according to the immunotherapy modules and examined the prognostic value of these scores. Indeed, the immunotherapy scores are significantly associated with patient survival, such that the expression of the PIT-up (down) signature is associated with lower (higher) survival rates (**Figure 24, 25**).

[0388] To examine the significance of this finding Applicants performed the same analysis with signatures that were previously identified based on the analysis of the single cell melanoma data (Tirosh *et al*, Dissecting the multicellular ecosystem of metastatic melanoma by single-cell RNA-seq. Science. 2016 Apr 8;352(6282):189-96). Applicants divided these signatures into two groups: (1) malignant signatures - signatures that describe the state of the malignant cells, as cell cycle, and the AXL and MITF signatures, which were previously shown to be associated with the response to targeted therapy; (2) tumor composition signatures that describe a specific cell type or the state of a non-malignant cell type within the tumor microenvironment. None of the malignant signatures is significantly associated with patient survival, indicating that mere variation across malignant cells is not sufficient to yield such results. The cell-type signatures are associated with patient survival, especially those that related to T-cell infiltration, though their prognostic signal is redundant when accounting for tumor purity. The latter is estimated based on CNVs.

[0389] Importantly, the prognostic value of the PIT scores is significant even when accounting for the tumor purity and T-cell infiltration scores. Interestingly, the PIT-up (down) scores are negatively (positively) correlated to the T-cell scores, as Applicants further describe herein. Nonetheless, the combination of the PIT and T-cell scores yields

significantly more accurate predictions of patient survival compared to those obtained when using each score separately, indicating that the PIT modules capture tumor properties that cannot be explained just by T-cell infiltration levels.

The post-immunotherapy modules are associated with response to anti-PD1 and anti-CTLA4 in the clinic and in mouse models

[0390] Immunotherapy introduces selective pressures that, in case of an unsuccessful treatment, are likely to increase the abundance of immunotherapy-resistant cells. The post-immunotherapy signatures Applicants derived might capture these resistant cell states, and, as such, may help to detect innate resistance to anti-PD-1 or anti-CTLA4 therapy - pretreatment. To examine this concept Applicants analyzed the gene expression profiles of responding ($n = 15$) and non-responding ($n = 13$) tumors sampled prior to anti-PD-1 therapy. Indeed, the tumors of responders overexpressed the PIT-down signature and underexpressed the PIT-up signature, resulting in accurate predictors of response to anti-PD-1 ($P = 3.38e-02$ and $5.5e-04$, Area Under the Receiver Operating Characteristic Curve (ROC-AUC) = 0.91 and 0.77. In another gene expression cohort of pre-anti-CTLA-4 melanoma tumors the signatures did not yield a significant separation between the responders and non-responders. Therefore, Applicants set out to test the signatures in a more controlled setting of a murine model, in which genetically identical mice that experienced the same environment and treatment display a dichotomous response to anti-CTLA4. Indeed, responders scored higher for the PIT-down signature and lower for the PIT-up signature, resulting in accurate predictors of response to anti-CTLA4 in this model ($P = 1.2e-05$, ROC-AUC = 0.99). The ITR signature was predictive of eventual outcome in both mouse and human data. First, in a bulk RNA-Seq study of anti-CTLA4 therapy in mouse, the malignant ITR score predicted well non-responders compared to responders. Applicants analyzed 27 patients associated with anti-PD1 response (Hugo et al., 2016). The malignant ITR was significantly lower in pre-treatment samples from patients with complete response compared to those with partial or no response (**Figure 26**). The (5) complete-responders in the data of Hugo et al. scored lower for the sc-resistance signature compared to the other 22 patients ($P = 9.37e-04$). These results indicate that the signatures identified capture cell states that are linked to anti-PD1 and anti-CTLA4 resistance.

[0391] Genes that were up-regulated in the resistant tumors (single cell) were down-regulated in CR vs. others ($P = 9.6e-14$) and C/PR vs. NR (NS) (**Figure 27**). Genes that were

down-regulated in the resistant tumors (single cell) were up-regulated in CR vs. others ($P = 2.8e-1$) and C/PR vs. NR ($P = 2.8e-03$) (**Figure 28**).

Associating melanoma-cell-intrinsic states with T-cell infiltration and exclusion.

[0392] Tumor infiltration with T cells is one of the strongest predictors of patient response to immune checkpoint inhibitors in various cancer types. Understanding the molecular mechanisms that underlie spontaneous T-cell infiltration could aid the development of therapeutic solutions for patients with non-inflamed tumors. Applicants leveraged the single-cell data and bulk gene expression cohorts of melanoma tumors to map malignant transcriptional states that are associated with T-cell infiltration or exclusion.

[0393] First, Applicants analyzed the single-cell data to derive a CD8 T-cell signature, consisting of genes that are primarily expressed by CD8 T-cells (Methods). Applicants used this signature to estimate the T-cell infiltration level of melanoma tumors based on their bulk gene expression profiles. Applicants show that patients with more T-cell infiltration, according to this measure, are more likely to respond to anti-CTLA4 and to MAGE-A3 antigen-specific immunotherapy, and have better overall survival. Next, Applicants identified based on the single-cell data genes that are expressed primarily by malignant melanoma cells. Applicants then searched for genes that are correlated with T cell abundance in the bulk TCGA gene expression cohort, while restricting the search only to the malignant-specific genes to derive an *initial* T-cell-infiltration signature (T cell exclusion signature (T-ex).

[0394] While the initial signature is informative, it is limited for two main reasons. First, there are only 384 genes that could be confidently defined as exclusively expressed by the malignant melanoma cells. Second, it cannot confidently identify genes whose expression in the malignant cells will exclude T-cells. To overcome these limitations, Applicants used the initial T-cell infiltration signature only as an anchor, and searched for genes whose expression level in the individual malignant cells is positively or negatively correlated to the overall expression of this initial signature. Applicants defined genes that are strongly positively (negatively) correlated to the initial signature as the infiltrated (non-infiltrated) module. Of note, non-malignant cells express most of the genes in these modules, and hence it would have been difficult to associate them with T-cell infiltration without leveraging the single-cell data.

[0395] The genes in the infiltrated module (exclusion-down) play a major role in antigen processing and presentation (ULA-A/B/C, B2M, TAPBP) and interferon gamma response (e.g., IFI27, IFI35, IRF4, IRF9, STAT2). In certain embodiments, the infiltrated module

includes the following genes: A2M, AEBP1, AHNAK, ANXA1, APOC2, APOD, APOE, ATP1A1, ATP1B1, C4A, CAPN3, CAV1, CD151, CD59, CD63, CDH19, CRYAB, CSPG4, CSRP1, CST3, CTSB, CTSD, DAG1, DDR1, DUSP6, ETV5, EVA1A, FBX032, FCGR2A, FGFR1, GAA, GATSL3, GJB1, GRN, GSN, HLA-B, HLA-C, HLA-F, HLA-H, IFI35, IGFBP7, IGSF8, ITGA3, ITGA7, ITGB3, LAMP2, LGALS3, LOXL4, LRPAP1, LY6E, LYRM9, MATN2, MFGE8, MIA, MPZ, MT2A, MTRNR2L3, MTRNR2L6, NPC1, NPC2, NSG1, PERP, PKM, PLEKHB1, PROS1, PRSS23, PYGB, RDH5, ROPN1, S100A1, S100A13, S100A6, S100B, SCARB2, SCCPDH, SDC3, SEMA3B, SERPINA1, SERPENTA3, SERPINE2, SGCE, SGK1, SLC26A2, SLC5A3, SPON2, SPP1, TIMP1, TIMP2, TIMP3, TM4SF1, TMEM255A, TMX4, TNFSF4, TPP1, TRIML2, TSC22D3, TXNIP, TYR, UBC and WBP2.

[0396] The non-infiltrated module (exclusion-up) is mainly enriched with MYC targets and MYC itself. It also includes STRAP, which is an inhibitor of TGF-beta signaling, and SMARCA4 (or BRG1) - a subunit of the BAF complex that has a key role in mediating beta-catenin signaling. The latter has been shown to promote T-cell exclusion in mice. In certain embodiments, the non-infiltrated module includes the following genes: AHCY, BZW2, CCNB1IP1, CCT6A, EEF2, EIF3B, GGCT, ILF3, IMPDH2, MDH2, MYBBPIA, NT5DC2, PAICS, PFKM, POLD2, PTK7, SLC19A1, SMARCA4, STRAP, TIMM13, TOP1MT, TRAP1 and USP22.

[0397] Interestingly, these results mirror and overlap the PIT signatures. When scoring the malignant cells according to these infiltration signatures Applicants find that the treatment naive malignant cells score significantly higher for infiltration compared to the post-treatment malignant cells. In other words, malignant cells having the ITR signature have higher exclusion signatures and treatment naive malignant cells have higher infiltration signatures (**Figure 29**). These results indicate that cells which survive post-immunotherapy either reside in less infiltrated niches within the tumor or have increased capacity to exclude T-cells from their immediate microenvironment. Not being bound by a theory, malignant cells that survive immunotherapy are either to begin with are in a T cell excluded TME or became T cell excluding.

Immunotherapy triggers significant transcriptional changes in CD8 T-cells

[0398] Next Applicants set out to map the transcriptional landscape of the immune cells and examine the association of these states with immunotherapy. Applicants performed the analysis separately for each cell type (CD8 T-cells, CD4 T-cells, B-cells, and macrophages).

First, Applicants performed an unbiased analysis to explore the main sources of heterogeneity in melanoma CD8 T-cells. To this end, Applicants applied Principle Component Analysis (PCA) followed by nonlinear dimensionality reduction (t-distributed stochastic neighbor embedding (t-SNE)). Interestingly, in the first PCs and the t-SNE dimensions, the CD8 T-cells are segregated according to their treatment history, such that post-treatment cells cluster together and apart from the treatment naive cells. These findings demonstrate that immunotherapy triggers significant transcriptional changes in CD8 T-cells, and highlight two additional and orthogonal sources of heterogeneity: one that is attributed to cell cycle, and another that is attributed to the expression of inhibitory checkpoints (**Figure 30, 31**).

[0399] Applicants performed supervised analyses to identify the genes and pathways that are differentially expressed in the post-immunotherapy CD8 T-cells compared to the treatment naive cells. The resulting signatures indicate that the post-treatment CD8 T-cells are more cytotoxic and exhausted, such that naive T-cell markers are downregulated, while IL-2 signaling, T-cell exhaustion and activation-dysfunction pathways are up regulated. Applicants then scored the CD8 T-cells according to these two signatures, revealing a spectrum of phenotypes also within the PIT and treatment naive populations, and within the CD8 T-cell population of the same tumor.

[0400] Applicants speculated that this spectrum might be related to clonal expansion. Clonal expansion occurs when T cells that recognize a specific (tumor) antigen proliferate to generate discernible clonal subpopulations defined by an identical T cell receptor (TCR) sequence. Applicants applied TraCeR to reconstruct the TCR chains of the T-cells and identify cells that are likely to be a part of the same clone (Stubbington et al., Nature Methods 13, 329-332 (2016)). Overall, Applicants identified 113 clones of varying sizes, three of which consist of more than 20 cells (**Figure 32**). Specifically, Applicants used the TcR sequence to determine the clone of each T cell, and distinguished four categories: treatment naive or ITR, and expanded or not. Applicants analyzed their gene expression and saw that cells vary in two ways. First CD8 T cells from ITR patients have distinct expression, and this is especially pronounced in expanded cells. All the major expanded clones were in ITR samples, and only very few cells were expanded in treatment naive patients. These few expanded cells look more like cells from the treated patients. Similar to results reported in mice there is an expanded population of Bcl6+Tcf7+ cells in the ITR samples, some also CXCR5+. When Applicants turn to their functional state, Applicants observed that across all

patients, regardless of treatment, some cells are more exhausted and others more naive.

[0401] These large clones are from post-treatment patients, indicating that immunotherapy is triggering T-cell activation and proliferation even when no objective clinical response is observed. Moreover, Applicants find that clonal expansion is strongly associated with the PIT scores, not only across all patients, but also when considering only the post-immunotherapy or treatment naive cells. Next Applicants compared clonally expanded T-cells to the other T-cells within the same tumor to derive signatures of clonal expansion. By leveraging intra-tumor T-cell heterogeneity in this manner Applicants were able to mitigate the problem of batch effects. In concordance with the previous results Applicants find that genes, which are over (under) expressed post-immunotherapy, are overrepresented in the up (down) regulated clonal-expansion module (**Figure 33**).

[0402] Not being bound by a theory, inhibition of genes, which are under expressed in the T-cells post immunotherapy, could potentially promote T-cell survival and expansion in the tumor microenvironment. Indeed, these genes are ranked significantly high in the results of an in-vivo shRNA screen that identified negative regulators of T-cell proliferation and survival in mice tumors ($P = 4.98e-03$). All in all, these results suggest that post-immunotherapy T-cells are more activated, even in this cohort of non-responders.

Table 4

Post-immunotherapy state in CD8 T-cells	Pathway	Genes
Up-regulated	Zinc TFs	<i>ZBTB24, ZNF526, ZNF528, ZNF543, ZNF620, ZNF652, ZSCAN2, ZSCAN22</i>
	IFN gamma signaling	<i>GBP2, GBP5, IRF1, PTPN2, STAT1</i>
	PD1 signaling	<i>CD3D, CD3E, CD3G, HLA-DQA1, HLA-DQA2, HLA-DRB5, PDCD1</i>
Down-regulated	Cell cycle	<i>BIRC5, BUB1, GMNN, MAD2L1, NDC80, UN, UBE2C, ZWINT</i>
	Negative regulators of T-cell survival/proliferation in the TME (Zhou et al. 2014)	<i>CBLB, WNK1, PDCD1</i>

[0403] Not being bound by a theory, immunotherapy is triggering transcriptional changes

both in the malignant cells and in the CD8 T-cells. The results suggest that the T-cells become more effective, while the malignant cells become more "immune-edited" (e.g., evasion (MHC-1) vs. T-cell exclusion).

Example 3 - C-map analysis

[0404] Drugs that could reduce the resistance signature were analyzed by c-map analysis. The analysis showed that the following drugs could reduce the immunotherapy resistance signature:

- PKC activators;
- NFkB pathway inhibitors;
- IGF 1R inhibitors; and
- Reserpine (Used to control high blood pressure & psychotic symptoms and blocks the vesicular monoamine transporter (VMAT)).

[0405] The signature is associated with drug response/effects. There was an association between the toxicity of different drugs and their resistance scores (according to the resistance signatures). C-map results indicated drugs that can sensitize/de-sensitize the cells to immunotherapy. The results of this analysis are summarized in Table 5-7.

Table 5. Drugs that modulate Gene Signature

The correlation between the resistance scores of the cell lines and their sensitivity (IC50) to the pertaining drug (based on the CCLE gene expression and the Garnett et al. Nature 2012)				
Negative R -> more toxic/selective to the immuno-resistant cells.				
Positive R -> less toxic/selective to the immuno-resistant cells.				
Drug	Adj. R	Adj. P	mtL:iiuim:i.U	mtL:iiuim:i.L
Pazopanib	-0.01	8.62E-01	-0.48	3.27E-02
Shikonin	-0.05	4.55E-01	-0.48	3.97E-02
Etoposide	-0.16	2.02E-02	-0.48	4.05E-02
JNK.9L	-0.13	4.97E-02	-0.39	1.00E-01
GSK.650394	-0.17	1.02E-02	-0.37	1.05E-01
X681640	-0.08	1.56E-01	-0.37	1.55E-01
Vinorelbine	-0.14	3.68E-02	-0.34	1.54E-01
AZD6482	0.16	1.46E-02	-0.34	1.56E-01
BIRB.0796	-0.11	6.17E-02	-0.33	2.13E-01
NVP.BEZ235	0.00	9.79E-01	-0.30	1.59E-01
Roscovitine	0.03	6.90E-01	-0.30	4.37E-01
Sunitinib	-0.04	6.12E-01	-0.30	4.37E-01
Gemcitabine	-0.05	4.18E-01	-0.29	2.19E-01
Epothilone.B	-0.05	4.40E-01	-0.29	2.21E-01
ATRA	-0.20	6.16E-04	-0.28	3.14E-01
VX.702	-0.16	6.16E-03	-0.27	2.62E-01
QS11	-0.17	7.40E-03	-0.27	2.50E-01
Lapatinib	0.29	4.69E-04	-0.27	4.93E-01
BMS.536924	0.32	7.64E-05	-0.25	5.21E-01
Vorinostat	-0.37	2.73E-11	-0.25	3.02E-01
PD.0332991	-0.06	2.82E-01	-0.22	3.75E-01
Parthenolide	0.08	3.55E-01	-0.22	5.81E-01
AZD.2281	-0.18	1.72E-03	-0.21	3.71E-01
FTL.277	0.18	6.29E-03	-0.21	3.85E-01
IPA.3	-0.08	2.14E-01	-0.21	3.75E-01
PF.562271	0.05	4.31E-01	-0.20	4.10E-01
PD.173074	-0.18	1.89E-03	-0.19	3.74E-01

Tipifarnib	-0.09	1.93E-01	-0.18	4.33E-01
A.770041	0.24	4.60E-03	-0.18	6.44E-01
Z.LLNle.CHO	0.23	5.71E-03	-0.18	6.44E-01
CEP.701	-0.10	9.73E-02	-0.17	4.75E-01
PAC.1	-0.09	1.52E-01	-0.17	4.76E-01
BI.2536	0.14	9.25E-02	-0.17	6.78E-01
GW843682X	0.05	5.52E-01	-0.17	6.78E-01
Midostaurin	0.06	3.70E-01	-0.16	5.03E-01
Metformin	-0.21	9.02E-05	-0.16	4.24E-01
ZM.447439	-0.09	1.27E-01	-0.14	5.21E-01
Elesclomol	0.07	2.48E-01	-0.14	6.21E-01
AZD7762	-0.08	1.48E-01	-0.14	5.68E-01
Sorafenib	-0.03	7.33E-01	-0.13	7.44E-01
XMD8.85	0.00	9.81E-01	-0.13	7.44E-01
BAY.61.3606	-0.05	4.84E-01	-0.13	5.81E-01
BI.D1870	-0.02	7.72E-01	-0.13	6.41E-01
Doxorubicin	-0.03	6.08E-01	-0.11	6.44E-01
DMOG	0.17	1.05E-02	-0.10	6.78E-01
BMS.509744	0.08	3.30E-01	-0.10	8.10E-01
Bosutinib	-0.05	3.91E-01	-0.09	7.05E-01
CMK	0.17	3.68E-02	-0.08	8.43E-01
KIN001.135	0.19	2.39E-02	-0.08	8.43E-01
WZ.1.84	0.21	1.47E-02	-0.08	8.43E-01
AZD8055	-0.11	5.79E-02	-0.08	7.33E-01
Paclitaxel	0.18	3.31E-02	-0.07	8.80E-01
VX.680	-0.01	9.30E-01	-0.07	8.80E-01
LFM.A13	0.12	5.87E-02	-0.06	8.11E-01
Methotrexate	-0.35	1.27E-09	-0.06	8.42E-01
NU.7441	0.10	1.02E-01	-0.06	8.39E-01
KU.55933	0.07	2.68E-01	-0.05	8.48E-01
JW.7.52.1	0.11	1.80E-01	-0.05	9.12E-01
OSI.906	0.06	3.67E-01	-0.05	8.36E-01
PD.0325901	0.23	4.75E-05	-0.04	8.51E-01
JNK.Inhibitor.VIII	0.03	6.13E-01	-0.04	9.00E-01
Gefitinib	-0.02	6.99E-01	-0.03	9.23E-01
BMS.754807	0.01	8.32E-01	-0.02	9.32E-01
BIBW2992	0.04	5.07E-01	-0.02	9.43E-01
Salubrinal	-0.11	1.93E-01	-0.02	9.82E-01
Camptothecin.3	0.03	6.44E-01	-0.01	9.57E-01
Camptothecin.5	0.03	6.44E-01	-0.01	9.57E-01
A.443654	0.14	9.40E-02	0.00	1.00E+00
Thapsigargin	-0.02	7.97E-01	0.00	9.92E-01
NSC.87877	-0.17	1.36E-02	0.01	9.86E-01
BX.795	0.03	6.53E-01	0.01	9.73E-01
X17.AAG	0.22	2.11E-04	0.03	9.26E-01
Mitomycin.C	-0.12	7.40E-02	0.03	9.11E-01
Temsirolimus	-0.12	4.14E-02	0.03	9.13E-01
Docetaxel	0.13	2.39E-02	0.03	8.84E-01
Cyclopamine	0.01	8.84E-01	0.03	9.48E-01
Camptothecin	-0.12	3.84E-02	0.04	8.74E-01
Camptothecin.4	-0.12	3.84E-02	0.04	8.74E-01
GDC0941	0.02	7.65E-01	0.04	8.41E-01
Obatoclox.Mesylate	-0.05	4.59E-01	0.05	8.41E-01
CGP.082996	-0.01	9.29E-01	0.07	8.80E-01
Bleomycin	-0.09	1.92E-01	0.08	7.53E-01
AS601245	-0.03	6.96E-01	0.08	7.29E-01
Bryostatin.l	-0.01	8.31E-01	0.08	7.29E-01
Embelin	-0.01	9.13E-01	0.09	7.05E-01
AKT.inhibitor.VIII	-0.10	1.35E-01	0.09	7.05E-01
AP.24534	0.13	6.29E-02	0.09	7.05E-01
RDEA119	0.27	1.44E-06	0.12	5.98E-01
Nilotinib	-0.09	1.34E-01	0.13	6.00E-01
CGP.60474	0.26	1.85E-03	0.13	7.44E-01
S.Trityl.L.cysteine	0.00	9.82E-01	0.13	7.44E-01
Erlotinib	0.18	4.08E-02	0.15	7.08E-01
ABT.888	-0.11	6.48E-02	0.15	5.17E-01
MK.2206	-0.09	1.47E-01	0.16	5.14E-01
Dasatinib	0.38	4.98E-06	0.17	6.78E-01

MG.132	0.25	2.24E-03	0.17	6.78E-01
PF.02341066	0.14	7.89E-02	0.17	6.78E-01
Cisplatin	-0.01	8.94E-01	0.18	5.12E-01
WH.4.023	0.23	5.25E-03	0.18	6.44E-01
CI.1040	0.09	1.24E-01	0.20	4.74E-01
SL.0101.1	-0.06	2.74E-01	0.20	4.56E-01
SB590885	-0.11	5.08E-02	0.21	3.61E-01
A.769662	0.06	3.85E-01	0.21	3.85E-01
AZ628	0.17	4.24E-02	0.22	5.81E-01
GSK269962A	0.21	1.14E-02	0.22	5.81E-01
MS.275	0.00	9.71E-01	0.22	5.81E-01
Cytarabine	-0.02	7.54E-01	0.22	4.10E-01
Axitinib	-0.19	1.11E-03	0.22	3.54E-01
Vinblastine	-0.07	2.38E-01	0.23	3.91E-01
Bicalutamide	0.02	7.59E-01	0.24	2.99E-01
PLX4720	0.07	2.41E-01	0.25	3.43E-01
RO.3306	0.11	6.07E-02	0.25	2.41E-01
AUY922	0.01	9.32E-01	0.26	2.75E-01
GNF.2	0.27	1.27E-03	0.27	4.93E-01
Lenalidomide	-0.11	5.30E-02	0.27	2.69E-01
GDC.0449	-0.12	3.17E-02	0.29	2.20E-01
AICAR	-0.16	3.97E-03	0.30	1.33E-01
AZD6244	0.17	4.19E-03	0.32	1.97E-01
Nutlin.3a	-0.09	1.18E-01	0.32	1.36E-01
Bexarotene	-0.01	9.08E-01	0.34	1.41E-01
Imatinib	0.15	6.78E-02	0.35	3.59E-01
Rapamycin	0.09	2.59E-01	0.35	3.59E-01
GW.441756	-0.09	1.17E-01	0.35	1.41E-01
ABT.263	-0.12	3.89E-02	0.37	8.43E-02
CHIR.99021	0.19	3.91E-03	0.38	1.10E-01
Bortezomib	0.36	6.13E-06	0.38	3.13E-01
Pyrimethamine	0.09	2.84E-01	0.38	3.13E-01
FH535	-0.24	1.51E-04	0.40	8.41E-02
AMG.706	-0.04	4.43E-01	0.45	3.14E-02
SB.216763	0.02	7.29E-01	0.46	4.84E-02
AZD.0530	0.31	1.05E-04	0.53	1.48E-01
PHA.665752	0.18	2.41E-02	0.68	5.03E-02
NVP.TAE684	0.21	8.27E-03	0.72	3.69E-02

Table 6. Top 200 drugs that induce downregulated genes in the signature

Rank	Score	Type (cp= compound, kd = knock-down, oe = over-expression, cc = cmap class)	ID	Name	Description
1	99.95	cc		PKC Activator	-
2	99.95	kd	CGS001-10538	BATF	basic leucine zipper proteins
3	99.95	kd	CGS001-25937	WWTR1	Hippo Signaling
4	99.95	kd	CGS001-7483	WNT9A	Wingless-type MMTV integration sites
5	99.95	kd	CGS001-2837	UTS2R	Urotensin receptor
6	99.95	kd	CGS001-7187	TRAF3	-
7	99.95	kd	CGS001-27242	TNFRSF21	Tumour necrosis factor (TNF) receptor family
8	99.95	kd	CGS001-7027	TFDP1	-
9	99.95	kd	CGS001-64783	RBM15	RNA binding motif (RRM) containing
10	99.95	kd	CGS001-8438	RAD54L	-
11	99.95	kd	CGS001-8624	PSMG1	-
12	99.95	kd	CGS001-53632	PRKAG3	AMPK subfamily
13	99.95	kd	CGS001-5184	PEPD	Methionyl aminopeptidase
14	99.95	kd	CGS001-4688	NCF2	Tetratricopeptide (TTC) repeat domain containing
15	99.95	kd	CGS001-11004	KIF2C	Kinesins
16	99.95	kd	CGS001-22832	KIAA1009	-
17	99.95	kd	CGS001-10014	HDAC5	Histone deacetylases
18	99.95	kd	CGS001-2355	FOSL2	basic leucine zipper

Rank	Score	Type (cp= compound, kd = knock-down, oe = over-expression, cc = cmap class)	ID	Name	Description
					proteins
19	99.95	kd	CGS001-2864	FFAR1	Fatty acid receptors
20	99.95	kd	CGS001-51719	CAB39	-
21	99.95	kd	CGS001-604	BCL6	BTB/POZ domain containing
22	99.95	kd	CGS001-326	AIRE	Zinc fingers, PHD-type
23	99.93	cp	BRD-K02526760	QS-11	ARFGAP inhibitor
24	99.92	kd	CGS001-23224	SYNE2	-
25	99.92	kd	CGS001-10267	RAMP1	Receptor (G protein-coupled) activity modifying proteins
26	99.92	kd	CGS001-4323	MMP14	Matrix metalloproteinase
27	99.92	kd	CGS001-9455	HOMER2	-
28	99.92	kd	CGS001-2852	GPER	-
29	99.92	kd	CGS001-694	BTG1	-
30	99.91	cc		NFKB Activation	-
31	99.91	oe	ccsbBroad304_00833	IFNG	Interferons
32	99.91	oe	ccsbBroad304_02889	WWTR1	Hippo Signaling
33	99.91	oe	ccsbBroad304_00832	IFNB1	Interferons
34	99.91	oe	ccsbBroad304_00259	CD40	Tumour necrosis factor (TNF) receptor family
35	99.91	oe	ccsbBroad304_05881	BCL2L2	Serine/threonine phosphatases / Protein phosphatase 1, regulatory subunits
36	99.91	oe	ccsbBroad304_05390	DUSP28	Protein tyrosine phosphatases / Class I Cys-based PTPs : Atypical dual specificity phosphatases
37	99.91	oe	ccsbBroad304_06021	KLF6	Kruppel-like transcription factors
38	99.91	oe	ccsbBroad304_00954	LYN	Src family
39	99.91	oe	ccsbBroad304_03926	SLC39A8	SLC39 family of metal ion transporters
40	99.89	cp	BRD-A52650764	ingenol	PKC activator
41	99.89	kd	CGS001-54472	TOLLIP	-
42	99.89	kd	CGS001-26472	PPP1R14B	Serine/threonine phosphatases / Protein phosphatase 1, regulatory subunits
43	99.89	kd	CGS001-6927	HNF1A	Homeoboxes / HNF class
44	99.87	kd	CGS001-79724	ZNF768	Zinc fingers, C2H2-type
45	99.87	kd	CGS001-6915	TBXA2R	GPCR / Class A : Prostanoid receptors
46	99.87	kd	CGS001-51588	PIAS4	Zinc fingers, MIZ-type
47	99.87	kd	CGS001-8974	P4HA2	-
48	99.87	kd	CGS001-283455	KSR2	RAF family
49	99.86	oe	ccsbBroad304_00880	IRF2	-
50	99.86	oe	ccsbBroad304_00771	HOXA5	Homeoboxes / ANTP class : HOXL subclass
51	99.86	oe	ccsbBroad304_06260	GATA3	GATA zinc finger domain containing
52	99.84	kd	CGS001-7106	TSPAN4	Tetraspanins
53	99.84	kd	CGS001-93487	MAPK11P1L	-
54	99.84	kd	CGS001-10112	KIF20A	Kinesins
55	99.84	kd	CGS001-3784	KCNQ1	Voltage-gated potassium channels
56	99.84	kd	CGS001-182	JAG1	CD molecules
57	99.84	kd	CGS001-1440	CSF3	Endogenous ligands
58	99.82	cp	BRD-K91145395	prostratin	PKC activator
59	99.82	cp	BRD-K32744045	disulfiram	Aldehyde dehydrogenase inhibitor
60	99.82	kd	CGS001-7525	YES1	Src family
61	99.82	kd	CGS001-7849	PAX8	Paired boxes
62	99.82	kd	CGS001-1845	DUSP3	Protein tyrosine

Rank	Score	Type (cp= compound, kd = knock-down, oe = over-expression, cc = cmap class)	ID	Name	Description
					phosphatases / Class I Cys-based PTPs : Atypical dual specificity phosphatases
63	99.82	kd	CGS001-1154	CISH	SH2 domain containing
64	99.81	oe	ccsbBroad304_04728	TWIST2	Basic helix-loop-helix proteins
65	99.81	oe	ccsbBroad304_02048	BCL10	-
66	99.8	kd	CGS001-10196	PRMT3	Protein arginine N-methyltransferases
67	99.79	cp	BRD-A15079084	phorbol-12-myristate-13-acetate	PKC activator
68	99.79	kd	CGS001-7090	TLE3	WD repeat domain containing
69	99.79	kd	CGS001-21	ABCA3	ATP binding cassette transporters / subfamily A
70	99.78	cc		Ribonucleotide Reductase Inhibitor	-
71	99.78	kd	CGS001-23057	NMNAT2	-
72	99.77	oe	ccsbBroad304_03232	VPS28	-
73	99.76	kd	CGS001-115509	ZNF689	Zinc fingers, C2H2-type
74	99.76	kd	CGS001-9928	KIF14	Kinesins
75	99.76	kd	CGS001-3417	IDH1	-
76	99.75	cp	BRD-K88429204	pyrimethamine	Dihydrofolate reductase inhibitor
77	99.75	cp	BRD-K25504083	cytochalasin-d	Actin polymerization inhibitor
78	99.75	cp	BRD-K47983010	BX-795	IKK inhibitor
79	99.74	kd	CGS001-6909	TBX2	T-boxes
80	99.74	kd	CGS001-5577	PRKAR2B	Protein kinase A
81	99.73	kd	CGS001-5469	MED1	-
82	99.72	oe	ccsbBroad304_07680	NEK6	NIMA (never in mitosis gene a)- related kinase (NEK) family
83	99.72	cp	BRD-A15010982	HU-211	Glutamate receptor antagonist
84	99.72	cp	BRD-K33106058	cytarabine	Ribonucleotide reductase inhibitor
85	99.71	kd	CGS001-6857	SYT1	Synaptotagmins
86	99.71	kd	CGS001-4482	MSRA	-
87	99.71	kd	CGS001-8321	FZD1	GPCR / Class F : Frizzled receptors
88	99.71	kd	CGS001-124583	CANT1	-
89	99.71	kd	CGS001-8312	AXIN1	Serine/threonine phosphatases / Protein phosphatase 1, regulatory subunits
90	99.71	kd	CGS001-8874	ARHGEF7	Rho guanine nucleotide exchange factors
91	99.68	oe	ccsbBroad304_03556	SMU1	WD repeat domain containing
92	99.68	oe	ccsbBroad304_06557	MAOA	Catecholamine turnover
93	99.68	oe	ccsbBroad304_08282	ATP6V1D	ATPases / V-type
94	99.66	kd	CGS001-8738	CRADD	-
95	99.65	kd	CGS001-29890	RBM15B	RNA binding motif (RRM) containing
96	99.63	kd	CGS001-3397	ID1	Basic helix-loop-helix proteins
97	99.63	kd	CGS001-26036	ZNF451	Zinc fingers, C2H2-type
98	99.63	kd	CGS001-9375	TM9SF2	-
99	99.63	kd	CGS001-10287	RGS19	Regulators of G-protein signaling
100	99.63	kd	CGS001-374291	NDUFS7	Mitochondrial respiratory chain complex / Complex I
101	99.63	kd	CGS001-51001	MTERFD1	-

Rank	Score	Type (cp= compound, kd = knock-down, oe = over-expression, cc = cmap class)	ID	Name	Description
102	99.63	oe	ccsbBroad304_06542	LTBR	Tumor necrosis factor receptor superfamily
103	99.61	cp	BRD-A54632525	BRD-A54632525	-
104	99.61	kd	CGS001-5654	HTRA1	Serine peptidases / Serine peptidases
105	99.61	kd	CGS001-2673	GFPT1	-
106	99.6	kd	CGS001-11057	ABHD2	Abhydrolase domain containing
107	99.58	kd	CGS001-4835	NQO2	-
108	99.58	kd	CGS001-11329	STK38	NDR family
109	99.58	kd	CGS001-1666	DECR1	Short chain dehydrogenase/reductase superfamily / Classical SDR fold cluster 1
110	99.58	kd	CGS001-4299	AFF1	-
111	99.58	oe	ccsbBroad304_07137	WT1	Zinc fingers, C2H2-type
112	99.55	kd	CGS001-22949	PTGR1	-
113	99.55	kd	CGS001-2071	ERCC3	General transcription factors
114	99.55	kd	CGS001-10668	CGRRF1	RING-type (C3HC4) zinc fingers
115	99.55	kd	CGS001-348	APOE	Apolipoproteins
116	99.54	oe	ccsbBroad304_00282	CDKN1A	-
117	99.54	oe	ccsbBroad304_01010	MGST2	Glutathione S-transferases / Microsomal
118	99.51	cp	BRD-K77908580	entinostat	HDAC inhibitor
119	99.5	kd	CGS001-7371	UCK2	-
120	99.5	kd	CGS001-5198	PFAS	-
121	99.5	kd	CGS001-51005	AMDHD2	-
122	99.47	kd	CGS001-5188	PET112	-
123	99.47	kd	CGS001-25836	NIPBL	-
124	99.47	kd	CGS001-5891	MOK	RCK family
125	99.47	kd	CGS001-1994	ELAVL1	RNA binding motif (RRM) containing
126	99.45	oe	ccsbBroad304_04891	TMEM174	-
127	99.44	cp	BRD-K73610817	BRD-K73610817	-
128	99.44	cp	BRD-K65814004	diphenyleneiodonium	Nitric oxide synthase inhibitor
129	99.44	oe	ccsbBroad304_01388	RELB	NFkappaB transcription factor family
130	99.42	kd	CGS001-8996	NOL3	-
131	99.42	kd	CGS001-64223	MLST8	WD repeat domain containing
132	99.41	kd	CGS001-929	CD14	CD molecules
133	99.4	oe	ccsbBroad304_07306	TNFRSF10A	Tumour necrosis factor (TNF) receptor family
134	99.4	cp	BRD-K26818574	BIX-01294	Histone lysine methyltransferase inhibitor
135	99.4	cp	BRD-K92991072	PAC-1	Caspase activator
136	99.39	cc		ATPase Inhibitor	-
137	99.37	kd	CGS001-1955	MEGF9	-
138	99.37	cp	BRD-K93034159	cladribine	Adenosine deaminase inhibitor
139	99.34	kd	CGS001-2063	NR2F6	COUP-TF-like receptors
140	99.33	cp	BRD-K50841342	PAC-1	-
141	99.32	cc		BCL2 And Related Protein Inhibitor	-
142	99.32	kd	CGS001-54386	TERF2IP	-
143	99.32	kd	CGS001-1852	DUSP9	Protein tyrosine phosphatases / Class I Cys-

Rank	Score	Type (cp= compound, kd = knock-down, oe = over-expression, cc = cmap class)	ID	Name	Description
					based PTPs : MAP kinase phosphatases
144	99.32	kd	CGS001-1212	CLTB	-
145	99.32	kd	CGS001-9459	ARHGEF6	Rho guanine nucleotide exchange factors
146	99.31	oe	ccsbBroad304_08010	FBXO5	F-boxes / other
147	99.3	kd	CGS001-9643	MORF4L2	-
148	99.29	kd	CGS001-22827	PUF60	RNA binding motif (RRM) containing
149	99.29	kd	CGS001-1349	COX7B	Mitochondrial respiratory chain complex
150	99.26	kd	CGS001-79885	HDAC11	Histone deacetylases
151	99.26	kd	CGS001-4046	LSP1	-
152	99.25	kd	CGS001-3177	SLC29A2	SLC29 family
153	99.24	kd	CGS001-3326	HSP90AB1	Heat shock proteins / HSPC
154	99.23	kd	CGS001-1643	DDB2	WD repeat domain containing
155	99.22	kd	CGS001-8986	RPS6KA4	MSK subfamily
156	99.22	cp	BRD-K26664453	cytochalasin-b	Microtubule inhibitor
157	99.21	cc		Aldo Keto Reductase	-
158	99.21	oe	ccsbBroad304_01710	TRAF2	RING-type (C3HC4) zinc fingers
159	99.21	oe	ccsbBroad304_05941	CBR3	Short chain dehydrogenase/reductase superfamily / Classical SDR fold cluster 1
160	99.21	kd	CGS001-5096	PCCB	Carboxylases
161	99.21	oe	ccsbBroad304_06392	HOXB7	Homeoboxes / ANTP class : HOXL subclass
162	99.18	kd	CGS001-22955	SCMH1	Sterile alpha motif (SAM) domain containing
163	99.17	oe	ccsbBroad304_00773	HOXA9	Homeoboxes / ANTP class : HOXL subclass
164	99.17	kd	CGS001-3108	HLA-DMA	Immunoglobulin superfamily / C1-set domain containing
165	99.17	oe	ccsbBroad304_05098	MAGEB6	-
166	99.14	oe	ccsbBroad304_01686	TNFAIP3	OTU domain containing
167	99.13	kd	CGS001-7690	ZNF131	BTB/POZ domain containing
168	99.13	kd	CGS001-23011	RAB21	RAB, member RAS oncogene
169	99.13	kd	CGS001-5106	PCK2	-
170	99.13	kd	CGS001-85315	PAQR8	-
171	99.12	oe	ccsbBroad304_01858	FOSL1	basic leucine zipper proteins
172	99.12	cp	BRD-K23984367	sorafenib	-
173	99.12	cp	BRD-K72264770	QW-BI-011	Histone lysine methyltransferase inhibitor
174	99.11	kd	CGS001-11116	FGFR10P	-
175	99.1	kd	CGS001-4804	NGFR	Tumour necrosis factor (TNF) receptor family
176	99.08	kd	CGS001-6676	SPAG4	-
177	99.08	kd	CGS001-63874	ABHD4	Abhydrolase domain containing
178	99.07	oe	ccsbBroad304_00389	CTBP1	-
179	99.05	kd	CGS001-7480	WNT10B	Wingless-type MMTV integration sites
180	99.05	kd	CGS001-80351	TNKS2	Ankyrin repeat domain containing
181	99.05	kd	CGS001-2264	FGFR4	Type V RTKs: FGF (fibroblast growth factor) receptor family

Rank	Score	Type (cp = compound, kd = knock-down, oe = over-expression, cc = cmap class)	ID	Name	Description
182	99.05	kd	CGSOOI-1725	DHPS	-
183	99.05	kd	CGSOOI-64170	CARD9	-
184	99.03	kd	CGSOOI-6259	RYK	Type XV RTKs: RYK
185	99.03	kd	CGSOOI-54566	EPB41L4B	-
186	99.02	kd	CGSOOI-308	ANXA5	Annexins
187	99.01	kd	CGSOOI-5257	PHKB	-
188	99	kd	CGSOOI-7764	ZNF217	Zinc fingers, C2H2-type
189	99	kd	CGSOOI-5451	POU2F1	Homeoboxes / POU class
190	98.98	cp	BRD-K30677119	PP-30	RAF inhibitor
191	98.98	kd	CGSOOI-23368	PPP1R13B	Ankyrin repeat domain containing
192	98.98	cp	BRD-A34208323	VU-0404997-2	Glutamate receptor modulator
193	98.97	kd	CGSOOI-4601	MXI1	Basic helix-loop-helix proteins
194	98.97	kd	CGSOOI-10247	HRSP12	-
195	98.95	kd	CGSOOI-8295	TRRAP	TRRAP subfamily
196	98.95	kd	CGSOOI-26064	RAI14	Ankyrin repeat domain containing
197	98.95	kd	CGSOOI-5710	PSMD4	Proteasome (prosome, macropain) subunits
198	98.95	kd	CGSOOI-3312	HSPA8	Heat shock proteins / HSP70
199	98.93	cp	BRD-K59456551	methotrexate	Dihydrofolate reductase inhibitor
200	98.93	kd	CGSOOI-10327	AKR1A1	Aldo-keto reductases

Table 7. Top 200 drugs that repress upregulated genes in the signature

Rank	Score	Type (cp = compound, kd = knock-down, oe = over-expression, cc = cmap class)	ID	Name	Description
8875	-99.95	kd	CGS001-10254	STAM2	-
8876	-99.95	kd	CGS001-5966	REL	NFkappaB transcription factor family
8877	-99.95	kd	CGS001-4609	MYC	Basic helix-loop-helix proteins
8878	-99.95	kd	CGS001-2079	ERH	-
8879	-99.95	kd	CGS001-2683	B4GALT1	Beta 4-glycosyltransferases
8880	-99.95	kd	CGS001-406	ARNTL	Basic helix-loop-helix proteins
8872	-99.92	cc		Aldo Keto Reductase	-
8873	-99.92	kd	CGS001-8644	AKR1C3	Prostaglandin synthases
8874	-99.92	kd	CGS001-2863	GPR39	GPCR / Class A : Orphans
8870	-99.91	oe	ccsbBroad304_03864	OVOL2	Zinc fingers, C2H2-type
8871	-99.91	oe	ccsbBroad304_08418	FBXL12	F-boxes / Leucine-rich repeats
8866	-99.89	kd	CGS001-114026	ZIM3	Zinc fingers, C2H2-type
8867	-99.89	kd	CGS001-51021	MRPS16	Mitochondrial ribosomal proteins / small subunits
8868	-99.89	kd	CGS001-3265	HRAS	RAS subfamily
8869	-99.89	kd	CGS001-1643	DDB2	WD repeat domain containing
8864	-99.88	kd	CGS001-6337	SCNN1A	Epithelial sodium channels (ENaC)
8865	-99.88	kd	CGS001-4191	MDH2	-
8861	-99.87	kd	CGS001-26137	ZBTB20	BTB/POZ domain containing
8862	-99.87	kd	CGS001-7227	TRPS1	GATA zinc finger domain containing
8863	-99.87	kd	CGS001-95	ACY1	-
8856	-99.86	oe	ccsbBroad304_0083	IFNB1	Interferons

Rank	Score	Type (cp= compound, kd = knock-down, oe = over-expression, cc = cmap class)	ID	Name	Description
			2		
8857	-99.86	oe	ccsbBroad304_0598 2	CDX2	Homeoboxes / ANTP class : HOXL subclass
8858	-99.86	oe	ccsbBroad304_0602 1	KLF6	Kruppel-like transcription factors
8859	-99.86	oe	ccsbBroad304_0124 9	PPARG	Peroxisome proliferator-activated receptors
8860	-99.86	oe	ccsbBroad304_0047 2	EBF1	-
8854	-99.84	kd	CGS001-7185	TRAF1	-
8855	-99.84	kd	CGS001-5562	PRKAA1	AMPK subfamily
8853	-99.83	kd	CGS001-7775	ZNF232	Zinc fingers, C2H2-type
8852	-99.82	kd	CGS001-10525	HYOU1	Heat shock proteins / HSP70
8851	-99.81	oe	ccsbBroad304_0736 3	AIFM1	-
8850	-99.79	cp	BRD-A81772229	simvastatin	HMGCR inhibitor
8847	-99.77	oe	ccsbBroad304_0074 7	HLF	-
8848	-99.77	oe	ccsbBroad304_0048 7	EGR1	Zinc fingers, C2H2-type
8849	-99.77	oe	ccsbBroad304_0427 1	MXD3	Basic helix-loop-helix proteins
8846	-99.76	kd	CGS001-5608	MAP2K6	MAPKK:STE7 family
8844	-99.75	cc		JAK Inhibitor	-
8845	-99.75	cp	BRD-K91290917	amodiaquine	Histamine receptor agonist
8843	-99.74	kd	CGS001-9296	ATP6V1F	ATPases / V-type
8841	-99.71	kd	CGS001-6389	SDHA	Mitochondrial respiratory chain complex
8842	-99.71	kd	CGS001-6275	S100A4	EF-hand domain containing
8839	-99.68	oe	ccsbBroad304_0083 3	IFNG	Interferons
8840	-99.68	oe	ccsbBroad304_0711 7	UGCG	Glycosyltransferase family 2 domain containing
8838	-99.67	kd	CGS001-8031	NCOA4	-
8836	-99.66	kd	CGS001-7167	TP11	-
8837	-99.66	kd	CGS001-3419	IDH3A	-
8835	-99.63	kd	CGS001-5469	MED1	-
8830	-99.61	cp	BRD-K52850071	JAK3-Inhibitor-II	JAK inhibitor
8831	-99.61	cp	BRD-K49049886	CGS-15943	Adenosine receptor antagonist
8832	-99.61	kd	CGS001-115650	TNFRSF13C	Tumour necrosis factor (TNF) receptor family
8833	-99.61	kd	CGS001-6493	SIM2	Basic helix-loop-helix proteins
8834	-99.61	kd	CGS001-7803	PTP4A1	Protein tyrosine phosphatases / Class I Cys-based PTPs : PRLs
8829	-99.59	cc		Aurora Kinase Inhibitor Grp2	-
8825	-99.58	cp	BRD-K37691127	hinokitiol	Tyrosinase inhibitor
8826	-99.58	kd	CGS001-5170	PDPK1	PDK1 family
8827	-99.58	kd	CGS001-4199	ME1	-
8828	-99.58	kd	CGS001-51295	ECSIT	Mitochondrial respiratory chain complex assembly factors
8822	-99.55	kd	CGS001-51520	LARS	Aminoacyl tRNA synthetases / Class I
8823	-99.55	kd	CGS001-2538	G6PC	-
8824	-99.55	kd	CGS001-2059	EPS8	-
8819	-99.54	cp	BRD-K58299615	RO-90-7501	Beta amyloid inhibitor

Rank	Score	Type (cp= compound, kd = knock-down, oe = over-expression, cc = cmap class)	ID	Name	Description
8820	-99.54	kd	CGS001-3485	IGFBP2	insulin-like growth factor (IGF) binding proteins
8821	-99.54	cp	BRD-K85606544	neratinib	EGFR inhibitor
8813	-99.53	kd	CGS001-54472	TOLLIP	-
8814	-99.53	kd	CGS001-4998	ORC1	ATPases / AAA-type
8815	-99.53	kd	CGS001-9020	MAP3K14	MAPKKK:STE-unique family
8816	-99.53	kd	CGS001-355	FAS	Tumour necrosis factor (TNF) receptor family
8817	-99.53	kd	CGS001-10327	AKR1A1	Aldo-keto reductases
8818	-99.53	kd	CGS001-178	AGL	-
8812	-99.52	cc		HOX Gene	-
8810	-99.51	cp	BRD-A19633847	perhexiline	Carnitine palmitoyltransferase inhibitor
8811	-99.51	cp	BRD-K47105409	AG-490	-
8809	-99.49	oe	ccsbBroad304_00706	GTF2B	General transcription factors
8806	-99.47	oe	ccsbBroad304_05980	CDKN1B	-
8807	-99.47	kd	CGS001-8226	HDHD1	-
8808	-99.47	kd	CGS001-5045	FURIN	Subtilisin
8805	-99.45	oe	ccsbBroad304_00772	HOXA6	Homeoboxes / ANTP class : HOXL subclass
8804	-99.44	kd	CGS001-3309	HSPA5	Heat shock proteins / HSP70
8803	-99.43	oe	ccsbBroad304_00838	IGFBP5	insulin-like growth factor (IGF) binding proteins
8802	-99.4	cp	BRD-K92991072	PAC-1	Caspase activator
8801	-99.39	kd	CGS001-35	ACADS	-
8800	-99.38	kd	CGS001-3122	HLA-DRA	Immunoglobulin superfamily / C1-set domain containing
8799	-99.37	cp	BRD-K66296774	fluvastatin	HMGCR inhibitor
8798	-99.36	kd	CGS001-7525	YES1	Src family
8797	-99.35	kd	CGS001-57178	ZMIZ1	Zinc fingers, MIZ-type
8795	-99.34	kd	CGS001-3635	INPP5D	Inositol polyphosphate phosphatases
8796	-99.34	kd	CGS001-3416	IDE	Pitriylisin
8794	-99.33	cp	BRD-K07881437	danusertib	Aurora kinase inhibitor
8793	-99.32	cp	BRD-A50675702	fipronil	GABA gated chloride channel blocker
8792	-99.29	kd	CGS001-998	CDC42	-
8791	-99.28	cc		PI3K Inhibitor	-
8787	-99.26	cc		DNA-dependent Protein Kinase	-
8788	-99.26	cp	BRD-K94441233	mevastatin	HMGCR inhibitor
8789	-99.26	oe	ccsbBroad304_02571	TOMM34	Tetratricopeptide (TTC) repeat domain containing
8790	-99.26	oe	ccsbBroad304_01579	SOX2	SRY (sex determining region Y)-boxes
8784	-99.24	kd	CGS001-5682	PSMA1	Proteasome subunits
8785	-99.24	kd	CGS001-53347	UBASH3A	-
8786	-99.24	kd	CGS001-2782	GNB1	WD repeat domain containing
8782	-99.23	oe	ccsbBroad304_11277	HAT1	Histone acetyltransferases (HATs)
8783	-99.23	kd	CGS001-4323	MMP14	Matrix metalloproteinase
8780	-99.2	kd	CGS001-79142	PHF23	Zinc fingers, PHD-type
8781	-99.2	kd	CGS001-2664	GD11	-
8778	-99.19	cp	BRD-K48974000	BRD-K48974000	-
8779	-99.19	kd	CGS001-4817	NIT1	-

Rank	Score	Type (cp= compound, kd = knock-down, oe = over-expression, cc = cmap class)	ID	Name	Description
8777	-99.18	kd	CGS001-7126	TNFAIP1	BTB/POZ domain containing
8775	-99.17	kd	CGS001-10497	UNC13B	-
8776	-99.17	kd	CGS001-57448	BIRC6	Inhibitors of apoptosis (IAP) protein family
8772	-99.15	cp	BRD-K13514097	everolimus	MTOR inhibitor
8773	-99.15	cp	BRD-K59331372	SB-366791	TRPV antagonist
8774	-99.15	cp	BRD-K78373679	RO-3306	CDK inhibitor
8770	-99.13	oe	ccsbBroad304_02451	HOXB13	Homeoboxes / ANTP class : HOXL subclass
8771	-99.13	kd	CGS001-7405	UVRAG	-
8769	-99.12	cp	BRD-K06217810	BRD-K06217810	-
8768	-99.11	cc		HMGCR Inhibitor	-
8765	-99.08	kd	CGS001-55781	RIOK2	RIO2 subfamily
8766	-99.08	kd	CGS001-7026	NR2F2	COUP-TF-like receptors
8767	-99.08	kd	CGS001-7994	KAT6A	Histone acetyltransferases (HATs)
8762	-99.07	oe	ccsbBroad304_06131	DUSP6	Protein tyrosine phosphatases / Class I Cys-based PTPs : MAP kinase phosphatases
8763	-99.07	kd	CGS001-4916	NTRK3	Type VII RTKs: Neurotrophin receptor/Trk family
8764	-99.07	oe	ccsbBroad304_06394	HOXC9	Homeoboxes / ANTP class : HOXL subclass
8761	-99.06	cp	BRD-K60623809	SU-11652	Tyrosine kinase inhibitor
8758	-99.03	oe	ccsbBroad304_03574	FBXW7	F-boxes / WD-40 domains
8759	-99.03	kd	CGS001-6772	STAT1	SH2 domain containing
8760	-99.03	kd	CGS001-6768	ST14	Serine peptidases / Transmembrane
8757	-99.02	kd	CGS001-64170	CARD9	-
8753	-98.98	oe	ccsbBroad304_02048	BCL10	-
8754	-98.98	cp	BRD-K50836978	purvalanol-a	CDK inhibitor
8755	-98.98	kd	CGS001-9601	PDIA4	Protein disulfide isomerases
8756	-98.98	cp	BRD-K46056750	AZD-7762	CHK inhibitor
8751	-98.97	kd	CGS001-1936	EEF1D	-
8752	-98.97	kd	CGS001-8192	CLPP	ATPases / AAA-type
8750	-98.96	kd	CGS001-5211	PFKL	-
8749	-98.95	kd	CGS001-23476	BRD4	Bromodomain kinase (BRDK) family
8746	-98.94	cp	BRD-K97399794	quercetin	Polar auxin transport inhibitor
8747	-98.94	oe	ccsbBroad304_10487	BPHL	-
8748	-98.94	cp	BRD-K64890080	BI-2536	PLK inhibitor
8745	-98.93	kd	CGS001-3927	LASP1	-
8742	-98.92	kd	CGS001-7541	ZFP161	-
8743	-98.92	kd	CGS001-56993	TOMM22	-
8744	-98.92	kd	CGS001-1326	MAP3K8	MAPKKK:STE-unique family
8739	-98.91	kd	CGS001-55038	CDCA4	-
8740	-98.91	kd	CGS001-7840	ALMS1	-
8741	-98.91	cp	BRD-A31159102	fluoxetine	Selective serotonin reuptake inhibitor (SSRI)
8736	-98.89	cc		MTOR Inhibitor	-
8737	-98.89	cc		IGF1R Inhibitor	-
8738	-98.89	oe	ccsbBroad304_01545	SLC3A2	SLC3 family
8735	-98.88	cp	BRD-A75769826	SDM25N	Opioid receptor antagonist
8733	-98.87	cc		EGFR Inhibitor	-

Rank	Score	Type (cp= compound, kd = knock-down, oe = over-expression, cc = cmap class)	ID	Name	Description
8734	-98.87	cp	BRD-K64881305	ispinesib	Kinesin-like spindle protein inhibitor
8731	-98.8	oe	ccsbBroad304_00100	RHOA	-
8732	-98.8	cp	BRD-K05350981	oligomycin-c	ATPase inhibitor
8730	-98.79	kd	CGS001-949	SCARB1	-
8729	-98.78	kd	CGS001-2114	ETS2	ETS Transcription Factors
8728	-98.77	cp	BRD-K73610817	BRD-K73610817	-
8725	-98.74	kd	CGS001-166793	ZBTB49	BTB/POZ domain containing
8726	-98.74	kd	CGS001-55176	SEC61A2	-
8727	-98.74	kd	CGS001-8313	AXIN2	-
8723	-98.73	cp	BRD-A81177136	KN-62	Calcium-calmodulin dependent protein kinase inhibitor
8724	-98.73	kd	CGS001-8792	TNFRSF11A	Tumour necrosis factor (TNF) receptor family
8722	-98.72	kd	CGS001-10600	USP16	Ubiquitin-specific peptidases
8720	-98.71	kd	CGS001-117289	TAGAP	Rho GTPase activating proteins
8721	-98.71	kd	CGS001-11230	PRAF2	-
8717	-98.7	oe	ccsbBroad304_06257	GATA2	GATA zinc finger domain containing
8718	-98.7	cp	BRD-K55070890	thiothixene	-
8719	-98.7	cp	BRD-K09499853	KU-0060648	DNA dependent protein kinase inhibitor
8715	-98.69	kd	CGS001-6777	STAT5B	SH2 domain containing
8716	-98.69	kd	CGS001-5184	PEPD	Methionyl aminopeptidase
8710	-98.66	oe	ccsbBroad304_06639	NFYB	-
8711	-98.66	cp	BRD-K68065987	MK-2206	AKT inhibitor
8712	-98.66	kd	CGS001-55872	PBK	TOPK family
8713	-98.66	kd	CGS001-1482	NKX2-5	Homeoboxes / ANTP class : NKL subclass
8714	-98.66	oe	ccsbBroad304_06393	HOXC4	Homeoboxes / ANTP class : HOXL subclass
8709	-98.62	cc		NFKB Pathway Inhibitor	-
8705	-98.61	kd	CGS001-6256	RXRA	Retinoid X receptors
8706	-98.61	kd	CGS001-8833	GMPS	-
8707	-98.61	kd	CGS001-2021	ENDO G	-
8708	-98.61	oe	ccsbBroad304_01291	MAP2K6	MAPKK:STE7 family
8703	-98.6	oe	ccsbBroad304_11796	ULK3	Unc-51-like kinase (ULK) family
8704	-98.6	kd	CGS001-5524	PPP2R4	Serine/threonine phosphatases / Protein phosphatase 2, regulatory subunits
8702	-98.59	kd	CGS001-27	ABL2	Abl family
8701	-98.58	kd	CGS001-54623	PAF1	-
8699	-98.57	kd	CGS001-11105	PRDM7	Zinc fingers, C2H2-type
8700	-98.57	oe	ccsbBroad304_08681	ADCK3	ABC1-B subfamily
8697	-98.52	kd	CGS001-5777	PTPN6	Protein tyrosine phosphatases
8698	-98.52	cp	BRD-K02130563	panobinostat	HDAC inhibitor
8696	-98.51	kd	CGS001-4223	MEOX2	Homeoboxes / ANTP class : HOXL subclass
8694	-98.5	oe	ccsbBroad304_00498	ELK1	ETS Transcription Factors
8695	-98.5	kd	CGS001-47	ACLY	-
8693	-98.48	kd	CGS001-5434	POLR2E	RNA polymerase

Rank	Score	Type (cp= compound, kd = knock-down, oe = over-expression, cc = cmap class)	ID	Name	Description
					subunits
8692	-98.47	kd	CGS001-4351	MPI	-
8691	-98.45	kd	CGS001-5710	PSMD4	Proteasome (prosome, macropain) subunits
8687	-98.43	cc		HSP90 Inhibitor	-
8688	-98.43	kd	CGS001-6259	RYK	Type XV RTKs: RYK
8689	-98.43	oe	ccsbBroad304_08879	CASD1	-
8690	-98.43	oe	ccsbBroad304_00283	CDKN2C	Ankyrin repeat domain containing
8686	-98.42	kd	CGS001-29957	SLC25A24	Mitochondrial nucleotide transporter subfamily
8683	-98.41	kd	CGS001-3312	HSPA8	Heat shock proteins / HSP70
8684	-98.41	cp	BRD-K36740062	GSK-1070916	Aurora kinase inhibitor
8685	-98.41	cp	BRD-K98548675	parthenolide	NFkB pathway inhibitor
8681	-98.39	kd	CGS001-527	ATP6V0C	ATPases / V-type
8682	-98.39	kd	CGS001-513	ATP5D	ATPases / F-type
8678	-98.38	oe	ccsbBroad304_02864	PRDX5	-
8679	-98.38	oe	ccsbBroad304_00817	IDH2	-
8680	-98.38	oe	ccsbBroad304_03232	VPS28	-
8677	-98.37	kd	CGS001-481	ATP1B1	ATPases / P-type
8676	-98.35	kd	CGS001-3113	HLA-DPA1	Immunoglobulin superfamily / C1-set domain containing
8672	-98.34	cp	BRD-K06147391	telenzepine	Acetylcholine receptor antagonist
8673	-98.34	cp	BRD-K78122587	NNC-55-0396	T-type calcium channel blocker
8674	-98.34	cp	BRD-K14618467	IKK-16	IKK inhibitor
8675	-98.34	kd	CGS001-26574	AATF	-

[0406] Applicants can also identify novel immunotherapy targets by looking for genes which are co-regulated with the immune-checkpoints (PDCDI, TIGIT, HAVCR2, LAG3, CTLA4) in CD4 and CD8 T-cells. For example, Applicants found CD27, an immune checkpoint and the target of an experimental cancer treatment (Varlilumab). The results of this analysis are for the top 200 genes summarized in Table 8.

Table 8. Top 200 genes that are co-regulated with immune-checkpoints

	Cd8.R	Cd8.I	Cd4.R	Cd4.I
PDCDI	0.66	1.59E-215	0.60	1.03E-119
CTLA4	0.63	4.88E-193	0.65	2.60E-145
TIGIT	0.63	1.11E-191	0.73	8.03E-204
HAVCR2	0.62	1.39E-183	0.32	7.85E-30
LAG3	0.55	7.66E-136		
LYST	0.42	5.22E-76	0.26	1.67E-20
CD8A	0.40	3.93E-66	-0.08	0.007523193
TNFRSF9	0.39	1.13E-64	0.09	0.001435974
CD27	0.39	6.38E-64	0.22	3.99E-15
FAM3C	0.34	1.47E-48		
CXCL13	0.34	1.47E-47	0.27	2.41E-21
SP47	0.33	1.43E-46	0.11	0.000202982
CBLB	0.33	7.16E-46	0.20	1.64E-12
SNX9	0.33	1.35E-45	0.11	6.89E-05
SIRPG	0.33	5.21E-45	0.33	2.62E-31
TNFRSF1B	0.33	1.09E-44	0.22	3.31E-15

FCRL3	0.32	1.36E-41	0.26	9.32E-20
VCAM1	0.31	3.44E-41		
DGKH	0.31	1.67E-39		
PRDM1	0.30	3.07E-38	0.20	2.24E-12
IGFLR1	0.30	6.12E-38	0.21	7.66E-14
ETV1	0.30	1.03E-37		
RGS1	0.30	4.15E-37	0.30	3.35E-27
WARS	0.30	1.32E-36	0.14	4.98E-07
MYO7A	0.30	3.10E-36		
ITM2A	0.29	2.65E-35	0.31	1.30E-27
GBP2	0.29	1.24E-34	0.21	3.93E-13
ENTPD1	0.28	1.21E-33	0.12	4.17E-05
TOX	0.28	2.39E-32	0.44	2.27E-58
DUSP4	0.28	2.48E-32	0.36	1.94E-38
TP53INP1	0.28	7.24E-32	0.23	2.04E-16
GAPDH	0.28	1.57E-31	0.36	1.21E-37
DFNB31	0.27	6.10E-31		
ATHL1	0.27	1.19E-30	0.01	0.71761873
TRAF5	0.27	2.83E-30	0.10	0.000897484
CLEC2D	0.27	5.88E-30	-0.02	0.535704689
SLA	0.26	6.03E-29	0.20	1.37E-12
CCL3	0.26	1.26E-28	0.04	0.161249379
IL6ST	0.26	2.25E-28	0.02	0.440674275
PCED1B	0.26	3.01E-28	0.21	3.65E-13
RAB27A	0.26	3.09E-28	0.13	6.49E-06
CD7	0.26	3.23E-28	0.06	0.049851187
ICOS	0.25	3.99E-27	0.31	2.87E-28
FUT8	0.25	1.41E-26	0.10	0.000314275
RNF19A	0.25	4.44E-26	0.29	1.51E-24
TBC1D4	0.25	1.16E-25	0.31	6.28E-29
FABP5	0.25	1.63E-25	0.18	2.19E-10
B1	0.24	3.89E-24	0.24	9.16E-18
TTN	0.24	6.97E-24		
SRGN	0.24	9.35E-24	0.36	1.61E-37
SARDH	0.24	2.50E-23	0.19	3.48E-11
IFNG	0.24	3.00E-23	0.14	4.84E-07
INPP5F	0.23	3.38E-23	0.14	4.75E-07
RGS2	0.23	4.50E-23	0.18	7.21E-10
CD38	0.23	5.61E-23	0.15	1.54E-07
ID3	0.23	1.34E-22	0.05	0.066457964
PHLDA1	0.23	1.35E-22	0.11	0.000184209
TIMD4	0.23	3.53E-22		
PAM	0.23	3.69E-22	0.28	2.82E-23
PTMS	0.23	1.99E-21		
CXCR6	0.22	6.84E-21	0.26	6.42E-20
LBH	0.22	1.48E-20	0.18	3.85E-10
PRF1	0.22	1.90E-20	0.09	0.001065922
ASB2	0.22	1.90E-20	0.29	8.22E-25
KIR2DL4	0.22	2.29E-20		
STAT3	0.22	4.75E-20	0.05	0.063080818
GLDC	0.22	5.92E-20		
MIR155HG	0.22	8.11E-20	0.15	9.54E-08
CD8B	0.22	1.10E-19	-0.14	2.30E-06
CD200	0.22	1.25E-19	0.25	1.49E-18
CD2BP2	0.21	1.79E-19	0.17	5.47E-09
CD84	0.21	2.59E-19	0.11	0.000105368
CD2	0.21	3.46E-19	0.32	5.24E-31
UBE2F	0.21	3.72E-19	0.06	0.035820564
TNS3	0.21	6.38E-19		
ATXN1	0.21	1.35E-18		
HNRPLL	0.21	1.51E-18	0.26	1.96E-20
FKBP1A	0.21	2.34E-18	0.19	2.16E-11
GALM	0.21	2.95E-18	0.19	3.98E-11
TOX2	0.20	6.98E-18	0.35	2.14E-35
AFAP1L2	0.20	1.90E-17		
GEM	0.20	2.64E-17	0.16	5.19E-08
HSPB1	0.20	2.75E-17	0.09	0.002636939
CCL3L3	0.20	3.71E-17		

CADMI	0.20	3.76E-17		
GFOD1	0.20	3.88E-17		
SH2D2A	0.20	3.90E-17	0.13	6.62E-06
PKM	0.20	4.16E-17	0.26	1.71E-19
HAPLN3	0.20	9.31E-17	-0.02	0.483961847
MTSS1	0.20	1.03E-16		
ZNF79	0.20	1.79E-16	0.03	0.275651913
EID1	0.19	2.53E-16	0.09	0.003034835
ZBED2	0.19	2.96E-16	0.14	1.69E-06
PTPN6	0.19	1.31E-15	0.04	0.210702886
HMOX1	0.19	1.51E-15		
SAMSN1	0.19	1.97E-15	0.10	0.00025252
SIT1	0.19	2.34E-15	0.08	0.007781849
CCDC64	0.19	2.65E-15	0.09	0.000993524
PTPN7	0.19	4.49E-15	0.25	3.66E-18
NDFIP2	0.19	6.66E-15	0.17	6.39E-09
CD74	0.19	7.63E-15	0.28	1.23E-22
CREM	0.18	1.94E-14	0.05	0.106041668
IRF4	0.18	1.98E-14	0.16	4.09E-08
ARNT	0.18	2.23E-14	0.10	0.000571869
TRPS1	0.18	2.93E-14		
ZC3H7A	0.18	3.28E-14	0.14	1.33E-06
RHOB	0.18	3.58E-14		
ASXL2	0.18	3.99E-14		
ITGA4	0.18	4.04E-14	0.08	0.008613713
CCL4L2	0.18	5.53E-14	0.11	0.000238679
CCL4L1	0.18	5.69E-14	0.11	0.000238679
IGF2R	0.18	1.06E-13		
SOD1	0.18	1.26E-13	0.18	4.99E-10
SYNGR2	0.18	1.31E-13	0.11	0.00010303
PDE3B	0.18	1.38E-13	-0.11	0.000178183
IFI16	0.18	1.43E-13	0.20	5.81E-12
PDE7B	0.18	1.46E-13		
SLC2A8	0.18	1.59E-13		
FYN	0.17	2.58E-13	0.23	2.55E-16
ARID5B	0.17	4.06E-13	0.22	2.72E-15
NFATC1	0.17	4.72E-13	0.10	0.000521207
TPI1	0.17	4.96E-13	0.17	2.07E-09
DTHD1	0.17	6.29E-13		
CD3E	0.17	7.13E-13	0.03	0.271016862
CRIM1	0.17	7.24E-13		
TMEM155	0.17	1.02E-12		
INPP4B	0.17	1.66E-12	-0.06	0.035577188
OSBPL3	0.17	1.74E-12	0.16	4.35E-08
LIMS1	0.17	1.76E-12	0.17	1.29E-09
KCNK5	0.17	1.76E-12		
KLRC2	0.17	2.17E-12		
RGS4	0.17	3.04E-12		
ACP5	0.17	3.13E-12	0.19	5.03E-11
DENND2D	0.17	3.30E-12	0.01	0.631199717
FAIM3	0.17	3.53E-12	0.04	0.189542882
DDX3Y	0.17	4.25E-12	0.00	0.907797482
HLA-H	0.16	4.66E-12	0.21	1.54E-13
GPR56	0.16	5.64E-12	0.11	6.30E-05
MAF	0.16	5.82E-12	0.36	2.14E-38
TRIM69	0.16	7.34E-12		
SEMA4A	0.16	9.52E-12		
IL2RG	0.16	1.04E-11	0.18	6.51E-10
TMEM140	0.16	1.11E-11	0.09	0.00163736
GMDS	0.16	1.18E-11	0.08	0.008326449
LITAF	0.16	1.19E-11	-0.05	0.063294972
HSPA1A	0.16	1.56E-11	0.11	0.000172577
PAPOLA	0.16	1.56E-11	-0.01	0.70579933
AH11	0.16	2.36E-11	0.16	9.85E-09
EZR	0.16	2.40E-11	0.14	1.92E-06
MIS18BP1	0.16	2.58E-11	0.17	6.15E-09
HLA-A	0.16	2.74E-11	0.32	9.78E-31
PSTPIP1	0.16	3.27E-11	0.11	9.40E-05

GBP5	0.16	3.71E-11	0.13	5.66E-06
RIN3	0.16	3.77E-11		
HIF1A	0.16	3.97E-11	0.06	0.048813828
HLA-DRB6	0.16	4.67E-11		
PAG1	0.16	5.87E-11	-0.08	0.003384546
AKAP5	0.16	6.76E-11		
KLRC3	0.16	6.90E-11		
RFX5	0.16	8.25E-11	0.07	0.014179979
UBB	0.15	8.74E-11	0.13	5.13E-06
TXNDC11	0.15	9.85E-11	0.14	1.74E-06
FOXN2	0.15	1.00E-10	0.05	0.082411107
DUSP16	0.15	1.15E-10	0.13	1.07E-05
CD82	0.15	1.38E-10	0.18	1.30E-10
PELI1	0.15	1.40E-10	0.20	6.92E-13
AMIG02	0.15	2.03E-10		
CCDC141	0.15	2.42E-10	0.06	0.036155173
TNIP3	0.15	2.63E-10	0.10	0.000563452
SAT1	0.15	2.71E-10	0.26	2.07E-20
LRBA	0.15	3.00E-10	0.12	2.66E-05
HLA-DMA	0.15	3.36E-10	0.20	2.02E-12
MAPRE2	0.15	3.48E-10	0.10	0.000867905
BIRC3	0.15	3.71E-10	-0.01	0.720398325
EPSTI1	0.15	4.13E-10	0.18	5.86E-10
NCALD	0.15	4.21E-10	0.22	5.12E-15
ID2	0.15	4.32E-10	-0.04	0.201480439
NFAT5	0.15	4.95E-10	0.14	5.55E-07
GOLIM4	0.15	6.33E-10		
ZBTB32	0.15	6.70E-10		
NDUFB3	0.15	6.70E-10	0.13	3.74E-06
CALM3	0.15	7.24E-10	0.22	2.32E-14
SHFM1	0.15	8.32E-10	0.09	0.000949937
HLA-DRB5	0.15	9.22E-10	0.17	1.46E-09
C21orf91	0.15	9.87E-10	0.07	0.011223721
CCND2	0.15	1.09E-09	0.02	0.530718461
BTLA	0.14	1.29E-09	0.16	1.30E-08
PRKCH	0.14	1.31E-09	0.12	3.11E-05
GALNT2	0.14	1.53E-09		
IKZF3	0.14	1.77E-09	0.12	3.13E-05
AMICA1	0.14	2.14E-09	-0.06	0.026070815
STAT1	0.14	2.64E-09	0.05	0.064028082
IRF8	0.14	2.81E-09		
ELF1	0.14	2.91E-09	0.02	0.548742854
CD3D	0.14	2.93E-09	0.16	5.77E-08
RBPJ	0.14	3.26E-09	0.12	2.32E-05
BATF	0.14	3.46E-09	0.34	3.15E-33
LRRC8D	0.14	3.57E-09	0.07	0.014705554
PMF1	0.14	3.60E-09	0.10	0.000379898
TNFSF4	0.14	4.01E-09		

Example 4 - Tumor microenvironment analysis in 26 melanoma tumors

[0407] T cells were also analyzed and the T cells contributed to the predicative value of the signature of the present invention (**Figure 30**).

[0408] The novel microenvironment cell-type signatures were very much associated with survival in both immunotherapy treated patients, and in general. The genes which are up/down regulated in the immune cells after immunotherapy (CD4 T-cells, CD8 T-cells, B cells, and macrophages) are shown in Table 9.

Table 9. All Cell Type Signatures

B cells	Macrophage	Malignant	T cells cd4	T cells cd8
---------	------------	-----------	-------------	-------------

B cells	Macrophage	Malignant		T cells cd4	T cells cd8
ADAM19	AIF1	ACOT7	MFGE8	AIM1	APOBEC3G
AKAP2	ALDH2	ACSL3	MF12	ANK3	CBLB
BACH2	ANPEP	ACTN1	MGST3	AQP3	CCL4
BANK1	C15orf48	ADAM15	MIA	CAMK4	CCL4L1
BCL11A	C1orf162	ADI1	MIF	CCR4	CCL4L2
BLK	C1QA	AEBP1	MITF	CCR8	CCL5
CD19	C1QB	AGPAT1	MLANA	CD28	CD27
CD1C	C1QC	AGRN	MLPH	CD40LG	CD8A
CD22	C3AR1	AHCY	MMP14	DGKA	CD8B
CD79A	CCR1	AIF1L	MORF4L2	EML4	CST7
CD79B	CD14	AKAP12	MORN2	FAAH2	CTSW
CLEC17A	CD163	AKT3	MPZL1	FBLN7	CXCL13
CNR2	CD300A	ANXA5	MRPL24	FKBP5	CXCR6
COL19A1	CD300C	APOA1BP	MT2A	FLT3LG	DTHD1
COL4A3	CD300LF	APOD	MTUS1	FOXP3	DUSP2
CPNE5	CD33	APOE	MX1	FXYD5	EOMES
CR2	CD86	ARL2	MYH10	IL6R	FASLG
CXCR5	CFP	ARNT2	MYO10	IL7R	FCRL3
EBF1	CLEC10A	ARPC1A	MYO1D	ITGB2-AS1	GBP5
ELK2AP	CLEC12A	ASPH	NAV2	JUNB	GZMA
FAM129C	CLEC4A	ATP1A1	NCKAP1	KLRB1	GZMB
FAM177B	CLEC5A	ATP1B1	NDST1	LEPROTL1	GZMH
FCER2	CMKLR1	ATP6V0A1	NENF	LOC100128420	GZMK
FCRL1	CSF1R	B3GNT1	NES	MAL	HCST
FCRL2	CSF2RB	BACE2	NGFRAP1	OXNAD1	HLA-A
FCRL5	CSF3R	BAIAP2	NGRN	PBXIP1	HLA-B
FCRLA	CSTA	BCAN	NHSL1	PIK3IP1	HLA-H
HLA-DOB	CXCL9	BIRC7	NID1	PIM2	ID2
IGJ	CXCR2P1	BTBD3	NME1	PRKCQ-AS1	IFNG
IGLL1	DSC2	C11orf24	NME2	RORA	IL2RB
IGLL3P	FAM26F	C17orf89	NME4	RPL35A	KLRK3
IGLL5	FBP1	C1orf198	NRP2	RPL4	KLRK4
KIAA0125	FCER1G	C1orf21	NRSN2	RPL6	KLRK4-KLRK1
KIAA0226L	FCGR1A	C1orf85	NSG1	RPS15A	KLRD1
LOC283663	FCGR1B	CALD1	OSBPL1A	RPS27	KLRK1
MS4A1	FCGR1C	CALU	P4HA2	RPS28	LAG3
P2RX5	FCGR3A	CAPN3	PACSN2	SEPT6	LSP1
PAX5	FCGR3B	CAV1	PAX3	SLAMF1	LYST
PNOC	FCN1	CBR1	PCDHGC3	SORL1	NKG7
POU2AF1	FOLR2	CCND1	PEG10	SPOCK2	PDCD1
POU2F2	FPR1	CCT3	PFDN2	SUSD3	PRF1
RASGRP3	FPR2	CD151	PFKM	TCF7	PSTPIP1
SEL1L3	FPR3	CD276	PFN2	TMEM66	PYHIN1
SNX29P1	GGTA1P	CD59	PGRMC1	TNFRSF18	RARRES3
ST6GAL1	GNA15	CD63	PHB	TNFRSF25	SH2D1A
STAP1	GPR84	CD9	PHLDB1	TNFRSF4	SH2D2A
SWAP70	HCK	CDC42BPA	PIR	TNFSF8	TARP
TCL1A	HK3	CDC42EP4	PKNOX2	TRABD2A	TIGIT
TMEM154	IGSF6	CDH19	PLEKHB1	TSC22D3	TNFRSF9
VPREB3	IL1B	CDK2	PLK2	TXK	TOX
	IL1RN	CDK2AP1	PLOD1		
	IL411	CECR7	PLOD3		
	ITGAM	CELSR2	PLP1		
	KYNU	CERCAM	PLS3		
	LGALS2	CERS2	PLXNA1		
	LILRA1	CHCHD6	PLXNB3		
	LILRA2	CHL1	PMEL		
	LILRA3	CHPF	PMP22		
	LILRA4	CLDN12	POLR2F		
	LILRB2	CLIC4	POLR2L		
	LILRB4	CNIH4	PON2		
	LILRB5	CNN3	PPT2		
	LST1	CNP	PRAME		
	MAFB	CNPY2	PRDX4		
	MARCO	COA3	PRDX6		
	MNDA	COL16A1	PRKCDBP		
	MRC1	COMT	PROS1		

B cells	Macrophage	Malignant		T cells cd4	T cells cd8
	MS4A4A	CRIP2	PRSS23		
	MS4A6A	CRNDE	PSMB5		
	MSR1	CRTAP	PTGFRN		
	NCF2	CRYAB	PTGR1		
	OLR1	CSAG1	PTK2		
	P2RY13	CSAG3	PTPLAD1		
	PILRA	CSPG4	PTPRM		
	PLAU	CSRP1	PTPRS		
	PLBD1	CTDSPL	PTRH2		
	PLXDC2	CTHRC1	PTTG1IP		
	PRAM1	CTNNAL1	PYCR1		
	RAB20	CTNNB1	PYGB		
	RAB31	CTSF	PYGL		
	RASSF4	CTSK	QDPR		
	RBM47	CTTN	QPCT		
	RGS18	CYB5R1	RAB13		
	S100A8	CYP27A1	RAB17		
	S100A9	CYSTEM1	RAB34		
	SECTM1	CYTH3	RAB38		
	SIGLEC1	DAAM2	RAI14		
	SIGLEC7	DCBLD2	RBFOX2		
	SIGLEC9	DCT	RCAN1		
	SLAMF8	DDR1	RCN1		
	SLC31A2	DDR2	RCN2		
	SLC43A2	DIP2C	RDX		
	SLC7A7	DLC1	RGS20		
	SLC8A1	DNAH14	RND3		
	SLCO2B1	DOCK7	ROBO1		
	SPI1	DST	ROPN1		
	STAB1	DSTN	ROPN1B		
	TBXAS1	DUSP6	RTKN		
	TFEC	ECM1	S100A1		
	TGFBI	EDNRB	S100A13		
	TLR2	EFNA5	S100A16		
	TLR4	EIF4EBP1	S100B		
	TLR8	EMP1	SCARB1		
	TMEM176A	ENTPD6	SCCPDH		
	TMEM176B	EPS8	SCD		
	TNFSF13	ERBB3	SDC3		
	TNFSF13B	ETV4	SDC4		
	TREM2	ETV5	SDCBP		
	TYROBP	EVA1A	SELENBP1		
	VSIG4	EXOSC4	SEMA3B		
	ZNF385A	FAM127A	SEMA3C		
		FAM127B	SEMA6A		
		FAM167B	SEPT10		
		FARP1	SERPINA3		
		FARP2	SERPINE2		
		FASN	SERPINH1		
		FKBP10	SGCD		
		FKBP4	SGCE		
		FKBP9	SHC1		
		FN1	SHC4		
		FNBP1L	SLC19A2		
		FRMD6	SLC24A5		
		FSTL1	SLC25A13		
		FXYD3	SLC25A4		
		G6PC3	SLC35B2		
		GALE	SLC39A1		
		GCSH	SLC39A6		
		GDF15	SLC45A2		
		GJB1	SLC6A15		
		GLI3	SLC7A8		
		GNG12	SMARCA1		
		GOLM1	SNAI2		
		GPM6B	SNCA		
		GPR143	SNHG16		

B cells	Macrophage	Malignant		T cells cd4	T cells cd8
		GPRC5B	SNRPE		
		GSTA4	SORT1		
		GSTP1	SOX10		
		GULP1	SOX13		
		GYG2	SOX4		
		H1FO	SPARC		
		HIBADH	SPR		
		HMCN1	SPRY4		
		HMG20B	SPTBN1		
		HOXB7	SRPX		
		HOXC10	SSFA2		
		HSBP1	ST3GAL4		
		HSP90AB1	ST5		
		HSPB1	ST6GALNAC2		
		HSPD1	STK32A		
		HSPG2	STMN1		
		IFI27	STXBP1		
		IGF1R	SYNGR1		
		IGFBP7	TANC1		
		IGSF11	TBC1D16		
		IGSF3	TBC1D7		
		IGSF8	TCEAL4		
		IMPDH2	TEAD1		
		ISYNA1	TENC1		
		ITFG3	TEX2		
		ITGA3	TFAP2A		
		ITGB3	TIMP2		
		KIRREL	TIMP3		
		LAMB1	TJP1		
		LAMB2	TMEM147		
		LAMC1	TMEM14C		
		LAPTM4A	TMEM9		
		LAPTM4B	TMEM98		
		LDLRAD3	TNFRSF19		
		LGALS1	TOM1L1		
		LGALS3BP	TRIM2		
		LINC00473	TRIM63		
		LINC00673	TSC22D1		
		LMNA	TSPAN3		
		LOC100126784	TSPAN4		
		LOC100130370	TSPAN6		
		LOC645166	TTL4		
		LOXL4	TUBB2A		
		LRP6	TUBB2B		
		MAGEA12	TUBB3		
		MAGEA2B	TYR		
		MAGEA3	UBL3		
		MAGEA6	VAT1		
		MAGED1	VIM		
		MAGED2	VKORC1		
		MAP1B	WASL		
		MARCKSL1	WBP5		
		MDK	WIPI1		
		MFAP2	WLS		
			XAGE1A		
			XAGE1B		
			XAGE1C		
			XAGE1D		
			XAGE1E		
			XYLB		
			YWJAE		
			ZNF462		

Table 10. Down-regulated and Up-regulated genes post-immunotherapy treatment in microenvironment

T.cdb.up		T.cdb.down		T.cd4.up		T.cd4.down		Macro.up		Macro.down	
AARS2	LYRM7	ACTN4	MAL	AARS2	ACTR2	APOC1	AREG				
ABHD15	MAP3K13	ADAM10	MAP1LC3A	ABI2	ADRBK1	APOE	ARF1				
ABI2	MAP7D3	AEN	MED21	APOBEC3A	ANAPC11	C17orf76-AS1	BRE-AS1				
AK3	MAPK13	AIM1	MGMT	APOL2	ANKRD36BP1	C1orf56	CD55				
AKAP5	MBOAT1	AIP	MKNK2	ARP6	ARAP2	CA2	CREM				
AKIP1	ME2	AKAP13	MPG	C17orf76-AS1	ASCC3	CD81	DUSP2				
ALG1	MED18	AKNA	MRPL47	C1orf56	ASMTL	CSTB	EREG				
ANKRD40	METTL16	AMD1	MRPL53	C1QB	ATXN2L	CXCL9	ETS2				
AP1G2	METTL2B	ANKRD11	MRPL54	CASP10	BCL6	DBNDD2	FKBP5				
AP3M1	MFSD11	ANKRD36BP1	MSI2	CCL5	C22orf34	DHRS412	FOSB				
AP3S2	MIAT	APBB1P	MT2A	CGND2	CALM3	DNAJC5B	GAPT				
APOL2	MLANA	APH1A	MXD4	CD68	CCNG1	DYNC112	HIF1A				
ARF6	MMS22L	APOBEC3G	MYCBP2	CEP41	CD200	DYNLL1	ICAM3				
ARIH2OS	MOC53	ARID1A	MYEOV2	CLUAP1	CD226	FABP3	IFI44L				
ARMC10	MREG	ARID2	MYH9	CNNM3	CD3E	FOLR2	IL1B				
ARSA	MRPL44	ARL1	NACA	CTBP1	CD40LG	FTL	LOC100130476				
ASB8	MS4A1	ARL4C	NAP1L1	CXCR3	CD58	FUCA1	MEF2C				
ATP6V0A2	MSH3	ASF1B	NDC80	CXCR6	CD6	GPNMB	NFIL3				
B2M	MTFMT	ATAD1	NDE1	DCAF10	CDC42EP3	HLA-J	NFKBIA				
BCL6	NAA16	ATP5E	NDUFA12	DNAJC14	CHI3L2	HSD11B1	NFKBIZ				
BLOC1S6	NDNL2	ATP5L	NDUFA13	FAM126B	COX7C	HSD3B7	NLRP3				
BMS1P1	NEK2	ATP5O	NDUFA2	FAM134A	CPSF1	HSPA7	NR4A2				
BMS1P4	NFKBIB	ATP6V0C	NDUFA4	FAM153C	CTSA	HSPB1	PPP1R15B				
BMS1P5	NME6	ATP6V0E2	NDUFA6	FGD5-AS1	CXCR5	KLHDC8B	REL				
BRIP1	NOL9	ATXN2L	NFATC2	GBP4	DDX39B	MGLL	RPSAP58				
C10orf32	NP1PL3	ATXN7L1	NFKBIA	GBP5	DDX3Y	MIR4461	THBS1				
C12orf65	NQO1	AURKB	NFKBIZ	GNRHR2	DHRS7	MRPS15	TNFAIP3				
C19orf40	NT5DC3	BCL11B	NINJ2	GPR56	EHD1	NOP10	ZBTB16				
C1orf174	NUAK2	BCL2	NIPBL	GSTM3	EIF3L	NUPR1	ZFP36				
C1orf210	OCN	BHLHE40-AS1	NIT2	GZMA	ERGIC3	PCBD1					
C1orf56	OPHN1	BIRC5	NOP56	HAUS2	EXOC1	PLA2G2D					
C1orf63	ORC6	BLMH	NPM1	HERC2P4	FAM172A	PLA2G7					
C1Q1NF6	PACS2	BLVRA	ORMDL3	HLA-DRA	GNG5	RAB20					
C5orf24	PAFAH1B2	BRK1	OST4	HLA-DRB1	GPRIN3	SCARB1					
C5orf55	PAICS	BTF3	PABPC1	HNRNPH1	HDDC2	SLRP					
C9orf3	PAN3	BTN3A2	PAIP2	INADL	HINT1	ST3GAL5					
C9orf85	PAR-SN	BUB1	PAM	KLRD1	HIST1H1D	TIMP2					
CACUL1	PARP11	BUB3	PARK7	LINC00439	HIST1H1E	TMSB10					
CAMLG	PARP3	C1D	PARP8	LOC100506469	HIVEP2	TRNAUIAP					
CCDC122	PARP9	CARD16	PCBP1	LOC284379	HNRNPC	UBD					
CCR6	PCGF5	CARS	PCBP2	LOC389641	HS3ST3B1	WSB2					
CD160	PDE12	CASP4	PDCD1	LOC644961	ICA1	XIST					
CD24	PER2	CASP8	PDCD5	LOC727896	ITM2A	YTHDF2					
CD68	PEX13	CBLB	PER1	MAP3K13	ITPR1						
CENPN	PIGX	CCDC141	PET117	MCTS1	KLF12						
CEP104	PKNOX1	CCDC167	PFDN5	NANOG	LCMT1						
CHP1	PMEL	CCDC23	PIK3IP1	NXNL2	LOC100216545						
CLCC1	POU2AF1	CCL4	PIK3R5	PIP4K2A	LOC100271836						
CLUAP1	PPP1R3B	CCNB2	PIN4	PLEKHA2	LOC285740						
CNNM3	PQLC2	CCND1	PLCB2	PPID	MAEA						
COA1	PRMT2	CCND3	PLEK	PRDM1	MAP2K3						
COX10-AS1	PSTPIP2	CCNH	PLEKHM1	PSTPIP2	MAP4K1						

T.cdb.up		T.cdb.down		T.cd4.up	T.cd4.down	Macro.up	Macro.down
COX18	PTPN2	CCNK	PLIN2	QRSL1	MED21		
CPPED1	QPR1	CCR1	POGZ	RASSF3	MKNK2		
CPT1A	RAB21	CCR4	PPIA	RBM43	MRPL33		
CRK	RAB33B	CCR5	PPM1G	RGS1	MRPS2		
CSAD	RAD1	CD2	PRDM1	RPP14	MTERFD2		
CSNK1G1	RASSF1	CD200R1	PRDX6	RUNX1-IT1	MTMR6		
CWC25	RBBP5	CD27	PRMT10	SBF2-AS1	MYEOV2		
CYB5D2	RBL1	CD320	PRPF8	SCAI	NAB1		
CYP4V2	RBMS2	CD37	PRR14L	SGOL1	NDUFA4		
DCP1A	RDH10	CD3D	PRRC2B	SLC25A51	NEK7		
DESI1	REL	CD3E	PTBP3	SLC35E1	NFATC1		
DGKD	RFC2	CD3G	PTPN4	SPDYE1	NFATC2		
DHODH	RFT1	CD4	PTRHD1	SPDYE2	NINJ2		
DIP2A	RHD	CD7	RAB1B	SPDYE2L	OST4		
DIS3	RIOK3	CD79A	RAPGEF1	SPDYE7P	P2RX5		
DIS3L	RNF14	CD81	RASA1	SWSAP1	PAPD4		
DNASE1	RNF141	CDC42SE1	RASA2	THAP5	PARL		
DND1	RPS6KA3	CDK1	RBM38	TMEM120B	PASK		
DTD2	RUNDC1	CENPK	RGS1	TMEM192	PCBP1		
EEF2K	S1PR2	CHCHD2	RGS10	TP53RK	PDCD1		
EIF5A2	SATB1	CHI3L2	RHBDD3	TRMT10B	PFKL		
ELMSAN1	SCAI	CIRBP	RHOA	TSNAX	PHF3		
ESYT2	SCAMP1	CITED2	RNASEK	TXNDC15	PHF8		
EYA3	SCML4	CLASP1	RPA3	UGT8	PIK3CG		
F11R	SEC23IP	CLDND1	RPL13A	UPK3BL	PLP2		
FAM126B	SEMA4D	CLECL1	RPL14	XIST	PON2		
FAM210B	SENP5	COX17	RPL18	ZNF253	PPP1CA		
FAM215A	SERPINB1	COX4I1	RPL22	ZNF276	PRKCH		
FAM217B	SERPINB6	COX6A1	RPL23	ZSWIM7	PRNP		
FAM73A	SGCB	COX7A2L	RPL27		PRRC2B		
FANCD2	SGK3	COX7C	RPL27A		PTBP3		
EASTKD2	SGOL1	COX8A	RPL29		RBM25		
FBLIM1	SH2D1B	CREB3L2	RPL31		RERE		
FBXL18	SIRT5	CSNK1D	RPL32		RGS3		
FBXW2	SKP2	CST7	RPL34		RPL13A		
FCRL3	SLAMF7	CTSC	RPL35		RPL14		
FCRL6	SLC25A15	CTSD	RPL35A		RPL27		
FDPSL2A	SLC25A32	CXCL13	RPL36		RPL37		
FLCN	SLC25A51	CXCR4	RPL36A		RPS26		
FLOT1	SLC2A3	CXCR6	RPL36AL		RPS4Y1		
FOXP1	SLC30A6	CYTIP	RPL37		RPS5		
FTO	SLC30A7	DDIT4	RPL37A		SARDH		
FXN	SLC31A1	DDX6	RPL38		SEC11C		
GALNT6	SLC35A3	DNAJB12	RPL39		SEC16A		
GATAD1	SLC48A1	DNAJC9	RPLP0		SELT		
GBP1	SLC50A1	DPM3	RPRD2		SF3B1		
GBP2	SLC7A5P2	DTHD1	RPS10		SFI1		
GBP4	SMIM14	DUSP4	RPS13		SMARCE1		
GBP5	SMYD4	EBP	RPS16		SMG1P1		
GCLM	SNAPC3	EEF1B2	RPS17		SNHG5		
GDAP2	SNIIG7	EEF1D	RPS17L		SNRPN		
GEMIN8	SNIP1	EEF2	RPS20		SRRM2		
GGPS1	SOAT1	EHMT1	RPS21		SSH2		
GLIPR1L2	SPAST	EIF3F	RPS23		STAU1		
GLUD1P7	SPRYD4	EIF3G	RPS24		TATDN1		
GMEB1	SRSF8	EIF4B	RPS26		TCF7		
GNE	SS18	ELK2AP	RPS28		THADA		
GNG4	STAT1	EMB	RPS29		TIAM1		
GNRHR2	STAT5B	ENSA	RPS4X		TIGIT		
GOLGA3	STOM	ERAP2	RPS5		TMEM59		
GPCPD1	STYX	ERGIC3	RPS7		TOX		
GPR82	SWSAP1	ERH	RPS9		TOX2		
GTF2H2C	TADA2B	ERN1	RPSA		TYK2		
GTPBP5	TADA3	ETS1	RBSN1		UBQLN1		
HAUS3	TANGO2	EVL	RUNX2		UQCR10		
HERC2P7	TARS2	FAM102A	RUNX3		UQCRH		
HIST1H2BG	TATDN3	FAM129A	S100A6		UTRN		

T.cd8.up		T.cd8.down		T.cd4.up	T.cd4.down	Macro.up	Macro.down
HIVEP3	TBC1D24	FAM53B	SELL		UXT		
HMHA1	TBCCD1	FAM78A	SF3A1		WNK1		
HOGA1	TERF1	FAU	SHISA9		WWP2		
HOPX	TERF2	FBXO5	SIRPG		ZFP36		
HSPA1B	THAP5	FKBP5	SLA		ZNF217		
ICA1L	TLE3	FNDC3A	SLC39A7				
ID3	TM7SF3	FOSB	SLC4A7				
IDO1	TMEM123	FOXP1	SMG7				
IER2	TMEM209	FRYL	SNORD10				
IFITM3	TMEM41A	G6PD	SNRNP200				
IFNAR1	TMEM41B	GAS5	SON				
IFNLR1	TNFAIP8L2-SCNM1	GINS2	SPOCK2				
IKBIP	TNFSF14	GLRX	SRRM2				
IL10	TPMT	GMCL1	SSR4				
INIP	TRIM5	GMFG	STK16				
INPP4B	TRIOBP	GMNN	SUMO2				
INPP5F	TSNAX	GNG5	SUPV3L1				
IRAK4	TTC39C	GPLY	SYNGR2				
IRF1	TUBGCP4	GOLGA8B	SYTL3				
IRF2BP2	TYMP	GPR183	TAF15				
ITGAX	UBB2Q2	GPR56	TAOK3				
ITK	UBOX5	GRN	TAP2				
KCNK5	UBXN2B	GSTM1	TK1				
KDELC2	UTP23	GSTP1	TLN1				
KDSR	VMP1	GTF2B	TMED9				
KIAA0355	WAC-AS1	GTF3C6	TMEM155				
KIAA1324	WDR92	GZMK	TMEM2				
KIAA1919	XIAP	H2AFZ	TNFAIP3				
KIF18B	XKR9	HDAC8	TNFSF4				
KIF3A	ZBTB24	HERC2P2	TNFSF8				
KIN	ZBTB43	HERPUD1	TOB1				
KLHL28	ZCHC4	HINT1	TOMM7				
KLRC2	ZFP14	HIST1H1E	TOX				
KLRC3	ZFP36L1	HIST1H3G	TP53INP1				
KLRD1	ZMYM5	HIST1H4C	TPX2				
KRAS	ZNF100	HLA-DQA1	TSC22D3				
LAIR1	ZNF124	HLA-DQA2	TSPAN14				
LDHA	ZNF160	HLA-DRB5	TSPYL2				
LDLR	ZNF321P	HLA-F	TSTD1				
LIAS	ZNF333	HLA-H	TTN				
LINC00476	ZNF37BP	HMBX1	TUBA4A				
LLGL1	ZNF483	HUWE1	TXK				
LOC100131067	ZNF526	IFIT5	TXNIP				
LOC100131089	ZNF528	IL6ST	TYMS				
LOC100132247	ZNF529	IQGAP1	UBA52				
LOC100190986	ZNF543	IQGAP2	UBE2C				
LOC100268168	ZNF548	ISCU	UBE2T				
LOC100271836	ZNF549	ISG20	UCP2				
LOC100505812	ZNF620	ITGAD	UGDH-AS1				
LOC100505876	ZNF652	ITGB1	UQCR11				
LOC100506083	ZNF665	ITGB2	UQCRB				
LOC100652772	ZNF669	ITM2B	UQCRH				
LOC202781	ZNF683	KDM5C	USB1				
LOC284023	ZNF721	KIAA1551	UXT				

T.cd8.up		T.cd8.down		T.cd4.up	T.cd4.down	Macro.up	Macro.down
LOC389641	ZNF793	KIR2DL4	VCAM1				
LOC727896	ZNF805	KLF12	VRK1				
LOC729603	ZNF814	KPNB1	WDR830 S				
LOC90834	ZSCAN2	LDHB	WNK1				
LRRRC57	ZSCAN22	LENG8	YEATS4				
LRRRC58	ZSCAN29	LINC00493	YWHAB				
LY9	ZSWIM7	LINC00612	ZBTB38				
		LNPEP	ZC3H12A				
		LOC643406	ZC3HC1				
		LOC643733	ZDHHC24				
		LOC646214	ZFP36L2				
		LRRRC37A4P	ZMYND8				
		LSM6	ZNF638				
		MAD2L1	ZWINT				
		MAEA					

Table 11. Top Genes from Table 10

T.cd8.up	T.cd8.down	T.cd4.up	T.cd4.down	Macro.up	Macro.down
AP1G2	AKNA	CASP10	CHI3L2	NUPR1	FKBP5
AP3M1	BCL2	CXCR3	COX7C		LOC100130476
APOL2	CARD16	CXCR6	CXCR5		NLRP3
ARF6	CCDC141	FAM153C	HIST1H1E		THBS1
C12orf65	COX4I1	FGD5-AS1	HIVEP2		TNFAIP3
CCDC122	COX8A	GBP5	ICA1		
CSAD	EIF3G	LOC727896	NEK7		
CWC25	FAU	NXNL2	NFATC2		
DHODH	G6PD	RBM43	NINJ2		
DIS3L	GLRX	RGS1	PASK		
FAM217B	GPLY	SLC35E1	RPL13A		
GBP2	GPR56	SPDYE1	TCF7		
GDAP2	HIST1H4C				
HOPX	HLA-DRB5				
IKBIP	HUWE1				
KIAA1919	ITGB2				
LOC727896	MGMT				
LOC90834	MKMK2				
LRRRC58	NDC80				
MAP7D3	NDUFA6				
MFSD11	PIK3R5				
MOCS3	RPL35A				
PER2	SYTL3				
POU2AF1	TNFSF4				
PQLC2	TOB1				
RAD1	UCP2				
SGCB	WNK1				
SGOL1					
SLC2A3					
SNAPC3					
SRSF8					
SS18					
STOM					
SWSAP1					
TANGO2					
TERF2					
TMEM123					
TMEM209					
ZBTB43					
ZNF160					
ZNF528					
ZNF543					

Example 5

Protein-Protein interactions between genes in the resistance signatures

[0409] In line with the co/anti-regulatory patterns of the PIT-Up (ICR-Up) and PIT-Down (ICR-down) modules, a significantly large number of protein-protein interactions occur within and between the two modules (253 interactions, $P = <1e-3$,) (Table 12). The number of interactions is ~7 times more than expected (empirical p-value)

Table 12.

GeneA	GeneB	GeneA	GeneB
ACAA2	PFN1	FOXRED2	OS9
ACAA2	ATP1B3	FXYD3	NR4A1
ACAA2	ISYNA1	G6PD	GBP2
ACSL4	PTPMT1	G6PD	TSTA3
ACSL4	HTATIP2	G6PD	IDH2
ADSL	UBC	GEM	LZTS2
ADSL	XPNPEP1	GLOD4	NR4A1
ADSL	PAICS	GLOD4	NNMT
AEN	LZTS2	GLOD4	PAICS
AHNAK	FN1	HDAC2	SMC3
AHNAK	S100A10	HDAC2	KLF4
ALDH1B1	UBC	HDAC2	RUVBL2
ALDH1B1	FN1	HDAC2	SNAI2
ALDH1B1	XPNPEP1	HDAC2	TSC22D3
ANXA1	UCHL5	HLA-A	TAPBP
ANXA1	FN1	HLA-A	TAP1
ANXA2	CTSB	HLA-A	UBC
ANXA2	S100A10	HLA-A	ITM2B
ANXA2	MIDI	HLA-A	HLA-C
ANXA2	FN1	HLA-A	HLA-E
ANXA2	LGALS1	HLA-C	UBC
ARHGEF1	CD44	HLA-C	HLA-F
ARHGEF1	FN1	HLA-C	HLA-E
ATF3	STAT1	HLA-C	ITGA6
ATF3	JUNB	HLA-E	HLA-F
ATP1A1	UBC	HLA-E	ITGA6
ATP1A1	ATP1B3	HSP90B1	OS9
ATP1B3	PTP4A3	HSP90B1	TPM1
ATP1B3	HLA-C	HSP90B1	RPN2
ATP1B3	RPL17	HSP90B1	TSR1
ATXN10	BSG	HSP90B1	STAT1
ATXN10	FN1	IDH2	UBC
ATXN10	MRPS16	IGF1R	IGFBP3
ATXN2L	GALNS	IGFBP3	TF
ATXN2L	PABPC1	ILF2	XRCC5
BCCIP	EIF6	ILF2	RPL17
BCCIP	FAM46A	ILF2	RPL10A
BCCIP	SORD	ILF2	RPS3
BCCIP	SMS	ILF2	SRSF7
BCL6	JUNB	ILF2	PRKCDBP
BCL6	HDAC2	ILF2	TOMM22
BCL6	PELII	ILF2	PTRF
BIRC3	UBC	ILF2	RUVBL2
BSG	OS9	ILF2	MYBBP1A
BSG	MYBBP1A	ILF2	KIAA0020
BSG	XP07	ITGA6	LGALS3BP

GeneA	GeneB
BSG	METAP2
BSG	PTPMT1
CALU	GAA
CALU	PRKCDBP
CALU	CTNNAL1
CALU	HSP90B1
CAV1	CD44
CAV1	PTRF
CD151	CD46
CD44	IGFBP3
CD44	FN1
CD44	NF2
CD46	CD9
CD9	LGALS3BP
CFB	FN1
CPSF1	POLR2A
CRELD1	EIF6
CRYAB	CS
CRYAB	SORD
CS	CTPS1
CST3	CTSB
CTSA	CTSD
CTSB	S100A10
CTSB	SPRY2
CTSD	UCHL5
CTSD	HSP90B1
DCBLD2	ITM2B
DCTN6	RPSA
ECHS1	UCHL5
ECHS1	ISYNA1
EGR1	JUNB
EIF4A1	PABPC1
EIF4A1	UCHL5
EIF4A1	RPSA
EIF4A1	TMEM43
EIF4A1	ILF2
EIF4A1	FN1
EIF6	PAICS
EIF6	PSME1
EIF6	FBL
EIF6	RPL17
EIF6	RUVBL2
EIF6	TSNAX
EIF6	KIAA0020
EMP1	SMIM3
EPDR1	NF2
FAM213A	HLA-C
FAM46A	PRSS23
FAM46A	SQRDL
FAM46A	FNDC3B
FBL	RUVBL2
FBL	KLF6
FBL	UBC
FBL	NOLC1
FBL	RPL17
FBL	RPS7
FBL	RPS3

GeneA	GeneB
KLF4	KLF6
LAMB1	UBC
LGALS1	LGALS3BP
LZTS2	TSNAX
LZTS2	SMIM3
MIDI	RPS3
MIDI	UBC
MTG1	PRNP
MYBBP1A	NR4A1
MYBBP1A	RPS3
MYBBP1A	PTRF
NCBP1	THOC5
NCBP1	SERPINE2
NF2	XRCC5
NF2	RPS3
NF2	RPS7
NF2	SMC3
NOLC1	PTRF
OXA1L	PTPMT1
PABPC1	RPSA
PABPC1	RBM4
PABPC1	RPL10A
PABPC1	RPL17
PELII	UBC
PFN1	UCHL5
POLR2A	XRCC5
POLR2A	SMC3
POLR2A	PSMB9
POLR2A	RUVBL2
PRAME	UBC
PRDX3	UCHL5
PRDX3	PSME1
PROS1	RPSA
PSMB9	PSME1
PSMB9	UCHL5
PTP4A3	XP07
RND3	SKP2
RPL10A	RPS3
RPL10A	RPL17
RPL10A	RPSA
RPL10A	S100A10
RPL10A	RPS7
RPL17	RPS3
RPL17	RPSA
RPN2	UBC
RPS3	RPS7
RPS3	RPSA
RPS3	TPM1
RPS3	TSR1
RPS3	UBC
RPS3	TSNAX
RPS7	RPSA
RPS7	TSR1
RPSA	TSR1
RUVBL2	SRCAP
RUVBL2	UCHL5
RUVBL2	UBC

Example 8 -Analysis of Single Cells from ER+ Metastatic Breast Cancer and Colon Cancer

[0412] Applicants also analyzed single cells in other cancers having an ICR signature, (see, e.g., **Figure 15A, B**). Applicants further extended the melanoma ecosystem studies to study response to immunotherapy, using massively parallel droplet scRNA-Seq to analyze cells from colon tumors, using snRNA-Seq methods to profile metastatic breast cancer samples and profiling pancreatic tumors. Cancer cells may be more or less resistant to immunotherapy based on uICR scores. Single cells in other cancers may be shifted to an immunotherapy sensitive signature by treating with CDK4/6 inhibitors. Analysis of this signature and measuring shifts in the signature after CDK4/6 inhibition can allow the proper administration of an immunotherapy in a combination treatment.

[0413] Applicants analyzed ER+ metastatic breast cancer using single nuclei RNA-seq (snRNA-seq) on fresh and frozen tissue samples (**Figure 38**). snRNA-seq as described herein is compatible with frozen tissue samples. Non-malignant cells clustered by cell type in both frozen and fresh tissue samples. Malignant cells clustered by patient.

[0414] Applicants analyzed 22 colon cancer samples using scRNA-seq (**Figure 39**). With strict quality control (QC) on the 22 samples analyzed Applicants obtained 12,215 epithelial cells and 17,143 non-epithelial cells.

Example 9 - Immunotherapy Resistance Signature

[0415] Immunotherapies have transformed the therapeutic landscape of several cancer types (Sharma and Allison, 2015). However, despite the durable responses in some patients, most patients' tumors manifest unpredictable resistance to immunotherapies (Gibney et al., 2016; Sharma et al., 2017). This hampers appropriate selection of patients for therapies, rational enrollment to clinical trials and the development of new therapeutic strategies that could overcome resistance (Sharma and Allison, 2015). Most non-responding patients manifest intrinsic resistance, reflected as continued tumor growth or occurrence of new metastatic lesions despite therapy, whereas some patients develop acquired resistance following an initial clinical disease regression. It is unknown whether these clinically discrete manifestations are associated with shared or distinct molecular mechanisms of resistance (Sharma et al., 2017).

[0416] Recent studies characterized resistance to immune checkpoint inhibitors (ICI) by analyzing Whole Exome Sequencing (WES) and transcriptional profiles of bulk tumors (Hugo et al., 2016; Mariathasan et al., 2018; Van Allen et al., 2015). These studies

demonstrated that tumors with a high mutational load (Van Allen et al., 2015) and a high level of immune cell infiltration (Riaz et al., 2017; Tumei et al., 2014) are more likely to respond, and linked ICI resistance in patients to functional immune evasion phenotypes, including defects in the JAK/STAT pathway (Zaretsky et al., 2016) and interferon gamma (IFN- γ) response (Gao et al., 2016; Zaretsky et al., 2016), impaired antigen presentation (Hugo et al., 2016; Zaretsky et al., 2016), and PTEN loss (Peng et al., 2016). While these studies significantly contributed to the understanding of the cancer-immune interplay, the resulting biomarkers were only partially predictive (Sharma et al., 2017). This may be due to the fact that they only reflect some facets of the causes of resistance (WES) or combine signals from malignant and non-malignant (immune and stroma) cells (RNA and copy-number variations).

[0417] Because immune checkpoint inhibitors target the interactions between different cells in the tumor, their impact depends on multicellular circuits between malignant and non-malignant cells (Tirosh et al., 2016a). In principle, resistance can stem from different compartment of the tumor's ecosystem, for example, the proportion of different cell types (*e.g.*, T cells, macrophages, fibroblasts), the intrinsic state of each cell (*e.g.*, memory or dysfunctional T cell), and the impact of one cell on the proportions and states of other cells in the tumor (*e.g.*, malignant cells inducing T cell dysfunction by expressing PD-L1 or promoting T cell memory formation by presenting neoantigens). These different facets are inter-connected through the cellular ecosystem: intrinsic cellular states control the expression of secreted factors and cell surface receptors that in turn affect the presence and state of other cells, and vice versa. In particular, brisk tumor infiltration with T cell has been associated with patient survival and improved immunotherapy responses (Fridman et al., 2012), but the determinants that dictate if a tumor will have high ("hot") or low ("cold") levels of T cell infiltration are only partially understood. Among multiple factors, malignant cells may play an important role in determining this phenotype (Spranger et al., 2015). Resolving this relationship with bulk genomics approaches has been challenging; single-cell RNA-seq (scRNA-seq) of tumors (Li et al., 2017; Patel et al., 2014; Tirosh et al., 2016a, 2016b; Venteicher et al., 2017) has the potential to shed light on a wide range of immune evasion mechanisms and immune suppression programs.

[0418] Here, Applicants used scRNA-seq and a new computational approach to identify immune evasion or suppression mechanisms in the melanoma ecosystem (**Figure 44A ,B**).

Applicants developed a data-driven approach that integrates scRNA-seq with other data sources to characterize malignant cell states that drive immune resistance in melanoma (**Figure 44B**). Applicants identified a program in malignant cells that is associated with T cell exclusion prior to immunotherapy, and with the melanoma cell states in patients who were resistant to immunotherapies. Applicants confirmed its presence *in situ* in tumors with multiplex protein imaging. This program predominantly reflects intrinsic resistance to immune checkpoint inhibitors (but not to RAF/MEK-targeted therapy) and its expression predicts responses to ICI and clinical outcomes in independent patient cohorts. Applicants further associated the CDK4/6 pathway with control of this program and showed that treatment with CDK4/6 inhibitors reverses it and promotes a senescent-like state. This work provides a new predictive biomarker for ICI response, suggests a new therapeutic modality that may re-sensitize malignant melanoma cells to ICI, and provides a general framework to study the effect of immunotherapies and other drugs on complex tumor ecosystems.

RESULTS

Systematic approach to discover malignant cell programs associated with immune cell infiltration or exclusion

[0419] To identify malignant cell programs that characterize "cold" melanoma tumors, Applicants devised a new strategy that combines scRNA-seq and bulk RNA-Seq data to relate the cellular state of one cell type (*e.g.*, malignant cell states) to the cellular composition of the tumors (*e.g.*, T cell infiltration *vs.* exclusion) (**Figure 44B**). For clarity, Applicants describe the strategy in this specific context, though it can be applied to any two cell-types of interest. Applicants first use scRNA-seq profiles to define cell type specific signatures of T cells and of malignant cells in melanoma tumors. Next, Applicants use the T cell signature to estimate T cell infiltration levels in each of hundreds of tumors, based on their bulk RNA-Seq profile. Applicants then define a "seed exclusion program" by identifying genes from the *malignant* cell signature whose expression is strongly correlated (positively or negatively) with the T cell infiltration level across those bulk tumors. Because the seed program is identified only among a few hundred genes that are exclusively expressed by scRNA-Seq in malignant cells, it avoids contamination from the tumor microenvironment; however, important genes that promote exclusion or infiltration may also be expressed by non-malignant cells (*e.g.*, MHC class I molecules). To recover these genes, Applicants finally return to the scRNA-seq data of the malignant cells and expand the seed program by

searching for genes that are correlated with it across the single malignant cells, irrespective of their expression in other cell types. In this way, Applicants derive a genome-scale, malignant-cell exclusion program, consisting of genes induced ("up") or repressed ("down") by malignant cells in "cold" vs. "hot" tumors. Applicants can then score each cell or tumor for expression of the program, such that overexpression of the program is defined as the overexpression of its induced part and underexpression of its repressed part, and vice versa (**Methods**).

Analysis of clinical scRNA-seq identifies a malignant cell program associated with T cell exclusion from melanoma tumors

[0420] Applicants applied the approach to 7,186 high-quality scRNA-seq profiles from the tumors of 31 melanoma patients, comprised of 2,987 cells from 16 newly collected patient tumors (**Figure 44A, Table SI** - note that only in this example (9) cohort 1 is referred to as cohort 2 and cohort 2 is referred to as cohort 1), and 4,199 cells from 16 patients that Applicants previously reported (Tirosh et al., 2016a), along with 473 bulk RNA-seq melanoma profiles from The Cancer Genome Atlas (TCGA) (Akpani et al., 2015). Applicants dissociated individual cells from fresh tumor resections, isolated immune and non-immune cells by FACS based on CD45 staining, and profiled them with a modified full-length SMART-Seq2 protocol (**Methods, Table S2**). Applicants distinguished different cell subsets and genetic clones both by their expression profiles and by their inferred CNV profiles (Tirosh et al., 2016a) (**Methods**), identifying: malignant cells, CD8 and CD4 T cells, B cells, NK cells, macrophages, Cancer Associated Fibroblasts (CAFs) and endothelial cells (**Figures 44C,D and 51, Tables S3 and S4**). Overall, malignant cells primarily grouped by their tumor of origin (**Figure 44C**), while the non-malignant cells grouped primarily by their cell type, and only then by their tumor of origin (**Figure 44D**), as Applicants have previously reported for melanoma and other tumor types (Puram et al., 2017; Tirosh et al., 2016a; Venteicher et al., 2017).

[0421] The resulting exclusion program (**Figure 44E, Table S6**) highlights the repression of diverse immune response pathways and the induction of a co-regulated gene module of Myc and CDK targets. The repressed genes were enriched for antigen processing and presentation genes (*B2M, CTSB, CTSL1, HLA-B/C/F, HSPA1A, HSPA1B*, $P = 4.19 \times 10^{-7}$, hypergeometric test), immune modulation genes ($P = 3.84 \times 10^{-9}$, e.g., *CD58* and the **NFKB** inhibitor, *NFKBIA*), and genes involved in the response to the complement system ($P =$

2.26×10^{-7} , e.g., *CD59* and *C4A*). *CD58* KO in malignant cells was recently shown to enhance the survival of melanoma cells in a genome-scale CRISPR screen of melanoma/T cell co-cultures (Patel et al., 2017), and its genetic loss or epigenetic inactivation are frequent immune evasion drivers in diffuse large B cell lymphoma (Challa-Malladi et al., 2011). The induced genes included *MYC* and Myc targets ($P = 2.8 \times 10^{-14}$), many *CDK7/8* targets ($P < 3 \times 10^{-9}$) (Oki et al., 2018), and transcription factors, such as *SNAI2* and *SOX4*. Myc-activation has been previously linked to increased expression of immunosuppressive signals, including the upregulation of *PD-L1* and β -catenin, which in turn inhibits dendritic cell recruitment to the tumor microenvironment via *CCL4* (Spranger et al., 2015).

The exclusion program characterizes individual malignant cells from patients who failed immunotherapy

[0422] To determine whether the malignant T cell exclusion program manifests in the context of immune checkpoint inhibitor therapy, Applicants leveraged the fact that the scRNA-seq cohort included both untreated patients and post-ICI patients who manifested intrinsic resistance. As clinical response rates to ICI vary, with up to 61% responders with combination therapies (Hodi et al., 2010; Larkin et al., 2015; Postow et al., 2015; Ribas et al., 2015), the untreated tumors Applicants profiled likely include both ICI sensitive and ICI resistant tumors, whereas the tumors from ICI resistant patients are expected to include primarily resistant malignant cells. Applicants thus turned to examine if the exclusion program is more pronounced in the malignant cells from ICI resistant vs. untreated patients. ScRNA-seq data provide particular power for such inter-patient comparisons, even when considering only a small number of tumors, because of the larger number of cells per tumor and because non-malignant cells in the tumor microenvironment do not confound the analyses.

[0423] Applicants thus independently identified a post-treatment transcriptional program, consisting of features that distinguish individual malignant cells from post-ICI resistant tumors compared to malignant cells from untreated tumors (**Table S6**). Applicants found a robust post-treatment program, consisting of genes induced (up) and repressed (down) by malignant cells from the post-treatment resistant vs. untreated patients, which is stable and generalizable in cross-validation (**Methods, Figure 45A**, AUC=0.83). In principle, the program might reflect both the overall impact of ICI therapy and intrinsic ICI resistance *per se*, but those cannot be directly distinguished based on the single-cell cohort, where Applicants did not have matched samples from the same patient or pre-treatment tumors from

responders and non-responders. Applicants address this below by analyzing two independent validation cohorts.

[0424] The post-treatment program substantially overlapped the exclusion program (**Figures 44E and 45B,C, Table S6**; $P < 10^{-16}$, hypergeometric test, Jaccard index = 0.27 and 0.23, for induced and repressed genes, respectively) and highlighted similar modules and pathways (**Figure 45D**), even though the exclusion program was identified without considering the treatment status of the tumors in the scRNA-seq data and with bulk RNA-Seq data of untreated patients. Both programs robustly classified individual cells as untreated or post-treatment (AUC = 0.83 and 0.86 for cross-validation post-treatment and exclusion, respectively, **Figure 45A,E**). In light of this congruence, Applicants defined a unified immune resistance program as the union of the corresponding post-treatment and exclusion programs, and used it in all subsequent analyses, unless indicated otherwise.

The immune resistance program reflects a coherent multifaceted state of immune evasion

[0425] The program is consistent with several hallmarks of active immune evasion, suppression and exclusion. First, it is more pronounced in uveal melanoma, which resides in an immune-privileged environment and has very low response rates to immunotherapy, compared to cutaneous melanoma (**Figure 46A**) (Algazi et al., 2016; Zimmer et al., 2015). Second, the inhibition of genes from the repressed component of the program in malignant melanoma cells conferred resistance to CD8 T cells in a genome-wide CRISPR KO screen ($P = 6.37 * 10^{-3}$, hypergeometric test) (Patel et al., 2017). Third, malignant cells which express the program substantially repress a significant number of interaction routes with other cell types in the tumor microenvironment, including MHC I:TCR (T cells), *CD58.CD2* (T cells), and *IL1RAP JLIB* (macrophages) (**Figure 46B, Methods**), as well as the overall Senescence Associated Secretory Phenotype (SASP) ($P = 4.3 * 10^{-166}$ and $3.6 * 10^{-3}$, one-sided t-test and mixed effects, respectively, **Figure 45D, right**).

[0426] The program genes appear to be under shared control by one or a few master regulators, with opposing effects on the repressed and induced components of the program. There was a strong positive correlation within the induced or repressed genes, and a strong anti-correlation between the induced and repressed genes, both across single cells in the same tumor and across TCGA tumors (**Figures 46C,D**). The co-variation patterns were remarkably reproducible within each one of the tumors in the cohort (**Figure 52**), such that any given aspect of the program {e.g., under-expression of MHC-1 genes in a cell) is coupled to the

state of the entire program. Moreover, there is a significant overlap between the perturbations that reverse the expression of the program's repressed and induced components (p -value= 2.33×10^{-14} , hypergeometric test), including the overexpression of IFN- γ and IFN- β and the knockdown of *MYC* (Subramanian et al., 2017). Indeed, *MYC* knockdown is among the top perturbation to repress the program, which is enriched for Myc targets.

Expression of resistance program features in malignant cells in T cell-depleted niches *in situ*

[0427] If the immune resistance program in malignant cells is associated with T cell exclusion, malignant and T cells should vary in their relative spatial distribution in tumors depending on the activity of the program. To explore this, Applicants used multiplexed immunofluorescence (t-CyCIF) (Lin et al., 2017) to stain histological sections of 19 tumors from the single-cell cohort for 14 proteins: six cell type markers (CD3, CD8, MHC-II, FOXP3, S100, and MITF) and eight members of the immune resistance program (induced: p53, CEP170, Myc, DLL3; repressed: HLA-A, c-Jun, SQSTM1, LAMP2). Following cell segmentation and estimation of antibody staining intensities (**Methods**), Applicants assigned cells (424,000 cells/image on average) into malignant cells (S100⁺, MITF⁺), T cells (CD3⁺) and cytotoxic T cells (CD8⁺); the rest were defined as uncharacterized.

[0428] To explore the association between the program markers and the "cold" phenotype, Applicants first generated a Delaunay neighborhood graph for each image (linking cells that are immediate neighbors) and computed the observed frequency of cell-to-cell interaction compared to that expected by chance, as recently described (Goltsev et al., 2017). Malignant cells were significantly more likely to reside next to other malignant cells, and significantly less likely to reside next to T cells ($P < 1 \times 10^{-16}$, binomial test, **Methods**). Next, for each frame in the imaged section (1,377 cells/frame on average; **Methods**), Applicants computed the fraction of T cells and the average expression of the different markers in the malignant cells. Applicants then quantified the association between expression of the immune resistance program markers and T cell infiltration levels across frames from the different images (**Methods**). Confirming this analysis approach, malignant cells in highly infiltrated niches had significantly higher levels of ULA-A (**Figure 47A**, $P = 2.61 \times 10^{-46}$, mixed-effects). Moreover, in line with the predictions, malignant cells in cold/hot niches had significantly lower/higher levels of c-Jun (repressed in the resistance program), respectively (**Figure 47B**, $P = 2.85 \times 10^{-12}$, mixed-effects), whereas p53, induced in the resistance program)

characterized cold niches ($P = 6.16 \times 10^{-7}$, mixed-effects). Applicants do note, however, that LAMP2 expression (repressed in the resistance program) was also associated with cold niches, potentially due to its post-transcriptional regulation (Feng et al., 2015).

[0429] Finally, since only a few markers were analyzed *in situ*, Applicants tested whether scRNA-seq and multiplex *in situ* protein profiles can be combined to jointly learn cell states, using a variant of canonical correlation analysis (CCA) (Butler and Satija, 2017) (**Methods**). The cells were primarily embedded and clustered based on their cell types, and not according to source, confirming the congruence of the two datasets, and that the markers tested can link global transcriptional cell states to spatial organization in tissue (**Figures 47C,D and 53**). Taken together, these results support the association between the expression of the immune resistance program and the cold phenotype.

The immune resistance program is intrinsic in melanoma cells prior to treatment and is enhanced specifically post-immunotherapy

[0430] Applicants hypothesized that the immune resistance program, while more pronounced in the malignant cell of patients after ICI, in fact reflects an intrinsic resistance mechanism, present even before immunotherapy. First, the program is detected in TCGA tumors, which were all untreated. Second, while the program is more predominant in the malignant cells of the post-treatment resistant patients, it is also overexpressed in a subset of the malignant cells from untreated patients (**Figure 44E and 45C**, right plots). This is aligned with clinical observations that intrinsic ICI resistance is more prevalent than acquired ICI resistance (Sharma et al., 2017). However, because the scRNA-seq cohort did not include matched samples from the same patient or pre-treatment tumors from subsequent responders vs. non-responders, Applicants could not directly distinguish intrinsic resistance from post-treatment effects.

[0431] To test this hypothesis, Applicants therefore analyzed an independent cohort of 90 specimens collected from 26 patients with metastatic melanoma who underwent ICI therapy, with bulk RNA-Seq from biopsies collected pre-treatment ($n = 29$), on-treatment ($n = 35$), and at the time of progression ($n = 26$) (**Figure 44A, validation cohort 1**). Applicants tested for changes in the program score during the course of treatment, while accounting for tumor composition (**Methods**). The program was induced in on- and post-treatment samples compared to pre-treatment samples from the same patient ($P = 1.36 \times 10^{-4}$ and 4.98×10^{-2} , immune resistance program, refined and non-refined, respectively, mixed-effect test, **Methods**), consistent with its overexpression in individual post-ICI malignant cells in the

unmatched single-cell cohort (**Figures 44E and 45C**). However, *inter-patient variation* in the program's expression was significantly higher than these intra-patient changes ($P < 10^{-8}$, ANOVA). This suggested that the major differences between the post-treatment and untreated tumors in the single-cell cohort reflect, at least in part, intrinsic differences between the two groups, which preceded the treatment, which Applicants turned to assess in a second validation cohort (below). Notably, Applicants did not observe an induction in the program following RAF/MEK-inhibition, indicating that the immune resistance state it defines is specific to ICI therapy and not merely a generic marker of any drug resistant tumor.

The immune resistance program predicts patient survival and clinical responses to ICI

[0432] The association of the program with T cell infiltration, its functional enrichment with immune evasion and exclusion mechanisms, its intrinsic expression in some malignant cells prior to treatment, and its further induction in post-ICI resistant lesions could make it a compelling biomarker for response to immunotherapy. To test this hypothesis, Applicants examined the program in multiple independent cohorts. Applicants used both the full program and one refined to the subset of genes that are co-regulated (positively) or anti-regulated (negatively) with genes whose inhibition desensitized melanoma cells to T cell mediated killing in functional screens (Patel et al., 2017) (**Table S6, Methods**) (The exclusion and post-treatment programs show similar signals and trends; **Figures 48E-H and 54-55**).

[0433] The underexpression of the program was strongly associated with improved survival in 473 TCGA melanoma patients (who did not receive ICI immunotherapy, **Figures 48A and 54**), even after controlling for tumor purity and inferred T cell infiltration (Azimi et al., 2012; Bogunovic et al., 2009). Furthermore, combining the program with inferred T cell infiltration levels yielded significantly more accurate predictions of patient survival than either alone (COX p-value = 1.4×10^{-8} , **Figure 48A, right**). Other proposed mechanisms, such as de-differentiation of melanoma cells (Landsberg et al., 2012), as reflected by an MITF-low signature, and other malignant cell signatures (*e.g.*, cell cycle or the AXL program) (Tirosh et al., 2016a), did not show an association with patient survival, indicating that mere biological variation across malignant cells is insufficient as a prognostic signature.

[0434] The program expression in published pre-treatment and early on-treatment bulk expression profiles also distinguished eventual ICI responders from non-responders in those studies (**Figures 48B,C**). In a lung cancer mouse model, the program expression in early on-treatment profiles clearly separated anti-CTLA-4 responders from non-responders ($P =$

3.6×10^{-7} , one-sided *t*-test, **Figure 48B**) (Lesterhuis et al., 2015). In bulk pre-treatment RNA-Seq data from 27 melanoma patients that were subsequently treated with Pembrolizumab (anti-PD-1) (Hugo et al., 2016), the program was underexpressed in the five complete responders, though just above statistical significance ($P = 6.3 \times 10^{-2}$, one-sided *t*-test, **Figure 48C**). In bulk pre-treatment RNA-Seq data from 42 melanoma patients that were subsequently treated with the CTLA-4 inhibitor ipilimumab (Van Allen et al., 2015), the program was significantly lower in the two complete responders ($P = 5.2 \times 10^{-3}$, one-sided *t*-test).

[0435] To test the predictive value of the program in a larger independent setting, Applicants assembled a validation cohort of 112 patients with metastatic melanoma who underwent a pre-treatment biopsy and bulk RNA-Seq followed by Pembrolizumab (anti-PD-1) therapy (**Figure 44A, validation cohort 2, Table SI**). The cohort was collected in a different hospital and country (Germany; **Methods**), and samples were processed and sequenced on the same platform (**Methods**). Applicants evaluated the program's performance in predicting anti-PD-1 responses as reflected by: (1) progression-free survival (PFS, recorded for 104 of the 112 patients), (2) clinical benefit (CB, defined as either partial or complete response by RECIST criteria), and (3) complete response (CR) (**Methods**). Applicants also compared the performance of the predictors to those of 32 other signatures, including the top hits of two functional CRISPR screens of resistance to T cells and ICI (Manguso et al., 2017; Patel et al., 2017) (**Table S10, Methods**).

[0436] The programs were predictive of PFS in the validation cohort (**Figures 48D and 55A-E**), even when accounting for other known predictors of ICI response, including inferred T cell infiltration levels and PD-L1 expression (**Figure 55E**). Although cell cycle alone is not associated with PFS (COX $P > 0.25$), filtering the cell-cycle component from the program score (**Methods**, and below) further improved PFS predictions (**Figure 48D, right**), suggesting that a tumor's immune resistance should be evaluated conditioning on its proliferation level. The program had a strong predictive value beyond T cell infiltration ($P = 3.37 \times 10^{-6}$, Wilcoxon-ranksum test), and was the only one negatively associated with PFS. Other alternative signatures were either not predictive or did not provide any additive predictive value once accounting for T cell infiltration levels (**Figure 48E**).

[0437] The program was underexpressed in patients with clinical benefit (CB) compared to those without benefit (no-CB) (**Figure 48F**). Nevertheless, some patients with clinical benefit had high pre-treatment expression of the program. Applicants hypothesized that these

patients might cease to respond quickly, due to pre-existing intrinsically resistant cells, like those Applicants observed in the single-cell cohort and in validation cohort 1. Indeed, among patients with clinical benefit, those with high expression of the program pre-treatment were significantly more likely to experience subsequent progressive disease (**Figure 48F**), and those with rapid progression (CB<6 months) had the highest scores of the program, even compared to those with no clinical benefit. Consistently, the program was most accurate in predicting patients with complete responses ($P < 6.31 \times 10^{-3}$, one-sided t-test, **Figures 48G and 55F**), outperforming all the other predictors ($P = 1.64 \times 10^{-8}$, Wilcoxon ranksum test), all of which, including clinically-used markers and inferred T cell infiltration levels, failed to predict complete response (**Figure 48H**).

The immune resistance program is coherently controlled by CDK4/6

[0438] Applicants reasoned that the program could be a compelling drug target: it was identified by its association with a critical process - T cell exclusion - that affects resistance to immunotherapy; it is a significantly predictive biomarker of ICI resistance; and it appears to be coherently regulated, such that a shared control mechanism could be targeted to reverse it.

[0439] To this end, Applicants identified drugs that were significantly more toxic to cell lines overexpressing the immune resistance program (controlling for cancer types, **Methods**), according to the efficacy measures of 131 drugs across 639 human cancer cell lines (Garnett et al., 2012). The top scoring drug was the CDK4/6-inhibitor palbociclib ($P = 6.28 \times 10^{-6}$, mixed-effects). Furthermore, the efficacy of CDK4/6 inhibition and the expression of the resistance program were also correlated in a study where the efficacies of CDK4/6 inhibitors palbociclib and abemaciclib were measured across a collection of cancer cell lines ($P = 7.15 \times 10^{-6}$, mixed-effects) (Gong et al., 2017).

[0440] Applicants further hypothesized that CDK4 and 6 may act as the master regulators of the immune resistance program. First, both CDK4 itself and multiple CDK target genes, are members of the of the induced program (**Figure 45C, Table S6**). Second, the program is more pronounced in cycling cells (where CDK4/6 are active), both within the same patient group and among cells of the same tumor (**Figures 44E, 45C, and 56A,B**, $P < 10^{-16}$, mixed effects model). Importantly, the program is not merely a proxy of the cell's proliferation state: there was no significant difference between the fraction of cycling cells in untreated *vs.* post-treatment tumors ($P = 0.696$, t-test), the program was nearly identical when identified only based on non-cycling cells, and - unlike the expression of the resistance program - the

expression of cell cycle signatures was not associated with the efficacy of CDK4/6 inhibitors across the cell lines. Finally, Applicants analyzed recently published expression profiles (Goel et al., 2017) of breast cancer cell lines and *in vivo* mouse models and found that CDK4/6 inhibition by abemaciclib represses the program (**Figures 49A-C and 56C**). Thus, multiple lines of evidence suggest that CDK4/6 inhibition could repress the expression of the immune resistance program and shift the cancer cell population to a less immune resistant state.

CDK4/6 inhibitors repress the immune resistance program in malignant melanoma cells

[0441] To test this hypothesis, Applicants studied the effect of abemaciclib on the immune resistance program in melanoma cell lines. Applicants selected three melanoma cell lines from the Cancer Cell Line Encyclopedia (Barretina et al., 2012) with a strong expression of the resistance program (**Table S12**), two of which are RBI -sufficient (IGR37, UACC257) and one is RBI-deficient (A2058). Applicants profiled each cell line with scRNA-seq before and after treatment with abemaciclib for 1 week (**Figures 49D-E**), analyzing over 23,000 cells in these and follow-up conditions (below).

[0442] **Table S12. The overall expression (OE) of the immune resistance signature across the CCLE melanoma cell lines.**

Melanoma cell line	Immune resistance OE
HMCB	0.818
LOXIMVI	0.72
UACC257	0.706
CHL1	0.698
IGR37	0.57
MELHO	0.522
COL0741	0.5
G361	0.476
COL0679	0.468
A2058	0.465
SKMEL3	0.443
GRM	0.431
SKMEL30	0.405
MELWO	0.371
A375	0.368
HS936T	0.339
K029AX	0.308
IPC298	0.261
IGRI	0.243
SKMEL1	0.238
SKMEL5	0.182
COL0783	0.174
COL0849	0.082

CJM	0.06
M EUUSO	0.049
COL0792	0.041
UACC62	0.015
M DAM B435S	0.005
IGR39	0
WM2664	-0.015
WM88	-0.045
HS944T	-0.053
RPMI7951	-0.067
WM983B	-0.09
W M 1799	-0.091
A101D	-0.097
HS895T	-0.126
SKM EL28	-0.152
SH4	-0.226
RVH421	-0.227
HT144	-0.23
SKM EL2	-0.242
COLO800	-0.251
HS294T	-0.264
WM793	-0.265
HS852T	-0.341
HS934T	-0.368
COL0829	-0.377
HS839T	-0.386
C32	-0.427
HS940T	-0.434
HS688AT	-0.435
HS939T	-0.464
HS600T	-0.464
COL0818	-0.466
HS695T	-0.5
W M 115	-0.513
MALME3M	-0.607
SKM EL31	-0.759
SKM EL24	-0.975

[0443] Consistent with the hypothesis, only in the RB-sufficient cell lines, abemaciclib dramatically decreased the proportion of cells overexpressing the immune resistance program and induced an immune response in the surviving cells. In the RBI -sufficient lines, IGR37 and UACC257, 10% of the cells had exceptionally strong expression of the immune resistance program ("immune resistant" cells) prior to treatment, decreasing to 2% and 1% of cells post-treatment, respectively ($P < 1 \times 10^{-30}$, hypergeometric test) (Figures 49D,E). In contrast, in the RBI-deficient line A2058 the treatment did not repress the immune resistant state ($P > 0.5$, one-sided t-test), consistent with the hypothesis that CDK4/6 inhibitors depend on RBI -sufficiency.

[0444] Moreover, in the two RB-sufficient lines, the remaining cells that underexpressed the immune resistance program, underwent substantial transcriptional changes, including the induction of key repressed component of the immune resistance program, such as the SASP. In particular, abemaciclib repressed the expression of DNMT1 ($P < 2.23 \times 10^{-106}$, likelihood-ratio test), consistent with previous observations (Goel et al., 2017) that CDK4/6 inhibition leads to DNMT1 repression, allowing the methylation of endogenous retroviral genes (ERVs), which in turn triggers a double-stranded RNA (dsRNA) response and stimulates type III IFN production (Goel et al., 2017). Following abemaciclib treatment there was also a higher portion of cells with increased expression of a MITF program (Tirosh et al., 2016a), which is repressed in "immune resistant" cells ($P < 3.33 \times 10^{-15}$, hypergeometric test, **Figure 49D,E**).

[0445] In particular, abemaciclib induced SASP, which is a major repressed component in the resistance program. First, the SASP module was significantly induced at the transcriptional level ($P < 3.91 \times 10^{-12}$, hypergeometric test, **Figures 49D,E**). Moreover, when Applicants measured 40 human cytokines and chemokines in the conditioned media of abemaciclib treated cancer cells, Applicants found it induced several secreted factors (**Figure 49F**), including macrophage inhibition factor (MIF), CX3CL1 (which induces migration and adhesion of T and NK cells and is linked to clinical outcomes in immunotherapy treatment (Herbst et al., 2014; Nelson and Muenchmeier, 2013)), and CCL20 (an important factor for T cell differentiation, which may enhance immunity in melanoma (Gordy et al., 2016)). Consistently, abemaciclib also induced alpha-galactosidase activity and morphological alterations that reflect cellular senescence (**Figure 49G**). Thus, unlike the mechanism described in breast cancer cells (Goel et al., 2017), abemaciclib might trigger SASP and cell differentiation in malignant melanoma cells.

[0446] Finally, Applicants tested if the effect of abemaciclib treatment on malignant cells is impacted by the presence of tumor infiltrating lymphocytes (TILs) in a patient-derived co-culture model of melanoma cells and *ex vivo* expanded TILs from the same metastatic melanoma lesion. After treating the malignant cells with abemaciclib for one week, Applicants added autologous TILs to the cultures. Applicants compared scRNA-seq profiles between these melanoma cells and cells from similar co-cultures but without abemaciclib treatment, or from cultures with neither abemaciclib treatment nor TILs. Exposure to TILs reduced the expression of the immune resistance program, both in the control and in the abemaciclib-treated cells ($P < 9.85 \times 10^{-14}$, one-sided t-test). Abemaciclib further intensified

these effects, as it further repressed the immune resistance program in both conditions (with and without the exposure to TILs, $P < 3.60 \times 10^{-7}$, one-sided t-test).

Discussion

[0447] Most melanoma patients have either intrinsic or acquired resistance to ICI, yet the systematic characterization of molecular resistance mechanisms has been limited. Here, Applicants leverage clinical scRNA-seq data and multiple cohorts to map malignant cell states associated with resistance to ICI, revealing a coherently co-regulated program that may be therapeutically targeted to overcome immune evasion and suppression.

[0448] The malignant cell resistance program showed prognostic and predictive power in several independent ICI cohorts, including a large new clinically annotated cohort of patients with pre-treatment (anti-PD-1) biopsies profiled by RNA-seq. The program outperformed other published biomarkers in the space, and may help to prospectively stratify patients to clinical trials and therapies. Even though the program was initially derived, in part, based on associations with inferred T cell infiltration levels, unlike many other biomarkers, it has a significant predictive value beyond T cell infiltration.

[0449] The program Applicants uncovered is primarily associated with intrinsic ICI resistance. It is manifested also in malignant cells of untreated patients in the single-cell cohort, and in bulk RNA-seq data from three independent cohorts of untreated patients: TCGA, a longitudinal cohort of ICI-treated patients (validation cohort 1), and a cohort of 112 pre-ICI patients (validation cohort 2). Among single cells of pre-treated patients, a subset (20.9% cells from 10 different patients) already overexpresses the program. In bulk samples collected before and after ICI, inter-patient variation exceeded intra-patient variation, further supporting an intrinsic role. In 112 melanoma patients, this pre-ICI inter-patient variation is tightly associated with ICI responses. Finally, the program is more pronounced after ICI failure, but not post targeted therapy, and thus it is unlikely to merely reflect the impact of any therapeutic intervention.

[0450] Some of the concepts established for drug resistance to targeted cancer therapies with RAF/MEK-inhibitors in melanoma may also be applicable to immunotherapies. Similar to the presence of a small sub-population of cells expressing a MITF-low program, which confers resistance to RAF/MEK-inhibitors, and rises in frequency under the pressure of a drug (Shaffer et al., 2017; Tirosh et al., 2016a, Hangauer et al., 2017; Viswanathan et al., 2017), patient tumors who have not been treated with ICI contain some cells expressing the immune resistance program. It is plausible that these cells are responsible for either intrinsic

resistance to ICI or lie in protected niches, and thus emerge in the context of ICI resistance. Selective targeting of these cells in combination with ICI may delay or prevent ICI resistance.

[0451] Applicants have focused on malignant cells, but T cell states or clones, beyond their extent of infiltration, might also predict the success of ICI. Within the limitation of the unmatched single-cell cohort, comparing the individual T cells of untreated *vs.* post-treatment (resistant) patients, suggested that treatment has activated the T cells and caused their expansion (data not shown). While Applicants cannot rule out the presence of other intrinsic T cell dysfunction mechanisms, this is consistent with a model where, at least partly, malignant cells cause ICI resistance despite at least some T cell functionality.

[0452] Because of the potential functional role of the program and its coherent underlying regulation, compounds that repress it may sensitize malignant cells to immunotherapy and/or T-cell mediated killing (**Figure 50**), especially in patients with a high intrinsic (pre-ICI) expression of the immune resistance program. Based on a systematic analysis of drug efficacies and the program features Applicants hypothesized that CDK4/6 inhibition could have such a sensitizing effect, and tested this in malignant melanoma cell lines and in co-cultures of patient cells with autologous TILs. CDK4/6 inhibition reversed the resistant transcriptional state: subpopulations of highly immune resistant cancer cells were dramatically reduced, either because the drug selectively eradicated them or because it triggered them to adopt a less immune resistant state. In parallel, CDK4/6 inhibition triggered the melanoma cells to adopt a senescent-like phenotype accompanied by secretion of key chemokines, which have been previously shown to enhance T cell responses (Gordy et al., 2016; Herbst et al., 2014; Nelson and Muenchmeier, 2013).

[0453] The malignant resistance programs may be relevant in other subtypes of melanoma as well as in other tumor types. Among different types of melanoma, uveal melanoma has more active resistance programs compared to cutaneous melanoma (**Figure 46A**); across cancers, the immune resistance program is lower in some of the more responsive tumors (head and neck, kidney, skin, lung) and higher in tumor types that are less responsive to immunotherapy and/or arise from immune-privileged tissues (eye, testis) (**Figure 57**). Interestingly, synovial sarcoma, which is driven by a single genomic aberration in the BAF complex, has the highest resistance scores. The BAF complex has been recently shown to play a key role in resistance to ICI immunotherapy (Miao et al., 2018; Pan et al., 2018). While this pan-cancer analysis is intriguing, it may still be impacted by the

composition of the tumor microenvironment, which is challenging to control without single-cell data.

[0454] Future similar studies of other tumors could apply the approach to identify other tumor-specific resistance programs. For example, Applicants performed such analysis with the recent head and neck cancer single cell cohort (Puram et al., 2017) and found that CAFs in cold tumors overexpressed genes up-regulated by TGFB1 ($P = 1.70 \times 10^{-7}$, hypergeometric test). Indeed, TGFB1 and TGFB signaling has been recently shown to be highly associated with lack of response to anti-PD-L1 treatment in urothelial cancer patients (Mariathasan et al., 2018). In line with the findings, co-administration of TGFB-blocking and anti-PD-L1 has been shown to modulated the tumor CAFs, which in turn facilitated T cell infiltration and tumor regression in mouse models (Mariathasan et al., 2018).

[0455] Overall, the analysis sheds light on the way cells shape and are being shaped by their microenvironment in tumors, and the approaches can be applied in other tumors to systematically map immune resistant malignant cell states, uncover improved biomarkers for patient selection, and reveal principles for the development of new therapeutics.

References

1. P. Sharma, J. P. Allison, The future of immune checkpoint therapy. *Science*. 348, 56-61 (2015).
2. F. S. Hodi, Kluger HM, Sznol M, Durable, long-term survival in previously treated patients with advanced melanoma who received nivolumab monotherapy in a phase I trial. 2016 AACR Annu. Meet. Abstr. CTOO1 Present. April 17 2016.
3. P. Sharma, S. Hu-Lieskovan, J. A. Wargo, A. Ribas, Primary, Adaptive, and Acquired Resistance to Cancer Immunotherapy. *Cell*. 168, 707-723 (2017).
4. E. M. Van Allen et al., Genomic correlates of response to CTLA-4 blockade in metastatic melanoma. *Science*. 350, 207-211 (2015).
5. W. Hugo et al., Genomic and Transcriptomic Features of Response to Anti-PD-1 Therapy in Metastatic Melanoma. *Cell*. 165, 35-44 (2016).
6. P. C. Tumeh et al., PD-1 blockade induces responses by inhibiting adaptive immune resistance. *Nature*. 515, 568-571 (2014).
7. N. Riaz et al., Tumor and Microenvironment Evolution during Immunotherapy with Nivolumab. *Cell*. 0 (2017), doi:10.1016/j.cell.2017.09.028.

8. J. M. Zaretsky et al., Mutations Associated with Acquired Resistance to PD-1 Blockade in Melanoma. *N. Engl. J. Med.* 375, 819-829 (2016).
9. J. Gao et al., Loss of IFN- γ Pathway Genes in Tumor Cells as a Mechanism of Resistance to Anti-CTLA-4 Therapy. *Cell.* 167, 397-404.e9 (2016).
10. W. Peng et al., Loss of PTEN Promotes Resistance to T Cell-Mediated Immunotherapy. *Cancer Discov.* 6, 202-216 (2016).
11. S. Spranger, R. Bao, T. F. Gajewski, Melanoma-intrinsic β -catenin signalling prevents antitumour immunity. *Nature.* 523, 231-235 (2015).
12. G. T. Gibney, L. M. Weiner, M. B. Atkins, Predictive biomarkers for checkpoint inhibitorbased immunotherapy. *Lancet Oncol.* 17, e542-e551 (2016).
13. I. Tirosh et al., Dissecting the multicellular ecosystem of metastatic melanoma by singlecell RNA-seq. *Science.* 352, 189-196 (2016).
14. A. P. Patel et al., Single-cell RNA-seq highlights intratumoral heterogeneity in primary glioblastoma. *Science.* 344, 1396-1401 (2014).
15. I. Tirosh et al., Single-cell RNA-seq supports a developmental hierarchy in human oligodendroglioma. *Nature.* 539, 309-313 (2016).
16. A. S. Venteicher et al., Decoupling genetics, lineages, and microenvironment in IDHmutant gliomas by single-cell RNA-seq. *Science.* 355 (2017), doi: 10.1126/science.aai8478.
17. H. Li et al., Reference component analysis of single-cell transcriptomes elucidates cellular heterogeneity in human colorectal tumors. *Nat. Genet.* 49, 708-718 (2017).
18. E. A. Eisenhauer et al., New response evaluation criteria in solid tumours: revised RECIST guideline (version 1.1). *Eur. J. Cancer Oxf. Engl.* 1990. 45, 228-247 (2009).
19. P. V. Kharchenko, L. Silberstein, D. T. Scadden, Bayesian approach to single-cell differential expression analysis. *Nat. Methods.* 11, 740-742 (2014).
20. P. Zhou et al., In vivo discovery of immunotherapy targets in the tumour microenvironment. *Nature.* 506, 52-57 (2014).
21. M. Singer et al., A Distinct Gene Module for Dysfunction Uncoupled from Activation in Tumor-Infiltrating T Cells. *Cell.* 166, 1500-1511.e9 (2016).
22. C. Zheng et al., Landscape of Infiltrating T Cells in Liver Cancer Revealed by Single-Cell Sequencing. *Cell.* 169, 1342-1356.e16 (2017).
23. M. J. T. Stubbington et al., T cell fate and clonality inference from single-cell transcriptomes. *Nat. Methods.* 13, 329-332 (2016).

24. R. Muthuswamy et al., NF- κ B hyperactivation in tumor tissues allows tumor-selective reprogramming of the chemokine microenvironment to enhance the recruitment of cytolytic T effector cells. *Cancer Res.* 72, 3735-3743 (2012).
25. E. Pikarsky et al., NF-kappaB functions as a tumour promoter in inflammation-associated cancer. *Nature.* 431, 461-466 (2004). 26. J. Lamb et al., The Connectivity Map: using gene-expression signatures to connect small molecules, genes, and disease. *Science.* 313, 1929-1935 (2006).
27. J. M. Taube et al., *Sci. Transl. Med.*, in press, doi:10.1126/scitranslmed.3003689.
28. S. J. Patel et al., Identification of essential genes for cancer immunotherapy. *Nature.* 548, 537-542 (2017).
29. M. Challa-Malladi et al., Combined genetic inactivation of p2-Microglobulin and CD58 reveals frequent escape from immune recognition in diffuse large B cell lymphoma. *Cancer Cell.* 20, 728-740 (2011).
30. S. Goel et al., CDK4/6 inhibition triggers anti-tumour immunity. *Nature.* 548, 471-475 (2017).
31. L. Zimmer et al., Phase II DeCOG-study of ipilimumab in pretreated and treatment-naive patients with metastatic uveal melanoma. *PloS One.* 10, e0118564 (2015).
32. A. P. Algazi et al., Clinical outcomes in metastatic uveal melanoma treated with PD-1 and PD-L1 antibodies. *Cancer.* 122, 3344-3353 (2016).
33. F. Azimi et al., Tumor-Infiltrating Lymphocyte Grade Is an Independent Predictor of Sentinel Lymph Node Status and Survival in Patients With Cutaneous Melanoma. *J. Clin. Oncol.* 30, 2678-2683 (2012).
34. D. Bogunovic et al., Immune profile and mitotic index of metastatic melanoma lesions enhance clinical staging in predicting patient survival. *Proc. Natl. Acad. Sci. U. S. A.* 106, 20429-20434 (2009).
35. J. Landsberg et al., Melanomas resist T-cell therapy through inflammation-induced reversible dedifferentiation. *Nature.* 490, 412-416 (2012).
36. W. J. Lesterhuis et al., Network analysis of immunotherapy-induced regressing tumours identifies novel synergistic drug combinations. *Sci. Rep.* 5, srep12298 (2015).
37. R. T. Manguso et al., In vivo CRISPR screening identifies Ptpn2 as a cancer immunotherapy target. *Nature.* 547, 413-418 (2017).

38. Akbani, R., Akdemir, K.C., Aksoy, B.A., Albert, M., Ally, A., Amin, S.B., Arachchi, H., Arora, A., Auman, J.T., Ayala, B., et al. (2015). Genomic Classification of Cutaneous Melanoma. *Cell* 161, 1681-1696.
39. Ayers, M., Luceford, J., Nebozhyn, M., Murphy, E., Loboda, A., Kaufman, D.R., Albright, A., Cheng, J.D., Kang, S.P., Shankaran, V., et al. (2017). IFN- γ -related mRNA profile predicts clinical response to PD-1 blockade. *J. Clin. Invest.* 127, 2930-2940.
40. Barretina, J., Caponigro, G., Stransky, N., Venkatesan, K., Margolin, A.A., Kim, S., Wilson, C.J., Lehar, J., Kryukov, G.V., Sonkin, D., et al. (2012). The Cancer Cell Line Encyclopedia enables predictive modelling of anticancer drug sensitivity. *Nature* 483, 603-607.
41. Benjamini, Y., and Hochberg, Y. (1995). Controlling the False Discovery Rate: A Practical and Powerful Approach to Multiple Testing. *J. R. Stat. Soc. Ser. B Methodol.* 57, 289-300.
42. Butler, A., and Satija, R. (2017). Integrated analysis of single cell transcriptomic data across conditions, technologies, and species. *BioRxiv* 164889.
43. Dobin, A., Davis, C.A., Schlesinger, F., Drenkow, J., Zaleski, C., Jha, S., Batut, P., Chaisson, M., and Gingeras, T.R. (2013). STAR: ultrafast universal RNA-seq aligner. *Bioinforma. Oxf. Engl.* 29, 15-21.
44. Ester, M., Kriegel, H.-P., Sander, J., and Xu, X. (1996). A density-based algorithm for discovering clusters a density-based algorithm for discovering clusters in large spatial databases with noise. In *Proceedings of the Second International Conference on Knowledge Discovery and Data Mining*, (Portland, Oregon: AAAI Press), pp. 226-231.
45. Fan, J., Salathia, N., Liu, R., Kaeser, G.E., Yung, Y.C., Herman, J.L., Kaper, F., Fan, J.-B., Zhang, K., Chun, J., et al. (2016). Characterizing transcriptional heterogeneity through pathway and gene set overdispersion analysis. *Nat. Methods* 13, 241-244.
46. Feng, Y., Yao, Z., and Klionsky, D.J. (2015). How to control self-digestion: transcriptional, post-transcriptional, and post-translational regulation of autophagy. *Trends Cell Biol.* 25, 354-363.
47. Fridman, W.H., Pages, F., Sautes-Fridman, C., and Galon, J. (2012). The immune contexture in human tumours: impact on clinical outcome. *Nat. Rev. Cancer* 12, 298-306.
48. Garnett, M.J., Edelman, E.J., Heidorn, S.J., Greenman, C.D., Dastur, A., Lau, K.W., Greninger, P., Thompson, I.R., Luo, X., Soares, J., et al. (2012). Systematic identification of genomic markers of drug sensitivity in cancer cells. *Nature* 483, 570-575.

49. Goel, S., DeCristo, M.J., Watt, A.C., BrinJones, H., Sceneay, J., Li, B.B., Khan, N., Ubellacker, J.M., Xie, S., Metzger-Filho, O., et al. (2017). CDK4/6 inhibition triggers anti-tumour immunity. *Nature* 548, 471-475.

50. Goltsev, Y., Samusik, N., Kennedy-Darling, J., Bhate, S., Hale, M., Vasquez, G., and Nolan, G. (2017). Deep profiling of mouse splenic architecture with CODEX multiplexed imaging. *BioRxiv* 203166.

51. Gong, X., Litchfield, L.M., Webster, Y., Chio, L.-C, Wong, S.S., Stewart, T.R., Dowless, M., Dempsey, J., Zeng, Y., Torres, R, et al. (2017). Genomic Aberrations that Activate D-type Cyclins Are Associated with Enhanced Sensitivity to the CDK4 and CDK6 Inhibitor Abemaciclib. *Cancer Cell* 32, 761-776.e6.

52. Gordy, J.T., Luo, K., Zhang, H., Biragyn, A., and Markham, R.B. (2016). Fusion of the dendritic cell-targeting chemokine MIP3a to melanoma antigen Gp100 in a therapeutic DNA vaccine significantly enhances immunogenicity and survival in a mouse melanoma model. *J. Immunother. Cancer* 4, 96.

53. Hangauer, M.J., Viswanathan, V.S., Ryan, M.J., Bole, D., Eaton, J.K., Matov, A., Galeas, J., Dhruv, H.D., Berens, M.E., Schreiber, S.L., et al. (2017). Drug-tolerant persister cancer cells are vulnerable to GPX4 inhibition. *Nature* 551, 247.

54. Herbst, R.S., Soria, J.-C, Kowanetz, M., Fine, G.D., Hamid, O., Gordon, M.S., Sosman, J.A., McDermott, D.F., Powderly, J.D., Gettinger, S.N., et al. (2014). Predictive correlates of response to the anti-PD-L1 antibody MPDL3280A in cancer patients. *Nature* 575, 563-567.

55. Hodi, F.S., O'Day, S.J., McDermott, D.F., Weber, R.W., Sosman, J.A., Haanen, J.B., Gonzalez, R., Robert, C, Schadendorf, D., Hassel, J.C., et al. (2010). Improved survival with ipilimumab in patients with metastatic melanoma. *N. Engl. J. Med.* 363, 711-723.

56. Holm, S. (1979). A Simple Sequentially Rejective Multiple Test Procedure. *Scand. J. Stat.* 6, 65-70.

57. Langmead, B., Trapnell, C, Pop, M., and Salzberg, S.L. (2009). Ultrafast and memory-efficient alignment of short DNA sequences to the human genome. *Genome Biol.* 10, R25.

58. Larkin, J., Chiarion-Sileni, V., Gonzalez, R., Grob, J.J., Cowey, C.L., Lao, C.D., Schadendorf, D., Dummer, R., Smylie, M., Rutkowski, P., et al. (2015). Combined Nivolumab and Ipilimumab or Monotherapy in Untreated Melanoma. *N. Engl. J. Med.* 373, 23-34.

59. Laurens Maaten (2009). Learning a Parametric Embedding by Preserving Local Structure. In Proceedings of the Twelfth International Conference on Artificial Intelligence and Statistics, David van Dyk, and Max Welling, eds. (PMLR), pp. 384-391.
60. Li, B., and Dewey, C.N. (2011). RSEM: accurate transcript quantification from RNA-Seq data with or without a reference genome. *BMC Bioinformatics* 12, 323.
61. Lin, J.-R., Izar, B., Mei, S., Wang, S., Shah, P., and Sorger, P. (2017). A simple open-source method for highly multiplexed imaging of single cells in tissues and tumours. *BioRxiv* 151738.
62. van der Maaten, L., and Hinton, G. (2008). Visualizing Data using t-SNE. 9, 2579-2605.
63. Mariathasan, S., Turley, S.J., Nickles, D., Castiglioni, A., Yuen, K., Wang, Y., Kadel III, E.E., Koepfen, H., Astarita, J.L., Cubas, R., et al. (2018). TGF β attenuates tumour response to PD-L1 blockade by contributing to exclusion of T cells. *Nature* 554, 544-548.
64. McDavid, A., Finak, G., Chattopadhyay, P.K., Dominguez, M., Lamoreaux, L., Ma, S.S., Roederer, M., and Gottardo, R. (2013). Data exploration, quality control and testing in single-cell qPCR-based gene expression experiments. *Bioinforma. Oxf. Engl.* 29, 461-467.
65. Miao, D., Margolis, C.A., Gao, W., Voss, M.H., Li, W., Martini, D.J., Norton, C., Bosse, D., Wankowicz, S.M., Cullen, D., et al. (2018). Genomic correlates of response to immune checkpoint therapies in clear cell renal cell carcinoma. *Science* 359, 801-806.
66. Nelson, P.J., and Muenchmeier, N. (2013). Membrane-anchored chemokine fusion proteins: A novel class of adjuvants for immunotherapy. *Oncoimmunology* 2, e26619.
67. Oki, S., Ohta, T., Shioi, G., Hatanaka, H., Ogasawara, O., Okuda, Y., Kawaji, H., Nakaki, R., Sese, J., and Meno, C. (2018). Integrative analysis of transcription factor occupancy at enhancers and disease risk loci in noncoding genomic regions.
68. Pan, D., Kobayashi, A., Jiang, P., Ferrari de Andrade, L., Tay, R.E., Luoma, A.M., Tsoucas, D., Qiu, X., Lim, K., Rao, P., et al. (2018). A major chromatin regulator determines resistance of tumor cells to T cell-mediated killing. *Science* 359, 770-775.
69. Postow, M.A., Chesney, J., Pavlick, A.C., Robert, C., Grossmann, K., McDermott, D., Linette, G.P., Meyer, N., Giguere, J.K., Agarwala, S.S., et al. (2015). Nivolumab and ipilimumab versus ipilimumab in untreated melanoma. *N. Engl. J. Med.* 372, 2006-2017.
70. Puram, S.V., Tirosh, L., Parikh, A.S., Patel, A.P., Yizhak, K., Gillespie, S., Rodman, C., Luo, C.L., Mroz, E.A., Emerick, K.S., et al. (2017). Single-Cell Transcriptomic

Analysis of Primary and Metastatic Tumor Ecosystems in Head and Neck Cancer. *Cell* 777, 1611-1624.e24.

71. Ramilowski, J.A., Goldberg, T., Harshbarger, T., Kloppmann, E., Lizio, M., Satagopam, V.P., Itoh, M., Kawaji, H., Carninci, P., Rost, B., et al. (2015). A draft network of ligand-receptor-mediated multicellular signalling in human. *Nat. Commun.* 6, 7866.

72. Ribas, A., Puzanov, I., Dummer, R., Schadendorf, D., Hamid, O., Robert, C., Hodi, F.S., Schachter, T., Pavlick, A.C., Lewis, K.D., et al. (2015). Pembrolizumab versus investigator-choice chemotherapy for ipilimumab-refractory melanoma (KEYNOTE-002): a randomised, controlled, phase 2 trial. *Lancet Oncol.* 16, 908-918.

73. Rosvall, M., and Bergstrom, C.T. (2008). Maps of random walks on complex networks reveal community structure. *Proc. Natl. Acad. Sci. U. S. A.* 105, 1118-1123.

74. Shaffer, S.M., Dunagin, M.C., Torborg, S.R., Torre, E.A., Emert, B., Krepler, C., Beqiri, M., Sproesser, K., Brafford, P.A., Xiao, M., et al. (2017). Rare cell variability and drug-induced reprogramming as a mode of cancer drug resistance. *Nature* 546, 431-435.

75. Shalek, A.K., Satija, R., Adiconis, X., Gertner, R.S., Gaublomme, J.T., Raychowdhury, R., Schwartz, S., Yosef, N., Malboeuf, C., Lu, D., et al. (2013). Single-cell transcriptomics reveals bimodality in expression and splicing in immune cells. *Nature* 498, 236-240.

76. Shalek, A.K., Satija, R., Shuga, J., Trombetta, J.J., Gennert, D., Lu, D., Chen, P., Gertner, R.S., Gaublomme, J.T., Yosef, N., et al. (2014). Single-cell RNA-seq reveals dynamic paracrine control of cellular variation. *Nature* 510, 363-369.

77. Shannon, P., Markiel, A., Ozier, O., Baliga, N.S., Wang, J.T., Ramage, D., Amin, N., Schwikowski, B., and Ideker, T. (2003). Cytoscape: a software environment for integrated models of biomolecular interaction networks. *Genome Res.* 13, 2498-2504.

78. Subramanian, A., Tamayo, P., Mootha, V.K., Mukherjee, S., Ebert, B.L., Gillette, M.A., Paulovich, A., Pomeroy, S.L., Golub, T.R., Lander, E.S., et al. (2005). Gene set enrichment analysis: a knowledge-based approach for interpreting genome-wide expression profiles. *Proc. Natl. Acad. Sci. U. S. A.* 102, 15545-15550.

79. Subramanian, A., Narayan, R., Corsello, S.M., Peck, D.D., Natoli, T.E., Lu, X., Gould, J., Davis, J.F., Tubelli, A.A., Asiedu, J.K., et al. (2017). A Next Generation Connectivity Map: L1000 Platform and the First 1,000,000 Profiles. *Cell* 777, 1437-1452.e17.

80. Trombetta, J.J., Gennert, D., Lu, D., Satija, R., Shalek, A.K., and Regev, A. (2014). Preparation of Single-Cell RNA-Seq Libraries for Next Generation Sequencing. *Curr. Protoc. Mol. Biol.* Ed. Frederick M Ausubel A1 107, 4.22.1-4.22.17.

81. Viswanathan, V.S., Ryan, M.J., Dhruv, H.D., Gill, S., Eichhoff, O.M., Seashore-Ludlow, B., Kaffenberger, S.D., Eaton, J.K., Shimada, K., Aguirre, A.J., et al. (2017). Dependency of a therapy-resistant state of cancer cells on a lipid peroxidase pathway. *Nature* 547, 453.

82. Wagner, A., Regev, A., and Yosef, N. (2016). Revealing the vectors of cellular identity with single-cell genomics. *Nat. Biotechnol.* 34, 1145-1160.

83. Waltman, L., and van Eck, N.J. (2013). A smart local moving algorithm for large-scale modularity-based community detection. *Eur. Phys. J. B* 86.

Example 10 - Materials and Methods

Patients

[0456] For the discovery cohort (single cell RNA-Seq), tissue was procured under Institutional Review Board (IRB) approved protocols at Brigham and Women's Hospital and Dana-Farber Cancer Institute, Boston, MA. Patients were consented to these protocols (11-104) in clinic visits prior to surgery/biopsy. Patients included in the initial study and newly collected specimens are highlighted in **table SI**.

[0457] For validation cohorts (bulk-RNA-seq), patient tissue was collected under IRB protocols of the University Hospital Essen, Germany and Massachusetts General Hospital, Boston, MA (protocol 11-181) and The Wistar Institute, Philadelphia, PA (Human subjects protocol 2802240). Demographics of validation Cohort 1 are summarized in **table SI**. Validation Cohort 2 included 90 samples from 26 patients, with multiple biopsies per patient, taken before, during, or after various treatment regimens, including both targeted therapies and immunotherapies. Twelve patients had both pre- and post/on- ICI samples (**table SI**).

Tissue handling and tumor disaggregation

[0458] Resected tumors were transported in DMEM (ThermoFisher Scientific, Waltham, MA) on ice immediately after surgical procurement. Tumors were rinsed with PBS (Life Technologies, Carlsbad, CA). A small fragment was stored in RNA-protect (Qiagen, Hilden, Germany) for bulk RNA and DNA isolation. Using scalpels, the remainder of the tumor was minced into tiny cubes $< 1 \text{ mm}^3$ and transferred into a 50 ml conical tube (BD Falcon, Franklin Lakes, NJ) containing 10 ml pre-warmed M199-media (ThermoFisher

Scientific), 2 mg/ml collagenase P (Roche, Basel, Switzerland) and 10U/ μ l DNase I (Roche). Tumor pieces were digested in this media for 10 minutes at 37°C, then vortexed for 10 seconds and pipetted up and down for 1 minute using pipettes of descending sizes (25 ml, 10 ml and 5 ml). If needed, this was repeated twice more until a single-cell suspension was obtained. This suspension was then filtered using a 70 μ m nylon mesh (ThermoFisher Scientific) and residual cell clumps were discarded. The suspension was supplemented with 30 ml PBS (Life Technologies) with 2% fetal calf serum (FCS) (Gemini Bioproducts, West Sacramento, CA) and immediately placed on ice. After centrifuging at 580g at 4°C for 6 minutes, the supernatant was discarded and the cell pellet was re-suspended in PBS with 1% FCS and placed on ice prior to staining for FACS.

FACS

[0459] Single-cell suspensions were stained with CD45-FITC (VWR, Radnor, PA) and live/dead stain using Zombie Aqua (BioLegend, San Diego, CA) per manufacturer recommendations. First, doublets were excluded based on forward and sideward scatter, then Applicants gated on viable cells (Aqua^{low}) and sorted single cells (CD45⁺ or CD45⁻) into 96-well plates chilled to 4°C, pre-prepared with 10 μ l TCL buffer (Qiagen) supplemented with 1% beta-mercaptoethanol (lysis buffer). Single-cell lysates were sealed, vortexed, spun down at 3,700 rpm at 4°C for 2 minutes, placed on dry ice and transferred for storage at -80°C.

Single cell RNA-seq

[0460] Whole Transcriptome amplification (WTA) was performed with a modified SMART-Seq2 protocol, as described previously (1, 2) with Maxima Reverse Transcriptase (Life Technologies) instead of Superscript II. Next, WTA products were cleaned with Agencourt XP DNA beads and 70% ethanol (Beckman Coulter, Brea, CA) and Illumina sequencing libraries were prepared using Nextera XT (Illumina, San Diego, CA), as previously described (2). The 96 samples of a multiwell plate were pooled, and cleaned with two 0.8X DNA SPRIs (Beckman Coulter). Library quality was assessed with a high sensitivity DNA chip (Agilent) and quantified with a high sensitivity dsDNA Quant Kit (Life Technologies).

[0461] For droplet-based scRNA-seq, experiments were performed on the 10x Genomics Chromium platform, with the Chromium Single Cell 3' Library & Gel Bead Kit v2 and Chromium Single Cell 3' Chip kit v2 according to the manufacturer's instructions in the Chromium Single Cell 3' Reagents Kits V2 User Guide. Briefly, ~6,000 cells were re-

suspended in PBS supplemented with 0.04% BSA and loaded to each channel. The cells were then partitioned into Gel Beads in Emulsion in the GemCode instrument, where cell lysis and barcoded reverse transcription of RNA occurred, followed by amplification, shearing and 5' adaptor and sample index attachment.

[0462] Barcoded single cell transcriptome libraries were sequenced with 38bp paired end reads on an Illumina NextSeq 500 Instrument.

RNA-capture and bulk RNA-seq of validation cohorts

[0463] RNA extraction from formalin-fixed, paraffin-embedded (FFPE) tissue slides was performed by the Genomics Platform of the Broad Institute (Cambridge, MA). For cDNA Library Construction total RNA was assessed for quality using the Caliper LabChip GX2 (Perkin Elmer). The percentage of fragments with a size greater than 200nt (DV200) was calculated and an aliquot of 200ng of RNA was used as the input for first strand cDNA synthesis using Illumina's TruSeq RNA Access Library Prep Kit. Synthesis of the second strand of cDNA was followed by indexed adapter ligation. Subsequent PCR amplification enriched for adapted fragments. The amplified libraries were quantified using an automated PicoGreen assay (Thermo Fisher Scientific, Cambridge, MA). 200ng of each cDNA library, not including controls, were combined into 4-plex pools. Capture probes that target the exome were added, and hybridized for the recommended time. Following hybridization, streptavidin magnetic beads were used to capture the library-bound probes from the previous step. Two wash steps effectively remove any nonspecifically bound products. These same hybridization, capture and wash steps are repeated to assure high specificity. A second round of amplification enriches the captured libraries. After enrichment, the libraries were quantified with qPCR using the KAPA Library Quantification Kit for Illumina Sequencing Platforms (Illumina) and then pooled equimolarly. The entire process is performed in 96-well format and all pipetting is done by either Agilent Bravo or Hamilton Starlet. Pooled libraries were normalized to 2nM and denatured using 0.1 N NaOH prior to sequencing. Flowcell cluster amplification and sequencing were performed according to the manufacturer's protocols using Illumina HiSeq 2000 or 2500 (Illumina). Each run was a 76bp paired-end with an eight-base index barcode read. Data was analyzed using the Broad Picard Pipeline (broadinstitute.github.io/picard/) which includes de-multiplexing and data aggregation.

RNA-Seq data pre-processing

[0464] BAM files were converted to merged, demultiplexed FASTQ files. The paired-end reads obtained with the SMART-Seq2 protocol were mapped to the UCSC hg19 human transcriptome using Bowtie (Langmead et al., 2009), and transcript-per-million (TPM) values were calculated with RSEM v1.2.8 in paired-end mode (Li and Dewey, 2011). The paired-end reads obtained with the IOx Genomics platform were mapped to the UCSC hg19 human transcriptome using STAR (Dobin et al., 2013), and gene counts/TPM values were obtained using the IOx Genomics computational pipeline (cellranger-2.1.0).

[0465] For bulk RNA-Seq data, expression levels of genes were quantified as $E_{ij} = \log_2(TPM_{ij} + 1)$, where $TPM_{i,j}$ denotes the TPM value of gene i in sample j . For scRNA-seq data, expression levels were quantified as $E_{i,j} = \log_2(TPM_{i,j}/10 + 1)$, where $TPM_{i,j}$ denotes the TPM value of gene i in cell j . TPM values were divided by 10 because the complexity of the single-cell libraries is estimated to be within the order of 100,000 transcripts. The 10^{-1} factoring prevents counting each transcript ~ 10 times, which would have resulted in overestimating the differences between positive and zero TPM values. The average expression of a gene i across a population of N cells, denoted here as P , was defined as

$$E_{i,p} = \log_2 \left(1 + \frac{\sum_{j \in P} TPM_{i,j}}{N} \right)$$

[0466] For each cell, Applicants quantified the number of genes with at least one mapped read, and the average expression level of a curated list of housekeeping genes (Tirosh et al., 2016a). Applicants excluded all cells with either fewer than 1,700 detected genes or an average housekeeping expression (E , as defined above) below 3 (Table S2). For the remaining cells, Applicants calculated the average expression of each gene (E_p), and excluded genes with an average expression below 4, which defined a different set of genes in different analyses depending on the subset of cells included. In cases where Applicants analyzed different cell types together, Applicants removed genes only if they had an average E_p below 4 in each of the different cell types that were included in the analysis. When analyzing CD45⁺ cells, Applicants excluded genes as described above only after the assignment of cells to cell types in order to prevent the filtering of genes that were expressed by less abundant cell types.

Data imputation and normalization

[0467] In all differential expression analyses, Applicants first modeled the read counts as a mixture of a negative binomial (NB) and Poisson components to estimate the expression levels, using SCDE (6) with the code provided in github.com/hms-dbmi/scde. The resulting normalized and imputed expression matrix, denoted as E' , was used in the differential expression analyses because, for single genes, it provides a more accurate and sensitive estimation of their expression. Analysis of droplet-based scRNA-seq data (10X Genomics Chromium, above) was performed with the Seurat package (<http://www.satijalab.org/seurat>), using the likelihood-ratio test for differential gene expression analyses (McDavid et al., 2013).

Identifying cell states associated with specific tumor compositions

[0468] Applicants combined scRNA-seq and bulk RNA-Seq data to characterize the state of a specific cell type in tumors with a specific cell type composition (**Figure IB**). The method takes as input scRNA-seq data and a cohort of RNA-Seq data, both collected from tumors of the same cancer type. For clarity Applicants describe the approach for malignant cells and T cells as applied here, though it can be applied to any pair of cell types.

[0469] **1. Analyze the scRNA-seq data:** (a) assign cells to cell types (see sections: *Classification of malignant and stromal cells* and *Classification of immune cells*); and (b) define a signature of malignant cells and a signature of T cells, consisting of genes which are primarily (specifically) expressed by malignant cells or T cells, respectively (see section: *Cell-type specific signatures*).

[0470] **2. Analyze the bulk RNA-Seq data:** (a) estimate the T cell infiltration level in each tumor by computing the overall expression (OE, see section: *Computing the OE of gene signatures*) of the T cell signature in each bulk sample; (b) compute the Spearman correlation coefficient between the expression of each of the genes in the malignant signature and the OE of the T cell signature across the bulk tumors; and (c) define the **seed exclusion-up (down)** signature as the top 20 malignant genes that are significantly negatively (positively) correlated in (b).

[0471] **3. Analyze the scRNA-seq data of the malignant cells:** (a) compute the OE of the seed exclusion signatures in each of the malignant cells; (b) compute the partial Spearman correlation coefficient between the expression of each gene and the OE of the seed exclusion signatures across the single malignant cells, while controlling for technical quality (the number of reads and genes that were detected in the cells).

[0472] **4. Derive the final genome-scale exclusion signatures,** defined as: (i) **exclusion-**

up: genes which were significantly positively correlated with the seed exclusion-up signature and significantly negatively correlated with the seed exclusion-down signature in the analysis described in (3); and **(ii) exclusion-down:** genes which were significantly positively correlated with the seed exclusion-down signature and significantly negatively correlated with the seed exclusion-up signature in the analysis described in (3). In this analysis, a gene is defined as significantly correlated with a signature if it was among the 200 topmost correlated genes, with p-value $< 10^{-10}$, and Pearson $|r| > 0.1$. Applicants implemented the approach with our clinical scRNA-seq melanoma data and bulk RNA-Seq data of 473 Skin Cutaneous Melanoma (SKCM) tumors from TCGA (as provided in xenabrowser.net/datapages/).

Computing the OE of gene signatures

[0473] Gene modules are more robust to noise and provide more coherent signals than the expression of single genes (Shalek et al., 2013, 2014; Wagner et al., 2016). To compute the OE of a gene module or signature Applicants used a scheme that filters technical variation and highlights biologically meaningful patterns. The procedure is based on the notion that the measured expression of a specific gene is correlated with its true expression (signal), but also contains a technical (noise) component. The latter may be due to various stochastic processes in the capture and amplification of the gene's transcripts, sample quality, as well as variation in sequencing depth (Wagner et al., 2016). The signal-to-noise ratio varies, depending, among other variables, on gene transcript abundance.

[0474] Applicants therefore computed the OE of gene signatures in a way that accounts for the variation in the signal-to-noise ratio across genes and cells. Given a gene signature and a gene expression matrix E (as defined above), Applicants first binned the genes into 50 expression bins according to their average expression across the cells or samples. The average expression of a gene across a set of cells *within* a sample is $E_{i,p}$ (see: **RNA-Seq data pre-processing**) and the average expression of a gene *across* a set of N tumor samples was defined as: $\mathbb{E}_j[E_{ij}] = \sum_j \frac{E_{ij}}{N}$. Given a gene signature S that consists of K genes, with k_b genes in bin b , Applicants sample random S -compatible signatures for normalization. A random signature is S -compatible with signature S if it consists of overall K genes, such that in each bin (b) it has exactly k_b genes. The OE of signature S in cell or sample j is then defined as:

$$OE_j = \frac{\sum_{i \in S} C_{ij}}{\mathbb{E}_{\tilde{S}}[\sum_{i \in \tilde{S}} C_{ij}]}$$

[0475] Where \tilde{S} is a random *S-compatible* signature, and C_y is the centered expression of gene i in cell or sample j , defined as $C_{ij} = E_{ij} - E[\mathcal{E}^{\wedge}]$. Because the computation is based on the centered gene expression matrix C , genes that generally have a higher expression compared to other genes will not skew or dominate the signal.

[0476] Applicants found that 100 random *S-compatible* signatures are sufficient to yield a robust estimate of the expected value $\mathbb{E}_{\tilde{S}}[\sum_{i \in \tilde{S}} C_{ij}]$. The distribution of the OE values was normal or a mixture of normal distributions, and, unlike the expression of a single gene, fulfilled the assumptions of the mixed effects models or hierarchical linear models that Applicants applied to study the differential expression of gene signatures (as described in the *Inter-patient single-cell differential expression analysis of gene sets* section).

[0477] In cases where the OE of a given signature has a bimodal distribution across the cell population, it can be used to naturally separate the cells into two subsets. To this end, Applicants applied the Expectation Maximization (EM) algorithm for mixtures of normal distributions to define the two underlying normal distributions. Applicants then assigned cells to the two subsets, depending on the distribution (high or low) that they were assigned to.

[0478] Applicants use the term a transcriptional *program* (e.g., the immune resistant program) to characterize cell states which are defined by a pair of signatures, such that one (*S-up*) is overexpressed and the other (*S-down*) is underexpressed. Applicants define the OE of such cell states as the OE of *S-up* minus the OE of *S-down*.

Classification of malignant and stromal cells

[0479] In the non-immune compartment (CD45⁻ cells), Applicants distinguished malignant and non-malignant cells according to three criteria: (1) their inferred CNV profiles (5, 10); (2) under-expression of different non-malignant cell-type signatures; and (3) higher similarity to melanoma tumors than to adjacent normal tissue, based on the comparison to bulk RNA-seq profiles. Specifically: (1) to infer CNVs from the scRNA-Seq data Applicants used the approach described in (10) as implemented in the R code provided in github.com/broadinstitute/inferCNV with the default parameters. Cells with an average absolute CNV level that was below the 0.1 quantile of the entire CD45⁻ cell population were considered as potentially non-malignant according to this criterion. (2) Applicants used signatures of endothelial cells, stromal cells, and Cancer Associated Fibroblasts (CAFs), as provided in **table S3**. The signatures combine well-established markers from two sources (www.biolegend.com/cell_markers and (5)). Applicants computed the OE of these three

signatures in each of the CD45⁻ cells, while controlling for the impact of technical cell quality (as described in section *Overall Expression (OE) of gene signatures*). CD45⁻ cells that expressed any one of these three signatures above the 0.95 quantile were considered as non-malignant according to this criterion. (3) Applicants downloaded the pan-cancer TCGA RNA-seqV2 expression data from xena.ucsc.edu, and log₂-transformed the RSEM-based gene quantifications. For each cell, Applicants computed the Spearman correlation between its profile (in TMP) and each bulk profile (in TPM) of 473 skin cutaneous melanoma samples and 727 normal solid tissues. Applicants then tested, for each cell, if it was more similar to the melanoma tumors compared to the normal tissues, by applying a one-sided Wilcoxon ranksum test on the correlation coefficients that were obtained for that cell. Cells that were more similar to the normal tissues ($P < 0.05$, Wilcoxon ranksum test) were considered as potentially non-malignant according to this criterion.

[0480] The cell assignments that were obtained by these three different criteria were highly consistent (Figures S1A,S1B, hypergeometric p-value < 10⁻¹⁷). Cells that were identified as potentially nonmalignant according to one or more of these three criteria were defined as nonmalignant, and were omitted from further analyses of the malignant cells. The nonmalignant CD45⁻ cells were further classified into CAFs and endothelial cells, if they overexpressed only one of the corresponding gene signatures, and as unresolved cells otherwise.

Table S3

Table S3. Cell type signatures that were used for cell classification.				
Macrophage	CCR5	CD14	CD163	CD33
Cytotoxic T cell	CC13	CC14	CD2	CD3D
T-reg	CCR4	CD4	CNGB1	CTLA4
TH22	AHR	CCR10	CCR4	CCR6
TH17	CCR4	CCR6	CD38	CD3D
TH9	CD3D	CD3E	CD3G	CD4
TH2	CCR3	CCR4	CCR7	CCR8
TH1	CCR1	CCR5	CD4	CD2
T Follicular Helper	BCL6	CD3D	CD3E	CD3G
Platelet	BSG	CC15	CCR3	CD109
Plasmacytoid Dendritic Cell	CCR7	CD1A	CD1B	CD1C
NK Cell	B3GAT1	CD244	CD69	IL2RB
Neutrophil	ANPEP	CSAR1	CD14	CD33
Naive T Cell	CCR7	CD3D	CD3E	CD3G
Myeloid Dendritic Cell	CCR7	CD1A	CD1B	CD1C
Megakaryocyte	CD9	GP1BA	ITGA2B	ITGAV
MDS	CCR7	CD1A	CD1B	CD1C
Mast Cell	ENPP3	KIT		
Erythrocyte	CD24	GYPA	PTPRC	
Eosinophil	CSAR1	CSAR1	CCR1	CCR3
B cell	BLK	CD19	CD2	CD22
Basophil	ANPEP	CCR3	CD44	CD63
CAF	FAP	THY1	DCN	COL1A1
Stromal Cell	MMF2	ICAM3	TLR3	MA1GAM1
Endothelial Cell	VWF	TEK	MCAM	CD34

CD68	CD80	CD86	CSF1R	ENG	FCGR1A	FUT4	ITGAL	ITGAM	ITGAX	LAMP2	LILRB4	TLR2	TLR4					
CD3E	CD3G	CD8A	CD8B	CST7	GZMA	GZMB	IFNG	NKG7	PRF1									
ENTPD1	FOXP3	IKZF2	IL2RA	ISG20	ITGAE	JAG3	JARCC2	NTSE	SELL	TNFRSF18	TNFRSF4							
CD3D	CD3E	CD3G	CD4															
CD3E	CD3G	CD4	IL17A	IL17F	IL1R1	IL21	IL22	KLRB1	LINC-ROR	STAT3								
GATA3	IRF4	STAT6																
CD4	CSF2	CXCR4	GATA3	HAVCR1	ICOS	IL10	IL13	IL1R1	IL4	IL5	IL6	PTGDR2						
CXCR3	DPP4	HAVCR2	IFNA1	IFNGR1	IL2	KLRD1	TNF	TNFRSF11										
CD4	CD40LG	CD84	CXCR5	ICOS	IL6R	PDCD1	SLAMF1	STAT3	TNFRSF4									
CD151	CD226	CD36	CD46	CD47	CD48	CD63	CD69	CD84	CD9	CNGB1	CSF3R	FCGR2A	FCGR2B	GPIBA	ICAM2	ITGA2	ITGA2B	
CD4	CD40	CD80	CD83	CD86	CD8A	CLEC4C	CMKLR1	IL3RA	ITGA4	ITGAM	ITGAX	NRP1	PDCD1LG2	TLR9				
ITGA2	ITGAM	ITGAX	KLRA1	KLRB1	KLRD1	KLRK1	NCAM1	NCR1	NKG2	SIGLEC7	SLAMF6	SLAMF7						
CEACAM8	CSF3R	CXCR1	CXCR2	FCGR1A	FUT4	ITGAM	ITGAX	MME	PEGAM1	SELL	TLR2							
CD4	SELL																	
CD207	CD209	CD4	CD40	CD80	CD83	CD86	CMKLR1	DCX	ITGA4	ITGAM	ITGAX	LY75	NRP1	PDCD1LG2				
ITGB3	PEGAM1	SELLP																
CD207	CD209	CD4	CD40	CD80	CD83	CD86	CMKLR1	HLA-DQA	HLA-DOB	HLA-DRA	HLA-DRB1	HLA-DRB5	HLA-DRB6	ITGA4	ITGAM	ITGAX	LY75	
CD244	CD52	CD53	CXCR3	FCER2	FUT4	IL9R	ITGA4	LAIR1	PTGDR2	S100A9	SIGLEC10	SIGLEC8						
CD40	CD5	CD69	CD70	CD79A	CD79B	CD80	CD86	CD93	FCER2	MSHA1	PAS5	PDCD1	SDC1	TNFRSF13B	TNFRSF13C	TNFRSF9	TNFRSF4	
CD69	ENPP3	ICAM1	IL3RA	LAMP1	TLR4													
COL1A2	COL6A1	COL6A2	COL6A3															
MMP1	PDGFRA	TLR4	THY1	KIT	TIMP1	ITGA4	MMP9	PDGFRB	MME	PEGAM1	TIMP2	TLR1	ITGB1	ICAM1	ICAM2	TLR2	VCAM1	
ITGB3	PROCR	CDH5	KDR	SELE	PEGAM1	ENG	ICAM1	FLT4	VCAM1									

potentially malignant or doublets of immune and malignant cells based on their inferred CNV profiles. To this end, Applicants defined the *overall CNV level* of a given cell as the sum of the absolute CNV estimates across all genomic windows. For each tumor, Applicants generated its *CNV profile* by averaging the CNV profiles of its malignant cells, when considering only those with the highest *overall CNV signal* (top 10%). Applicants then evaluate each cell by two values: (1) its *overall CNV level*, and (2) the Spearman correlation coefficient obtained when comparing the cell CNV profile to the CNV profile of its tumor. These two values were used to classify cells as malignant, non-malignant, and unresolved cells that were excluded from further analysis (**fig. 5C-E**).

[0483] Next, Applicants applied two different clustering approaches to assign immune (CD45⁺) cells into cell types. In the first approach, Applicants clustered the CD45⁺ cells according to 194 well-established markers of 22 immune cell subtypes (**table S3**; assembled from www.biolegend.com/cell_markers and (5)). The clustering was performed in three steps: (1) Applicants computed the Principle Components (PCs) of the scRNA-seq profiles, while restricting the analysis to the 194 biomarker genes. Applicants used the top PCs that captured more than 50% of the cell-cell variation. In this case 10 PCs were used, but the results were robust and stable when using the first 5-15 PCs. (2) Applicants applied t-SNE (t-Distributed Stochastic Neighbor Embedding) to transform these first 10 PCs to a two-dimensional embedding, using the R implementation of the t-SNE method with the default parameters, as provided in lvdmaaten.github.io/tsne/. (3) Applicants applied a density clustering method, DBscan (77), on the two-dimensional t-SNE embedding that was obtained in (2). This process resulted in six clusters for which the top preferentially expressed genes included multiple known markers of particular cell types (**fig. 6**).

[0484] To map between clusters and cell types Applicants compared (one sided *t*-test) each cluster to the other clusters according to the OE of the different cell-type signatures (**table S3**). The cell-type signature that was most significantly (*t*-test *p*-value <10⁻¹⁰) overexpressed in the cluster compared to all other clusters was used to define the cluster identity. In this manner, Applicants annotated the clusters as CD8 and CD4 T cells, B cells, macrophages, and neutrophils (**Fig. 1C**). Cells that clustered with the CD8 T-cells and did not express CD8A or CD8B were labeled as NK cells if they overexpressed NK markers, otherwise they were considered as unresolved T-cells. T-cells that were clustered together with the CD4 T-cells and expressed CD8A or CD8B were also considered as unresolved T-cells. Unresolved T-cells were not used in further analyses of CD4 or CD8 T cells.

[0485] To assess the robustness of the assignments, Applicants applied another approach, and determined the concordance between the two assignments. In the second approach, Applicants first made initial cell assignments based on the OE of well-established cell-type makers: T-cells (CD2, CD3D, CD3E, CD3G), B-cells (CD19, CD79A, CD79B, BLK), and macrophages (CD163, CD14, CSF1R). Across all the CD45⁺ cells, the OE levels of these signatures had binomial distributions. Applicants used the bimodal OE of each signature to assign cells to cell types (as described in section *Overall Expression (OE) of gene signatures*). Cells that were assigned to more than one cell type at this point were considered as unresolved. Cells that were defined as T-cells according to this measure were further classified as CD8 or CD4 T-cells if they expressed CD8 (CD8A or CD8B) or CD4, respectively. T-cells that expressed both CD4 and CD8 were considered as unresolved. As a result, 67.3% of the cells had an initial cell-type assignment.

[0486] Next, Applicants clustered the cells with the Infomap algorithm (12). Infomap decomposes an input graph into modules by deriving a compressive description of random walks on the graph. The input to the algorithm was an unweighted *k*-NN graph (*k* = 50) that Applicants generated based on the expression of the 194 biomarker genes across the CD45⁺ cells. Infomap produced 22 clusters, separating the different CD45⁺ cells not only according to cell types but also according to various cell states. For each cluster, Applicants examined if it was enriched with cells of a specific cell type, according to the initial assignments. Nineteen clusters were enriched with only one cell type. The cells within these clusters were assigned to the cell type of their cluster, unless their initial assignment was different, and in this case, they were considered as unresolved.

[0487] The cell-type assignments that were obtained by the two approaches were highly concordant: 97% of the cells had the same assignment with both approaches.

Data-driven signatures of specific cell-types

[0488] To identify cell-type signatures Applicants performed pairwise comparisons between the nine different cell types that Applicants identified: malignant cells, CD8 and CD4 T-cells, NK cells, B-cells, macrophages, neutrophils, CAFs, and endothelial cells. Applicants then performed pairwise comparisons between the different cell types via one-sided Wilcoxon ranksum-tests on the imputed and normalized data *E'* (see *Data imputation and normalization*). Genes that were overexpressed in a particular cell subtype compared to all other cell subtypes (Wilcoxon ranksum-test p-value <10⁻⁵) were considered as cell-type specific. For cell types with less than 1,000 cells Applicants also ranked the genes based on

the maximal p-value that was obtained when comparing the cell type to each of the other cell types; the bottom 100 genes that also passed the first filter were considered as cell type specific. As CD8 T-cells and NK cells had similar expression patterns, Applicants excluded NK cells from the analysis when identifying T-cell specific genes. In the analyses described above Applicants considered the CD4 and CD8 as one entity of T-cells, but also derived CD4 and CD8 specific signatures, by considering as separated entities. The lists of cell-type specific genes are provided in **table S4**.

Differential expression between TN and ICR

[0489] To identify potential signatures of resistance, Applicants searched for transcriptional features that distinguish between the cells of TN and ICR patients, for each cell category separately. Applicants analyzed each cell type that had a sufficient number (>100) of cells: malignant cells, macrophages, B cells, CD8 and CD4 T cells.

[0490] Applicants used sampling to mitigate the effects of outliers and prevent tumors with a particularly large number of cells of a given cell type from dominating the results. In each sampling, Applicants selected a subset of the tumors, subsampled at most 30 cells of the given type from each tumor, and identified differentially expressed genes between the ICR and TN cells. Differentially expressed genes were identified by applying SCDE (73), a Bayesian method that was specifically developed to detect single-cell differential expression. As input to SCDE Applicants used the normalized and imputed expression matrix E' (see *Data imputation and normalization*).

[0491] Applicants repeated the sampling procedure 500 times, and computed for each gene g the fraction of subsamples in which it was found to be significantly under ($F_{down,g}$) or over ($F_{up,g}$) expressed in the ICR population compared to the TN population ($|z\text{-score}| > 1.96$). Genes with $F_{down,g}$ values larger than the 0.9 quantile of the F_{down} distribution were considered as potentially down-regulated in the respective ICR population. Likewise, genes with $F_{up,g}$ values larger than the 0.9 quantile were considered as potentially up-regulated in the respective ICR population.

[0492] Applicants further filtered the signatures with two additional statistical tests that Applicants applied on the full scRNA-seq data (E') of the respective cell type (6). The first test was SCDE followed by multiple hypotheses correction (Holm-Bonferroni (14)). The second was a non-parametric empirical test, where Applicants performed a one-sided Wilcoxon ranksum test to examine if a given gene is differentially expressed in the ICR vs. TN cells. Applicants used E' and not the raw counts or log transformed TPM, as non-ordinal

values violate the Wilcoxon ranksum assumptions. Applicants corrected for multiple hypotheses testing using the Benjamini & Hochberg approach (75), and obtained empirical p-values to ensure the differences in expression were not merely reflecting differences in cell quality (*i.e.*, the number of aligned reads per cell). To this end Applicants generated 1,000 random permutations of the gene expression matrix E' , such that each permutation preserves the overall distribution of each gene, as well as the association between the expression of each gene and cell quality. Applicants performed the Wilcoxon ranksum test on the permuted E' matrixes to compute the empirical p-values.

[0493] To assemble the final signatures, Applicants selected genes that fulfilled the subsampling criteria described above and were most significantly differentially expressed according to both the SCDE and empirical tests (top 200 genes with corrected $P < 0.05$).

Mixed effect model for testing the differential expression of gene signatures

[0494] To test the ability of a given gene signature to distinguish between the ICR and TN patients Applicants modeled the data with a mixed-effects model that accounts for the dependencies and structure in the data. Applicants used a hierarchical linear model (HLM) with two levels: (1) cell-level, and (2) sample-level. The sample-level controlled for the dependency between the scRNA-seq profiles of cells that were obtained from the same patient, having a sample-specific intercept. The model had overall five covariates. Level-1 covariates were the number of reads (log-transformed) and the number of genes that were detected in the respective cell. Level-2 covariates were the patient's gender, age, and treatment group, and a binary covariate that denotes if the sample was a metastatic or primary lesion. In the analyses of malignant cells, Applicants added another level-1 covariate that denoted which cells were cycling, based on the bimodal OE of the cell cycle signatures defined in (7) (see section *Overall Expression (OE) of gene signatures*).

[0495] To examine if a given signature was differentially expressed in the ICR compared to the TN group Applicants used the HLM model to quantify the significance of the association between each of the model covariates and the OE of the signature across the cells. Applicants applied this approach to examine the association between the treatment and the OE of the ICR and exclusion signatures. Applicants also tested annotated gene sets that Applicants downloaded from MSigDB v6.0 (16) to examine if certain pre-defined pathways and biological functions were differentially expressed in the ICR vs. TN cells (table S9, Fig. 2C).

[0496] Applicants implemented the HLM model in R, using the *lme4* and *ImerTest*

packages (CRAN.R-project.org/package=lme4, CRAN.R-project.org/package=lmerTest).

Cross validation analysis

[0497] To examine the generalizability of the oncogenic-ICR (mICR) signatures Applicants performed a cross-validation procedure. In each cross-validation round the test set consisted of all the cells of one patient, and the training set consisted of the data from all the other patients in the cohort. In each round Applicants used only the training data to generate mICR signatures (as described in *Differential expression between TN and ICR*), and computed the OE of the resulting mICR signatures in the cells of the test patient to obtain their resistance scores (mICR-up minus mICR-down). To center the expression matrix for the computation of the OE values, Applicants used all the malignant cells in the data, such that the resistance scores of one patient were relative to those of the other patients.

Integrating the exclusion and post-treatment programs

[0498] Applicants combined the post-treatment and exclusion programs with a simple union of the matching signatures, into the immune resistance gene program (**Table S5**). Applicants further refined the immune resistance program by integrating the scRNA-seq data with the results of a genome-scale CRISPR screen that identified gene KOs which sensitize malignant melanoma cells to T cell killing (Patel et al., 2017). Applicants defined our single malignant cells as putatively "*resistant*" if they underexpressed (lowest 1%) of one of the top hits of the screen: B2M, CD58, HLA-A, MLANA, SOX10, SRP54, TAP2, TAPBP. This underexpression did not reflect low cell quality, because these "*resistant*" cells had a higher number of genes and reads. These cells had significantly higher immune resistance scores ($P = 2.24 \times 10^{-18}$ and 1.59×10^{-3} , t-test and mixed effects, respectively), and were enriched with cycling cells ($P = 1.74 \times 10^{-13}$, hypergeometric test). Applicants identified the topmost differentially expressed genes by comparing the "*resistant*" cells to other malignant cells, and included in the refined immune resistance-up (down) signature only 25 (35) immune resistance-up (down) genes that pass this additional differential expression test.

[0499] Applicants report the performances of all the resistance program subsets: exclusion, post-treatment, and their union (**Figures S4-S5**). As comparators, Applicants used the hits of the co-culture screen along with other potentially prognostic signatures, to generate competing predictors of patient survival and response (**Figures 5E,H, Table S7**, see section *Competing ICI response predictors*).

[0500]

T cell cytotoxicity and exhaustion signature analysis

[0501] The analysis of T-cell exhaustion *vs.* T-cell cytotoxicity was performed as previously described (5), with six different exhaustion signatures, as provided in (7) and (77). First, Applicants computed the cytotoxicity and exhaustion scores of each CD8 T cell. Next, to control for the association between the expression of exhaustion and cytotoxicity markers, Applicants estimated the relationship between the cytotoxicity and exhaustion scores using locally-weighted polynomial regression (LOWESS, black line in Fig. IE and fig. S4B). Based on these values, Applicants defined T cells as functional if they fulfilled two criteria: (1) their cytotoxicity score was at the top 20% of the CD8 T cell population (across all patients), and (2) their exhaustion scores were lower than expected given their cytotoxicity scores (below the dashed line in Fig. IE and fig. 4SB). Applicants then applied a hypergeometric test to examine if the CD8 T cells of a given patient were enriched with functional cells.

Identifying T cell clones and estimating the fraction of clonally expanded T-cells

[0502] Applicants reconstructed the T-cell Receptors (TCRs) using TraCeR (75), with the Python package provided in github.com/Teichlab/tracer. TCR reconstruction significantly improved in the new cohort compared to previously analyzed patients (**table SI**): 92% CD8 T-cells had reconstructed TCRs, compared to only 50% such cells in the previously published cohort (**fig. 9A**). This is likely due to shorter read length and lower sequencing depth in the previous study (7). Applicants assigned T cells to the clones defined in the TraCeR output. Reassuringly, cells from different patients were never falsely assigned to the same clone, and CD8 and CD4 T-cells were always assigned to different clones, even when they were obtained from the same tumor. In the CD8 T-cells Applicants detected 137 clones (**Fig. IF**). In the CD4 T-cells Applicants detected only 29 clones, with at most 3 cells per clone.

[0503] The size and number of clones that Applicants identified in each tumor is affected by the number of T-cells that were sequenced from that tumor, and the success rate of TCR reconstruction. To estimate the fraction of clonally expanded T-cells in a given tumor Applicants therefore sampled its T-cells as follows. First, Applicants restricted the analysis to tumors with at least 20 CD8 T-cells with a full-length reconstructed TCR. Next, Applicants repeatedly sampled 20 cells from each tumor, such that, in each iteration, Applicants computed for every tumor the fraction of clonally expanded cells, namely, the fraction of sampled cells that shared their TCR with another cell within the sampled population. The average fraction of clonally expanded cells was used as an estimate of the T-cell clonal expansion level (**fig. 9B**).

Cell cycle analysis

[0504] Applicants performed the following analysis to identify gene modules that characterize cycling cells specifically in CD8 T-cells (**table S8**). First, Applicants identified cycling cells in the CD8 T-cells and in the malignant cells based on the bimodal OE of a cell-cycle signature (the GO gene set *cell cycle process*, as defined in the **Overall Expression (OE) of gene signatures** section). Applicants then identified differentially expressed genes (with SCDE (13)) between the cycling and non-cycling cells, separately in the CD8 T-cells and in the malignant cells. Lastly, Applicants filtered from the resulting CD8 T-cell cycling signatures the genes that were also included in the corresponding malignant signatures.

Characterizing malignant cells in non-infiltrated tumors

[0505] Applicants developed an approach that combines scRNA-seq and bulk RNA-seq data to characterizes the state of a specific cell type in tumors with a specific cell-type composition. Applicants applied it to identify oncogenic programs that are induced or repressed in malignant cells that reside in tumors or niches with low T-cell infiltration levels. For clarity, Applicants describe the approach for this specific application, but note that it can also be applied in various other settings, as long as the tumor composition can be well-defined, and the cell type of interest is adequately represented in the single cell data.

[0506] Applicants implemented the following step-wise approach (**Fig. 2F**):

1. Applicants provided as input the signature of malignant cells and the signature of T-cells, defined above (section: **Cell-type specific signatures**).
2. Applicants obtained the bulk RNA-Seq data of 473 Skin Cutaneous Melanoma (SKCM) tumors from TCGA (as provided in xenabrowser.net/datapages/). On this bulk data Applicants (a) estimated of the T-cell infiltration level in each tumor by computing the OE of the T-cell signature in each of the bulk samples; (b) computed the Spearman correlation coefficient between the expression of each of the genes in the malignant signature and the OE of the T-cell signature across the 473 bulk tumors; and (c) defined the **seed exclusion-up (down)** signature as the top 20 malignant genes that were significantly negatively (positively) correlated in (b).
3. Applicants analyzed the scRNA-Seq data of the *malignant cells* in the following way. (a) Applicants computed the OE of the seed T_{exc} signatures in each of the malignant cell profiles; (b) Applicants computed the partial Spearman correlation coefficient between the expression of each gene and the OE of the seed T_{exc} signatures across the single malignant cells, while controlling for technical quality (the number of reads and genes that were detected in the

cells).

4. Applicants derived the final genome-scale exclusion signatures, defined as: (i) **exclusion-up**: Genes which are significantly positively correlated with the seed $T_{\text{exc-up}}$ signature and significantly negatively correlated with the seed $T_{\text{exc-down}}$ signature; and (ii) **exclusion-down**: Genes which are significantly positively correlated with the seed $T_{\text{exc-down}}$ signature and significantly negatively correlated with the seed exclusion-up signature. In this analysis, a gene was defined as significantly correlated with a signature if it was among the 200 topmost correlated genes, with P-value $< 10^{-10}$, and $|R| > 0.1$.

Integration of the exclusion and oncogenic-ICR signatures

[0507] Applicants combined the mICR and T_{exc} signatures with a simple union of the matching signatures, into the uICR gene signatures. Applicants further refined the uICR signatures by identifying putative "*resistant*" malignant cells as those that under-expressed (lowest 1%) one of the top hits of a CRISPR screen (19) in malignant melanoma for resistance to T-cell killing: B2M, CD58, HLA-A, MLANA, SOX10, SRP54, TAP2, TAPBP. (This under-expression did not reflect low cell quality, because these "*resistant*" cells had a higher number of genes and reads. These cells had significantly higher uICR scores ($P = 2.24 \times 10^{-18}$ and 1.59×10^{-3} , t-test and mixed effects, respectively), and were enriched with cycling cells ($P = 1.74 \times 10^{-13}$, hypergeometric test).) Applicants the topmost differentially expressed genes by comparing the "*resistant*" cells to other malignant cells (13), and included in the refined uICR-up (down) signature only 25 (35) uICR-up (down) genes that pass this additional differential expression test.

[0508] Applicants report the performances of all the resistance signatures: oncogenic-ICR, exclusion, and their union (uICR), with and without this additional refinement (**figs. 11-13**). For comparison, Applicants used the hits of the co-culture screen along with other potentially prognostic signatures, to generate competing predictors of patient survival and response (**Fig. 4, E,H, tables S10**, see section *Competing ICR predictors*).

Cell-cell interaction network

[0509] Applicants generated genome-scale cell-cell interactions networks by integrating (1) protein-protein interactions that were previously assembled by (20) as cognate ligand-receptor pairs, with (2) cell-subtype specific signatures from the single cell profiles, identified as described above. The resulting network maps the physical interactions between the different cell subtypes that Applicants characterized. Each cell subtype and protein are represented by a node in the network. An edge between a cell subtype node and a ligand or

receptor node denotes that this protein is included in the cell subtype signatures. An edge between two proteins denotes that they can physically bind to each other and mediate cell-cell interactions. A path from one cell subtype to another represents a potential route by which the cells can interact. For each cell subtype, Applicants defined a 'communication signature', which includes all the surface proteins that bind to the cell subtype signature proteins. To examine if the ICR malignant cells suppress their interactions with other cell subtypes Applicants examined if the different oncogenic resistance signatures were enriched (hypergeometric test) with genes from the different immune and stroma 'communication signatures' (Fig. 3E). An interactive map of the cell-cell interaction network is provided as **supplementary files**, and can be explored with Cytoscape (21) provided in www.cytoscape.org.

Survival and ICI-response predictions

[0510] To test if a given signature can predict survival or progression free-survival (PFS) Applicants first computed the OE of the signature in bulk RNA-Seq in each patient tumor. Next, Applicants used a Cox regression model with censored data to compute the association and its significance. To examine if the signature's predictive value was significant beyond T-cell infiltration levels Applicants computed for each sample the OE of the T-cell signature (above), used this as another covariate in the Cox regression model, and computed another p-value for the given signature, based on its association with survival or PFS in this two-covariate model.

[0511] To visualize the predictions of a specific signature in a Kaplan Meier (KM) plot, Applicants stratified the patients into three groups according to the OE of the signature: high or low expression correspond to the top or bottom **25%** of the population, respectively; intermediate expression is between the upper and lower quartiles (**26%-74%**, interquartile range). Applicants used a one-sided logrank test to examine if there was a significant difference between these three patient groups in terms of their survival or PFS rates.

[0512] CB was defined according to the RESICT criteria, such that patients with a complete or partial response were defined as CB patients. Patients with progressive disease were defined as non-CB, and patients with more ill-defined response, as stable disease or marginal responses were excluded from this analysis. Applicants further stratified the CB patients according to the duration of the response: (1) less than **6** months, (2) more than **6** months and less than a year, and (3) more than a year (long-term CB). Applicants then applied one-sided t-tests to examine if the OE of the different signatures were differentially

expressed in the CB *vs.* non-CB patients, or in the long-term CB patients compared to the non-CB patients. Finally, Applicants tested the ability of the different signatures to predict complete response by comparing (t-test) between the complete responders and the all other patients with a RECIST annotation (n = 101, **Fig. 4H and fig. 14**), and computing the Area Under the Curve (AUC) of the resulting Receiver Operating Characteristic (ROC) curve.

Multiplexed, tissue cyclic immunofluorescence (t-CyCIF) of FFPE tissue slides

[0513] Formalin-fixed, paraffin-embedded (FFPE) tissue slides, 5 μm in thickness, were generated at the Brigham and Women's Hospital Pathology Core Facility from tissue blocks collected from patients under IRB-approved protocols (DFCI 11-104). Multiplexed, tissue cyclic immunofluorescence (t-CyCIF) was performed as described recently (Lin et al., 2017). For direct immunofluorescence, Applicants used the following antibodies: CEP 170 (Abeam, ab84545), LAMP2 (R&D technologies, AF6228), MITF (Abeam, ab3201), DLL3 (Abeam, ab103102, Rab), MITF (Abeam, ab3201, Ms), S100a-488 (Abeam, ab207367), CD3-555 (Abeam, ab208514), CD8a-660 (eBioscience, 50-0008-80), cJUN-488 (Abeam, ab193780), cMyc-555 (Abeam, ab201780), HLAA-647 (Abeam, ab199837), TP53-488 (Cell Signaling, 5429), SQSTM1-555 (Abeam, ab203430). Stained slides from each round of CycIF were imaged with a CyteFinder slide scanning fluorescence microscope (RareCyte Inc. Seattle WA) using either a 10X (NA=0.3) or 40X long-working distance objective (NA = 0.6). Imager5 software (RareCyte Inc.) was used to sequentially scan the region of interest in 4 fluorescence channels. Image processing, background subtraction, image registration, single-cell segmentation and quantification were performed as previously described (Lin et al., 2017).

Mapping cell-cell interactions based on imaging data

[0514] Given the processed imaging data, Applicants assigned cells into cell types by discretizing the log-transformed expression levels of the cell type markers (S100, MITF, CD3, and CD8). Applicants applied the EM algorithm for mixtures of normal distributions to characterize the two normal distributions for each of these cell type marker intensities. S100⁺/MITF⁺/CD3⁺CD8⁻ cells were defined as malignant cells; S100⁺/MITF⁻/CD3⁺/CD8⁻ cells were defined as T cells, and S100⁻/MITF⁻/CD3⁺/CD8⁺ cells were defined as CD8 T cells; other cells were defined as uncharacterized.

[0515] For each image Applicants constructed a Delaunay (Gabriel) graph, where two cells are connected to each other if there is no other cell between them. Following the approach presented in (Goltsev et al., 2017), Applicants examined if cells of certain types

were less/more likely to be connected to each other in the graph. To this end, Applicants computed the odds ratio of cell-cell interactions of cell type A and cell type B by computing the observed frequency of interactions divided by the expected theoretical frequency (calculated as the total frequency of edges incident to type A multiplied by the total frequency of edges incident to type B). Two cell types are less or more likely to interact than expected by chance if the log-transformed odds ratio is less or more than 0, respectively. The significance of the deviation from zero was tested using the binomial distribution test.

[0516] Next, Applicants examined the association between the expression of the different markers in the malignant cells and the level of T cell infiltration. Each image in our data was composed of a few hundred frames (119-648 frames/image), where each frame consists of 1,377 cells on average. In each frame, Applicants computed the fraction of T cells and the average expression of the different markers in the malignant cells. Applicants then used a hierarchical logistic regression model to quantify the associations. The independent variables included the average expression of the marker in the malignant cells of the frame (level-1), the average expression of normalization markers in the malignant cells of the frame (level-1), and the image the frame was sampled from (level-2). The dependent variable was the discretized T cell infiltration level of the frame, defining frames with high/low lymphocyte-fraction as "hot"/"cold", respectively. Applicants used different cutoffs to define hot/cold frames, such that a frame with a T cell fraction $< Q$ was defined as cold. Applicants report the results that were consistent across multiple definitions of Q , and provide the p-value obtained with $Q =$ the median T cell fraction across all frames from all images.

Integrating scRNA-seq and spatial data

[0517] Applicants integrated the scRNA-seq and multiplexed immunofluorescence (t-CyCIF) data via a variant of Canonical Correlation Analysis (CCA), using the code provided in the R toolkit Seurat (Butler and Satija, 2017). CCA aims to identify shared correlation structures across datasets, such that each dataset provides multiple measurements of a gene-gene covariance structure, and patterns which are common to both datasets are identified. Cells from both sources are then represented in an aligned-CCA space (Butler and Satija, 2017).

[0518] In our application, each cell in the t-CyCIF data was represented by the log-transformed intensities of 14 markers. Each cell in the scRNA-seq data was represented by the imputed expression of the genes encoding the same 14 proteins. To impute the scRNA-seq data Applicants identified a signature for each marker, consisting of the top 50 genes

which were mostly correlated with the marker expression across the cell population in the scRNA-seq data. Applicants then used the OE of the marker signature as a measure of its activity in the scRNA-seq data.

[0519] The cells from both sources were represented in the resulting aligned-CCA space. Next, Applicants used the first five aligned-CCA dimensions to cluster the cells and represented them in a 2D t-SNE embedding (Laurens Maaten, 2009). Clustering was performed using a shared nearest neighbor (SNN) modularity optimization based clustering algorithm, which calculates k-nearest neighbors, constructs an SNN graph, and optimizes the modularity function to determine clusters (Waltman and van Eck, 2013).

[0520] To examine if cells clustered according to cell type or according to source Applicants computed the expected number of cells from each two categories to be assigned to the same cluster by chance, assuming a random distribution of cells into clusters. Applicants then used the observed *vs.* expected co-clustering ratio to quantify the deviation from the random distribution, and used the binomial test to compute the statistical significance of this deviation from random.

Survival and ICI-response predictions

[0521] To test if a given signature predicts survival or progression free-survival (PFS) Applicants first computed the OE of the signature in each tumor based on the bulk RNA-Seq data. Next, Applicants used a Cox regression model with censored data to compute the significance of the association between the OE values and prognosis. To examine if the signature's predictive value was significant beyond T cell infiltration levels Applicants computed for each sample the OE of our T cell signature (above), used this as another covariate in the Cox regression model, and computed another p-value for each signature, based on its association with survival or PFS in this two-covariate model.

[0522] To visualize the predictions of a specific signature in a Kaplan Meier (KM) plot, Applicants stratified the patients into three groups according to the OE of the signature: high or low expression correspond to the top or bottom 25% of the population, respectively, and intermediate otherwise. Applicants used a one-sided log-rank test to examine if there was a significant difference between these three patient groups in terms of their survival or PFS rates.

[0523] CB was defined according to RESICT criteria, such that patients with a complete or partial response were defined as CB patients. Patients with progressive disease were defined as non-CB, and patients with more ill-defined response, such as stable disease or

marginal responses, were excluded from this analysis. Applicants further stratified the CB patients according to the duration of the response: (1) less than 6 months, (2) more than 6 months and less than a year, and (3) more than a year (long-term CB). Applicants applied one-sided t-tests to examine if the OE of the different signatures were differentially expressed in the CB vs. non-CB patients, or in the long-term CB patients compared to the non-CB patients. Finally, Applicants tested the ability of the different signatures to predict complete response by comparing (t-test) between the complete responders and all other patients with a RECIST annotation (n = 101, **Figures 5H and S5F**), and computing the Area Under the Curve (AUC) of the resulting ROC curve.

Controlling for cell cycle effects in the resistance OE scores

[0524] The single-cell data demonstrated that cycling cells have higher expression of resistance states, according to the oncogenic-ICR, exclusion, and uICR signatures. Since the tumor proliferation rate may be a dynamic and context-dependent property, it might be advisable to compare between tumors based on their *basal resistance level*, namely, after controlling for the cell cycle effect. To this end, Applicants compute for each tumor the OE of two cell cycle signatures (G1/S and G2/M signatures in **table S10**). Applicants then fitted a linear model to estimate the expected OE of the resistance signature, when using the OE of the two cell cycle signatures as covariates. The residuals of this linear model, which quantify the deviation from the expected resistance OE values, were considered as the *basal resistance level*. Applicants performed this analysis with different resistance signatures (e.g., uICR, exclusion, etc.).

Alternative ICR predictors

[0525] To compare the predictive value of the resistance signature to that of other signatures, Applicants repeated the prediction process, as describe in *Survival and ICI-response predictions*, for each of the following gene signatures (**table S10**): (1) Cell-type specific signatures identified from the scRNA-Seq (as described in the *Cell-type specific signatures* section); (2) Signatures that characterize oncogenic cell states in melanoma (the AXL-high, MITF-high, and cell cycle states from (7)); (3) Six different sets of genes whose guides were found to be differentially (FDR < 0.05) depleted or enriched in the *in vivo* CRISPR screen of (22), designed to identify key regulators of immune evasion and ICR in melanoma, based on the pairwise comparisons of three experimental settings. The data was obtained from **Table SI** of (22); (4) The genes whose guides were most preferentially and significantly enriched (top 10 and top 50) in the co-culture conditions in the genome-scale

CRISPR screen of (19), also designed to identify key regulators of immune evasion and ICR in melanoma; (5) Immune-related signatures that were identified based on the analysis of multiple Pembrolizumab clinical datasets, and were shown to predict the response to Pembrolizumab in an independent cohort (23); (6) The Fluidigm Advanta™ Immunology Gene Expression signatures (www.fluidigm.com/applications/advanta-immuno-oncology-gene-expression-assay); and (7) PDL1 expression.

[0526] Applicants summarize in **table S10** the predictive value of each of these signatures when applied to predict melanoma (TCGA) patient survival, and the PFS, clinical benefit (CB), and complete response in the melanoma patients of the aPDL1 cohort.

Comparison of pre- and post-treatment samples in validation Cohort 2

[0527] Applicants used a mixed-effects model to represent the data and examine the association between the expression of various gene signatures and different treatment categories. The model included two levels. The first, sample-level, had 12 covariates, the first three denote whether the sample was exposed to: (1) targeted therapy (on/post RAF/MEK-inhibitors), (2) ICI (on/post), with or without an additional immunotherapy, (3) non-ICI immunotherapy (NK antibodies, IL2, IFN, or GM-CSF) without ICI. The other 9 sample-level covariates control for potential changes in the tumor microenvironment by providing the OE of the different non-malignant cell subtype signatures that Applicants identified (**table S4**). The second, patient-level, controlled for the dependency between the scRNA-seq profiles of samples that were obtained from the same patient, having a patient-specific intercept that provided the baseline level for each patient.

[0528] Applicants used the mixed effects model to quantify the association between the different ICR signatures and the exposure to ICI or targeted therapy (the second and first sample-level covariates, respectively). When testing the association between the tumor composition and the treatments Applicants used the model described above without the 9 TME covariates.

[0529] Applicants implemented the HLM model in R, using the lme4 and lmerTest packages (CRAN.R-project.org/package=lme4, CRAN.R-project.org/package=lmerTest).

[0530] For each resistance signature, Applicants applied ANOVA to test if the inter-patient variation in the OE values was significantly greater than the intra-patient variation, and reported the least significant ANOVA p-value that was obtained.

Searching for immune sensitizing drugs

[0531] Applicants performed the following analysis to identify drugs that could selectively eradicate malignant cells with a high expression of the resistance program, using efficacy measures of 131 drugs across 639 human cancer cell lines (Garnett et al., 2012). For each drug, Applicants defined sensitive cell lines as those with the lowest (bottom 10%) IC50 values. Applicants then used the gene expression provided in (Garnett et al., 2012), computed the OE of the resistance program in each of the 639 cells, and defined "resistant" cell lines as those with the highest OE values (top 10%). Next, for each drug Applicants built a hierarchical logistic regression model, where the dependent variable is the cell line's (drug-specific) binary sensitivity assignment, and the independent variables are the cell lines' "resistance" assignments (level-1) and cancer types (level-2). Drugs then were ranked based on the one-tailed p-values that quantify the significance of the positive association between the drug sensitivity (dependent) variable and the immune resistance (independent) variable.

Abemaciclib treatment of melanoma cell lines

[0532] Established melanoma cell lines IGR39, UACC62 and A2058 were acquired from the Cancer Cell Line Encyclopedia (CCLE) from the Broad Institute. Cells were treated every 3 days with 500 nM abemaciclib (LY2835219, MedChemExpress) or DMSO control. The doubling time of each cell line was established and lines were seeded such that cells collected for scRNA-seq were derived from culture dishes with ~50-60% confluency on day 7 of treatment. Cells were lifted of culture dishes using Versene solution (Life Technologies), washed twice in 1x PBS, counted and resuspended in PBS supplemented with 0.04% BSA for loading for scRNA-seq with the 10X Genomics platform.

Melanoma-TIL co-culture

[0533] An autologous pair of melanoma and TIL culture was provided by MD Anderson Cancer Center and were established using previously described protocols (Peng et al., 2016). Melanoma cells were pre-treated with 500 nM abemaciclib or DMSO control for 7 days followed by co-culture with autologous TILs (with an effector to target ratio of 5:1) for 48 hours. TILs were removed by pipetting of the supernatant, and the remaining melanoma cells were washed twice with PBS, lifted off the culture dish, and resuspended in PBS supplemented with 0.04% BSA for loading for scRNA-seq with the 10X Genomics platform.

Data availability

[0534] Processed scRNA-seq data generated for this study is currently provided through the single-cell portal in a 'private' mode. To access the data login to the portal (portals.broadinstitute.org/single_cell) via the email account icr.review1@gmail.com, with

the password *icrreviewl*, and use the following link to view or download the data portals.broadinstitute.org/single_cell/study/melanoma-immunotherapy-resistance. The processed data will also be available through the Gene Expression Omnibus (GEO), and raw scRNA-seq data will be deposited in dbGAP.

References for Materials and Methods

1. I. Tirosh et al., Dissecting the multicellular ecosystem of metastatic melanoma by single-cell RNA-seq. *Science* 352, 189-196 (2016).
2. S. Picelli et al., Smart-seq2 for sensitive full-length transcriptome profiling in single cells.
3. J. J. Trombetta et al., Preparation of Single-Cell RNA-Seq Libraries for Next Generation Sequencing.
4. B. Langmead, M. Trapnell C Fau - Pop, S. L. Pop M Fau - Salzberg, S. L. Salzberg, Ultrafast and memory-efficient alignment of short DNA sequences to the human genome.
5. B. Li, C. N. Dewey, RSEM: accurate transcript quantification from RNASeq data with or without a reference genome.
6. J. Fan et al., Characterizing transcriptional heterogeneity through pathway and gene set overdispersion analysis. *Nat Meth* 13, 241-244 (2016).
7. A. K. Shalek et al., Single-cell transcriptomics reveals bimodality in expression and splicing in immune cells. *Nature* 498, 236-240 (2013).
8. A. Wagner, A. Regev, N. Yosef, Revealing the vectors of cellular identity with single-cell genomics. *Nat Biotech* 34, 1145-1 160 (2016).
9. A. K. Shalek et al., Single-cell RNA-seq reveals dynamic paracrine control of cellular variation. *Nature* 510, 363-369 (2014).
10. A. P. Patel et al., Single-cell RNA-seq highlights intratumoral heterogeneity in primary glioblastoma. *Science (New York, N.Y.)* 344, 1396-1401 (2014).
11. M. Ester, H.-P. Kriegel, #246, r. Sander, X. Xu, paper presented at the Proceedings of the Second International Conference on Knowledge Discovery and Data Mining, Portland, Oregon, 1996.
12. M. Rosvall, C. T. Bergstrom, Maps of random walks on complex networks reveal community structure. *Proceedings of the National Academy of Sciences* 105, 1118-1 123 (2008).

13. P. V. Kharchenko, L. Silberstein, D. T. Scadden, Bayesian approach to single-cell differential expression analysis. *Nat Meth* 11, 740-742 (2014).
14. S. Holm, A Simple Sequentially Rejective Multiple Test Procedure. *Scandinavian Journal of Statistics* 6, 65-70 (1979).
15. Y. Benjamini, Y. Hochberg, Controlling the False Discovery Rate: A Practical and Powerful Approach to Multiple Testing. *Journal of the Royal Statistical Society. Series B (Methodological)* 57, 289-300 (1995).
16. A. Subramanian et al., Gene set enrichment analysis: A knowledge-based approach for interpreting genome-wide expression profiles. *Proceedings of the National Academy of Sciences* 102, 15545-15550 (2005).
17. C. Zheng et al., Landscape of Infiltrating T Cells in Liver Cancer Revealed by Single-Cell Sequencing.
18. M. J. T. Stubbington et al., T cell fate and clonality inference from single cell transcriptomes. *Nat Meth* 13, 329-332 (2016).
19. S. J. Patel et al., Identification of essential genes for cancer immunotherapy. *Nature* 548, 537-542 (2017).
20. J. A. Ramilowski et al., A draft network of ligand-receptor-mediated multicellular signalling in human. 6, 7866 (2015).
21. P. Shannon et al., Cytoscape: A Software Environment for Integrated Models of Biomolecular Interaction Networks. *Genome Research* 13, 2498-2504 (2003).
22. R. T. Manguso et al., In vivo CRISPR screening identifies Ptpn2 as a cancer immunotherapy target. *Nature* 547, 413-418 (2017).
23. M. Ayers et al., IFN- γ -related mRNA profile predicts clinical response to PD-1 blockade. *The Journal of Clinical Investigation* 127, 2930-2940 (2017).
24. S. Goel et al., CDK4/6 inhibition triggers anti-tumour immunity. *Nature* 548, 471-475 (2017).

* * *

[0535] Various modifications and variations of the described methods, pharmaceutical compositions, and kits of the invention will be apparent to those skilled in the art without departing from the scope and spirit of the invention. Although the invention has been described in connection with specific embodiments, it will be understood that it is capable of further modifications and that the invention as claimed should not be unduly limited to such

specific embodiments. Indeed, various modifications of the described modes for carrying out the invention that are obvious to those skilled in the art are intended to be within the scope of the invention. This application is intended to cover any variations, uses, or adaptations of the invention following, in general, the principles of the invention and including such departures from the present disclosure come within known customary practice within the art to which the invention pertains and may be applied to the essential features herein before set forth.

CLAIMS

What is claimed is:

1. A method of detecting an immune checkpoint inhibitor resistance (ICR) gene signature in a tumor comprising, detecting in tumor cells obtained from a subject in need thereof the expression or activity of a malignant cell gene signature comprising:

a) one or more genes or polypeptides selected from the group consisting of C1QBP, CCT2, CCT6A, DCAF13, EIF4A1, ILF2, MAGEA4, NONO, PA2G4, PGAM1, PPA1, PPIA, RPL18A, RPL26, RPL31, RPS1 1, RPS15, RPS21, RPS5, RUVBL2, SAE1, SNRPE, UBA52, UQCRH, VDAC2, AEBP1, AHNAK, APOC2, APOD, APOE, B2M, C10orf54, CD63, CTSD, EEA1, EMP1, FBX032, FYB, GATSL3, HCP5, HLA-A, HLA-B, HLA-C, HLA-E, HLA-F, HLA-H, ITGA3, LAMP2, LYRM9, MFGE8, MIA, NPC2, NSG1, PROS1, RDH5, SERPINA1, TAPBP, TIMP2, TNFSF4 and TRIML2; or

b) one or more genes or polypeptides selected from the group consisting of ACAT1, ACP5, ACTB, ACTG1, ADSL, AEN, AK2, ANP32E, APP, ASAPI, ATP5A1, ATP5D, ATP5G2, BANC1, BCAN, BZW2, C17orf76-AS1, C1QBP, C20orf1 2, C6orf48, CA14, CBX5, CCT2, CCT3, CCT6A, CDK4, CEP170, CFL1, CHP1, CNRIP1, CRABP2, CS, CTPS1, CYC1, DAP3, DCAF13, DCT, DDX21, DDX39B, DLL3, EDNRB, EEF1D, EEF1G, EEF2, EIF1AX, EIF2S3, EIF3E, EIF3K, EIF3L, EIF4A1, EIF4EBP2, ESRP1, FAM174B, FAM178B, FAM92A1, FBL, FBLN1, FOXRED2, FTL, FUS, GABARAP, GAS5, GNB2L1, GPATCH4, GPI, GRWD1, GSTO1, H3F3A, H3F3AP4, HMGA1, HNRNPA1, HNRNPAIPIO, HNRNPC, HSPA8, IDH2, IFI16, ILF2, IMPDH2, ISYNA1, ITM2C, KIAA0101, LHFPL3-AS1, LOC100190986, LYPLA1, MAGEA4, MARCKS, MDH2, METAP2, MIDI, MIR4461, MLLT1 1, MPZL1, MRPL37, MRPS12, MRPS21, MYC, NACA, NCL, NDUFS2, NF2, NIDI, NOLC1, NONO, NPML, NUCKS1, OAT, PA2G4, PABPC1, PAFAH1B3, PAICS, PFDN2, PFN1, PGAM1, PIH1D1, PLTP, PPA1, PPIA, PPP2R1A, PSAT1, PSMD4, PTMA, PYCARD, RAN, RASA3, RBM34, RNF2, RPAIN, RPL10, RPL10A, RPL1 1, RPL12, RPL13, RPL13A, RPL13AP5, RPL14, RPL17, RPL18, RPL18A, RPL21, RPL26, RPL28, RPL29, RPL3, RPL30, RPL31, RPL35, RPL36A, RPL37, RPL37A, RPL39, RPL4, RPL41, RPL5, RPL6, RPL7, RPL7A, RPL8, RPLPO, RPLP1, RPS10, RPS1 1, RPS12, RPS15, RPS15A, RPS16, RPS17, RPS17L, RPS18, RPS19, RPS2, RPS21, RPS23, RPS24, RPS26, RPS27, RPS27A, RPS3, RPS3A, RPS4X, RPS5,

RPS6, RPS7, RPS8, RPS9, RPSA, RSL1D1, RUVBL2, SAE1, SCD, SCNM1, SERBP1, SERPINF1, SET, SF3B4, SHMT2, SKP2, SLC19A1, SLC25A3, SLC25A5, SLC25A6, SMS, SNAI2, SNHG16, SNHG6, SNRPE, SORD, SOX4, SRP14, SSR2, TIMM13, TIMM50, TMC6, TOP1MT, TP53, TRAP1, TRPM1, TSR1, TUBAIB, TUBB, TUBB4A, TULP4, TXLNA, TYRP1, UBA52, UCK2, UQCRFS1, UQCRH, USP22, VCY1B, VDAC2, VPS72, YWHAE, ZFAS1, ZNF286A, A2M, ACSL3, ACSL4, ADM, AEBP1, AGA, AHNAK, ANGPTL4, ANXA1, ANXA2, APLP2, APOC2, APOD, APOE, ARF5, ARL6IP5, ATF3, ATP1A1, ATP1B1, ATP1B3, ATRAID, B2M, BACE2, BBX, BCL6, C10orf54, C4A, CALU, CASP1, CAST, CAV1, CBLB, CCND3, CD151, CD44, CD47, CD58, CD59, CD63, CD9, CDH19, CHI3L1, CHN1, CLIC4, CLU, CPVL, CRELD1, CRYAB, CSGALNACT1, CSPG4, CST3, CTSA, CTSB, CTSD, CTSL1, DAG1, DCBLD2, DDR1, DDX5, DPYSL2, DSCR8, DUSP4, DUSP6, DYNLRB1, ECMI, EEAI, EGRI, EMP1, EPHX2, ERBB3, EVAIA, EZHI, EZR, FAM3C, FBX032, FCGR2C, FCRLA, FGFRI, FLJ43663, FOS, FYB, GAA, GADD45B, GATSL3, GEM, GOLGB1, GPNMB, GRN, GSN, HCP5, HLA-A, HLA-B, HLA-C, HLA-E, HLA-F, HLA-H, HPCAL1, HSPA1A, HSPA1B, HTATIP2, ID2, IFI27L2, IFI35, IGF1R, ILIRAP, IL6ST, ISCU, ITGA3, ITGA6, ITGA7, ITGB1, ITGB3, ITM2B, JUN, KCNN4, KLF4, KLF6, KRT10, LAMP2, LEPROT, LGALS1, LGALS3, LGALS3BP, LOC100506190, LPL, LRPAP1, LTBP3, LYRM9, MAEL, MAGEC2, MAPIB, MATN2, MFGE8, MFI2, MIA, MRPS6, MT1E, MT1M, MT1X, MT2A, NDRG1, NEAT1, NFKBIA, NFKBIZ, NNMT, NPC1, NPC2, NR4A1, NSG1, OCIAD2, PAGE5, PDK4, PERP, PKM, PLP2, PRKCDBP, PRNP, PROS1, PRSS23, PSAP, PSMB9, PTRF, RDH5, RNF145, RPS4Y1, S100A13, S100A6, S100B, SAT1, SCARB2, SCCPDH, SDC3, SEL1L, SEMA3B, SERPINA1, SERPINA3, SERPINE2, SGCE, SGK1, SLC20A1, SLC26A2, SLC39A14, SLC5A3, SNX9, SOD1, SPON2, SPRY2, SQSTM1, SRPX, STOM, SYNGR2, SYPL1, TAPBP, TAPBPL, TF, TGOLN2, THBD, TIMP1, TIMP2, TIMP3, TIPARP, TM4SF1, TMBIM6, TMED10, TMED9, TMEM66, TMX4, TNC, TNFSF4, TPP1, TRIML2, TSC22D3, TSPYL2, TXNIP, TYR, UBC, UPP1, XAGE1A, XAGE1B, XAGE1C, XAGE1D, XAGE1E, ZBTB20 and ZBTB38; or

c) one or more genes or polypeptides selected from the group consisting of ANP32E, CTPS1, DDX39B, EIF4A1, ESRP1, FBL, FUS, HNRNPA1, ILF2, KIAA0101, NUCKS1, PTMA, RPL21, RUVBL2, SET, SLC25A5, TP53, TUBAIB, UCK2, YWHAE, APLP2, ARL6IP5, CD63, CLU, CRELD1, CTSD, CTSL1, FOS, GAA, GRN, HLA-F,

ITM2B, LAMP2, MAPIB, NPC2, PSAP, SCARB2, SDC3, SEL1L, TMED10 and TSC22D3; or

d) one or more genes or polypeptides selected from the group consisting of MTIE, MTIM, MTIX and MT2A.

2. The method according to claim 1, wherein said ICR signature comprises a ICR-down signature, said signature comprising one or more genes selected from the group consisting of:

a) AEBPI, AHNAK, APOC2, APOD, APOE, B2M, C10orf54, CD63, CTSD, EEAI, EMPI, FBX032, FYB, GATSL3, HCP5, HLA-A, HLA-B, HLA-C, HLA-E, HLA-F, HLA-H, ITGA3, LAMP2, LYRM9, MFGE8, MIA, NPC2, NSG1, PROS1, RDH5, SERPINA1, TAPBP, TIMP2, TNFSF4 and TRIML2; or

b) A2M, ACSL3, ACSL4, ADM, AEBPI, AGA, AHNAK, ANGPTL4, ANXA1, ANXA2, APLP2, APOC2, APOD, APOE, ARF5, ARL6IP5, ATF3, ATP1A1, ATP1B1, ATP1B3, ATRAID, B2M, BACE2, BBX, BCL6, C10orf54, C4A, CALU, CASP1, CAST, CAV1, CBLB, CCND3, CD151, CD44, CD47, CD58, CD59, CD63, CD9, CDH19, CHI3L1, CHNI, CLIC4, CLU, CPVL, CRELD1, CRYAB, CSGALNACT1, CSPG4, CST3, CTSA, CTSB, CTSD, CTSL1, DAG1, DCBLD2, DDR1, DDX5, DPYSL2, DSCR8, DUSP4, DUSP6, DYNLRB1, ECM1, EEAI, EGRI, EMPI, EPHX2, ERBB3, EVA1 A, EZHI, EZR, FAM3C, FBX032, FCGR2C, FCRLA, FGFR1, FLJ43663, FOS, FYB, GAA, GADD45B, GATSL3, GEM, GOLGB1, GPNMB, GRN, GSN, HCP5, HLA-A, HLA-B, HLA-C, HLA-E, HLA-F, HLA-H, HPCAL1, HSPA1A, HSPA1B, HTATIP2, ID2, IFI27L2, IFI35, IGF1R, ILIRAP, IL6ST, ISCU, ITGA3, ITGA6, ITGA7, ITGB1, ITGB3, ITM2B, JUN, KCNN4, KLF4, KLF6, KRT10, LAMP2, LEPROT, LGALS1, LGALS3, LGALS3BP, LOC100506190, LPL, LRPAP1, LTBP3, LYRM9, MAEL, MAGEC2, MAPIB, MATN2, MFGE8, MFI2, MIA, MRPS6, MTIE, MTIM, MTIX, MT2A, NDRG1, NEAT1, NFKBIA, NFKBIZ, NNMT, NPC1, NPC2, NR4A1, NSG1, OCIAD2, PAGE5, PDK4, PERP, PKM, PLP2, PRKCDBP, PRNP, PROS1, PRSS23, PSAP, PSMB9, PTRF, RDH5, RNF145, RPS4Y1, S100A13, S100A6, S100B, SAT1, SCARB2, SCCPDH, SDC3, SEL1L, SEMA3B, SERPINA1, SERPINA3, SERPINE2, SGCE, SGK1, SLC20A1, SLC26A2, SLC39A14, SLC5A3, SNX9, SOD1, SPON2, SPRY2, SQSTM1, SRPX, STOM, SYNGR2, SYPL1, TAPBP, TAPBPL, TF, TGOLN2, THBD, TIMP1, TIMP2, TIMP3, TIPARP, TM4SF1,

TMBIM6, TMEDIO, TMED9, TME66, TMX4, TNC, TNFSF4, TPP1, TRIML2, TSC22D3, TSPYL2, TXNIP, TYR, UBC, UPP1, XAGE1A, XAGE1B, XAGE1C, XAGE1D, XAGE1E, ZBTB20 and ZBTB38; or

c) APLP2, ARL6IP5, CD63, CLU, CRELD1, CTSD, CTS1, FOS, GAA, GRN, HLA-F, ITM2B, LAMP2, MAPIB, NPC2, PSAP, SCARB2, SDC3, SELIL, TMEDIO and TSC22D3,

wherein said ICR-down signature is downregulated in a tumor with a high ICR score and upregulated in a tumor with a low ICR score.

3. The method according to claim 1, wherein said ICR signature comprises a ICR-up signature, said signature comprising one or more genes selected from the group consisting of:

a) C1QBP, CCT2, CCT6A, DCAF13, EIF4A1, ILF2, MAGEA4, NONO, PA2G4, PGAM1, PPA1, PPIA, RPL18A, RPL26, RPL31, RPS1 1, RPS15, RPS21, RPS5, RUVBL2, SAE1, SNRPE, UBA52, UQCRH and VDAC2; or

b) ACAT1, ACP5, ACTB, ACTG1, ADSL, AEN, AK2, ANP32E, APP, ASAP1, ATP5A1, ATP5D, ATP5G2, BANC1, BCAN, BZW2, C17orf76-AS1, C1QBP, C20orf1 2, C6orf48, CA14, CBX5, CCT2, CCT3, CCT6A, CDK4, CEP170, CFL1, CHP1, CNRIP 1, CRABP2, CS, CTPS1, CYC1, DAP3, DCAF13, DCT, DDX21, DDX39B, DLL3, EDNRB, EEF1D, EEF1G, EEF2, EIF1AX, EIF2S3, EIF3E, EIF3K, EIF3L, EIF4A1, EIF4EBP2, ESRP1, FAM174B, FAM178B, FAM92A1, FBL, FBLN1, FOXRED2, FTL, FUS, GABARAP, GAS5, GNB2L 1, GPATCH4, GPI, GRWD1, GSTO1, H3F3A, H3F3AP4, HMGAI, HNRNP1A1, HNRNP1A1P1, HNRNP1C, HSPA8, IDH2, IFI16, ILF2, IMPDH2, ISYNA1, ITM2C, KIAA0101, LHFPL3-AS1, LOC100190986, LYPLA1, MAGEA4, MARCKS, MDH2, METAP2, MIDI, MIR4461, MLLT1 1, MPZL1, MRPL37, MRPS12, MRPS21, MYC, NACA, NCL, NDUFS2, NF2, NID1, NOLC1, NONO, NPM1, NUCKS1, OAT, PA2G4, PABPC1, PAFAH1B3, PAICS, PFDN2, PFN1, PGAM1, PIH1D1, PLTP, PPA1, PPIA, PPP2R1A, PSAT1, PSMD4, PTMA, PYCARD, RAN, RASA3, RBM34, RNF2, RPAIN, RPL10, RPL10A, RPL1 1, RPL12, RPL13, RPL13A, RPL13AP5, RPL14, RPL17, RPL18, RPL18A, RPL21, RPL26, RPL28, RPL29, RPL3, RPL30, RPL31, RPL35, RPL36A, RPL37, RPL37A, RPL39, RPL4, RPL41, RPL5, RPL6, RPL7, RPL7A, RPL8, RPLPO, RPLP1, RPS10, RPS1 1, RPS12, RPS15, RPS15A, RPS16, RPS17, RPS17L, RPS18,

RPS19, RPS2, RPS21, RPS23, RPS24, RPS26, RPS27, RPS27A, RPS3, RPS3A, RPS4X, RPS5, RPS6, RPS7, RPS8, RPS9, RPSA, RSL1D1, RUVBL2, SAEI, SCD, SCNM1, SERBP1, SERPINF1, SET, SF3B4, SHMT2, SKP2, SLC19A1, SLC25A3, SLC25A5, SLC25A6, SMS, SNAI2, SNHG16, SNHG6, SNRPE, SORD, SOX4, SRP14, SSR2, TIMM13, TIMM50, TMC6, TOP1MT, TP53, TRAP1, TRPM1, TSR1, TUBAIB, TUBB, TUBB4A, TULP4, TXLNA, TYRP1, UBA52, UCK2, UQCRFS1, UQCRH, USP22, VCY1B, VDACC2, VPS72, YWHAE, ZFAS1 and ZNF286A; or

c) ANP32E, CTPS1, DDX39B, EIF4A1, ESRP1, FBL, FUS, HNRNPA1, ILF2, KIAA0101, NUCKS1, PTMA, RPL21, RUVBL2, SET, SLC25A5, TP53, TUBAIB, UCK2 and YWHAE,

wherein said ICR-up signature is upregulated in a tumor with a high ICR score and downregulated in a tumor with a low ICR score.

4. A method of detecting an immune checkpoint inhibitor resistance (ICR) gene signature in a tumor comprising, detecting in tumor cells obtained from a subject in need thereof the expression or activity of a malignant cell gene signature comprising:

a) one or more genes or polypeptides selected from the group consisting of ACTB, AEN, ANP32E, ATP5A1, ATP5G2, BZW2, C17orf76-AS1, C1QBP, C20orf112, CA14, CBX5, CCT2, CCT3, CDK4, CFL1, CNRIP1, CRABP2, CS, CTPS1, DCAF13, DCT, DDX39B, DLL3, EEF1G, EIF2S3, EIF3K, EIF4A1, EIF4EBP2, FAM174B, FBL, FBLN1, FOXRED2, FTL, FUS, GABARAP, GAS5, GNB2L1, GPATCH4, GPI, GRWD1, H3F3A, H3F3AP4, HMGA1, HNRNPA1, HNRNPA1P10, HNRNPC, HSPA8, IDH2, ILF2, ISYNA1, ITM2C, KIAA0101, MAGEA4, MDH2, METAP2, MIDI, MIR4461, MLLT11, MPZL1, MRPS21, NACA, NCL, NDUFS2, NOLC1, NONO, PA2G4, PABPC1, PAFAH1B3, PFDN2, PFN1, PGAM1, PIH1D1, PPA1, PPIA, PPP2R1A, PSMD4, PTMA, RAN, RBM34, RNF2, RPAIN, RPL10A, RPL11, RPL12, RPL13, RPL13A, RPL13AP5, RPL17, RPL18, RPL18A, RPL21, RPL26, RPL28, RPL29, RPL3, RPL31, RPL36A, RPL37, RPL37A, RPL39, RPL4, RPL41, RPL5, RPL6, RPL8, RPLPO, RPLP1, RPS10, RPS11, RPS12, RPS15A, RPS16, RPS17, RPS17L, RPS18, RPS19, RPS21, RPS23, RPS24, RPS26, RPS27, RPS27A, RPS3, RPS4X, RPS5, RPS6, RPS7, RPS8, RPS9, RPSA, RUVBL2, SAEI, SCD, SCNM1, SERPINF1, SET, SF3B4, SHMT2, SKP2, SLC25A3, SMS, SNAI2, SNHG6, SNRPE, SOX4, SRP14, SSR2, TIMM50, TMC6, TP53, TRPM1, TSR1, TUBAIB, TUBB,

TULP4, UBA52, UQCRFS1, UQCRH, USP22, VCY1B, VDAC2, VPS72, YWHAE, ZNF286A, A2M, ACSL3, ACSL4, ADM, AEBP1, AGA, AHNAK, ANGPTL4, ANXA1, ANXA2, APLP2, APOD, APOE, ARL6IP5, ATF3, ATP1A1, ATP1B1, ATP1B3, B2M, BACE2, BBX, BCL6, CALU, CASPI, CAST, CAVI, CCND3, CD151, CD44, CD47, CD58, CD59, CD63, CD9, CDH19, CHI3L1, CLIC4, CRELD1, CRYAB, CSGALNACT1, CSPG4, CST3, CTSA, CTSB, CTSD, CTSL1, DAG1, DCBLD2, DDR1, DDX5, DPYSL2, DUSP4, DUSP6, ECM1, EEA1, EGR1, EMP1, EPHX2, ERBB3, EVA1A, EZH1, FAM3C, FBX032, FCGR2C, FCRLA, FGFR1, FLJ43663, FOS, GAA, GADD45B, GEM, GOLGB1, GPNMB, GRN, GSN, HLA-A, HLA-B, HLA-C, HLA-E, HLA-F, HLA-H, HPCAL1, HSPA1A, HTATIP2, IFI35, IGFIR, ILIRAP, IL6ST, ITGA3, ITGA6, ITGB1, ITGB3, ITM2B, JUN, KCNN4, KLF4, KLF6, LAMP2, LEPROT, LGALS1, LGALS3, LGALS3BP, LPL, LRPAP1, MAGEC2, MFGE8, MFI2, MIA, MTIE, MTIM, MTIX, MT2A, NEAT1, NFKBIA, NFKBIZ, NNMT, NPC1, NPC2, NR4A1, NSG1, PDK4, PLP2, PRKCDBP, PRNP, PROS1, PRSS23, PSAP, PSMB9, PTRF, RNF145, RPS4Y1, S100A6, S100B, SAT1, SCARB2, SCCPDH, SDC3, SEL1L, SEMA3B, SERPINA3, SERPINE2, SGCE, SGK1, SLC20A1, SLC26A2, SLC39A14, SLC5A3, SOD1, SPRY2, SQSTM1, SRPX, STOM, SYNGR2, SYPL1, TAPBP, TAPBPL, TF, TGOLN2, TIMP1, TIMP2, TIMP3, TIPARP, TM4SF1, TMED10, TMED9, TMEM66, TMX4, TNC, TPP1, TSC22D3, TYR, UBC, UPP1, ZBTB20 and ZBTB38; or

b) one or more genes or polypeptides selected from the group consisting of AEN, ATP5A1, C20orf112, CCT2, DCAF13, DDX39B, ISYNA1, NDUFS2, NOLC1, PA2G4, PPP2R1A, RBM34, RNF2, RPL6, RPL21, SERPINF1, SF3B4, SMS, TMC6, VPS72, ANXA1, ATF3, BCL6, CD58, CD9, CTSB, DCBLD2, EMP1, HLA-F, HTATIP2, ILIRAP, ITGA6, KCNN4, KLF4, MTIE, MTIM, MTIX, MT2A, NNMT, PRKCDBP, S100A6 and TSC22D3; or

c) one or more genes or polypeptides selected from the group consisting of ACTB, ANP32E, CBX5, FUS, HNRNP1A1, IDH2, KIAA0101, NCL, PFN1, PPIA, PTMA, RAN, RPLP0, TUBA1B, TUBB, VCY1B, A2M, APOD, BCL6, CD44, CD59, CD63, CDH19, CHI3L1, CTSA, CTSB, CTSD, FOS, GPNMB, GRN, HLA-A, HLA-B, HLA-H, ITM2B, LGALS3BP, NEAT1, PDK4, PSAP, SCARB2, SERPINA3, SLC26A2, TAPBPL, TMEM66 and TYR; or

d) one or more genes or polypeptides selected from the group consisting of MT1E, MT1M, MT1X and MT2A.

5. The method according to claim 4, wherein said ICR signature comprises an ICR-down signature, said signature comprising one or more genes selected from the group consisting of:

a) A2M, ACSL3, ACSL4, ADM, AEBP1, AGA, AHNAK, ANGPTL4, ANXA1, ANXA2, APLP2, APOD, APOE, ARL6IP5, ATF3, ATP1A1, ATP1B1, ATP1B3, B2M, BACE2, BBX, BCL6, CALU, CASP1, CAST, CAV1, CCND3, CD151, CD44, CD47, CD58, CD59, CD63, CD9, CDH19, CHI3L1, CLIC4, CRELD1, CRYAB, CSGALNACT1, CSPG4, CST3, CTSA, CTSB, CTSD, CTSL1, DAG1, DCBLD2, DDR1, DDX5, DPYSL2, DUSP4, DUSP6, ECM1, EEA1, EGR1, EMP1, EPHX2, ERBB3, EVA1A, EZH1, FAM3C, FBX032, FCGR2C, FCRLA, FGFR1, FLJ43663, FOS, GAA, GADD45B, GEM, GOLGB1, GPNMB, GRN, GSN, HLA-A, HLA-B, HLA-C, HLA-E, HLA-F, HLA-H, HPCAL1, HSPA1A, HTATIP2, IFI35, IGFIR, ILIRAP, IL6ST, ITGA3, ITGA6, ITGB1, ITGB3, ITM2B, JUN, KCNN4, KLF4, KLF6, LAMP2, LEPROT, LGALS1, LGALS3, LGALS3BP, LPL, LRPAP1, MAGEC2, MFGE8, MFI2, MIA, MT1E, MT1M, MT1X, MT2A, NEAT1, NFKBIA, NFKBIZ, NNMT, NPC1, NPC2, NR4A1, NSG1, PDK4, PLP2, PRKCDBP, PRNP, PROS1, PRSS23, PSAP, PSMB9, PTRF, RNF145, RPS4Y1, S100A6, S100B, SAT1, SCARB2, SCCPDH, SDC3, SEL1L, SEMA3B, SERPINA3, SERPINE2, SGCE, SGK1, SLC20A1, SLC26A2, SLC39A14, SLC5A3, SOD1, SPRY2, SQSTM1, SRPX, STOM, SYNGR2, SYPL1, TAPBP, TAPBPL, TF, TGOLN2, TIMP1, TIMP2, TIMP3, TIPARP, TM4SF1, TMED10, TMED9, TMEM66, TMX4, TNC, TPP1, TSC22D3, TYR, UBC, UPP1, ZBTB20 and ZBTB38; or

b) ANXA1, ATF3, BCL6, CD58, CD9, CTSB, DCBLD2, EMP1, HLA-F, HTATIP2, ILIRAP, ITGA6, KCNN4, KLF4, MT1E, MT1M, MT1X, MT2A, NNMT, PRKCDBP, S100A6 and TSC22D3; or

c) A2M, APOD, BCL6, CD44, CD59, CD63, CDH19, CHI3L1, CTSA, CTSB, CTSD, FOS, GPNMB, GRN, HLA-A, HLA-B, HLA-H, ITM2B, LGALS3BP, NEAT1, PDK4, PSAP, SCARB2, SERPINA3, SLC26A2, TAPBPL, TMEM66 and TYR,

wherein said ICR-down signature is downregulated in a tumor with a high ICR score and upregulated in a tumor with a low ICR score.

6. The method according to claim 4, wherein said ICR signature comprises an ICR-up signature, said signature comprising one or more genes selected from the group consisting of:

a) ACTB, AEN, ANP32E, ATP5A1, ATP5G2, BZW2, C17orf76-AS1, C1QBP, C20orf12, CA14, CBX5, CCT2, CCT3, CDK4, CFL1, CNRIP1, CRABP2, CS, CTPS1, DCAF13, DCT, DDX39B, DLL3, EEF1G, EIF2S3, EIF3K, EIF4A1, EIF4EBP2, FAM174B, FBL, FBLN1, FOXRED2, FTL, FUS, GABARAP, GAS5, GNB2L1, GPATCH4, GPI, GRWD1, H3F3A, H3F3AP4, HMGA1, HNRNPA1, HNRNPA1P10, HNRNPC, HSPA8, IDH2, ILF2, ISYNA1, ITM2C, KIAA0101, MAGEA4, MDH2, METAP2, MIDI, MIR4461, MLLT1, MPZL1, MRPS21, NACA, NCL, NDUFS2, NOLC1, NONO, PA2G4, PABPC1, PAFAH1B3, PFDN2, PFN1, PGAM1, PIH1D1, PPA1, PPIA, PPP2R1A, PSMD4, PTMA, RAN, RBM34, RNF2, RPAIN, RPL10A, RPL11, RPL12, RPL13, RPL13A, RPL13AP5, RPL17, RPL18, RPL18A, RPL21, RPL26, RPL28, RPL29, RPL3, RPL31, RPL36A, RPL37, RPL37A, RPL39, RPL4, RPL41, RPL5, RPL6, RPL8, RPLPO, RPLP1, RPS10, RPS11, RPS12, RPS15A, RPS16, RPS17, RPS17L, RPS18, RPS19, RPS21, RPS23, RPS24, RPS26, RPS27, RPS27A, RPS3, RPS4X, RPS5, RPS6, RPS7, RPS8, RPS9, RPSA, RUVBL2, SAE1, SCD, SCNM1, SERPINF1, SET, SF3B4, SHMT2, SKP2, SLC25A3, SMS, SNAI2, SNHG6, SNRPE, SOX4, SRP14, SSR2, TIMM50, TMC6, TP53, TRPM1, TSR1, TUBA1B, TUBB, TULP4, UBA52, UQCRFS1, UQCRH, USP22, VCYIB, VDAC2, VPS72, YWHAE and ZNF286A; or

b) AEN, ATP5A1, C20orf12, CCT2, DCAF13, DDX39B, ISYNA1, NDUFS2, NOLC1, PA2G4, PPP2R1A, RBM34, RNF2, RPL6, RPL21, SERPINF1, SF3B4, SMS, TMC6, VPS72; or

c) ACTB, ANP32E, CBX5, FUS, HNRNPA1, IDH2, KIAA0101, NCL, PFN1, PPIA, PTMA, RAN, RPLPO, TUBA1B, TUBB and VCYIB,

wherein said ICR-up signature is upregulated in a tumor with a high ICR score and downregulated in a tumor with a low ICR score.

7. The method according to any of claims 1 to 6, wherein the ICR signature is detected in cycling cells and/or expanded cells.

8. A method of detecting an immune cell exclusion gene signature in a tumor comprising, detecting in tumor cells obtained from a subject in need thereof the expression or

activity of a malignant cell gene signature comprising:

a) one or more genes or polypeptides selected from the group consisting of ACAT1, ACP5, ACTG1, ADSL, AK2, APP, ASAP1, ATP5D, BANCR, BCAN, BZW2, C17orf76-AS1, C1QBP, C6orf48, CA14, CCT3, CCT6A, CEP170, CHP1, CTPS1, CYC1, DAP3, DCT, DDX21, EDNRB, EEF1D, EEF1G, EEF2, EIF1AX, EIF2S3, EIF3E, EIF3K, EIF3L, EIF4A1, ESRP1, FAM178B, FAM92A1, FTL, GAS5, GNB2L1, GPI, GSTO1, IFI16, ILF2, IMPDH2, LHFPL3-AS1, LOC100190986, LYPLA1, MARCKS, MDH2, MRPL37, MRPS12, MYC, NCL, NF2, NIDI, NOLCI, NPM1, NUCKS1, OAT, PABPC1, PAICS, PLTP, PSAT1, PYCARD, RASA3, RPL10, RPLIOA, RPL11, RPL12, RPL13, RPL13A, RPL13AP5, RPL14, RPL17, RPL18, RPL18A, RPL28, RPL29, RPL3, RPL30, RPL35, RPL37A, RPL39, RPL4, RPL5, RPL6, RPL7, RPL7A, RPL8, RPLPO, RPLP1, RPS10, RPS11, RPS15, RPS15A, RPS16, RPS17, RPS17L, RPS18, RPS19, RPS2, RPS24, RPS27, RPS3, RPS3A, RPS4X, RPS5, RPS7, RPS8, RPS9, RPSA, RSLIDI, SCD, SERBP1, SERPINF1, SLC19A1, SLC25A5, SLC25A6, SNAI2, SNHG16, SNHG6, SORD, SOX4, TIMM13, TIMM50, TOP1MT, TRAP1, TUBB4A, TXLNA, TYRP1, UCK2, UQCRFS1, ZFAS1, A2M, AGA, AHNAK, ANXA1, APLP2, APOC2, ARF5, ATP1A1, ATP1B1, ATRAID, B2M, C10orf54, C4A, CBLB, CCND3, CD151, CD47, CD58, CD59, CDH19, CHN1, CLU, CPVL, CST3, CTSB, CTSD, CTSL1, DDR1, DPYSL2, DSCR8, DUSP6, DYNLRB1, EMP1, EZR, FAM3C, FGFR1, FYB, GAA, GATSL3, GRN, GSN, HCP5, HLA-B, HLA-C, HLA-F, HLA-H, HSPA1A, HSPA1B, ID2, IFI27L2, ISCU, ITGA3, ITGA7, ITGB3, KCNN4, KRT10, LOC100506190, LTBP3, LYRM9, MAEL, MAP1B, MATN2, MFGE8, MFI2, MIA, MRPS6, MT2A, NDRG1, NFKB1A, NPC1, OCIAD2, PAGE5, PERP, PKM, RDH5, S100A13, S100A6, SERPINA1, SERPINA3, SERPINE2, SGCE, SLC26A2, SLC5A3, SNX9, SPON2, THBD, TIMP1, TM4SF1, TMBIM6, TNFSF4, TPP1, TRIML2, TSC22D3, TSPYL2, TXNIP, UBC, XAGE1A, XAGE1B, XAGE1C, XAGE1D and XAGE1E; or

b) one or more genes or polypeptides selected from the group consisting of ACTG1, ADSL, C17orf76-AS1, C1QBP, CTPS1, EIF2S3, EIF3E, ILF2, NCL, NF2, NOLCI, PABPC1, PAICS, RPLIOA, RPL18, RPL6, RPS24, RSLIDI, SERPINF1, SOX4, AHNAK, ANXA1, CCND3, CD151, CD47, CD58, CST3, CTSB, CTSD, EMP1, FGFR1, HLA-C, HLA-F, ITGB3, KCNN4, MIA, MT2A, S100A6, SLC5A3, TIMP1 and TSC22D3;

or

c) one or more genes or polypeptides selected from the group consisting of C17orf76-AS1, CIQBP, CTPS1, EIF2S3, ILF2, NCL, NOLC1, PABPC1, RPL10A, RPL18, RPL6, RPS24, SERPINF1, SOX4, AHNAK, ANXA1, CCND3, CD151, CD47, CD58, CST3, CTSB, CTSD, EMP1, FGFR1, HLA-C, HLA-F, ITGB3, KCNN4, MIA, MT2A, S100A6, SLC5A3, TIMP1 and TSC22D3.

9. The method according to claim 8, wherein said exclusion signature comprises an exclusion-down signature, said signature comprising one or more genes selected from the group consisting of:

a) A2M, AGA, AHNAK, ANXA1, APLP2, APOC2, ARF5, ATP1A1, ATP1B1, ATRAID, B2M, C10orf54, C4A, CBLB, CCND3, CD151, CD47, CD58, CD59, CDH19, CHN1, CLU, CPVL, CST3, CTSB, CTSD, CTSL1, DDR1, DPYSL2, DSCR8, DUSP6, DYNLRB1, EMP1, EZR, FAM3C, FGFR1, FYB, GAA, GATSL3, GRN, GSN, HCP5, HLA-B, HLA-C, HLA-F, HLA-H, HSPAIA, HSPAIB, ID2, IFI27L2, ISCU, ITGA3, ITGA7, ITGB3, KCNN4, KRT10, LOC100506190, LTBP3, LYRM9, MAEL, MAPIB, MATN2, MFGE8, MFI2, MIA, MRPS6, MT2A, NDRG1, NFKBIA, NPC1, OCIAD2, PAGE5, PERP, PKM, RDH5, S100A13, S100A6, SERPINA1, SERPINA3, SERPINE2, SGCE, SLC26A2, SLC5A3, SNX9, SPON2, THBD, TIMP1, TM4SF1, TMBIM6, TNFSF4, TPP1, TRIML2, TSC22D3, TSPYL2, TXNIP, UBC, XAGE1A, XAGE1B, XAGE1C, XAGEID and XAGE1E); or

b) AHNAK, ANXA1, CCND3, CD151, CD47, CD58, CST3, CTSB, CTSD, EMP1, FGFR1, HLA-C, HLA-F, ITGB3, KCNN4, MIA, MT2A, S100A6, SLC5A3, TIMP1 and TSC22D3,

wherein said exclusion-down signature is downregulated in a tumor with T cell exclusion and is upregulated in a tumor with T cell infiltration.

10. The method according to claim 8, wherein said exclusion signature comprises an exclusion-up signature, said signature comprising one or more genes selected from the group consisting of:

a) ACAT1, ACP5, ACTG1, ADSL, AK2, APP, ASAP1, ATP5D, BANCN, BCAN, BZW2, C17orf76-AS1, CIQBP, C6orf48, CA14, CCT3, CCT6A, CEP170, CHP1,

CTPS1, CYC1, DAP3, DCT, DDX21, EDNRB, EEF1D, EEF1G, EEF2, EIF1AX, EIF2S3, EIF3E, EIF3K, EIF3L, EIF4A1, ESRP1, FAM178B, FAM92A1, FTL, GAS5, GNB2L1, GPI, GSTO1, IFI16, ILF2, IMPDH2, LHFPL3-AS1, LOC100190986, LYPLA1, MARCKS, MDH2, MRPL37, MRPS12, MYC, NCL, NF2, NIDI, NOLC1, NPM1, NUCKS1, OAT, PABPC1, PAICS, PLTP, PSAT1, PYCARD, RASA3, RPL10, RPL10A, RPL11, RPL12, RPL13, RPL13A, RPL13AP5, RPL14, RPL17, RPL18, RPL18A, RPL28, RPL29, RPL3, RPL30, RPL35, RPL37A, RPL39, RPL4, RPL5, RPL6, RPL7, RPL7A, RPL8, RPLPO, RPLP1, RPS10, RPS11, RPS15, RPS15A, RPS16, RPS17, RPS17L, RPS18, RPS19, RPS2, RPS24, RPS27, RPS3, RPS3A, RPS4X, RPS5, RPS7, RPS8, RPS9, RPSA, RSLIDI, SCD, SERBP1, SERPINF1, SLC19A1, SLC25A5, SLC25A6, SNAI2, SNHG16, SNHG6, SORD, SOX4, TIMM13, TIMM50, TOP1MT, TRAP1, TUBB4A, TXLNA, TYRP1, UCK2, UQCERS1 and ZFAS1; or

b) ACTG1, ADSL, C17orf76-AS1, C1QBP, CTPS1, EIF2S3, EIF3E, ILF2, NCL, NF2, NOLC1, PABPC1, PAICS, RPL10A, RPL18, RPL6, RPS24, RSLIDI, SERPINF1 and SOX4; or

c) C17orf76-AS1, C1QBP, CTPS1, EIF2S3, ILF2, NCL, NOLC1, PABPC1, RPL10A, RPL18, RPL6, RPS24, SERPINF1 and SOX4,

wherein said exclusion-up signature is upregulated in a tumor with T cell exclusion and is downregulated in a tumor with T cell infiltration.

11. The method according to any of claims 1 to 10, further comprising detecting tumor infiltrating lymphocytes (TIL).

12. The method according to any of claims 1 to 11, wherein the gene signature is detected in a bulk tumor sample, whereby the gene signature is detected by deconvolution of bulk expression data such that gene expression is assigned to malignant cells and non-malignant cells in said tumor sample.

13. The method according to any of claims 1 to 12, wherein detecting the gene signature comprises detecting downregulation of the down signature and/or upregulation of the up signature, and wherein not detecting the gene signature comprises detecting upregulation of the down signature and/or downregulation of the up signature.

14. The method according to any of claims 1 to 13, wherein detecting the

signature and/or TILs indicates lower progression free survival and/or resistance to checkpoint blockade therapy, and wherein not detecting the signature and/or TILs indicates higher progression free survival and/or sensitivity to checkpoint blockade therapy.

15. The method according to any of claims 1 to 14, wherein detecting the gene signature indicates a 10-year survival rate less than 40% and wherein not detecting the signature indicates a 10-year survival rate greater than 60%.

16. The method according to any of claims 1 to 15, wherein detecting an ICR signature in a tumor further comprises detecting in tumor infiltrating lymphocytes (TIL) obtained from the subject in need thereof the expression or activity of a CD8 T cell gene signature, said signature comprising one or more genes or polypeptides selected from the group consisting of CEP19, EXO5, FAM153C, FCRL6, GBP2, GBP5, HSPA1B, IER2, IRF1, KLRK1, LDHA, LOC100506083, MBOAT1, SEMA4D, SIRT3, SPDYE2, SPDYE2L, STAT1, STOM, UBE2Q2P3, ACP5, AKNA, BTN3A2, CCDC141, CD27, CDC42SE1, DDIT4, FAU, FKBP5, GPR56, HAVCR2, HLA-B, HLA-C, HLA-F, IL6ST, ITGA4, KIAA1551, KLF12, MIR155HG, MTA2, MTRNR2L1, MTRNR2L3, PIK3IP1, RPL26, RPL27, RPL27A, RPL35A, RPS1 1, RPS16, RPS20, RPS26, SPOCK2, SYTL3, TOB1, TPT1, TTN, TXNIP, WNK 1 and ZFP36L2.

17. The method according to any of claims 1 to 16, wherein detecting an ICR signature in a tumor further comprises detecting in macrophages obtained from the subject in need thereof the expression or activity of a macrophage gene signature, said signature comprising one or more genes or polypeptides selected from the group consisting of APOL1, CD274, CSTB, DCN, HLA-DPB2, HLA-DQA1, HLA-G, HSPA8, HSPB1, IL18BP, TMEM176A, UBD, A2M, ADAP2, ADORA3, ARL4C, ASPH, BCAT1, C11orf11, C3, C3AR1, C6orf62, CAPN2, CD200R1, CD28, CD9, CD99, COMT, CREM, CRTAP, CYFIP1, DDOST, DHRS3, EGFL7, EIF1AY, ETS2, FCGR2A, FOLR2, GATM, GBP3, GNG2, GSTT1, GYPC, HIST1H1E, HPGDS, IFI44L, IGFBP4, ITGA4, KCTD12, LGMN, LOC441081, LTC4S, LYVE1, MERTK, METTL7B, MS4A4A, MS4A7, MTSS1, NLRP3, OLFML3, PLA2G15, PLXDC2, PMP22, POR, PRDX2, PTGS1, RNASE1, ROCK1, RPS4Y1, S100A9, SCAMP2, SEPPI, SESN1, SLC18B1, SLC39A1, SLC40A1, SLC7A8, SORL1, SPP1, STAB1, TMEM106C, TMEM86A, TMEM9, TNFRSF1B, TNFRSF21, TPD52L2, ULK3 and ZFP36L2.

18. A method of stratifying cancer patients into a high survival group and a low survival group comprising detecting the expression or activity of an ICR and/or exclusion signature in a tumor according to any of claims 1 to 17, wherein if the signature is detected the patient is in the low survival group and if the signature is not detected the patient is in the high survival group.

19. The method according to claim 18, wherein patients in the high survival group are immunotherapy responders and patients in the low survival group are immunotherapy non-responders.

20. A method of treating a cancer in a subject in need thereof comprising detecting the expression or activity of an ICR and/or exclusion signature according to any of claims 1 to 17 in a tumor obtained from the subject and administering a treatment,

wherein if an ICR and/or exclusion signature is detected the treatment comprises administering an agent capable of reducing expression or activity of said signature, and

wherein if an ICR and/or exclusion signature is not detected the treatment comprises administering an immunotherapy.

21. The method according to claim 20, wherein the agent capable of reducing expression or activity of said signature comprises a CDK4/6 inhibitor, a drug selected from Table 3, a cell cycle inhibitor, a PKC activator, an inhibitor of the NF κ B pathway, an IGF1R inhibitor, or Reserpine.

22. The method according to claim 20, wherein the agent capable of reducing expression or activity of said signature comprises an agent capable of modulating expression or activity of a gene selected from the group consisting of MAZ, NF κ B1, MYC, ANXA1, SOX4, MT2A, PTP4A3, CD59, DLL3, SERPINE2, SERPINF1, PERP, EGR1, SERPINA3, SEMA3B, SMARCA4, IFNGR2, B2M, and PDL1.

23. The method according to claim 20, wherein the agent capable of reducing expression or activity of said signature comprises an agent capable of targeting or binding to one or more up-regulated secreted or cell surface exposed ICR and/or exclusion signature genes or polypeptides.

24. The method according to any of claims 20 to 23, wherein the method further comprises detecting the expression or activity of an ICR and/or exclusion signature according to any of claims 1 to 17 in a tumor obtained from the subject after the treatment and administering an immunotherapy if said signature is reduced or below a reference level.

25. The method according to claim 24, wherein the agent capable of reducing expression or activity of said signature is a CDK4/6 inhibitor.

26. The method according to any of claims 20 to 23, wherein the method further comprises detecting the expression or activity of an ICR and/or exclusion signature according to any of claims 1 to 17 in a tumor obtained from the subject before the treatment and administering an immunotherapy if said signature is not detected or below a reference level.

27. The method according to any of claims claim 20 to 23, wherein the method further comprises administering an immunotherapy to the subject administered an agent capable of reducing the expression or activity of said signature.

28. The method according to any of claims 20 to 27, wherein the immunotherapy comprises a check point inhibitor or adoptive cell transfer (ACT).

29. The method according to claim 28, wherein adoptive cell transfer comprises a CAR T cell or activated autologous T cells.

30. The method according to claim 28, wherein the checkpoint inhibitor comprises anti-CTLA4, anti-PD-L1 and/or anti-PD1 therapy.

31. A method of treating a cancer in a subject in need thereof comprising detecting the expression or activity of an ICR and/or exclusion signature according to any of claims 1 to 17 in a tumor obtained from the subject, wherein if an ICR and/or exclusion signature is detected the treatment comprises administering an agent capable of modulating expression or activity of one or more genes or polypeptides in a network of genes disrupted by perturbation of a gene selected from the group consisting of MAZ, NFKBIZ, MYC, ANXA1, SOX4, MT2A, PTP4A3, CD59, DLL3, SERPINE2, SERPINF1, PERP, EGR1, SERPINA3, SEMA3B, SMARCA4, IFNGR2, B2M, and PDL1.

32. A method of treating a cancer in a subject in need thereof comprising

administering to the subject a therapeutically effective amount of an agent:

- a) capable of modulating the expression or activity of one or more ICR and/or exclusion signature genes or polypeptides according to any of claims 1 to 17; or
- b) capable of targeting or binding to one or more cell surface exposed ICR and/or exclusion signature genes or polypeptides, wherein the gene or polypeptide is up-regulated in the ICR and/or exclusion signature; or
- c) capable of targeting or binding to one or more receptors or ligands specific for a cell surface exposed ICR and/or exclusion signature gene or polypeptide, wherein the gene or polypeptide is up-regulated in the ICR and/or exclusion signature; or
- d) comprising a secreted ICR and/or exclusion signature gene or polypeptide, wherein the gene or polypeptide is down-regulated in the ICR and/or exclusion signature; or
- e) capable of targeting or binding to one or more secreted ICR and/or exclusion signature genes or polypeptides, wherein the genes or polypeptides are up-regulated in the ICR and/or exclusion signature; or
- f) capable of targeting or binding to one or more receptors specific for a secreted ICR and/or exclusion signature gene or polypeptide, wherein the secreted gene or polypeptide is up-regulated in the ICR and/or exclusion signature; or
- g) comprising a CDK4/6 inhibitor, a drug selected from Table 3, a cell cycle inhibitor, a PKC activator, an inhibitor of the **NFKB** pathway, an IGFIR inhibitor, or Reserpine.

33. The method according to claim 32, wherein said agent comprises a therapeutic antibody, antibody fragment, antibody-like protein scaffold, aptamer, protein, CRISPR system or small molecule.

34. The method according to claim 32, wherein said agent capable of targeting or binding to one or more cell surface exposed ICR and/or exclusion signature polypeptides or one or more receptors specific for a secreted ICR and/or exclusion signature gene or

polypeptide comprises a CAR T cell capable of targeting or binding to one or more cell surface exposed ICR and/or exclusion signature genes or polypeptides or one or more receptors specific for a secreted ICR and/or exclusion signature gene or polypeptide.

35. The method according to claim 32, wherein said agent capable of modulating the expression or activity of one or more ICR and/or exclusion signature genes or polypeptides comprises a CDK4/6 inhibitor.

36. The method according to claim 35, wherein the CDK4/6 inhibitor comprises abemaciclib.

37. The method according to claim 35 or 36, wherein the method further comprises administering an immunotherapy to the subject.

38. The method according to claim 37, wherein the immunotherapy comprises a check point inhibitor.

39. The method according to claim 38, wherein the checkpoint inhibitor comprises anti-CTLA4, anti-PD-L1 and/or anti-PD1 therapy.

40. A method of monitoring a cancer in a subject in need thereof comprising detecting the expression or activity of an ICR and/or exclusion gene signature according to any of claims 1 to 17 in tumor samples obtained from the subject for at least two time points.

41. The method according to claim 40, wherein at least one sample is obtained before treatment.

42. The method according to claim 40 or 41, wherein at least one sample is obtained after treatment.

43. The method of any one of claims 1 to 42, wherein the cancer is melanoma or breast cancer.

44. The method of any one of claims 1 to 17, wherein the ICR and/or exclusion signature is expressed in response to administration of an immunotherapy.

45. A method of detecting an ICR signature in a tumor comprising, detecting in

tumor cells obtained from a subject in need thereof who has been treated with an immunotherapy the expression or activity of a malignant cell gene signature comprising:

- a) one or more down regulated genes selected from the group consisting of genes associated with coagulation, apoptosis, TNF- α signaling via NF κ b, Antigen processing and presentation, metallothionein and IFNGR2; and/or
- b) one or more up regulated genes selected from the group consisting of genes associated with negative regulation of angiogenesis and MYC targets.

46. A kit comprising reagents to detect at least one ICR and/or exclusion signature gene or polypeptide according to any of claims 1 to 17.

47. The kit according to claim 46, wherein the kit comprises at least one antibody, antibody fragment, or aptamer.

48. The kit according to claim 46, wherein the kit comprises primers and/or probes for quantitative RT-PCR or fluorescently bar-coded oligonucleotide probes for hybridization to RNA.

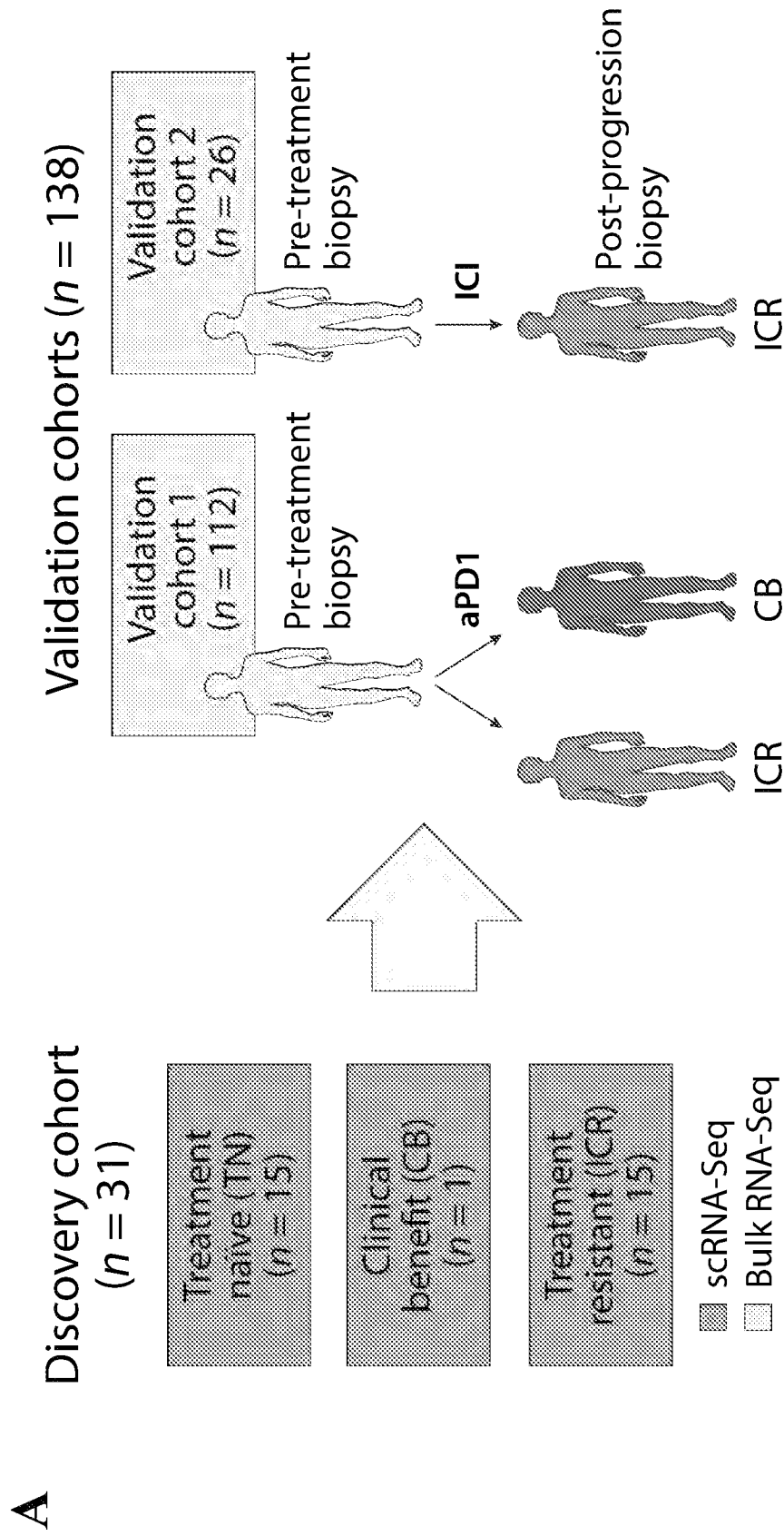
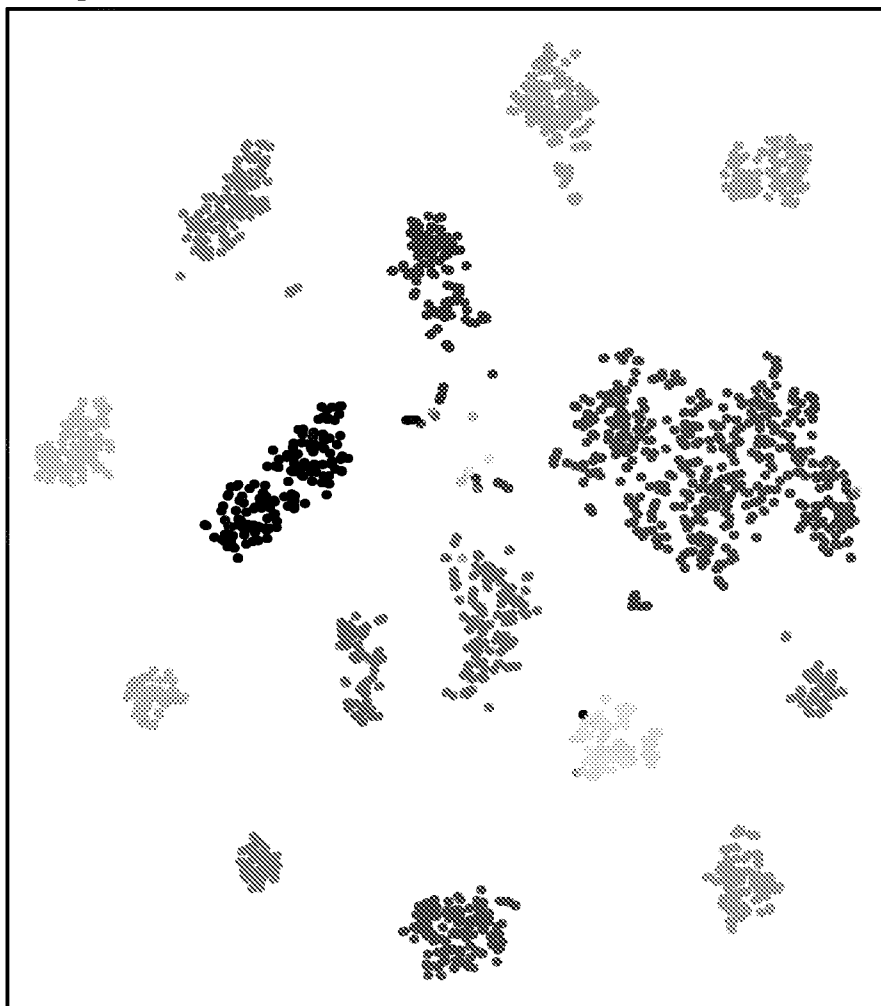


FIG. 1A

B

Malignant cells



- Tumor
- Mel78
 - Mel79
 - Mel88
 - Mel71
 - Mel81
 - Mel80
 - Mel89
 - Mel194
 - Mel102
 - Mel110
 - Mel103
 - Mel106
 - Mel98
 - Mel129pa

FIG. 1B

C

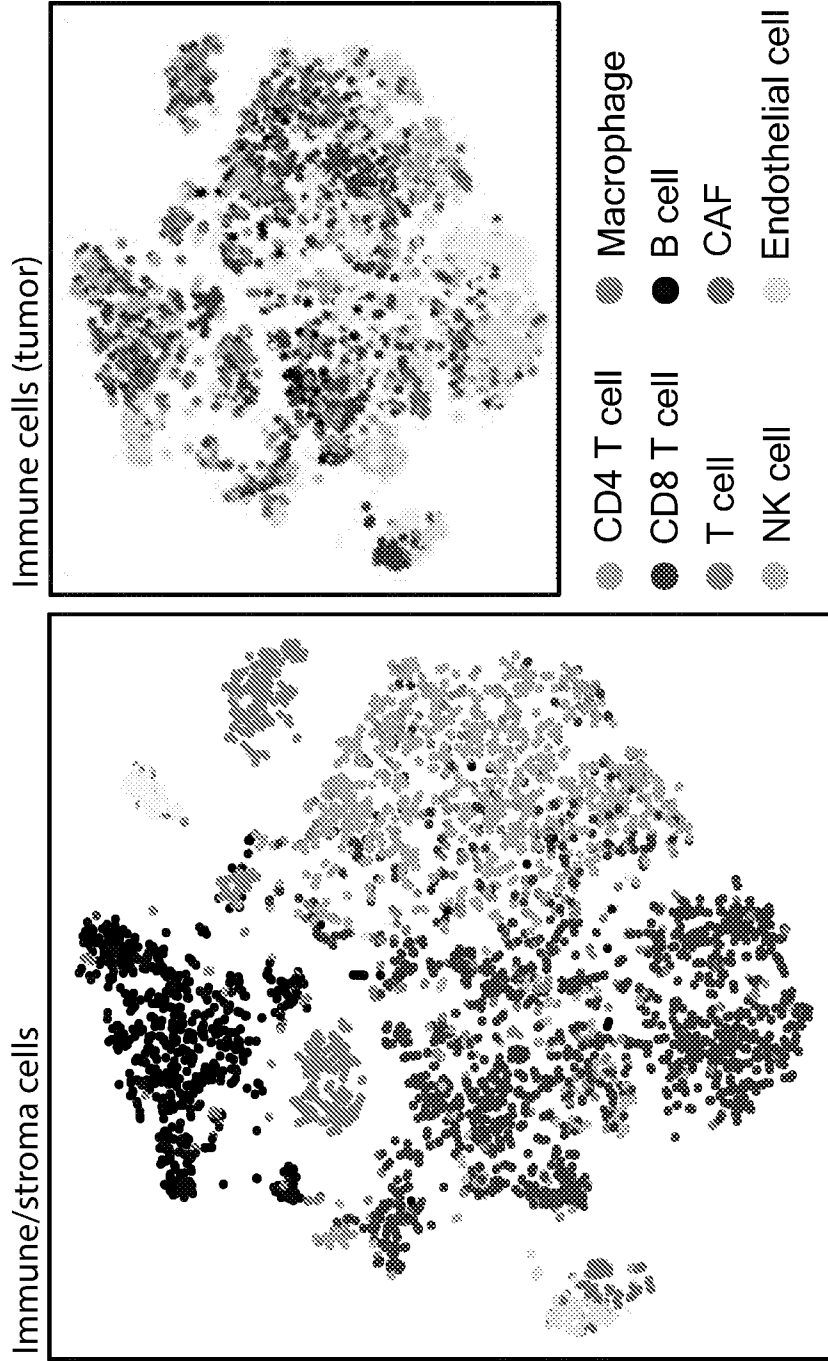


FIG. 1C

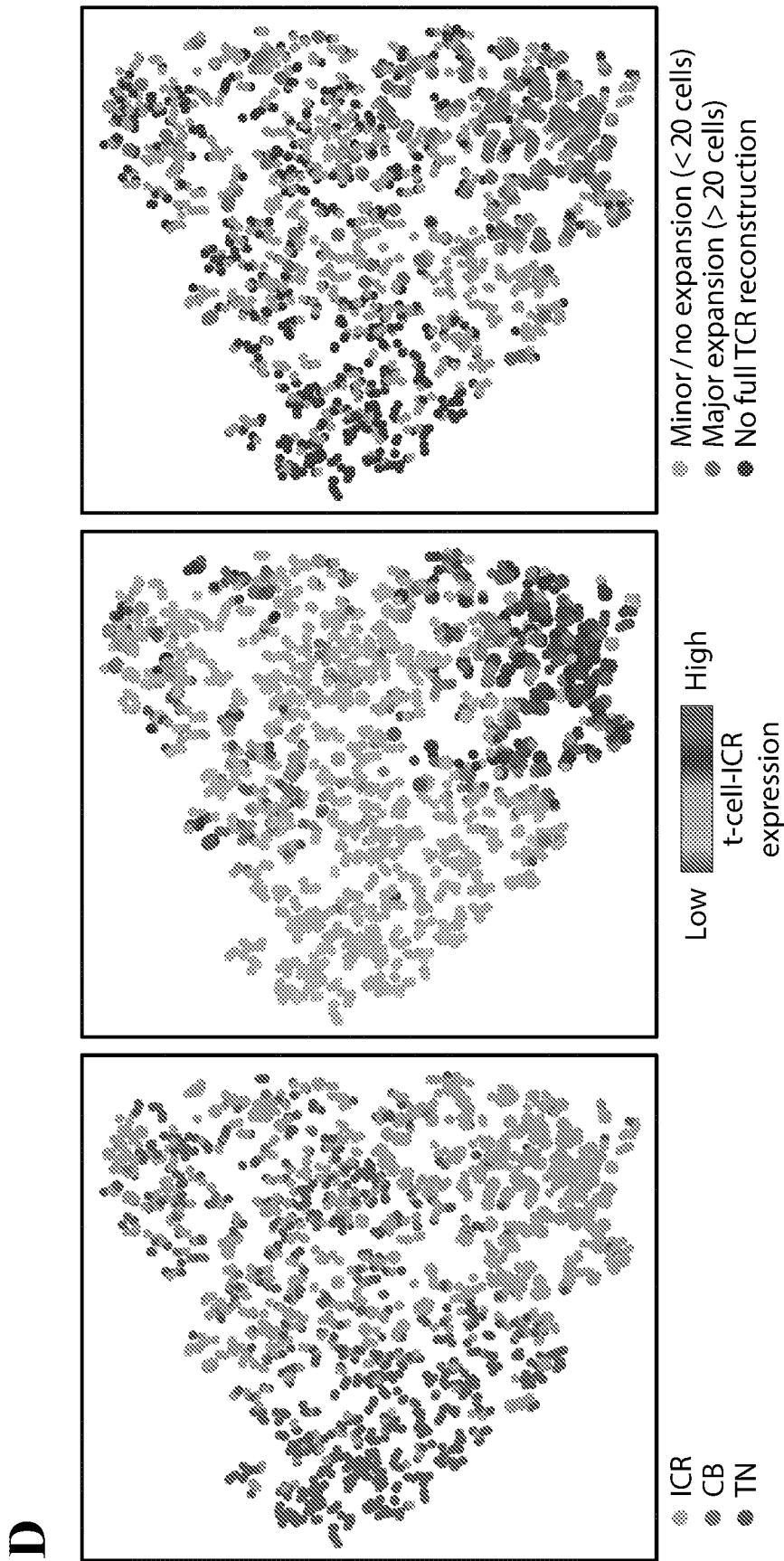


FIG. 1D

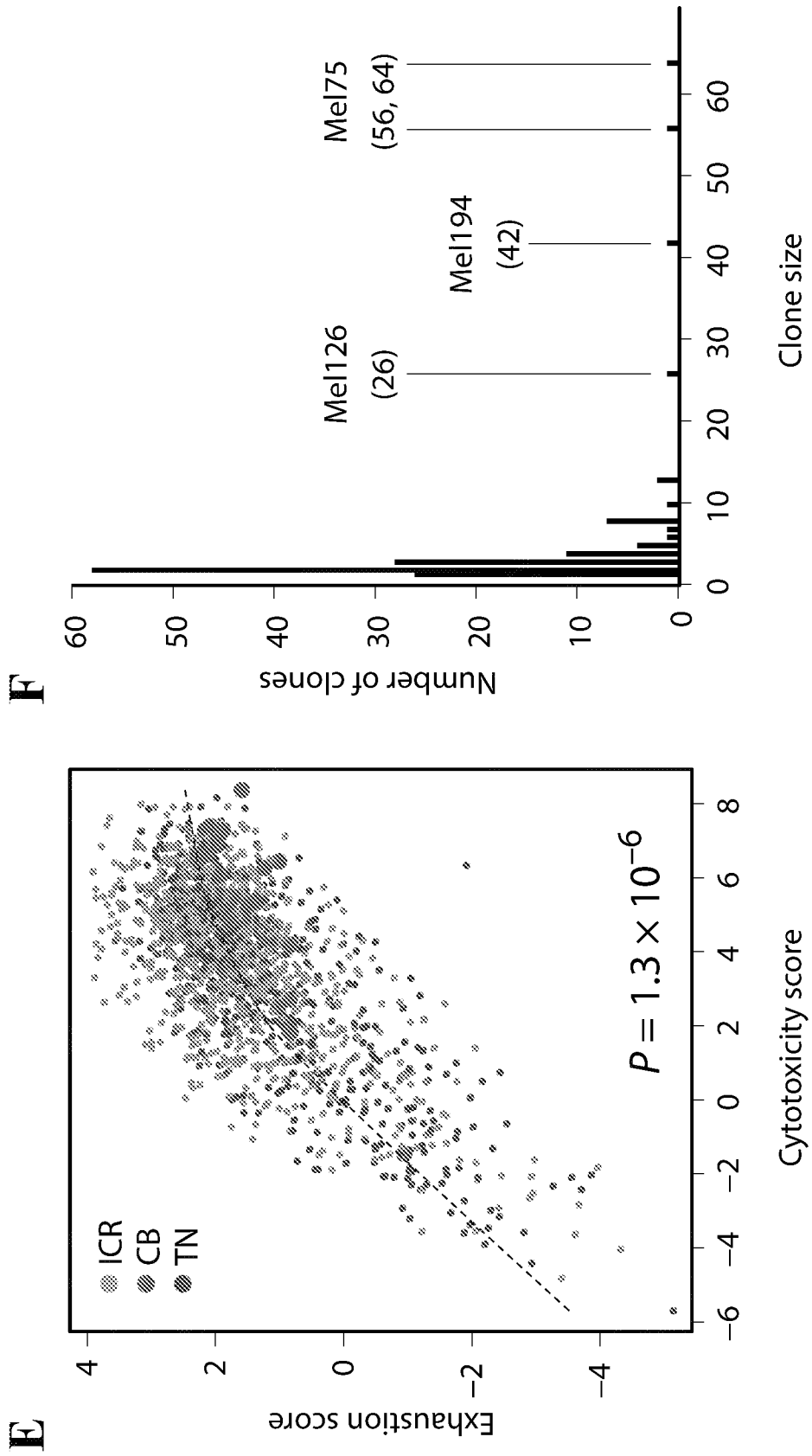


FIG. 1E-F

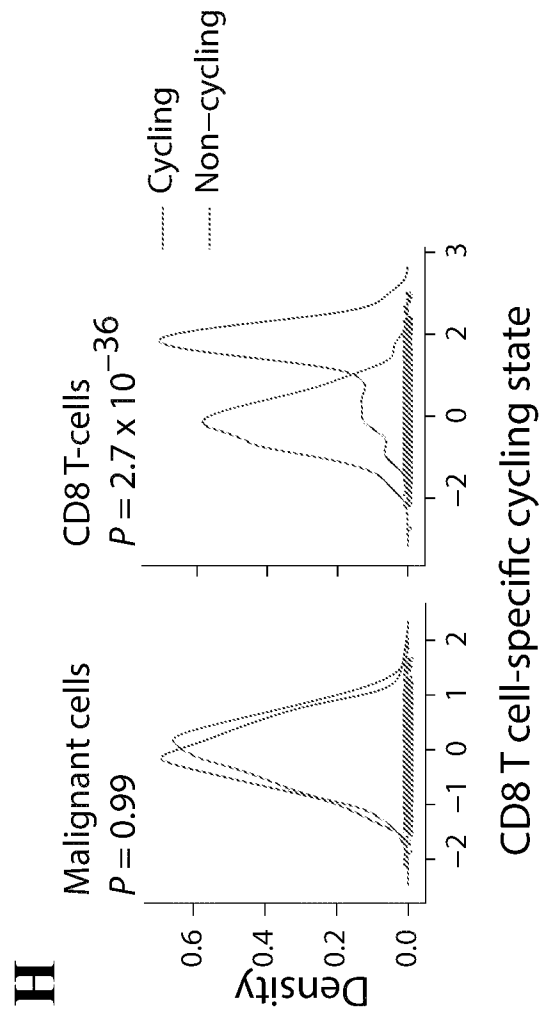
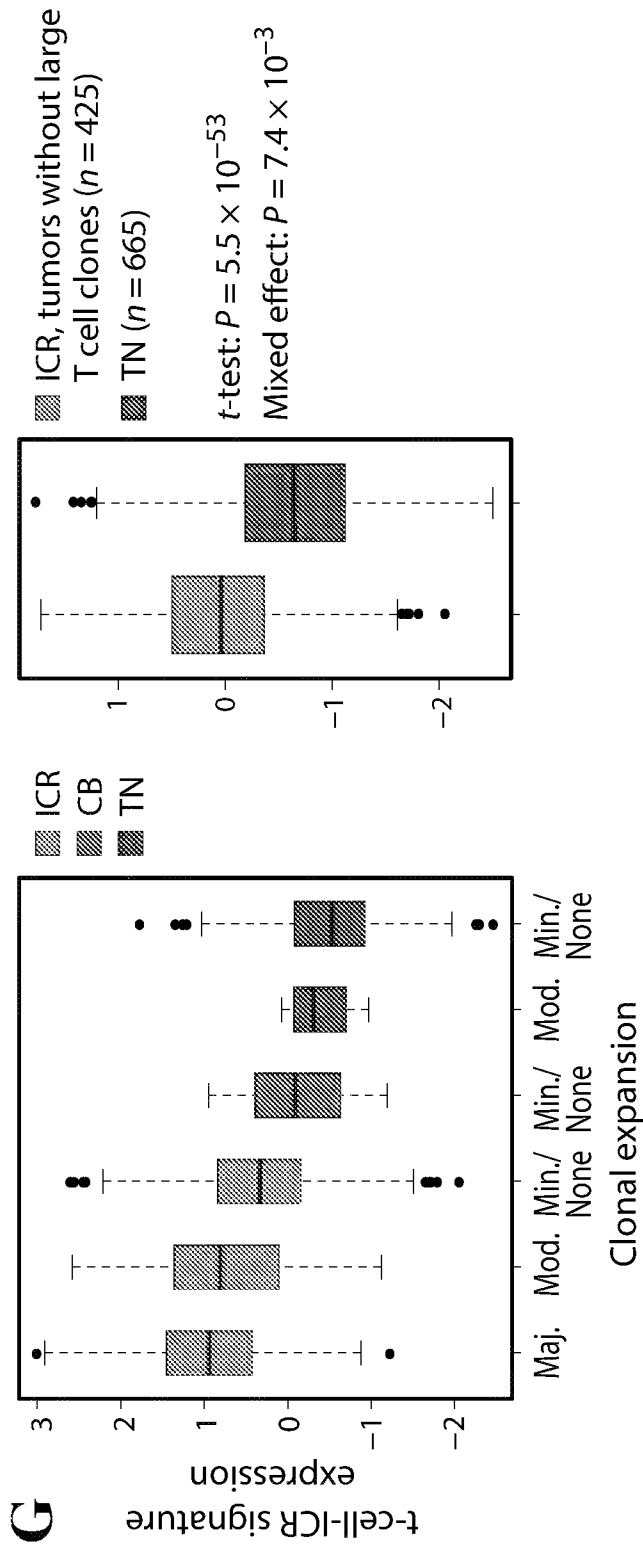


FIG. 1G-H

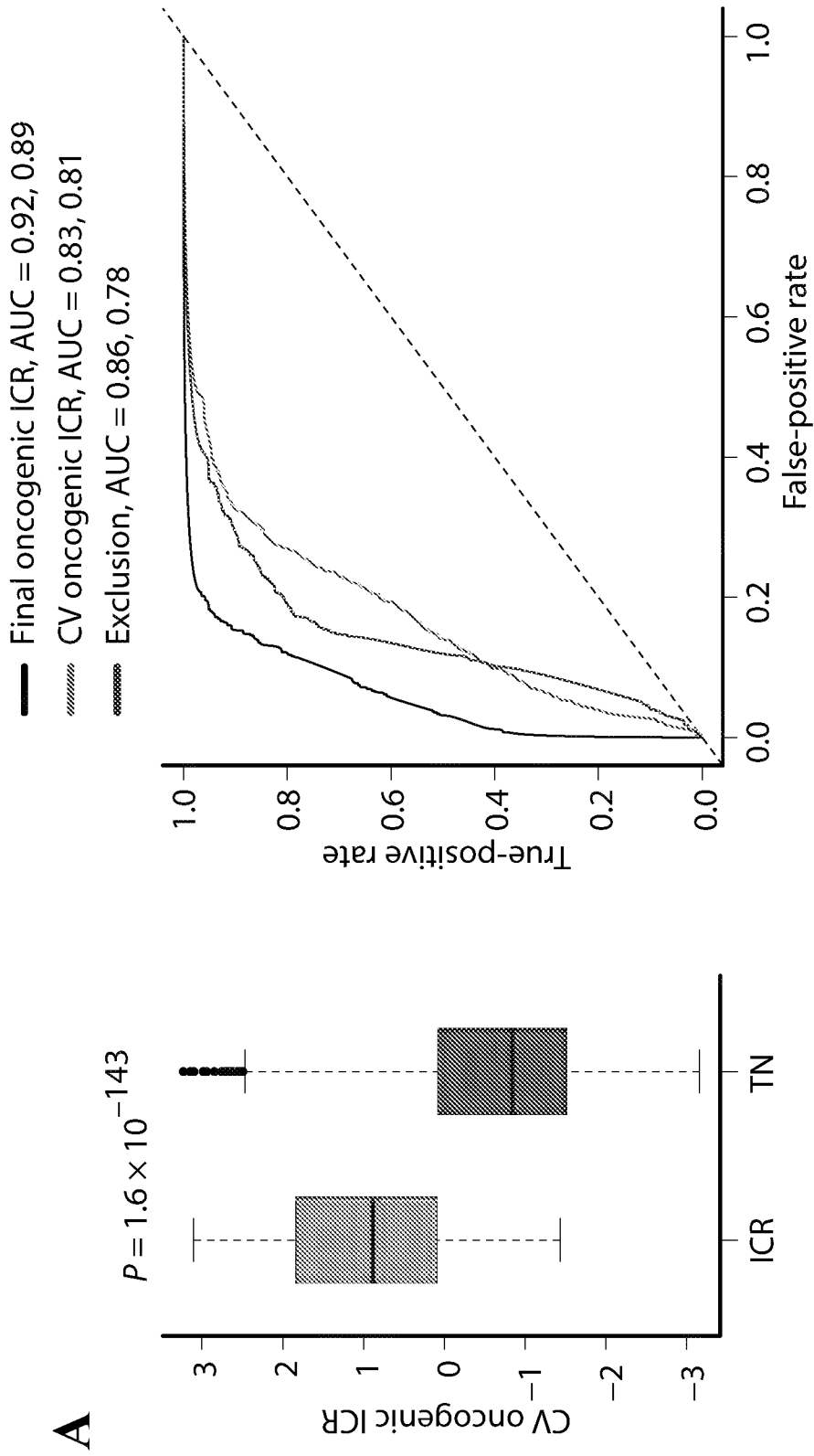


FIG. 2A

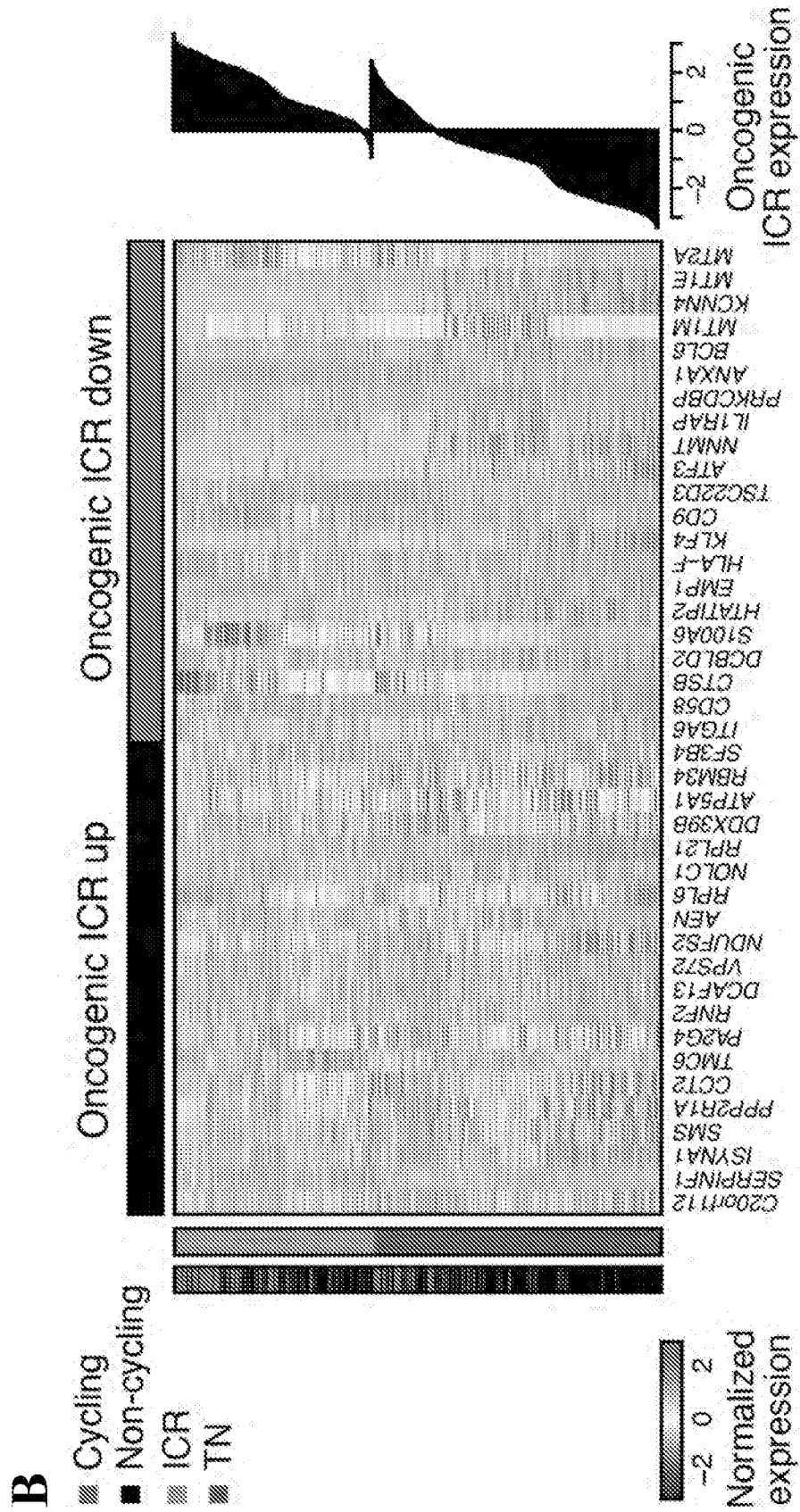


FIG. 2B

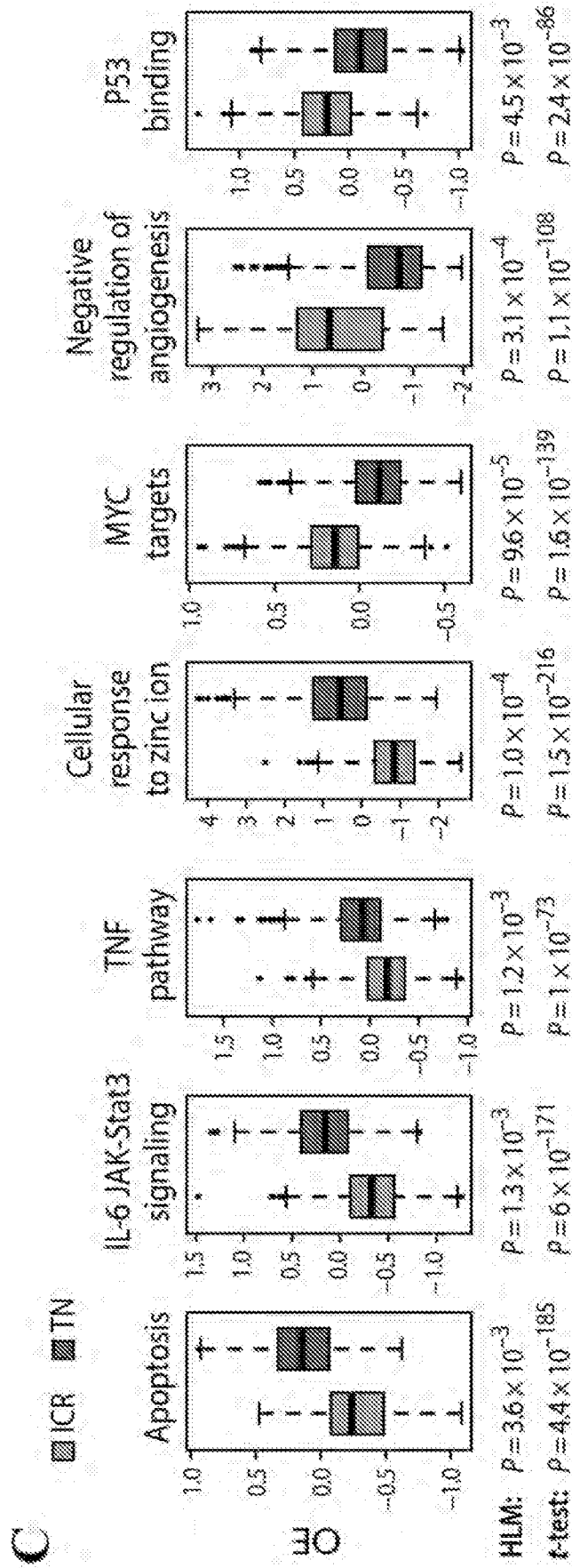


FIG. 2C

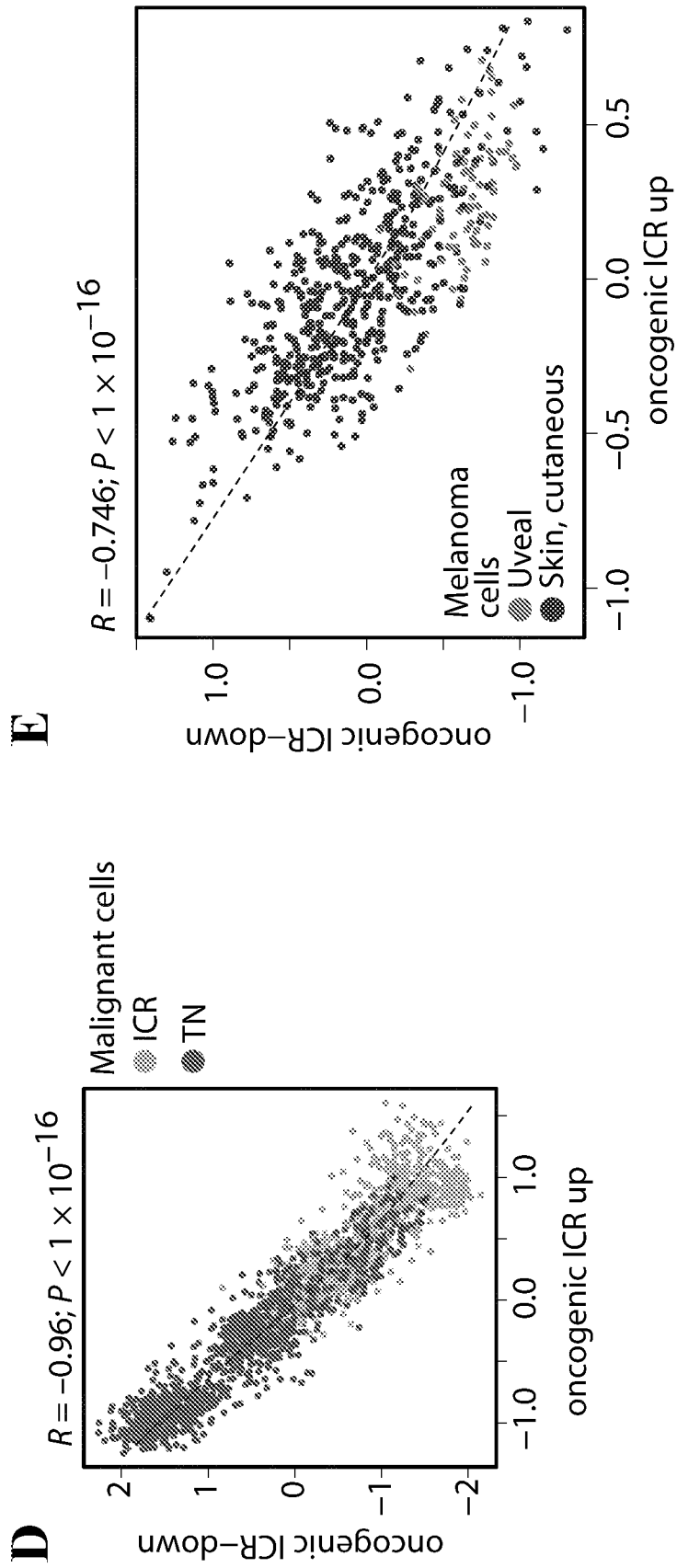


FIG. 2D-E

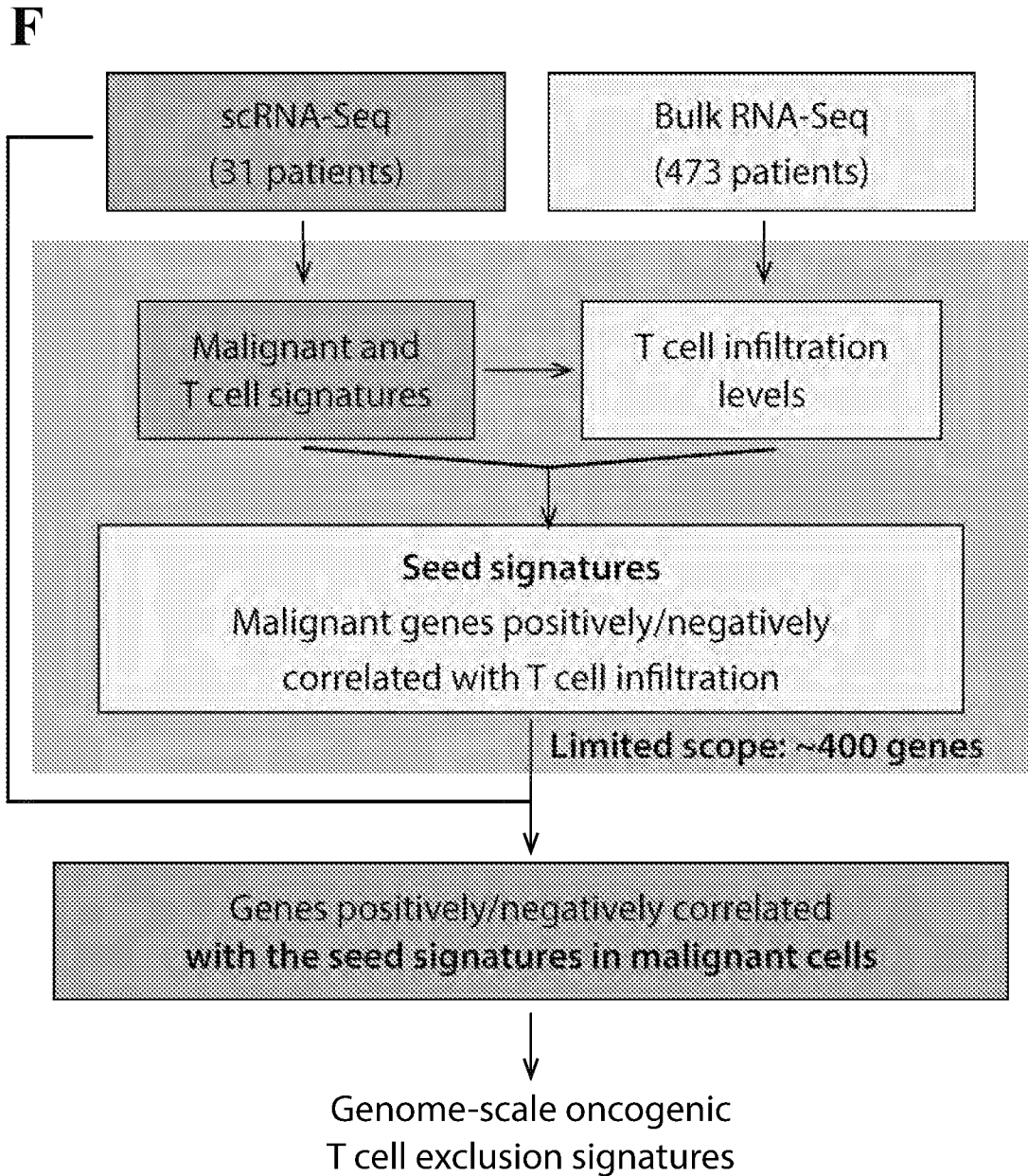
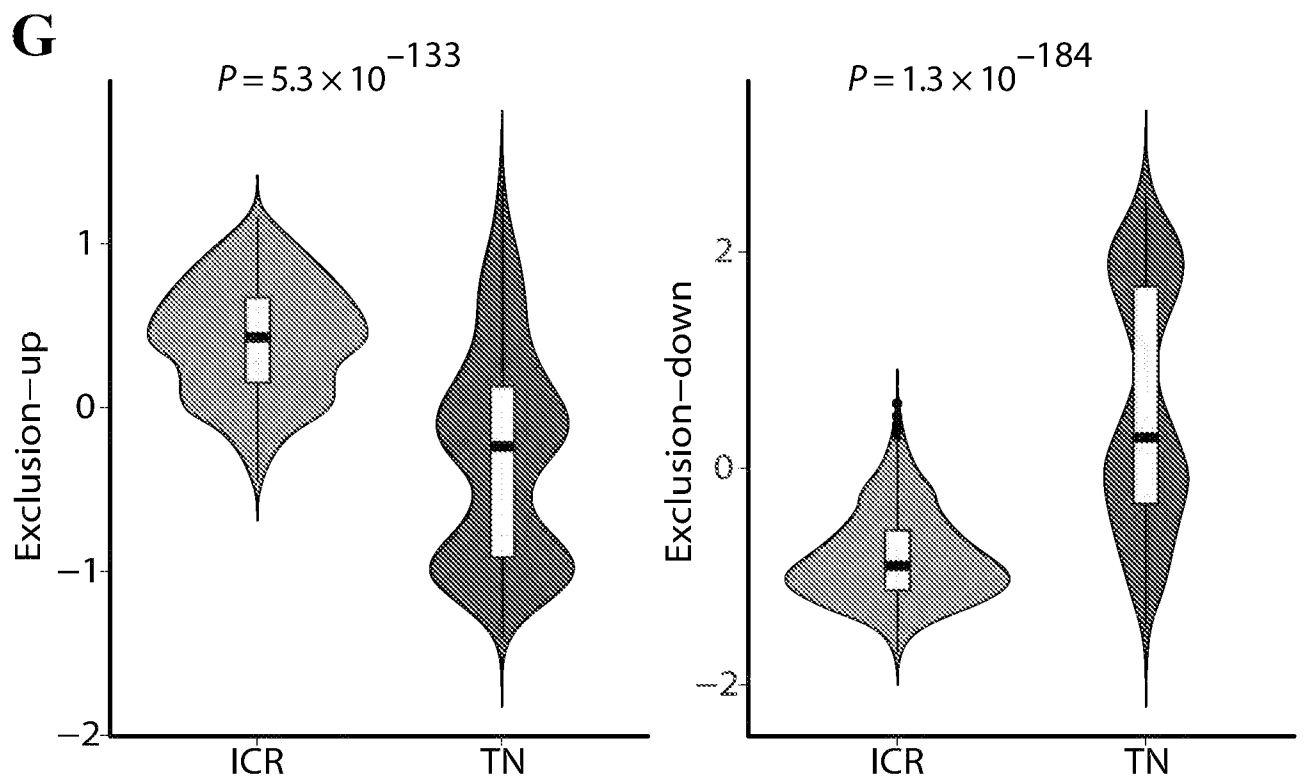


FIG. 2F

**FIG. 2G**

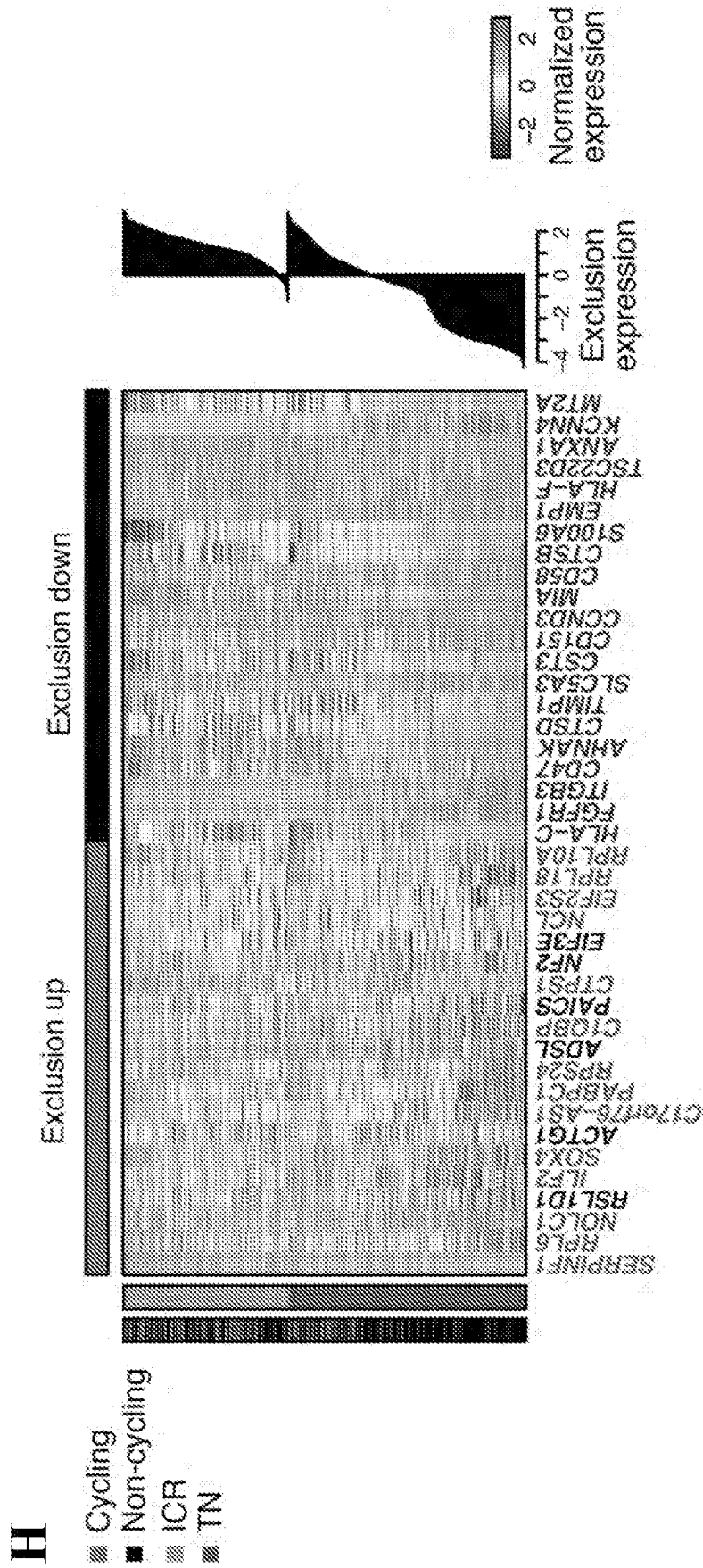


FIG. 2H

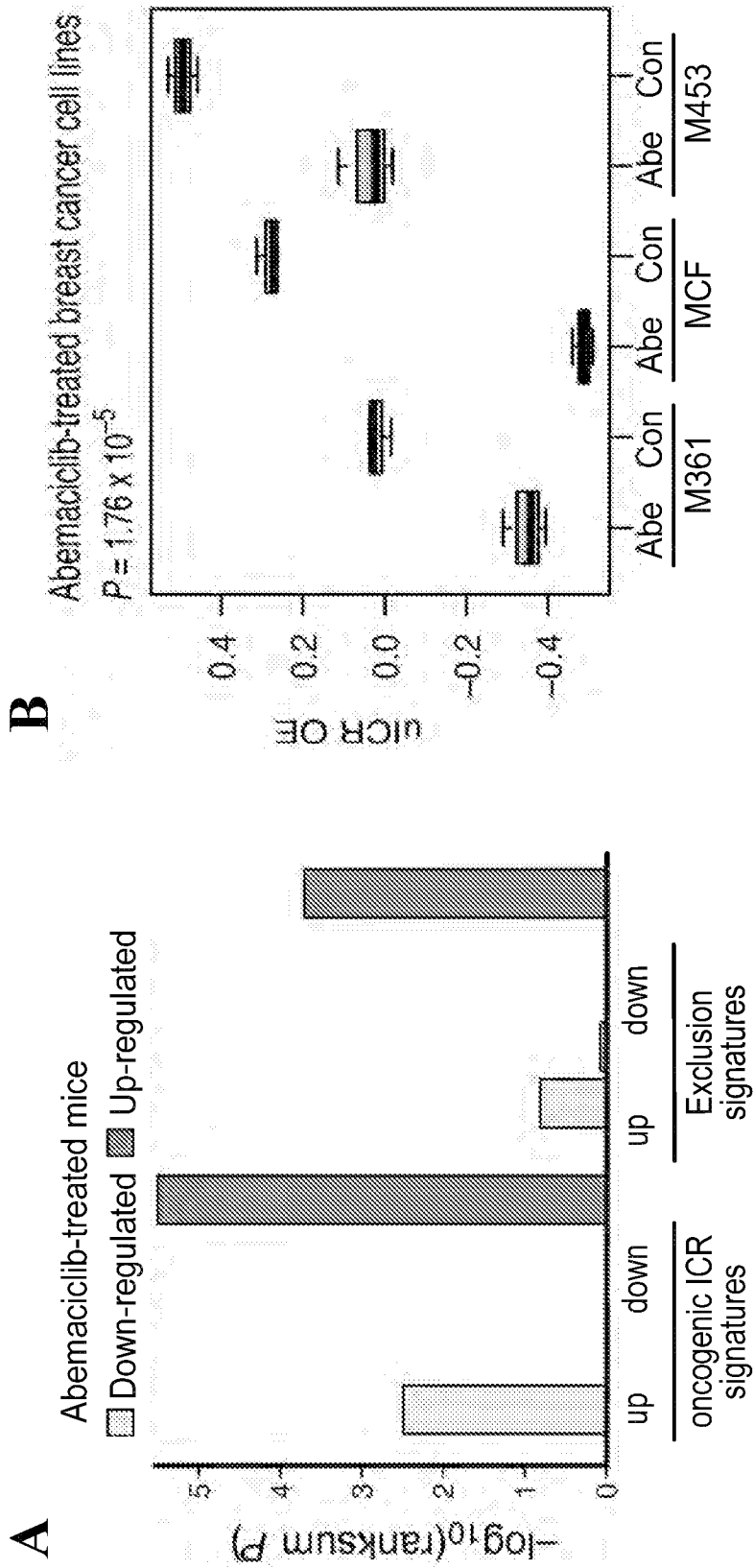


FIG. 3A-B

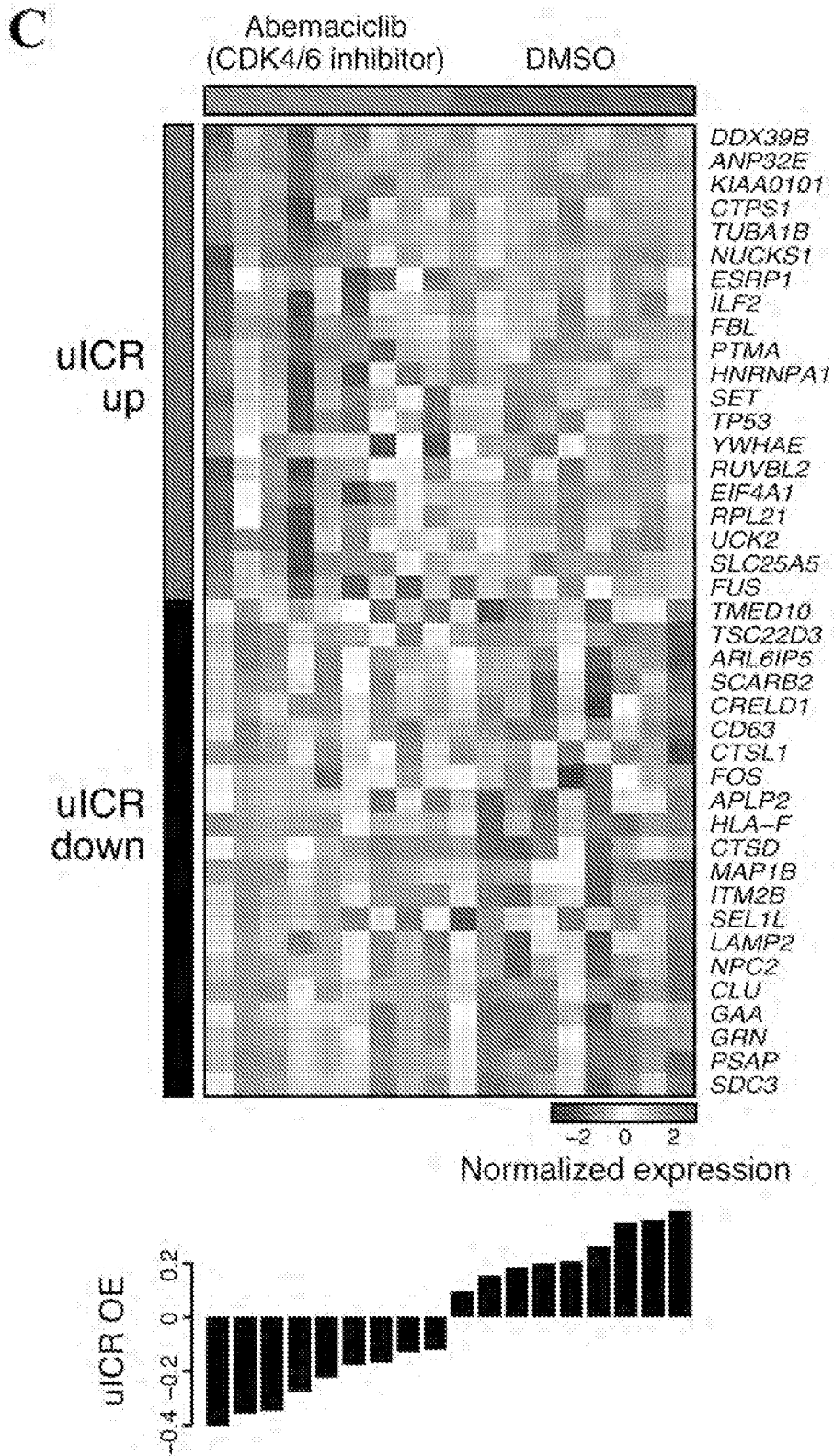


FIG. 3C

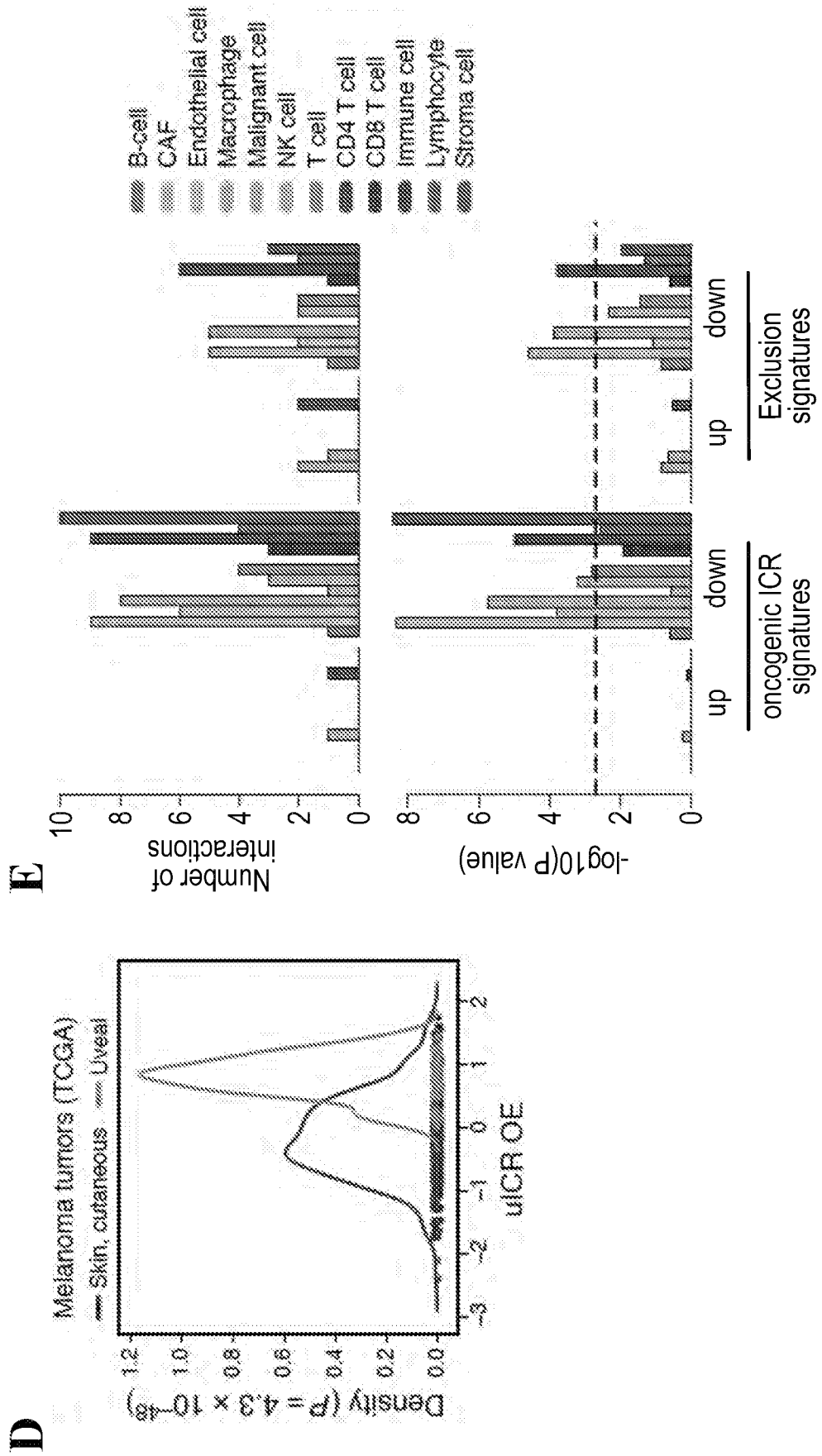


FIG. 3D-E

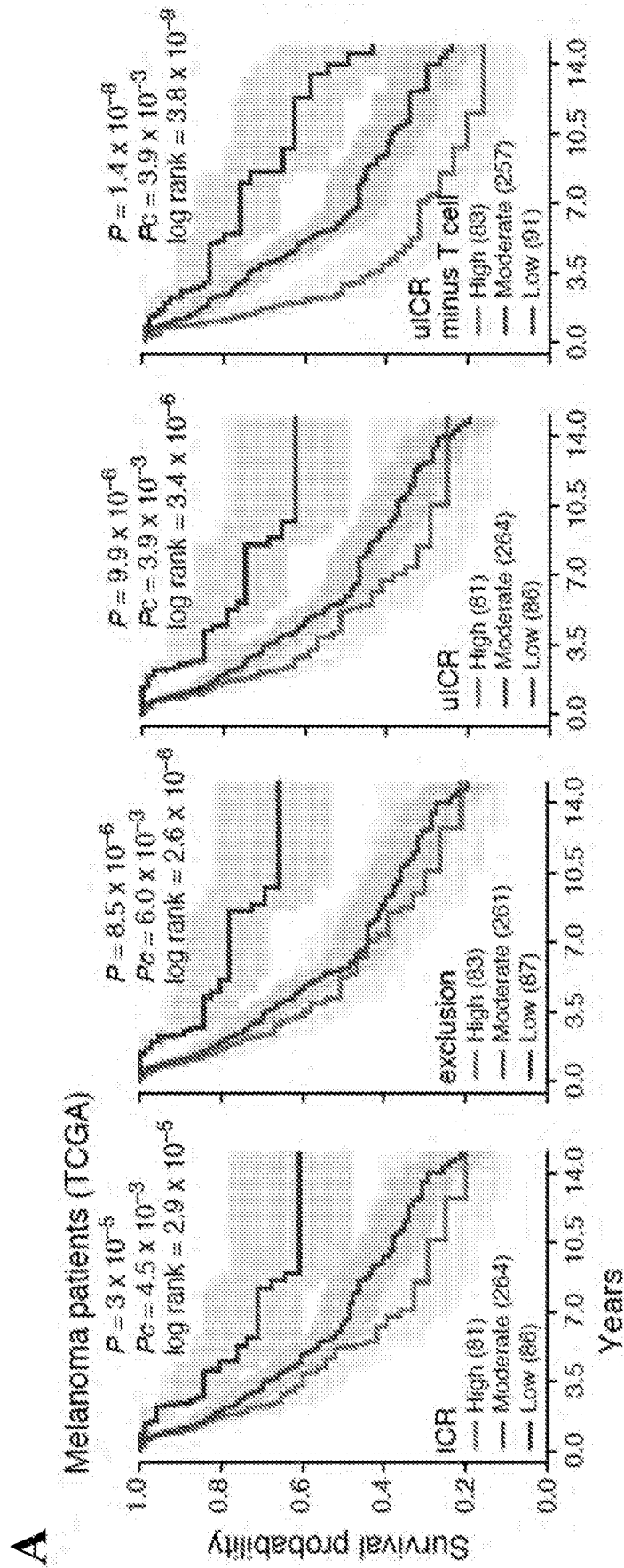
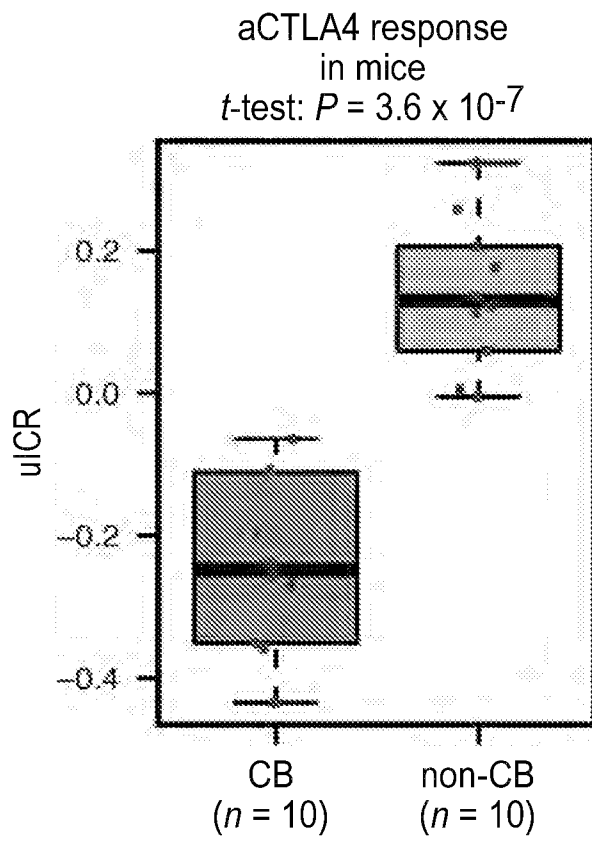


FIG. 4A

B



C

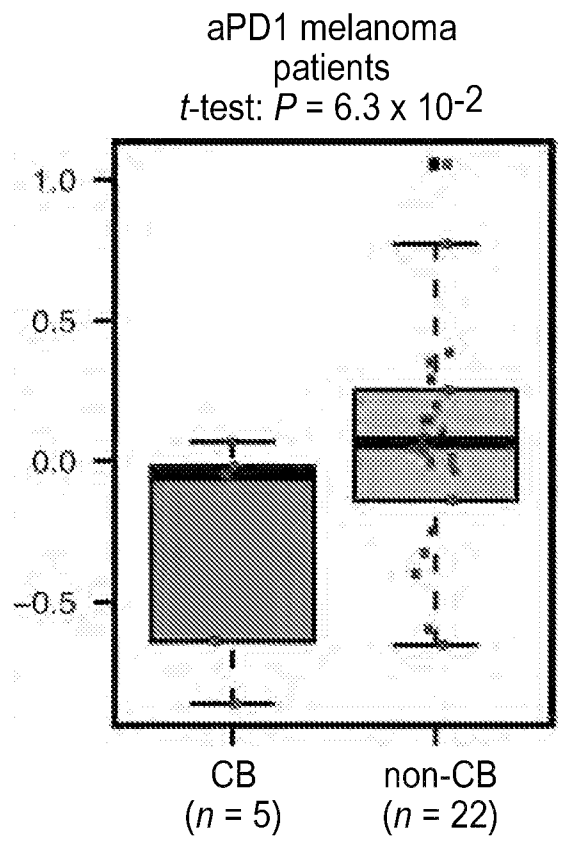


FIG. 4B-C

D

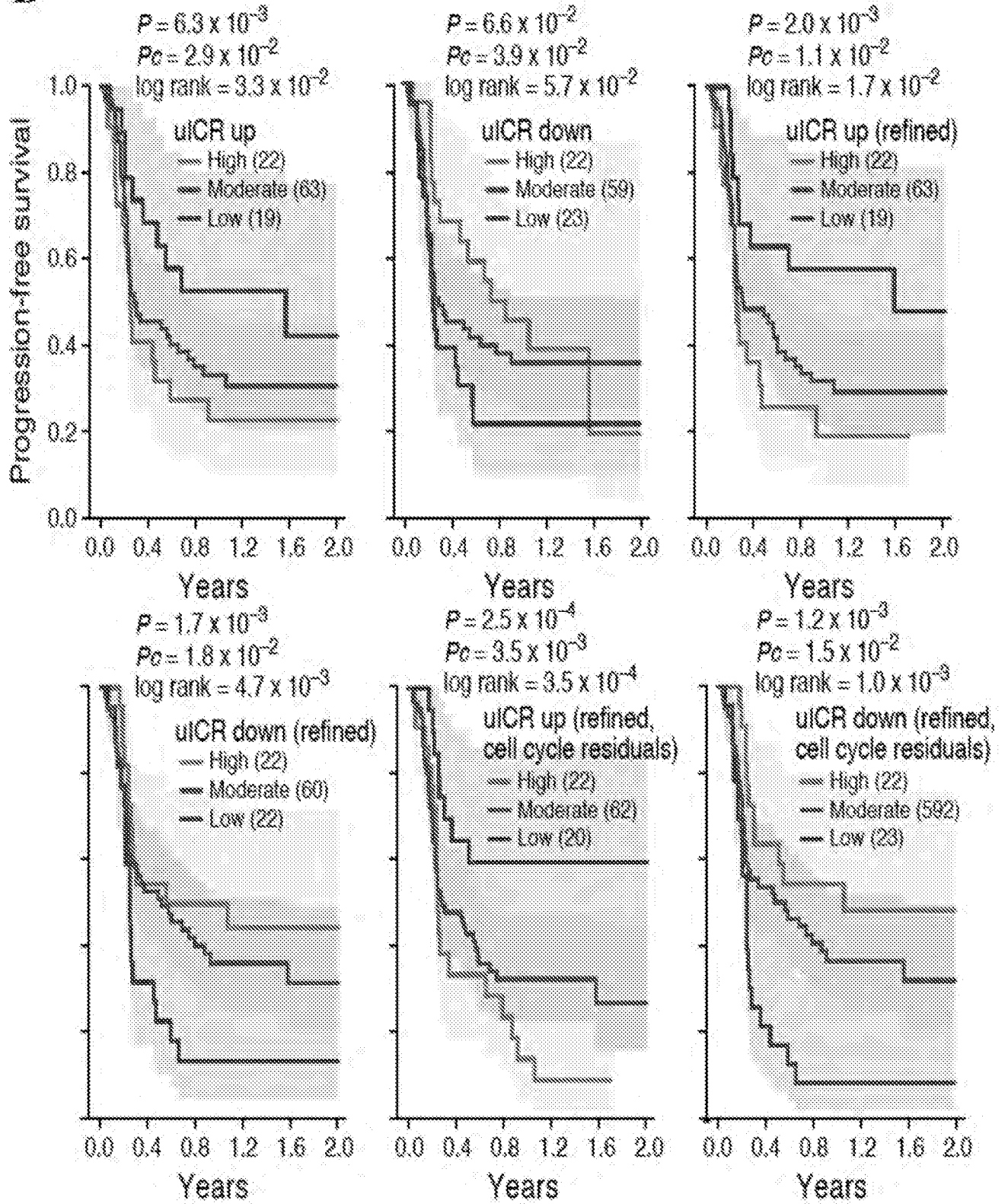


FIG. 4D

E

Progression-free survival ($P = 2.25 \times 10^{-6}$)
 104 aPD1-treated melanoma patients
 Predictive value given T cell infiltration levels

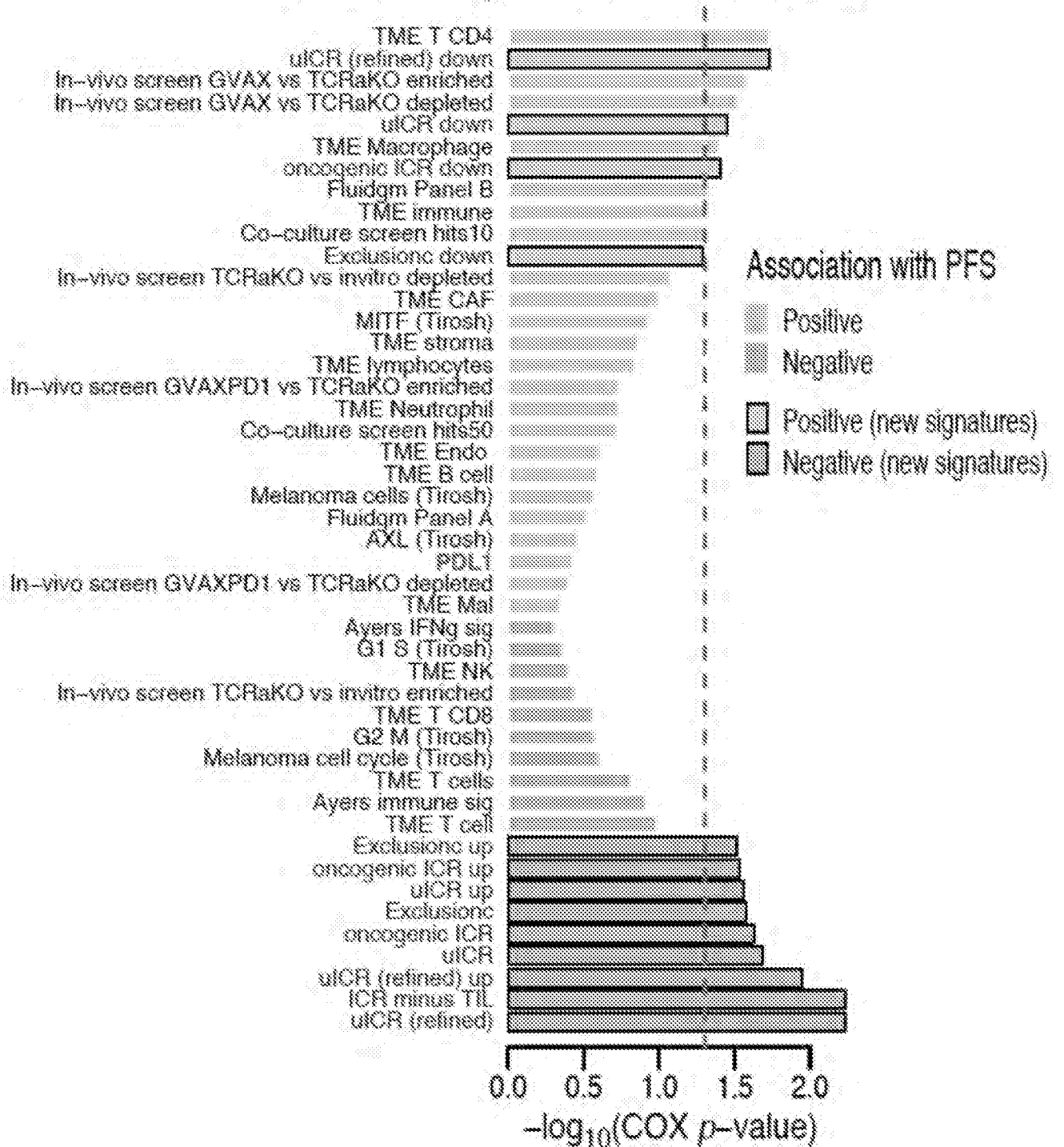
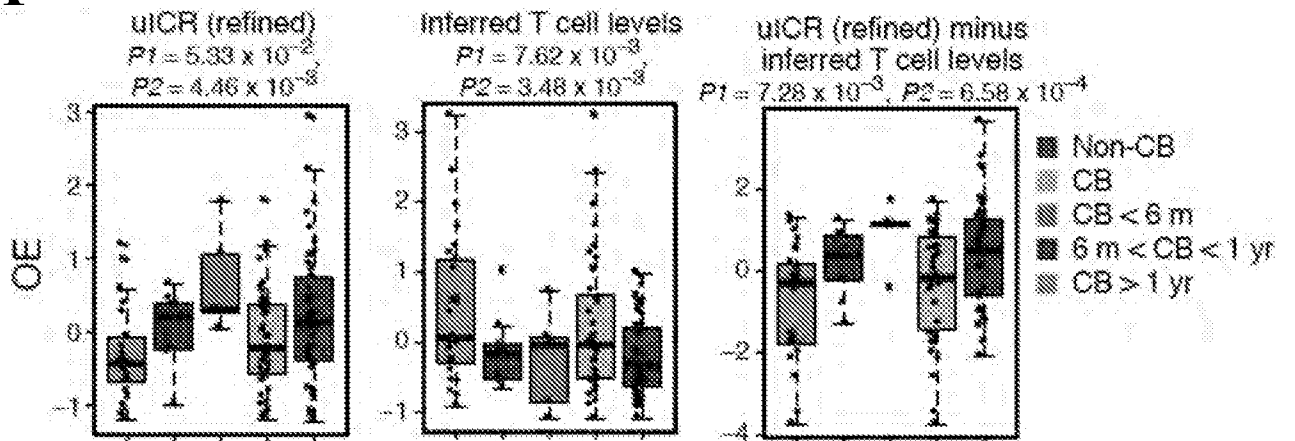


FIG. 4E

F



G

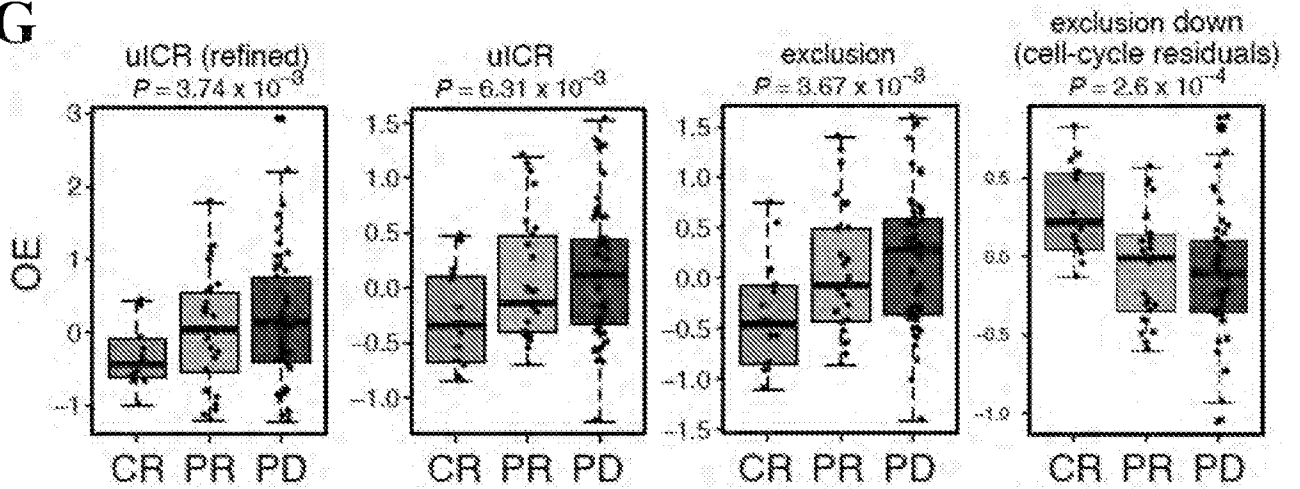


FIG. 4F-G

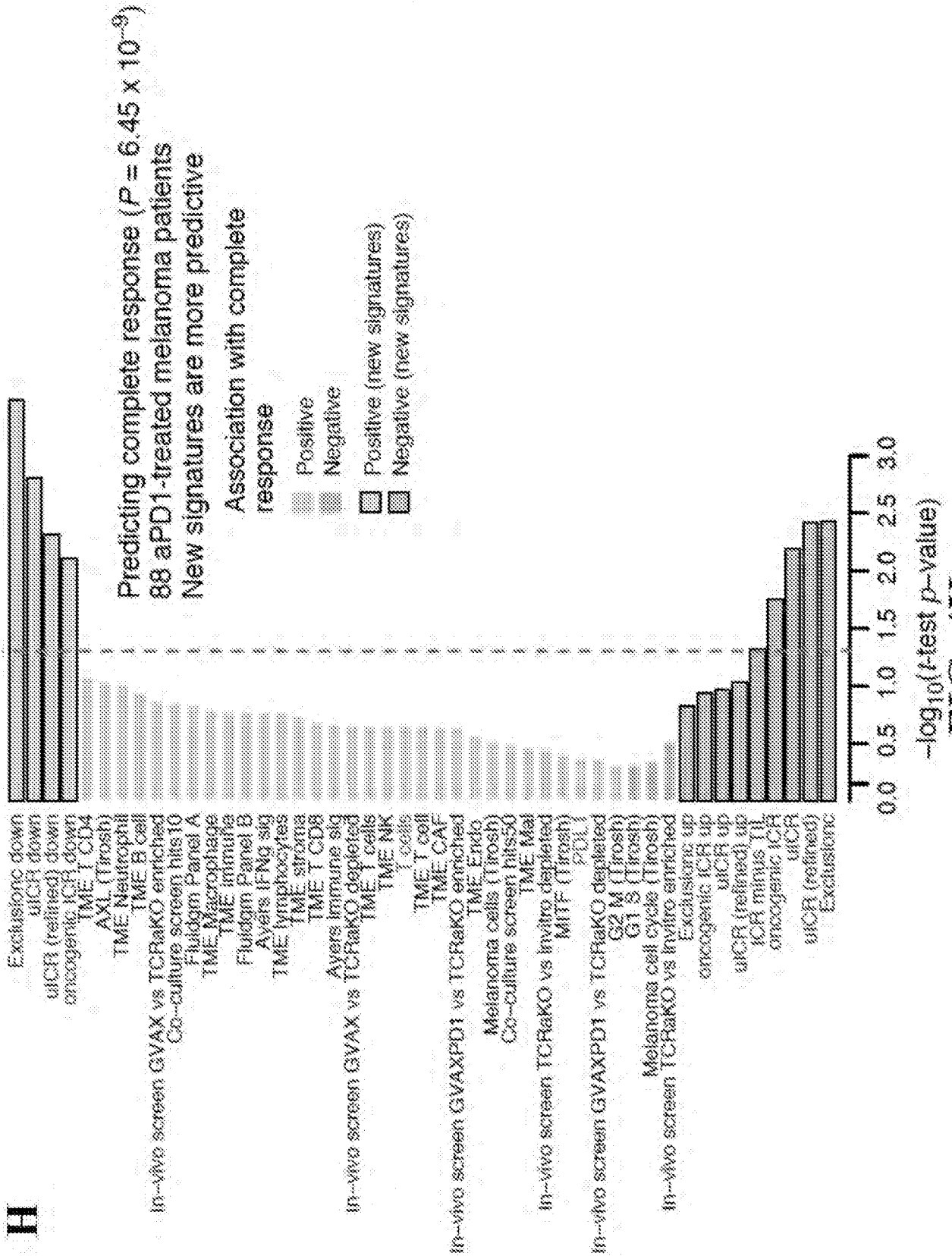


FIG. 4H

I

Treatment cohort ($n = 31$);
scRNA-Seq

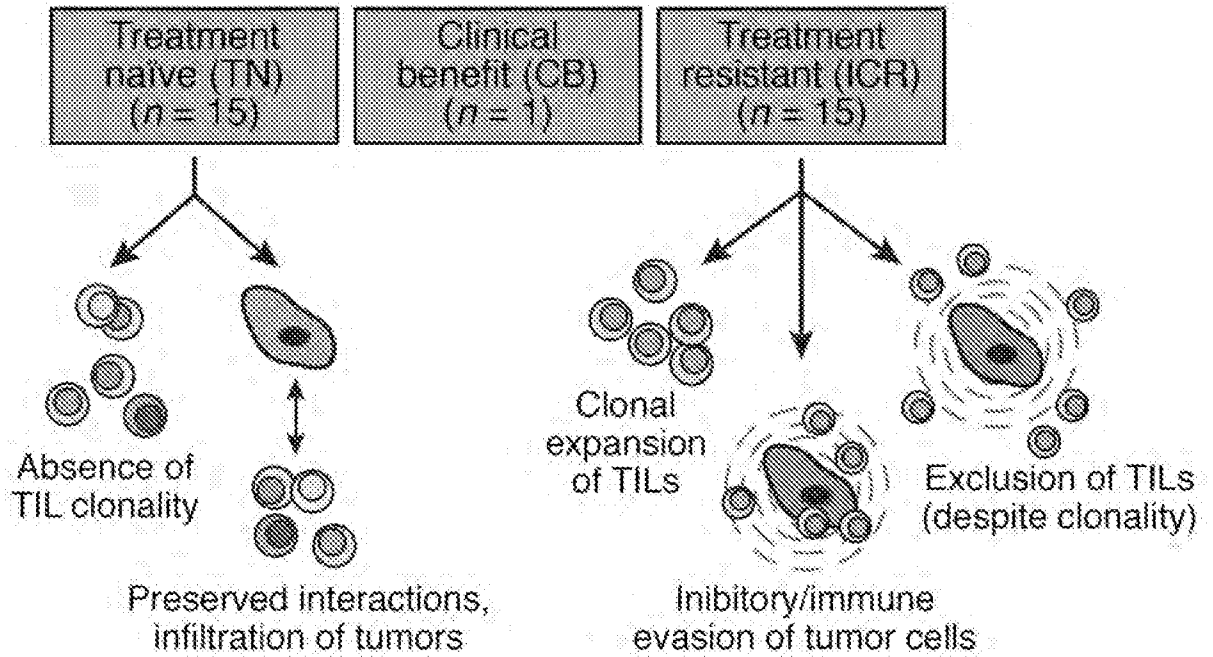


FIG. 4I

A

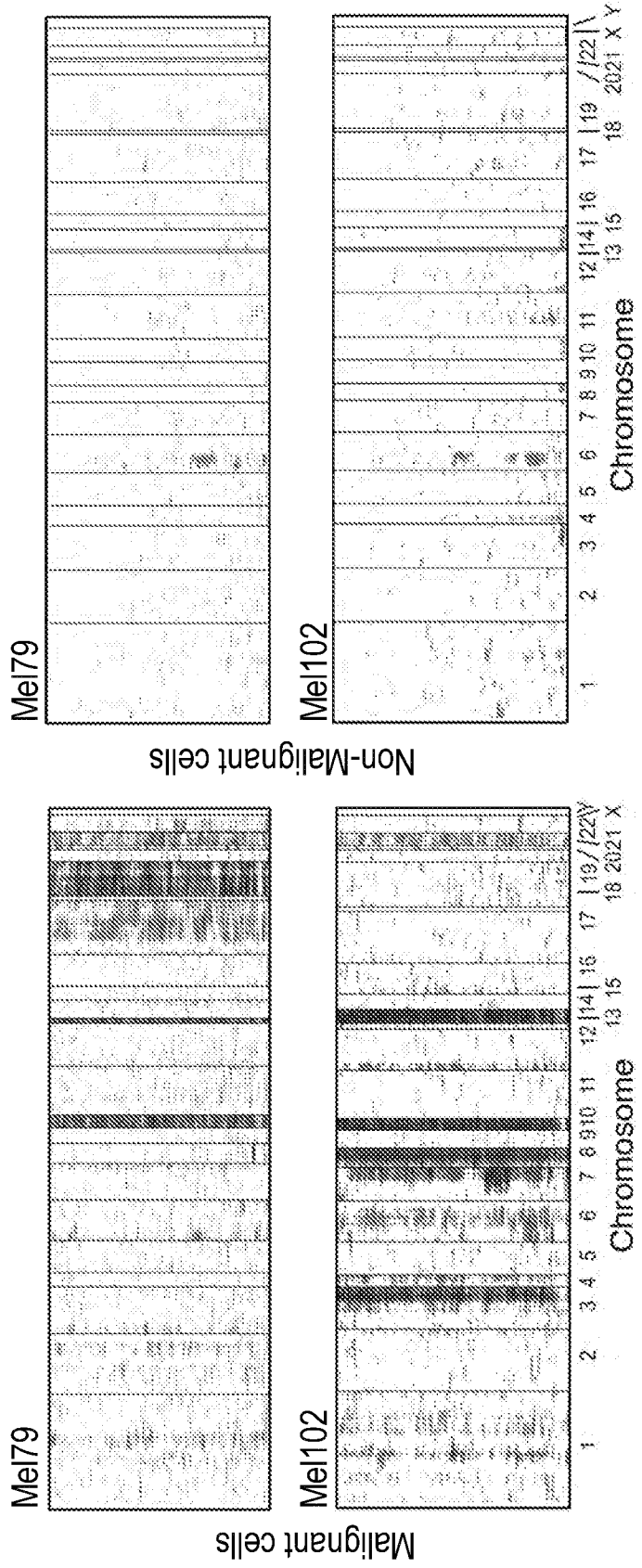


FIG. 5A

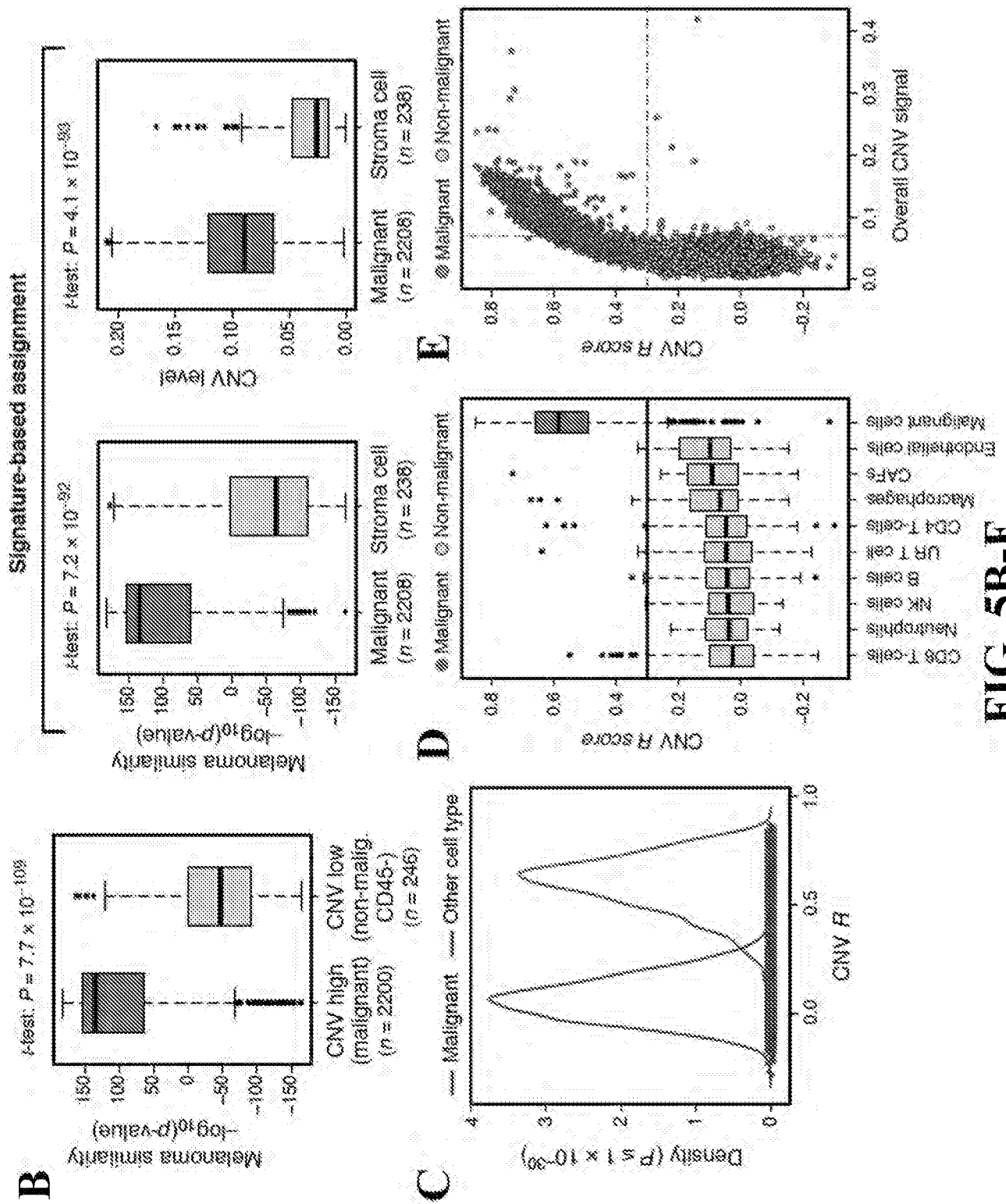


FIG. 5B-E

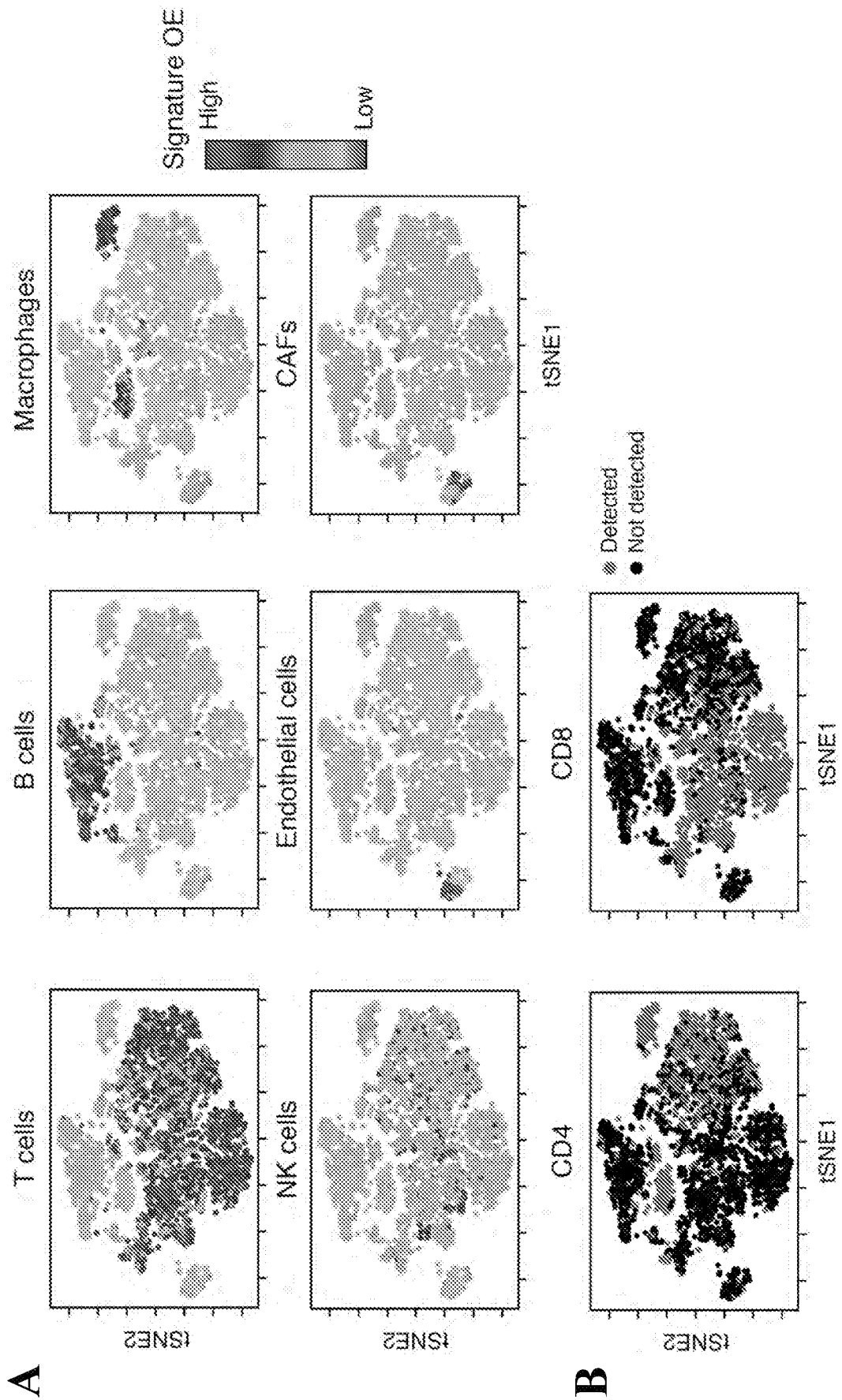


FIG. 6A-B

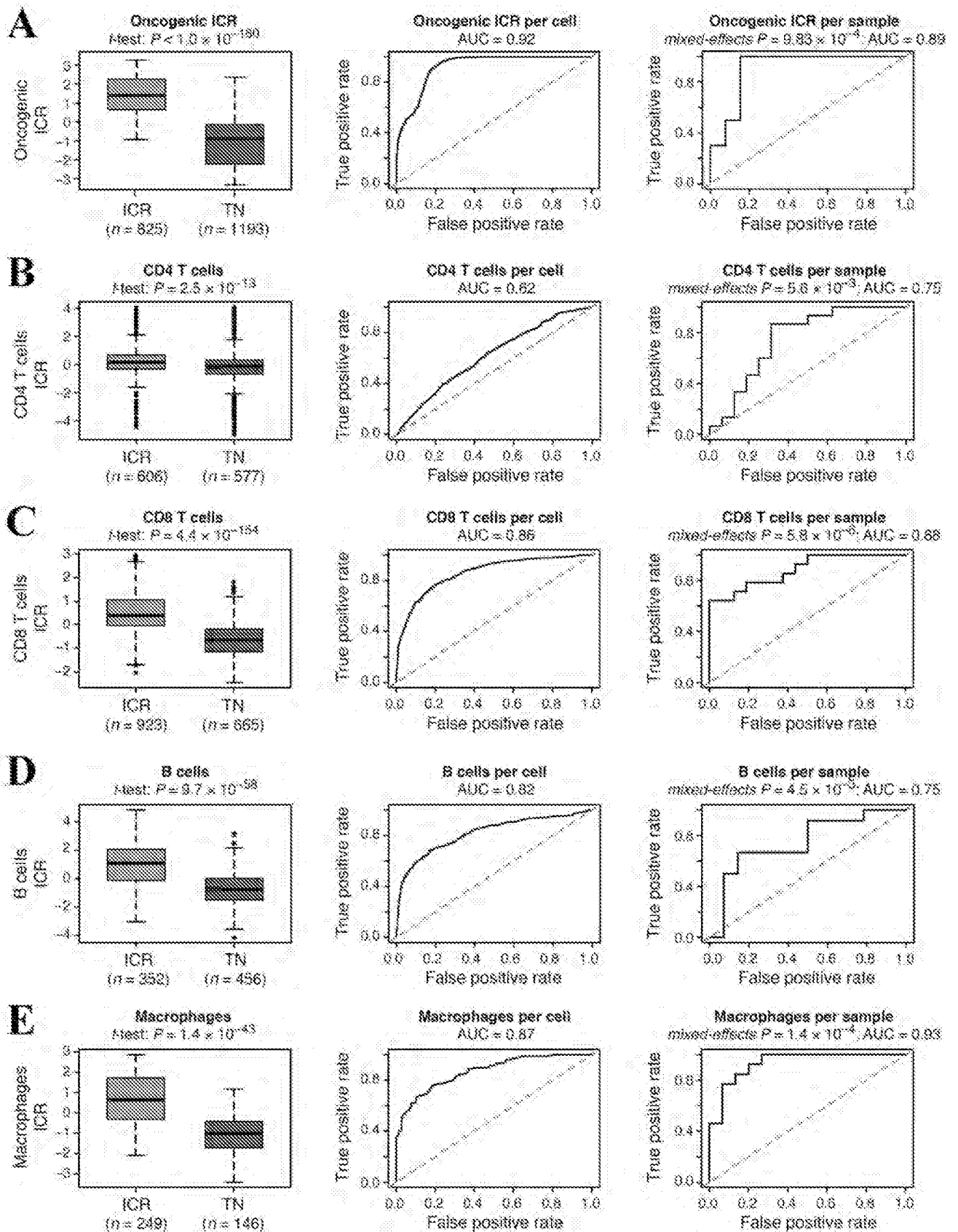


FIG. 7A-E

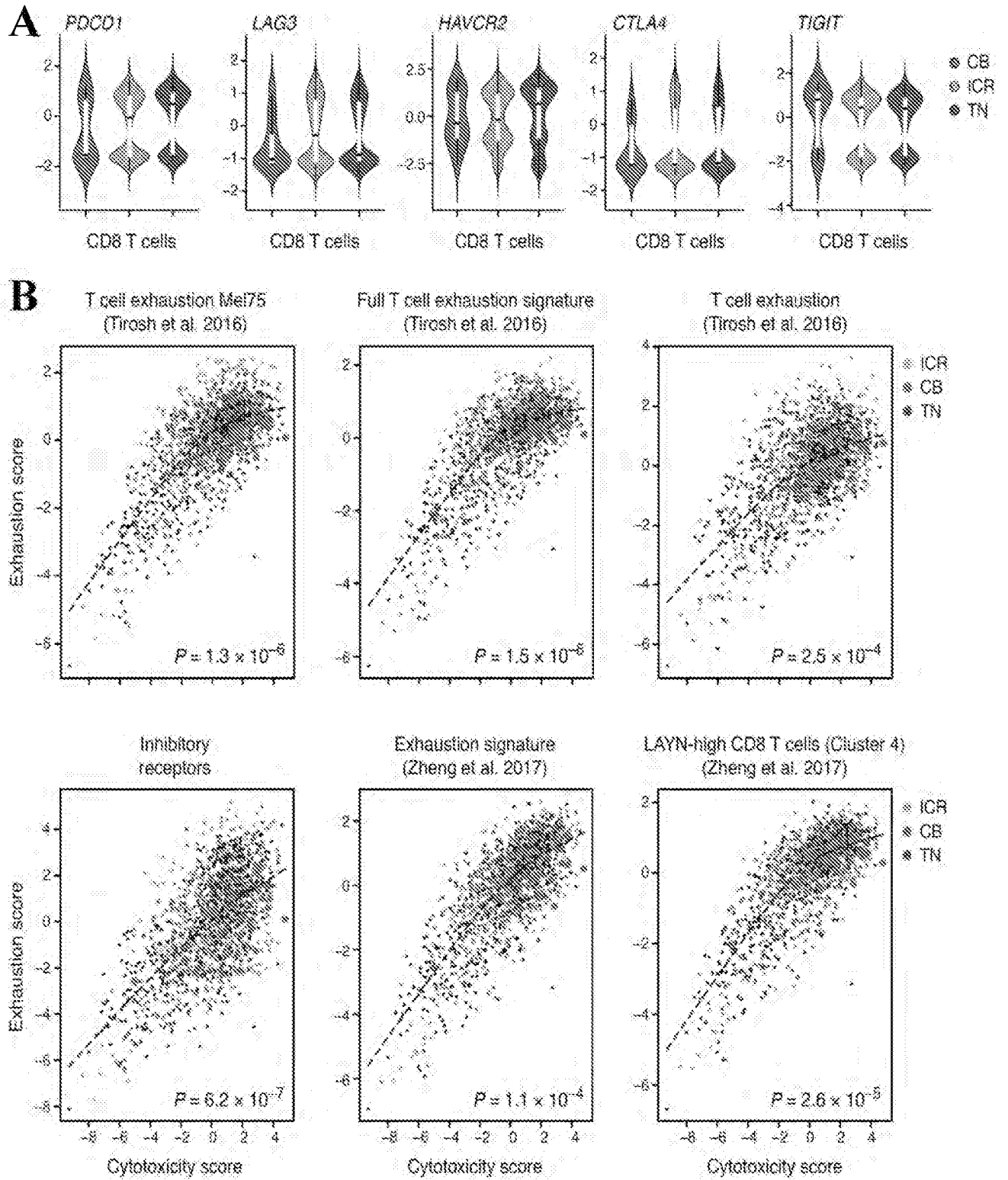


FIG. 8A-B

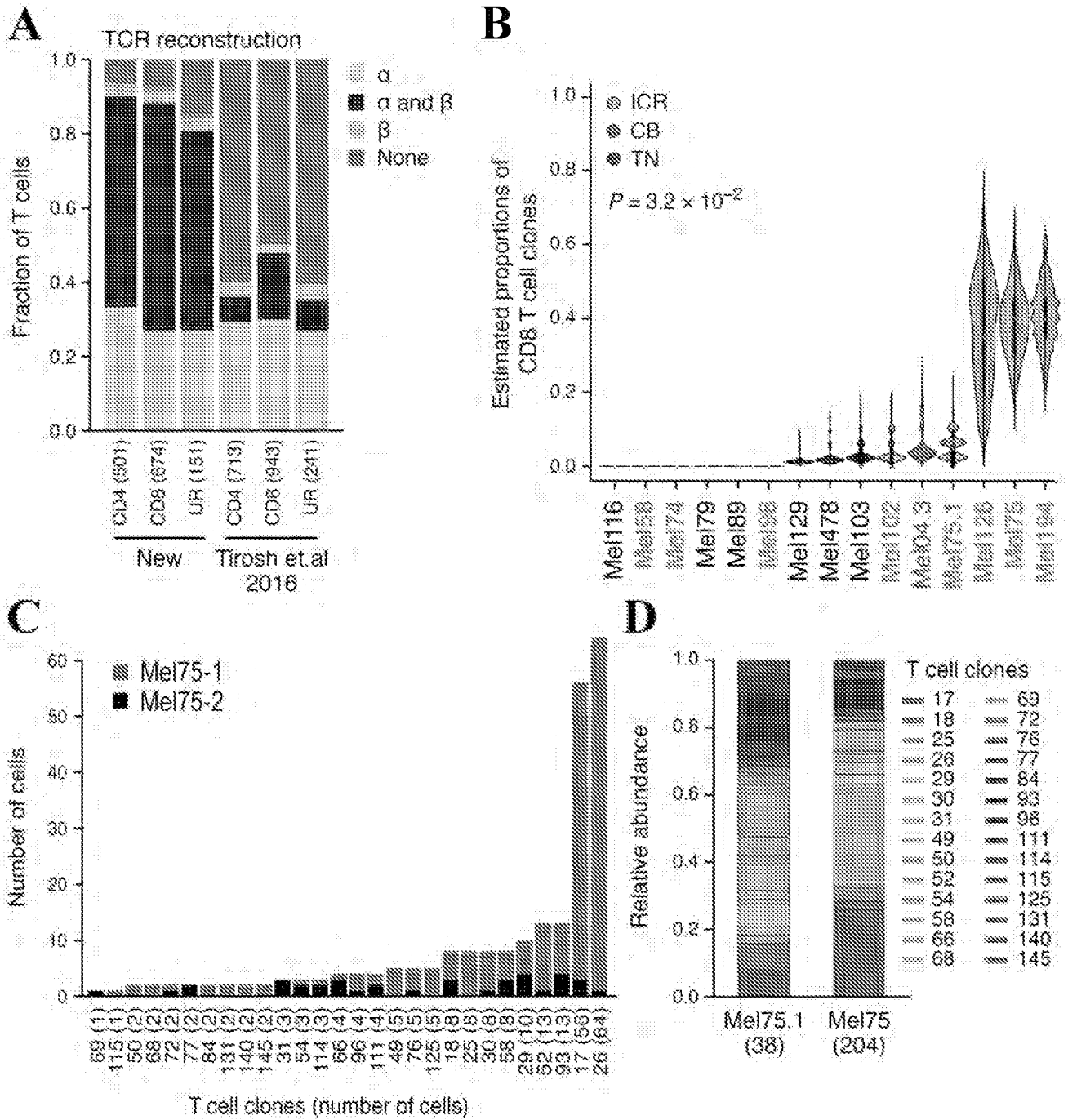


FIG. 9A-D

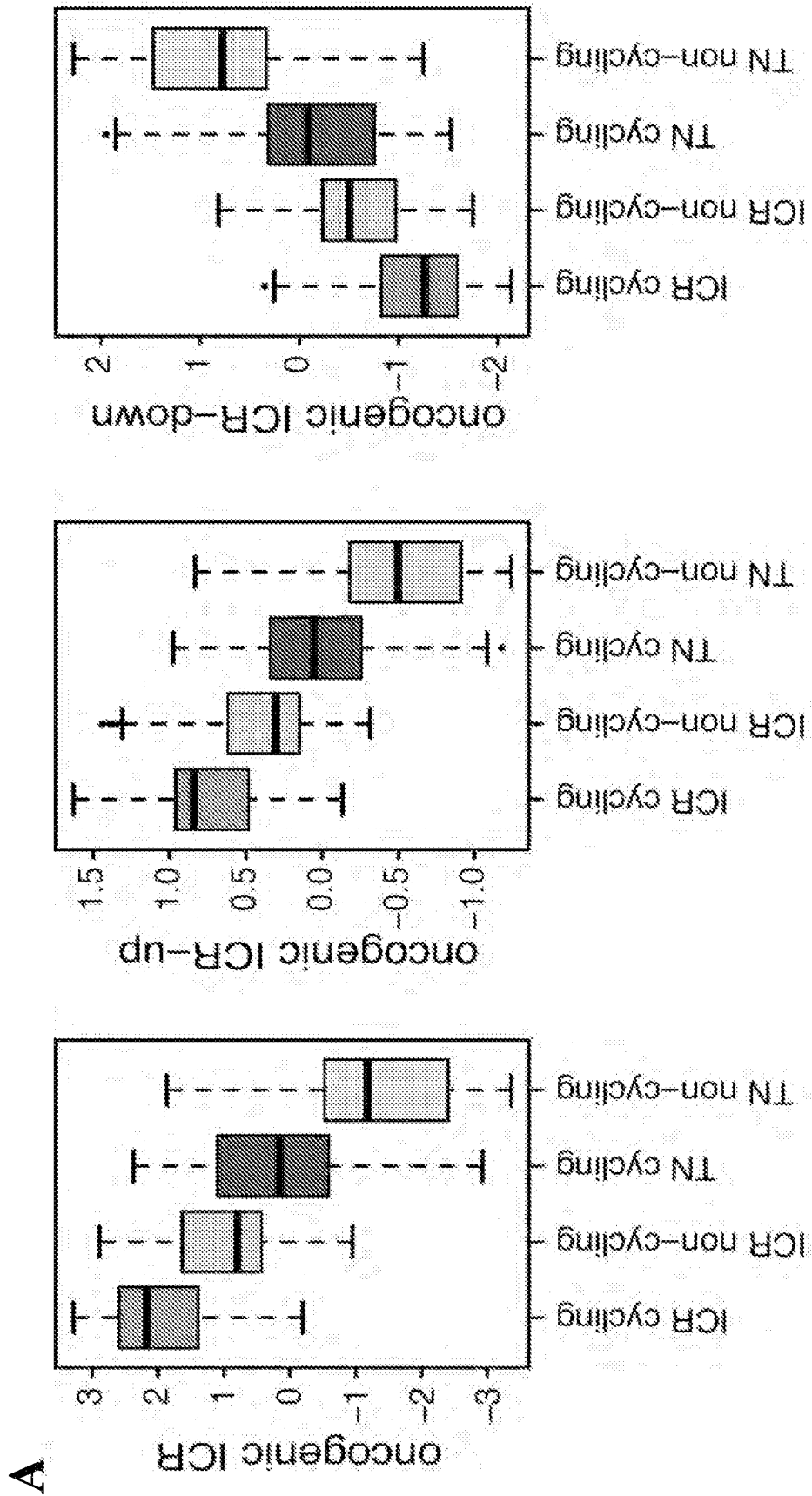
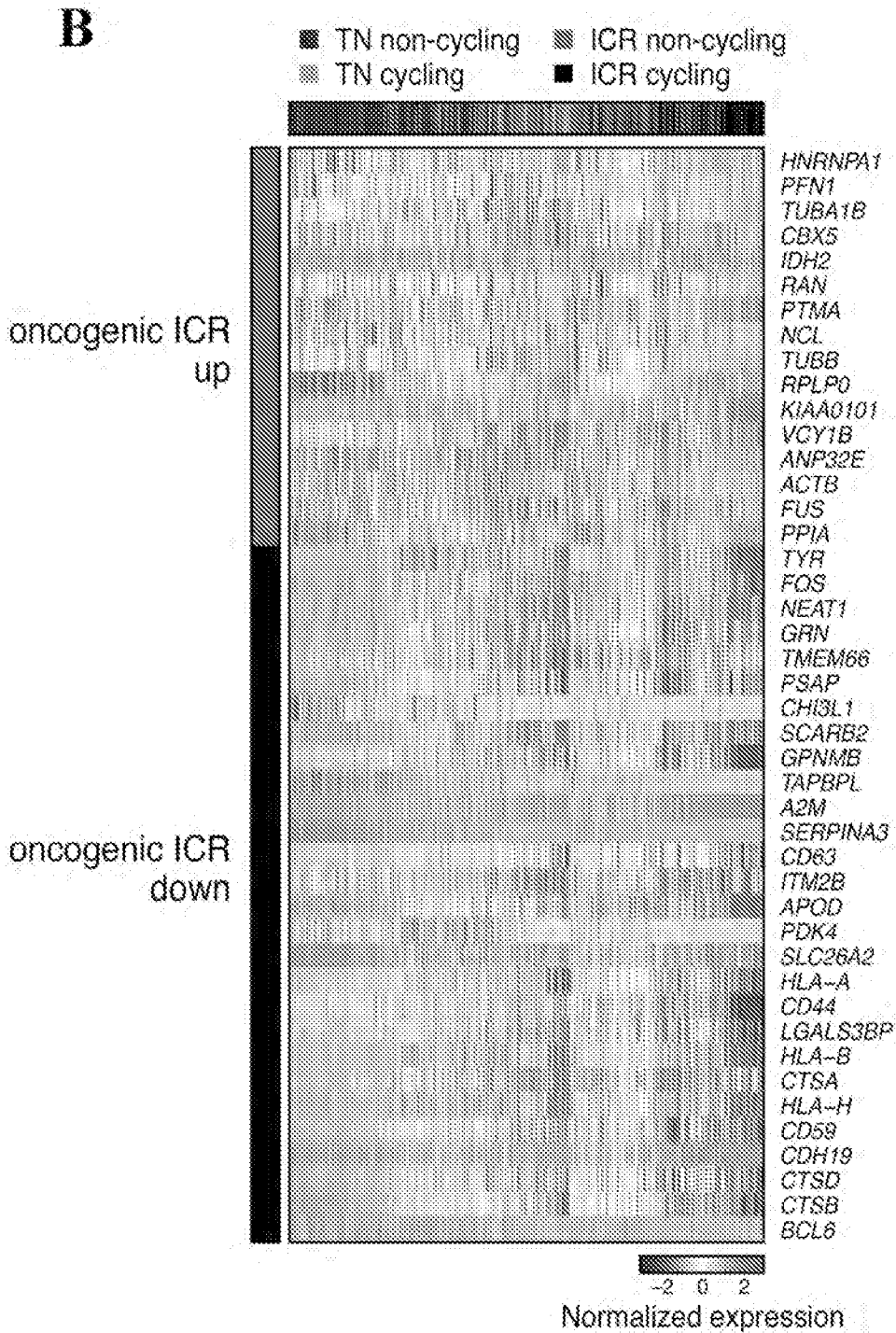


FIG. 10A



Malignant melanoma cells

FIG. 10B

C

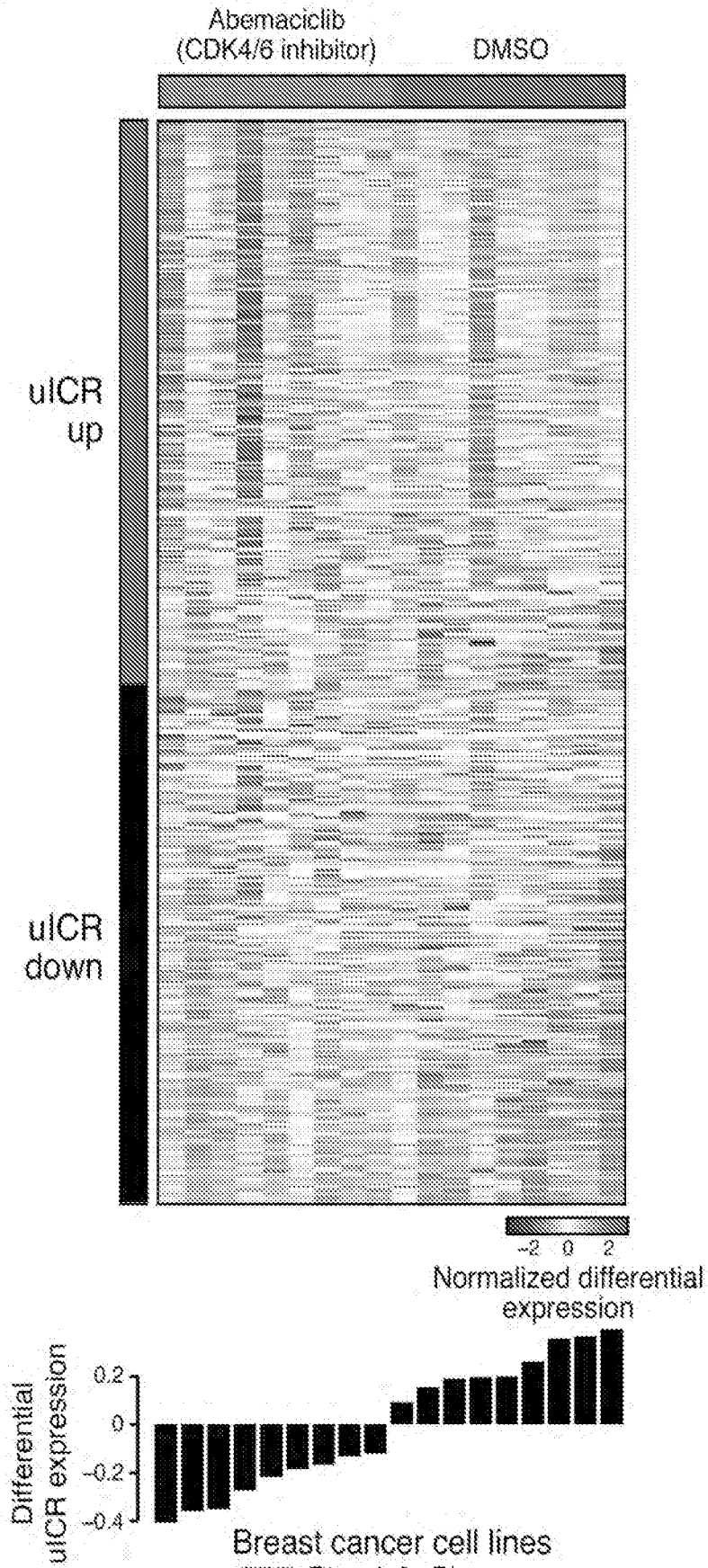


FIG. 10C

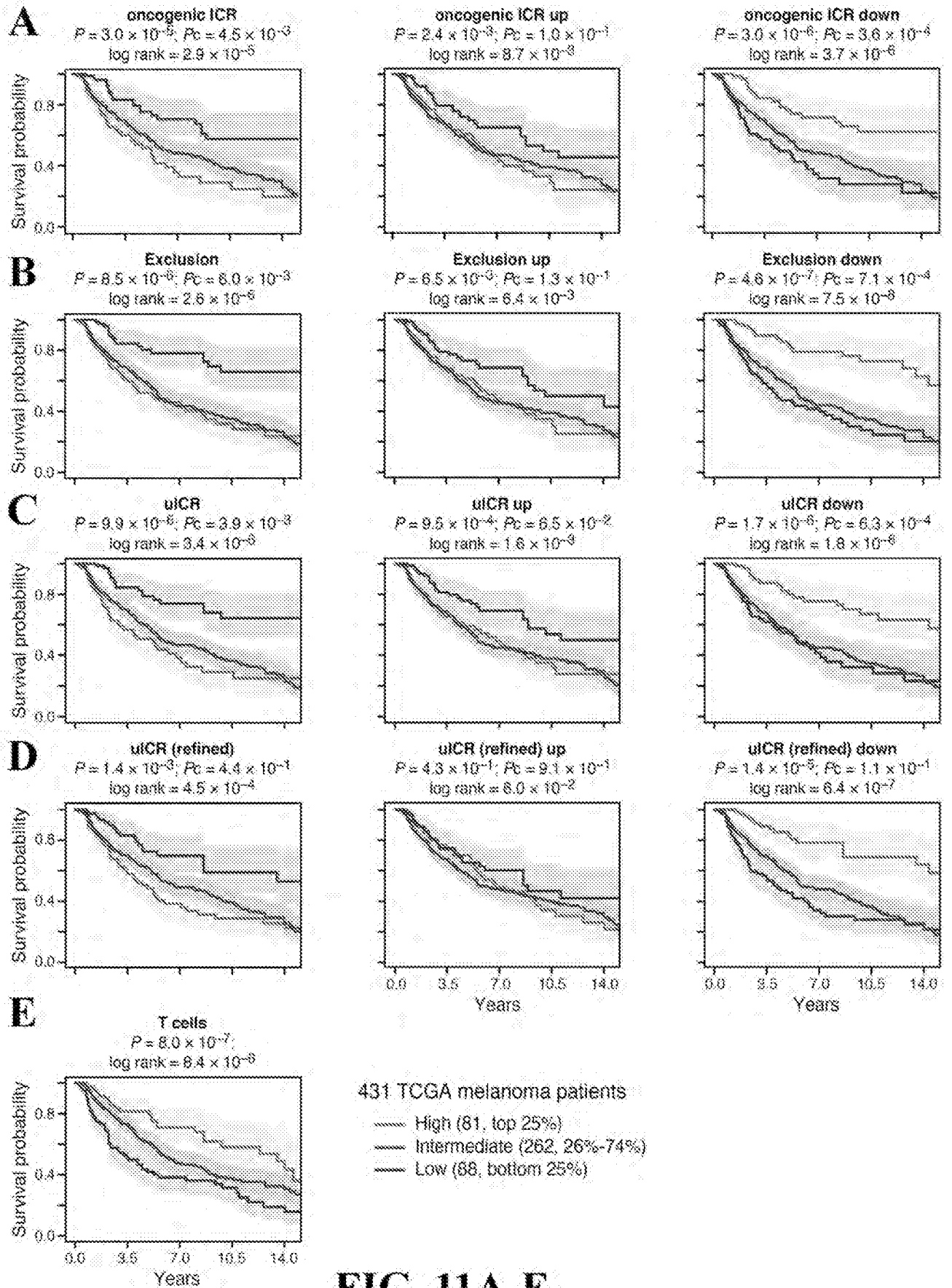


FIG. 11A-E

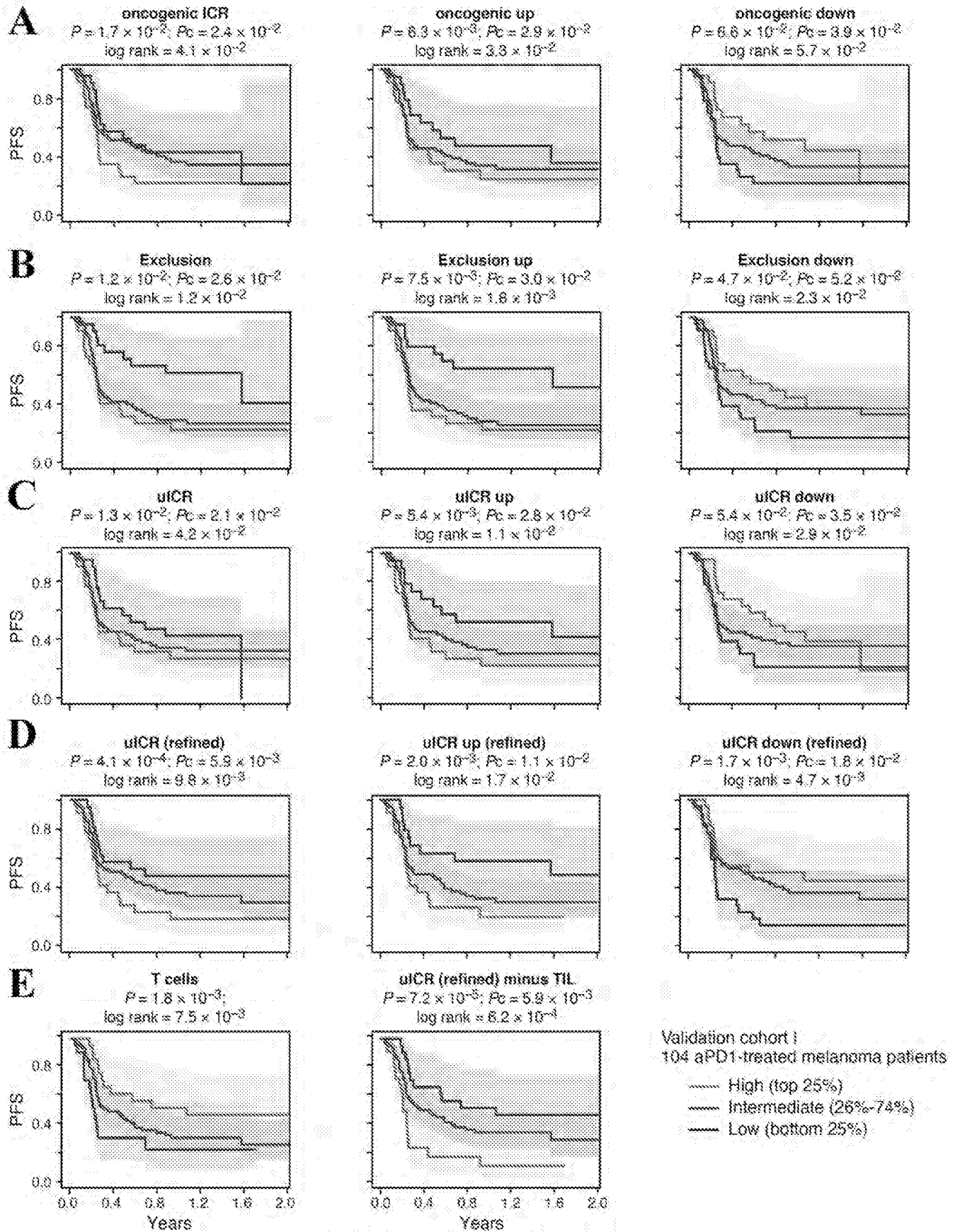


FIG. 12A-E

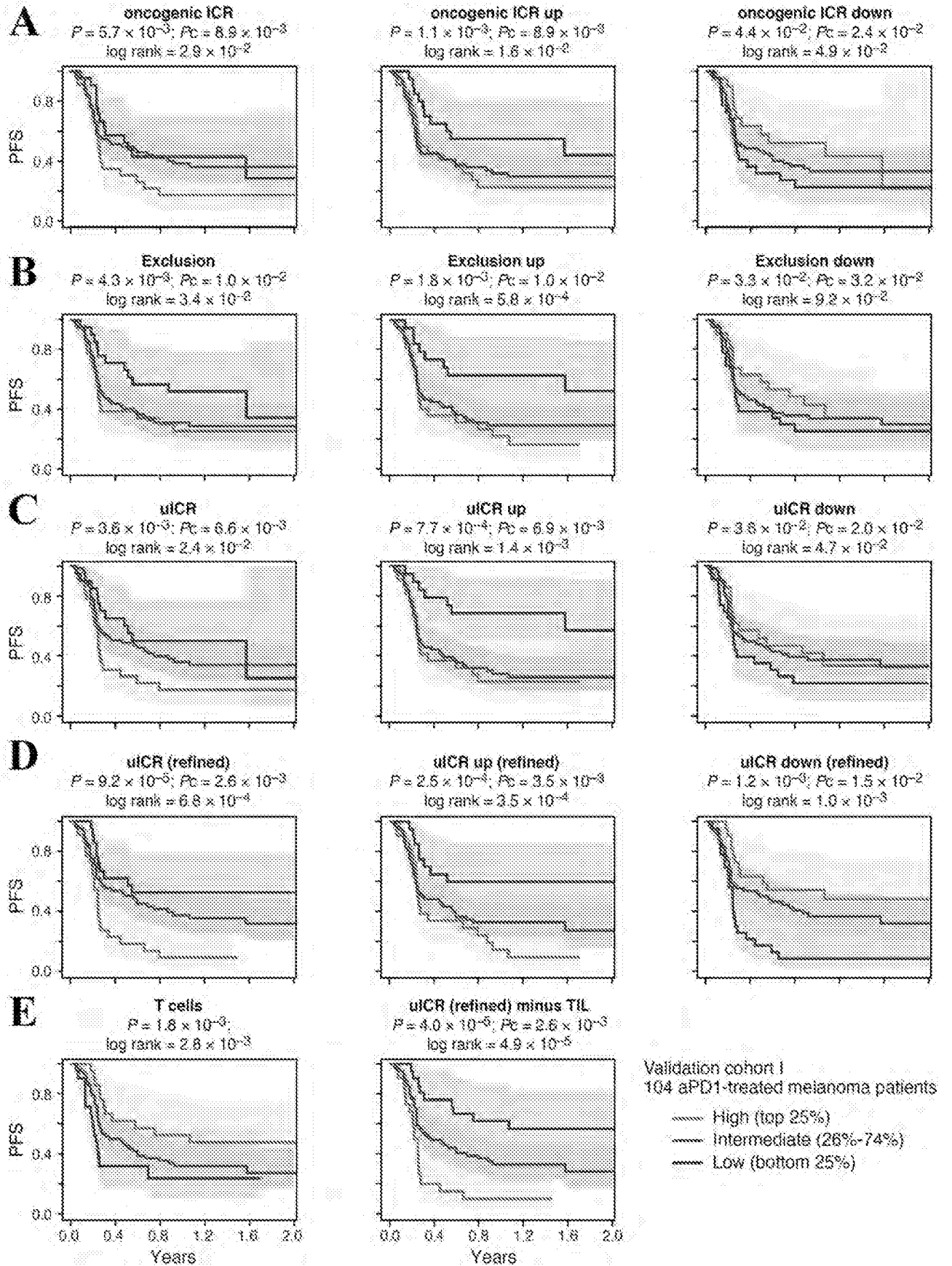


FIG. 13A-E

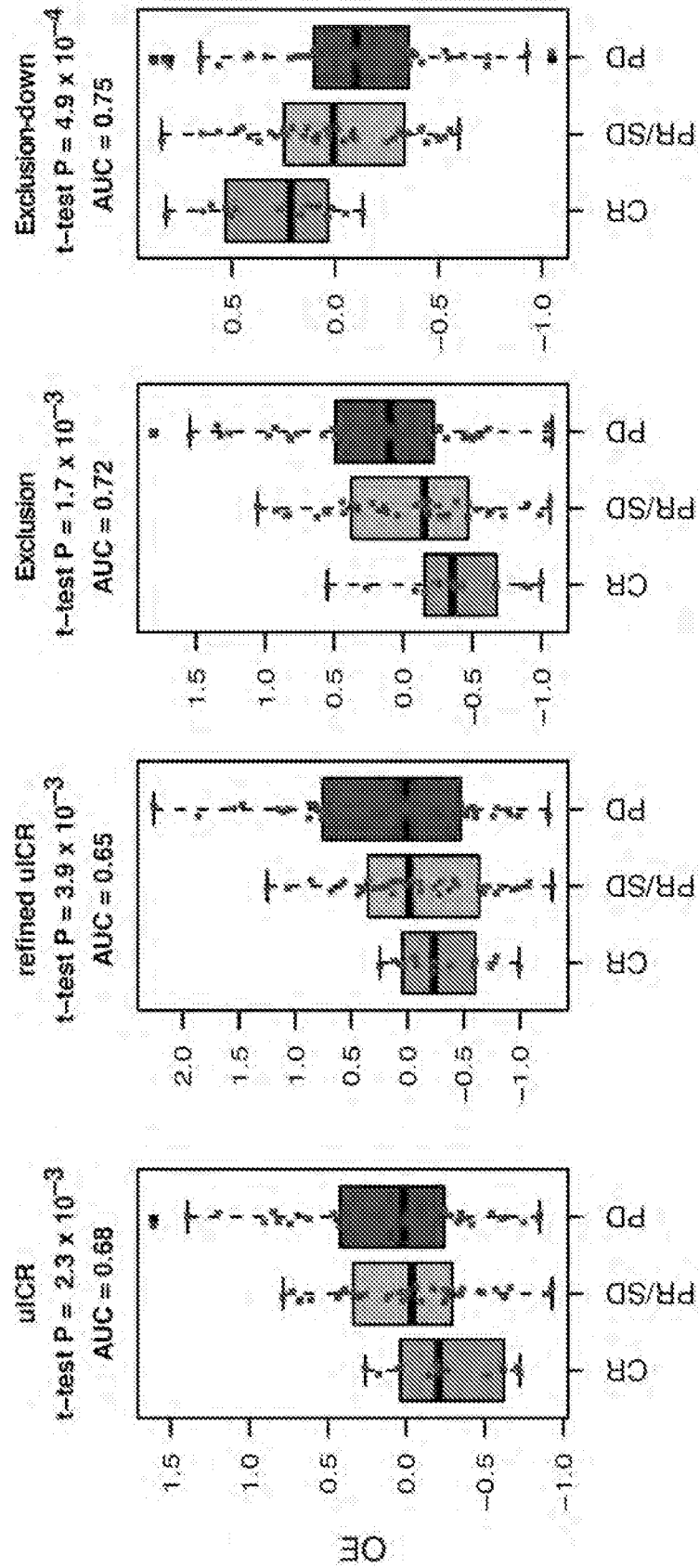


FIG. 14

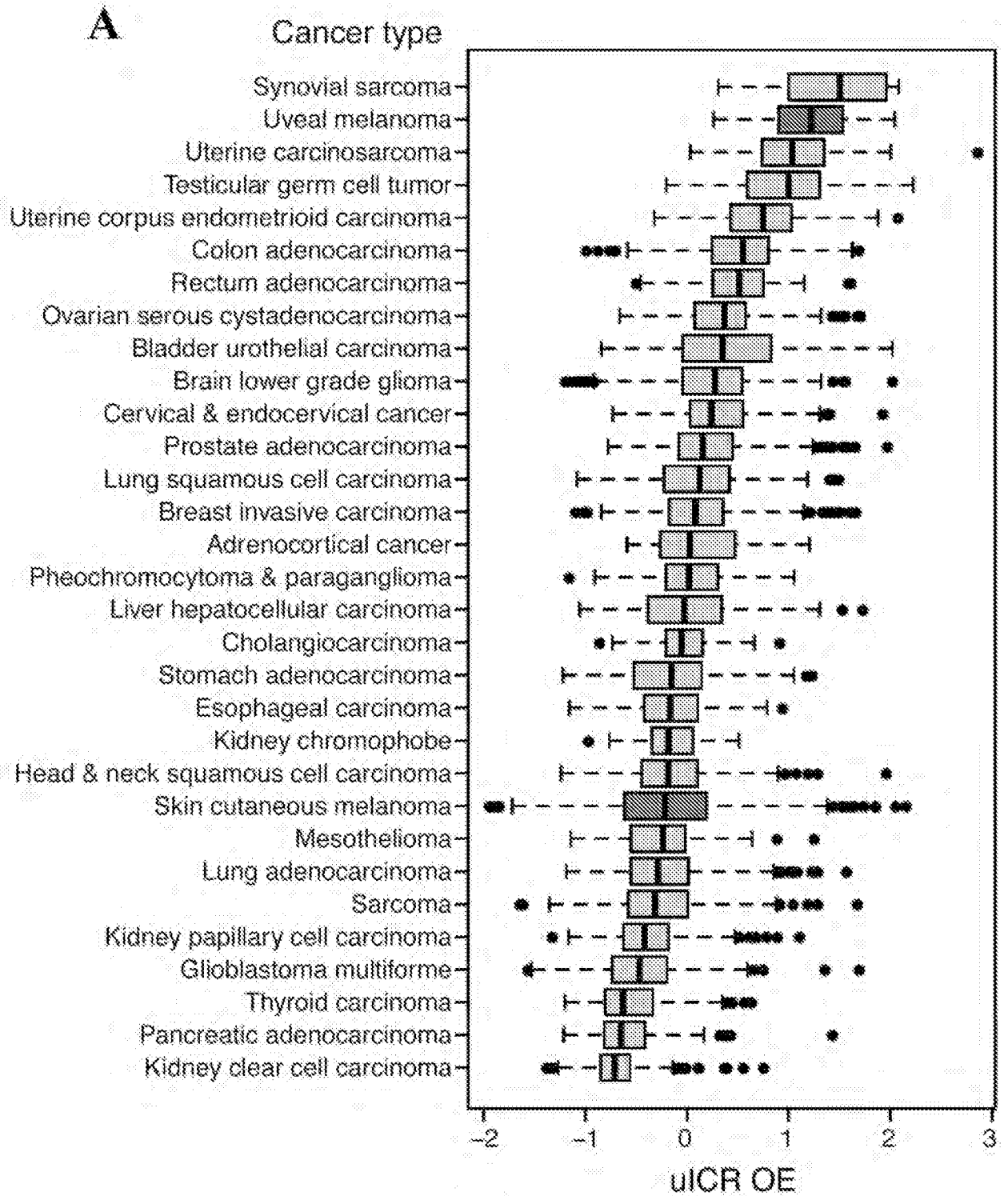


FIG. 15A

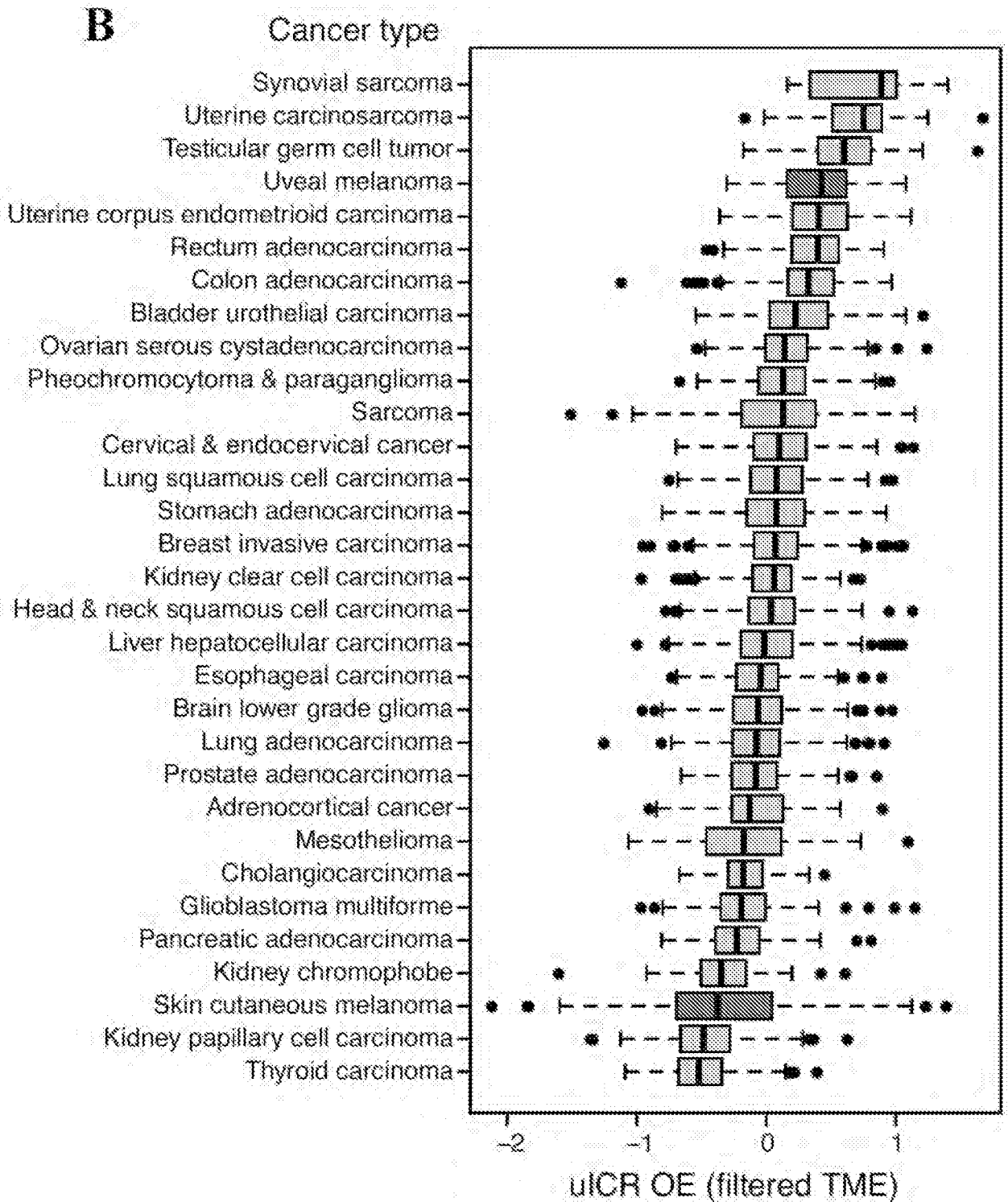


FIG. 15B

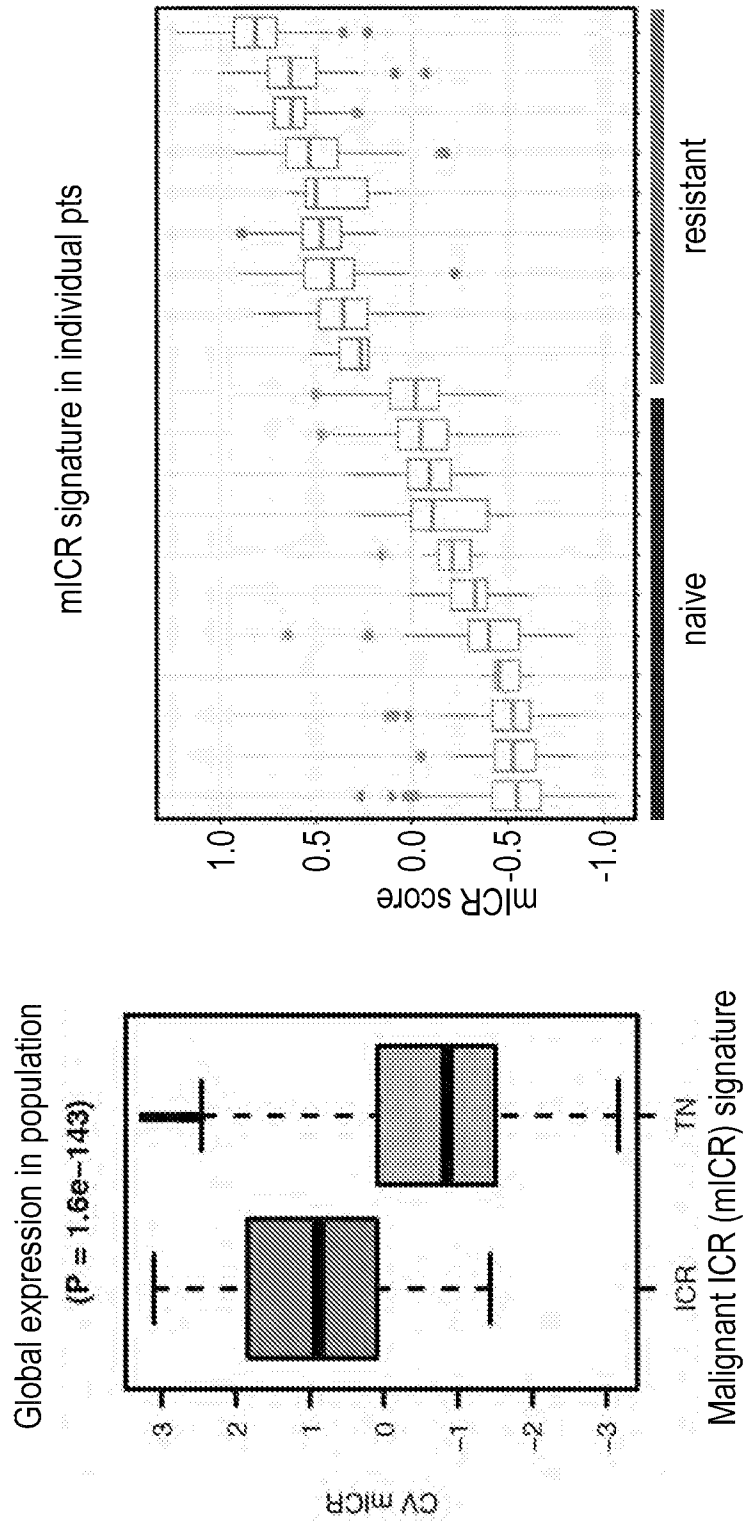
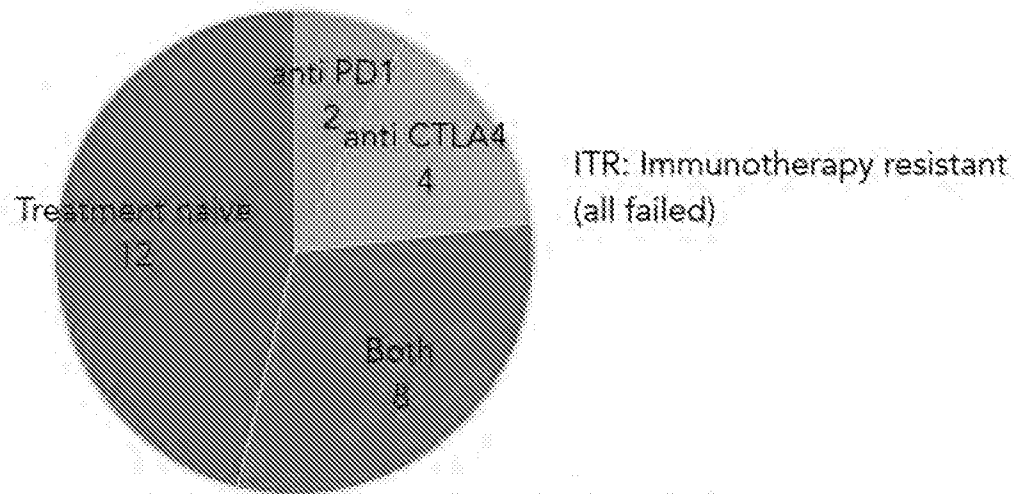


FIG. 16

Treatment naive vs. immunotherapy resistant (ITR) patients



26 tumors (16+10); 11,800 cells (3,300+8,500)

FIG. 17

Treatment is the main source of *inter-tumor* variation in
malignant cells

$$P < 1.46 \times 10^{-173}$$

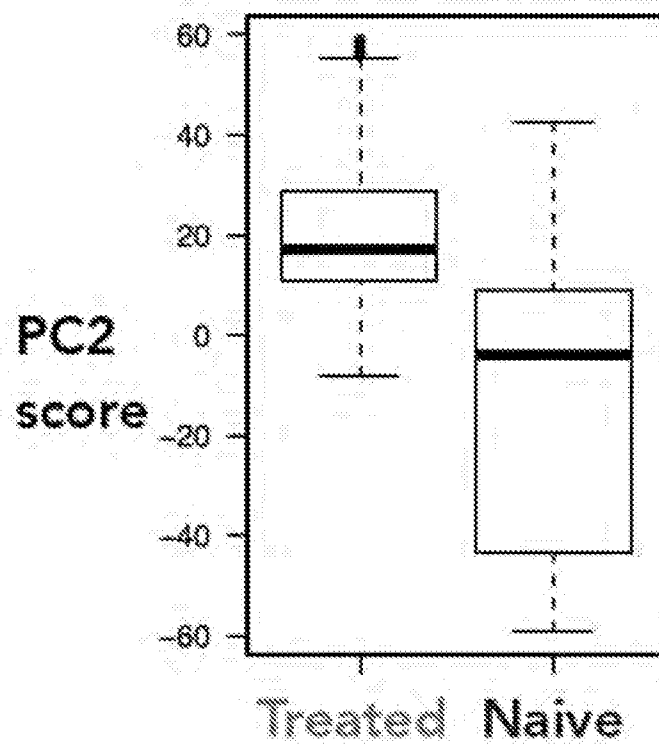


FIG. 18

Treated
Untreated

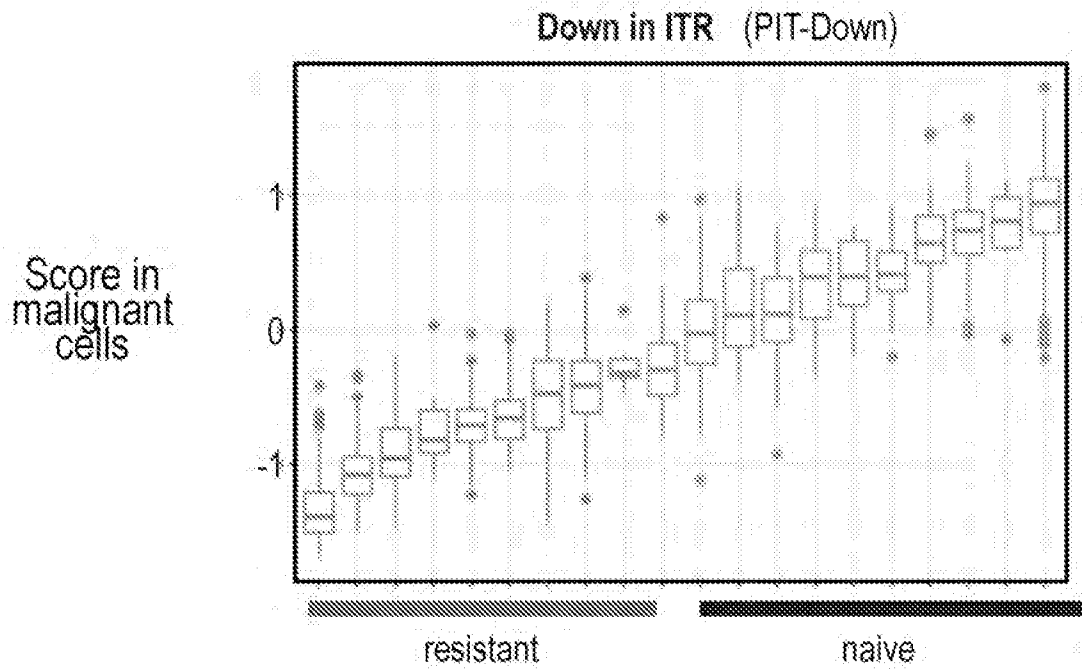
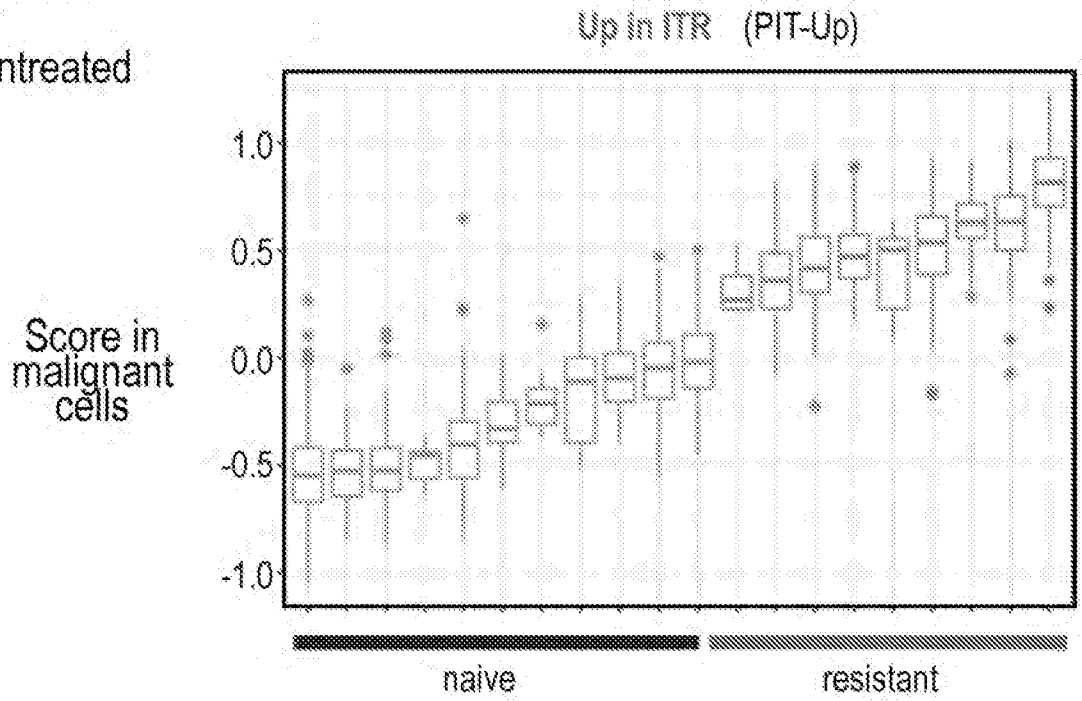
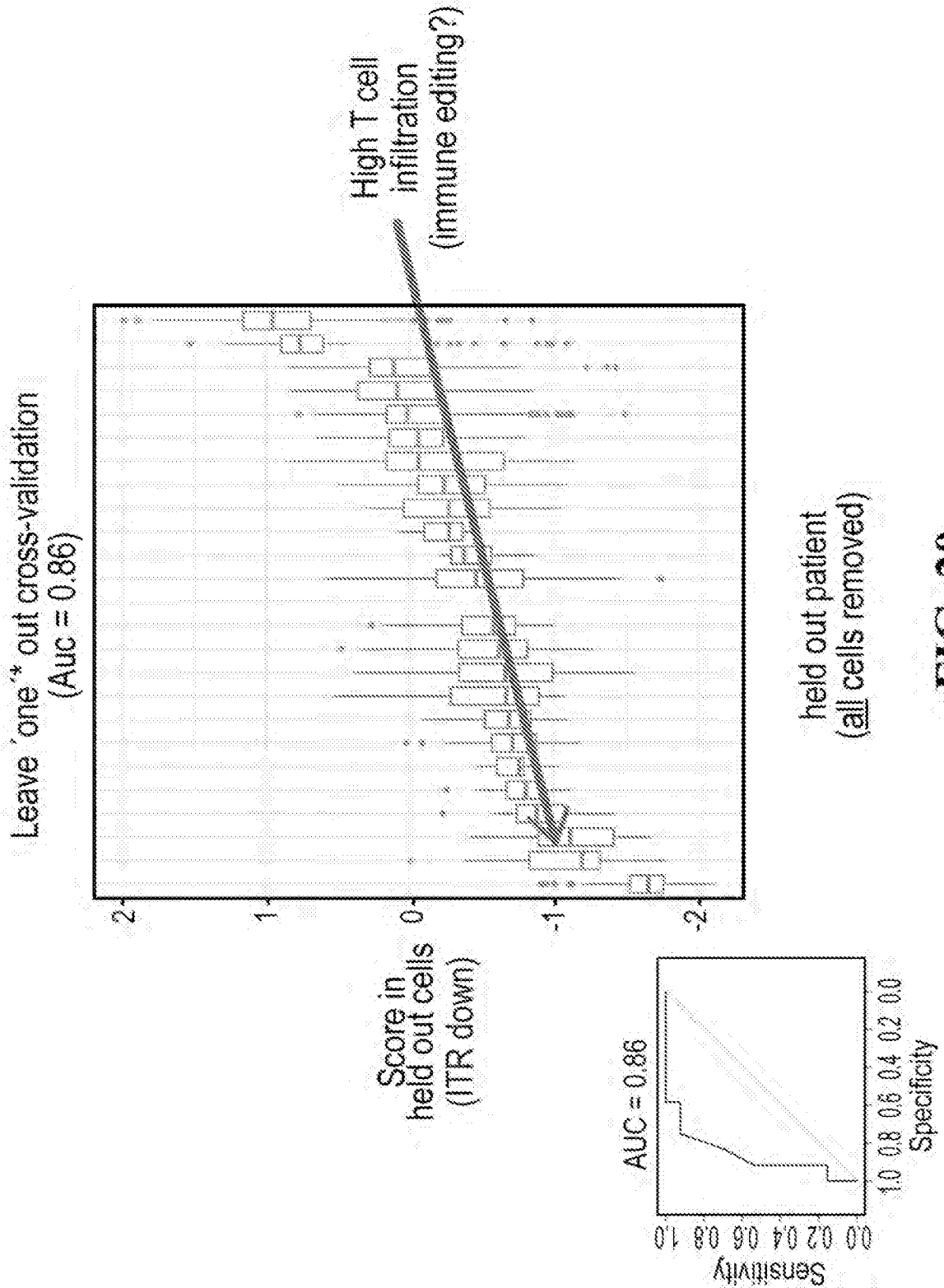


FIG. 19



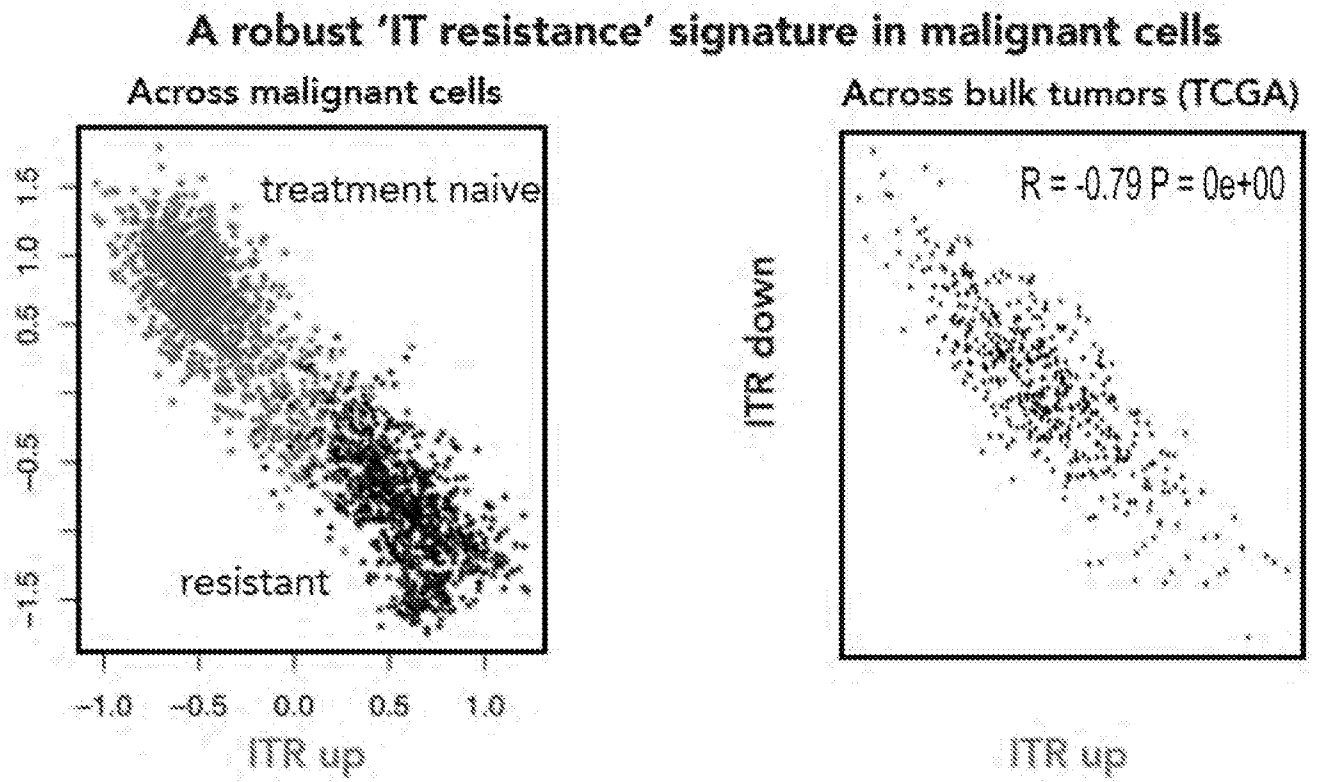


FIG. 21

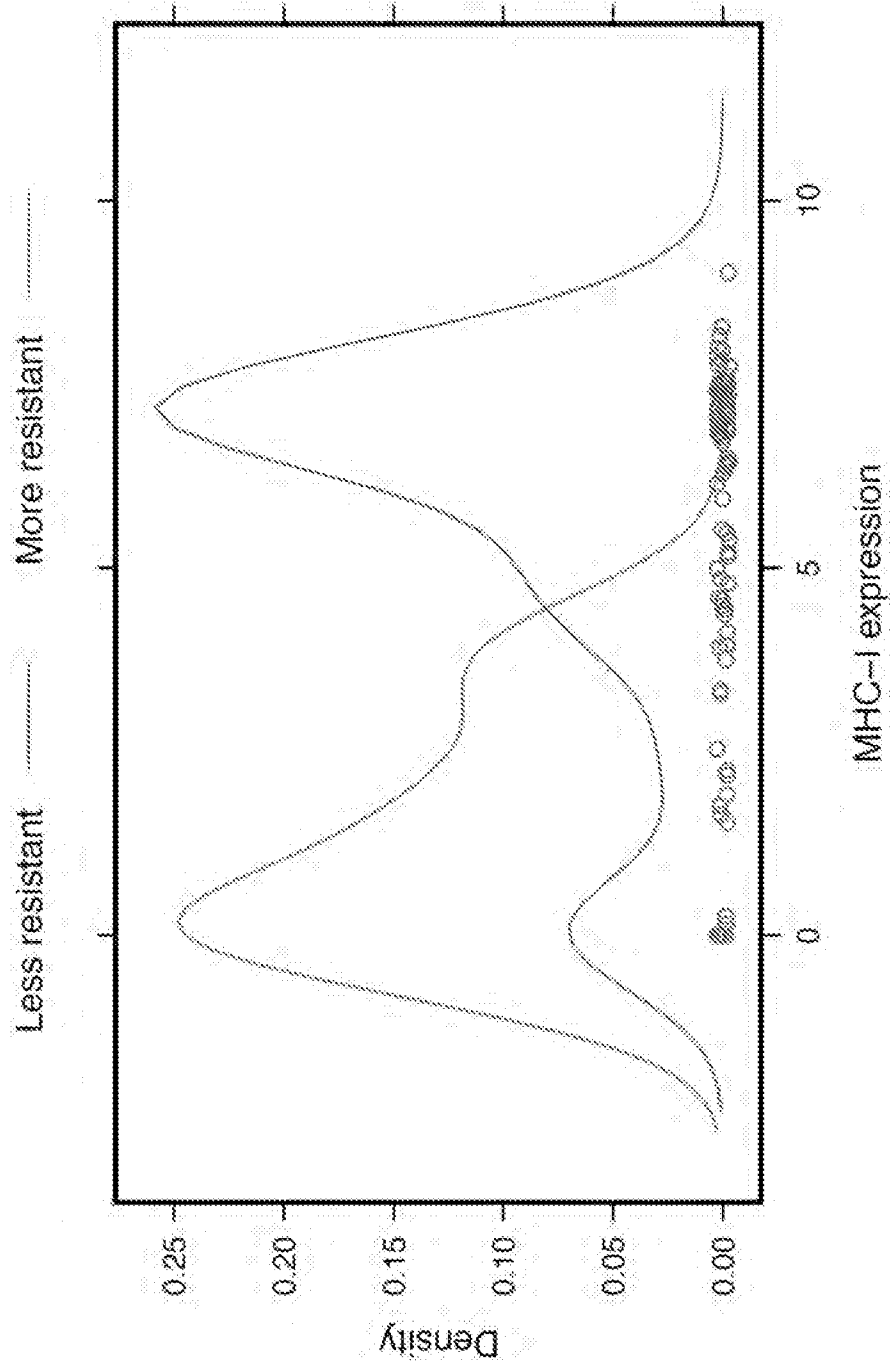


FIG. 22

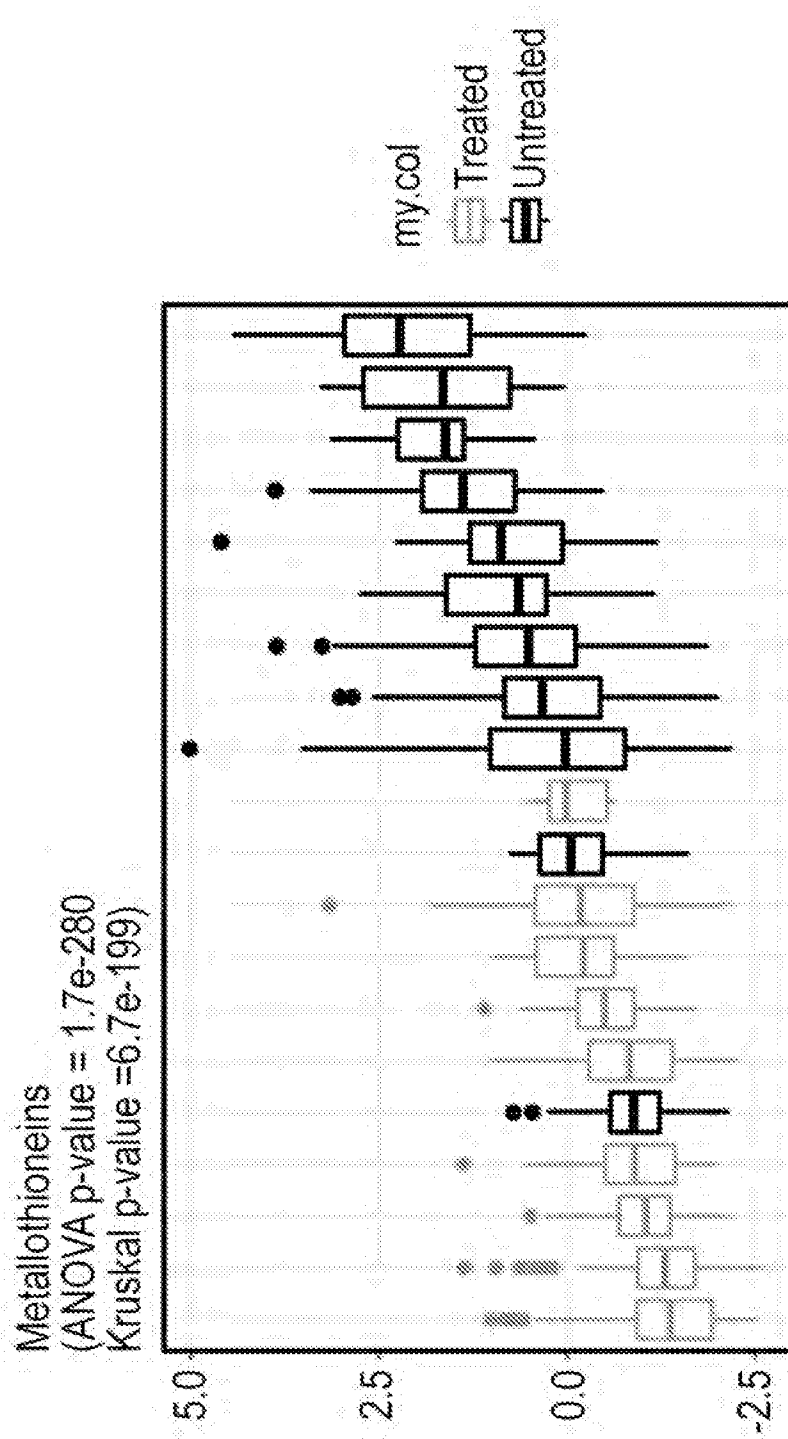


FIG. 23

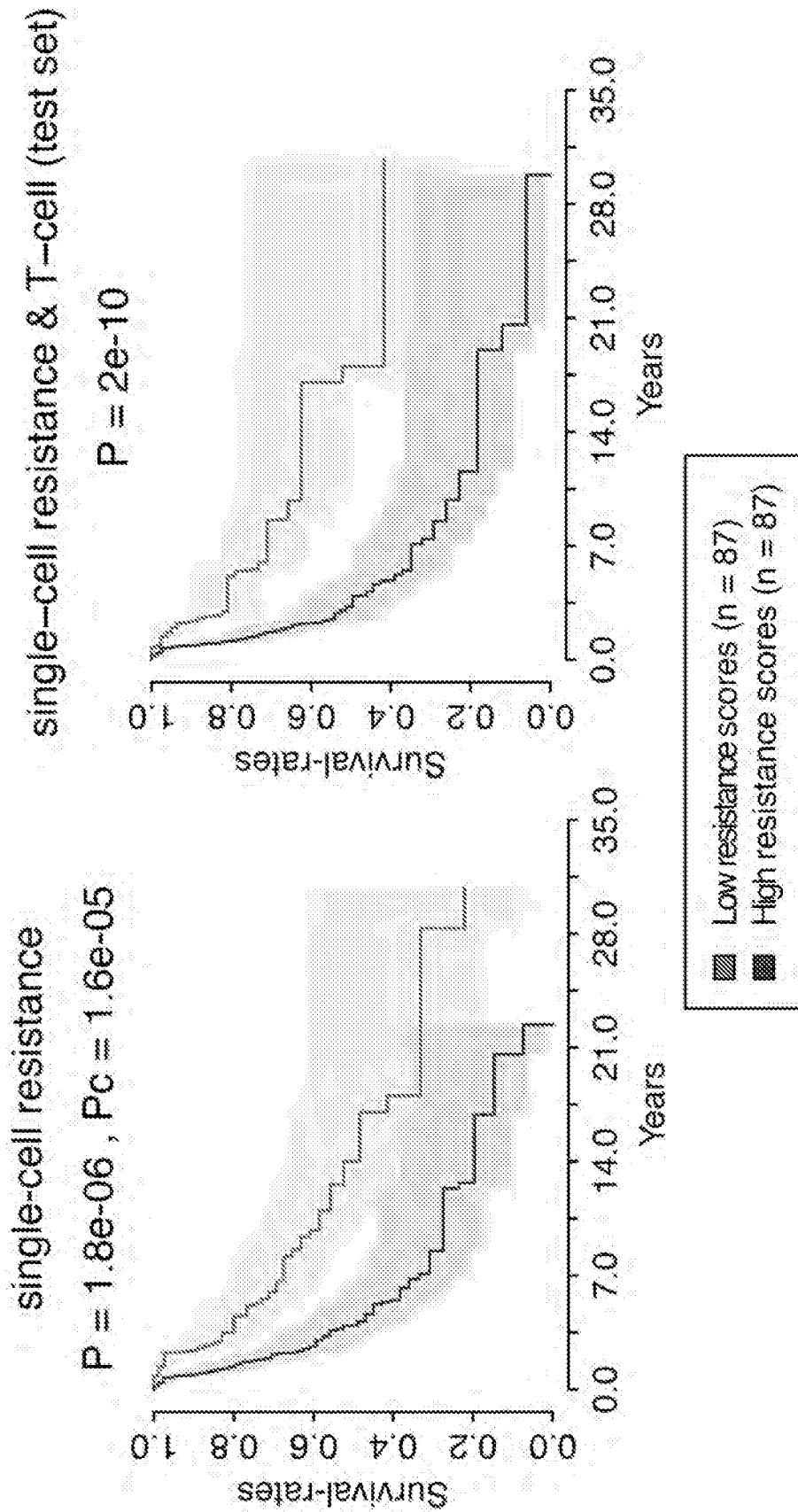


FIG. 24

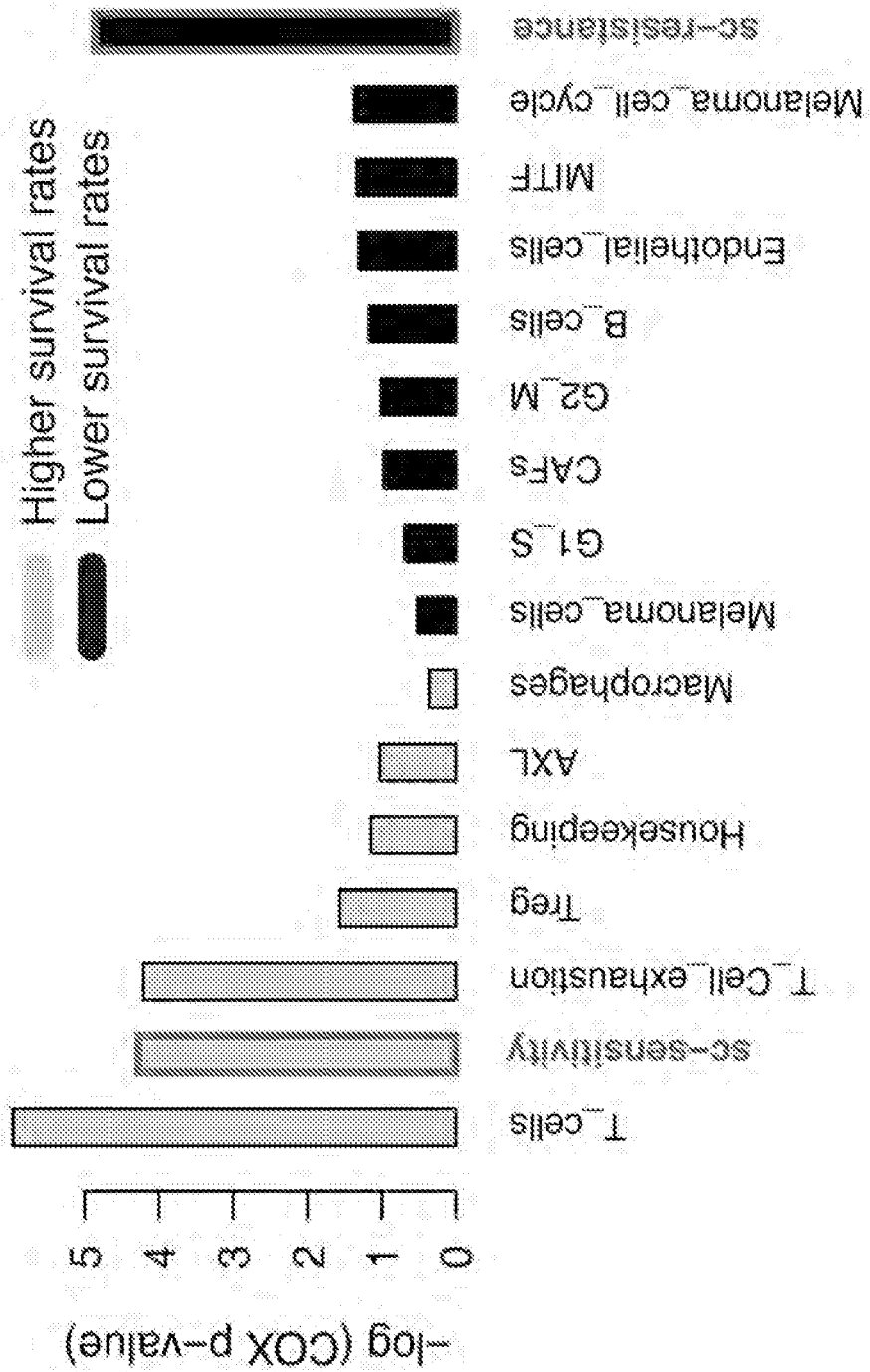


FIG. 25

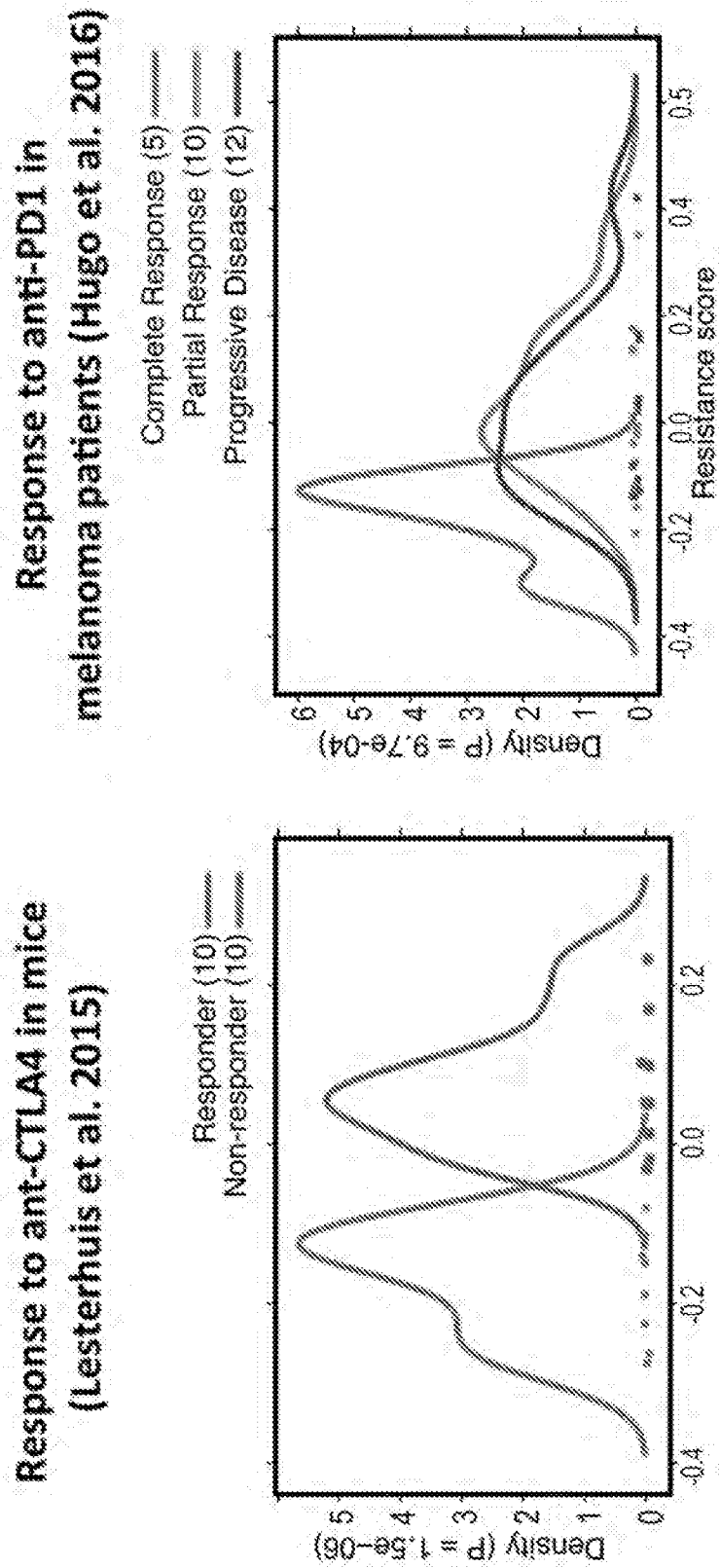


FIG. 26

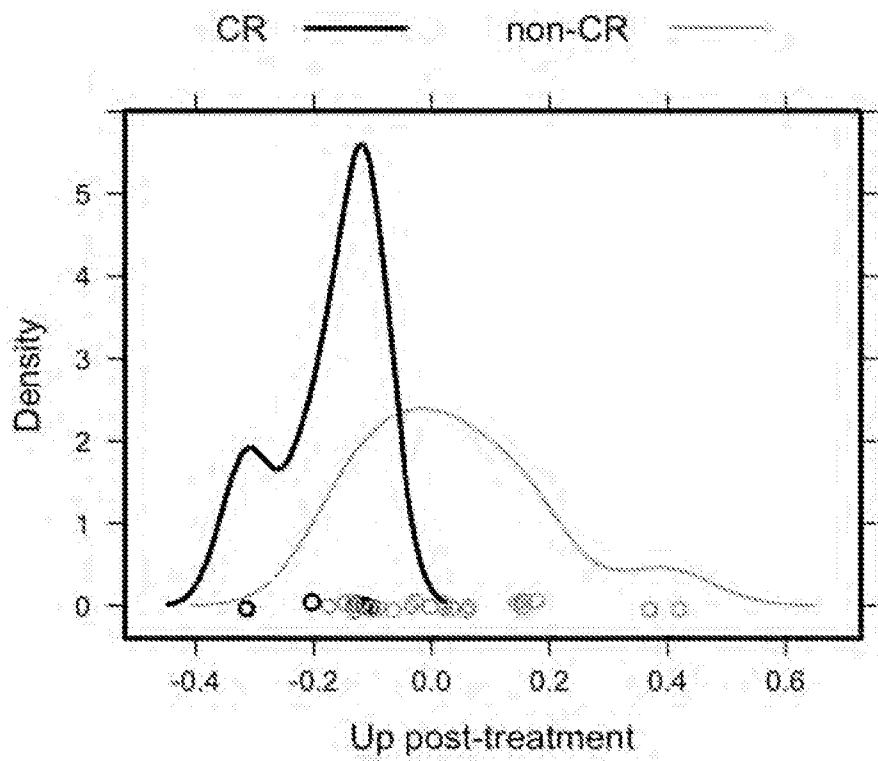


FIG. 27

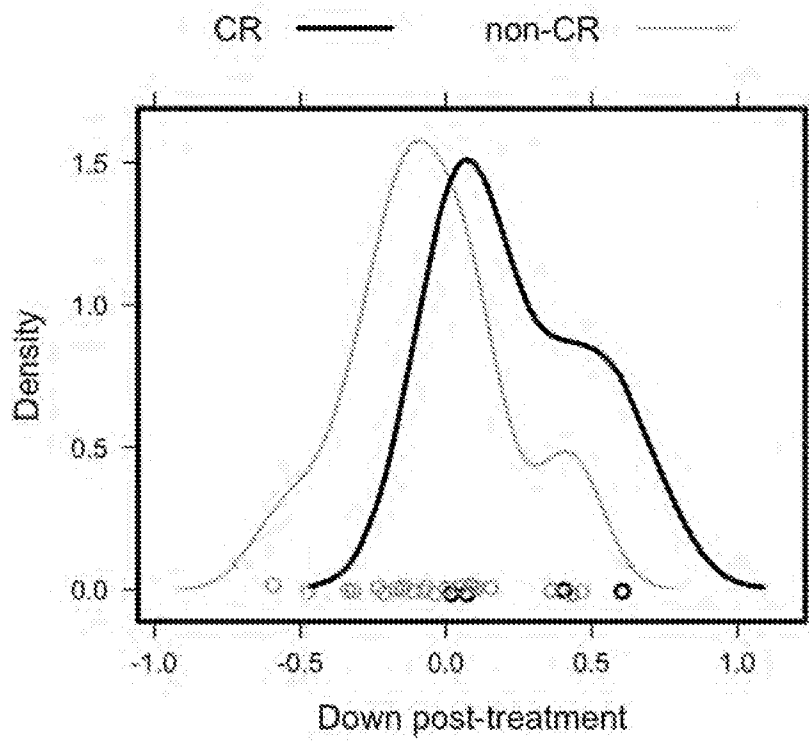


FIG. 28

**Malignant cells ITR have higher exclusion signatures;
treatment naïve have higher infiltration signatures**

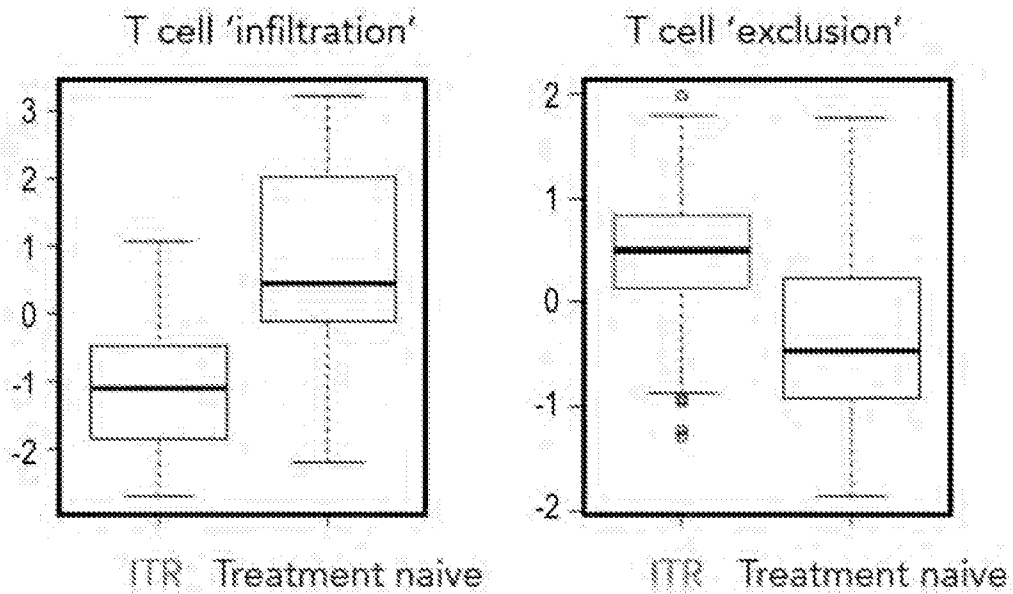


FIG. 29

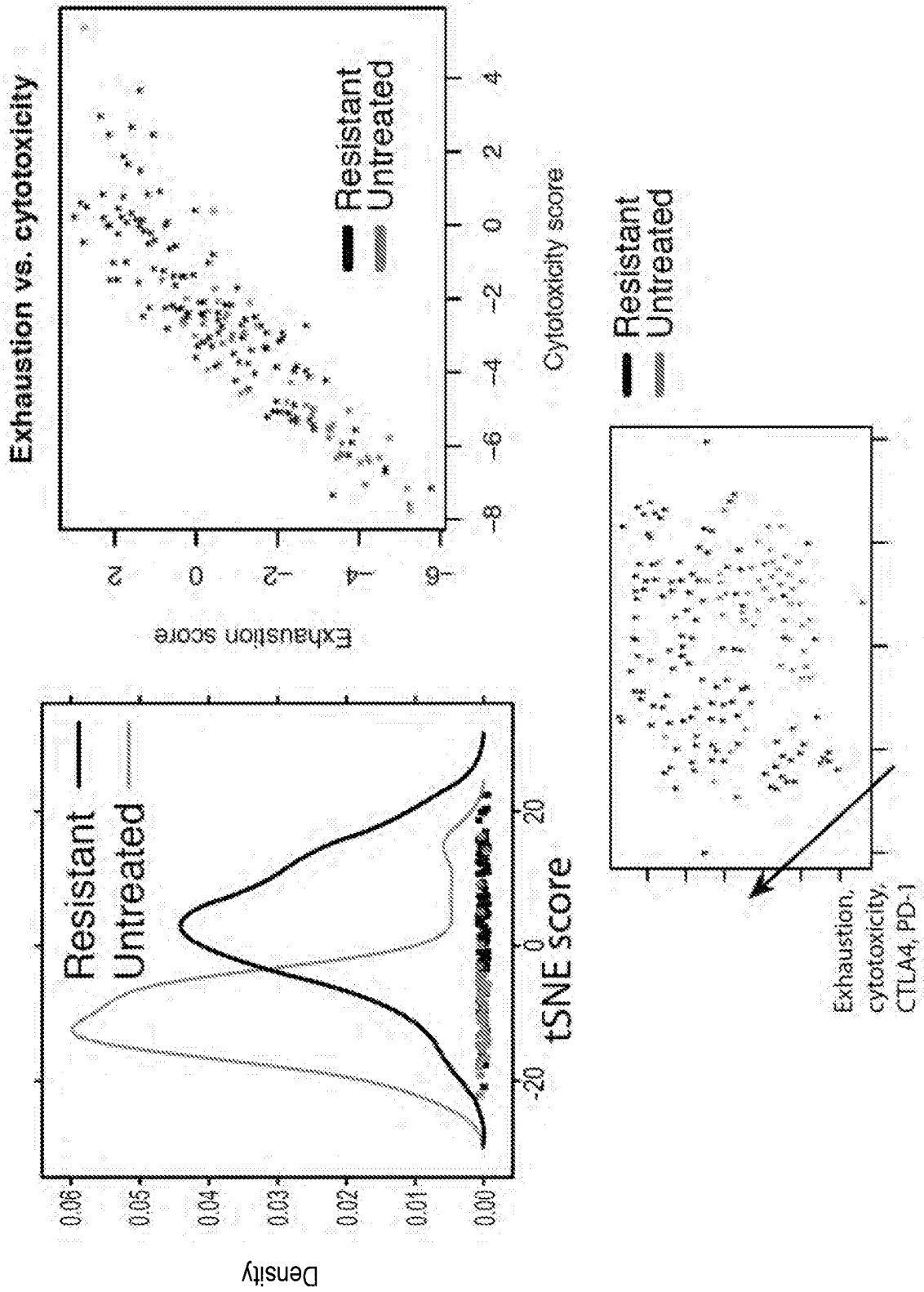


FIG. 30

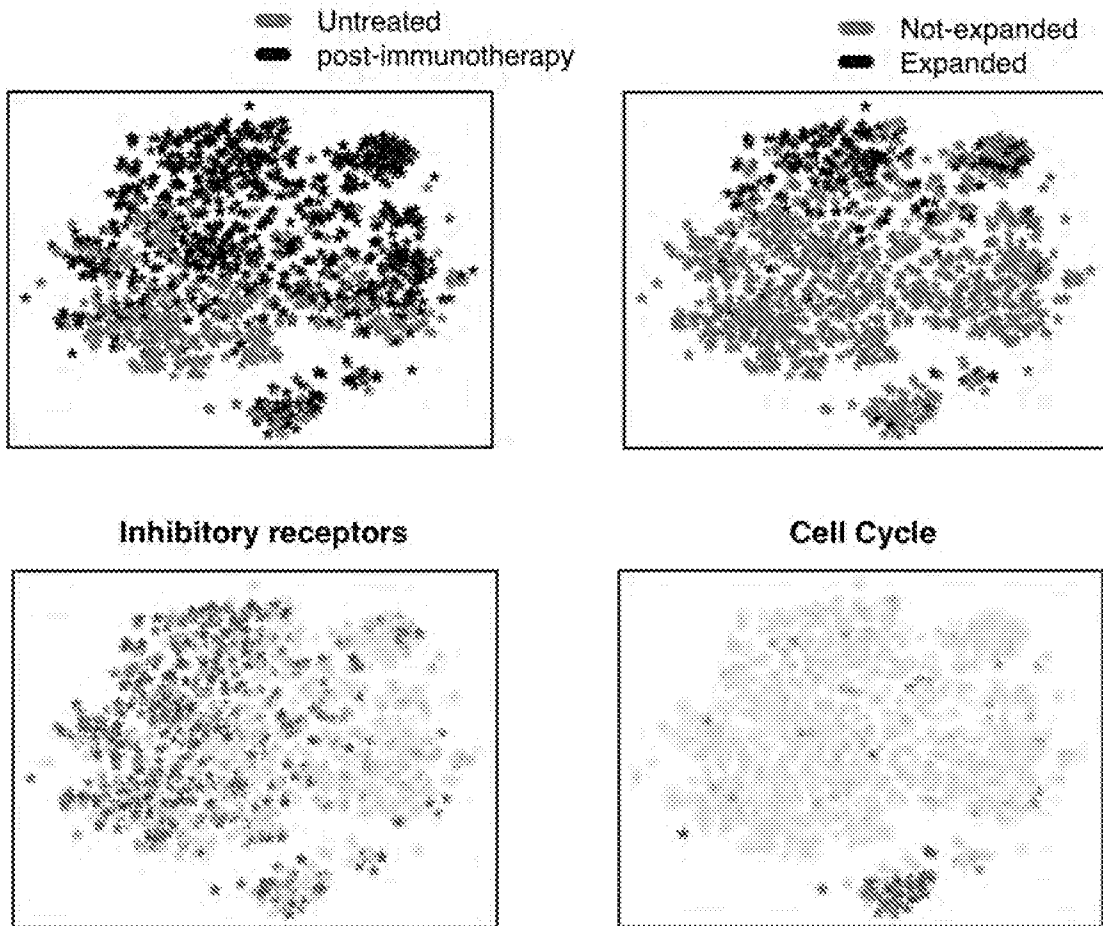
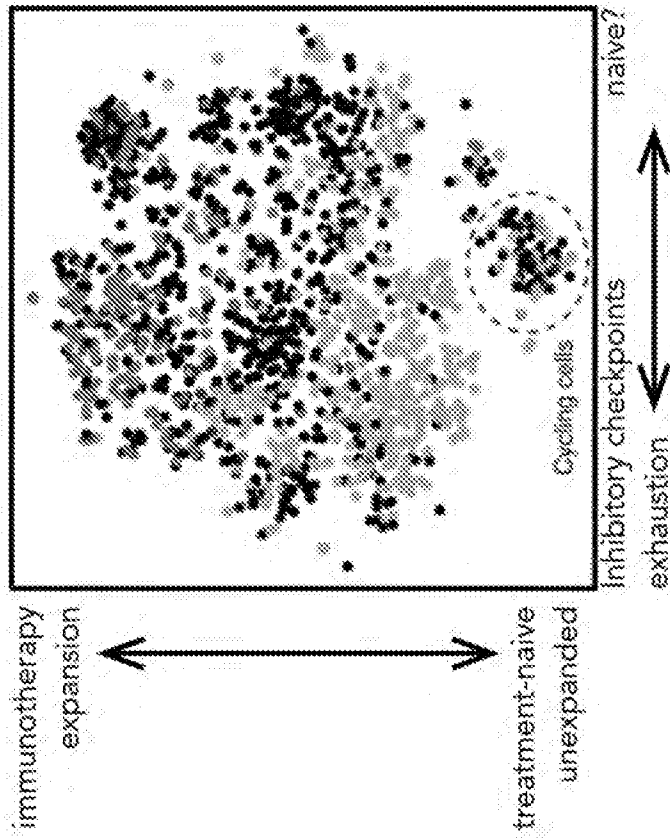


FIG. 31

Major changes in T cell programs post immunotherapy

113 clones by TcR; 3 @ >20 cells, all in treated patients

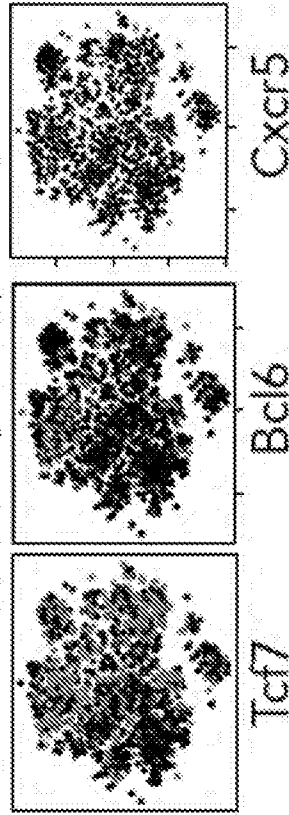


- ITR; expanded
- ITR; not expanded
- Treatment naive; expanded (v few)
- Treatment naive; not expanded

Tcf7⁺Bcl6⁺(Cxcr5⁺) expanded ITR

Mouse: Im et al., Nature 2016, R. Ahmed lab

$P = 2.09 \times 10^{-10}$ (3.41×10^{-3})



co-inhibitors (PDL1, TIM3, CTLA4, TIGIT, LAG3, HVEM)

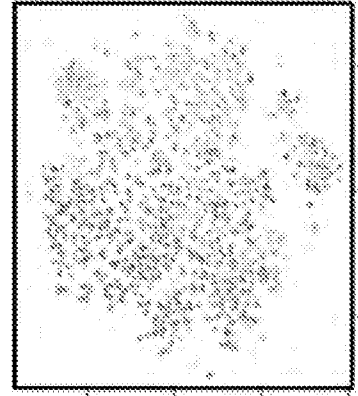


FIG. 32

CD8 ITR signature is strongly associated with clonal expansion

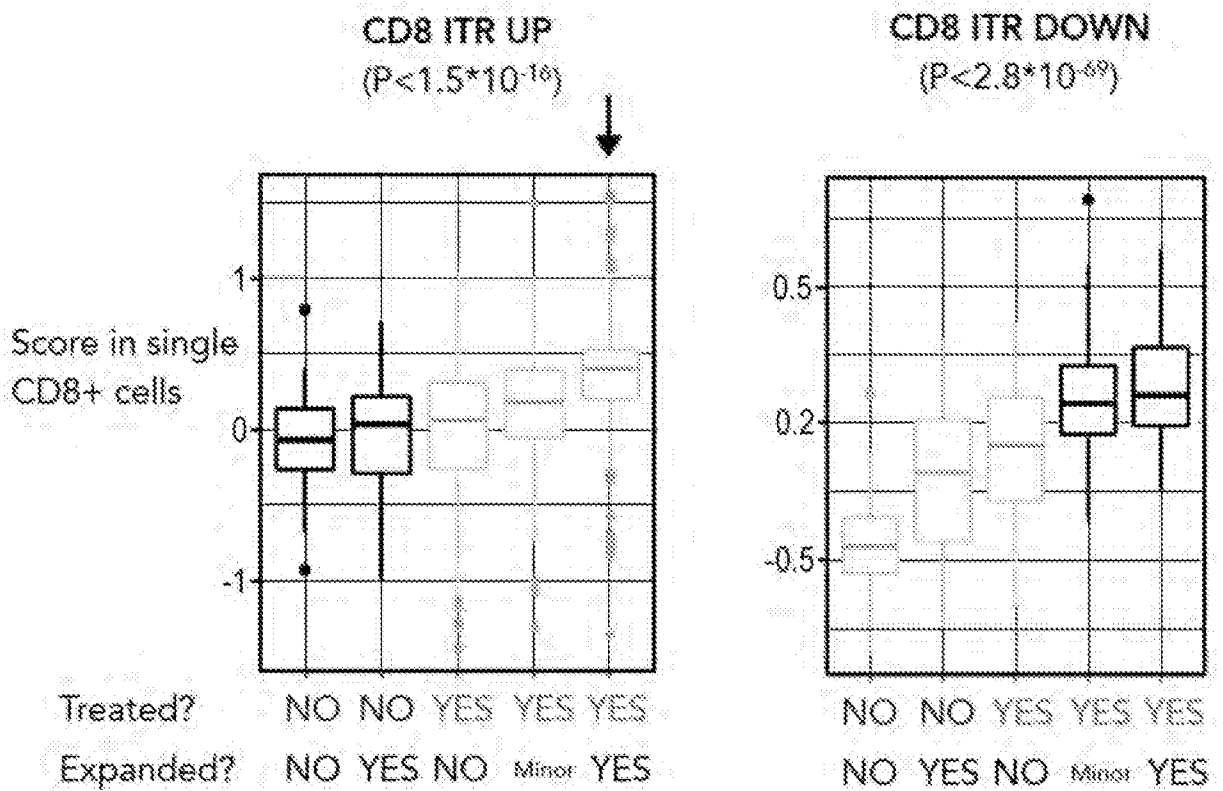


FIG. 33

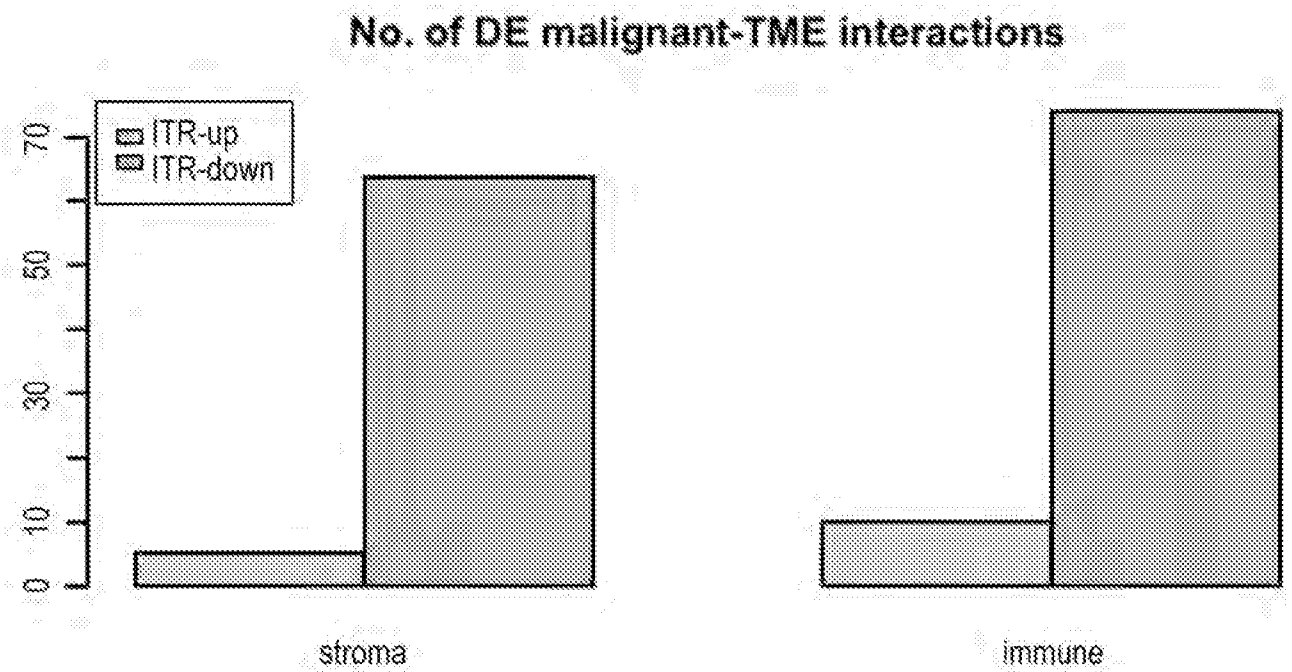


FIG. 35

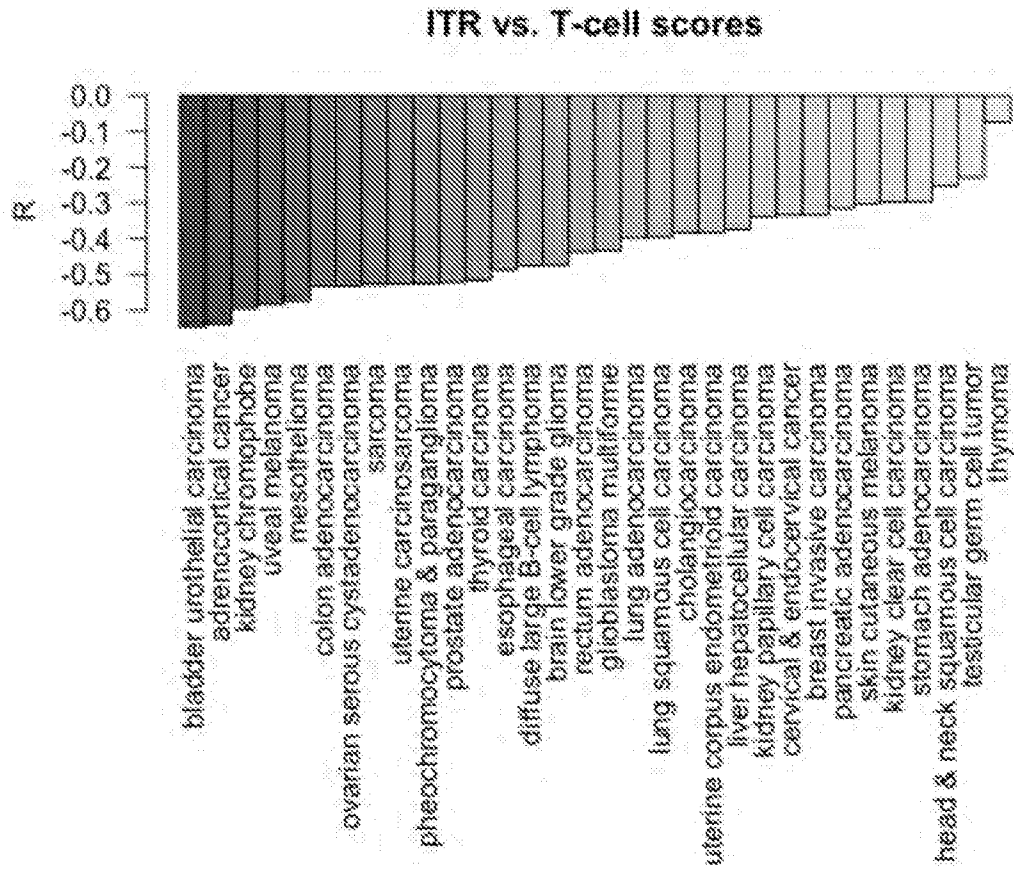


FIG. 36

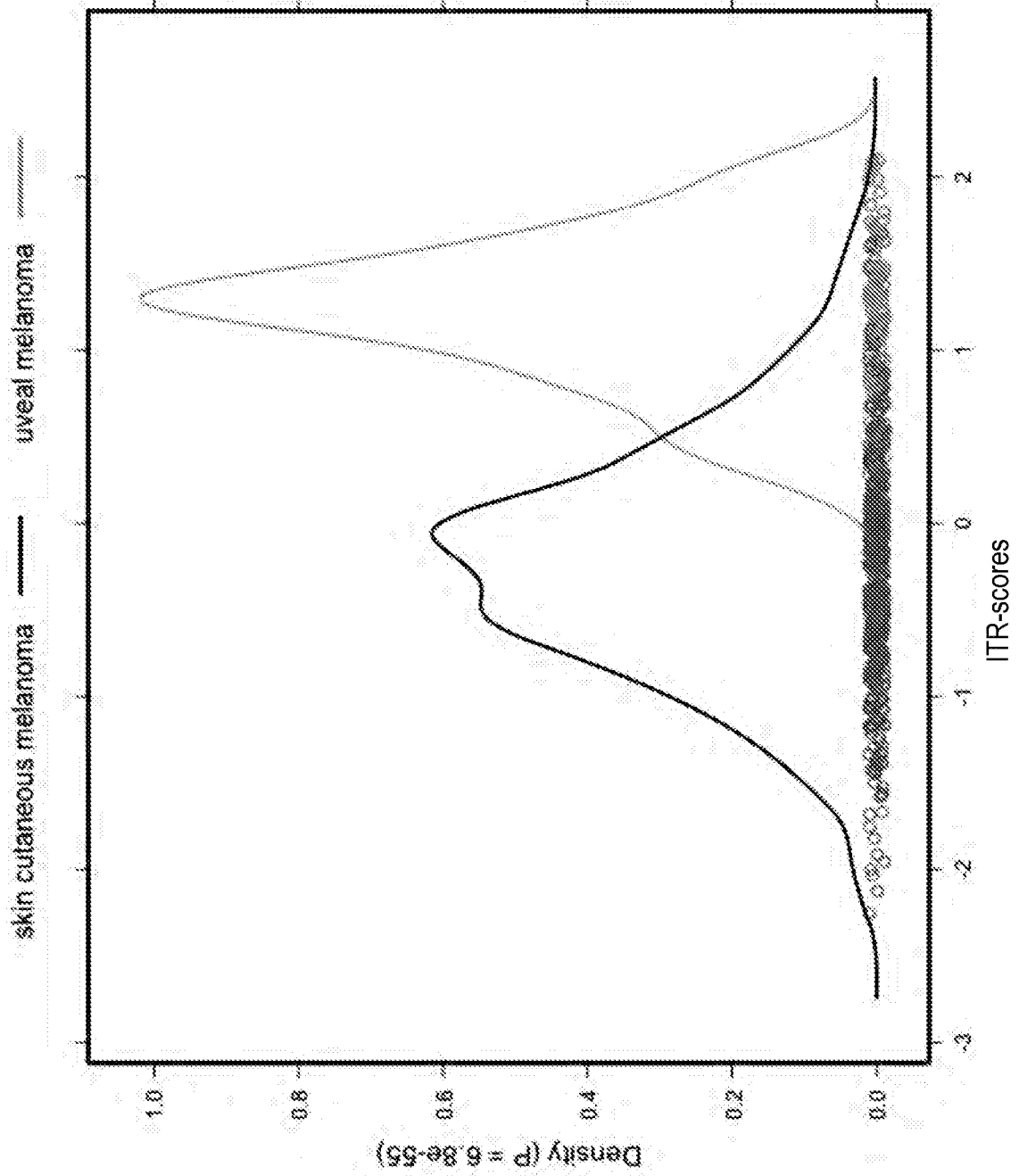


FIG. 37

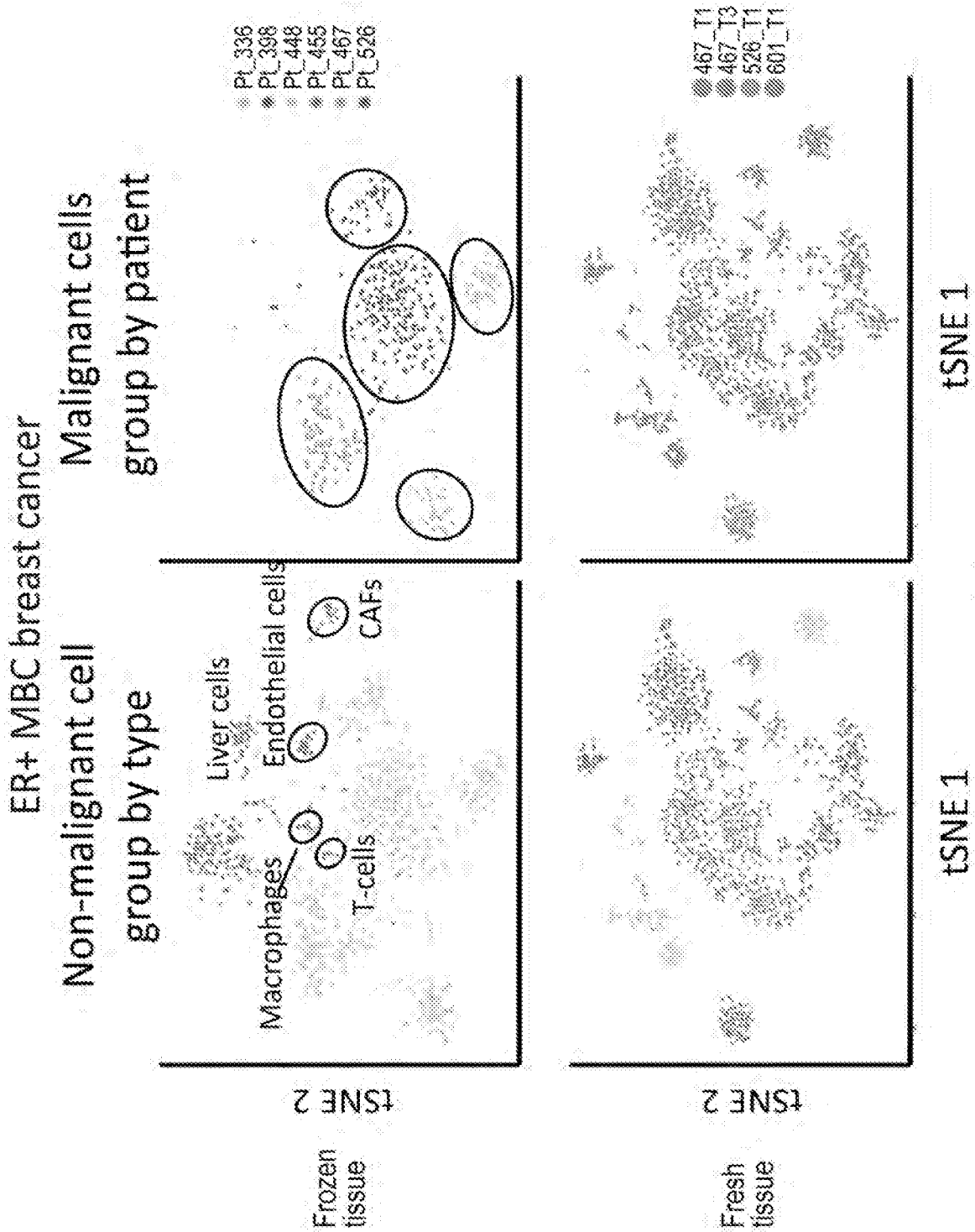


FIG. 38

Colon cancer

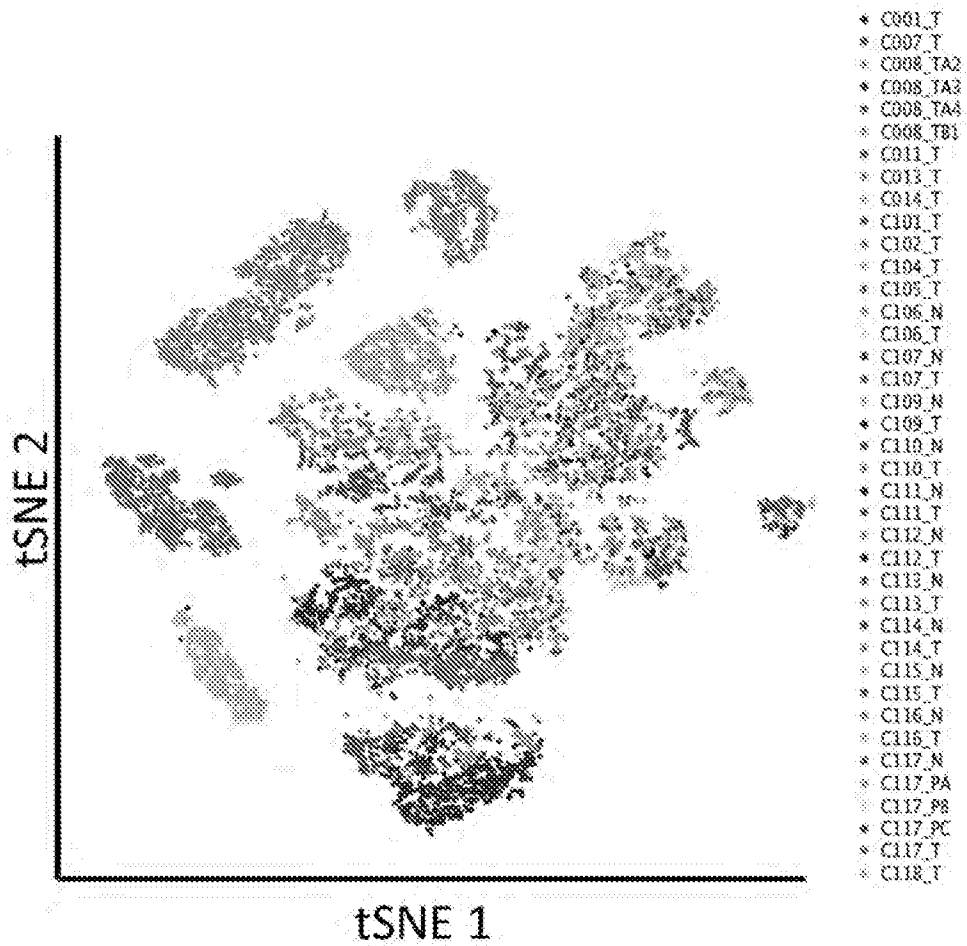


FIG. 39

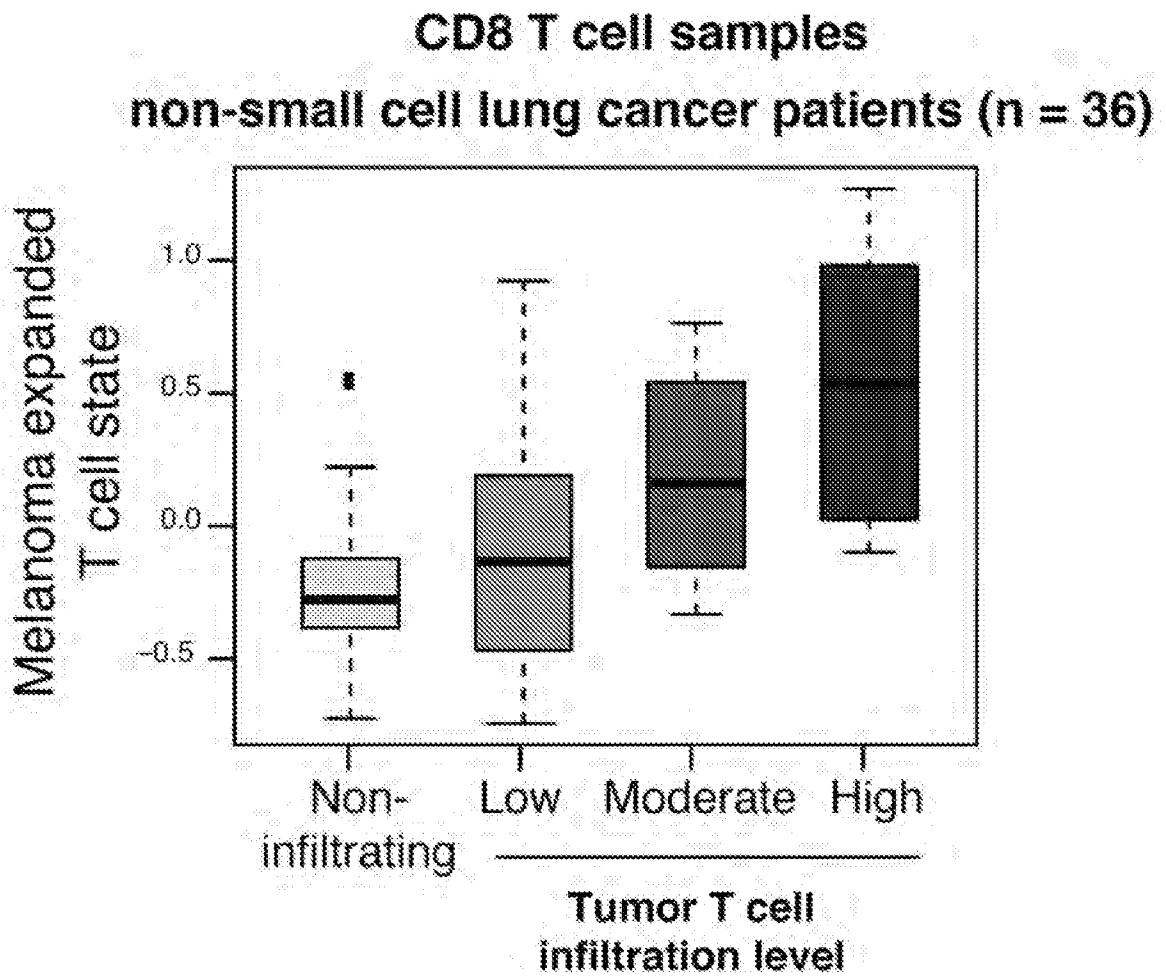


FIG. 40

CDK4/6 inhibitors sensitize melanoma cells

- Short term melanoma culture (P = 4.4e-23) ✓
- Melanoma cell lines
 1. IGR37 (P = 1.7e-36) ✓
 2. UACC257 (P = 4.9e-240) ✓
 3. A2058 (RB1-deficient) (P = 1) X

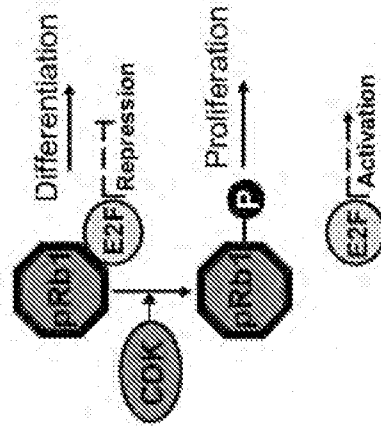


FIG. 41

CDK4/6 inhibitors induce markers of differentiation, senescence and immunogenicity in melanoma

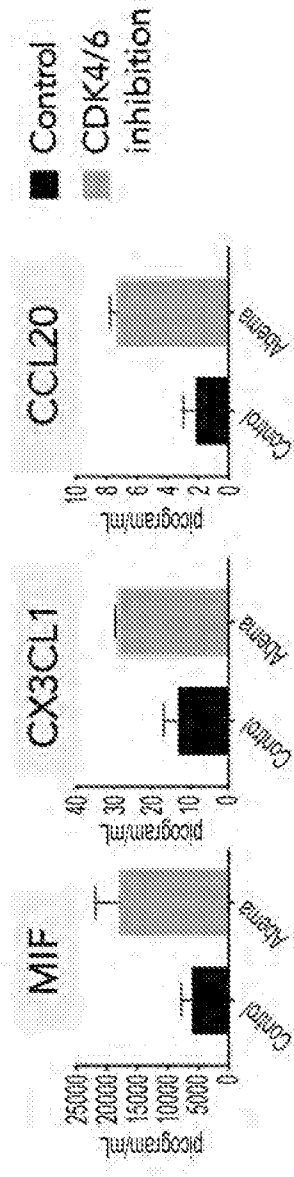
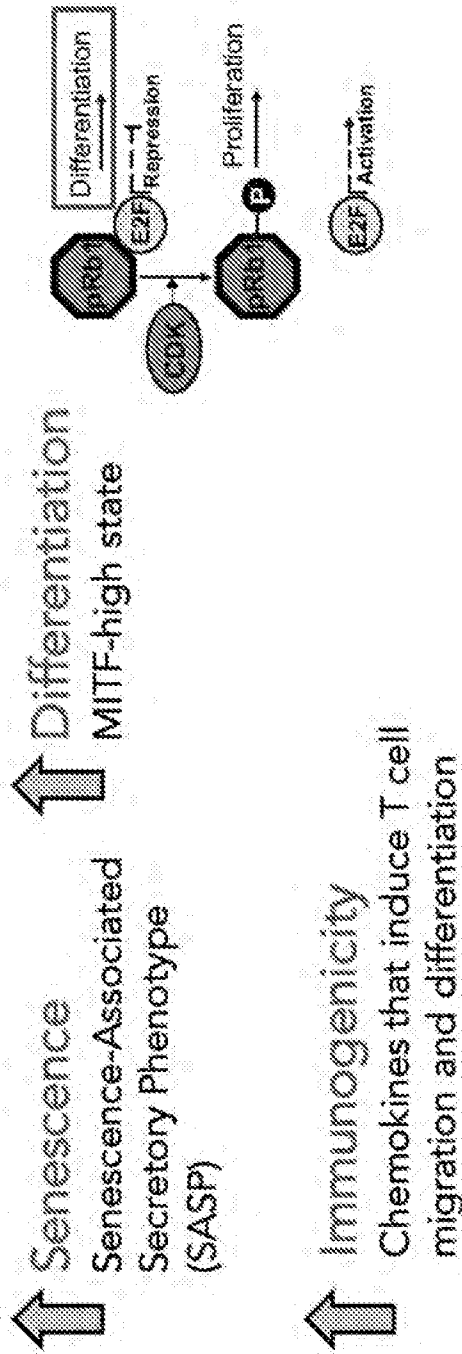


FIG. 42

CDK4/6 inhibitors eliminated a resistant subpopulation

Melanoma cells (IGR37)

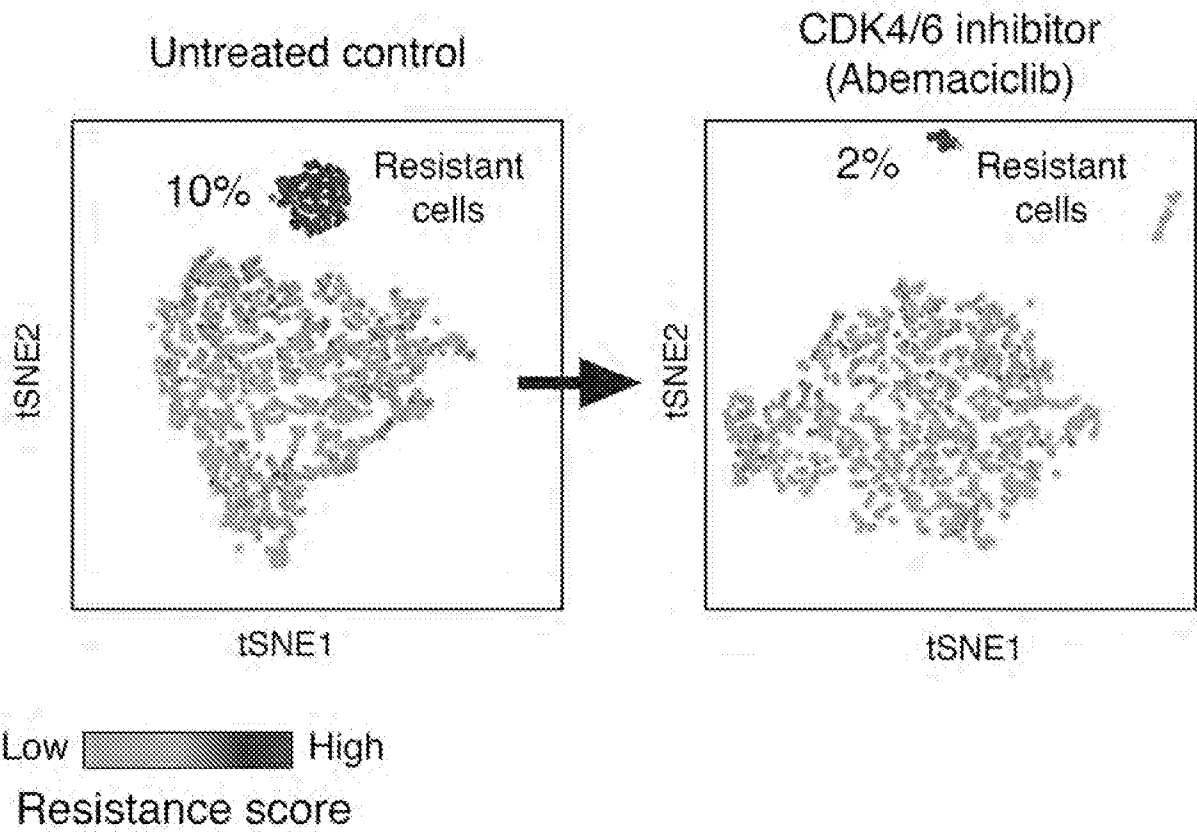


FIG. 43

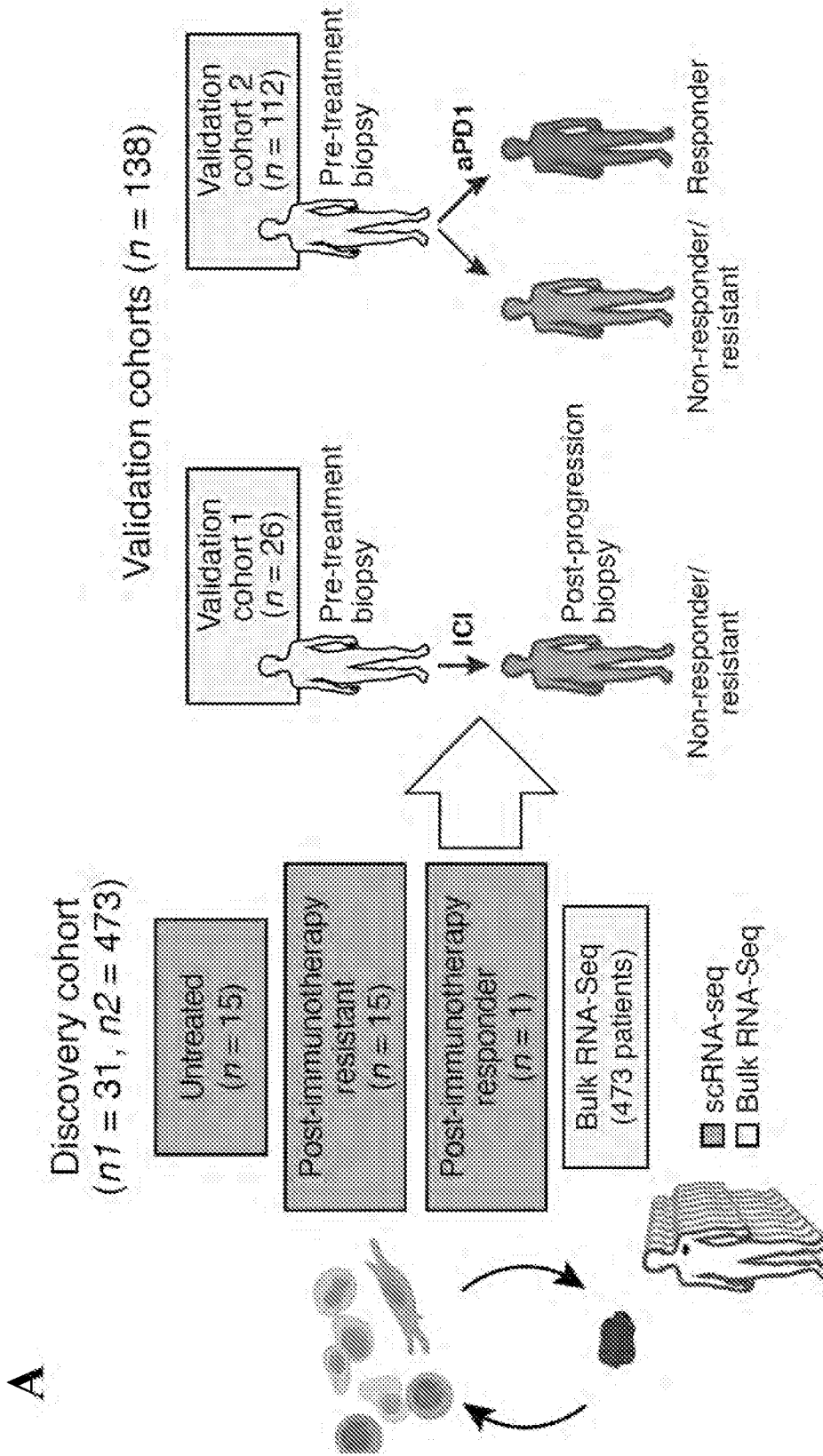


FIG. 44A

B

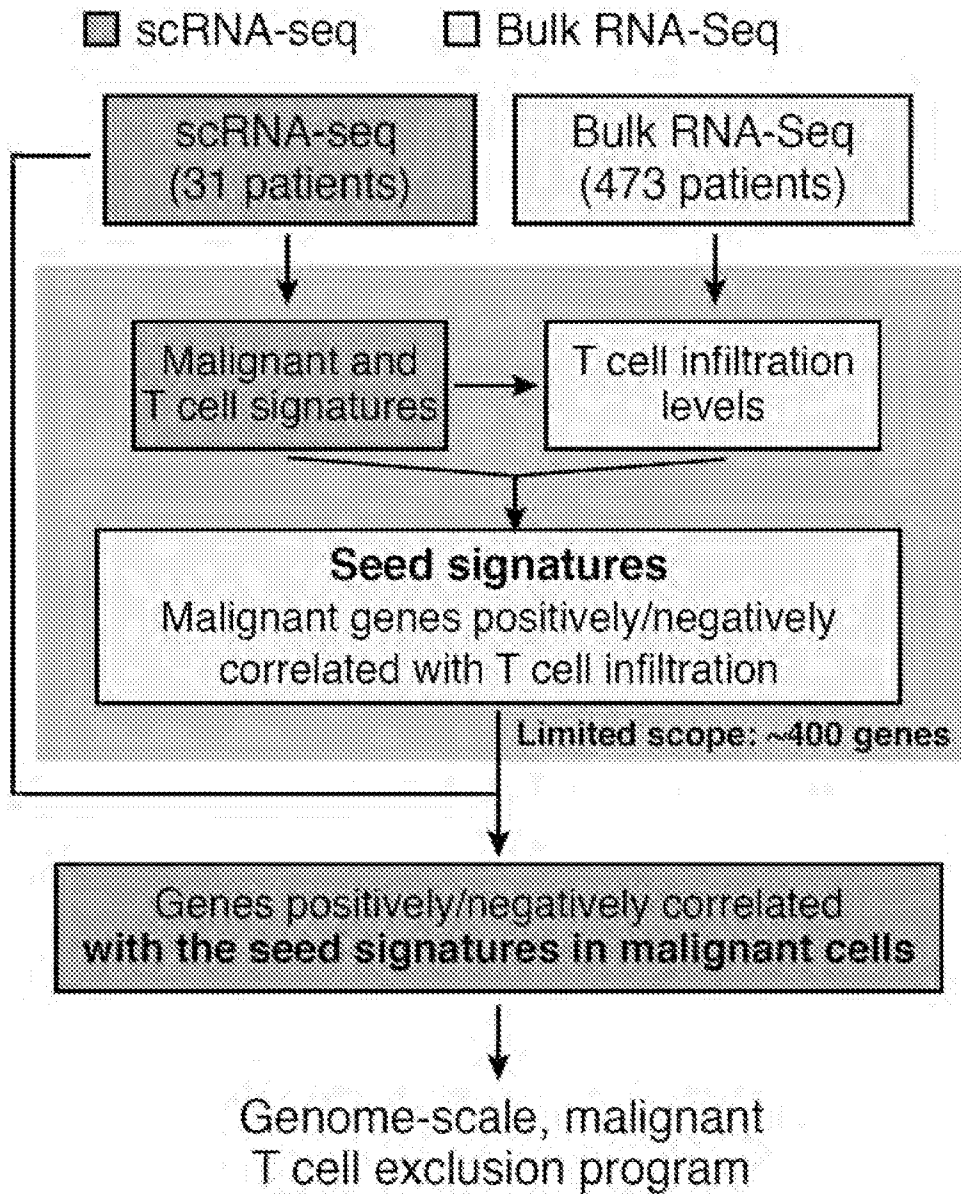


FIG. 44B

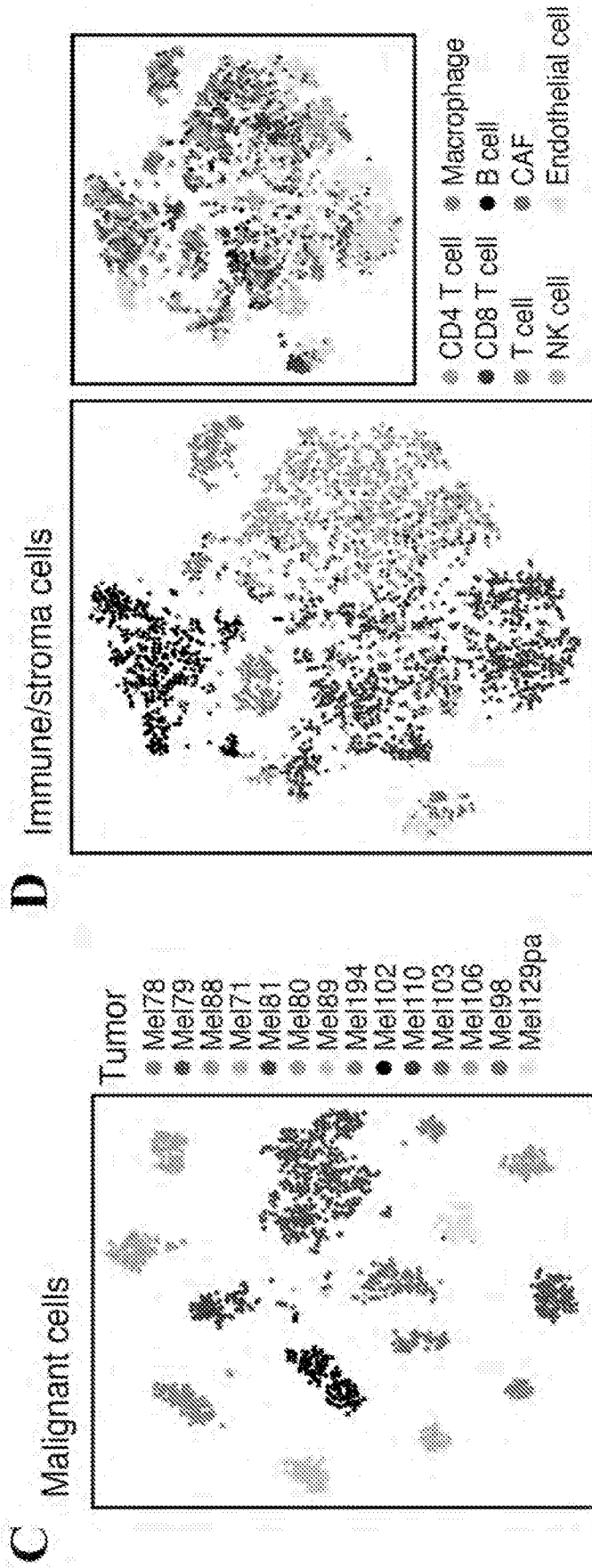


FIG. 44C-D

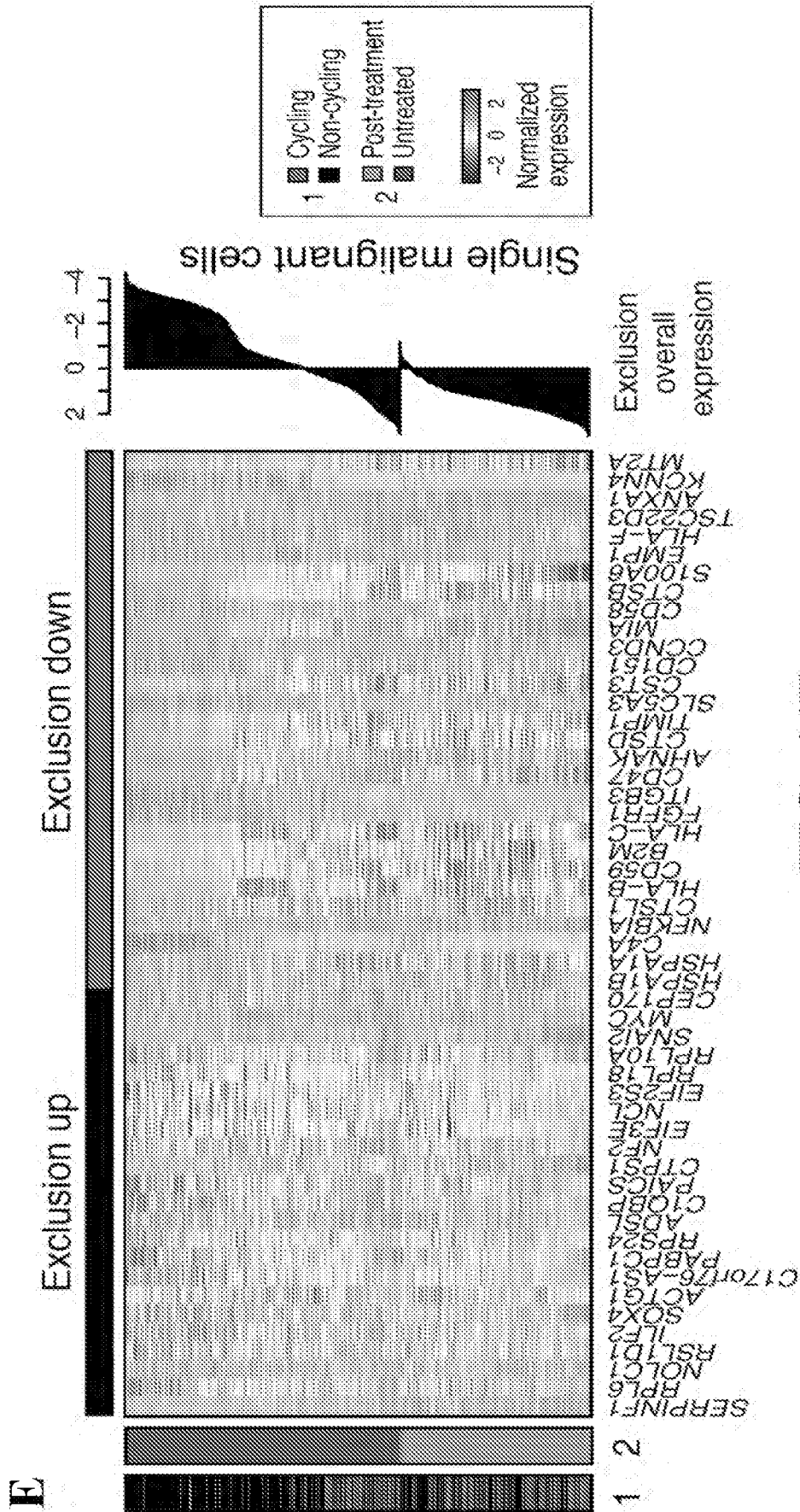


FIG. 44E

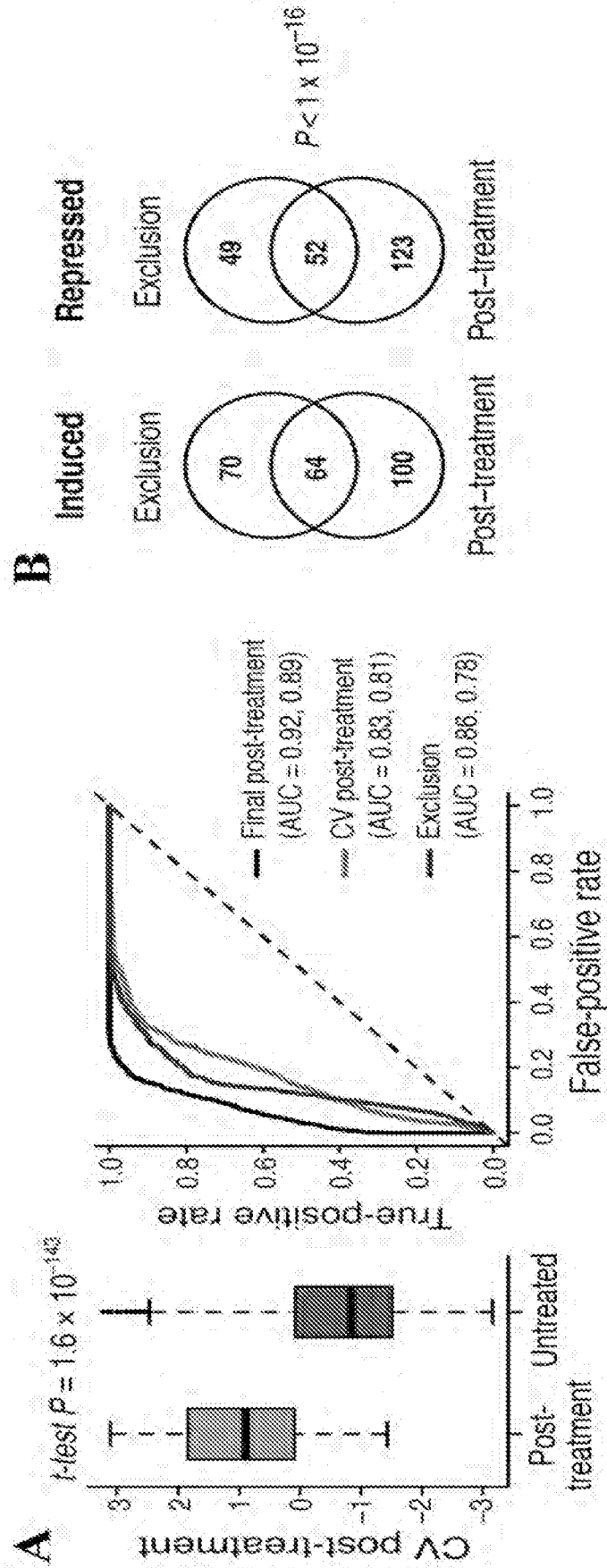


FIG. 45A-B

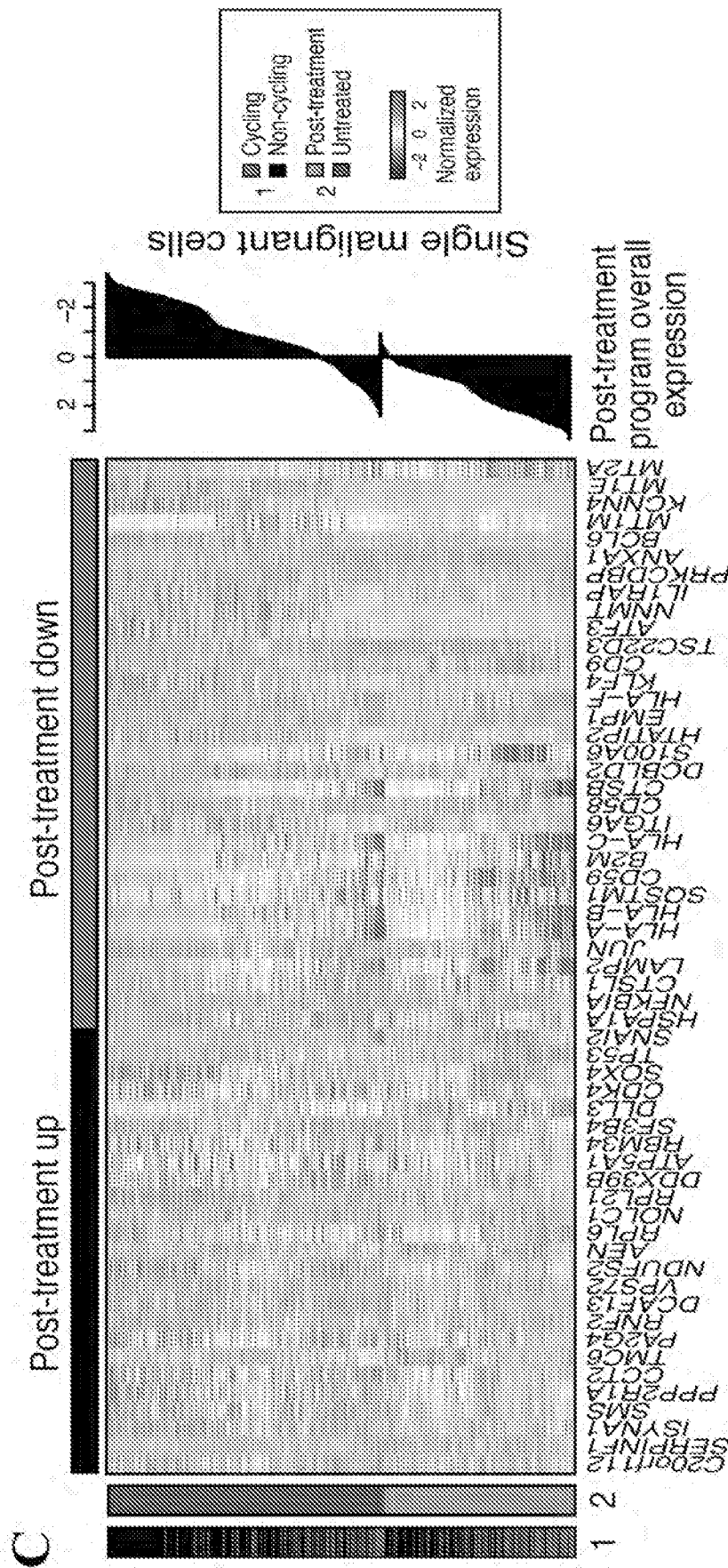


FIG. 45C

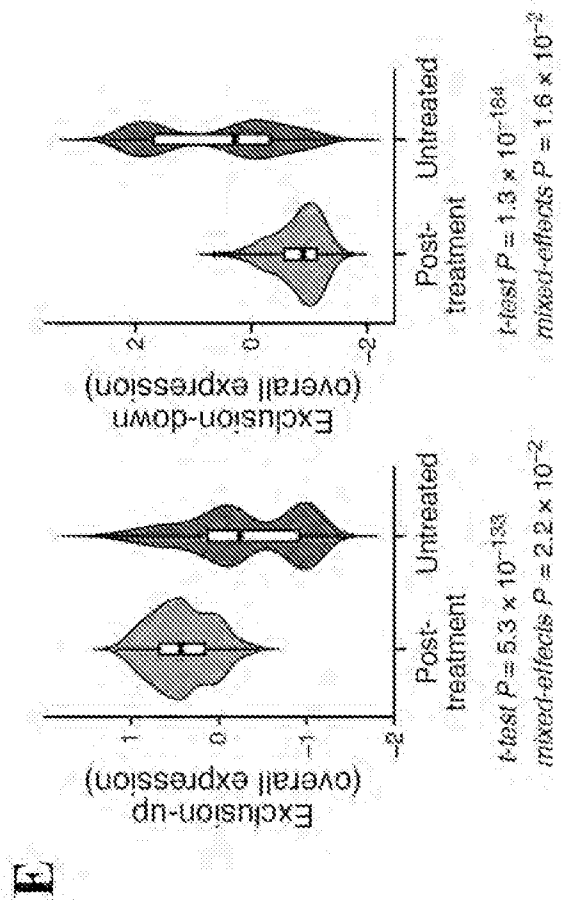
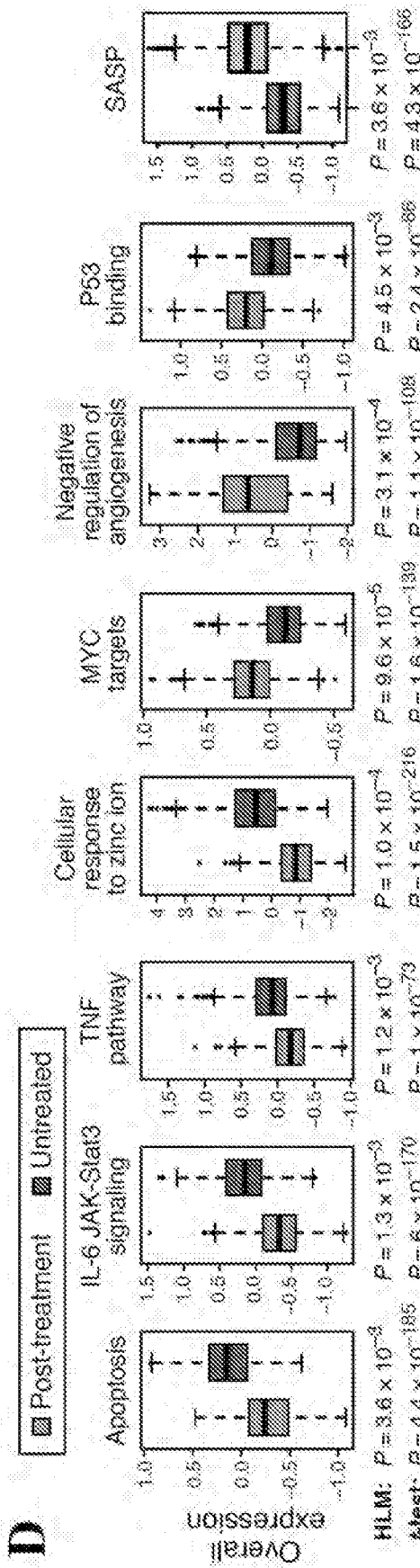


FIG. 45D-E

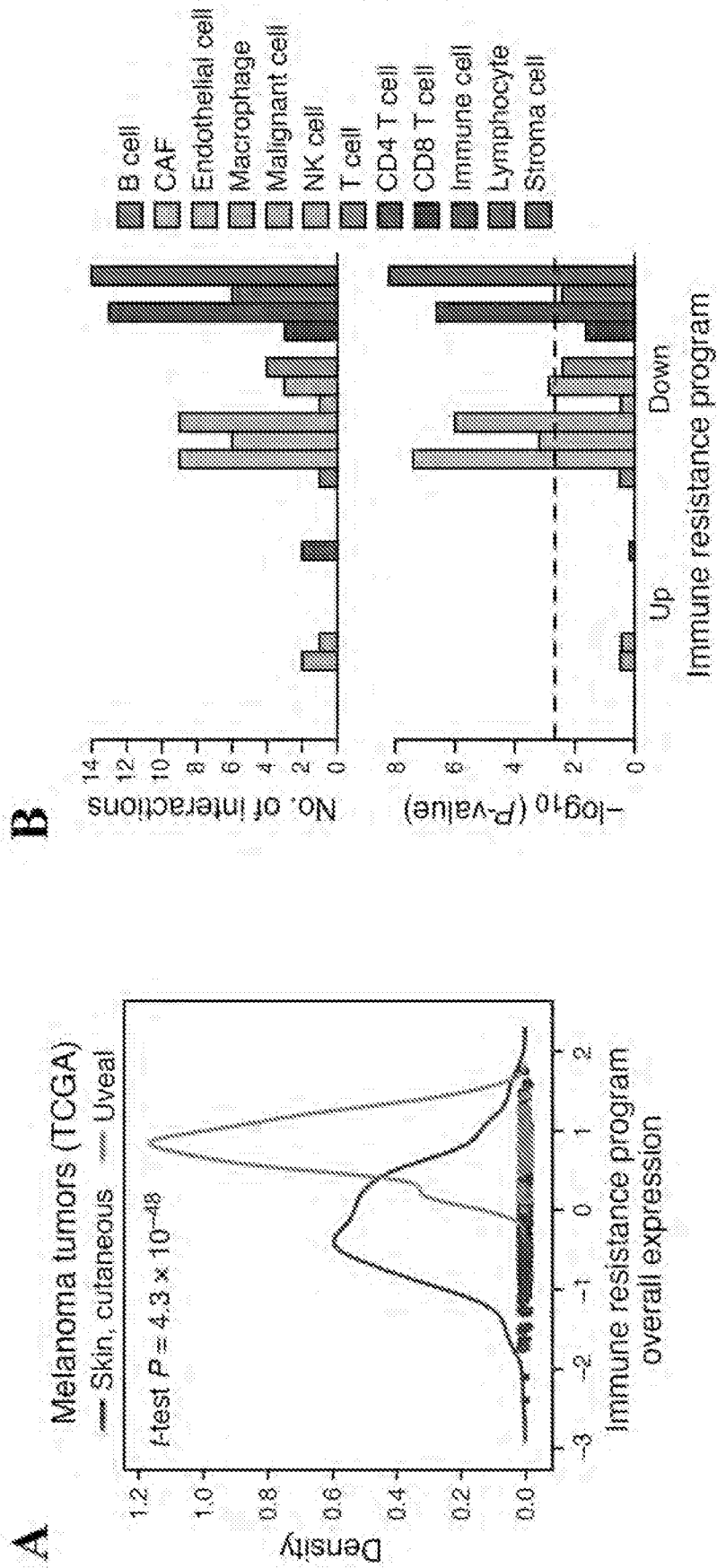
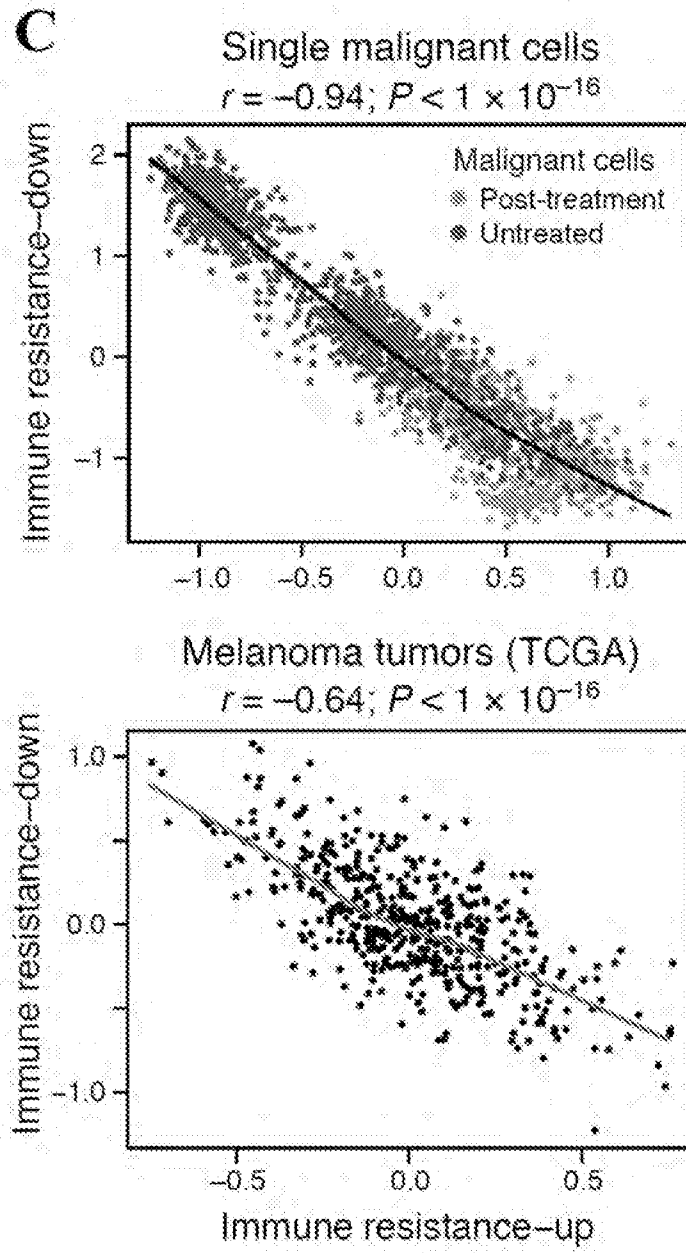


FIG. 46A-B

**FIG. 46C**

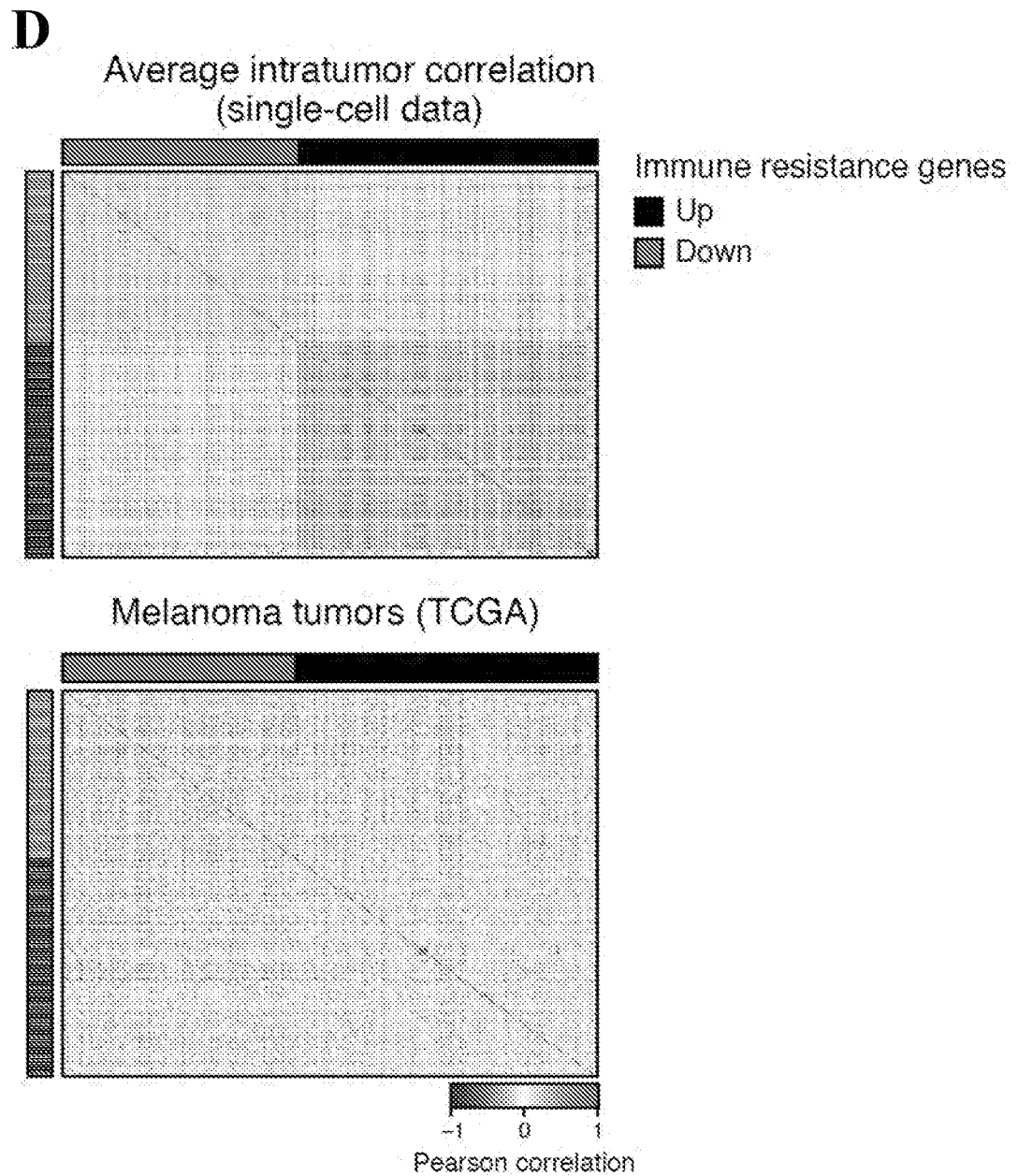


FIG. 46D

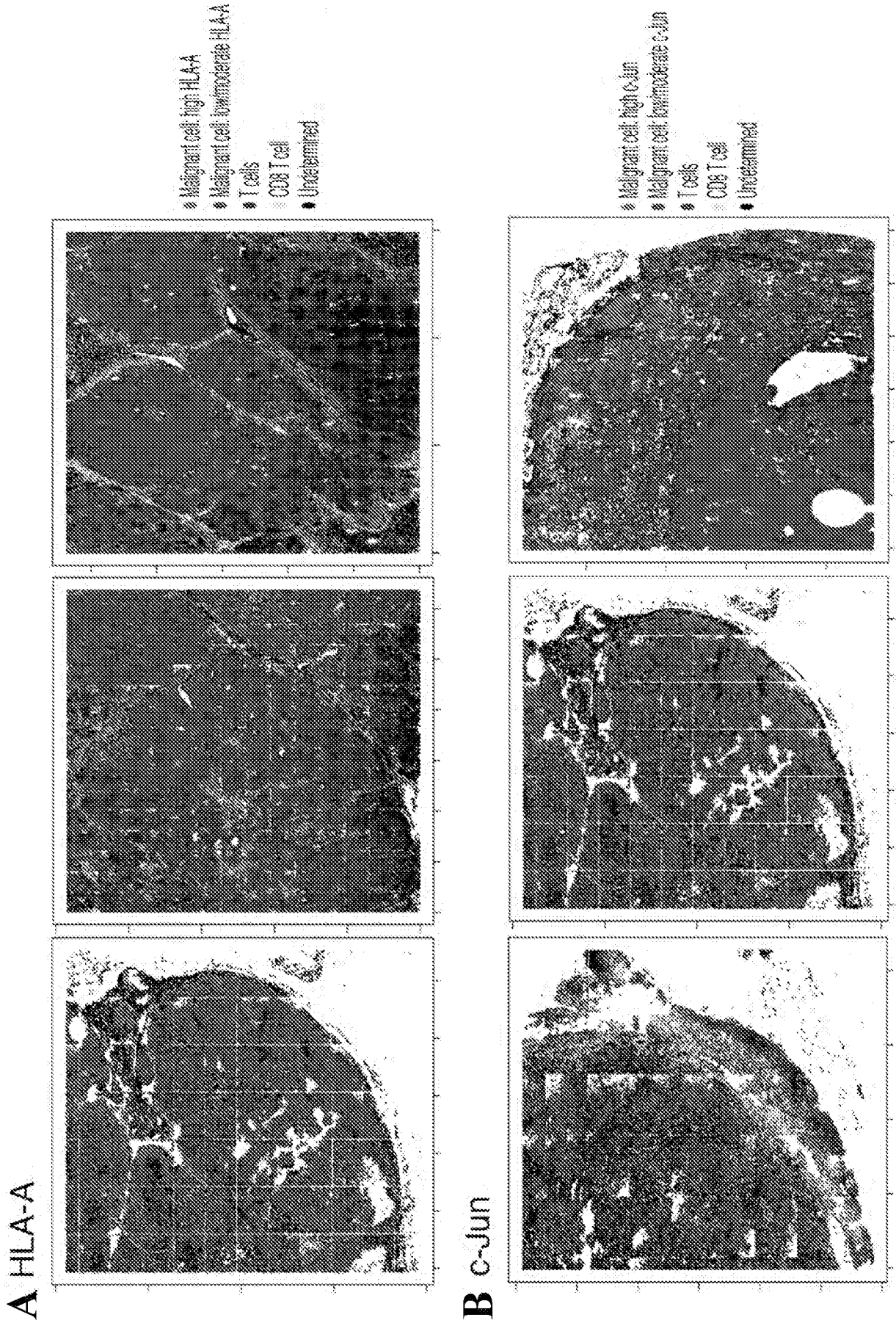


FIG. 47A-B

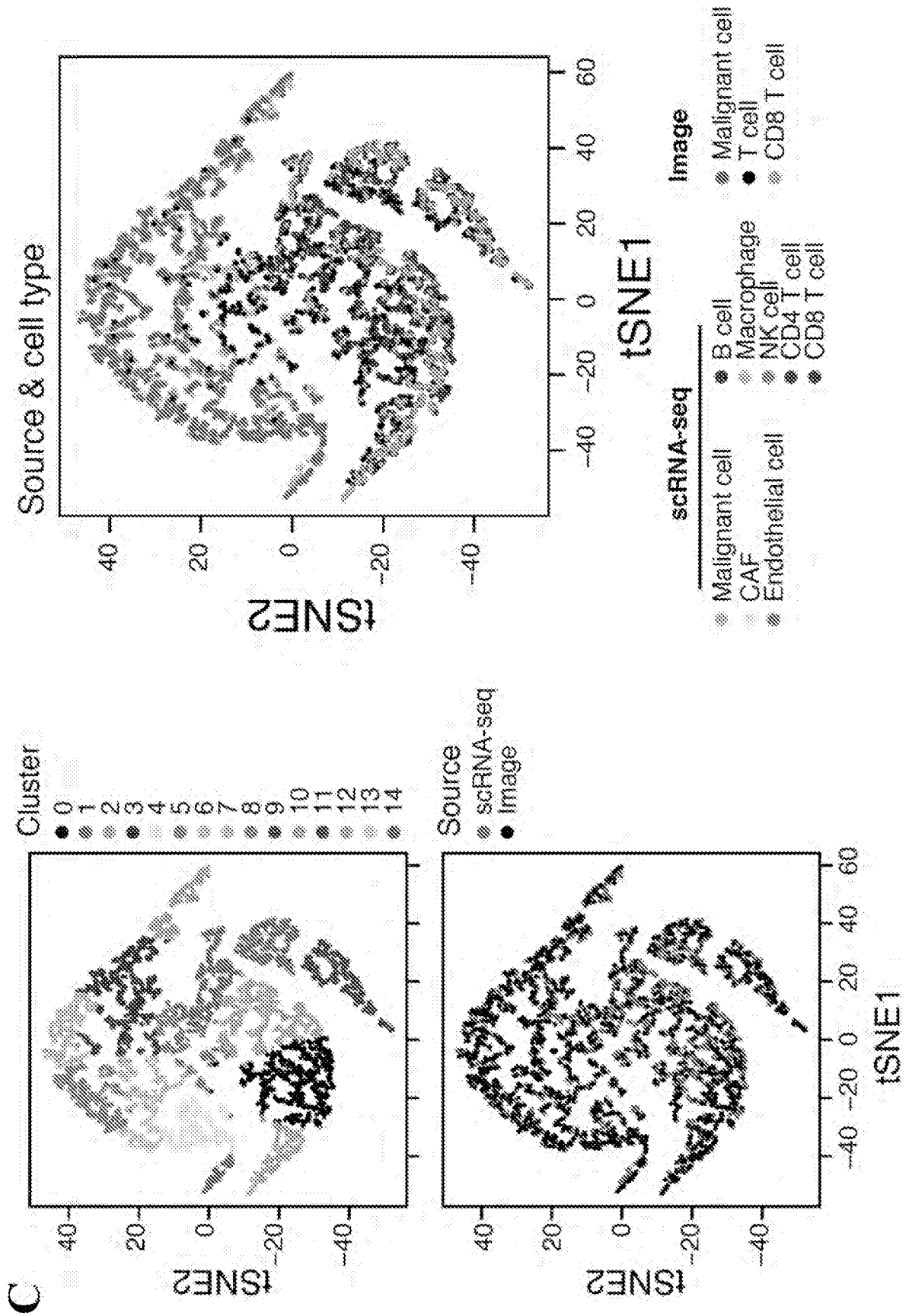


FIG. 47C

D

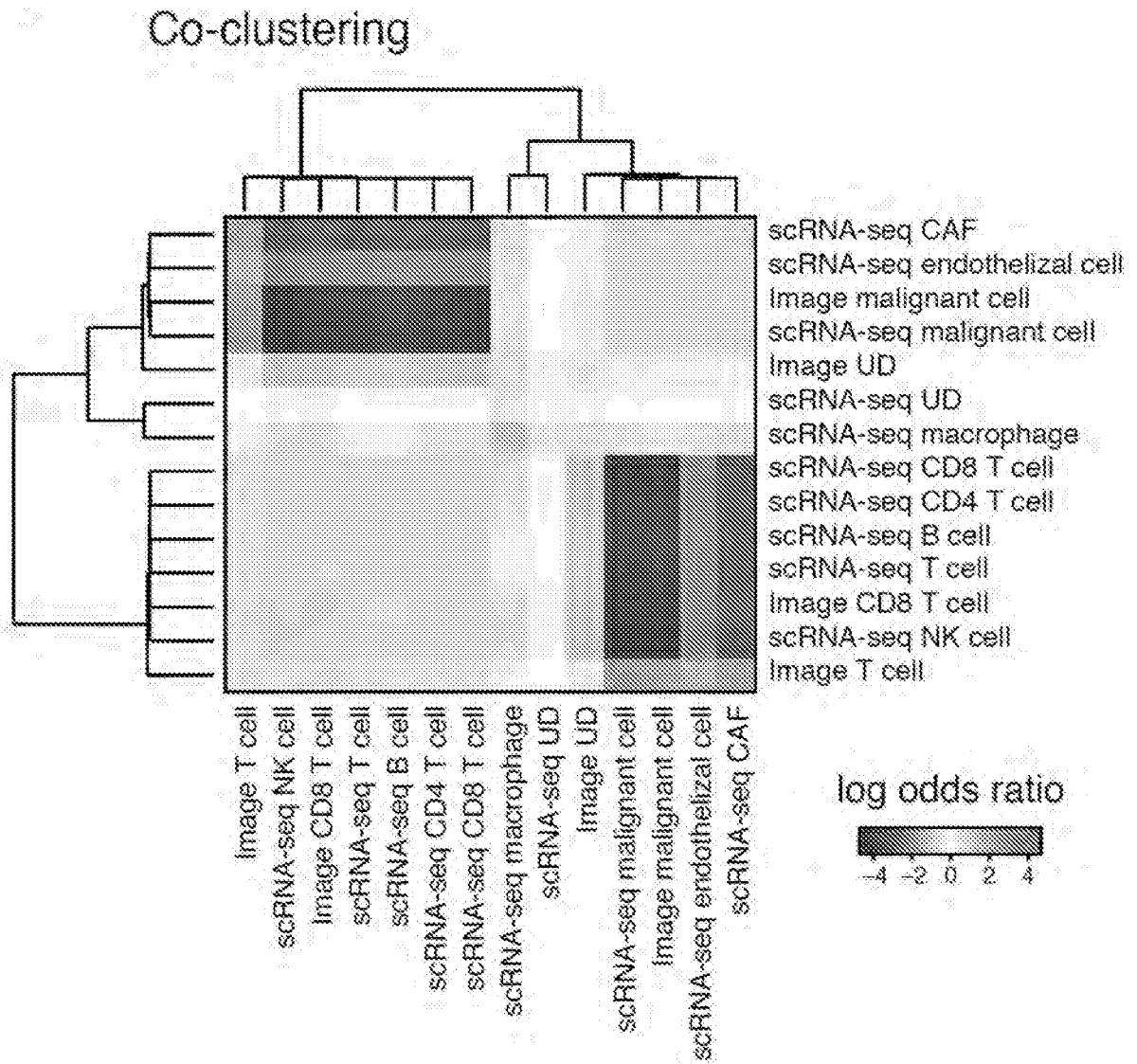


FIG. 47D

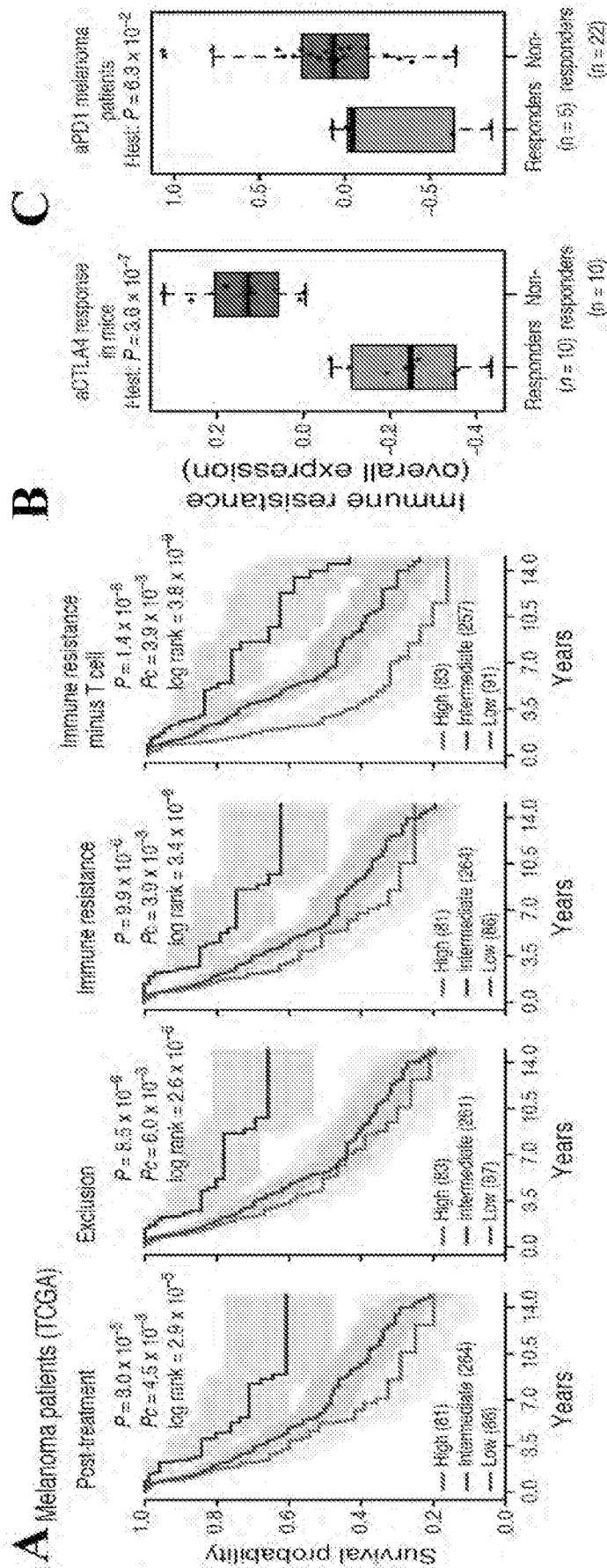


FIG. 48A-C

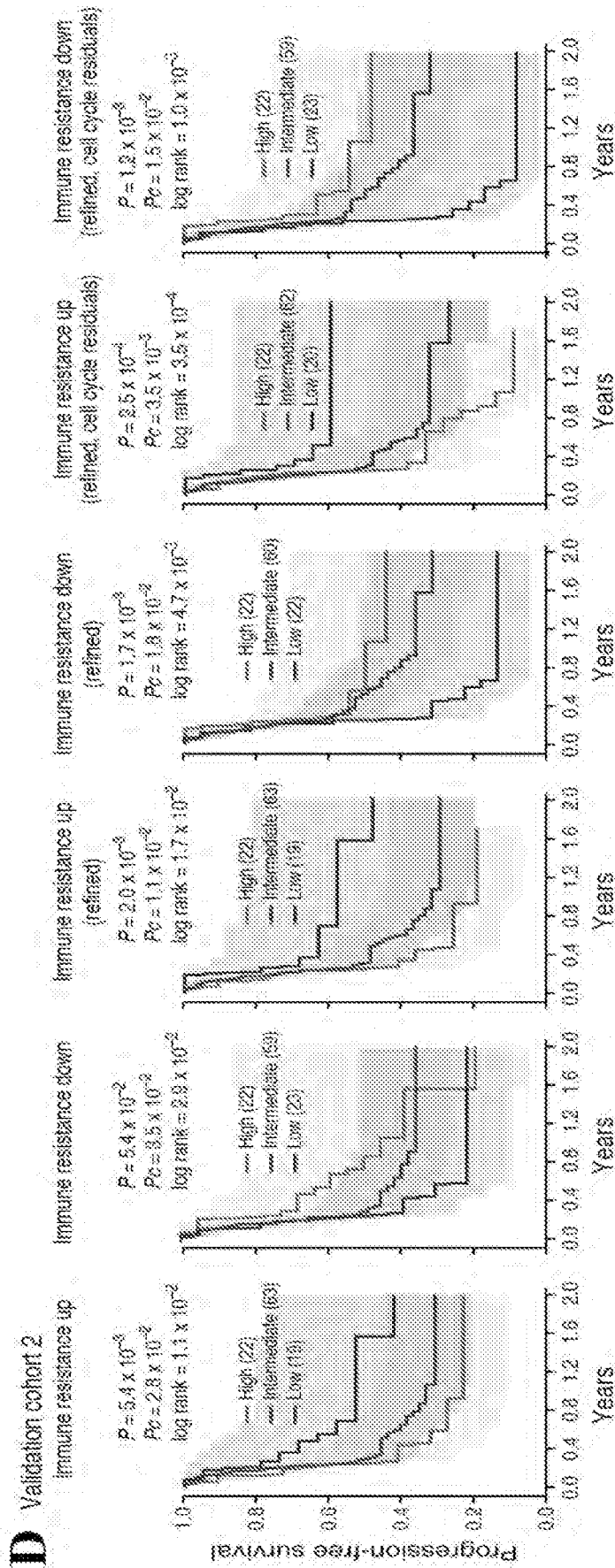


FIG. 48D

E

Predicting progression-free survival given T cell infiltration levels
104 aPD1-treated melanoma patients

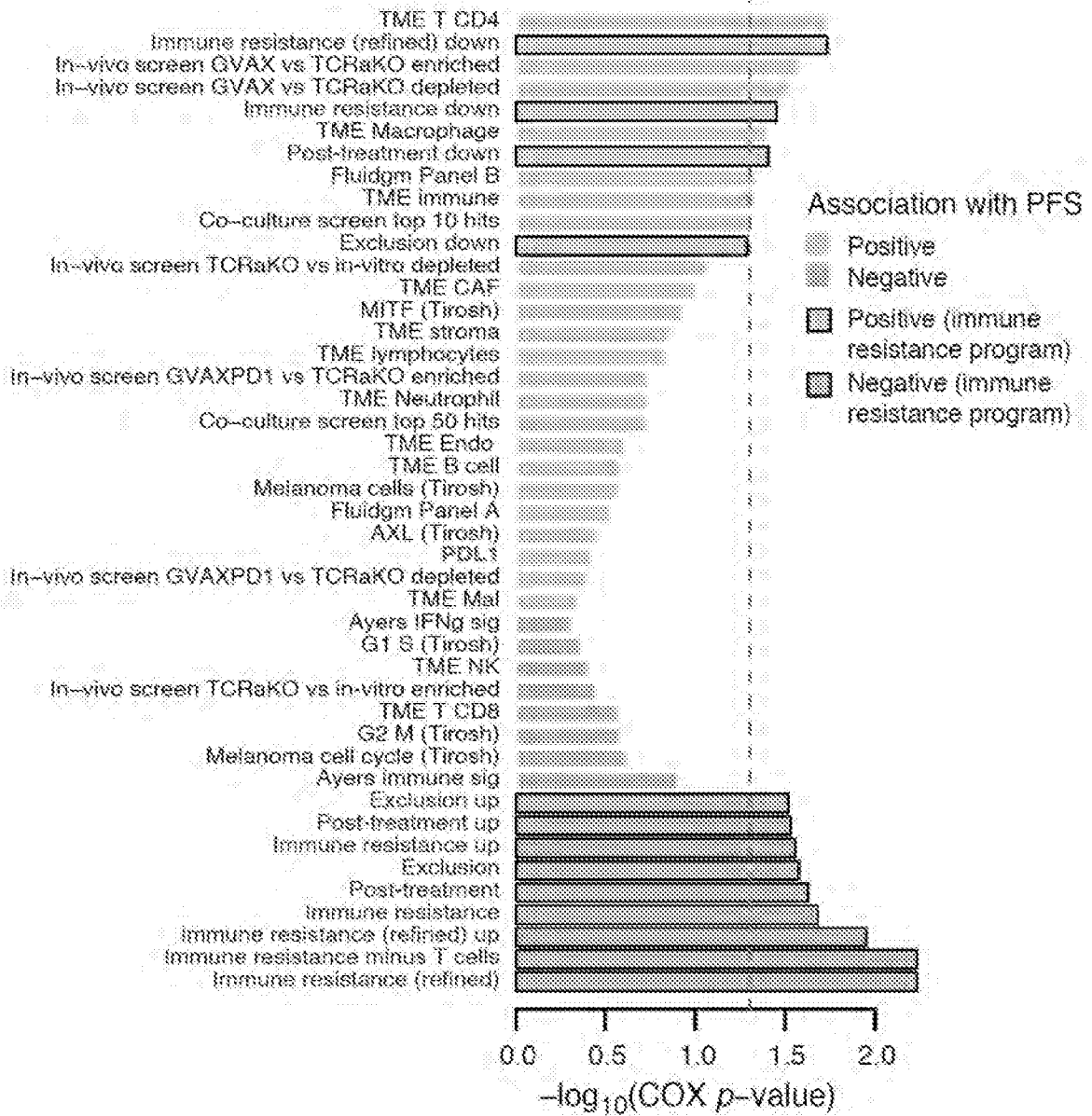


FIG. 48E

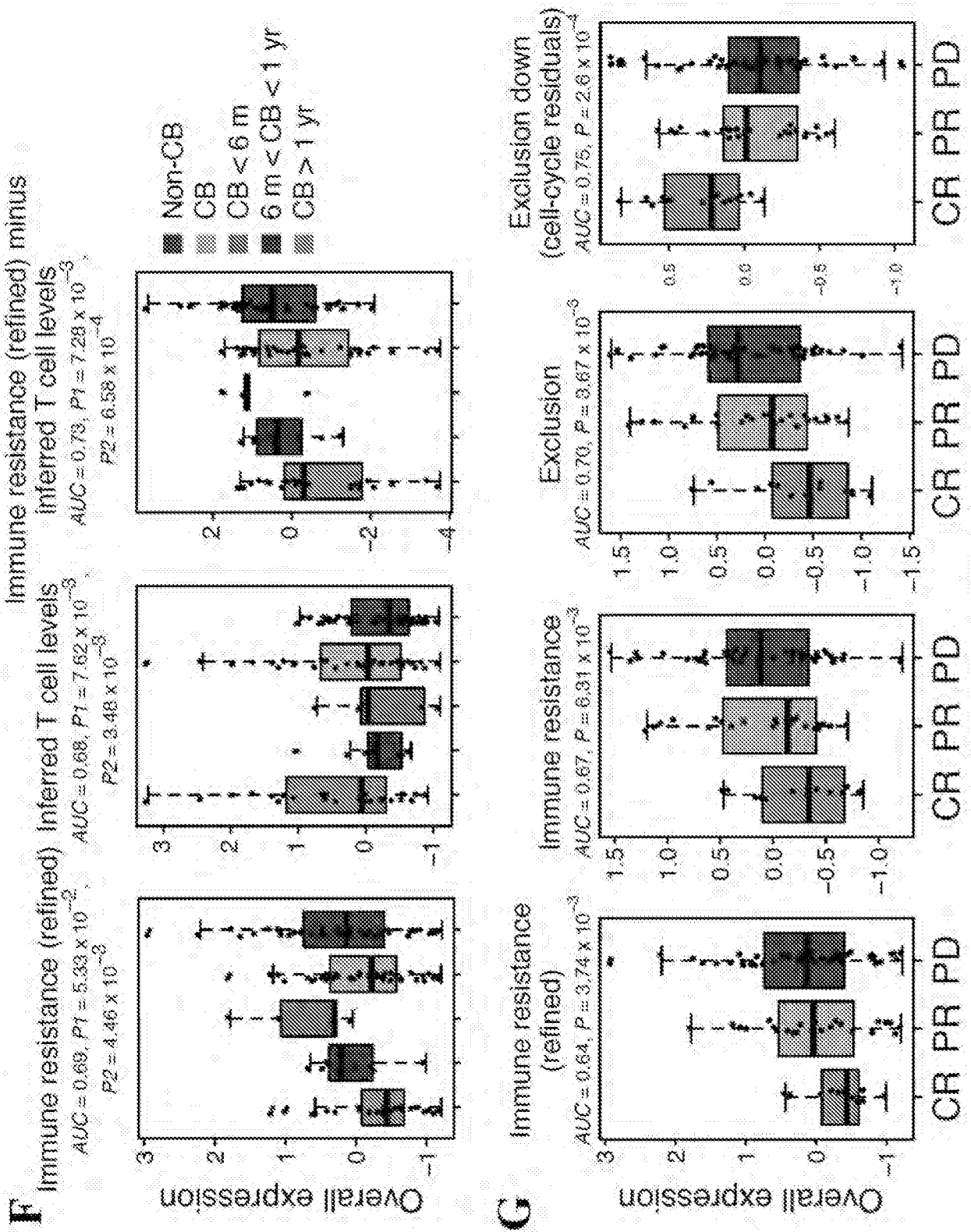


FIG. 48F-G

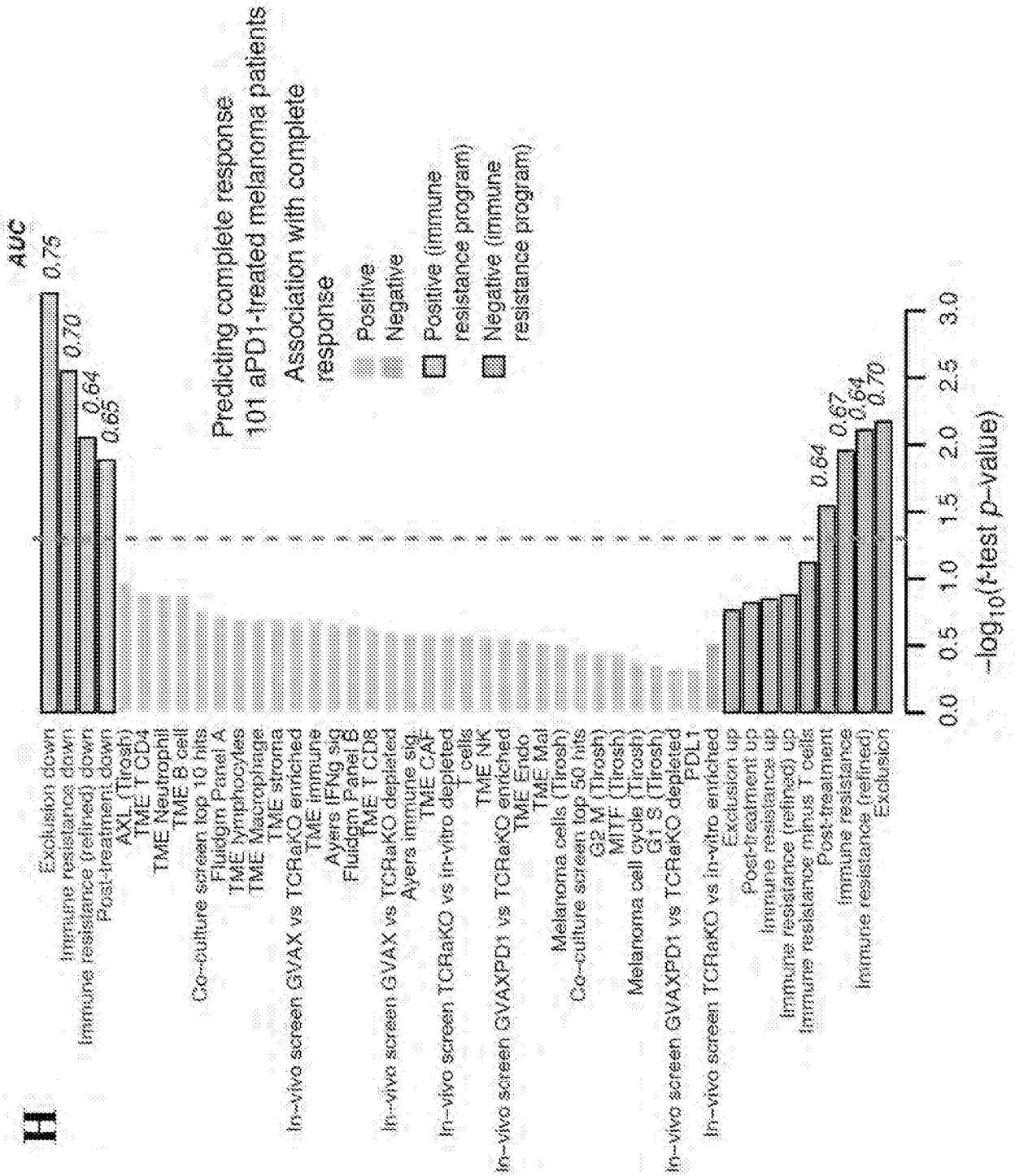


FIG. 48H

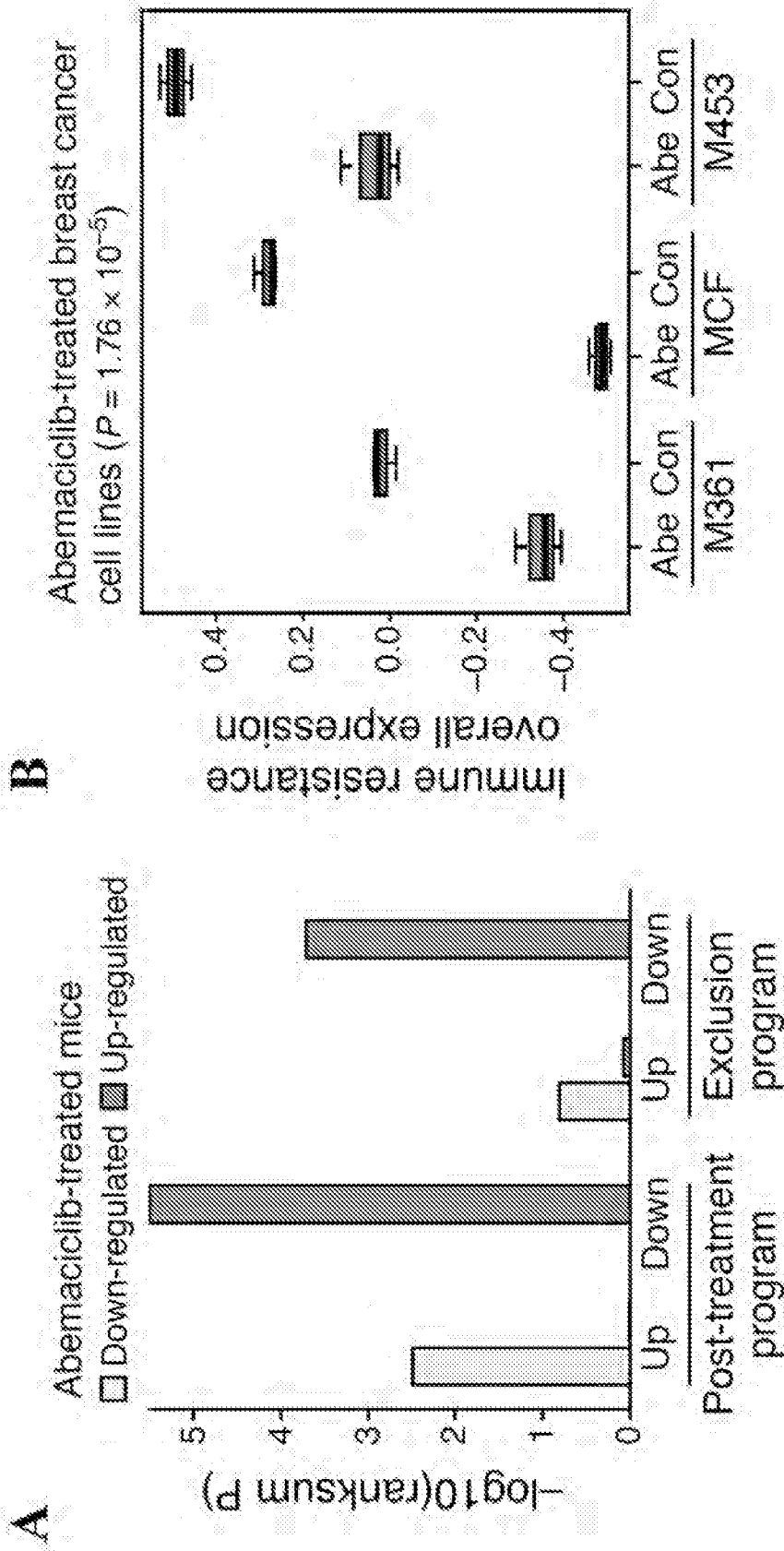


FIG. 49A-B

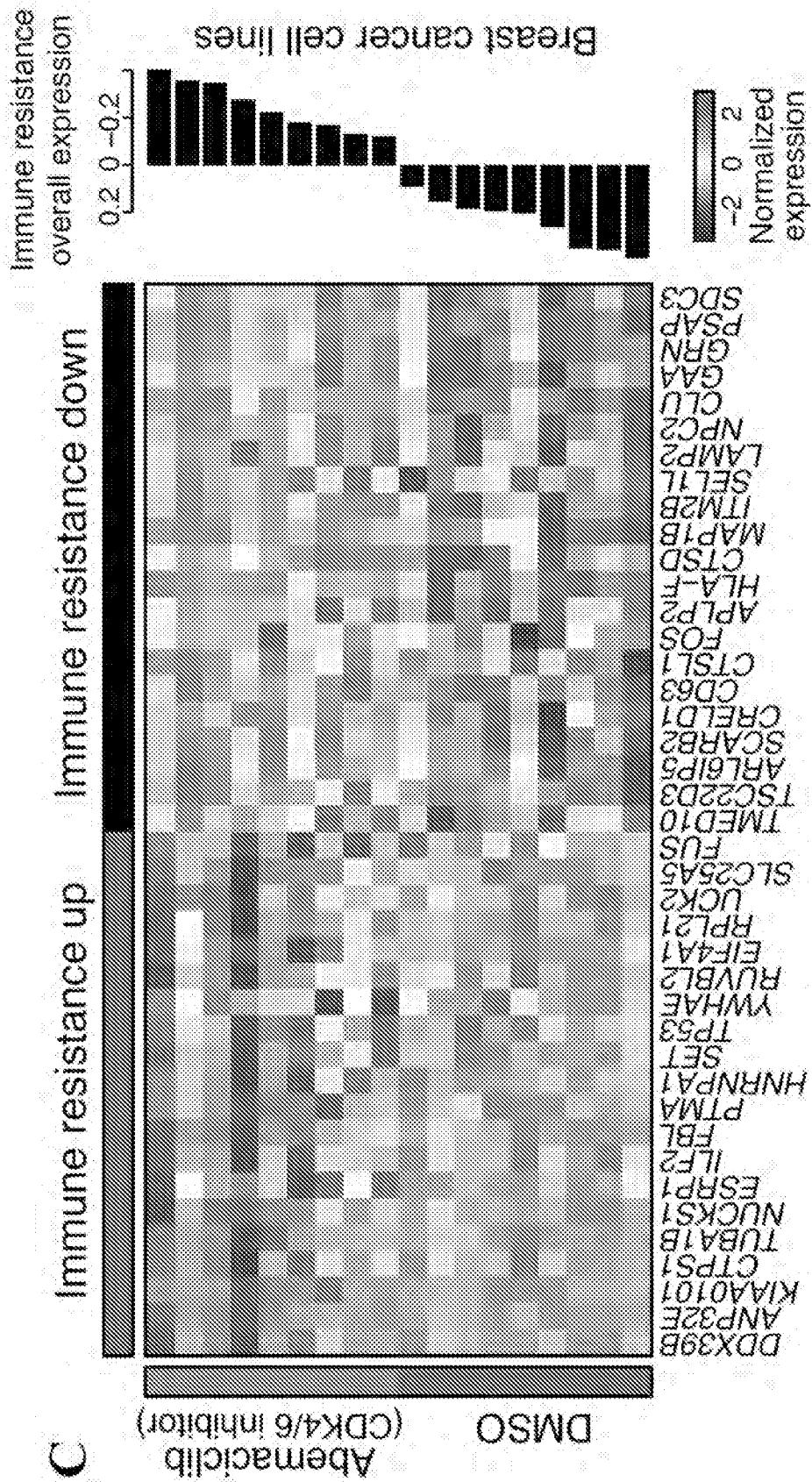


FIG. 49C

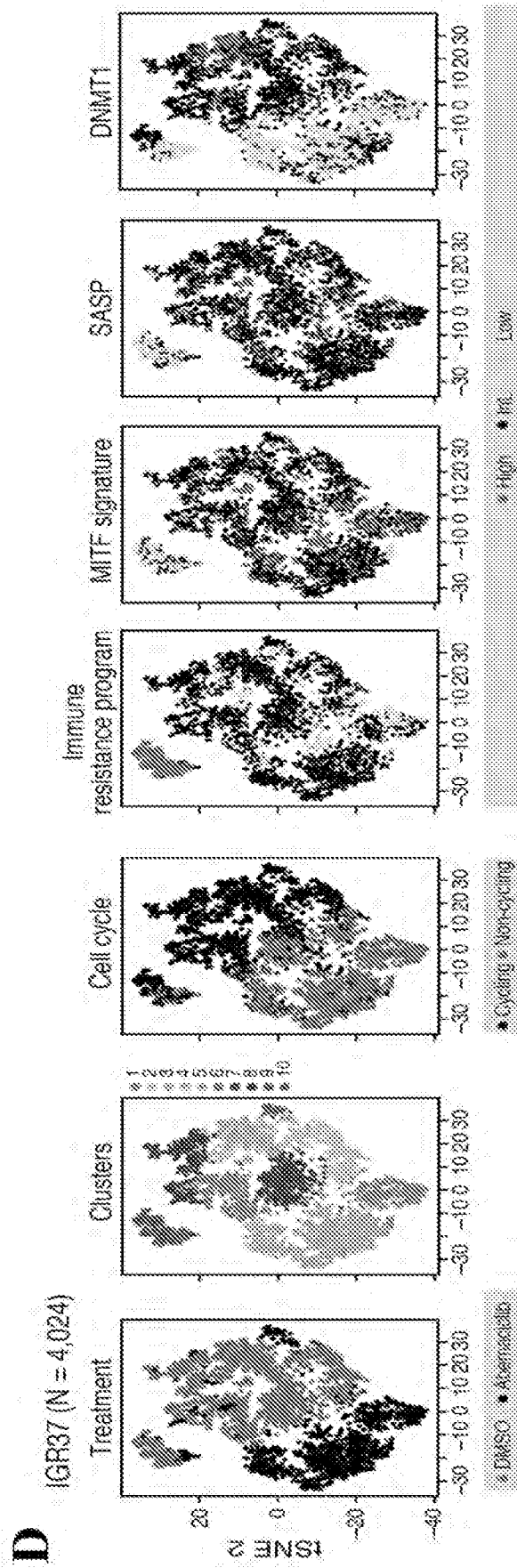


FIG. 49D

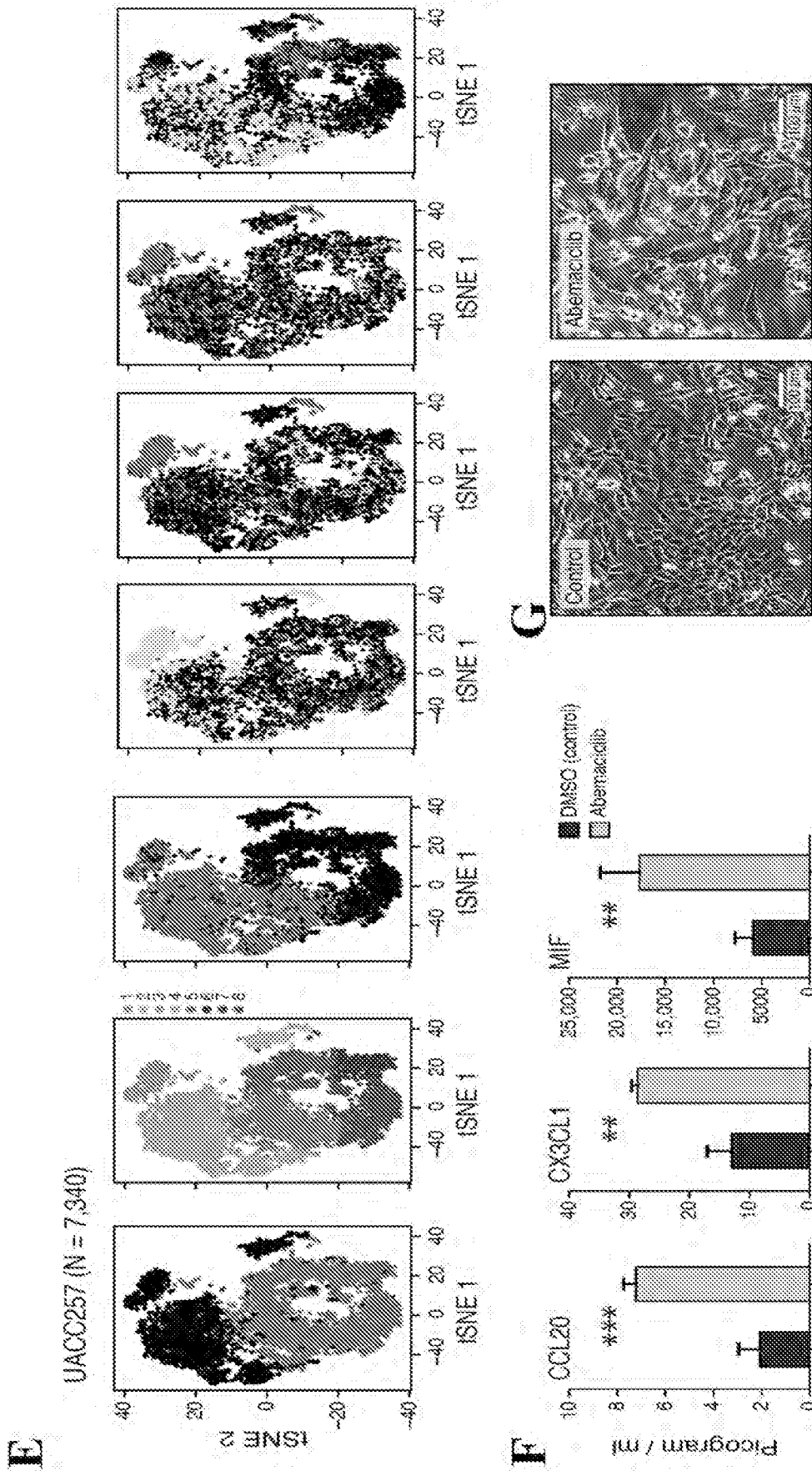


FIG. 49E-G

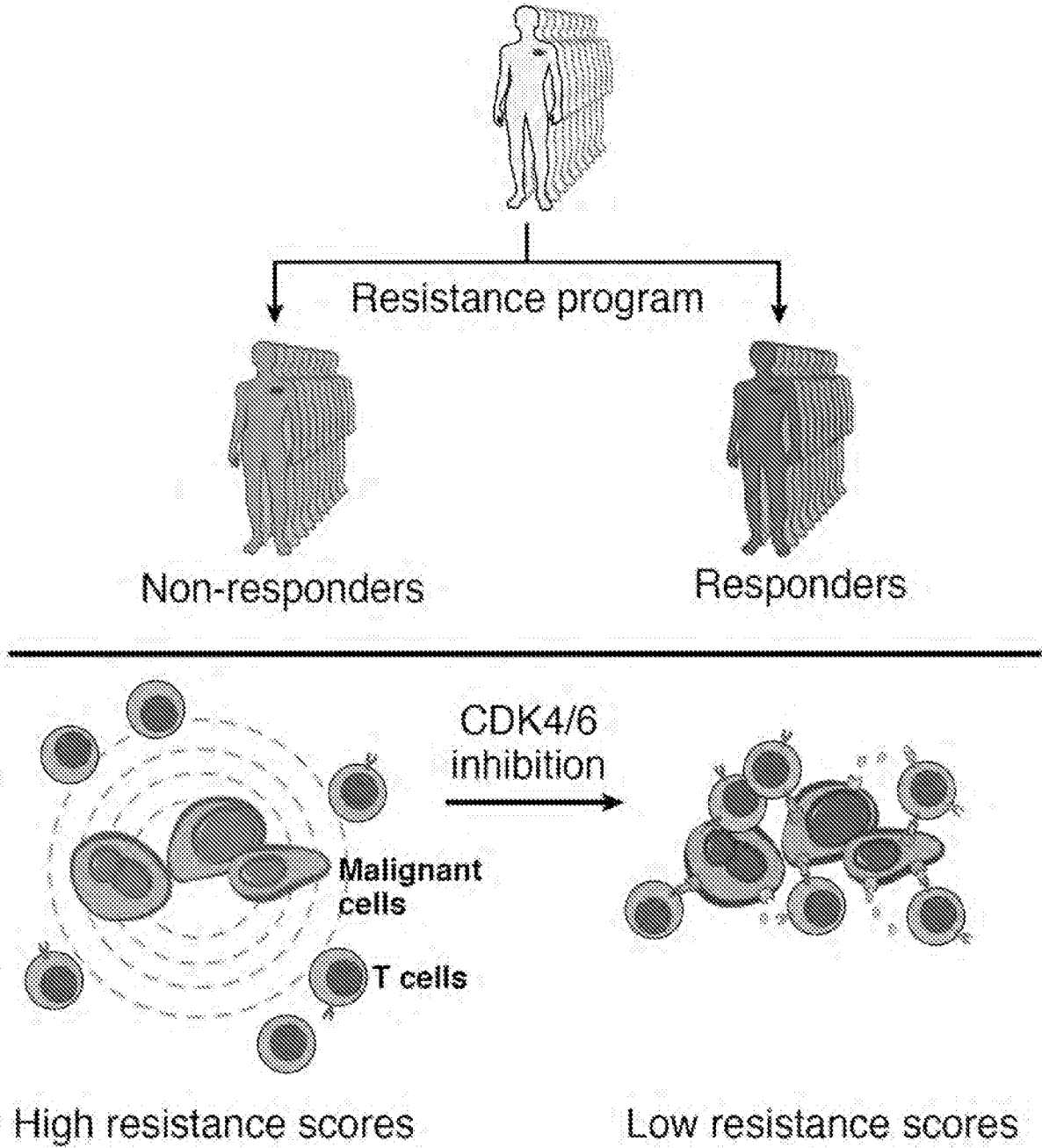


FIG. 50

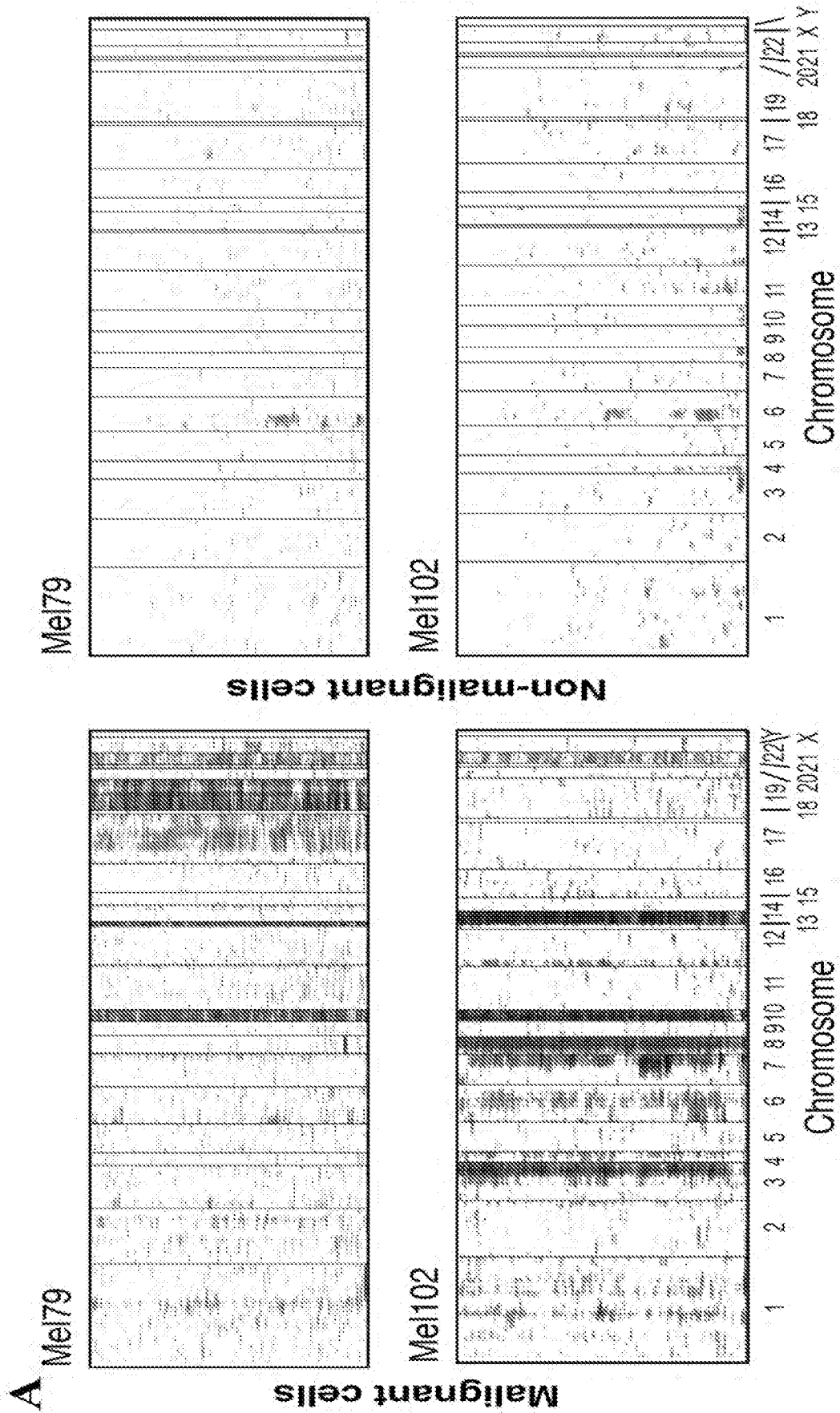


FIG. 51A

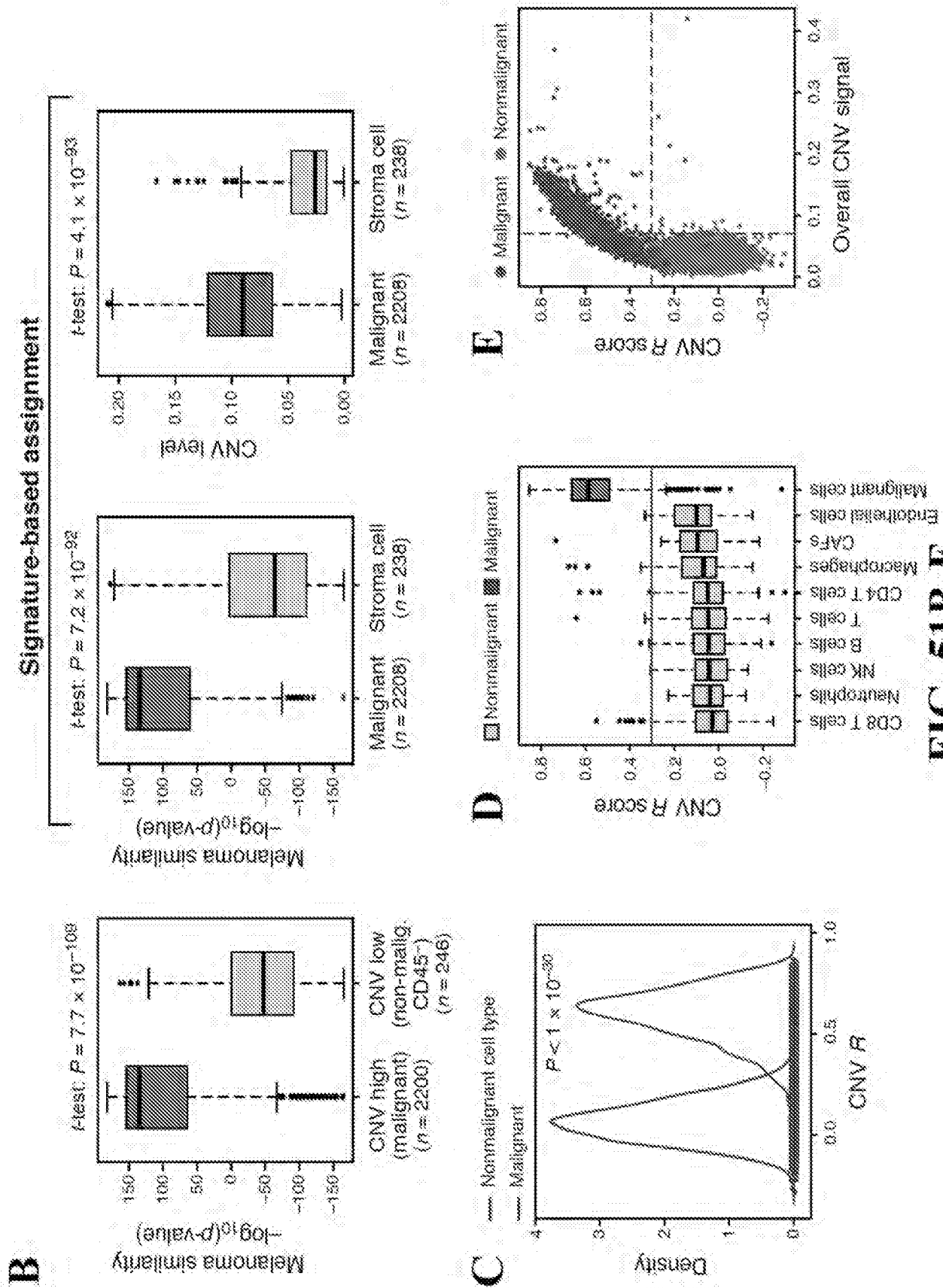


FIG. 51B-E

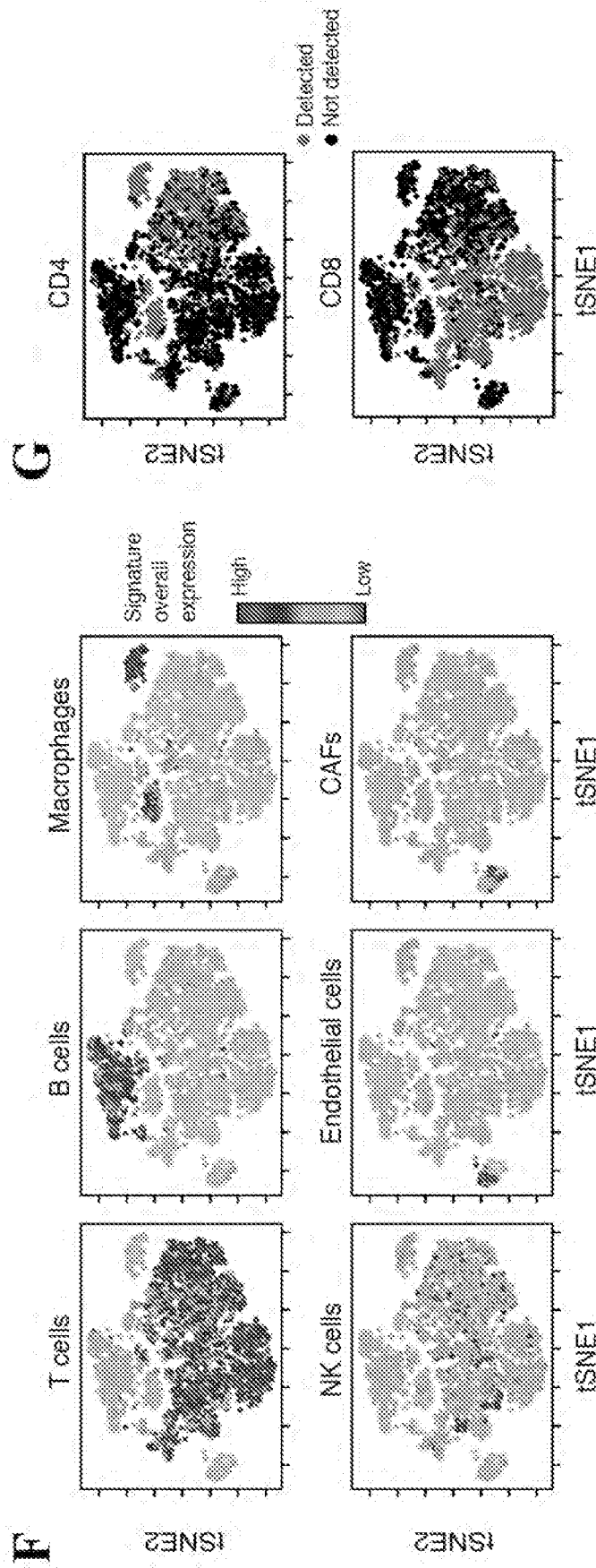


FIG. 51F-G

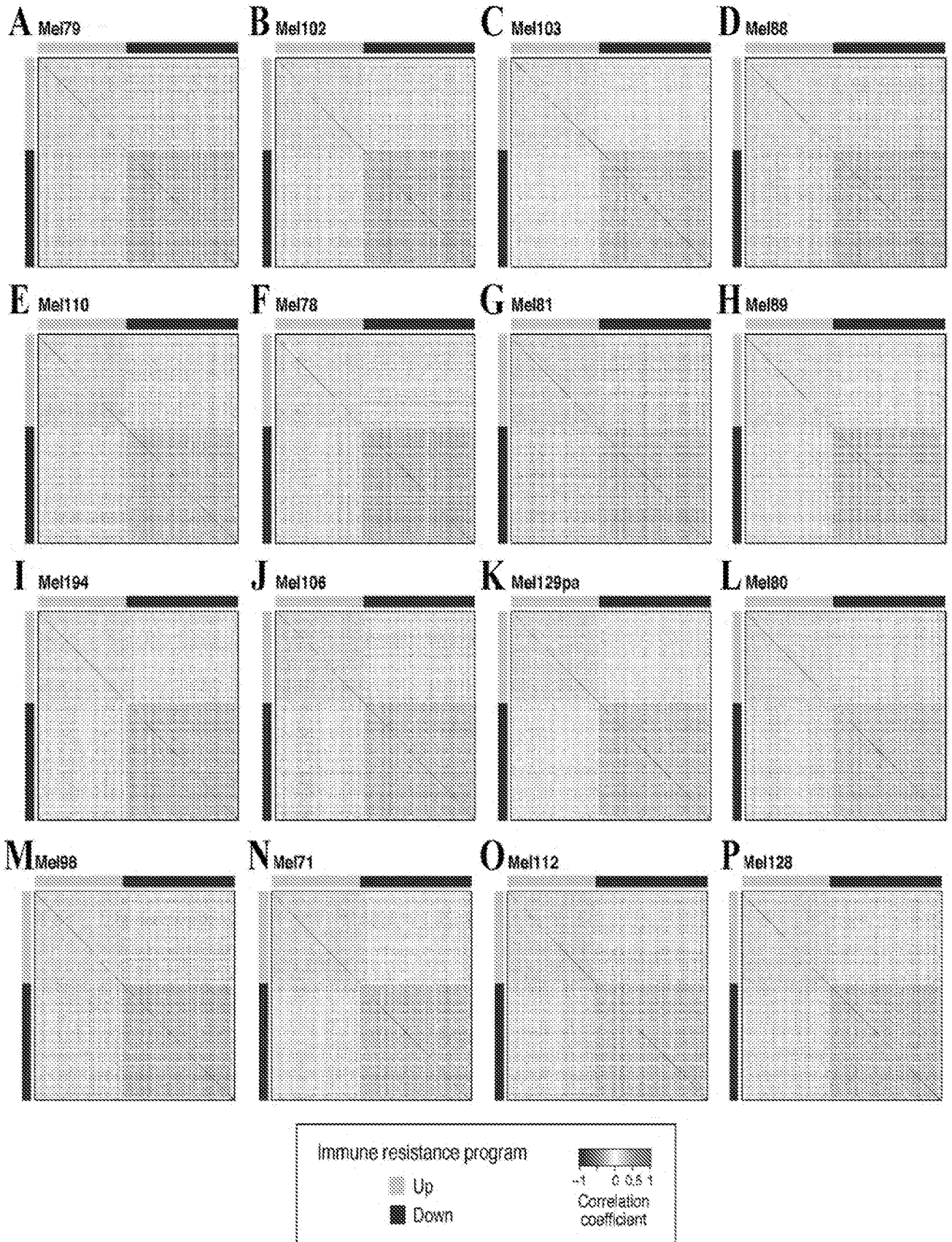


FIG. 52A-P

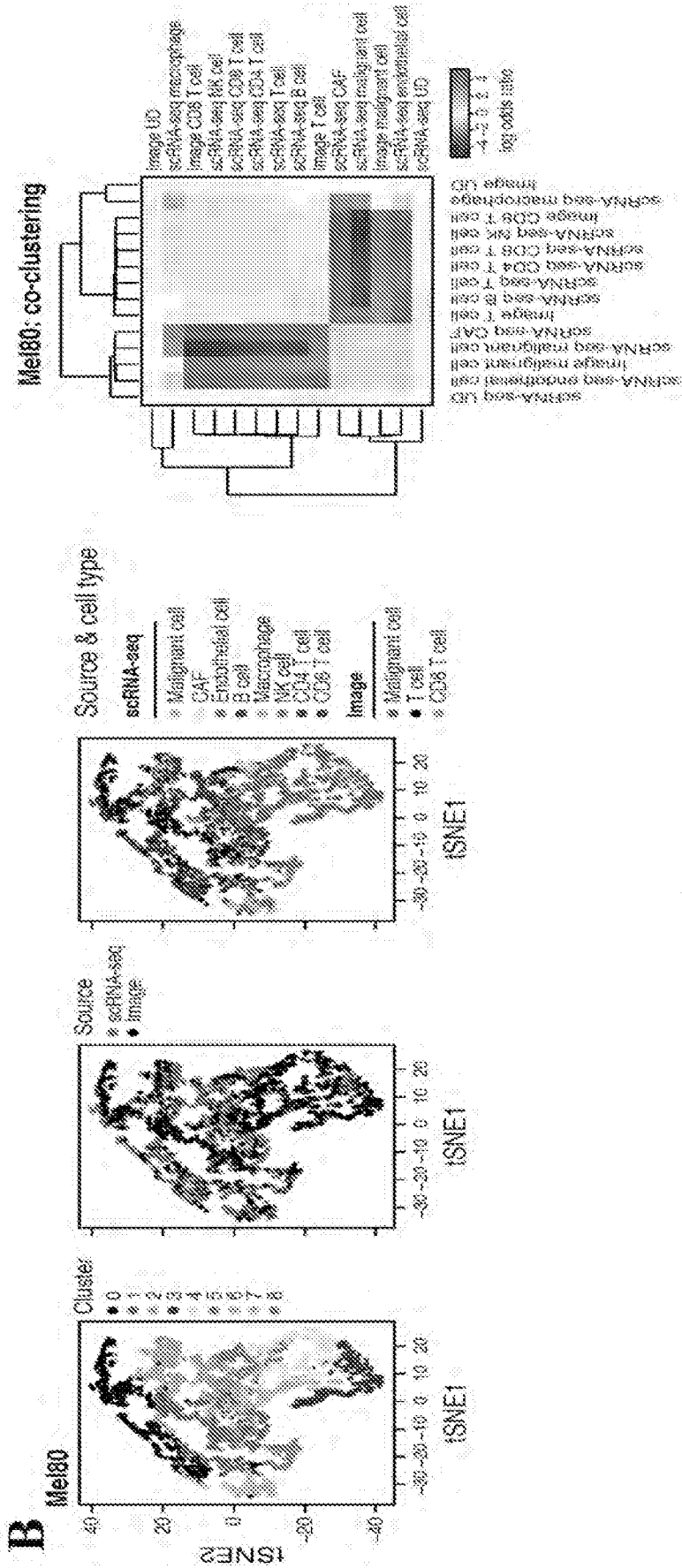


FIG. 53B

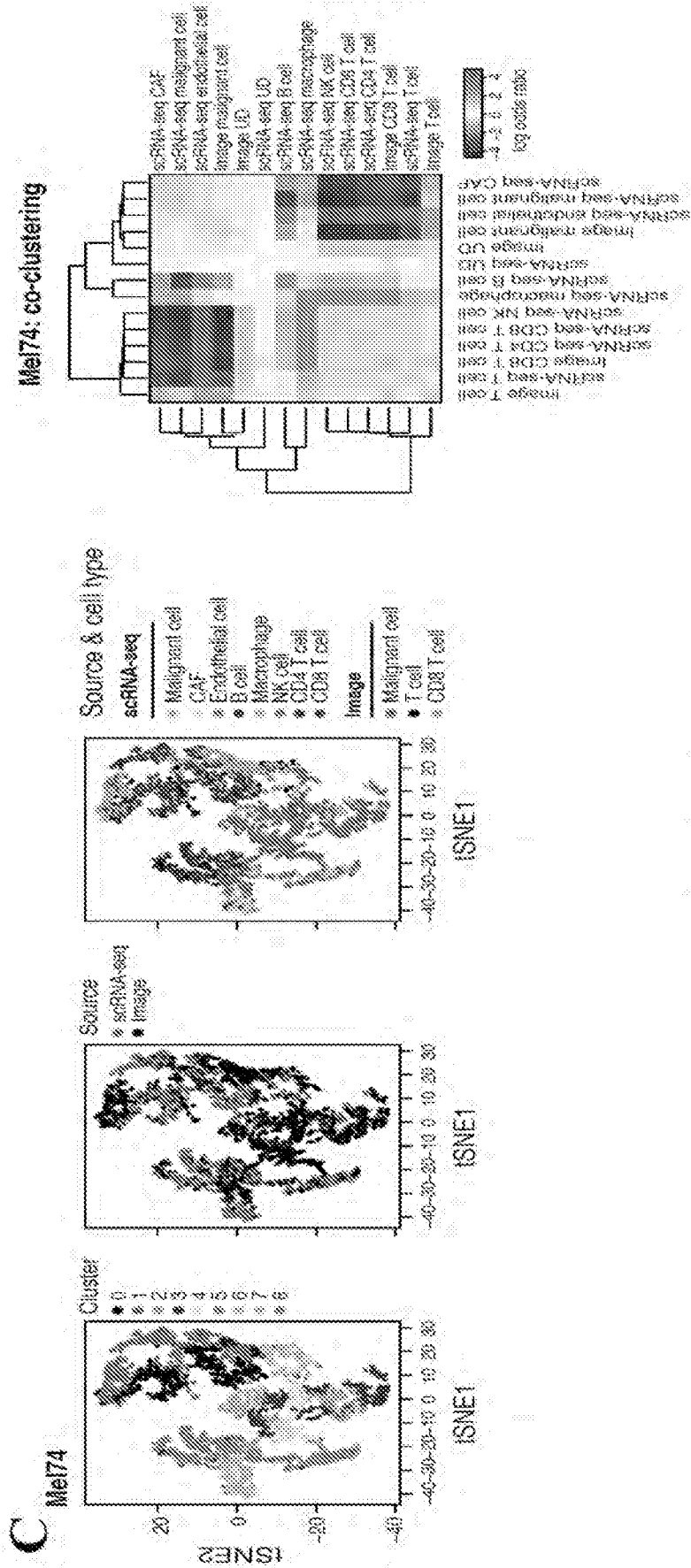


FIG. 53C

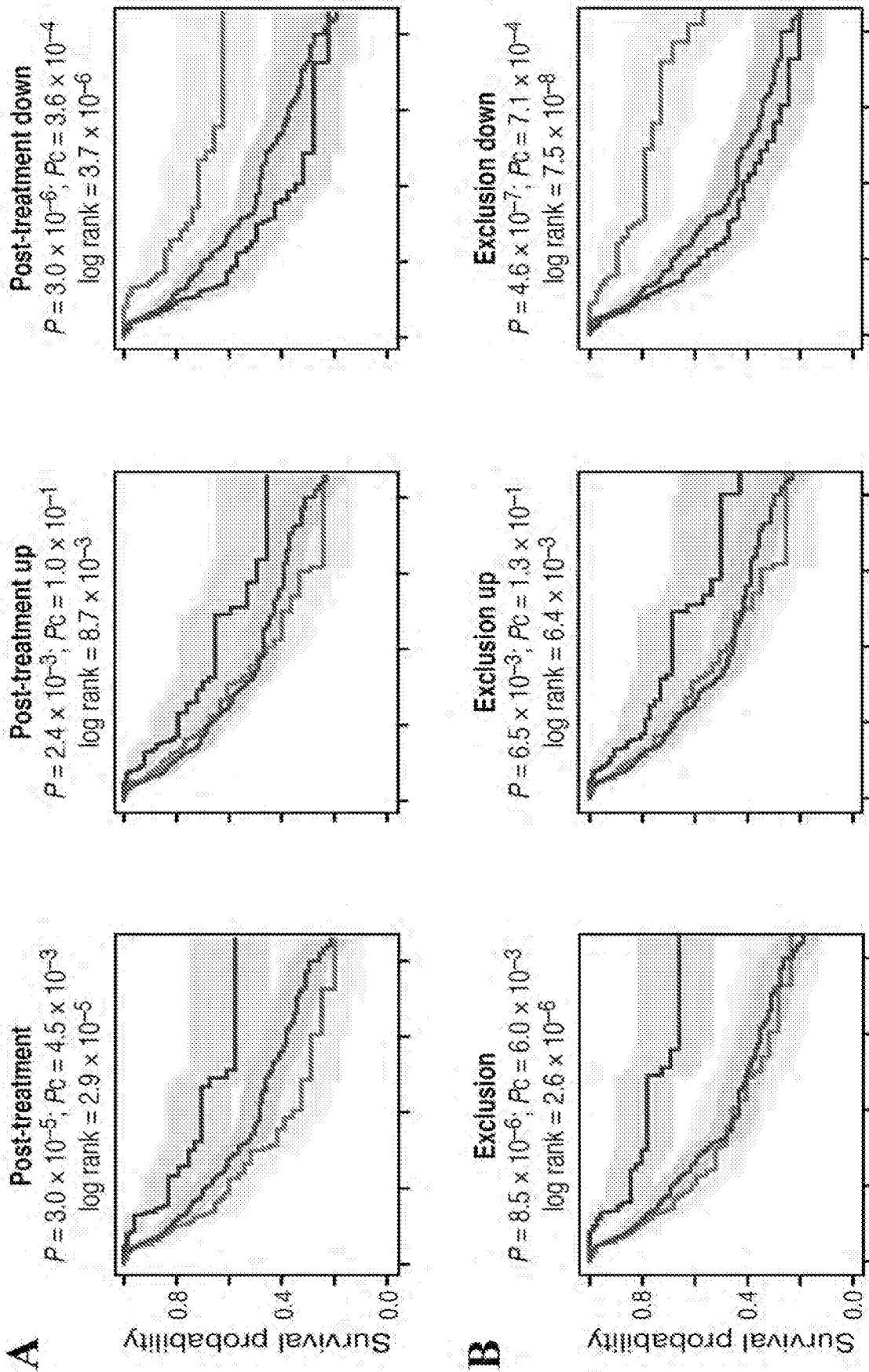


FIG. 54A-B

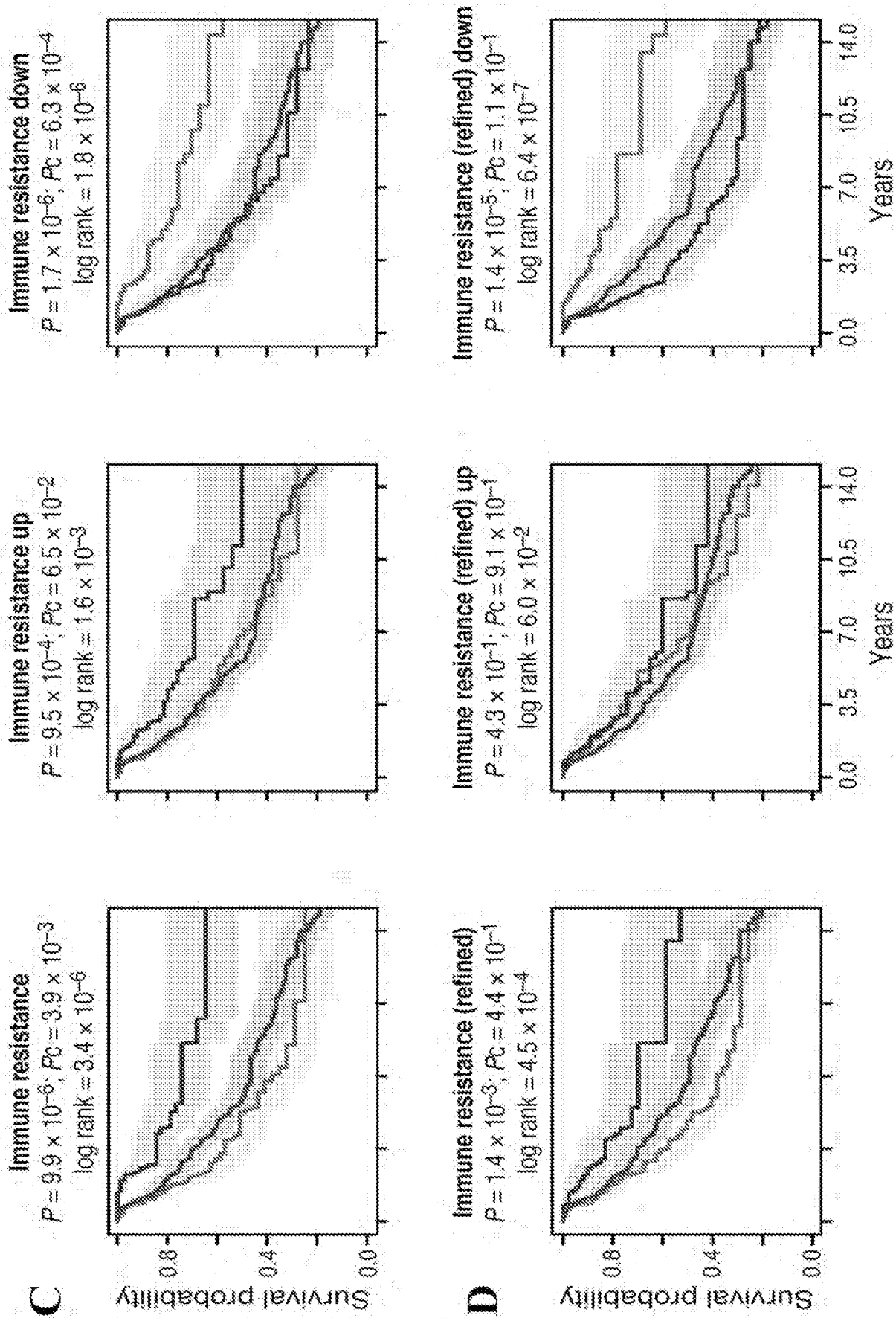


FIG. 54C-D

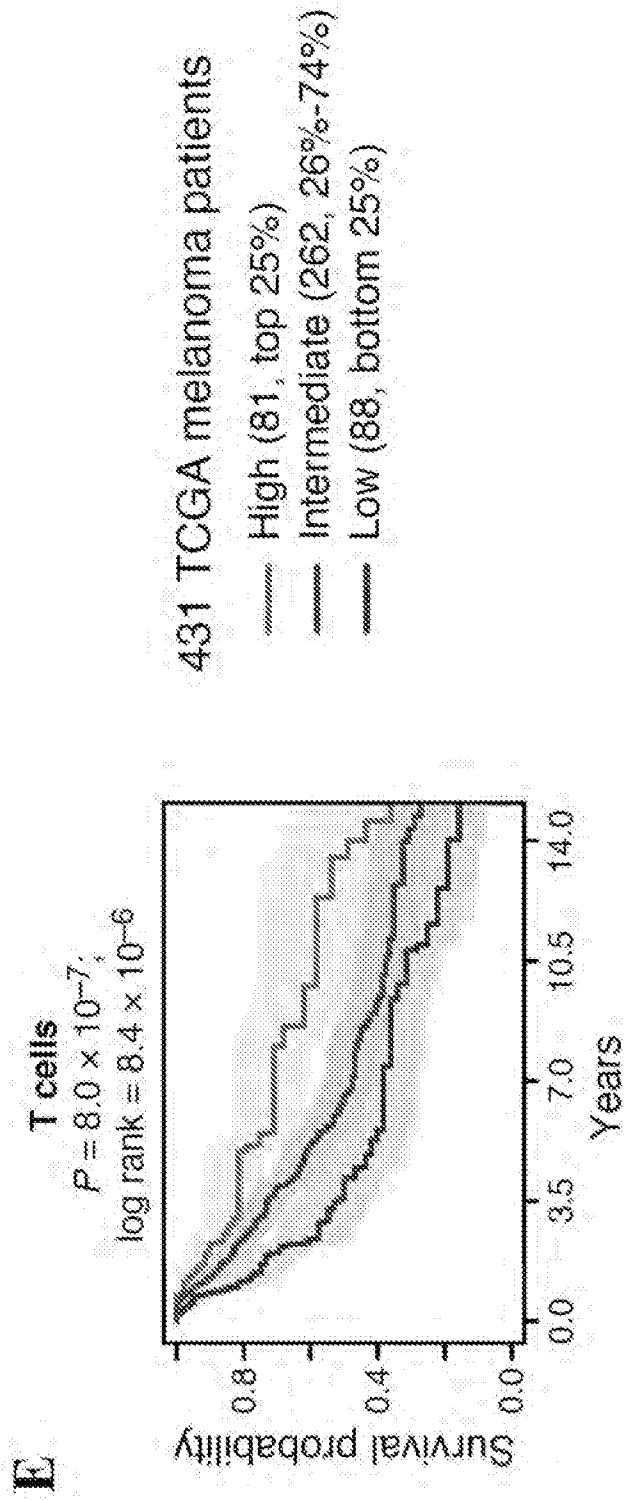


FIG. 54E

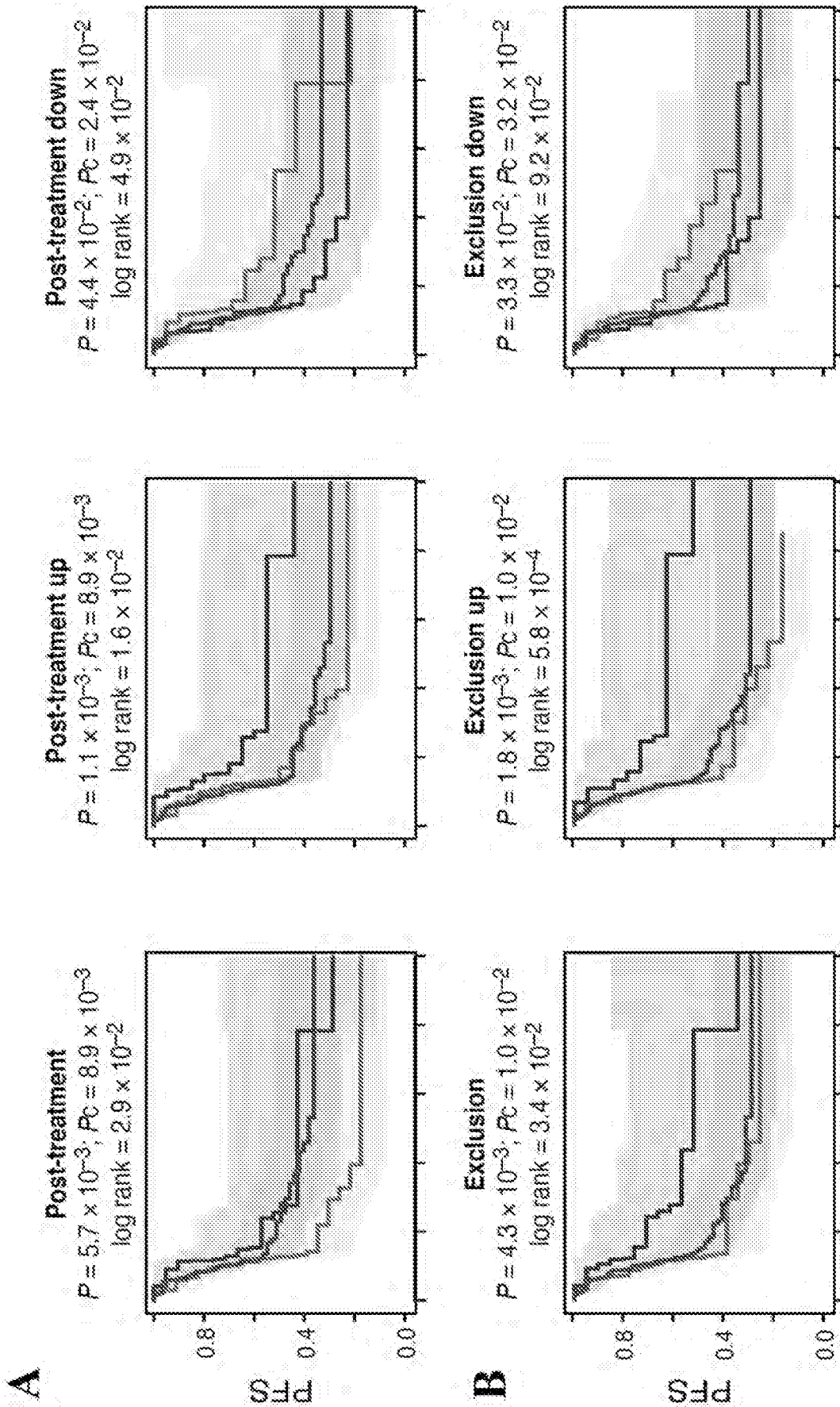


FIG. 55A-B

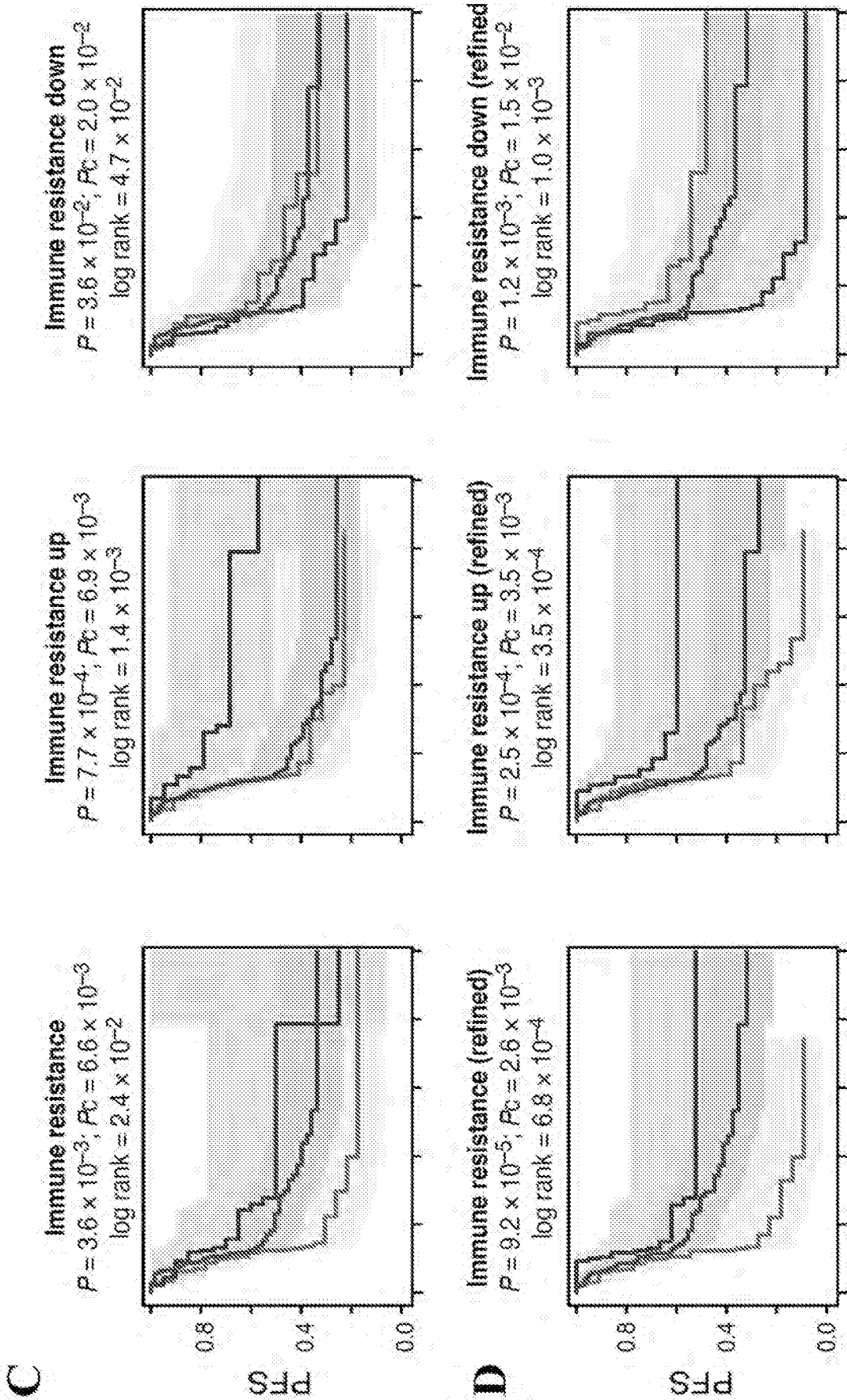
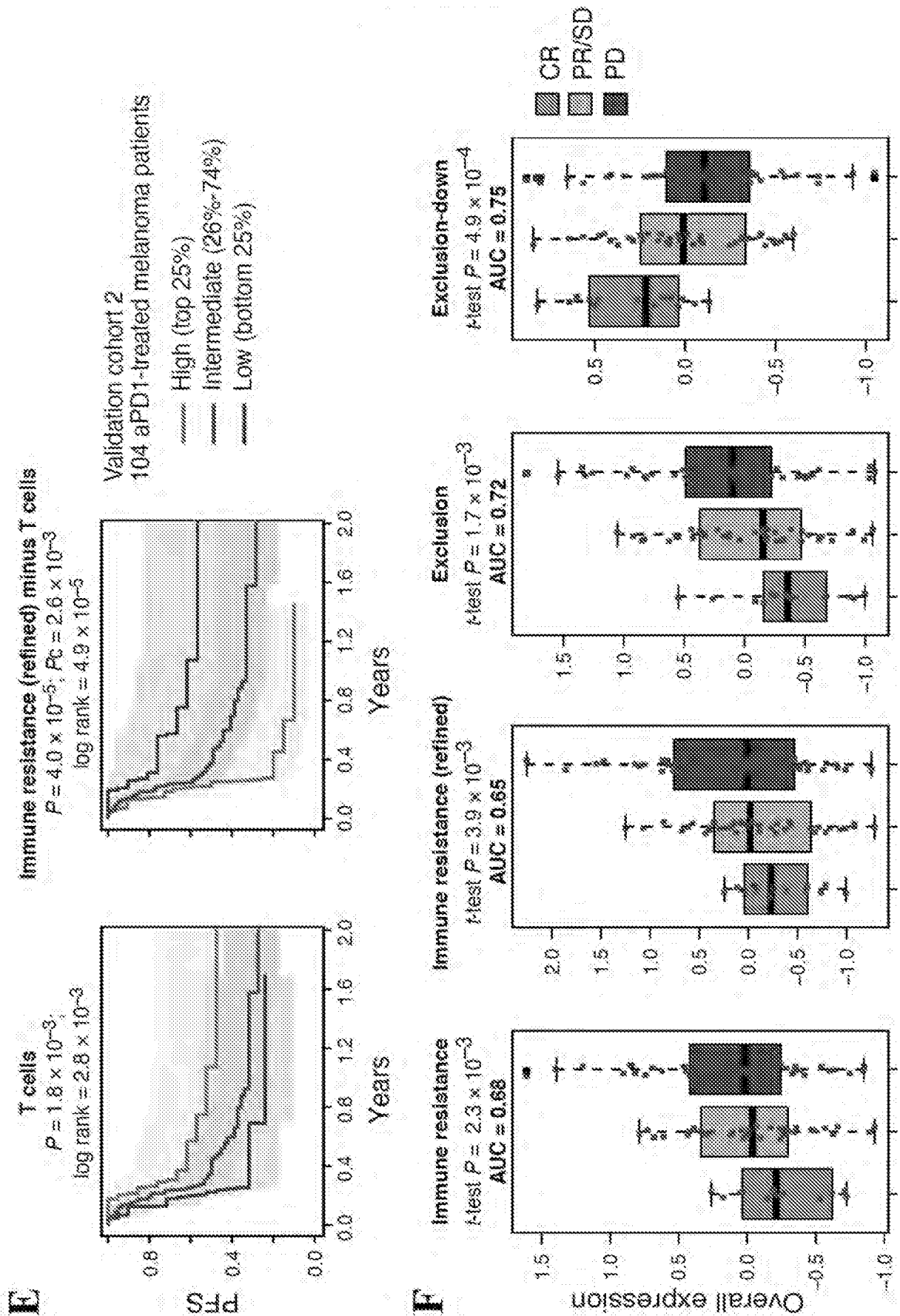


FIG. 55C-D



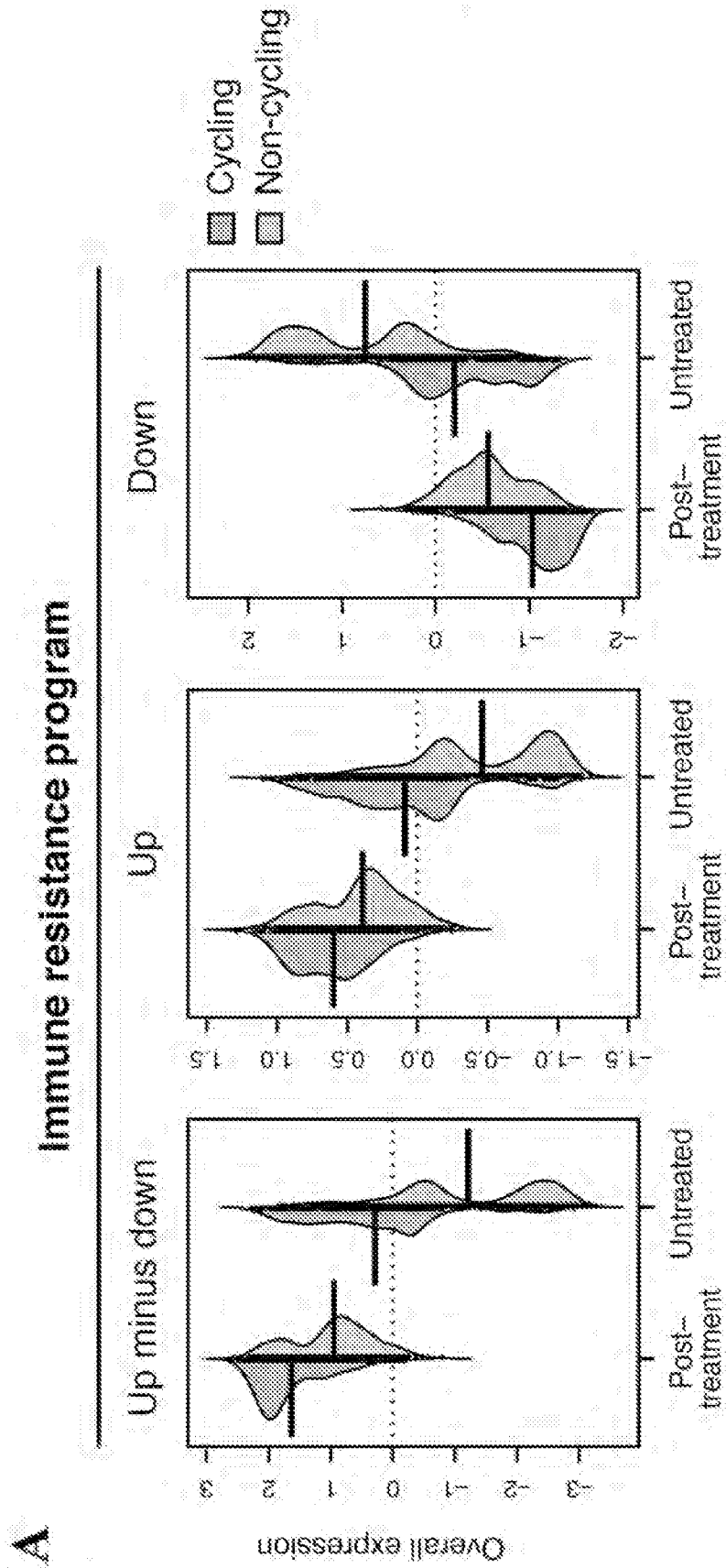
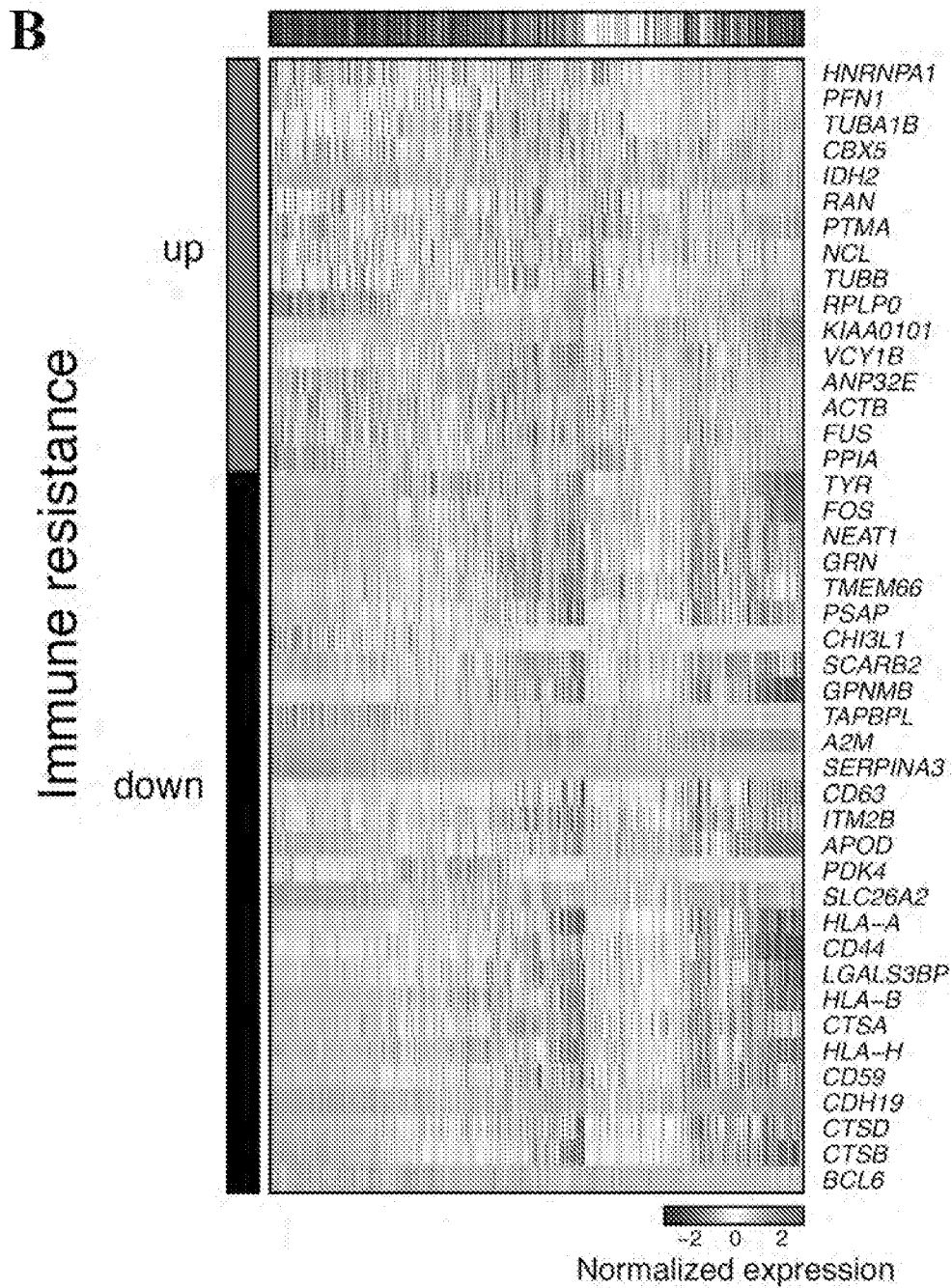


FIG. 56A



- Post-treatment cycling
- Post-treatment non-cycling
- Untreater cycling
- Untreater non-cycling

FIG. 56B

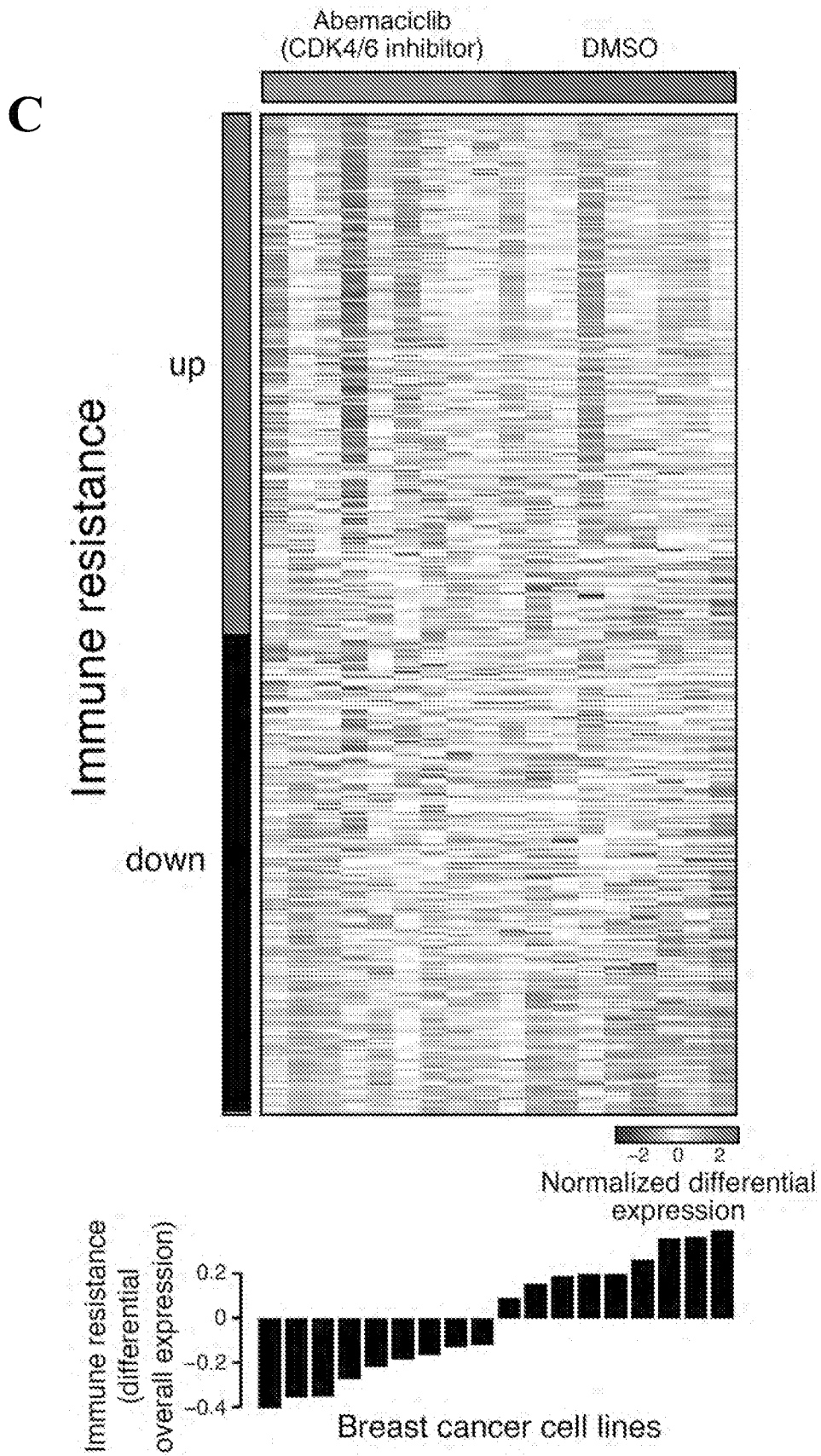


FIG. 56C

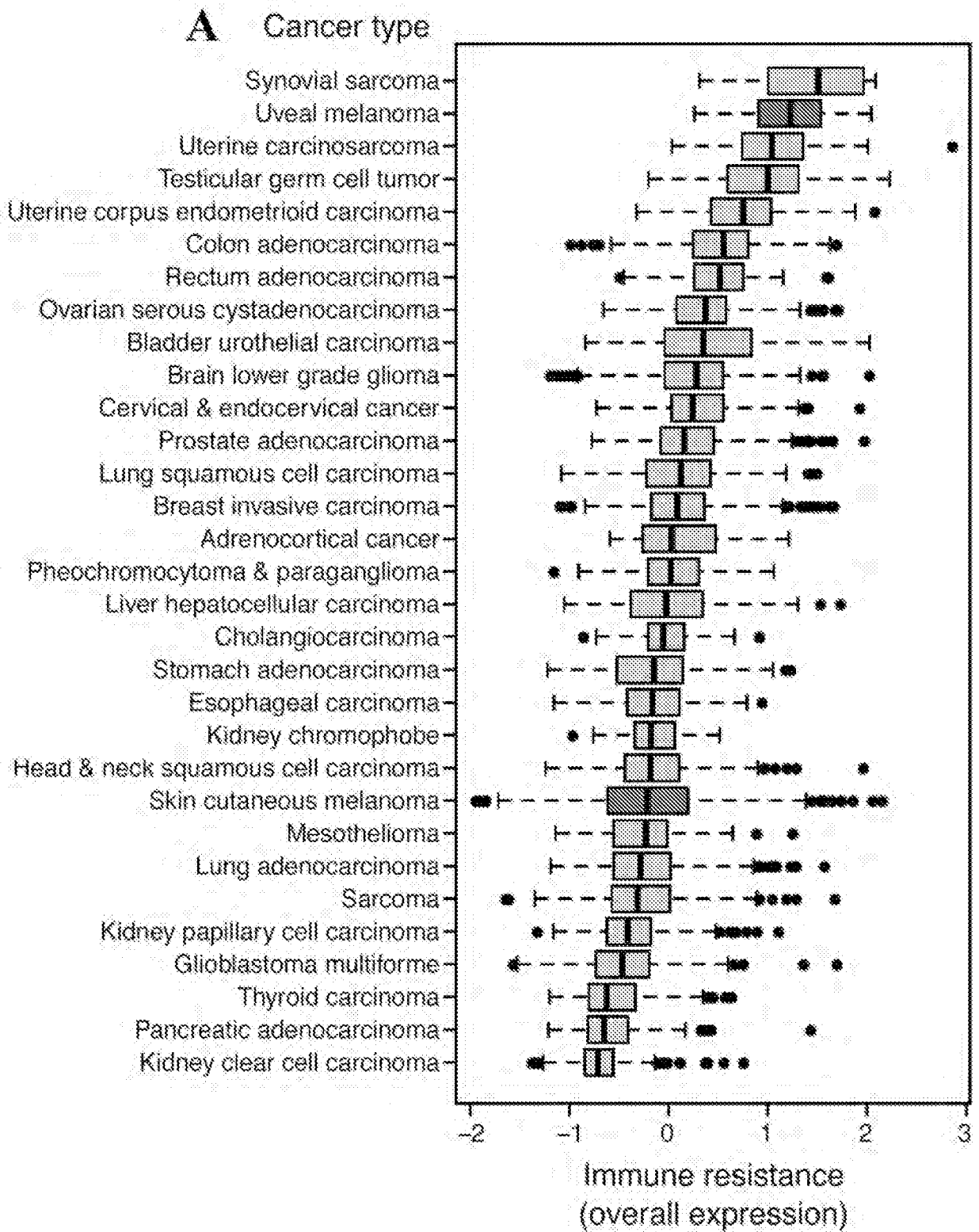


FIG. 57A

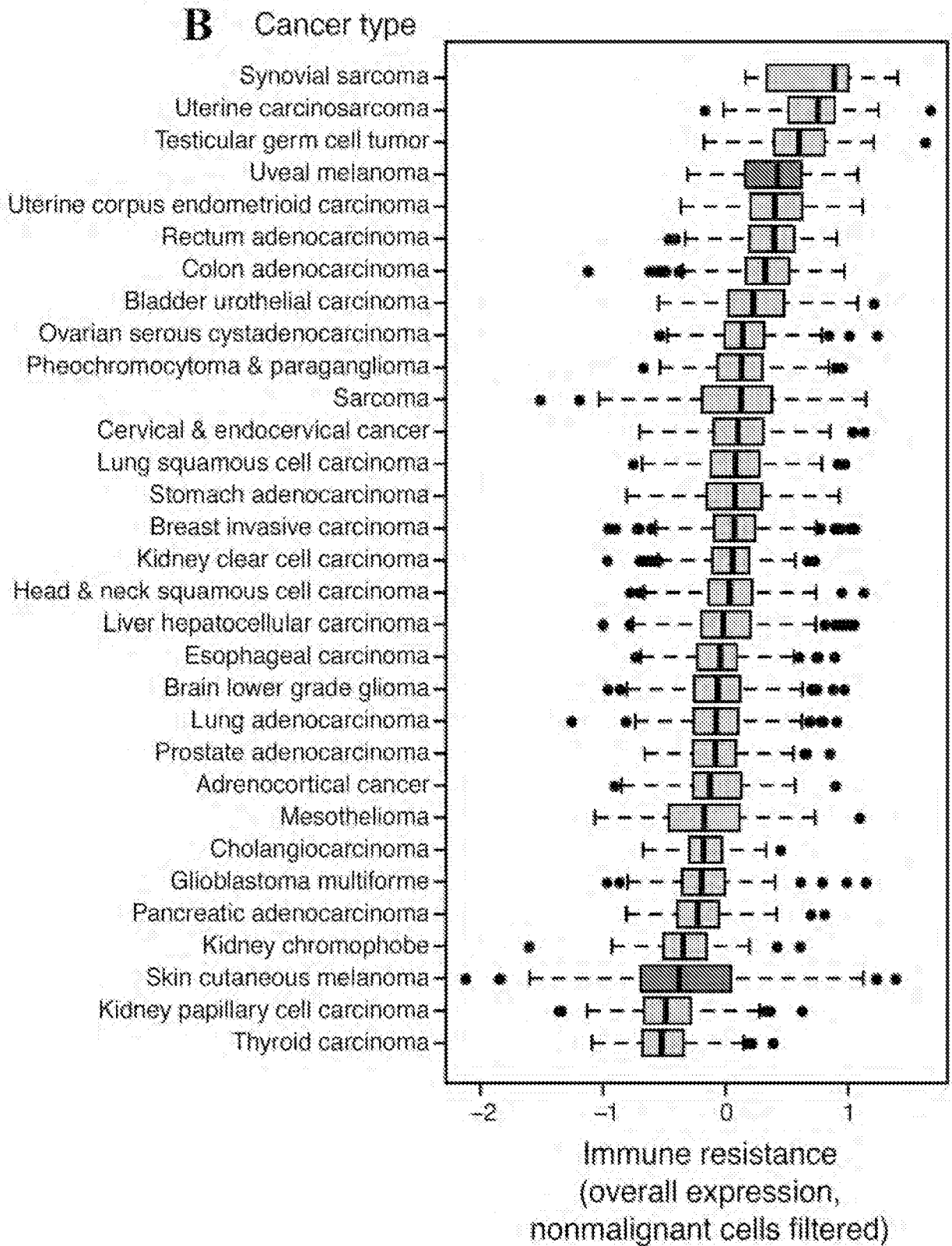


FIG. 57B

INTERNATIONAL SEARCH REPORT

International application No.
PCT/US 18/25507

A. CLASSIFICATION OF SUBJECT MATTER
IPC(8) - A61 K 31/40, A61 K 31/401 5, A61 K 31/4035 (201 8.01)
CPC - C12Q 2600/1 56, A61 K 31/4439

According to International Patent Classification (IPC) or to both national classification and IPC

B. FIELDS SEARCHED

Minimum documentation searched (classification system followed by classification symbols)
 See Search History Document

Documentation searched other than minimum documentation to the extent that such documents are included in the fields searched
 See Search History Document

Electronic data base consulted during the international search (name of data base and, where practicable, search terms used)
 See Search History Document

C. DOCUMENTS CONSIDERED TO BE RELEVANT

Category*	Citation of document, with indication, where appropriate, of the relevant passages	Relevant to claim No.
X	WO 2016/057705 A1 (NOVARTIS AG) 14 April 2016 (14.04.2016) p. 2, ln 19-25; p. 7, ln 24-30; p.5, ln 10 to p. 6, ln 10; p. 10, ln 5 to p. 11, ln 8; p. 13, ln 8-9; p. 14, ln 3-21 ; p. 68, ln 27-28; p. 132, ln 6-20; p. 141, ln 16-22; p. 181, ln 20-24; p. 221, ln 20-26; p. 241 , ln 13-20; Table 7A.	1, 3, 4, 6, 7/(1,3,4,6), 8, 10, 45
A	WO 2015/164743 A2 (DANA FARBER CANCER INSTITUTE INC) 29 October 2015 (29.10.2015) full document, especially abstract.	1, 3, 4, 6, 7/(1,3,4,6), 8, 10, 45
X,P	US 2018/0051347 A1 (UNIVERSITY OF CALIFORNIA) 22 February 2018 (22.02.2018) full document, especially abstract.	1, 3, 4, 6, 7/(1,3,4,6), 8, 10, 45

Further documents are listed in the continuation of Box C. See patent family annex.

* Special categories of cited documents:	"T" later document published after the international filing date or priority date and not in conflict with the application but cited to understand the principle or theory underlying the invention
"A" document defining the general state of the art which is not considered to be of particular relevance	"X" document of particular relevance; the claimed invention cannot be considered novel or cannot be considered to involve an inventive step when the document is taken alone
"E" earlier application or patent but published on or after the international filing date	"Y" document of particular relevance; the claimed invention cannot be considered to involve an inventive step when the document is combined with one or more other such documents, such combination being obvious to a person skilled in the art
"L" document which may throw doubts on priority claim(s) or which is cited to establish the publication date of another citation or other special reason (as specified)	"&" document member of the same patent family
"O" document referring to an oral disclosure, use, exhibition or other means	
"P" document published prior to the international filing date but later than the priority date claimed	

Date of the actual completion of the international search 07 August 2018	Date of mailing of the international search report 28 AUG 2018
---	--

Name and mailing address of the ISA/US Mail Stop PCT, Attn: ISA/US, Commissioner for Patents P.O. Box 1450, Alexandria, Virginia 22313-1450 Facsimile No. 571-273-8300	Authorized officer: Lee W Young PCT Helpdesk: 571-272-4300 PCT OSP: 571-272-7774
---	--

INTERNATIONAL SEARCH REPORT

International application No.

PCT/US 18/25507

Box No. **I** Nucleotide and/or amino acid sequence(s) (Continuation of item 1.c of the first sheet)

1. With regard to any nucleotide and/or amino acid sequence disclosed in the international application, the international search was carried out on the basis of a sequence listing:

a. forming part of the international application as filed:

in the form of an Annex C/ST.2₅ text file.

on paper or in the form of an image file.

b. furnished together with the international application under PCT Rule 13ter.1(a) for the purposes of international search only in the form of an Annex C/ST.25 text file.

c. furnished subsequent to the international filing date for the purposes of international search only:

in the form of an Annex C/ST.25 text file (Rule 13/er.1(a)).

on paper or in the form of an image file (Rule 13ter.1(b) and Administrative Instructions, Section 713).

2. In addition, in the case that more than one version or copy of a sequence listing has been filed or furnished, the required statements that the information in the subsequent or additional copies is identical to that forming part of the application as filed or does not go beyond the application as filed, as appropriate, were furnished.

3. Additional comments:

INTERNATIONAL SEARCH REPORT

International application No.

PCT/US 18/25507

Box No. II Observations where certain claims were found unsearchable (Continuation of item 2 of first sheet)

This international search report has not been established in respect of certain claims under Article 17(2)(a) for the following reasons:

- 1. [] Claims Nos.: because they relate to subject matter not required to be searched by this Authority, namely:
2. [] Claims Nos.: because they relate to parts of the international application that do not comply with the prescribed requirements to such an extent that no meaningful international search can be carried out, specifically:
3. [X] Claims Nos.: 11-44, 46-48 because they are dependent claims and are not drafted in accordance with the second and third sentences of Rule 6.4(a).

Box No. III Observations where unity of invention is lacking (Continuation of item 3 of first sheet)

This International Searching Authority found multiple inventions in this international application, as follows: This application contains the following inventions or groups of inventions which are not so linked as to form a single general inventive concept under PCT Rule 13.1. In order for all inventions to be examined, the appropriate additional examination fees must be paid.

Group I+, claims 1-10 and 45, directed to a method of detecting an immune checkpoint inhibitor resistance (ICR) gene signature in a tumor. The method will be searched to the extent that the gene signature encompasses C1QBP. It is believed that claims 1, 3, 4, 6, 7(in part), 8, 10 and 45 encompass this first named invention, and thus these claims will be searched without fee to the extent that the gene signature encompasses C1QBP. Additional gene signature gene(s) or polypeptide(s) will be searched upon the payment of additional fees. Applicants must specify the claims that encompass any additionally elected gene signature gene(s) or polypeptide(s). Applicants must further indicate, if applicable, the claims which encompass the first named invention, if different than what was indicated above for this group. Failure to clearly identify how any paid additional invention fees are to be applied to the "+" group(s) will result in only the first claimed invention to be searched. An exemplary election would be CCT2 (claims 1, 3, 4, 6 and 7(in part), 45).

-continued on extra sheet-

- 1. [] As all required additional search fees were timely paid by the applicant, this international search report covers all searchable claims.
2. [] As all searchable claims could be searched without effort justifying additional fees, this Authority did not invite payment of additional fees.
3. [] As only some of the required additional search fees were timely paid by the applicant, this international search report covers only those claims for which fees were paid, specifically claims Nos.:
4. [X] No required additional search fees were timely paid by the applicant. Consequently, this international search report is restricted to the invention first mentioned in the claims; it is covered by claims Nos.: 1, 3, 4, 6, 7/(1,3,4,6), 8, 10, 45, limited to C1QBP

Remark on Protest

- [] The additional search fees were accompanied by the applicant's protest and, where applicable, the payment of a protest fee.
[] The additional search fees were accompanied by the applicant's protest but the applicable protest fee was not paid within the time limit specified in the invitation.
[] No protest accompanied the payment of additional search fees.

-continued from Box III: Observations where unity of invention is lacking--

The inventions listed as Group I+ do not relate to a single special technical feature under PCT Rule 13.1 because, under PCT Rule 13.2, they lack the same or corresponding special technical features for the following reasons:

Special technical features

The inventions of Group I+ each include the special technical feature of a unique amino acid sequence. Each amino acid sequence encodes a unique peptide, and is considered a distinct technical feature.

Shared technical features

The inventions of Group I+ share the common technical features of a method of detecting an immune checkpoint inhibitor resistance (ICR)/an immune cell exclusion gene signature in a tumor comprising, detecting in tumor cells obtained from a subject in need thereof the expression or activity of a malignant cell gene signature comprising one or more genes or polypeptides;

wherein the subject has been treated with an immunotherapy;

wherein the malignant cell gene signature comprises: a) one or more down regulated genes selected from the group consisting of genes associated with coagulation, apoptosis, TNF- α signaling via NF κ B, Antigen processing and presentation, metallothionein and IFNGR2; and/or b) one or more up regulated genes selected from the group consisting of genes associated with negative regulation of angiogenesis and MYC targets.

However, these shared technical features are previously disclosed by WO 2016/057705 A1 to NOVARTIS AG (hereinafter Novartis).

Novartis teaches a method of detecting an immune checkpoint inhibitor resistance (ICR) gene signature in a tumor comprising, detecting in tumor cells obtained from a subject in need thereof the expression or activity of a malignant cell gene signature (p. 2, In 19-25 "genes, whose expression, at the transcriptional and protein levels, are correlated with CLL and ALL progression, e.g., as a way of predicting a response to a Chimeric Antigen Receptor (CAR)-expressing cell therapy (e.g., a therapy comprising a cell (e.g., an immune effector cell or population of cells)...a biomarker listed in Table 1A, Table 1B, Table 7A"; p. 7, In 24-30 "a method of, or assay for, identifying a subject having a cancer as having an increased or decreased likelihood to respond to a treatment...providing, e.g., acquiring, a sample from the subject; (2) determining a level or activity of one or more biomarkers listed in Table 1A, Table 1B, Table 7A...wherein a difference, e.g., a statistically significant difference, between the determined level compared to a reference level is predictive of the subject's responsiveness to the CAR- expressing cell therapy"; p. 14, In 15-21 "a non-responder has, or is identified as having, a greater percentage of an immune cell exhaustion marker, e.g., one, two or more immune checkpoint inhibitors (e.g., PD-1, TIM-3 and/or LAG-3)" comprising:

a) one or more genes or polypeptides selected from the group consisting of C1QBP (p. 10, In 21-30 "the value of responder or relapse status comprises a measure of a combination of a gene signature and a biomarker. In some embodiments, the value of the responder or relapse status comprises a measure of a CD 19 CAR-expressing cell gene set signature and a combination of one or more of: a biomarker listed in Table 1A, Table 1B, Table 7A...the expression profile includes one or more gene signatures based on mRNA expression levels of selected genes obtained from the apheresis sample or a manufactured CD 19 CAR-expressing cell product (e.g., CTL019). In one embodiment, the expression profile includes one, two, three, four, five, ten, twenty or more of a biomarker listed in Table 1A, Table 1B, Table 7A"; p. 255, Table 7A ("Exemplary genes that predict patient response to CTL019 therapy...C1QBP Hs.555866 NM_001212 (at p. 256)"; p. 181, In 20-24 "the method further includes administering the mTOR inhibitor and/or the CAR in combination with one or more checkpoint inhibitors described here, such as, e.g., a Pdlinhibitor"; p. 10, In 1-5 "the population of immune effector cells (e.g., cells expressing a CAR molecule described herein) is administered in combination with an inhibitor of an immune checkpoint molecule chosen from one or more of PD1, PD-L1, PD-L2, CTLA4"), wherein the subject has been treated with an immunotherapy (p. 38, In 1-5 "a subject identified as a partial responder or non-responder and who has been subsequently treated with an agent that increases the number of naive T cells in the subject, e.g., the subject has been treated with a kinase inhibitor, e.g., an mTOR inhibitor, e.g., as described herein, and/or a checkpoint inhibitor, e.g., as described herein").

Novartis further teaches wherein the malignant cell gene signature comprises: a) one or more down regulated genes selected from the group consisting of genes associated with coagulation, apoptosis, TNF- α signaling via NF κ B, Antigen processing and presentation, metallothionein and IFNGR2; and/or b) one or more up regulated genes selected from the group consisting of genes associated with negative regulation of angiogenesis and MYC targets (p. 14, In 3-21 "a complete responder has, or is identified as having, a greater percentage of one, two, three, or more (e.g., all) of resting TEFF cells...compared to a reference value, e.g., a non-responder number of resting TEFF cells...a non-responder has, or is identified as having, a greater percentage of an immune cell exhaustion marker, e.g., one, two or more immune checkpoint inhibitors (e.g., PD-1, TIM-3 and/or LAG-3). In one embodiment, a non-responder has, or is identified as having, a greater percentage of PD-1 or LAG-3 expressing immune effector cells (e.g., CD4+ T cells and/or CD8+ T cells) (e.g., CAR-expressing CD4+ cells and/or CD8+ T cells) compared to the percentage of PD-1 or LAG-3 expressing immune effector cells from a responder"; p. 241, In 13-20 "Exemplary genes according to Table 2 downregulated in Teff at 16 h vs 0 h include...ANXA1"; applicant specification p. 183, Table 1. ANXA1 is listed as a coagulation gene); p. 240, In 20 to p. 241, In 12 "Exemplary genes according to Table 2 downregulated in Treg compared with Teff at 0h include ABCB1, ACSL6, ADAMTS10, ADD2, AIF1, AIF1, AIF1, AK5, AKR1 E2, ALS2CL, ANK3, ANKRD55, APBA2, AREG, ATHL1, AXIN2, B4GALNT4, BACH2, BCL7A, BEND5, BHLHE40, BPGM, C10orf47, C16orf54, Clorf228, C2orf89, CA6"; p. 16, In 27-31 "any of the aforesaid methods and compositions for use, a TEFFcell (e.g., an activated TEFFcell) has upregulated expression of one or more (e.g., at least 10, 20, 30, 40, 50, 60, 70, or all) of the following biomarkers: AIM2, ALAS1, B4GALT5, BATF, C3orf26, C4orf43, CCL3, CCL4").

As the technical features were known in the art at the time of the invention, they cannot be considered special technical features that would otherwise unify the groups.

Therefore, Group I+ inventions lack unity under PCT Rule 13 because they do not share the same or corresponding special technical feature.

NOTE, claims 11-44 and 46-48 are held unsearchable because they are dependent claims and are not drafted in accordance with the second and third sentences of Rule 6.4(a).